ANNUAL REVIEW

INSTITUTE FOR MOLECULAR SCIENCE

1990

ANNUAL REVIEW

INSTITUTE
FOR
MOLECULAR
SCIENCE
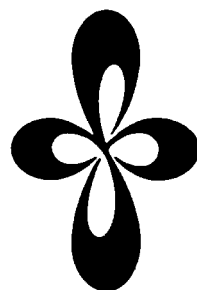
1990

IMS 1990

Institute for Molecular Science was established in 1975. Because 15 years has passed since the establishment of IMS, we are making plans for the coming 15 years. The faculty of IMS has thoroughly discussed what research subjects should be pursued at IMS and what kind of research organization is most appropriate for the future. After extensive discussions we have decided to reorganize our research departments. Briefly, our fisrst step is to establish research groups to carry out research using vacuum ultraviolet light from our Ultraviolet Synchrotron Orbital Radiation facility (UVSOR).

Our synchrotorn radiation light source, which was commissioned in 1984, has been used actively as an excellent tunable light source by about 500 users, including visiting scientists as well as our in-house staff. In order to accelerate the on-going research projects and to further explore new research fields in the vacuum UV region, where molecules can strongly interact with the light, we have focused our efforts to the establishment of a new research department named the Department of Vacuum Ultraviolet Radiation Science. Thanks to the great support of the Ministry of Education, Science, and Culture, in 1991 we expect to reorganize the present research departments, in particular the Department of Molecular Assemblies, from the present five research departments and seven facilities to six research departments and seven research facilities. In order to advance the research by the new department to be established, extensive use of lasers is anticipated.

The turnover in personnel to and from IMS has been very active. Professor Eizi Hirota, who had headed Laboratory of Molecular Structure I, moved to the Graduate University for Advanced Studies, as a Vice President of the University. The names of the other researchers and technical associates who have moved from or joined the IMS since Sept. 1, 1989 till Aug. 31, 1990 are listed in the list of staff.

December, 1990

Hiroo INOKUCHI

CONTENTS

ORGANIZATION AND STAFF

Organization

The Institute for Molecular Science comprises twenty one research laboratories—each staffed by a professor, an associate professor, two research associates and several technical associates—, two research laboratories with foreign visiting professors, and six research facilities. The laboratories are grouped into five departments and one facility for coordination chemistry:

Department of Theoretical Studies	Theoretical Studies I
	Theoretical Studies II
	Theoretical Studies III[1]
Department of Molecular Structure	Molecular Structure I
	Molecular Structure II[1]
	Molecular Dynamics
Department of Electronic Structure	Excited State Chemistry
	Excited State Dynamics
	Electronic Structure[1]
	Molecular Energy Conversion[2]
Department of Molecular Assemblies	Solid State Chemistry
	Photochemistry
	Molecular Assembly Dynamics
	Interface Molecular Science
	Molecular Assemblies[1]
	Synchrotron Radiation Research[2]
Department of Applied Molecular Science	Applied Molecular Science I
	Applied Molecular Science II[1]
	Physical Organic Chemistry
Coordination Chemistry Laboratories	Synthetic Coordination Chemistry
	Complex Catalysis
	Functional Coordination Chemistry
	Coordination Bond[1]
Research facilities are:	Computer Center
	Chemical Materials Center
	Instrument Center
	Low-Temperature Center
	Equipment Development Center
	Ultraviolet Synchrotron Orbital Radiation
	(UVSOR) Facility.

1) Professors and associate professors are adjunct professors from other universities.
2) Research Laboratories with foreign visiting professors.

Scientific Staff

Hiroo INOKUCHI   Professor, Director-General

Department of Theoretical Studies
Theoretical Studies I

Keiji MOROKUMA	Professor
Iwao OHMINE	Associate Professor
Koichi YAMASHITA	Research Associate
Masaki SASAI	Research Associate
Norihiro SHIDA	Research Associate (April '90—)
Yoshiaki AMATATSU	Technical Associate
Shinji SAITO	Technical Associate (April '90—)
Andrea DORIGO	JSPS Post-doctral Fellow (—July '90)
Simon MATHIEU	JSPS Post-doctral Fellow (—March '90)
Yanbo DING	Graduate Student (—June '90)
Kyoichi SAWABE	Graduate Student from Univ. of Tokyo* (—March '90)
Toshiaki FUJII	Graduate Student (April '90—)
Tamiki KOMATSUZAKI	Graduate Student (April '90—)
Hiroo FUKUNAGA	Visiting Research Fellow from Fuji Photo Film Co.
Hiroshi KURIBAYASHI	Visiting Research Fellow from Sumitomo Chemical Co.
Jun ENDO	Visiting Research Fellow from Mitsubishi Petrochemical Co.
Tadahiro OZAWA	Visiting Research Fellow from Kao Corp.
Katsuhiro HASHIMOTO	Visiting Research Fellow from Sumitomo Pharmaceutical Co.

Theoretical Studies II

Hiroki NAKAMURA	Professor
Keiichiro NASU	Associate Professor
Masahiro IWAI	Research Associate
Kaoru IWANO	Research Associate (June '90—)
Akihiko OHSAKI	Technical Associate (—Nov. '89) Research Associate (December '89—April '90)[1]
Masato SUZUKI	Technical Associate (April '90—)
Shoji TAKADA	Graduate Student (April '90—)

Theoretical Studies III

Michio MATSUZAWA	Adjunct Professor from The University of Electro-Communications (—March '90)
Kimihiko HIRAO	Adjunct Professor from Nagoya University (April '90—)
Shigeyoshi SAKAKI	Adjunct Professor from Kumamoto University (April '90—)
Yuzo SHINOZUKA	Adjunct Associate Professor from Yamaguchi University (—March '90)
Nobuaki KOGA	Research Associate
Kiyohiko SOMEDA	Research Associate

Department of Molecular Structure
Molecular Structure I

Eizi HIROTA	Professor (−January '90)[2]
Norio MORITA	Associate professor
Chikashi YAMADA	Research Associate (−April '90)[3]
Asuka FUJII	Research Associate (September '89−)
Mitsutaka KUMAKURA	Technical Associate
Wyn LEWIS-BEVAN	Visiting Scientist (−November '89)

Molecular Structure II

Takashi KUSHIDA	Adjunct Professor from Osaka Univ.
Yasuki ENDO	Adjunct Associate Professor from Univ. of Tokyo (−March '90)
Tsutomu YABUZAKI	Adjunct Associate Professor from Kyoto Univ. (April '90−)
Takashi OGURA	Research Associate
Toshinori SUZUKI	Research Associate (−September '90)[4]
Misaki OKUNISHI	Research Associate (May '90−)

Molecular Dynamics

Teizo KITAGAWA	Professor
Yasuo UDAGAWA	Associate Professor
Keiji KAMOGAWA	Research Associate
Kazuyuki TOHJI	Research Associate
Takanori MIZUSHIMA	Technical Associate
Shin'ichiro SATO	Technical Associate
Eleni ANNI	EC Post-doctoral Fellow (−October '89)
Jiři HUDEČEK	Visiting Scientist from Charles Univ., Czechoslovakia (−August '90)
Paul CHAMPION	Visiting Scientist (May '90−August '90)
Scott L. ANDERSON	Visiting Scientist (−February '90)
Shoji KAMINAKA	JSPS Post-doctoral Fellow
Masashi NAKAGAWA	JSPS Post-doctoral Fellor (−December '89)[5]
Tsuyoshi EGAWA	Graduate Student from Tokyo Metropolitan Univ.*
Takeshi MIKI	Graduate Student from Toyohashi Univ. of Tech.* (−March '90)
Naoyuki TAKAHASHI	Graduate Student from Toyohashi Univ. of Tech.* (−March '90)
Hisashi HAYASHI	Graduate Student
Yasuhisa MIZUTANI	Graduate Student
Yoshinao SAKAN	Graduate Student
Satoshi TAKAHASHI	Graduate Student

Department of Electronic Structure
Excited State Chemistry

Keitaro YOSHIHARA	Professor
Yoshiyasu MATSUMOTO	Associate Professor (March '90−)
Hrvoje PETEK	Research Associate
Tohru KOBAYASHI	Technical Associate
Hideki KANDORI	Post-doctoral Fellow (April '90−)
Takeshi SUZUMOTO	Visiting Research Fellow from Fuji Photo Film Co. Ltd.
Ryoji INABA	Graduate Student from the Univ. of Tokyo* (April '90−)
Ronald L. CRISTENSEN	Visiting Scientist (February−May '90)
Rachel HOWELL	Visiting Graduate Student (October '89−December '89)

Excited State Dynamics

Ichiro HANAZAKI	Professor
Nobuyuki NISHI	Associate Professor
Masao TAKAYANAGI	Research Associate
Minoru SUMITANI	Research Associate (—September '90)[6]
Kazuhiko OHASHI	Research Associate
Teruhiko NISHIYA	Technical Associate
Yoshihito MORI	Technical Associate
Kazunori YAMAMOTO	Technical Associate (—January '90)[7]
Prem K. SRIVASTAVA	Visiting Scientist
Pascal LABLANQUIE	Visiting Scientist (April '90—)
Nam-Soo LEE	Visiting Scientist (July '90—August '90)
Fushi ZHANG	Visiting Scientist (October '89—December '89)
Kazuhiro HONDA	Graduate Student
Takumi KOHNO	Graduate Student
Tetsuo SEKIGUCHI	Graduate Student

Electronic Structure

Michiya ITOH	Adjunct Professor from Kanazawa Univ. (April '90—)
Koichi ITO	Adjunct Professor from Osaka Univ. (—March '90)
Masaharu OKAZAKI	Adjunct Professor from Government Industrial Research Institute, Nagoya
Ryoichi NAKAGAKI	Research Associate (—March '90)[8]
Hiromi OKAMOTO	Research Associate (—September '90)[9]
Kaoru SUZUKI	Research Associate (August '90—)

Molecular Energy Conversion

John H.D. ELAND	Visiting Professor from Oxford Univ., United Kingdom (—August '89)
Georg JOHANSSON	Visiting Professor from Royal Inst. of Technology, Sweden
Vaclav KUBEČEK	Visiting Associate Professor from Technical Univ. of Prague, Czechoslovakia (August '90—)
Ramakrishna RAMASWAMY	Visiting Associate Professor from Jawaharlal Nehru Univ., India (October '89—August '90)

Department of Molecular Assemblies

Solid State Chemistry

Kyuya YAKUSHI	Professor
Inosuke KOYANO	Associate Professor (—March '90)[10]
Takashi IMAMURA	Research Associate
Akito UGAWA	Research Associate
Ken-ichi IMAEDA	Technical Associate
Shinzo SUZUKI	Technical Associate (—March '90)[11]
Takashi IDA	Technical Associate
Atsushi KAWAMOTO	IMS Fellow (April '90—)
Hideo YAMAKADO	Graduate Student
Kentaro IWASAKI	Graduate Student (April '90—)
Hideji ISHII	Graduate Student from Univ. of Tokyo* (April '90—)

Photochemistry

Katsumi KIMURA	Professor
Kosuke SHOBATAKE	Associate Professor
Kiyohiko TABAYASHI	Research Associate
Katsuhiko OKUYAMA	Research Associate

Masahiko TAKAHASHI	Technical Associate
Kohji KAMIYA	IMS Fellow
Kunikazu KONDO	Graduate Student from Nagoya Univ.*
Tatsuya MIYAKE	Graduate Student from Toyohashi Univ. of Technology* (April '90—)
Hiroyuki OZEKI	Graduate Student
Haruhiko OHASHI	Graduate Student from Toyohashi Univ. of Technology*
Hiroshi YOSHIKAWA	Graduate Student (April '90—)
Kenichi KATOH	Graduate Student from Toyohashi Univ. of Technology* (October '89—April '90)
Toshiyasu TSUBOUCHI	Graduate Student from Toyohashi Univ. of Technology* (—March '90)
Yasuhiro IWANO	Graduate Student from Toyohashi Univ. of Technology*

Molecular Assemblies Dynamics

Yusei MARUYAMA	Professor
Masatoshi SATO	Associate Professor (—March '90)[12]
Tamotsu INABE	Research Associate
Masashige ONODA	Research Associate (—March '90)[13]
Masafumi SERA	Research Associate (—March '90)[14]
Hajime HOSHI	Technical Associate
Shin-ichi SHAMOTO	Technical Associate
Toshifumi TERUI	Graduate Student
Isabelle GAUTIER-LUNEAU	Graduate Student (—October '90)
Shin-ichi YAMAGATA	Graduate Student from Nagoya Univ.* (—March '90)
Hironori OGATA	Graduate Student (April '90—)
Yoshihisa MORI	Graduate Student (April '90—)
Chikako NAKANO	Visiting Research Fellow
Naoki NAKAMURA	Visiting Research Fellow from Toyota Motor Co., Ltd. (April '90—)

Interface Molecular Science

Shinri SATO	Associate Professor
Tatsuo MATSUSHIMA	Associate Professor
Tadayoshi OHMORI	Research Associate
Yuichi OHNO	Research Associate
Yuji UKISU	Technical Associate
Kiyoshi NAGAI	Visiting Research Fellow (April '90—)

Molecular Assemblies

Yuuji OHASHI	Adjunct Professor from Tokyo Inst. of Technology.
Youji ACHIBA	Adjunct Associate Professor from Tokyo Metropolitan Univ.
Takehiko MORI	Research Associate
Shin-ichi NAGAOKA	Research Associate (—October '89)[15]
Kenji FURUYA	Research Associate (April '90—)

Synchrotron Radiation Research

Robert J. FLEMING	Visiting Professor from Monash Univ., Australia (—November '89)
Xin SUN	Visiting Professor from Fudan Univ., China (June '90—)
Ellak I. VON NAGY-FELSOBUKI	Visiting Associate Professor from Univ. of Newcastle, Australia (—August '89)
S. NESPUREK	Visiting Associate Professor from Czechoslovakia Sci. Acad. Inst. of Macromolecular Chem., Czechoslovakia (March '90—)

Department of Applied Molecular Science

Applied Molecular Science I

Kazuhiro NAKASUJI	Professor
Kiyoshi ISOBE	Associate Professor
Koshiro TORIUMI	Research Associate
Yoshiki OZAWA	Research Associate
Yasushi MORITA	Research Associate (June '90−)
Yoshihito HAYASHI	Technical Associate
Jiro TOYODA	Technical Associate
Toshikazu KITAGAWA	IMS Fellow (−December '89)[16]
Toshi NAGATA	Visiting Scientist (January '90−March '90)[17]
Haruo AKASHI	JSPS Post-doctoral Fellow (April '90−)
Ken-ichi SUGIURA	Graduate Student
Takeshi OOMAE	Graduate Student
Amelio VAZQUEZ de MIGUEL	Visiting Professor from Univ. of Alecala de Henares, Spain, (June '90−December '90)
Youngkyu DO	Visiting Professor from Korea Advanced Institute of Science and Technology, Korea (July '90−August '90)

Applied Molecular Science II

Hideki SAKURAI	Adjunct Professor from Tohoku Univ.
Eiichi NAKAMURA	Adjunct Associate Professor from Tokyo Inst. of Tech.
Hiroki OSHIO	Research Associate

Physical Organic Chemistry

Yuho TSUNO	Professor
Junji INANAGA	Associate Professor
Masaaki MISHIMA	Research associate
Takeshi HANAMOTO	Research Associate (January '90−)
Hiroshi IMAHORI	Graduate Student from Kyoto Univ.* (−March '90)
Yuji MIKATA	Graduate Student from Kyoto Univ.* (April '90−)
Kenji TAKEHARA	Graduate Student from Kyushu Univ.* (April '90−)
Katsuya SAKO	Graduate Student from Kyushu Univ.* (April '90−)
Yoshihiro SAEKI	Graduate Student from Kyushu Univ.* (October '89−)
Izumi AKASAKA	Graduate Student from Kyushu Univ.* (October '89−)
Yasuo YOKOYAMA	Graduate Student from Kyushu Univ.* (October '89−)
Yoshiyasu BABA	Graduate Student from Kyushu Univ.* (October '89−)
Kazuhide NAKATA	Graduate Student from Kyushu Univ.* (April '90−)

Coordination Chemistry Laboratories

Hitoshi OHTAKI	Director

Synthetic Coordination Chemistry

Eiichi KIMURA	Professor (−March '90)[18]
Yoshihiko KUSHI	Professor (April '90−)
Ryuichi IKEDA	Associate Professor (−March '90)[19]
Fumio KAWAIZUMI	Associate Professor (April '90−)
Cynthia J. BURROWS	JSPS Visiting Associate Professor from State Univ. of New York (−February '90)
L.S. Prabhu MIRASHI	Visiting Scientist from Poona Univ., India (October '89−December '89)
Hideki MASUDA	Research Associate
Mitsuhiko SHIONOYA	Research Associate (−March '90)[20]
Tatsuya KAWAMOTO	Research Associate (April '90−)

Hiromasa KUROSAKI	Technical Associate (−July '90)
	Visiting Scientist (August '90−)
Yasuhisa KUROGI	Graduate Student from Hiroshima Univ.* (−March '90)
Tamotsu SUGIMORI	Graduate Student from Nagoya Univ.* (April '90−)

Complex Catalysis

Hitoshi OHTAKI	Professor
Toshikatsu YOSHIDA	Adjunct Professor from Univ. Osaka Pref. (−March '90)
Eiichi KIMURA	Adjunct Professor from Hiroshima Univ. (April '90−)
Reiko KURODA	Adjunct Associate Professor from Univ. of Tokyo (−March '90)
Ryuichi IKEDA	Adjanct Associate Professor from Nagoya Univ. (April '90−)
Kiyohiko NAKAJIMA	Research Associate
Atsushi YAGASAKI	Technical Associate
Yusuke TAMURA	IMS Fellow
Kwang O. KOH	Visiting Research Fellow from Soonchunhyang Univ. in Korea (December '89−February '90)
Dominique N. LUNEAU	JSPS Post-Doctoral Fellow (−December '89)
Nobuhiro FUKUSHIMA	Graduate Student from Tokyo Inst. of Tech.* (−March '90)
Kenji WAIZUMI	Graduate Student from Tohoku Univ.*

Functional Coordination Chemistry

Koji TANAKA	Professor (March '90−)
Hirotaka NAGAO	Research Associate (July '90−)
Nobutoshi KOMEDA	Graduate Student from Osaka Univ.* (April '90−)

Coordination Bond

Masanobu HIDAI	Adjunct Professor from Univ. of Tokyo
Toshio YAMAGUCHI	Adjunct Associate Professor from Fukuoka Univ.

Research Facilities

Computer Center

Keiji MOROKUMA	Director
Kazuo KITAURA	Associate Professor
Umpei NAGASHIMA	Research Associate
Shigeyoshi YAMAMOTO	Technical Associate (−April '90)[21]
Kazuhiko HONDA	Technical Associate (April '90−)

Chemical Materials Center

Kazuhiro NAKASUJI	Director
Yoshiro YAMASHITA	Associate Professor
Shoji TANAKA	Research Associate
Masaaki TOMURA	Technical Associate

Instrument Center

Ichiro HANAZAKI	Director
Kiyokazu FUKE	Associate Professor
Keisaku KIMURA	Research Associate
Fuminori MISAIZU	Research Associate
Shunji BANDOW	Research Associate (October '90−)
Keizo TSUKAMOTO	Graduate Student from Keio Univ.* (October '89−)

Low-Temperature Center

Yusei MARUYAMA	Director
Kunio AWAGA	Research Associate

Equipment Development Center

Teizo KITAGAWA	Director
Tadaoki MITANI	Associate Professor
Yoshihiro TAKAGI	Research Associate
Hiroshi OKAMOTO	Research Associate

Ultraviolet Synchrotron Orbital Radiation Facility

Katsumi KIMURA	Director
Makoto WATANABE	Associate Professor
Goro ISOYAMA	Associate Professor (October '89—)
Masao KAMADA	Associate Professor (January '90—)
Kazuhiko SEKI	Adjunct Associate Professor from Hiroshima Univ.
Hiroto YONEHARA	Research Associate (—April '90)[22]
Kazutoshi FUKUI	Research Associate (—April '90)[23]
Atsunari HIRAYA	Research Associate
Shin-ichiro TANAKA	Research Associate (May '90—)
Shirou TAKANO	Research Associate (May '90—)

Technical Staff

Akira UCHIDA	Technical Division Head
Keiichi HAYASAKA	Technical Section Chief
Kusuo SAKAI	Technical Section Chief
Satoshi INA	Technical Section Chief
Fumio NISHIMOTO	Computer Center (Unit Chief)
Fumitsuna TESHIMA	Computer Center
Kunihiko TANAKA	Computer Center
Junko KIRITOOSHI	Chemical Materials Center
Takaya YAMANAKA	Instrument Center
Masahiro SAKAI	Instrument Center
Kiyonori KATO	Low-Temperature Center (Unit Chief)
Takashi TAKAYAMA	Low-Temperature Center
Kazuo HAYAKAWA	Equipment Development Center (Unit Chief)
Hisashi YOSHIDA	Equipment Development Center
Masashi NAGATA	Equipment Development Center
Kouichi UCHIYAMA	Equipment Development Center
Toshio HORIGOME	Equipment Development Center (Unit Subchief)
Norio OKADA	Equipment Development Center
Mitsukazu SUZUI	Equipment Development Center
Nobuo MIZUTANI	Equipment Development Center
Shinji KATO	Equipment Development Center
Osamu MATSUDO	UVSOR Facility (Unit Chief)
Toshio KINOSHITA	UVSOR Facility
Masami HASUMOTO	UVSOR Facility

Jun-ichiro YAMAZAKI   UVSOR Facility

Eiken NAKAMURA   UVSOR Facility

* Carries out graduate research of IMS on the Cooperative Education Program of IMS with graduate schools.

1) Present Address: Dept. of Applied Physics, Faculty of Engineering, Miyazaki Univ., 1-1, Gakuen Kibanadai Nishi, Miyazaki 889-21
2) Present Address: The Graduate University for Advanced Studies, 4259, Nagatsuta, Midori, Yokohama 227
3) Present Address: Optoelectronics Tech. Res. Lab., 5-5, Tohkodai, Tsukuba 300-26
4) Present Address: Dept. of Chemistry, Baker Laboratory, Cornell Univ., Ithaca, New York 14853-1301, U.S.A.
5) Present Address: Faculty of Medicine, Univ. of Tokyo, 7-3-1, Hongo, Bunkyo-ku, Tokyo 113
6) Present Address: Shizuoka Institute of Science & Technology, 2200-2, Toyosawa, Fukuroi, Shizuoka 437
7) Present Address: The National Institute for Environmental Studies, 16-2, Onogawa, Tsukuba 305
8) Present Address: Faculty of Pharmaceutical Science, Kanazawa Univ., 13-1, Takara-machi, Kanazawa 920
9) Present Address: Dept. of Chemistry, Univ. of Tokyo, 7-3-1, Hongo, Bunkyo-ku, Tokyo 113
10) Present Address: Dept., of Material Science, Faculty of Science, Himeji Institute of Technology, 2167, Shosha, Himeji 671-22
11) Present Address: Dept., of Chemistry, Faculty of Science, Tokyo Metropolitan Univ., 2-1-1, Fukazawa, Setagaya-ku, Tokyo 158
12) Present Address: Dept., of Physics, Faculty of Science, Nagoya Univ., Furo-cho, Chikusa-ku, Nagoya 464
13) Present Address: Institute of Physics, Univ. of Tsukuba, 1-1-1, Tennodai, Tsukuba 305
14) Present Address: Dept., of Physics, Faculty of Science, Nagoya Univ., Furo-cho, Chikusa-ku, Nagoya 464
15) Present Address: Dept. of Chemistry, Faculty of Science, Ehime Univ., 2-5, Bunkyo-cho, Matsuyama 790
16) Present Address: Dept., of Hydrocarbon Chemistry, Faculty of Engineering, Kyoto Univ., Yoshida Honmachi, Sakyo-ku, Kyoto 606
17) Present Address: Dept., Chemistry, Faculty of Science, Kyoto Univ., Kitashirakawa Oiwake-cho, Sakyo-ku, Kyoto 606
18) Present Address: Dept. of Pharmaceutical Science, School of Medicine, Hiroshima Univ., 1-2-3, Kasumi, Minami-ku, Hiroshima 734
19) Present Address: Dept. of Chemistry, Univ. of Tsukuba, 1-1-1, Tennodai, Tsukuba, Ibaraki 305
20) Present Address: Dept. of Pharmaceutical Science, School of Medicine, Hiroshima Univ., 1-2-3, Kasumi, Minami-ku, Hiroshima 734
21) Present Address: Faculty of Culture, Chukyo Univ., 101, Yukadachi, Kaizu-cho, Toyota 470-03
22) Present Address: Tokai Research Establishment, Japan Atomic Energy Research Institute, Tokai-mura, Naka-gun, Ibaraki 319-11
23) Present Address: Dept., of Electrical and Electronics Engineering, Faculty of Engineering, Fukui Univ., 3-9-1, Bunkyo, Fukui 910

COUNCIL

Hiroo INOKUCHI   Director-General

Councillors

Chairman	Kenichi FUKUI	President, Institute for Fundamental Chemistry
Vice-Chairman	Yutaka TOYOZAWA	Professor, Chuo University
	Hirotsugu AKAIKE	President, The Institute of Statistical Mathematics
	Hideaki CHIHARA	Professor Emeritus, Osaka University
	Eiichi FUJITA	President, Osaka University of Pharmaceutical Sciences
	Sachio HAYAKAWA	President, Nagoya University
	Namio HONDA	Professor, Nagoya University of Commerce and Business Administration
	Sho ITO	Professor, Tokushima Bunri University
	Kouzou KUCHITU	Professor, Nagaoka University of Technology
	Michio KURATA	Professor Emeritus, Kyoto Univesity
	Akira MIKAZUKI	Professor Emeritus, University of Tokyo
	Masatoshi MORITA	Chief Executive Officer, Toyota Central Research & Development Laboratories, INC
	Haruo NISHIHARA	President, Waseda University
	Kazuo SAITO	Professor, International Christian University
	Kenji TAMARU	Professor, Science University of Tokyo
	Ikuzou TANAKA	Professor Emeritus, Tokyo Institute of Technology
	Teijiro YONEZAWA	Professor, Kinki University
	John C. POLANYI	Professor, University of Toronto
	Heinz A. STAAB	President, Max-Planck Society for the Advancement of Science, F.R.G.

The Council is the advisory board for the Director-General. Two of the councillors are selected among distinguished foreign scientists.

Distinguished Research Consultants

Kenichi FUKUI	President, Institute for Fundamental Chemistry
Masao KOTANI	Professor Emeritus, University of Tokyo (−April '90)
Yonezo MORINO	Professor Emeritus, University of Tokyo; Director and Supreme Consultant, Sagami Chemical Research Center (−April '90)
Saburo NAGAKURA	President, The Graduate University for Advanced Studies
Kenji TAMARU	Professor, Science University of Tokyo (April '90−)
Yasutada UEMURA	Chancellor, Musashi Gakuen

Administration Bureau

Toshio UENO	Director-General, Administration Bureau
Satoshi HUJISAWA	Director, General Affairs Department
Jitsuo SUZUKI	Director, Finance and Facilities Department (−April '90)
Yasuyoshi NONAKA	Director, Finance and Facilities Department (April '90−)
Nobuaki SHIMIZU	Head, General Affairs Division
Makoto SUZUKI	Head, Personnel Division
Tsunetaka GIMA	Head, Research Cooperation and International Affairs Division
Masaaki TSUJITA	Head, Budge Division
Kaoru KATO	Head, Accounts Division (−April '90)
Saigyo KAMIYAMA	Head, Accounts Division (April '90−)
Masakazu SASAKI	Head, Construction Division
Motokazu FURUYA	Head, Equipment Division (−April '90)
Kunikatsu SYOJI	Head, Equipment Division (April '90−)

11

BUILDINGS AND CAMPUS

The IMS campus covering 62,343 m^2 is located on a low hill in the middle of Okazaki City. The inequality in the surface of the hill and growing trees are preserved as much as possible, and low-storied buildings are adopted for conservation of the environment. The buildings of IMS are separated according to their functions as shown in the map. The Research Office Building and all Research Facilities except for the Computer Center are linked organically to the Main Laboratory Building by corridors. Computer Center, Library, and Administration Buildings are situated between IMS and the neighboring National Institute for Basic Biology and National Institute for Physiological Sciences, because the latter two facilities are common to these three institutes.

The lodging facility of IMS called Yamate Lodge, located within 10 min walk, has sleeping accommodations for 19 guests and two families. Mishima Lodge, located within four minutes' walk east of IMS can accommodate 68 guests and ten families. Scientists who visit IMS as well as the two other institutes can make use of these facilities. Foreign visiting scientists can also live at these lodgings with their families during their stays.

The Institute for Molecular Science

1. Research Office Building
2. Main Laboratory Building
3. Equipment Development Center
4. Instrument Center
5. Chemical Materials Center
6. Low-Temperature Center
7. Computer Center
8. Library
9. Central Administration
10. UVSOR Facility
11. Power Station
12. Waste-Water Disposition Facilities
13. Faculty Club
14. South Laboratory Building
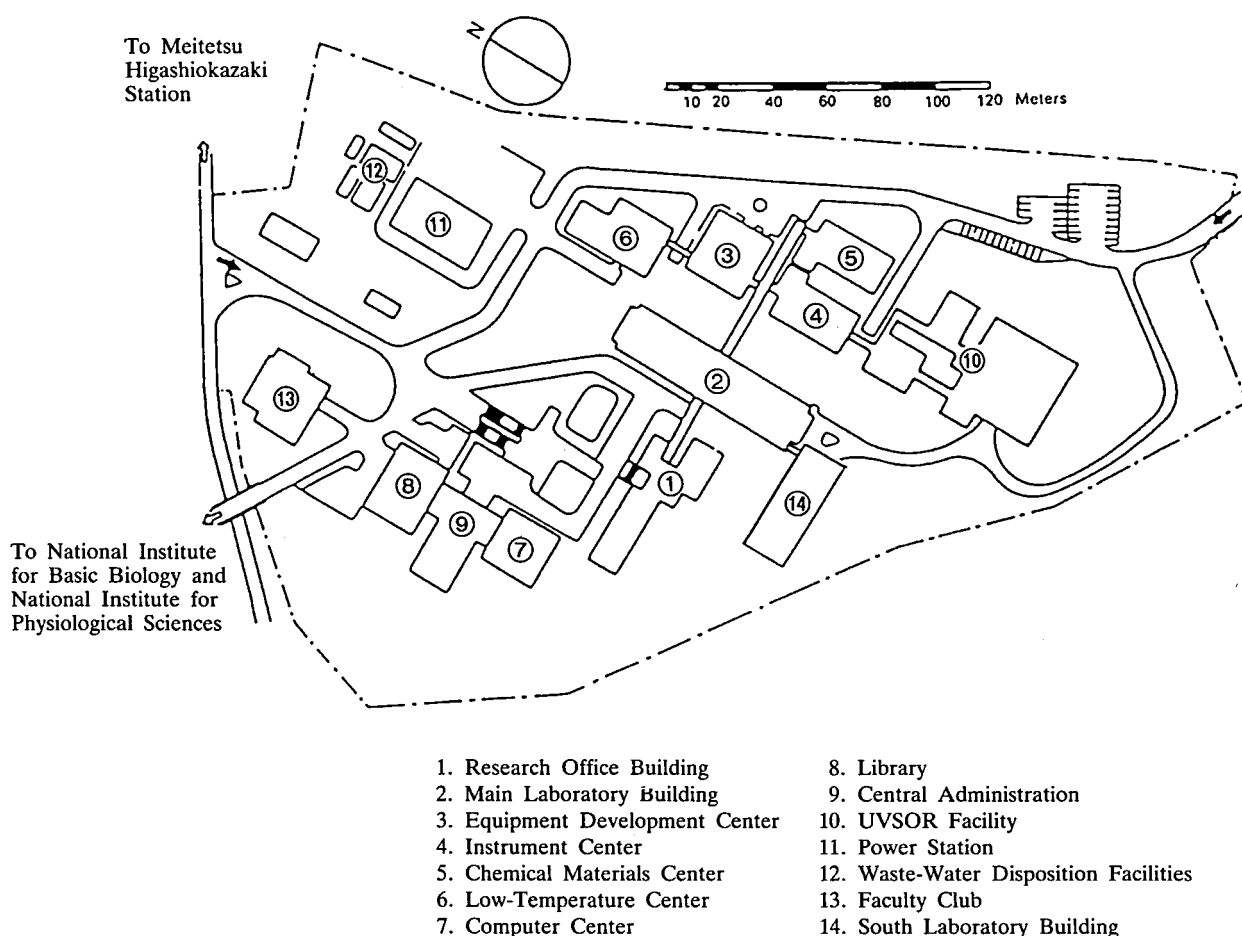
Okazaki (population 300,000) is 260 km southwest of Tokyo, and can be reached by train in about 3 hours from Tokyo via New Tokaido Line (Shinkansen) and Meitetsu Line.

The nearest large city is Nagoya, about 40 km west of Okazaki.
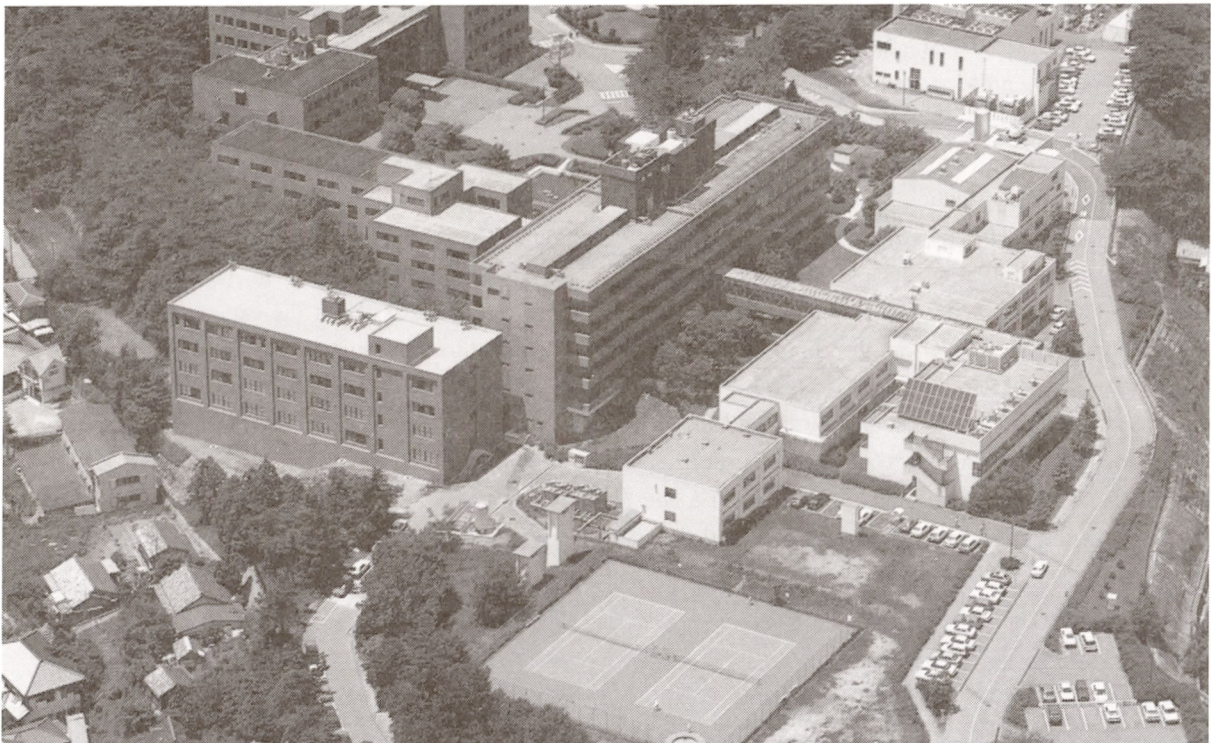
RESEARCH ACTIVITIES I
Department of Theoretical Studies

I—A Potential Energy Surfaces and Dynamics of Elementary Chemical Reactions

Fascinating new varieties of experiments, called generally "transition state spectroscopy", try to probe the reaction system spectroscopically during chemical reactions. However, very little experimental information is available about the nature of states involved and their behavior in the region where reorganization of bonds is taking place. Theoretical potential energy surfaces and dynamics on them are indispensable for interpretation and design of the transition state spectroscopy. Extending our involvement in this field in the past few years, we have studied this year several new systems relevant to the transition state spectroscopy experiment, including Na+HCl, ClHCl$^-$, O_3, ICN and CH_3I. The major figures in this project are Dr. K. Yamashita, a veteran Research Associate, Mr. Y. Amatatsu, a Technical Associate just finishing up his PhD thesis and Dr. S. Yabushita, a former colleague now at Hiroshima University.

I-A-1 Theoretical Study of Laser-Catalyzed Na+HCl Reaction: A Possibility of Transition State Spectroscopy

Koichi YAMASHITA and Keiji MOROKUMA

The reaction between the Na(3S, 3P) atom and the HCl molecule, and its laser-catalyzed process are theoretically investigated. The potential energy surfaces (PESs) of the ground $1^2A'$, and excited $2^2A'$, states of this reactive scattering process are calculated by the ab initio configuration interaction (CI) method. Surface-hopping trajectory calculations are performed to investigate the Na(3P)+HCl quenching reaction as well as the laser-catalyzed reaction which involves two types of nonadiabatic processes, laser-absorption and quenching. Analysis of the theoretical absorption and excitation spectra, based on the laser-dressed PES which governs the nuclear motion under the laser-field, has demonstrated a possibility of "transition state spectroscopy", that is, it may be possible to probe the PES and dynamics at the transition complex region of the excited state.

I-A-2 Ab Initio Study of Transition State Spectroscopy: ClHCl$^-$ Photodetachment Spectrum

Koichi YAMASHITA and Keiji MOROKUMA

Ab initio CASSCF-MRCI calculation with the [7s6p3d1f/4s3p1d] contracted Gaussian basis sets are performed to investigate the photodetachment spectrum of ClHCl$^-$ observed experimentally by Neumark et al. [*J. Chem. Phys.* **88**, 1463 (1988); *J. Phys. Chem.* **94**, 1377 (1990)]. The theoretical asignments for the ClHCl$^-$ and ClDCl$^-$ spectra based on one-dimensional Franck-Condon calculations are qualitatively in good agreement with the experiment. It is found by calculations that some peaks in the experimental spectra are assignable to transitions to the vibrational states of the first electronically excited $^2\Pi$ state in addition to those of the ground $^2\Sigma^+$ state in the transition state region of the neutral complex.

I-A-3 New Ab Initio Potential Energy Surfaces and Quantum Exact Three-Dimensional Dynamics of Ozone Photodissociation

Koichi YAMASHITA, Claude LEFORESTIER *(Univ. of Paris-Sud, France)* and Keiji MOROKUMA

New ab initio potential energy surfaces (PESs) of the ground and B_2 states of ozone which can describe its three- dimensional photodissociation processes were calculated. The CASSCF-MRCI calculations were performed with the DZP basis set using the MOLPRO program by Werner and Knowles. The orbitals for CI calculations were optimized in the state-averaged CASSCF calculation, where 12 electrons were distributed among 9 active orbitals, with equal weights for the four A′ states. The CI calculations were performed including all the single excitations from the resulting 1292 reference configurations. The dissociation energy of the ground state and the barrier height of the B_2 state were calculated to be 0.886 and 1.219 eV, in better agreement with the experimental values of 1.05 and 0.97 eV than those by Hay, Pack, Walker, and Heller. In order to see how the ozone photodissociation dynamics is sensitive to potential energy surfaces, the correlation function which is the Fourier transform of the total cross section was calculated based on the quantum exact three-dimensional formalism using our new PES fitted to Murrell-Sorbie analytical functions as well as using the Sheppard and Walker PES.

I-A-4 Ab initio Potential Energy Surface for Rotational Excitation of CN Product in the A-Band Photodissociation of ICN

Satoshi YABUSHITA *(Hiroshima Univ.)* and Keiji MOROKUMA

Potential energy surfaces of low-lying excited states of ICN have been calculated for linear and bent dissociation using the ab initio spin-orbit CI method with the effective spin-orbit Hamiltonian. Contrary to popular belief, all the relevant excited surfaces are bent in the Franck-Condon region and a conical intersection is found at a longer C-I distance, i.e. 2.70 Å. Based on the calculated surfaces, we propose a new model for the photodissociation dyanmics.

I-A-5 Ab initio Potential Energy Surfaces and Trajectory Studies of A-band Photodissociation Dynamics: $CH_3I^* \to CH_3 + I$ and $CH_3 + CH_3 + I^*$

Yoshiaki AMATATSU, Satoshi YABUSHITA *(Hiroshima Univ.)* and Keiji MOROKUMA

Ab initio contracted Spin-Orbit Configuration Interaction (SOCI) calculations have been carried out to obtain potential energy surfaces of $^3Q_0$ and $^1Q_1$ excited states of methyl iodide as functions of all the geometrical parameters except for the 3 C-H stretches. The results are fitted to 6 dimensional diabatic potential functions and their couplings. Classical trajectory calculations have been performed using these potential functions. The rotation of the CH_3 product in the I-channel has been calculated to be perpendicular to the top axis and to have a peak at $N=5$ and extend up to $N=7$, whereas it is cold in the I^*-channel, in good agreement with recent experiments. The CH_3 rotation is excited by the time trajectories arrive at the conical intersection region; this excitation is retained in the I-channel product because the $^1Q_1$ surface has a small bending force constant outside the conical intersection, whereas it is damped in the I^*-channel because $^3Q_0$ still has a large bending force constant. The calculated distribution in the ν_2 umbrella vibrational mode of the CH_3 product is hot and has a peak at $v=2$ for the I-channel, and is cool for the I^*-channel, in good agreement with recent experiments. This channel selectivity is due to the difference in the preferred structure of CH_3 outside the conical intersection region; while the $^3Q_0$ surface prefers a bent CH_3 until the CH_3-I distance becomes very large, $^1Q_1$ wants a planar CH_3. The location of conical intersection and the ground-excited energy difference there are in good agreement with those deduced from experiment, if a dynamical effect is taken into account.

I-A-6 The Role of C-H Stretches in ab Initio Potential Energy Surfaces and A-band Photodissociation Dynamics: $CH_3I^* \rightarrow CH_3 + I$ and $CH_3 + I^*$

Yoshiaki AMATATSU, Satoshi YABUSHITA (Hiroshimia Univ.) and Keiji MOROKUMA

In our preceeding study of potential energy surfaces (PESs) and dynamics of CH_3I A-band photodissociation, we have recognized the potential importance of C-H stretches, as has been found experimentally as an excitation of the product CH_3 ν_1 symmetric stretch mode. Therefore, we have calculated full 9-dimensional PESs of $^1Q_1$ and $^3Q_0$ states as functions of three C-H stretches, as well as six coordinates used in the preceeding study. The behavior of PESs with respect to the degenerate asymmetric stretch, S_{4a} and S_{4b}, are nearly same as that with respect to the corresponding modes of the product CH_3. On the other hand, the PESs with respect to of S_1 behave quite differently between the reactant and the product; in the Franck-Condon region, the C-H distance is longer and has a larger anharmonicity than in the CH_3 product. This behavior could be related to the ν_1 mode excitation. It has been found that the coupling elements, which determine the I/I^* ratio, obey a good additivity with respect to the internal parameters. Therefore, the inclusion of the C-H stretches in the dynamics is expected to decrease from the previous 0.92 to the experimental value (0.7-0.8).

I-A-7 A Theoretical Study of Transition State Spectroscopy: Laser Dressed Potential Energy Surface and Surface Hopping Trajectory Calculations on K + NaCl and Na + KCl

Koichi YAMASHITA and Keiji MOROKUMA

Spectroscopy during the chemical reactions, K + NaCl and its reverse, has been studied by surface hopping trajectory calculations. Laser absorption and emission processes are modeled as the transitions between the laser-dressed ground and excited state potential energy surfaces (PESs), which are constructed from ab initio potential energy and transition dipole funcions. The theoretical excitation spectrum measured by Na-D emission intensity as a funcion of laser wavelength agrees qualitatively with the experiment by Maguire et al. [J. Chem. Phys. 85, 844 (1986)]. The excitation spectrum is found to be very different from the absorption spectrum, because only a small portion of excited trajectories reaches the Na* product due to the endothermicity of the excited state reaction. Therefore the excitation spectrum reflects only the excited state dynamics but not the transition state spectroscopy. The laser wavelength dependence of the spectra is well explained by a characteristic shift of the crossing seam accompanied with changes in laser wavelength. We have also predicted the absorption and excitation spectra for the reverse reaction and found that in this case the intensity of the product emission as a function of laser wavelength reflects to a large extent the true transition state spectroscopy.

I-A-8 Ab Initio Potential Energy Surfaces of Charge-transfer Reactions: $F^+ + CO \rightarrow F + CO^+$

Koichi YAMASHITA, Keiji MOROKUMA, Yasushi SHIRAISHI* and Isao KUSUNOKI* (*Tohoku Univ.)

Ab initio potential energy surfaces (PESs) of the charge-transfer reaction $F^+ + CO \rightarrow F + CO^+$, studied experimentally by Kusunoki and Ishikawa [J. Chem. Phys. 82, 4991 (1985)], are calculated by the MRSD-CI method using the DZP basis set. Six low-lying triplet A' and six A'' states, correlated to the initial state $F^+(^3P) + CO(X^1\Sigma^+)$, the final state $F(^2P) + CO^+(A^2\Pi)$ and the ground state $F(^2P) + CO^+(X^2\Sigma^+)$, are investigated for full three-dimensional interactions between the F atom and the CO molecule. The mechanism of charge-transfer is disucussed based on the PES characteristics and the nonadiabatic coupling elements between the initial and relevant final states. A simple theoretical model which emphasizes the importance of the nonadiabatic transition along the CO vibrational coordinate is presented to interpret the vibrational excitation of the product $CO^+(A)$.

I—B   Theoretical Studies of Structure and Spectroscopy

I-B-1   Theoretical Potential Energy and Electric Dipole Moment Functions of HCF (X^1A' and a^3A'')

Bernhard WEIS*, Pavel ROSMUS* (*Univ. of Frankfurt, FRG), Koichi YAMASHITA and Keiji MOROKUMA

Highly correlated CEPA electronic wave funcions have been used to calculate the three-dimensional potential energy and electric dipole moment funcions of the X^1A' and a^3A'' states of HCF. The analytic expansions of these functions have been employed in variational and perturbational calculations of the vibrational band origins and spectroscopic constants. For the singlet ground state the vibrational band origins agree with available experiments within 2 to 20 cm^{-1}, the rotational constants to within 0.04 cm^{-1}. Theoretical spectroscopic constants of similar accuracy are presented also for the triplet state. The singlet-triplet separation is calculated to be 13.9 kcal/mol, in agreement with the experimental upper bound of 14.7 kcal/mol. The dipole moments have been calculated to be 1.394 D (X^1A') or 1.049 D (a^3A''), respectively, and vibrational radiative transition probabilities are also given. Anomalous variations of radiative lifetimes in some low-lying vibrational levels have been found in the singlet state of HCF which are due to anharmonic coupling effects.

I-B-2   Solvent Effect on Vibrational Structure in (n, π^*) Transition of Formaldehyde

Hiroo FUKUNAGA (Fuji Photo Film Co. and IMS) and Keiji MOROKUMA

Intermolecular potential functions between formaldehyde in the ground and excited (n, π^*) state and a water molecule determined before have been improved by adding some points near the local minima and changing functional forms. The potentials are expressed in terms of r^{-1}, r^{-3}, and r^{-12}. The new potential functions reproduce the minima on the ab initio potential, without phantom minima.

Monte Carlo simulation based on an NVT ensemble has been carried out to obtain the distribution of the (n, π^*) transition energies of formaldehyde complexed with one to several water molecules.

I-B-3   A Simple Scheme of Estimating Substitution or Substituent Effects in the ab Initio MO Method Based on the Shift Operator

Nobuaki KOGA and Keiji MOROKUMA

A simple scheme for changing the Coulomb integral of a chosen orbital in the ab initio method is proposed based on the energy shift operator. The scheme, compatible with the energy derivatives, provides a simple procedure for estimating substitution or substituent effects on the structure, energy and other electronic properties.

I-B-4   Analytic Second Derivatives with Model Potentials at SCF and MP2 Levels.

Dylan JAYATILAKA,* Roger D. AMOS* (*Univ. of Cambridge, UK) and Nobuaki KOGA

We report the implementation of analytic first and second derivatives using the model potential method of Bonifacic and Huzinaga. Applications to CH_3Br and $Zn(CH_3)_2$ are discussed. The predicted geometries and spectroscopic constants are very good compared to all-electron calculations, thus confirming that the method may be used as a cheap alternative to all-electron calculations.

I—C   Theoretical Studies of Reaction Mechanisms and Struture of Organic Compounds

We have tackled varieties of problems in reactions and structure of organic compounds. Dr. A. Dorigo, a JSPS postdoc from US, continued to work on stereoselectivity in the reaction of CC double bonds. Dr. S. Mathieu, another JSPS postdoc from France, and Mr. T. Ozawa, a trainee from Kao, have studied structure and reactivity of compounds containing hypervalent sulfur, phosphorus and silicon. We have also studied reactions involving biradical or biradicaloid intermediates. Some of organic chemistry projects are supported by a Ministry of Education grant on priority area of "Organic Unusual Valency" and another of "Molecular Design".

I-C-1   Influence of the π-Complexation of $(CH_3)_2CuLi$ with $CH_2=CH-CH_2X$ Molecules on the S_N2' Reaction Stereochemistry. An ab Initio MO Study

Andrea E. DORIGO and Keiji MOROKUMA

The complexation of $(CH_3)_2CuLi$ with allylic systems $CH_2=CH-CH_2X$ (X=Cl, OH, and OCOH) has been investigated by ab initio molecular orbital methods. The X group is found to prefer the anti position to the outside position in the complex, which is in line with the observed stereochemical outcome of S_N2' reactions in these systems. An energy decomposition analysis indicates that charge transfer from the cuprate to the olefin is the term which is most responsible for the stabilization of the anti complex.

I-C-2   Stereoselectivity in Addition Reactions of Simple Nucleophiles to α, β-Unsaturated Carbonyl Compounds. An ab Initio MO Study

Andrea E. DORIGO and Keiji MOROKUMA

Nucleophilic additions of the OH^- and NH_2^- anions to acrolein, 2-butenal, and 4-hydroxy-2-pentenal have been studied by ab initio molecular orbital methods. These calculations predict a stereochemical outcome which is opposite to that obtained in the addition of alkylmetals.

I-C-3   Equatophilicity in the Structural Preference in Trigonal Bipyramids. Ab Initio Study

Simon MATHIEU and Keiji MOROKUMA

Ab initio molecular orbital calculations on pentacoordinated phosphorus and silicon compounds composed of combinations of hydrogen, fluorine and chlorine ligating atoms are used to establish the origin of the structural preference in trigonal bipyramidal compounds. In agreement with experimental observations, halides are shown to exhibit apical preference over hydride. However, the apical bond has been found to be relatively weak and the apical bond energy shows very small difference between the M-H and the M-X bond. On the other hand, the equatorial bond in stronger, and the binding energy of the M-H bond is larger than that of the M-X bond. Therefore, this structure preference should be attributed to the equatophilicity, i. e. the less electronegative group prefers the equatorial position to the apical position, rather than to the popularly believed apicolilicity, i. e. the more electronegative group prefers the apical position.

I-C-4   Hydrosilylation by Pentacoordinate Silicon Compound. An ab Initio MO Study

Tadahiro OZAWA *(Kao Corp. and IMS)*, **Nobuaki KOGA and Keiji MOROKUMA**

The reaction of tetracoordinate silicon compounds with ketone and aldehyde would not take place without catalyst, whereas that of pentacoordinate silicon compounds recently synthesized has been found to take place under the mild conditions without catalyst. In order to elucidate the origin of this high reactivity of the pentacoordinate silicon compounds, we compared model reaction 1 and 2 of the tetracoordinate and pentacoordinate compounds, respectively, by using the ab initio MO method.

$$HSi(OH)_3 + HCHO \rightarrow CH_3OSi(OH)_3 \qquad (1)$$
$$HSi(OH)_4^- + HCHO \rightarrow CH_3OSi(OH)_4^- \qquad (2)$$
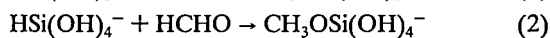
We carried out the RHF geometry optimizations to find that reaction 1 is synchronous via four-centered transition state (TS), while reaction 2 is asynchronous, which passes through the three-centered TS with the hydride transfer occurring, followed by the Si-O bond formation. The MP4SDQ energy calculations at the RHF optimized structures were performed to show that the activation energy for reaction 2 is 34 kcal/mol lower than that for reaction 1; reaction 2 is easier. The three-centered TS is more favorable for hydrosilylation because of the smaller steric (exchange) repulsion and the smaller deformation energy. The hydride transfer at the three-centered TS for reaction 2 leads to CH_3O^-...Si $(OH)_4$; $CH_3O^- + Si(OH)_4$ is in fact 8.3 kcal/mol lower in energy than the TS at the RHF level. The hydride transfer in reaction 1 would give less stable CH_3O^-...$Si(OH)_3^+$, and thus reaction 1 takes the four-centered TS.

I-C-5 Comparison of Biradical Formation between Enediyne and Eneyne-Allene. Ab Initio CASSCF and MRSDCI Study

Nobuaki KOGA and Keiji MOROKUMA

We theoretically compared energetics of the Bergman type biradical formation between enediyne and eneyne-allene. The structures of transition states as well as reactants and products for the reaction of (Z)-hexa-1,5-diyn-3-ene, **1**, and (Z)-hepta-1,2,4-triene-6-yne, **2**, are determined at the CASSCF level. Energy calculations at the CASSCF and the MRSDCI level show that the reaction of eneyne-allene, **2**, is more exothermic and its activation energy is lower than that of enediyne, **1**, consistent with the experiments. The reaction of eneyne-allene is more exothermic, since a π radical on the benzylic methylene group in the product of eneyne-allene is more stable than the σ radical of the product of enediyne, partly because of the conjugation with the aromatic ring and partly because of the intrinsically stronger aryl-H bond than the alkyl-H bond. This conjugation, however, does not take place at the eneyne-allene transition state where the methylene remains perpendicular. Thus, the lower acti-

vation energy for eneyne- allene is not ascribed to the conjugation but to the smaller four-electron repulsion between the in-plane π bonds than that for enediyne.

I-C-6 Ab Initio MCSCF and CI Calculations of the Singlet-Triplet Energy Differences in Oxyallyl and in Dimethyloxyallyl

Michael B. COOLIDGE*, Koichi YAMASHITA, Keiji MOROKUMA and Weston T. BORDEN*
(*Univ. of Washington)

Ab initio MCSCF and multi-reference CI calculations predict a very small singlet-triplet energy splitting in oxyallyl (**1**). The largest calculations find the triplet to be the ground state by 1-2 kcal/mol. The reason for the small singlet-triplet energy difference in **1** is discussed. The pair of alkyl substituents dimethyloxyallyl (**2**) are computed to confer a singlet ground state on this diradical. Multi-reference CI calculations, which include correlation between and π electrons, give a singlet- triplet energy separation in **2** of about 5 kcal/mol.

I-C-7 Ab Initio Calculations of the Effects of Cyano Substituents on the Cope Rearrangement

David A. HROVAT*, Weston T. BORDEN* *(*Univ. of Washington)*, **Robert L. VANCE†, Nelson G. RONDAN†** *(†Dow Chemical Co.)*, **K. N. HOUK** *(Univ. of California, Los Angeles)* and **Keiji MOROKUMA**

Ab initio calculations have been performed with the 3-21G basis set on the transition states (**1-3**) for the chair Cope rearrangement of 1,5-hexadiene and its 2,5-dicyano and 1,4-dicyano derivatives. Both the SCF and CI optimized values of the interallylic bond length, R, increase in the order 2 < 1 < 3. This finding supports the interpretation of Conrad and Gajewski of the secondary kinetic isotope effects measured by them, in terms of a structure for the Cope transition state that varies with the position of radical stabilizing substituents. However analysis of the CI wavefunction for

transition state **2** shows that, despite the 8.3 kcal/mol lowering of the MP2 energy of activation for the Cope rearrangement by the cyano substituents at C-2 and C-5, **2** is not a diradical and is best described as a closed-shell, "aromatic", species.

I—D   Structure and Reactions of Transition Metal Complexes

Our continued effort in this field centered mainly on the CH bond activation and on the second full catalytic cycle to be studied with the ab initio method in our group, olefin hydroformylation, both by a rhodium catalyst, as well as chemistry of early transition metals, in particular Zr. The work was spear-headed by Dr. N. Koga, a Research Associate, in collaboration with Mr. Y. Ding, a Chinese graduate student who has gone to US this June to continue his PhD study, and Mr. Endo and Mr. Kuribayashi, two industrial trainees.

I-D-1   CH Bond Activation of Ethylene by CpRh(PH₃) and Conversion from Vinyl Hydride to Ethylene Complex. A Theoretical Study

Nobuaki KOGA, Feliu MASERAS *(Univ. of Autonoma de Barcelona and IMS)*, **and Keiji MOROKUMA**

As a continuation of our previous study of the CH bond activation of ethylene by $CpRh(RH_3)$, we studied with the MP2 energy gradient method this activation process and the conversion from the vinyl hydride complex, $CpRh(PH_3)(H)(C_2H_3)$, **1**, the CH bond activation product, to the ethylene complex, $CpRh(PH_3)(C_2H_4)$, **2**. The basis set used for the geometry optimization consists of 3-21G for ethylene, DZ and ECP for Rh, and STO-3G for Cp and PH_3. At the RHF level, we found the σ complex, in which one of the ethylene CH bonds interacts with the central Rh atom, and the transition state between the σ complex and **1**. However, when the electron correlation was taken into account at the MP2 level, the reaction path leading to **1** was found to be down-hill. At the transition state between **1** and **2**, both the CH σ and the π orbital interact with the Rh atom. At the RHF level, such a transition state does not exist; the correlation effect is quite large. The conversion from **1** to **2** requires the activation energy of 25 kcal/mol and is exothermic by 24 kcal/mol at the MP2 level with the larger basis set. The transition state lies below the dissociation limit, $CpRh(PH_3)$ + C_2H_4, by 21 kcal/mol, suggesting the intramolecular rearrangement.

I-D-2   Potential Energy Surface of Olefin Hydroformylation Catalyzed by Rhodium Complex HRh(CO)₂(PR₃): Electron Correlation Effect

Yanbo DING *(IMS and Beijing Normal Univ.)*, **Nobuaki KOGA and Keiji MOROKUMA**

As a continuation of our previous study, we calculated the potential energy profile for the hydroformylation catalytic cycle by $HRh(CO)_2(PH_3)$ with the MP2 method at the RHF optimized structures. This catalytic cycle consists of PR_3 dissociation, olefin coordination, olefin insertion, PR_3 coordination, CO insertion, H_2 oxidative addition, aldehyde reductive elimination, aldehyde dissociation, and CO coordination. In the model cycle we studied, PH_3 and ethylene were used as PR_3 and olefin. The MP2 energy calculations showed that the catalytic cycle is rather smooth without high activation barrier and too stable intermediates, as we have found in the study of olefin hydrogenation by the Wilkinson catalyst. The two insertion steps, olefin insertion and carbonyl insertion, require the substantial activation enegy of 22 and 26 kcal/mol, respectively. On the other hand, the propionaldehyde dissociation is quite endothermic by 32 kcal/mol. Since this step is up-hill, this endothermicity corresponds to the activation energy. Therefore, this aldehyde dissociation may be rate-determining. Experimentally, the rate-determining step is believed to be the H_2 oxidative addition, the calculated activation energy of which is only 1.5 kcal/mol.

I-D-3 A Theoretical Study on Stereoselectiv-Soc.ity in Olefin Insertion into a Zr-Me bond of Silano-bridged Zirconocene System

Hiroshi KURIBAYASHI *(Sumitomo Chemical Co. and IMS)*, Nobuaki KOGA and Keiji MOROKUMA

Some silano-bridged zirconocene complexes with methyl and t-butyl substituents on Cp rings have been known experimentally to catalize propylene polymerization to give isotactic polypropylene selectively. It has been proposed that the steric bulkiness of substituents controls the stereochemistry at the transition state of monomer insertion. We are presently studying potential energy surfaces of the following model reaction with an ab initio MO method.

$$(Cp_2SiH_2)ZrCH_3^+ + C_2H_4 \rightarrow$$
$$(Cp_2SiH_2)ZrCH_3(C_2H_4)^+ \rightarrow (TS) \rightarrow$$
$$(Cp_2SiH_2)ZrC_3H_7^+ \qquad (1)$$
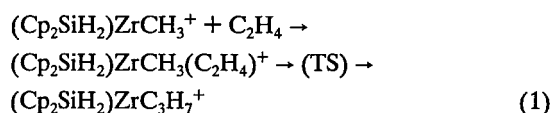
We have optimized the geometries of the stationary points for ethylene insertion reaction (1) at the RHF/3-21G(Zr:ECP) level. The ethylene binding energy in the π complex is 19.1 kcal/mol and the activation energy from the complex is 16.7 kcal/mol at RHF level. In comparison with the data of the $CH_3TiCl_2^+ + C_2H_4$ reacting system we have previously studied, the present ethylene binding energy is smaller by about 20 kcal/mol, but the activation energy is larger only by a few kcal/mol. While the reactant and the π complex have C_s symmetry, the four-centered transition state is slightly nonplanar with the torsional angle of 3°, which is smaller by about 7° than that of the Ti system. We are planing to study the corresponding reaction with propylene and to examine the steric effect of substituents with the use of molecular mechanics.

I-D-4 A Theoretical Study of Hydrozirconation

Jun ENDO *(Mitsubishi Petrochemical CO. and IMS)*, Nobuaki KOGA and Keiji MOROKUMA

Hydrozirconation (eq.1) can be considered to be a model reaction of olefin polymerization by zirconocene/methylaluminoxine system.

$$Cp_2Zr(H)Cl + C_2H_4 \rightarrow Cp_2Zr(C_2H_5)Cl \qquad (1)$$
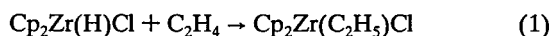
As a continuation of our previous theoretical study, we studied the electron correlation effect on energetics of hydrozirconation with the MP2 method. Ethylene can attack two sites of $Cp_2Zr(H)Cl$; the one site is trans to Cl and cis to H (path a) and the other is between H and Cl (path b). At the RHF level, path b requires the activation energy of 15 kcal/mol and is 24 kcal/mol exothermic, while the activation energy and exothermicity for path a were calculated to be 28 and 21 kcal/mol, respectively. Path b is kinetically and thermodynamically more favorable. The electron correlation effect at the MP2 level, calculated at the RHF optimized structures, makes both path a and b more exothermic by 6 kcal/mol and lowers the activation energy by 14 and 16 kcal/mol for path a and b, respectively. These results show that hydrozirconation takes place with a very low activation energy through path b. We calculated the energies at several ethytlene-Zr distances at the MP2 level to find that the ethylene complex does not exist; energy monotonically increases up to the transition state, when ethylene approaches the Zr fragment. In addition, these calculations suggest that the MP2 transition state would be much earlier than the RHF transition state.

I-D-5 Ab Initio Calculations on $(H_3P)_2Pt(C_2H_4)$. The Effect of Alkene Pyramidalization on Internal Rotation and Alkene Binding Energies

Keiji MOROKUMA and Weston T. BORDEN *(Univ. of Washington)*

Ab initio calculations have been performed on the title compound at both planar (1) and tetrahedral (2) coordination geometries. Calculations at these geometries have also been performed on a $(H_3P)_2Pt(C_2H_4)$ model, in which the ethylene fragment was constrained to have a pyramidalization angle of 60.6°, a model for the recently established $(Ph_3P)_2Pt$ complex of tricyclo[3.3.1.0^{3,7}]undec-3(7)-ene. The model calculations predict that in $(Ph_3P)_2Pt$ complexes, where the alkene is constrained to be highly pyramidalized, the barrier to internal rotation from **1** to **2** will be found to be higher than in $(Ph_3P)_2Pt$ complexes of unconstrained alkenes. However, on alkene pyramidalization, the increase in the energy that is required for internal rotation is calculated not to be nearly as large as the increase in the

alkene binding energy. It is shown that the computational results are consistent with the expected effect of pyramidalization on the ability of the alkene π^* LUMO to accept electron density from a filled metal d orbital.

1-D-6 Facile Regioselective Ligand Substitution for the In-Plane Bridging Acetates in Octakis (μ-acetato-O,O')tetraplatinum (II)

Tadashi YAMAGUCHI*, Yoichi SASAKI*, Akira NAGASAWA*, Tasuku ITO* (*Tohoku Univ.), Nobuaki KOGA and Keiji MOROKUMA

Octakis(μ-acetato-O,O')tetraplatinum(II), **1**, undergoes rapid regioselective ligand substitution for the in-plane acetates with free carboxylic acids in solution. EHMO calculations have been carried out for a model compound, $Pt_4(HCOO)_8$, **2**, and its fragments. The MO's of **2** derived from dσ orbitals (predominantly $d_{x^2-y^2}$ and d_{z^2} characters) of each Pt, give four essentially bonding orbitals to result in the Pt-Pt single bonds. The regioselectivity has been explained by the fact that the lower three orbitals are predominantly of $d_{x^2-y^2}$ character and antibonding for in-plane ligands, and only the highest one is of d_{z^2} character and antibonding for out-of-plane ligands. An EHMO calculation further indicates that $[Pt_4(HCOO)_7]^+$, where one

of the in-plane ligand is removed from **2**, is substantially more stable than that without one out-of-plane ligand.

1-D-7 Study of the Effect of Structural Factors on the Magnetism of Di-μ-alkoxodicopper(II) Complexes by ab Initio MO Calculations

M. HANDA*, N. KOGA, and S. KIDA* (*Kyushu Univ.)

The effect of variation of structural factors on the spin-exchange interaction between copper(II) centers in dialkoxy-bridged dinuclear copper complexes were studied by the ab initio MO method with UHF formalism. The calculations were performed on di-μ-methoxotetraamminedicopper(II). The J-values were obtained as functions of Cu-O-Cu angle, dihedral angle between two coordination planes, planarity of bonds on the bridging oxygens, tetrahedral distortion of coordination planes, and the tilt of O-C bond from the O-O axis. The results demonstrated that the Cu-O-Cu angle most effectively affect the J-value but the other factors are less effective.

I—E Theoretical Studies of Chemical Reactions on Solid Surfaces

Though the progress is not as fast as we hoped for, we have been learning quite a lot on the chemisorption on the MgO surface, in particular, on the site dependency and cooperativity, due to the effort of Mr. K. Sawabe, a graduate student from the University of Tokyo who is finishing his PhD before long. We hope to continue the project with new postdoctoral fellows.

I-E-1 An ab Initio MO Study of The Electron Correlation Effect on the H_2 Adsorbed on the MgO Surface

Kyoichi SAWABE (Univ. of Tokyo and IMS), Nobuaki KOGA, Yasuhiro IWASAWA (Univ. of Tokyo) and Keiji MOROKUMA

We have implemented the local MP2 method by

P.Pulay[1] in which the occupied orbitals are localized and the corresponding virtual space can be locally described. This method gives a better chemical insight into the correlation effect than the normal canonical orbital MP2 method. In addition, the local MP2 allows a substantial saving of computer time in calculating the energy difference between the reactants and the product, if the correlation energy difference can be

described by a local domain around the chemisorption sites. For instance, there is only 0.2 kcal/mol difference in relative energy for the $H_2(MgO)_6$ system between the canonical MP2 result and the Local MP2 result, where only the atoms of the adsorption sites and the next neighbor atoms are included into the local domain.

For the $H_2(MgO)_4$ system, the energies of the chemisorbed complex relative to $H_2 + (MgO)_4$ are −34.3 kcal/mol at RHF, −20.3 kcal/mol at MP2, −28.3 kcal/mol at MP3 and −22.4 kcal/mol at MP4SDQ, with the basis sets 6-31G for Mg atoms, 6-31+G for O atoms and 6-31G++G** for H atoms. The correlation effect is large, but the MP2 level of calculation seems to be a good compromise between the cost and the accuracy for larger models.

Reference
1) S.Saebo and P.Pulay, *J. Chem. Phys.*, **86**, 914 (1986).

I-E-2 An ab Initio MO Study of Cooperativity of Chemisorption on MgO Surface

Kyoichi SAWABE *(Univ. of Tokyo and IMS)*, Nobuaki KOGA, Yasuhiro IWASAWA *(Univ. of Tokyo)* and Keiji MOROKUMA

The cooperativity of coadsorbed gases on the MgO surface was investigated using $(MgO)_4$ and $(MgO)_6$ clusters as models of catalytic surface. With the $(MgO)_4$ cluster model, H_2, NH_3 and H_2O are ionically dissociated on the adsorption site of the MgO surface, like $H^--Mg-O-H^+$, $H_2N-Mg-O-H^+$ and $HO^--Mg-O-H^+$. When a new H_2 is chemisorbed on the site next to such a pre-adsorbed site, the chemisorption energy of this new H_2 is larger than that of the first H_2. The additional stability, i.e. the cooperativity, is almost same, around 21-22 kcal/mol(RMP2/3-21+G), regardless of the first adsorbed species. The H_2-CO coadsorbed system, in which CO is adsorbed undissociatively, does not show much cooperativity (1 kcal/mol). The cooperativity above is partly due to the electrostatic attraction between the coadsorbed ionic species and partly due to the enhanced charge transfer interaction of the second H_2 with the preadsorbed MgO surface.

I—F Structures and Reactions of Manybody Chemical Systems

Electronic structure and dynamical behavior of large systems such as liquids and polymers are investigated theoretically. (a) Collective motions and fluctuations in liquid and cluster (b) Chemical reactions and energy relaxations in liquid and clusters, and (c) Electronic structures and dynamical behaviors of polyenes and polyacetylenes, are analyzed.

I-F-1 Potential Energy Surfaces for Water Dynamics II: Vibrational mode excitations, mixing, and relaxations

Iwao OHMINE and Hideki TANAKA *(Kyoto Univ.)*

[*J. Chem. Phys.*, in press]

Dynamical behavior of liquid water is investigated by analyzing the potential energy surface involved. Multidimensional properties of the potential energy surface are explored in terms of vibrational mode excitations at its local energy minima, called inherent structures. The vibrational mode dynamics, especially mechanism of mode relaxation and structure transitions, is analyzed. It shows very strong excitation energy dependence and mode dependence. There are three kinds of vibrational coupling among modes. For excitations of energy near the room temperature, most modes (more than 90% of total modes) individually interact with only one or two other modes, and yield near-recurrence of the mode energy in a few tens pico seconds (very slow relaxation). Spatially localized modes in the intermediate frequency range couple with many delocalized modes, yielding fast relaxation. The coupling is governed by atomic displacement overlaps and frequency matching. Each mode couples with nearby

frequency or double frequency modes through the Fermi resonance. Lowest frequency modes almost always lead to transitions from a potential energy well to neighbor potential wells, called inherent structure transitions. In high energy excitation, some intermediate frequency modes also yield such transitions. There exist very low energy paths involving single or few water molecule displacements at almost every inherent structures, indicating that certain facile molecular movements occur even in very low temperature states. Different energy excitations of a low frequency mode result in different inherent structure transitions; transitions caused by high energy excitations involve many large molecular displacements. These inherent structure transitions are source of the binding structural reorganization dynamics.

I-F-2 Potential Energy Surfaces for Water Dynamics I: Reaction Coordinates, Transition States and Normal Mode Analyses

Hideki TANAKA *(Kyoto Univ.)* and Iwao OHMINE

Potential energy surface involved in the water dynamics is investigated in terms of the reaction coordinates, transition state energy distribution and normal mode analyses. The reaction coordinates connecting between the inherent structures, successively visited by the system in the trajectory, and their barrier heights are determined. We have analyzed the normal modes and their anharmonicity, and related them to the reaction coordinates. The classification of the inherent structure transitions is made by defining the distance matrix.

I-F-3 Structural transitions of Argon cluster

Osamu KITAO *(Kyoto Univ.)* and Iwao OHMINE

Dynamics of Ar cluster is studied by analyzing the potential energy surface involved. A potential surface of a manybody system consists of many potential energy wells. Each well is represented its energy minimum call an inherent structure. We have determined the reaction coordinates (RC) connecting between in-

herent structures and the transition state energy barrier height distribution of RCs. The normal mode analysis along RC are also performed. Classification of inherent structures and of whole potential energy surfaces is systematized for small cluster systems by intensive quenching search. Collective motions associated with transitions between the inherent structure in large clusters are classified as surface dislocations and core rearrangements. The energy barrier height for these motions are determined to analyze their temperature dependence. Long time scale motions, shape deformations, of large clusters are also studied by a nanoseconds trajectory calculations. The energy relaxation processes of vibrationally excited molecules in these clusters are investigated to find the threshold behavior of the relaxation rate; the amplitude threshold for the energy relaxation by 'hard' collisions and the mechanism of the 'resonance type' relaxation and their mutual onsets are being carefully studied.

I-F-4 Ab Initio study of the C=C stretching mode in the $2^1A_g^-$ Stete of ppolyenes

Mutsumi AOYAGI, Iwao OHMINE and Bryan Kohler *(Univ. of California, Reverside)*

The frequency increase of the C=C a_g stretching mode of polyenes on going from the ground state $(1^1A_g^-)$ to the excited $(2^1A_g^-)$ state as well as on the chain length is investigated by using Ab initio MCSCF calculations for Butadiene, Hexatriene and Octatetraene. A MCSCF with the CAS (the completely active space) for $N \pi$ electrons is used and molecular geometries are optimized for both states with the energy gradient technique. The calculation well produces the frequency increase of the C=C stretching and shows that this increase comes from couplings this mode and the C-C single bond stretches and C-C-H bends.

I-F-5 Instabilities of Hydrogen Bond Network in Liquid Water

Masaki SASAI

A new model of the hydrogen bond network in liquid water is developed. Using the technique of polymer science, the grand canonical partition function of water is expressed by the functional integral of the field variables. The method is applied to anomalies of liquid water. Using the mean-field lattice-gas approximation it is shown that there are two instability lines, one in the supercooled region and the other in the stretched $(P<0)$ region. Approaching the instability line in the supercooled region, the fluctuation of ice-likeness grows anomalously large and liquid water becomes unstable to be ice. Approaching the instability line in the stretched region, the fluctuation of the concentration of non-hydrogen-bonded sites grows large and liquid water becomes unstable to be gas. Divergence of the thermodynamic response functions and the mean-field values of exponents are discussed.

I-F-6 Molecular Theory of Associative Memory Hamiltonian Models of Protein Folding

Masaki SASAI and Peter G. WOLYNES *(Univ. of Illinois)*

There are two difficulties in determining protein structure from the amino acid sequence by computer simulation. Correct free energy functions are riddled with local minima, unrelated structurally to the folded protein. There is also the problem of finding the correct free energy function. Both the local minima problem and the problem of finding the energy function can be studied using spin glass theory. A concrete realization of these ideas is provided by associative memory Hamiltonian models.[1]

In this work, a molecular level theory of the phase diagram of folding proteins is developed and applied to associative memory Hamiltonian models. Equilibrium collapse, folding, and glass transitions are described with a unified variational treatment. Cold denaturation of protein is described as a reentrant transition from the folded state to the glassy state. Quantitative estimates of the capacity of recall are found.

Reference
1) M. Friedrichs and P.G. Wolynes, *Science*, **246**, 371 (1989).

I—G Theoretical Studies of Chemical Reaction Dynamics

The purposes of the theoretical reaction dynamics studies are to understand the effects of potential energy hypersurface topography and mass combination of the reactants on the dynamics, and also to clarify the role of each internal degree of freedom or of the internal energy in each degree of freedom. One of the basic ideas we employ is a separate treatment of vibrational transition and rotational transition. This is reasonable, because the mechanisms of the vibrational transitions in reaction are different from those of the rotational transitions. As for vibrational transition, the sudden and adiabatic approximations reformulated in terms of the hyperspherical coordinates have been applied to various reaction systems. For rotational transition, the IOS-DW and the independent events approximations have been proposed and applied to some systems. The reaction mechanisms can be clarified by these treatments. Exact calculations of 3-D reactions are also now becoming possible in our group. Another new line of our reaction dynamics studies is to figure out a way of separating collisional and vibrational variables. This is useful not only for understanding the mechanisms qualitatively, but also for attacking the larger reaction systems.

I-G-1 Application of the Independent Events Approximation to Rotational Transitions in the $H+H_2$ and $D+H_2$ Reactions

Masato NAKAMURA and Hiroki NAKAMURA

Rotational transitions in the reactions $H+H_2$ and $D+H_2$ are investigated by using the previously pro-

posed independent events approximation in which the overall rotational state distribution is expressed as a sum of products of the transition probabilities for the initial and final rotationally inelastic half-collisions and the rearrangement in the reaction zone. This approach can clarify the roles of these three processes in reaction. Numerical results are compared with other calculations, and are encouraging for the simplicity of the approximation.

I-G-2 Quantum Mechanical Study of the Light-Atom Transfer Reactions, $O(^3P)+XCl \rightarrow OX+Cl(X=H,D)$. I. Reactions in the Ground Vibrational States

Seung C. PARK *(Kangweon National Univ., Korea)*, Hiroki NAKAMURA and Akihiko OHSAKI *(Miyazaki Univ.)*

We present a three-dimensional quantum mechanical study of the light atom transfer reaction $O(^3P)+XCl(\nu_i=0) \rightarrow OX(\nu_f=0)+Cl(X=H,D)$, where ν_α represents the vibrational state in the α channel. The adiabatic-bend approximation reformulated in terms of the hyperspherical coordinates is employed to calculate the cross sections and rate constants. The potential energy surface used here is the Persky- Broida's LEPS-I. The results are compared with the available experimental data and quasiclasical trajectory calculations. A discrepancy is found between the present results and the quasiclassical trajectory results at low collision energies (low temperatures). This is a clear manifestation of the quantum mechanical tunneling effect. The present results of the rate constants and the kinetic isotope effect are generally in better agreement with experiment. The previously proposed constant centrifugal potential approximation (CCPA) is directly demonstrated to work well.

I-G-3 Separation of Collisional and Vibrational Variables in Chemical Reactions: Decoupling Surface in Phase Space

Kiyohiko SOMEDA and Hiroki NAKAMURA

A method for decoupling the collisional and vibrational variables in collision process is developed. The present procedure of decoupling is based on canonical transformation in phase space. The basic principle employed is the "maximal decoupling condition", $[\partial H/\partial u]_{u=v=0}=[\partial H/\partial v]_{u=v=0}=0$, where H is the Hamiltonian, and u and v represent new vibrational coordinates and momenta. "Decoupling surface" is defined as the surface determined by u=v=0. The partial differential equation to be satisfied by this decoupling surface is derived. This partial differential equation can be easily solved by utilizing classical trajectories. Local vibrational frequencies along the decoupling surface are defined, and their stability analysis is shown to provide the criterion for the separability. "Adiabatic approximation" which assumes the conservation of locally defined actions of the new vibrational variables leads to an "effective Hamiltonian" that describes the collision process under a given set of the initial vibrational actions. The present theory is applied to the collinear $H+H_2 \rightarrow H_2+H$ chemical reaction. Analysis of the local frequencies shows that the instability occurs in the following two regions depending on the collision energy: (1) When the collision energy is just above the activation energy, the instability occurs around the saddle point of the potential energy surface, and (2) at the higher collision energies, this unstable region disappears, but another one appears in the region where the reactive trajectories touch the ridge of the potential just after passing through the saddle point. In these unstable regions, bifurcation of the trajectories occurs. Analysis of the effective Hamiltonian can indicate the existence of a resonance structure corresponding to a temporal trapping of trajectory. This resonance structure is analogous to that in the coupled-oscillator problems, and we can expect that the so called irregular motion, or a stochastic layer, exists around the separatrix connected to this resonance structure.

I—H Theoretical Studies of Highly Excited States
of Atoms and Molecules

Highly (either electronically or vibrationally) excited states show various intriguing properties and participate in a variety of dynamic processes. We believe that they will open a new challenging world of science. The ultimate purpose of our studies is to find and understand the new collective motions in these states and their isomorphism among the various systems of different kinds. We also want to have a unified view of the various dynamic processes involving the highly excited states.

I-H-1 Ionization of Low-Rydberg-State He Atoms by Dipole-Forbidden Rotational Deexcitation of NH_3

Toshizo SHIRAI *(Japan Atomic Energy Research Institute)* and Hiroki NAKAMURA

A theoretical study of the ionization of He(n=14 ^{1}P) atoms in thermal collisions with NH_3 was carried out within the semiquantal approximation. The charge-dipole Glauber differential cross section was employed for the electron-molecule rotational deexcitation process. Calculated thermally averaged cross sections show quite a strong n dependence, especially for $n \le 17$. A comparison is made between the present results and recent experiments.

I-H-2 What are the Basic Mechanisms of Electronic Transitions in Molecular Dynamic Processes?

Hiroki NAKAMURA

The basic mechanisms of electronic transitions in molecular processes and their theoretical treatments are summarized and reviewed. These are the non-adiabatic (either radially or rotationally induced) transitions and the decay (auto-ionization) mechanisms of 'superexcited states'. The interdisciplinarity of the concept of non-adiabatic transition is emphasized, and the present status of the semiclassical theory is inclusively summarized together with some numerical applications. Particular emphasis is put on the non-adiabatic tunneling process which is supposed to be an important key mechanism for state (or phase) change in various fields. Definitions of two kinds of superexcited state are given, and their peculiarities and richness in their participating dynamic processes are explained. The multi-channel quantum defect theory is outlined and recommended as a powerful theoretical tool for dealing with the various dynamic processes such as photo-ionization, photodissociation, autoionization, dissociative recombination and associative ionization. Some numerical applications are also presented in order to promote the understanding of the mechanisms. The underlying philosophy throughout this paper is to try to clarify the basic mechanisms of electronic transitions and to formulate them in a unified way as much as possible.

I-H-3 Theoretical Study of the Dissociative Recombination of NO^+ with Slow Electrons

Hosung SUN *(Pusan National Univ. and IMS)* and Hiroki NAKAMURA

The multi-channel quantum defect theory (MQDT) has been applied to the dissociative recombination of NO^+ by collisions with slow electrons. The Rydberg states (superexcited states of second kind) are fully incorporated by using the quantum defect functions. Five valence-type dissociative superexcited states of first kind ($A'^2\Sigma^+$, $I^2\Sigma^+$, $B^2\Pi$, $L^2\Pi$, $B'^2\Delta$) are all considered as the dissociation channels. Since the recently obtained quite reliable information on the superexcited states is employed in the calculation, the present results are considered to be the most accurate ones at this moment. Energy dependence of the cross sections shows intriguing resonance structures and varies from state to state, reflecting the relative dominance of the three

basic important quantities: quantum defect function, electronic coupling and Franck-Condon factor. The results are compared with other calculations and the available experiments.

I—I   Theory for High-Tc Superconductivity

To clarify the origin of Cu-O type and Bi-O type high-temperature superconductivities, we theoretically study their microscopic electronic structures and the nature of electron-phonon couplings in these materials.

I-I-1 Discontinuous Change of Superconducting Transition Temperature from BCS-type to Bipolaron-type in Strongly Coupled Electron-phonon Systems

Keiichiro NASU

A new unified theory for superconducting transition temperature T_c of electron-phonon coupled systems has been derived, so as to clarify the natures of the intermediated region of coupling strength, as well as the weak (BCS) region and the strong (bipolaronic) one. This theory is mainly based on the polaron picture, and takes the thermal fluctuation of pairing order into account within the coherent potential approximation. In the weak coupling limit, it reduces to the Eliashberg theory and gives such T_c that increases as the coupling increases. While, in the strong coupling region, it reduces to a pseudo-spin type theory of bipolarons, and T_c decreases as the coupling increases. Thus, T_c takes its maximum value in the intermediated region of coupling strength. It is shown, however, that this change of T_c from the BCS region to the bipolaronic one becomes discontinuous when the band-width of electron is greater than the phonon energy. While, in the opposite case, it changes continuously. The calculated results of the former case are discussed in connection with the insulator-superconductor transition of $Ba_{1-x}K_xBiO_3$.

I—J   Nonlinear Excitations in Halogen-Bridged Mixed-Valence Metal Complexes

To clarify the natures of elementary optical excitations and other nonlinear excitations in one-dimensional charge-density wave state, we study singlet excitons, solitons and polarons in one-dimensional halogen-bridged mixed-valence metal complexes.

I-J-1   Spectral Shapes of Optical Absorption in the Extended Peierls-Hubbard Model

Kaoru IWANO and Keiichiro NASU

In order to clarify the origin of the light absorption bands of halogen-bridged mixed-valence metal complexes (HMMC), we calculate the shapes of charge-transfer excitation spectra within the Franck-Condon approximation, by using the extended Peierls-Hubbard model. There are two essential factors dominating the shapes. One is the electron-correlation effect beyond the mean field approximation, and the other is the fluctuation of the halogen lattice around the dimerization. However, there has been no theoretical study that takes both of them into account simultaneously. Thus, as the first trial, we have calculated the spectra, assuming that only one electron is excited and the lattice fluctuation is classical. When the intersite electron-electron repulsion V is weak enough, the charge-transfer exciton is only weakly bound. The interband continuum (free electrons and free holes) still possesses an amount of oscillator strength comparable to that of the exciton. When V is strong enough, on the other hand, the con-

tribution from the interband continuum becomes negligible. In this case, the spectra mainly come from the lowest excitons and become asymmetric Lorentzian. The most of HMMC's seem to correspond to the latter cases. Moreover, we have clarified the temperature dependence. In low temperatures, the thermal fluctuations of the halogen lattice coordinates are governed by a Gaussian distribution because of their harmonic motions. In higher temperaures, on the other hand, the anharmonicity which originates from the degeneracy of the ground states becomes important. We have also clarified the natures of the low-energy tail, in relation to the Urbach rule.

I—K   Theory for Charge Separation of Exciton in Alkali Halides

To clarify the microscopic mechanism of charge separation of exciton into electron-hole pair, we study the nature of adiabatic potential energy surface of an electron-hole pair, asymmetrically coupling to the lattice.

I-K-1 Dichotomization Processes of Self-Trapped Exciton into Asymmetric Electron-Hole Pair

Shinichiro, NAGASAKA *(Univ. of Yamagata)* and **Keiichiro, NASU**

Problems related with optical excitations and their lattice relaxation processes in various nonmetallic solids are the subject of considerable interest in these twenty years. Especially, the lattice relaxation processes of an exciton in alkali halides have been studied intensively, since it shows a very strong exciton-lattice coupling. Through a number of experimental and theoretical investigations for this problem over these two decades, it has become clear that there are at last two types of states, to which the exciton reaches after the lattice relaxation. The one is the ordinary self-trapped exciton (OSTE), being composed of a self-trapped hole (STH), and an electron in a s-like symmetric bound state centered at this STH. The other is the dichotomic self-trapped exciton (DSTE) without parity, being composed of a STH and an electron localized at a neighboring lattice site of this STH. Since the DSTE has a long life time for the radiative recombination as compared with the OSTE, it plays important roles as a starting state of the various photochemical reactions, such as the photographic effect, the optical composition and decomposition, the defect formation, degrading or damaging by laser light, and so on. For these reasons, we have studied relative stability between these two relaxed states of an exciton: the DSTE and the OSTE, as well as the possible conversion process between them. We have shown that in alkali halides the OSTE and the DSTE coexist with a very low energy barrier in between. The singlet state is shown to split off from the triplet ones by the exchange interaction between the electron and the hole, and the magnitude of this splitting becomes maximum in the OSTE but becomes very small in the DSTE.

I—L   Study on The Electronic Structure Theory

I-L-1   Electron Correlation Problems

Kimihiko HIRAO *(Nagoya Univ. and IMS)*

The need for a reliable, yet simple and feasible treatment of the correlation problems for molecules is becoming more and more urgent. Configuration Interaction (CI) is the most straightforward and most generally applicable method for an approximate solution of the Schrödinger equation. However, the convergence becomes rather slow if one strives at "chemical accuracy". There are two sources of the slow convergence of the CI expansion; the combinatorial problem and the partial wave expansion. It is now understood how to get along the combinatorial problem. Our cluster expansion theory (SAC and SAC-CI) is one of the most

promising approaches to this problem. By now the SAC and SAC-CI approaches have been well tested for numerous ground state and excited states. The slow convergence of the second source is a consequence of the Coulomb singurality of the electron interaction. A wave function, including r_{12} dependent terms, which takes care of the correlation cusp, is introduced to allow a closed summation of the slowly convergent contributions. We have studied a simple method to avoid difficult integrals without a significant loss of accuracy.

I-L-2 Floating Wavefunctions

Kimihiko HIRAO *(Nagoya Univ. and IMS)*

The Hellmann-Feynman theorem plays an important role in many area of molecular quantum theory, e.g., studies of molecular geometries, force constants, chemical reactions and dynamics. The theorem often leads to very classical and intuitive pictures and in this connection there is a potentially important point. In spite of its great theoretical significance, the Hellmann-Feynman theorem has been of surprisingly little value for practical calculations, since the validity of the theorem requires some condition when approximate wavefunctions are employed. As pointed out by Hurley, the floating functions obeys the Hellmann-Feynman theorem. As a price for translational invariance and for the force theorem, the atomic orbitals of the floating functions may have their cusps off the nuclei. The standard computer program for geometry optimization is adapted to yield floating functions. This provides a

great conceptual simplification and leads to practical advantages for the calculation of the higher-order energy derivative. The method is tested by detailed calculations for numerous molecules.

I-L-3 Miscellaneous Applications of the ab initio Calculations

Kimihiko HIRAO *(Nagoya Univ. and IMS)*

The mechanism of pseudo-rotation of penta-coordinated compounds having been extensively studied experimentally and theoretically, still remains unresolved. We have studied pseudo-rotation reactions of some phosphorous compounds using ab initio method and discussed the mechanism of the pseudo-rotation.

Recently IR spectra of the protonated ethane have been recorded by the Lee's group at Berkeley. The spectrum changes dramatically as a function of the pressure behind the nozzle in the ion source. The observed IR frequencies are compared with predicted frequencies for already known classical and bridged structures of the protonated ethane. However, there exist serious conflicts between theory and experiment. In order to interpret these spectrum features, we have carried out ab initio calculations on the protonated ethane. We found the new weakly bound $C_2H_7^+$ in addition to already known classical and bridged isomers. The experimentally observed different behavior can be attributed to the changing ratio of the weakly bound complex to the bridged protonated ethane being probed spectroscopically.

I—M   Geometries, Electronic Structure, and Reactions of Transition metal complexes

Transition metal complexes are of much interest because of their varieties in geometries, electronic structures, reactions, and catalytic activities. Theoretical investigation of transition metal complexes concerning those issues is important and useful in understanding chemistry of transition metal complexes and finding new catalysts. In this work, ab Initio MO studies are carried out on such transition metal complexes as nickel(0) and nickel(I) complexes with carbon dioxide, platinum(0)- and platinum(II)-complexes with silene and disilene, and oxidative addition of Si-H bond with Pt(0) complexes. These complexes are chosen here from following reasons. Coordination of carbon dioxide have received recent attention in catalytic fixation of carbon dioxide because transition metal complexes are expected to activate carbon dioxide through coordination. Silene and disilene complexes, which have been recently synthesized and isolated, are interesting as models of intermediates in various syntheses of Si compounds. Also, Si-H

oxidative addition with transition metal complex is expected to be one of key steps in syntheses of Si compounds.

I-M-1 An ab Initio MO and SD-CI Study of $Ni(PH_3)_2(CO_2)$. Electron Correlation Effects on Geometry, Binding energy, and Electronic Structure

Shigeyoshi SAKAKI *(Kumamoto Univ., IMS),* **Nobuaki KOGA and Keiji MOROKUMA**

Ab initio Hartree-Fock, single-reference single-double configuration interaction (SD-CI) and multi-reference SD-CI calculations were carried out for $Ni(PH_3)_2(CO_2)$. Introduction of electron correlation lengthens the $Ni-CO_2$ coordinate bond distance of the η^2-side-on complex and decreases the CO_2 binding energy. These correlation effects are opposite to those found in M(CO) (M=Ni, Pd, or Pt), $Ni(PH_3)_2(\eta^1-N_2)$ and $Ni(PH_3)_2(C_2H_4)$. The difference in correlation effects between them comes from their different feature of HOMO. The electronic structure of $Ni(PH_3)_2(\eta^2-CO_2)$ is analyzed in detail at the Hartree-Fock and SD-CI levels.

I-M-2 Can CO_2 Coordinate to a Ni(I) Complex? An ab Initio MO/SD-CI Study

Shigeyoshi SAKAKI *(Kumamoto Univ., IMS)*

$Ni^IF(NH_3)_4(CO_2)$ **1**, $[Ni^I(NH_3)_4(CO_2)]^+$ **2**, and $[Ni^{II}F(NH_3)_4(CO_2)]^+$ **3** are investigated with ab Initio MO/SD-CI method. These complexes can be viewed as models of an intermediate which has been propsoed in electrocatalytic reduction of CO_2 with Ni^{II}(cyclam)Cl_2. In **1**, the η^1-CO_2 coordination is calculated to have a considerably large binding energy (22 kcal/mol at Hartree-Fock (HF) level and 48 kcal/mol at the SD-CI level), while negative binding energy is obtained for the η^2-side-on CO_2 coordination. Considerably negative binding energies are also calculated for **2** and **3** which are assumed to take the same structure as **1**. This suggests that CO_2 coordination needs three conditions; the reduction of Ni(II) to Ni(I), neutralization of positive charge, and the presence of a counter ligand (or

adsorption to the electrode). These conditions would destabilize the Ni d_{z^2} orbital in energy, which allows strong charge-transfer to CO_2 from Ni. At the same time, the charge neutralization would decrease the charge-dipole repulsion between the distorted CO_2 and Ni(I). In **1**, these conditions are satisfied. Therefore, **1** possesses a strong Ni $\rightarrow$ CO_2 charge-transfer interaction and forms a stable η^1-CO_2 complex. Such strong charge-transfer in **1** significantly increases the negative charge on the O atom of CO_2, which would facilitate proton attack to the coordinated CO_2.

I-M-3 Geometries and Coordinate Bond Nature of Silene and Disilene complexes with platinum(0) and platinum(II)

Shigeyoshi SAKAKI *(Kumamoto Univ., IMS),* **Masami IEKI** *(Kumamoto Univ.)*

An ab Initio/MP4 and SD-CI studies are carried out on $Pt(PH_3)_2(CH_2=SiH_2)$, $Pt(PH_3)_2(SiH_2=SiH_2)$, and $PtCl_3(SiH_2=SiH_2)$, in a comparison with well known ethylene analogues. Optimized distances of C=C, Si=C, and Si=Si bonds at Hartree-Fock level are in good agreement with experimental values. Binding energy of their coordination increases in the order ethylene < silene < disilene in both platinum(0) and platinum(II) complexes, and platinum(0) < platinum(II) in ethylene and disilene complexes. This increasing order results from the fact that both donating and back-donating abilities increase in the same order. One of characteristic features of silene and disilene coordination is the Pt-P and Pt-Cl bond trans to Si are longer than those trans to C, which indicates that the trans-influence effect of Si is stronger than that of C.

I-M-4 Oxidative Addition of Si-H Bond with Platinum(0) Complex. An ab Initio MO Study

Shigeyoshi SAKAKI *(Kumamoto Univ., IMS),* **Masami IEKI** *(Kumamoto Univ).*

Oxidative addition of SiH_4 to $Pt(PH_3)_2$ is investigated with ab Initio MO/MP4 method, and compared

with a similar oxidative addition of CH_4 with $Pt(PH_3)_2$. Geometries of reactants, $Pt(PH_3)_2$ and SiH_4, product, cis-$Pt(H)(SiH_3)(PH_3)_2$, and transition state are optimized at Hartree-Fock level. SiH_4 oxidative addition is significantly exothermic (28.3 kcal/mol at MP2 and 26.4 kcal/mol at MP4 level), while CH_4 oxidative addition is endothermic (5.2 kcal/mol at MP2 and 6.5 kcal/mol at MP4 levels). Corresponding to this difference, SiH_4 oxidative addition proceeds with more early transition state than the CH_4 oxidative addition.

The activation barrier of CH_4 oxidative addition is calculated to be 25.9 kcal/mol at MP2 level and 28.1 kcal/mol at MP4 level. On the other hand, the activation barrier of SiH_4 oxidative addition is -1.9 kcal/mol at MP2 and -1.6 kcal/mol at MP4 levels. These small negative values are changed to very small positive values by correcting basis set superposition error. This critical difference between CH_4 and SiH_4 additions indicates the larger reactivity of Si-H bond than that of C-H bond.

RESEARCH ACTIVITIES II
Department of Molecular Structure

II—A High Resolution Spectroscopy of Transient Molecules and Ions

During the course of chemical reactions many transient molecules and ions appear as intermediates. Because of their high reactivities, i.e. their short lifetimes, these transient species have remained to be explored and some of them have even escaped detection. Many of these molecules have open-shell electronic structure, which characterizes them as free radicals. Unpaired electrons in a molecule cause splittings in high resolution spectra of such species through fine and hyperfine interactions, and, when properly analyzed, these splittings provide us with information on the electronic properties of the molecule which is not obtainable for molecules without unpaired electrons. High resolution spectroscopy not only provides molecular constants of transient molecules at very high precision, but also allows us to unambiguously identify chemical species occuring in reaction systems and to unravel the details or reaction mechanisms, in particular, when it is combined with some time-resolved detection methods. The present project will also be of some significance in related fields such as astrophysics and environmental sciences, and even in semiconductor fabrication.

II-A-1 The Microwave Spectrum and the Molecular Structure of the SSCl Radical

Masaharu FUJITAKE and Eizi HIROTA

The measurement of the microwave spectrum of the SSCl radical generated by a dc glow discharge in an S_2Cl_2/Ar or SCl_2/Ar mixture has been extended to yield molecular constants with high precision, which are listed in Table I. The ^{37}Cl species has also been studied in a similar way, and the results are displayed in Table I. The spin-rotation interaction constants are substituted in Curl's relation $g=2.0023-\epsilon/2B$ to calculate $g_{aa}=2.0386$, $g_{bb}=2.0237$, and $g_{cc}=2.0027$, which are favorably compared with the ESR values[1]: $g_{aa}=2.0384$, $g_{bb}=2.0225$, and $g_{cc}=2.0019$. The observed rotational constants lead to the structure parameters: r(S-S)=1.937Å, r(S-Cl)=2.037Å, and θ(SSCl)=110.6°.

Reference

1) F.G. Herrig et al., *J. Chem. Phys.* **57**, 4564 (1972).

Table I. Molecular constants of the SSCl Radical (MHz)[a]

Constant	SS^{35}Cl	SS^{37}Cl
A	18 319.775 (21)	18 183.16 (224)
B	2 827.5490 (16)	2 748.1368 (462)
C	2 445.9326 (10)	2 383.9196 (40)
Δ_J	1.1504 (4) 10^{-3}	1.1283 (6) 10^{-3}
Δ_{JK}	−1.8011 (11) 10^{-2}	−2.0588 (270) 10^{-2}
Δ_K	2.7117 (11) 10^{-1}	[2.7117 10^{-1}][b]
δ_J	2.5118 (20) 10^{-4}	[2.5118 10^{-4}][b]
δ_K	4.5350 (217) 10^{-3}	[4.5350 10^{-3}][b]
ϵ_{aa}	−1 329.03 (91)	[−1319.12][c]
ϵ_{bb}	−121.24 (12)	[−117.84][c]
ϵ_{cc}	1.75 (11)	1.75 (2)
$|(\epsilon_{ab}+\epsilon_{ba})/2|$	18.62 (193)	—
Δ^s_N	1.22 (29) 10^{-4}	[1.22 10^{-4}][b]
Δ^s_{NK}	−2.04 (58) 10^{-3}	[−2.04 10^{-3}][b]
Δ^s_K	2.20 (37) 10^{-2}	[2.20 10^{-2}][b]
δ^s_N	6.50 (54) 10^{-5}	[6.50 10^{-5}][b]

a. Values in parentheses denote standard deviations and apply to the last digits of the constants.
b. Fixed.
c. Calculated by $\epsilon(^{37}Cl) = \epsilon(^{35}Cl)B(^{37}Cl)/B(^{35}Cl)$.

II-A-2 The $CH_4 + O(^1D$ and $^3P) \rightarrow CH_3$ + OH Reaction Investigated by Infrared Diode Laser Kinetic Spectroscopy

Toshinori SUZUKI and Eizi HIROTA

In view of the fundamental importance of the reaction in the title we have examined it in detail mainly through the time-resolved observation of the ν_2 band of the CH_3 radical as a product. We generated $O(^1D)$ by the photolysis of N_2O at 193 nm, of NO_2 at 193 nm or of O_3 at 248 nm, with the maximum available energy of 7300, 3500, and 2800 cm^{-1}, respectively, whereas $O(^3P)$ was obtained by photolyzing SO_2 at 193 nm, leaving 2500 cm^{-1} as an upper limit of available energy. The total pressure of the precursor/methane mixture was fixed to 200 mTorr. The rotational temperature of CH_3 was found to reach about 400 K a few μs after the photolysis, except for the SO_2 case for which it was likely to be about 600 K at an initial stage of the process. The CH_3 radical generated did not show any population inversion among the $\nu_2=0$ to 4 states; the vibrational population deviated considerably from the statistical distribution, more favoring lower states, i.e. the population decreased with the increasing ν_2 quantum number much faster than expected from a statistical model. In contrast, the OH radical in the case of $O(^1D)$ was much excited. These observations indicate that the process is a direct hydrogen abstraction reaction for both the $O(^1D)$ and $O(^3P)$ cases.

II-A-3 Laser Induced Fluorescence Spectroscopy of the $\tilde{A}^1A''-\tilde{X}^1A'$ Transition of HGeCl

Haruhiko ITO, Eizi HIROTA, and Kozo KUCHITSU (Nagaoka Univ. Tech.)

Germanium-containing transient molecules have recently attracted much interest, presumably because of their important roles as intermediate species in Ge CVD processes. However, little has been known on these molecules, in sharp contrast with the corresponding C and Si analogues. The present study was initiated to detect such Ge-containing intermediates, and the (000)-(000), (010)-(000), and (020)-(000) bands of the $\tilde{A}^1A''-\tilde{X}^1A'$ transition of the HGeCl molecule were observed by laser induced fluorescence spectroscopy. The K-subband heads were resolved, and the transition wavenumbers of these heads were measured with a resolution of 0.04 cm^{-1}. The molecular constants of the relevant vibronic levels were determined by a least-squares analysis of the observed wavenumbers, and are listed in Table I.

Table I. Molecular Constants for the $\tilde{A}^1A''$ and $\tilde{X}^1A'$ States of HGeCl (cm^{-1})

Stete	ν_0	$A\text{-}\bar{B}$	D_K
$\tilde{A}^1A''$ (000)	21 515.08	7.844	0.0040
(010)	21 946.14	8.025	0.0052
(020)	22 355.01	8.170	0.0069
$\tilde{X}^1A'$ (000)	0.0	6.622	0.0022

II-A-4 Laser Induced Fluorescence Spectroscopy of the $\tilde{A}^1A''-\tilde{X}^1A'$ Transition of HGeBr

Haruhiko ITO, Eizi HIROTA, and Kozo KUCHITSU (Nagaoka Univ. Tech.)

As in the case of HGeCl, HGeBr molecules were generated by the reaction of GeH_4 with microwave discharge products of Br_2 diluted with Ar. A laser-induced-fluorescence (LIF) spectrum was observed in 400-500 nm region and was assigned to the $\tilde{A}$-$\tilde{X}$ transition of HGeBr. Two vibronic bands (010)- (000) and (020)-(000) were resolved into K-subbands. Figure 1 shows the $K'=6\leftarrow K''=5$ subband of (020)-(000) as an example of the observed spectrum. The observed subband heads were analyzed using the following energy level expression:

$$F(K) = \nu_0 + (A\text{-}\bar{B})K^2 - D_K K^4,$$

where ν_0 was set to zero for the $\tilde{X}(000)$ state. The ν_0, $(A\text{-}\bar{B})$, and D_K constants thus determined are 21471.82, 8.394, and 0.0063 for $\tilde{A}(020)$, 21 079.79, 8.326, and 0.0052 for $\tilde{A}(010)$, and 0, 6.693, and 0.0016 for $\tilde{X}(000)$, all in cm^{-1}.

21598.0160   21600.8051 cm^{-1}

Te$_2$
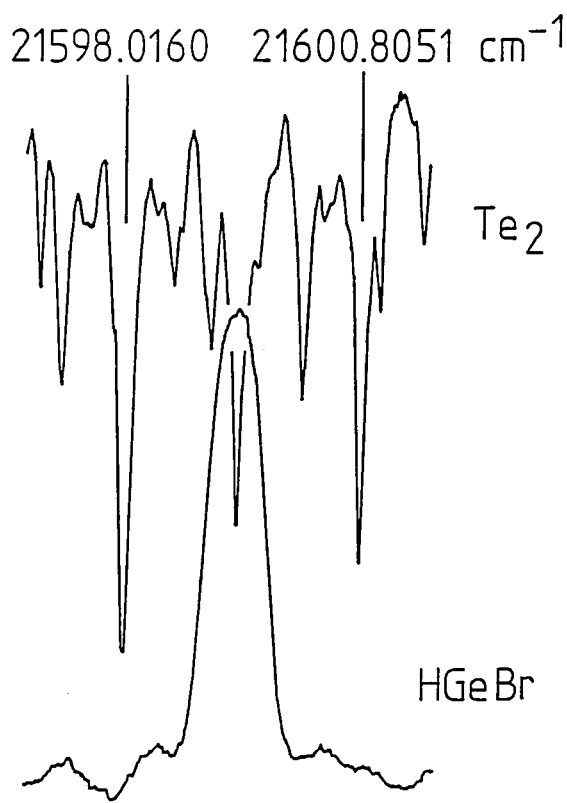
HGeBr

Figure 1. The $K'=6 \leftarrow K''=5$ subband of the $\tilde{A}\,^1A''(020) \leftarrow$ $\tilde{X}\,^1A'(000)$ transition of HGeBr, observed by LIF. The upper trace is the LIF spectrum of Te$_2$ simultaneously recorded to calibrate the HGeBr spectrum.

II-A-5   The Microwave Spectrum of NaK

Chikashi YAMADA and Eizi HIROTA

In contrast with homonuclear diatomic molecules of alkali atoms, only a few spectroscopic studies have been carried out on heteronuclear diatomics. For NaK, Ross et al.[1] reported the D-X and D-a bands excited by an Ar$^+$ laser and observed as dispersed fluorescence, while Wormsbecher et al.[2] measured a few rotational transitions by a microwave-optical double-resonance (MODR) technique combined with an Ar$^+$ laser. Degdigian and Wharton[3] found by a molecular beam electric resonance method the dipole moment of NaK to be quite large. Therefore, we decided to detect this molecule by millimeter-wave spectroscopy. The spectrum, if observed, would be of great use in identifying this species in interstellar space.

The heterodimer was generated directly in a stainless-steel absorption cell 10 cm in diameter and 110 cm long, by loading Na and K with nearly 1:1 weight ratio

and then by heating the central part of the cell over about 50 cm up to 500°C; Ar gas of 20 mTorr was slowly pumped through the cell to suppress the flow of alkali vapor. The rotational transitions of $J=45-44$ up to $J=70-69$ were observed for the $v=0-6$ states. The Dunham coefficients reported in Ref.1 were combined with the present data to improve the molecular constants, as shown in Table I. The harmonic frequency was calculated to be 124.045 cm^{-1}, in good agreement with the observed value 124.012 cm^{-1}. The equilibrium internuclear distance was determined to be 3.499 04 Å, which agreed well with the sum of the covalent radii, 1.54 + 1.96 Å, but was much longer than the ionic radius sum, 2.28 Å.

References
1) A.J. Ross, C. Effantin, J. d'Incan, and R.F. Barrow, *Mol. Phys.* **56**, 903 (1985).
2) R.F. Wormsbecher, M.M. Hessel, and F.J. Lovas, *J. Chem. Phys.* **74**, 6983 (1981).
3) P.J. Dagdigian and L. Wharton, *J. Chem. Phys.* **57**, 1487 (1972).

Table I.   Molecular Constants of NaK (MHz)[a]

Constant	Reference 1	Present
Y_{01}	2854.92[b]	2854.9007 (33)
Y_{11}	−13.478 (16)	−13.4434 (30)
Y_{21}	−0.077 1 (47)	−0.0756 (12)
Y_{31}	−0.73 (17) 10^{-3}	−0.85 (20) 10^{-3}
Y_{41}	−0.35 (12) 10^{-4}	−0.34 (15) 10^{-4}
Y_{51}	0.78 (22) 10^{-6}	0.79 (52) 10^{-6}
Y_{61}	0.123 (15) 10^{-7}	0.123 (37) 10^{-7}
Y_{02}	0.6872 (37) 10^{-2}	0.673 026 (83) 10^{-2}
Y_{12}	−0.347 (36) 10^{-4}	−0.462 9 (36) 10^{-4}
Y_{22}	0.79 (33) 10^{-6}	−0.35 (12) 10^{-6}
Y_{32}	−0.19 (15) 10^{-7}	−0.27 (13) 10^{-7}
Y_{42}	0.111 (21) 10^{-9}	0.108 (50) 10^{-9}
Y_{03}	0.244 (28) 10^{-7}	0.146 82 (79) 10^{-7}

a. Values in parentheses denote one standard deviation and apply to the last digits of the constants.
b. Fixed to the value reported in Ref.3.

II-A-6   Millimeter-Wave Spectroscopy of Excited Vibrational States of Aminoborane, NH$_2$BH$_2$

Wyn LEWIS-BEVAN *(Southern Illinois Univ. and IMS)*, **Chikashi YAMADA, and Eizi HIROTA**

Aminoborane is a planar molecule of C$_{2v}$ symmetry; it has three lowest modes v_6 (A$_2$), v_8 (B$_1$), and v_{12} (B$_2$)

at 742, 613, and 836 cm^{-1} respectively which are strongly coupled each other by Coriolis interaction. These perturbations combined with the fact that v_6 is infrared inactive make the analysis of high resolution Fourier transform spectra previously measured[1] extremely difficult. The present study was initiated to obtain further information on the three states through the observation of the rotational spectrum.

The molecule was produced by the two-stage thermal decomposition of borane-ammonia, $NH_3 \cdot BH_3$ (s). The gaseous products were continuously pumped through an absorption cell of a millimeter-wave spectrometer operated in the frequency range between 90 and 390 GHz. Very strong signals of low J and K_a pure rotational transitions from all the three vibrational states were observed and assigned, with noticeable deviations from the ground-state frequencies, especially for v_6 and v_{12}. Significant hyperfine structure was also observed. The observed data are being analyzed with the infrared spectra to explain the numerous perturbations observed in the v_8 and v_{12} bands as well as those reported for v_4[2].

References
1) W. Lewis-Bevan, D.M. Steunenberg, A.J. Merer, and M.C.L. Gerry, to be published.
2) M.C.L. Gerry, W. Lewis-Bevan, A.J.Merer, and N.P.C. Westwood, J. Mol. Spectrosc. 110, 153 (1985).

II-A-7 Infrared Diode Laser Spectroscopy of the Bending Fundamental (v_3) of the DCO Radical

Wyn LEWIS-BEVAN (Southern Illinois Univ. and IMS), Toshinori SUZUKI, and Eizi HIROTA

There is considerable interest in understanding the potential energy surface of the formyl radical. The interest results mainly from the weak nature of the C-H or C-D bond, which is considerably anharmonic. There have been numerous spectroscopic studies of both HCO and DCO. In particular, Lowe and McKellar[1] studied the C-D and C=O stretching fundamental bands of DCO using laser magnetic resonance spectroscopy. They reported a significant change in the A rotational constant upon excitation of the C-D fundamental mode. It was expected that an even larger magnitude change should be observed in the study of

the DCO bending fundamental band. This band is the last to be characterized at high resolution in the infrared.

We employed infrared diode laser kinetic spectroscopy to observe the DCO lowest lying band. The radical was produced by the flash photolysis of fully deuterated acetaldehyde by XeCl excimer laser radiation at 308 nm. Spectral data were recorded between 820 and 890 cm^{-1}, and over one hundred transitions were observed, which were mainly P-branch transitions of a parallel, i.e. a-type band. No b-type transitions have been assigned. The observed lines were assigned to transitions with quantum numbers up to $J=10$ and $K_a=4$.

Reference
1) R.S. Lowe and A.R.W. McKellar, J. Chem. Phys. 74, 2686 (1981).

II-A-8 The Vibrational Distribution of Methyl Radicals Produced by the Photolysis of CH$_3$I at 248 nm

Toshinori SUZUKI, Hideto KANAMORI (Univ. Tokyo), and Eizi HIROTA

The photodissociation of methyl iodide in the $\tilde{A}$ state consists of cleavage of the C-I bond and opening of the HCH angles; the latter would result in considerable excitation of the methyl radical v_2 band. In fact, all previous studies using time-of-flight mass spectrometry[1] and infrared emission observation[2] concluded that the CH$_3$ vibrational population peaks at $v_2=2$. However, we found that all the bands $v_2=1$-0 up to 4-3 appeared as absorptions, eliminating any possibility of population inversion in the v_2 manifold[3]. We have repeated measurements by focussing attention to a spike appearing in the time profile of the signal for a few μs after the photolysis. We previously ascribed this spike to complicated vibration and rotation relaxation processes[3], but it is better interpreted as CH$_3$ products moving out from the infrared monitoring beam because of their large velocity right after the photolysis. Within the spike of a few μs, the line shape did not change, indicating that the internal state distribution was not affected in this time interval. The rotational temperature was found to be in a range 600-750 K, irrespective of the vibrational state. Figure 1 shows the vibrational

population of CH_3 radicals thus determined with those of Refs. 1 and 2.

References
1) R.K. Sparks, K. Shobatake, L.R. Carlson, and Y.T. Lee, *J. Chem. Phys.* **75**, 3838 (1981).
2) H.W. Hermann and S.R. Leone, *J. Chem. Phys.* **76**, 4766 (1982).
3) H. Kanamori, S.R. Leone, and E. Hirota, *IMS Ann. Rev.* 1988 II-A-9.
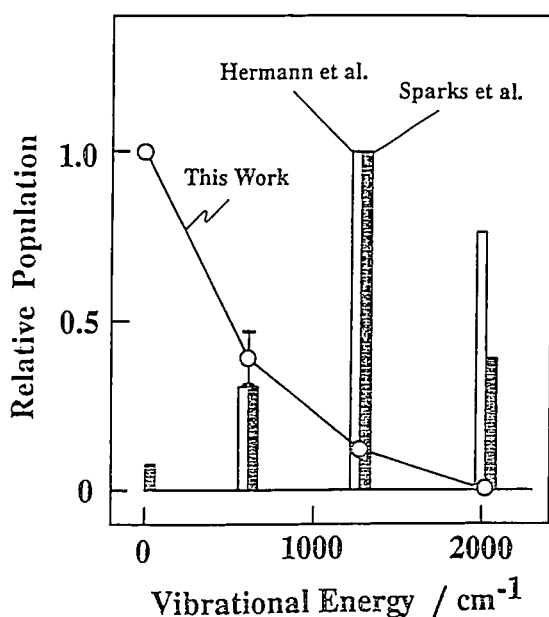
Figure 1. Vibrational (ν_2) population of CH_3 radicals produced by the 248 nm photolysis of CH_3I.

II-A-9 Millimeter-Wave Spectroscopy of the GeF$^+$ Ion

Keiichi TANAKA *(Kyushu Univ.),* **Yasunobu AKIYAMA** *(Kyushu Univ.),* **Takehiko TANAKA** *(Kyushu Univ.),* **Chikashi YAMADA,** and **Eizi HIROTA**

[*Chem. Phys. Lett.* **171**, 175 (1990)]

In a previous paper Akiyama et al.[1] reported the observation of the vibration-rotation band of GeF$^+$. However, because the precursor GeF$_4$ absorbed in the P-branch region strongly, no unique *J* assignment could be made. The present study aimed at resolving this ambiguity through the observation of pure rotational transitions.

The GeF$^+$ ion was generated in a free-space absorption cell by the hollow-cathode discharge in a GeF$_4$/Ar mixture. We employed the magnetic field to discriminate ion signals against those of neutrals. The observed transition frequencies were combined with the vibration-rotation transition data reported in Ref.1 and were analyzed by a least-squares method yielding the following Dunham coefficients: Y_{10}=815.558 (91) cm^{-1}, Y_{20}=−3.208 (45) cm^{-1}, Y_{01}=12 064.265 (46) MHz, Y_{11}=−75.505 (91) MHz, Y_{02}=−11.754 (27) kHz, and Y_{12}=39 (53) Hz with one standard deviation in parentheses, which applies to the last digits of the constants. The equilibrium bond length was calculated to be 1.664 821 0 (38) Å.

Reference
1) Y. Akiyama, K. Tanaka, and T. Tanaka, *Chem. Phys. Lett.* **165**, 335 (1990).

II-A-10 The Microwave Spectrum of the CsO Radical

Chikashi YAMADA and Eizi HIROTA

We have extended our studies on alkali monoxides to a last member CsO. As in the case of RbO, this radical was found to have the $^2\Sigma$ ground electronic state. The method of producing the radical was also similar; 20 g of Li metal and the corresponding mole of CsCl were placed at the central part of a stainless-steel absorption cell and were heated to about 500°C. The spin splitting was large in the ground and low-lying vibrational states, but decreased as the vibrational quantum number increased, making hyperfine splitting more conspicuous in higher vibrational states. The coupling scheme also changed from b$_{\beta J}$ to b$_{\beta S}$ as v increased. The analysis of the observed spectrum yielded molecular constants, as listed in Table I. The equilibrium internuclear distance was calculated to be 2.3007 Å, and the B_e and D_e constants led to a harmonic frequency of 357.5 cm^{-1}. The ground-state spin-rotation coupling constant gave an estimate for the lowest $^2\Pi$ state excitation energy to be 6200 cm^{-1}.

Table I. Molecular Constants of the CsO Radical (MHz)[a]

Constant	$\nu=0$	$\nu=1$	$\nu=2$	$\nu=3$
B	6668.0312(12)	6628.9651(14)	6589.5879(17)	6549.4925(15)
D	0.0104712(24)	0.0105334(27)	0.0106457(39)	0.0107914(34)
$H\times10^8$	0.17(15)	−0.46(17)	0.76(25)	−0.44(21)
γ	432.251(69)	371.62(14)	286.00(16)	144.65(13)
$\gamma_D\times10^2$	0.4998(96)	0.745(17)	1.119(23)	2.147(18)
$\gamma_H\times10^6$	−0.167(58)	0.166(92)	−0.30(13)	−1.03(10)
b	426.23(52)	427.3(22)	411.4(15)	409.34(49)
c	118.05(93)	112.0(36)	127.8(31)	120.30(16)
c_1	0.068(14)	−0.072(12)	−0.017(13)	−0.037(10)
eQq	−23.1(47)	22.(11)	19.(15)	56.(12)
σ	0.067	0.079	0.089	0.091

a. Values in parentheses denote one standard deviation and apply to the last digits of the constants.

II-A-11 Infrared Diode Laser Spectroscopy of Aluminum Hydride

Chikashi YAMADA and Eizi HIROTA

Deutsch et al.[1] observed the $\nu=2 \rightarrow 0$ to $\nu=8 \rightarrow 6$ bands of aluminum hydride using a Fourier transform spectrometer. Tipping[2] pointed to us that the dipole-moment derivative of AlH was exceptionally large and its detection by infrared diode laser spectroscopy was worth being tried.

In an initial stage, a crucible was employed to produce aluminum vapor at around 1500°C in the atmosphere of hydrogen. It was later replaced by a sheet of carbon less than 1 mm thick inserted in an alumina tube 60 mm in diameter. A piece of Al was placed at the central part of the cell, which was filled with hydrogen of 500 mTorr. The cell was then heated up to 1500°C. The region 1400 to 1700 cm^{-1} was scanned, and 8,4,4, and 5 lines were observed for the $\nu=1-0$, 2-1, 3-2, and 4-3 bands, respectively. An attempt was also made to observe the $J=1-0$ transition at 377 737 MHz, but failed; the permanent dipole moment is likely to be small. The observed vibration-rotation transition wavenumbers were combined with the Fourier data of Ref.1 and were analyzed by a least-squares method to derive molecular parameters, as listed in Table I. The expansion of the vibrational term value in $\nu+1/2$ was found to be slow-convergent.

References
1) J.L. Deutsch, W.S. Neil, and D.A. Ramsay, *J. Mol. Spectrosc.* **125**, 115 (1987).
2) R.H. Tipping. private communication.

Table I. Vibration-rotation Constants of Aluminum Hydride (cm^{-1})[a]

Constant	Reference 1	Present
B_e	6.393 7 (4)	6.393 78 (10)
α_e	0.186 85 (30)	0.187 057 (59)
γ_e	0.001 73 (5)	0.001 822 (32)
$10^4 D_e$	3.683 (10)	3.684 7 (42)
$10^4 \beta_e$	−0.063 5 (3)	0.064 1 (11)
$10^8 H_e$	1.48 (6)	1.476 (72)
ω_e	1682.435	1682.379 (11)
$\omega_e x_e$	29.106	29.053 4 (50)
$\omega_e y_e$	0.266 5	0.248 2 (30)
$\omega_e z_e$	−0.004 07	−0.004 7 (52)
$\omega_e \tau_e$	−	−0.000 129 (22)

a. Values in parentheses denote three standard deviations and apply to the last digits of the constants.

II-A-12 Infrared Diode Laser Spectroscopy of the CCD Radical in 2500 to 2800 cm^{-1} Region

Hideto KANAMORI (Univ. Tokyo) and Eizi HIROTA

Although a number of high-resolution spectroscopic studies have already been carried out on the ethynyl radical, the lowest excited electronic state has not been located precisely. Furthermore, the ν_1 fundamental band has not been identified, presumably because of overlap with the $\tilde{A}$-$\tilde{X}$ electronic band. In order to solve this problem, we decided to detect the ν_1 band of the CCD species; because of the isotope shift, the ν_1 band will appear around 2800 cm^{-1}, without being much perturbed by vibronic interactions with the $\tilde{A}$

state.

The CCD radical was produced by the 193 nm photolysis of deuterated acetylene, and its vibration-rotation bands were recorded by kinetic spectroscopy. Two bands were readily observed around 2800 cm^{-1}, one of $^2\Sigma$-$^2\Sigma$ type and the other of $^2\Pi$-$^2\Sigma$ type. The lower state of the former was shown to be identical to the $\tilde{X}^2\Sigma(001)$ state, and the upper state was also likely to be a vibrational state primarily associated with $\tilde{X}^2\Sigma$, because its rotational constant was typical of $\tilde{X}$, rather than of $\tilde{A}$. The $^2\Pi$-$^2\Sigma$ band appeared around the wavenumber region where Jacox[1] observed a band in a low-temperature matrix thought to be the ν_1 band. However, the upper state was shown to be of $^2\Pi$ symmetry, and thus could not be assigned to ν_1; the upper state was tentatively ascribed to $\tilde{X}^2\Sigma(110)$, while the lower state was confirmed to be the ground vibronic state. Two more bands were observed around 2500 cm^{-1}, one of $^2\Sigma$-$^2\Sigma$ type and the other of $^2\Pi$-$^2\Sigma$ type. The lower state of the former was again shown to be $\tilde{X}^2\Sigma(001)$, whereas both the upper and lower states of the latter band have not been known heretofore. Table I summarizes molecular constants of the three bands.

Reference

1) M.E. Jacox and W.B. Olson, *J. Chem. Phys.* **86**, 3134 (1987).

Table I. Molecular Parameters of Four Bands of CCD (cm^{-1})[a]

$^2\Sigma$-$^2\Sigma$ 2850 cm^{-1} band

B'	1.188 43 (3)	γ' 10^3	-3.7 (1)
D' 10^5	-1.9 (2)	γ_D' 10^6	2.3 (4)
H' 10^8	-4.29 (7)		
L' 10^{11}	3.3 (7)	T_v'	4594.4996 (9)

[The lower-state parameters were fixed to those of $\tilde{X}$ $^2\Sigma(001)$.]

$^2\Pi$-$^2\Sigma$ 2795 cm^{-1} band

B'	1.191 701 (6)	p' 10^4	1.1 (4)
D' 10^6	2.86 (2)	q' 10^2	1.038 (1)
A'	-0.701 (2)	q_D' 10^7	-2.5 (2)
γ' 10^3	-1.90 (8)	T_v'	2796.0340 (5)

[The lower-state parameters were fixed to those of $\tilde{X}$ $^2\Sigma(000)$.]

$^2\Sigma$-$^2\Sigma$ 2500 cm^{-1} band

B'	1.177 238 (5)	γ' 10^3	-4.00 (5)
D' 10^5	0.297 (2)	T_v'	4218.4751 (8)

[The lower-state parameters were fixed to those of $\tilde{X}$ $^2\Sigma(001)$.]

$^2\Pi$-$^2\Sigma$ 2500 cm^{-1} band (No detailed analysis has been made.)

a. Values in parentheses denote one standard deviation and apply to the last digits of the constants.

II-A-13 A Re-Investigation of the NO_3 1492 cm^{-1} Band

Kentarou KAWAGUCHI *(Nobeyama Radio Observatory)*, **Eizi HIROTA**, **Takashi ISHIWATA** *(Tokyo Inst. Tech.)*, **and Ikuzo TANAKA** *(Tokyo Inst. Tech.)*

Ishiwata et al. [*J. Chem. Phys.* **82**, 2196 (1985)] have recently observed an infrared diode laser spectrum of NO_3 in 1492 cm^{-1} region and have assigned it to the ν_3 band in the $\tilde{X}^2A_2'$ state. However, some of the derived constants did not conform well with expected values. In the present study the observation was extended so as to take combination differences, which led us to revise the previous assignment slightly and to remove all the anomalies in the lower (i.e. ground) state. A most important result of the present study is that a spin-orbit interaction constant $a_{eff}|<L_z>|$=0.17 cm^{-1} is indispensable to explain the spin-splitting observed for the upper state. The first-order Coriolis coupling constant of the upper state (ζ=0.19) remains essentially the same as in the previous study and differs considerably from the value calculated for the ν_3 state (ζ=0.7). Possible explanations of these data are discussed in some detail to obtain more information on the molecular structure of the NO_3 radical.

II-A-14 Vibronic Interactions in the NO_3 Radical

Eizi HIROTA *(Grad. Univ. Advanced Studies)*, **Kentarou KAWAGUCHI** *(Nobeyama Radio Observatory)*, **Takashi ISHIWATA** *(Tokyo Inst. Tech.)*, **and Ikuzo TANAKA** *(Tokyo Inst. Tech.)*

A few anomalies observed in the 1492 cm^{-1} band of NO_3 have been explained mainly in terms of the vibronic interaction of the $\tilde{X}^2A_2'\nu_3$=1 state with an excited electronic state of $^2E'\tau$ symmetry. The interaction Hamiltonian may be expressed as

$$H = V_1\,q\,(e^{i(\theta-\alpha)} + \text{c.c.}) + V_2\,q^2\,(e^{i(\theta+2\alpha)} + \text{c.c.}) + ...$$

where q denotes the amplitude of the degenerate N-O stretching coordinate and θ and α stand for the azimuthal angles of the unpaired electron and the N-O vibration stretching coordinates, respectively. The first term will mix the $\tilde{X}$ ν_3=1 state with the $^2E'$ state, transferring the spin-orbit interaction term in the latter state to

the former. The effective spin-orbit interaction constant a_{eff} is given by $(h_1/\Delta E)^2 A_{so}$, where h_1 denotes the matrix element of the first term in H' between $\tilde{X}^2 A_2'$ and $^2 E'$ and ΔE and A_{so} represent the excitation energy and the spin-orbit interaction constant of the $^2 E'$ state, respectively. When A_{so}=150, ΔE=15000, and a_{eff}= 0.173 cm^{-1} are employed, $|h_1|$ is about 500 cm^{-1}. Then H' is employed to derive an effective vibrational potential function in the $\tilde{X}^2 A_2'$ ground electronic state; Van Vleck transformation of H' yields additional terms to the ordinary potential function, namely $-[|h_1|^2/\Delta E]q_+ q_- - [|h_1 h_2|/\Delta E](q_+{}^3 + q_-{}^3) + ...$, where $q_{\pm}$ $= q\exp(\pm i\alpha)$. The second term modulates the azimuthal motion of the degenerate N-O stretching mode which is otherwise free, and thus reduces the first-order Coriolis coupling constant. The observed ζ constant can be reproduced when $|h_2|$ of about 2658 cm^{-1} is assumed. Obviously this $q_+{}^3 + q_-{}^3$ term does not affect the ground vibrational state, preserving D_{3h} symmetry in this state, in accord with the experimental observation.

II-A-15   The Microwave Spectrum of Sodium Borohydride

Yoshiyuki KAWASHIMA *(Kanagawa Tech. Univ.)*, **Chikashi YAMADA, and Eizi HIROTA**

Sodium borohydride is a well-known reducing reagent, but its molecular structure in the gas phase has not been known. We have succeeded in observing millimeter-wave spectra, by simply heating solid material in a stainless-steel absorption cell. The observed spectrum showed the pattern of a symmetric-top molecule; the transitions of J=10 ← 9 up to 21 ← 20 and of K=0-12 were observed, yielding molecular constants, as listed in Table I. The rotational constants of the ^{11}B and ^{10}B species led to the bond lengths r(Na-B) and r(B-H) to be 2.3135 Å and 1.172 Å, respectively, assuming tetrahedral symmetry for the BH$_4$ group. The Na-B distance is considerably shorter than the corresponding value 3.08 Å in a crystal[1]. Two additional sets of satellites were observed, one with a larger D_{JK} constant and the other with a negative D_{JK} constant, and both showed K=0, 1, and 2 lines deviating from the ordinary symmetric-top pattern. Most of the K-components of the former set are split into two components. The two sets are ascribed to the excited states of the BH$_4$ internal motion.

Reference
1) B.D. James and M.G.H. Wallbridge, *Progr. Inorg. Chem.* **11**, 99 (1970).

Table I. Molecular Constants of Sodium Borohydride (MHz)[a]

Constant	Na^{11}BH$_4$	Na^{10}BH$_4$
B	9652.494 (4)	10036.079 (5)
D_J	0.021 083 (8)	0.022 619 (9)
D_{JK}	0.241 25 (10)	0.261 56 (15)
H_{JK}	3.95 (13) 10^{-6}	4.44 (24) 10^{-6}
H_{KJ}	3.2 (6) 10^{-6}	1.7 (7) 10^{-6}

a. Values in parentheses denote three standard deviations and apply to the last digits of the constants.

II-A-16   Internal Motions in MBH$_4$ (M=Alkali)

Eizi HIROTA *(Grad. Univ. Advanced Studies and IMS)*

In order to facilitate analyzing the rotational spectra recently observed for alkali borohydride (II-A-15), a Hamiltonian was set up which included the overall rotation and the BH$_4$ group internal-rotation terms, as follows:

$$H/h = (A-B')J_z^2 + B'J^2 - 2B'(J_x p_x + J_y p_y) + F(p_x^2 + p_y^2) + V,$$

where $A=h/8\pi^2 I_a$, $B'=h/8\pi^2 I_{\perp}'$, $F=(h/8\pi^2)(I_{\perp}/I_a I_{\perp}')=A + B'$, $I_{\perp}=I_a + I_{\perp}'$, and I_a and $I_{\perp}$ represent the moments of inertia, respectively, of BH$_4$ (T$_d$ symmetry assumed) and of the entire molecule about the x and y axes that are perpendicular to z, the symmetry axis. The internal-motion potential function V will take a complicated form when the rotations about x and y are considered. Instead three equivalent, mutually perpendicular axes 1, 2, and 3 were employed; the internal angular momenta are given by $p_1 = (1/\sqrt{3})J_z + (2/\sqrt{6})p_x$, $p_2 = (1/\sqrt{3})J_z - (1/\sqrt{6})p_x + (1/\sqrt{2})p_y$, and $p_3 = (1/\sqrt{3})J_z - (1/\sqrt{6})p_x - (1/\sqrt{2})p_y$, and the potential function in zero-th order by $\Sigma_i(V_2/2)(1-\cos 2\alpha_i)$. Each internal-motion state is expressed as $|v_1\sigma_1, v_2\sigma_2, v_3\sigma_3 >$, where v_i denotes the vibrational quantum number in a high-barrier limit and σ_i=0 or 1 depending upon symmetric or antisymmetric with respect to C$_2$ operation of α_i. The fact that one of 1,2, and 3 is dummy is

expressed by the relation $\sigma_i + \sigma_j = \sigma_k$ (mod 1). The coupling term between the overall and internal rotations becomes $- (2/3)F\Sigma_i p_i J_z - 2B'(J_x p_x + J_y p_y)$, which is treated by perturbation. The reesults are in qualitative agreement with the observation.

II-A-17　Spatial Distribution of SiH₃ Radicals in RF Silane Plasma

Naoshi ITABASHI *(Nagoya Univ.)*, Nobuki NISHIWAKI *(Nagoya Univ.)*, Mitsuo MAGANE *(Nagoya Univ.)*, Susumu NAITO *(Nagoya Univ.)*, Toshio GOTO *(Nagoya Univ.)*, Akihisa MATSUDA *(Electrotech. Lab.)*, Chikashi YAMADA, and Eizi HIROTA

Infrared diode laser absorption spectroscopy (IRLAS) was applied to the measurement of SiH₃ in a RF silane P=CVD chamber with parallel plate electrodes. The spatial distribution of SiH₃ radicals between the electrodes was measured to obtain the incident flux density of SiH₃ to the electrode surface. The growth rate of a-Si:H was also measured in the same plasma. These data were used to estimate the contribution of SiH₃ to a-Si:H thin-film growth.

II-A-18　SiH₃ Radical Density in Pulsed Silane Plasma

Naoshi ITABASHI *(Nagoya Univ.)*, Nobuki NISHIWAKI *(Nagoya Univ.)*, Mitsuo MAGANE *(Nagoya Univ.)*, Toshio GOTO *(Nagoya Univ.)*, Akihisa MATSUDA *(Electrotech. Lab.)*, Chikashi YAMADA, and Eizi HIROTA

The SiH₃ radical density in pulsed silane discharge plasma was measured by infrared diode laser absorption spectroscopy [IRLAS] for three buffer gases and also as functions of the sample pressure and the pulse width. They were compared with the SiH and SiH₂ radical densities. The growth rate of a-Si:H thin film was compared with the SiH₃ radical density on various plasma conditions. These data were employed to discuss the contribution of SiH₃ to a-Si:H thin-film growth.

II-A-19　Measurements of the CF Radical in DC Pulsed CF₄/H₂ Discharge Plasma Using Infrared Diode Laser Absorption Spectroscopy

Mitsuo MAGANE *(Nagoya Univ.)*, Naoshi ITABASHI *(Nagoya Univ.)*, Nobuki NISHIWAKI *(Nagoya Univ.)*, Toshio GOTO *(Nagoya Univ.)*, Chikashi YAMADA, and Eizi HIROTA

Infrared diode laser absorption spectroscopy (IRLAS) was established as the measurement method for the CF radical density. The absolute density of the CF radical and its pressure dependences were measured in DC pulsed CF₄/H₂ discharge plasma. Moreover, from the analysis of the decay parts of the observed transient absorption waveforms of the CF radical, the CF radical was shown to be removed mainly by a diffusion process in the present plasma, yielding the diffusion coefficients D(CF in H₂) and D(CF in CF₄).

II—B　Development of New Instruments and New Experimental Methods for High Resolution Spectroscopy

The scope of a research is limited by the techniques and the capabilities of instruments available to a researcher. This is particularly true for spectroscopic investigations of simple molecules, free radicals, and ions, which are main research themes this Department is interested in. The high precision with which we determine molecular parameters often unravels new features of molecular structure which have previously escaped experimental observation. The diversity of molecular systems which we can detect and analyze is often limited by the sensitivity of the spectrometer employed. It is thus imperative for us to steadily improve our research facilities and to develop equipments of radically new conceptual design. The rewards of these efforts will include not only the detailed knowledge of the mole-

cules under investigation, but also contributions to related fields. Various technical problems need to be solved to attain these goals. In this respect the collaboration of the Equipment Development Center is indispensable. New instruments developed in this program promise to open new research area in the field of molecular science.

II-B-1 A Molecular Beam Apparatus for Infrared Diode Laser Spectroscopy

Toshinori SUZUKI and Eizi HIROTA

We have previously constructed a molecular beam apparatus for infrared diode laser spectroscopy[1]. The sensitivity we achieved with this apparatus was not high enough to be applied to detection of transient molecules generated by the photolysis. Therefore, we decided to modify the design completely and set up a new one; Figure 1 shows a schematic diagram of the new apparatus. It is equipped with a supersonic nozzle, a pair of nearly parallel mirrors for efficient infrared absorption, and a quadrupole mass analyzer to monitor photofragments. We have two types of nozzles, one consisting of a piezo element which can be used up to 300 Hz repetition rate and the other being a conventional fuel injector which withstands the cycle up to 20 Hz. The quadrupole mass filter has the resolution of 500. One of the mirrors for multiple reflection of the infrared beam is concave with $R=2000$, whereas the other is flat; they are spaced by about 10 cm, and seven to eight traversals are easily achieved. The main chamber is pumped by a 2000 ℓ mechanical booster pump followed by a 500 ℓ rotary pump; the pressure is about 10^{-7} Torr without molecular beam and increases to 2×10^{-5} Torr when a sample gas of 2 atm stagnation pressure is injected through an 800 μmϕ orifice with a repetition rate of 150 Hz. The quadrupole mass section is pumped separately by two turbo-molecular pumps. We have tested several types of nozzle including slit-type ones, but could not have found any large difference in efficiency.

We have applied the apparatus to SO generated by the 193 nm photolysis of SO_2 diluted with Ar to 10%; the signal-to-noise ratio of about 10 was achieved.

Reference
1) *IMS Ann. Rev.* 1988, II-B-1.
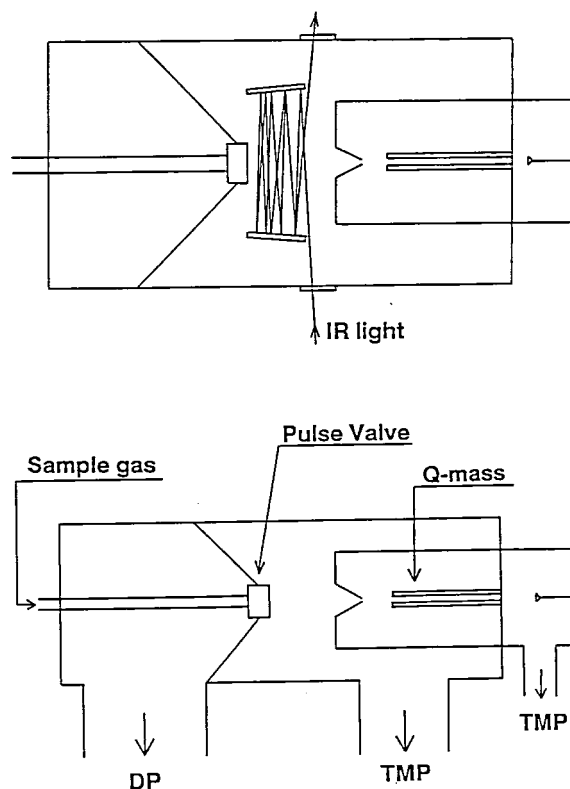
Figure 1. Schematic diagram of a molecular beam apparatus for infrared diode laser spectroscopy.

II—C High Resolution Spectroscopy of Molecules of Fundamental Importance

The need for high quality spectroscopic data has recently been increasing, especially for molecules of fundamental importance. Perhaps such spectroscopic data have been accumulated in the past because of interest in precise molecular structure determination. However, research activities in other related fields such as reaction kinetics, environmental sciences, plasma chemistry and physics, astronomy, and semiconductor technology have recently been

advanced such that precise spectroscopic data are indispensable as a means of monitoring molecules. Spectroscopic data which are available at present are not necessarily good enough and must often be replaced by new data that meet necessary requirements. Such spectroscopic data on chemically stable molecules of fundamental importance will be presented in this section.

II-C-1 Harmonic Potential Contributions to Vibration-Rotation Interactions

Eizi HIROTA

The vibration-rotation interaction parameters are complicated functions of harmonic as well as third-order potential constants; the relations are so much complicated that it is extremely hard to assess even the contributions of the harmonic potential. Only numerical analyses are feasible. However, if there are some constraints on these relations, they must be fully appreciated, and, in many cases, they simplify the relations. The present study points out the fact that the l matrix is proportional to the L matrix employed in the normal coordinate analysis in the sense that the proportionality factor contains only the masses of atoms and the geometry, and therefore the l matrix provides us with only $n(n-1)/2$ pieces of information on the harmonic potential constants, where n denotes the number of the normal coordinates belonging to a symmetry species. For $n=1$, there is no freedom, in other words, l is completely determined by mass and geometry. For $n=2$, we expect to get one piece of information, etc. As an example, a C_{2v} XY_2 type molecule is considered.

There are three normal modes; two of them belong to a_1 and the last to b_2. Therefore, all vibration-rotation interaction parameters are determined by one parameter (except for averages of the normal coordinates, which are given in terms of the normal mode frequencies). As shown in Table I, the coefficients of the moments of inertia expanded in terms of the normal coordinates, a and A, the Coriolis coupling constants, and the centrifugal distortion constants are all expressed by one parameter γ.

Table I. Vibration-Rotation Interaction Parameters for a C_{2v} XY_2 type Molecules

Normal mode	a_1		b_2
	1	2	3
$a_s^{(aa)}$	$2\sqrt{I_{aa}}\,\sin\gamma$	$-2\sqrt{I_{aa}}\,\cos\gamma$	0
$a_s^{(bb)}$	$2\sqrt{I_{bb}}\,\cos\gamma$	$2\sqrt{I_{bb}}\,\sin\gamma$	0
$a_s^{(ab)}$	0	0	$2[I_{aa}I_{bb}/I_{cc}]^{1/2}$

$A_{13}^{(ab)} = [C/A]^{1/2}\cos\gamma,\ A_{13}^{(ba)} = [C/B]^{1/2}\sin\gamma$

$\zeta_{23}^{(c)} = -\sin(\gamma+\gamma_0),\ \zeta_{13}^{(c)} = -\cos(\gamma+\gamma_0)$
$\cos\gamma_0 = (C/A)^{1/2},\ \sin\gamma_0 = (C/B)^{1/2}$

$\tau_{aaaa} = -16\,A^3\,[\sin^2\gamma/\omega_1^2 + \cos^2\gamma/\omega_2^2]$
$\tau_{bbbb} = -16\,B^3\,[\cos^2\gamma/\omega_1^2 + \sin^2\gamma/\omega_2^2]$
$\tau_{aabb} = -16\,[A^3B^3]^{1/2}\,\sin\gamma\cos\gamma\,(1/\omega_1^2 - 1/\omega_2^2)$

II—D Laser Investigation of Autoionizing and Predissociating States of Atoms and Small Molecules

Highly excited electronic states of molecules and atoms play important roles in inelastic collision processes including chemical reactions. In those states of molecules, many dissociation and ionization channels are generally open and strongly compete with each other, so that dominating channels in a particular state tend to differ from state to state. Therefore, 'state-resolved' measurements of dynamical behaviors of those highly excited states are expected to give us a lot of knowledge on the complicated channel competition, which may provide useful information on photochemical reactions. In atoms, on the other hand, doubly excited states are of particular interest because they do not only play an important role in photoionization processes but they also intrinsically involve electron correlation effects, which may lead to cooperative electronic motions. In this study, with the above interest, highly excited states of molecules and atoms are spectroscopically investigated through laser multiphoton and/or multistep excitation methods together with the aid of some theoretical analyses.

43

II-D-1 Predissociation Dynamics of Highly Excited Rydberg States of NO

Asuka FUJII and Norio MORITA

Predissociation dynamics of highly excited Rydberg states of NO molecule has been investigated by multiphoton ionization (MPI) detection of fragment atoms. We applied a two-color double resonance technique to produce the highly excited states of NO. The first laser excited the molecule to the $A^2\Sigma^+(v=1)$ state, and the molecule in the A state was successively pumped to autoionizing ns, np and nf $(n=8-12, v=1)$ Rydberg states by the second laser. Nitrogen atoms resulting from predissociation of the Rydberg states was detected by $(2+1)$ resonant enhanced MPI with the third laser. We used a time-of-flight mass-spectrometer to separate N^+ ions from NO^+ ions.

Production of the excited $N(^2D)$ atom was observed. It proves that the $B^2\Pi$ and/or $L^2\Pi$ states, which dissociate to the $N(^2D) + O(^3P)$ limit, contribute to the predissociation of the Rydberg states as predicted by theoretical calculations. We measured the fragment-yield-spectrum of the N atom by scanning the second pumping laser. A comparison of this spectrum with a two-color MPI spectrum of NO molecule, which was separately observed (monitoring NO^+ ion), shows that a predissociation process dominates the decay of the np Rydberg states while in the ns states the main decay process is autoionization.

II-D-2 R-Matrix Calculation and Charge Density Plots of Doubly Excited $^1S^e$ States of Ca Atom below 7s Threshold

Norio MORITA

Photoionization spectra of the $^1S^e$ states of atomic calcium below the 7s threshold have been calculated by the eigenchannel R-matrix method and the multichannel quantum defect theory. The calculated spectra have been compared with experimental spectra of the 7sns $(9 \leq n \leq 13)$ states observed in our previous study, and it has been found that both spectra agree well with each other. Based on this agreement, charge density plots of the nsns states have also been drawn using the calculated eigenvectors, and they have been compared with those obtained by our previous CI calculation. Both results agree well with each other except in the 7s7s state, in which the most probable e^--Ca^{2+}-e^- structure appears to have a bent form in the result of the R-matrix calculation, while it has a linear form in the result of the CI calculation. A reason for this difference has been discussed, and the validity of the present result has been proved. Considering similar bent forms observed in the 7s7p $^3P^o$, 7s6d $^1D^e$ and 7s7d $^1D^e$ states calculated by CI method, the present result suggests the existence of a collective motion of two excited electrons with nearly keeping a bent e^--Ca^{2+}-e^- structure.

II—E   Laser Cooling of Neutral Atoms

Light does not have its mass but has its own momentum, so that an atom can be accelerated or decelerated when the atom absorbs or emits light. On the other hand, a strong radiation field can modify the internal energy of an atom, so that an atom in an inhomogeneous radiation field is subjected to a force. Using those mechanisms, the translational motion of a neutral atom cannot only be controlled but also be cooled to an extremely low temperature by laser radiation. As an atom is cooled and its temperature goes down to a nanokelvin region, its translational de Broglie wavelength becomes a macroscopic size. At this stage, macroscopic quantum-mechanical collective motions of an atomic assembly can be expected to occur in a very thin gas. Taking a main interest in this point, we have started a study on the laser cooling of neutral atoms. Besides this interest, once neutral atoms are controllable by lasers, there will be many applications in various research fields.

II-E-1 Laser Cooling of Metastable Helium Atom by Using an LNA Laser

Mitsutaka KUMAKURA and Norio MORITA

Laser cooling of helium atomic beam in a meta-

stable state has been tried by using a tunable LNA ($La_{1-x}Nd_xMgAl_{11}O_{19}$) laser, which can generate a wavelength resonant with a transition from a metastable $2s^3S$ state to $2p^3P$ ($\lambda=1.083$ μm). When the atomic beam is subjected to a counter-propagating laser beam, the atom is decelerated through many absorption-fluorescence cycles. The resonant frequency of the atomic transition, which is red-shifted by the Doppler effect, was tuned to the laser frequency by the Zeeman effect. A parabolically varying magnetic field for the Zeeman tuning assures the continuous cooling. The initial atomic beam was produced with a liquid-nitrogen-cooled supersonic nozzle source in order to make the cooling path as short as possible and the magnetic field as low as possible. The metastable state was produced through electron bombardment by an electron gun.

By applying another laser beam which crosses the atomic beam at an angle of 1.5° and excites the $2p^3P \rightarrow 3d^3D$ transition ($\lambda=588$ nm), fluorescence of this transition was monitored to observe a velocity distribution along the beam. This excitation spectrum could be observed when either the cooling laser beam or the magnetic field was absent. On the contrary, when both the cooling beam and the field were applied, the spectrum disappeared. This can be considered a proof of the cooling along the beam, because the atomic beam is expected to diverge significantly when the longitudinal velocity is decelerated enough to be comparable to the transverse velocity.

II—F   Raman Spectroscopy and Its Application

Raman spectroscopy reveals the vibrational spectrum of molecules which is sensitive to geometrical as well as electronic structures. We have applied this technique to study the following projects; 1) a mechanism of oxygen activation by enzymes, 2) an electron- and a proton-transfer mechanism through protein, 3) structure-function relationship of biomolecules, 4) structure of transient species, and 5) solution structure. For (1)-(4), we take advantage of resonance enhancement of Raman intensity by bringing the excitation wavelength into the absorption band. This resonance effect enables us to observe the vibrational spectra of chromophores of large molecules selectively with a small amount of dilute solution. Various kinds of hemeproteins, retinoid proteins, metalloproteins, phytochrome, and their model compounds have been investigated. Currently, we focus our attention to reaction intermediates of bacteriorhodopsin, cytochrome oxidase, peroxidase, and cytochrome P-450. Recently we succeeded in observing the ultraviolet (200-240 nm) excited resonance Raman spectra of proteins in time resolution of 10 ns. In order to determine a molecular structure in transient states with a time resolution of μs to ps, the pump/probe technique with two pulsed lasers are used. Currently photoreduction of ironporphyrins and dynamics of protein higher order structures are pursued with this technique. We also developed an improved method for fluorescence rejection by using a gated diode array detector. The project (5) intends to evaluate relative magnitudes of solvent-solvent and solvent-solute interactions and their properties for various binary mixtures. A Raman difference spectrometer was constructed for this purpose and has been applied to detect a frequency shift upon isotope mixing.

II-F-1   Identification of the Long-Lived L' Species of Bacteriorhodopsin to be the N Intermediate by Raman/Absorption Quasi-simultaneous Measurements

Masashi NAKAGAWA, Akio MAEDA (Kyoto Univ.), Takashi OGURA and Teizo KITAGAWA

A device for measuring quasi-simultaneously the absorption and Raman spectra of bacteriorhodopsin (bR) in the spinning cell was constructed. The quasi-simultaneously observed Raman and absorption spectra demonstrated that the long-lived L' species, which had been pointed out in our previous study to accumulate in the spinning cell during the Raman measurements of alkaline bR, is identical with the N intermediate recently proposed from kinetic experiments [Kouyama et al. Biochemistry 27, 5855 (1988)]. Examinations with 12, 14-dideuterated retinal-containing bR revealed that the L'(N) intermediate has predominantly the $C_{13}=C_{14}$ cis form, and the deuteration shift of the Schiff base C=N

stretching mode established that the L'(N) intermediate has the protonated Schiff base, in agreement with the recent report about the N intermediate by Fodor et al. (*Biochemistry* 27, 7097 (1988)). Therefore, an overall chromophore structure and the strength of hydrogen bond at the Schiff base of the L'(N) intermediate are very close to those of L_{550}. However, L'(N) intermediate exhibited appreciable fluorescence in the wavelength region longer than 620 nm in contrast with L_{550}, suggesting that geometrical arrangements of aromatic residues near the retinal chromophore and thus the protein tertiary structure are different between L'(N) and L_{550}.

II-F-2 Observation of the Fe^{II}-O_2 Stretching Raman Band for Cytochrome Oxidase Compound A at Ambient Temperature

Takashi OGURA, Satoshi TAKAHASHI, Kyoko SHINZAWA-ITOH *(Himeji Inst. Tech.)*, Shinya YOSHIKAWA *(Himeji Inst. Tech.)* and Teizo KITAGAWA

Resonance Raman scattering from an early intermediate in dioxygen reduction at 5°C catalyzed by cytochrome oxidase was observed by using the 'Artificial Cardiovascular System' (Ogura et al., *Biochemistry* 1989, 8022-8027). The absorption spectrum simultaneously observed under resonance Raman measurements indicates that the intermediate is compound A placed under physiological conditions. Upon excitation at 425.0 nm, we observed a Raman band at 569 cm^{-1} for the $^{16}O_2$ derivative which shifted to 540 cm^{-1} for the $^{18}O_2$ derivative. Accordingly, the 569 cm^{-1} band was assigned to the Fe^{II}-O_2 stretching vibration. This provides decisive evidence for Compound A to be the dioxygen-bound form. The magnitude of the ^{18}O isotopic frequency shift as well as the frequency itself are very close to those of oxyhemoglobin, suggesting that the binding geometry of O_2 in Compound A resembles that of oxyhemoglobin.

II-F-3 Observation of the Fe^{4+}=O Stretching Raman Band for Cytochrome Oxidase Compound B at Ambient Temperature

Takashi OGURA, Satoshi TAKAHASHI, Kyoko SHINZAWA-ITOH *(Himeji Inst. Tech.)*, Shinya YOSHIKAWA *(Himeji Inst. Tech.)* and Teizo KITAGAWA

Resonance Raman and visible absorption spectra were simultaneously observed for cytochrome oxidase reaction intermediates at 5°C by using the Artificial Cardiovascular System (Ogura et al. *Biochemistry* 28, 8022-8027 (1989)) and Device for Raman/Absorption Simultaneous Measurements (Ogura and Kitagawa, *Rev. Sci. Instrum.* 59, 1316-1320 (1989)). The Fe^{4+}=O stretching (ν_{FeO}) Raman band was observed at 788 cm^{-1} for compound B for the first time. This band showed the $^{16}O/^{18}O$ isotopic frequency shift ($\Delta\nu_{FeO}$) by 40 cm^{-1}, in agreement with that for horseradish peroxidase compound II (ν_{FeO}=787 cm^{-1} and $\Delta\nu_{FeO}$=34 cm^{-1}). In the time region when the Fe^{II}-O_2 stretching band for compound A and the ν_{FeO} band for compound B were coexistent, a Raman band assignable to the Fe^{3+}-O-O-Cu^{2+} linkage was not recognized.

II-F-4 Alcohol Catalyzed Photoreduction of Iron Porphyrin Complexes Revealed by Resonance Raman and Absorption Spectroscopies

Takashi OGURA, Vlastimil FIDLER, Yukihiro OZAKI *(Kwansei Gakuin Univ.)* and Teizo KITAGAWA

Photoreduction of Fe^{III}(OEP)(2-MeIm) (OEP: Octaethylporphyrine; 2-MeIm: 2-methylimidazole) was found to be catalyzed by a trace amount of MeOH present in CH_2Cl_2 as a stabilizer. Absence of either 2-MeIm or MeOH in the CH_2Cl_2 solution of Fe^{III}(OEP)X (X=Cl$^-$, Br$^-$ or I$^-$) leads to no photoreduction. Presence of MeOH in the Fe^{III}(OEP)(2-MeIm) solution results in appearance of a new absorption band at 585 nm, and when Raman scattering was excited at 590 nm, a new Raman band appeared at 524 cm^{-1}. This band exhibited an upshift by 4 cm^{-1} with ^{54}Fe(OEP)(2-MeIm)(CH$_3$OH) and a downshift by 12 cm^{-1} with ^{56}Fe(OEP)(2-MeIm)(CD$_3$OD) and was therefore assigned to the Fe^{III}-(MeOH) stretching vibration. The excitation profile of this band gave a peak

around 585 nm and accordingly, the new absorption band at 584 nm was assigned to a charge transfer (CT) band from MeOH to the Fe^{III} ion. It was most unexpected that the photoreduction did not occur upon laser illumination within the CT band.

II-F-5 Resonance Raman Study on Oxygen Binding Site of an Allosteric Hemerythrin

Shoji KAMINAKA, Hideo TAKIZAWA *(Tokyo Sci. College)*, Takashi HANDA *(Tokyo Sci. College)*, Hiroshi KIHARA *(Jichi Medical School)* and Teizo KITAGAWA

Resonance Raman spectra were observed for the oxy and azidomet forms of an allosteric hemerythrin (Hr) isolated from *L.unguis* and a nonallosteric Hr from *S.cumanense*. For the allosteric Hr, the O-O stretching frequency of the oxyHr was lower and the symmetric Fe-O-Fe stretching frequency of azidometHr was higher in the high affinity form (high pH form) than in the low affinity form (low pH form), while the $Fe-O_2$ and $Fe-N_3$ stretching frequencies remained unchanged between the two forms. The nonallosteric Hr did not show any pH dependence about those frequencies. Upon the exchange of solvent from H_2O to D_2O, the O-O and $Fe-O_2$ stretching modes were shifted to higher and lower frequencies, respectively, and their sizes were the same between the high- and low-affinity forms and also same as those of the nonallosteric Hr. Possible structural mechanism for the cooperative oxygen binding is discussed.

II-F-6 Solution Structures and Phase Separation in Fluoroalcohol/Water Mixtures; A Study with Raman Difference and ^{13}C NMR Spectroscopy

Yasuhisa MIZUTANI, Keiji KAMOGAWA, Teizo KITAGAWA, Akio SHIMIZU *(Ritsumeikan Univ.)*, Yoshihiro TANIGUCHI *(Ritsumeikan Univ.)* and Koichiro NAKANISHI *(Kyoto Univ.)*

The static and dynamic structures of aqueous solutions of 2- propanol (IPA), 1,1,1-trifluoro-2-propanol (TFIPA), and 1,1,1,3,3,3-hexafluoro-2-propanol (HFIPA) were investigated with Raman difference- and ^{13}C NMR spectroscopies to understand the phase separation in intermediate concentrations of TFIPA solution. Concentration dependences of the frequency shifts of the CH stretching vibrations of the alcohols were analyzed in terms of the homogeneous ($\Delta\nu_{AA}$) and heterogeneous ($\Delta\nu_{AB}$) interaction factors proposed previously. In the IPA/water and HFIPA/water systems, $\Delta\nu_{AA}$ gradually decreased upon dilution by water similar to the cases of other aqueous solutions of water-soluble organic molecules and accordingly, suggested the formation of a micelle-like assembly with alkyl groups inside. In the TFIPA/water system, $\Delta\nu_{AA}$ remained zero until the concentration where phase separation occurs, suggesting its disability to form the micelle-like assembly. In highly dilute aqueous solutions of TFIPA, $\Delta\nu_{AA}$ was positive in contrast with negative values in two other alcohol solutions. The rotational correlation time of TFIPA, which was obtained from the measurements of the spin-lattice relaxation time of ^{13}C and the nuclear Overhauser enhancements, decreased upon dilution by wate until the phase separation. This implied that the hydrogen-bonding partner of the alcoholic OH groups was replaced from TFIPA to water similar to other aqueous alcohol solutions. Consequently, occurrence of phase separation was attributed to very low affinity between the CH_3 and CF_3 groups, which prohibits TFIPA from forming the micelle-like assembly.

II-F-7 A Synthetic Model for Dioxygen Binding Site of Non-heme Iron Proteins: X-ray Structure of Fe(OBz)(MeCN)[HB(3,5-iPr$_2$pz)$_3$] and Resonance Raman Evidence for Reversible Formation of Peroxo Adduct

Nobumasa KITAJIMA *(Tokyo Inst. Tech.)*, Yoshihiko MOROOKA *(Tokyo Inst. Tech.)*, Hideno FUKUI *(Tokyo Inst. Tech.)*, Yasuhisa MIZUTANI, Teizo KITAGAWA

A mononuclear five-coordinate complex Fe(OBz)[HB(3,5- iPr$_2$pz)$_3$] (1) [HB(3,5-iPr$_2$pz)$_3$ = hydrotris(3,5-diisopropyl-1-pyrazolyl) borate; OBz = benzoate] was synthesized as a plausible synthetic analogue for the dioxygen binding site of non-heme iron

proteins. Complex **1** readily forms an adduct with MeCN or pyridine and the molecular structure of the MeCN adduct was determined by x-ray crystallography. Dioxygen binds to **1** reversibly in toluene at $-20°C$ and the resonance Raman spectrum of the adduct located its O-O and $Fe-O_2$ stretching vibrations at 890 and 419 cm^{-1}, respectively, suggesting the μ-peroxo bridged structure. This is consistent with the manometric measurements of O_2 uptake which was 0.5 mole per a mole of **1**.

II-F-8 Resonance Raman Pursuit of the Change from Fe^{II}- O_2 to Fe^{III}-OH via Fe^{IV}=O in Autoxidation of Ferrous Iron-porphyrin

Yasuhisa MIZUTANI, Shinji HASHIMOTO, Yoshiyuki TATSUNO *(Osaka Univ.)* and Teizo KITAGAWA

Resonance Raman (RR) and visible absorption spectra were observed for autoxidation intermediates of ferrous tetramesitylporphyrin [$(TMP)Fe^{II}$] to the ferric hydroxy derivative [$(TMP)Fe^{III}OH$] via $(TMP)Fe^{II}$-O_2, $(TMP)Fe^{III}$-O-O-$Fe^{III}(TMP)$, and $(TMP)Fe^{IV}$=O. The O-O stretching [$\nu(O_2)$] and Fe^{II}-O_2 stretching [$\nu(Fe^{II}$-$O_2)$] Raman bands were simultaneously observed at 1171 and 522 cm^{-1}, respectively for the $(TMP)Fe^{II}$-O_2 in toluene solution at $-100°C$ for the first time. The present data together with the reported IR data for the solution samples indicate a linear inverse correlation between $\nu(O_2)$ and $\nu(Fe^{II}$-$O_2)$ frequencies similar to that between $\nu(CO)$ and $\nu(Fe^{II}$-CO), but the data from heme proteins fall off the line. Upon raising the sample temperature to $-70°C$, formation of $(TMP)Fe^{III}$-O-O-$Fe^{III}(TMP)$ was confirmed by ^1H NMR and its visible absorption spectrum was determined. However the peroxo-bridged dimer was so photolabile that it was decomposed into $(TMP)Fe^{IV}$=O by laser illumination even at $-70°C$ and therefore, no oxygen isotope-sensitive RR band assignable to $(TMP)Fe^{III}$-O-O-$Fe^{III}(TMP)$ was identified. $(TMP)Fe^{IV}$=O was also photolabile and yielded the photoproduct, the same as the case of thermal decomposition, but $(TMP)Fe^{IV}$=O gave the Fe^{IV}=O stretching [$\nu(Fe^{IV}$=O)] Raman band at 843 cm^{-1}, which is in agreement with the value reported for the five coordi-

nate oxoferryl complex. Reduction rate of $(TMP)Fe^{IV}$=O to $(TMP)Fe^{III}$-OH was different between the toluene-h_8 and $-d_8$ solutions, suggesting that it proceeds via hydrogen abstraction from toluene. Presumably, the Fe^{IV}=O bond has a partial radical character, which increases upon electronic excitation, and this is the reason why decomposition of $(TMP)Fe^{IV}$=O is accelerated by laser illumination.

II-F-9 Resonance Raman Study on Mutant Cytochrome P-450 Obtained by Site Directed Mutagenesis

Tsuyoshi EGAWA, Yoshiro IMAI *(Univ. Osaka Prefect.)*, Takashi OGURA, and Teizo KITAGAWA

Resonance Raman spectra were observed for the threonine-301 to serine or valine mutant as well as the wild type of rabbit liver microsomal cytochrome P-450 [laurate (ω-1)- hydroxylase][P-450 (ω-1)], which were prepared through site-directed mutagenesis. The high-spin marker RR bands became similarly stronger for all the P-450s examined in the oxidized form upon addition of laurate, and the RR spectra in the higher frequency region of the oxidized, reduced, and CO-adduct forms did not distinctly differ among the P-450s examined. Nevertheless, the Fe-CO stretching mode (ν_{Fe-CO}) of the CO adduct exhibited upshift for the valine mutant, suggesting positional proximity of Thr-301 to bound CO like Thr-252 of P-450_{cam}, in agreement with the expectation from the sequence analysis. The ν_{Fe-CO} band was shifted to higher frequency upon binding of normal alkyl fatty acids with C_{10} or longer alkyl chain but little affected by binding of shorter fatty acids.

II-F-10 Resonance Raman Spectra of Large Pea Phytochrome at Ambient Temperature: Difference in Chromophore Protonation between Red and Far red-Absorbing Forms

Satoru TOKUTOMI *(NIBB)*, Yasuhisa MIZUTANI, Helen ANNI and Teizo KITAGAWA

Resonance Raman (RR) scattering from large pea phytochrome was observed at ambient temperature for the first time by using a micro-spinning cell and the two color excitation technique. The relative population of the red-absorbing form (P_r), the far red-absorbing form (P_{fr}), and the bleached intermediate (I_{bl}) under laser illumination was estimated from the absorption spectra. The RR spectrum of P_r obtained by the 363.8 nm excitation under the 740.0 nm pumping, exhibited a frequency shift between the H_2O and D_2O solutions, but those of P_{fr} and I_{bl} obtained by the 406.7 nm excitation under the 632.8 nm pumping did not it, indicating distinct difference in their protonation levels, presumably in protonation of ring C.

II-F-11 Resonance Raman Study on Photoreduction of Iron-Porphyrins: A Novel Insight into the Ligand-Aided Process

Vlastimil FIDLER, Takashi OGURA, Sin-ichiro SATO, Katsuhiro AOYAGI *(Fukushima Natl. College Univ.)*, and Teizo KITAGAWA

Photoreduction of Fe(OEP)(OEP: octaethylporphyrin) in organic solvents by visible light was demonstrated to be a ligand-aided process in which simultaneous coordinations of a base such as 2-methylimidazole (2-MeIm) and an aliphatic alcohol to two axial positions of the iron ion were required. Coordination of an alcohol was evidenced from the observation of the Fe-alcohol stretching ($\nu_{Fe-alcohol}$) resonance Raman (RR) band. Since this band exhibited an appreciable frequency shift between ROH and ROD, coordination of the alcohol in a protonated form was suggested. When a primary or secondary alcohol was added to the CH_2Cl_2 solution of Fe^{III}(OEP)Cl, a new absorption band appeared around 560-590 nm and the $\nu_{Fe-alcohol}$ RR band was most intensified at the maximum of the new absorption band. Therefore, the new absorption was assigned to the alcohol to Fe^{III} charge transfer (CT) band. Tertiary alcohol gave neither the new absorption band nor the $\nu_{Fe-alcohol}$ RR band, suggesting no coordination, and photoreduction did not take place. This photoreduction was not apparently recognized in the presence of oxygen. However, flash photolysis experiments demonstrated that the photoreduction occurs irrespective of the presence or absence of oxygen but rapid reoxidation results in apparent no effect.

II-F-12 Unusual CO-Binding Geometry in Abnormal Subunits of Hemoglobin M Boston and Hemoglobin M Saskatoon

Masako NAGAI *(Kanazawa Univ.)*, Yoshimasa YONEYAMA *(Kanazawa Univ.)* and Teizo KITAGAWA

In order to explore a role of proximal (F8) histidine (His), distal (E7) His, and E11 valine (Val), resonance Raman (RR) spectra of carbonmonoxide adduct of hemoglobins (Hbs) M in which one of these residues was genetically replaced to another amino acid in either α or β subunit. In the fully reduced state, all Hbs M exhibited ν_3 frequencies at 1487-1499 cm^{-1} and ν_{Fe-His} frequencies at 214-218 cm^{-1}, indicating that they have a pentacoordinate heme structure and the heme iron is bound to E7 or F8 His. The porphyrin skeletal vibrations of the COHb M were essentially unchanged by replacement of E7- or F8-His with Tyr and of E11-Val with Glu. The ν_{CO}, ν_{Fe-CO} and δ_{Fe-C-O} frequencies of the CO adducts of Hb M Iwate (αF8His → Tyr), Hb M Hyde Park (βF8His → Tyr), and Hb M Milwaukee (βE11Val → Glu) were nearly identical with those of COHb A. However, the RR spectra of CO adducts of Hb M Boston (αE7His → Tyr) and Hb M Saskatoon (βE7His → Tyr) gave two new RR bands derived from the abnormal subunits, this is, ν_{Fe-CO} at 490 cm^{-1} and ν_{CO} at 1972 cm^{-1} in addition to those from the normal subunits at 505 cm^{-1} (ν_{Fe-CO}) and 1952 cm^{-1} (ν_{CO}). The additional CO adduct is distinct from the normal species regarding photodissociability; the 490 cm^{-1} species exhibits apparently no photodissociation upon CW excitation in a stationary cell in which the 505 cm^{-1} species is completely photodissociated. From normal coordinate analysis, the Fe-C-O bond in abnormal subunits in Hb M Boston and Hb M Saskatoon was suggested to be nearly normal to the heme plane.

II-F-13 Resonance Raman Characterization of Ferric- and Ferrylporphyrin π Cation Radicals and the Fe^{IV}=O Stretching Frequency

Shinji HASHIMOTO, Yasuhisa MIZUTANI, Yoshitaka TATSUNO *(Osaka Univ.)* and Teizo KITAGAWA

Resonance Raman (RR) spectra of porphyrin π cation radicals were investigated for the Fe^{III} and Fe^{IV} states by using tetramesitylporphyrinato-iron complexes [(TMP)Fe]. Vibrational modes were assigned on the basis of the isotopic frequency shifts upon ^{15}N and meso-^{13}C substitution and the reported normal coordinate analysis. For both the Fe^{III} and Fe^{IV} porphyrin π cation radicals, the ν_4 band was significantly shifted to lower frequency and thus the previous assignment by Kincaid et al. [*J. Am. Chem. Soc.* **111**, 735 (1989)] should be modified. The RR spectra did not exhibit temperature dependence between $-100°C$ and $+10°C$, and between $-100°C$ and $-80°C$ for the Fe^{III}- and Fe^{IV}-porphyrin π cation radicals, respectively, indicating the presence of one type of radicals, presumably the a_{2u} radical judging from the low frequency shifts of the ν_2 mode. The controversy about the $Fe^{IV}=O$ stretching mode ($\nu_{Fe=O}$) of the $Fe^{IV}=O$ porphyrin π cation radical was clarified by demonstrating that the two $\nu_{Fe=O}$ RR bands appear at 831 and 801 cm^{-1} in the presence of EtOH and n-PrOH while a single band appears at 831 or 801 cm^{-1} in the presence of MeOH or BuOH, respectively. The difference between the $\nu_{Fe=O}$

frequencies in the presence and absence of MeOH was interpreted reasonably in terms of the effect of the fifth ligand.

II-F-14 Systematic Interpretation of Hydration Shifts of the C-H Stretching Vibrations of Organic Liquids upon Mixing with Water: Novel Insight into Hydrophobic Interaction

Keiji KAMOGAWA and Teizo KITAGAWA

Frequency shifts of the C-H stretching vibrations of 1,4-dioxane and dimethylsulfoxide upon mixing with water were observed as a function of concentration by using the dual beam multichannel Raman difference spectrometer developed recently. From the concentration dependence of the frequency shifts, two parameters, $\Delta\nu_{AA}$ and $\Delta\nu_{AB}$, that reflect the magnitude of the A-A and A-B interactions, respectively (A: organic species, B: water), were obtained. Here we propose a new idea for interpreting the concentration dependence of $\Delta\nu_{AA}$ and $\Delta\nu_{AB}$ in terms of the solute shift and rearrangement shift. This idea was found to be able to explain all the $\Delta\nu_{AA}$ and $\Delta\nu_{AB}$ data reported so far consistently except for those of methanol/water mixture.

II—G Structure of Noncrystalline Solids

Amorphous materials often have various interesting and useful properties, which are closely related with their structures. EXAFS (extended x-ray absorption fine structure) is best suited to determine structures of amorphous materials, because it can determine the local structures around a selected element irrespective of the phase. In this laboratory efforts to develop EXAFS spectroscopy have been made as well as EXAFS studies on the structures of amorphous materials, in particular, supported catalysts.

In the past year, fluorescence detection was developed to extend the possibilities of EXAFS spectroscopy. As a result, it is now possible to obtain EXAFS spectra of as low as 5 mM aqueous solution of iron compounds or 1000 Å thick films. In-situ EXAFS studies have been continued in order to reveal the nature of catalysis by structural study.

The following is the abstracts of the manuscripts submitted to several journals in the past year.

II-G-1 An EXAFS and IR Study of CO Adsorption-Induced Morphology Change in Ru Catalysts

Takanori MIZUSHIMA, Kazuyuki TOHJI, Yasuo UDAGAWA, and Akifumi UENO *(Toyohashi Univ. Technology)*

EXAFS(extended x-ray absorption fine structure) and IR studies were performed on Ru catalysts supported on γ-Al_2O_3, MgO, SiO_2, and TiO_2 to elucidate the mechanism of the CO adsorption-induced disruption of metal clusters. EXAFS results show that after

reduction, Ru atoms exist on all the supports as small metal clusters, but the particle sizes and metal-support interactions vary with the support. CO adsorption onto Ru/γ-Al$_2$O$_3$ and Ru/MgO leads to the disruption of Ru-Ru bonds. By comparing with IR spectroscopic observations it is concluded that new species like O-Ru-CO and O- Ru(CO)$_2$ on γ-Al$_2$O$_3$ and O-Ru-CO and (O-Ru)$_2$- CO (n=3-4) on MgO are formed after CO admission. On the other hand, no evidence of disruption of Ru clusters by CO adsorption was obtained in Ru/SiO$_2$ and Ru/TiO$_2$. IR study showed, contrary to previously proposed models, that no H$_2$ evolution takes place during the CO adsorption-induced disruption. A new reaction scheme which is consistent with our observations is presented, which is shown in Figure 1.
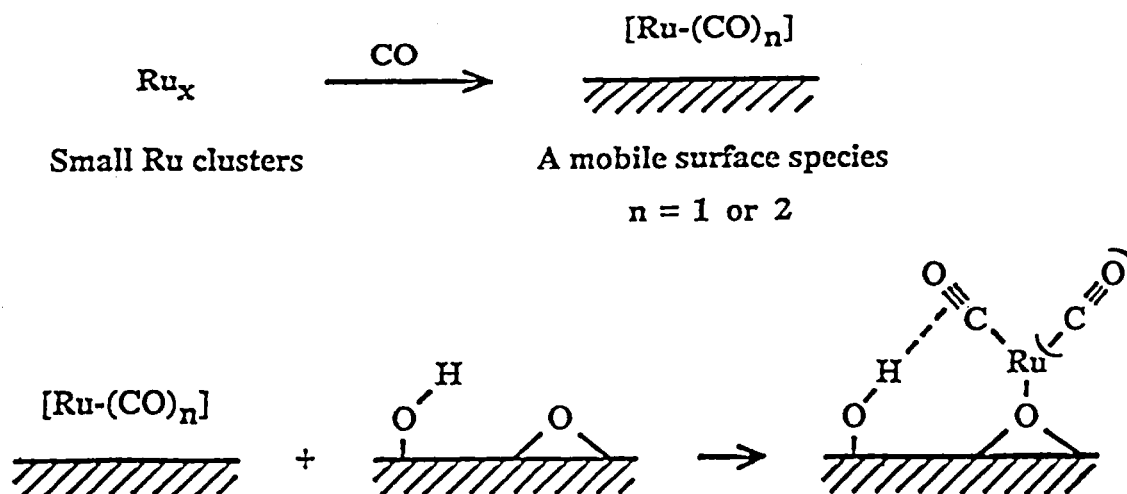
Figure 1. A proposed mechanism of the CO adsorption-induced oxidative disruption of small Ru clusters on γ-Al$_2$O$_3$. The broken line represents a hydrogen bond between CO adsorbed on Ru and surface OH group.

II-G-2 Growth/Restructuring of Pd Clusters Induced by CO Adsorption

Scott L. ANDERSON, Takanori MIZUSHIMA, and Yasuo UDAGAWA

Highly dispersed palladium catalysts supported on alumina and silica were prepared and studied by EXAFS and IR spectroscopy. The Pd-Pd EXAFS oscillations for the freshly reduced catalysts are only about one fourth as strong as those observed for bulk Pd, indicating that the Pd particles in the catalysts are either very small, highly disordered, or both. Exposure to CO at room temperature causes the Pd-Pd EXAFS intensity to increase dramatically, in some cases to nearly the bulk Pd value. This increase is irreversible with respect to CO removal. IR spectra show CO binding only in the expected two- fold bridging and linear sites. The increase was observed on both SiO$_2$ and Al$_2$O$_3$ supports but varied in magnitude with support

and support condition. Exposure to water vapor did not affect the Pd-Pd EXAFS.

Several possible explanations for the EXAFS intensity increases are discussed. The most likely appears to be that CO increases the mobility of Pd atoms over the support, and allows growth of the Pd clusters present after reduction. This result may have implications for the interpretation of the commonly used CO adsorption method for measuring catalyst dispersion.

II-G-3 Laboratory EXAFS by Fluorescence Detection

Kazuyuki TOHJI, Takanori MIZUSHIMA, and Yasuo UDAGAWA

It is demonstrated that a slight modification of a laboratory EXAFS(extended x-ray absorption fine structure) spectrometer for fluorescence detection can

greatly lower the limit of dilution compared with that attainable by the conventional transmission method. It can also extend samples studied to thin films on x-ray opaque substrates.

Basically the system consists of a laboratory EXAFS spectrometer equipped with two NaI scintillation counters combined with filters, and an SSD (solid state detector). Optimum experimental conditions are chosen by monitoring the output of the SSD, and then scintillation counters are used for measurements by making use of the large aperture. The procedures leading to the optimum conditions for Fe EXAFS measurements are described in detail.

The performance of this system was tested by taking 5 and 50 mM aqueous solutions of $Fe(NO_3)_3$ as examples. Then 1000 and 5000 Å thick iron film deposited on glass substrates were examined. Neat and 6 mM solutions of octaethylporphyrin iron (III) chloride (Fe(OEP)Cl) were also studied. A comparison of the extracted EXAFS oscillations, which are shown in Figure 1, clearly shows that the local structure around the central iron atom changes by dissolution.

II-G-4 Enhancement of Fluorescent Intensity of a SiO_2:Sm Glass by Al co-Doping and Local Structure Around Sm by an EXAFS Study

Ryuichi MORIMO*, Takanori MIZUSHIMA, Yasuo UDAGAWA, Hiroaki OKUMURA**, Noriyoshi KAKUTA**, Akifumi UENO**, and Hiroshi NAMIKAWA*** (*Miyakonojo National College of Technology and IMS, **Toyohashi Univ. Technology, ***Nihon Sanso Co.)

Al co-doped SiO_2:Sm phosphors were prepared by the alkoxide method, which starts from a hydrolysis of silicon ethoxide and the metal nitrates at low temperature and minimized the contamination of impurities. An addition of Al ions into SiO_2:Sm is found to increase emission intensity from Sm ion more than an order of magnitude. EXAFS study revealed that local structures around Sm ions in the phosphors with and without dopant is significantly different; in the SiO_2:Sm phosphor Sm atoms are well dispersed at low Sm concentrations and Sm atoms agglomerate at high concentrations, while in the Al co-doped phosphor Sm atoms are coordinated by Al through Sm-O-Al bonding. This provides a direct structural evidence of the role of the co-dopant.

Figure 1. Observed Fe K edge absorption spectra and extracted oscillations of (a) neat and (b) a 6 mM solution of Fe(OEP)Cl.

RESEARCH ACTIVITIES III
Department of Electronic Structure

III—A Photochemical Isomerization of Model Chemical Systems in Clusters and under Isolated Conditions

Due to interesting photochemical properties, availability and stability, stilbene has been a paradigm for *cis-trans* isomerization reactions. *cis*-Stilbene is of particular interest because it can isomerize to form either *trans*-stilbene or dihydrophenanthrene (DHP). Although previous work on the non-radiative decay of S_1 state of *cis*-stilbene only considers the *cis-trans* isomerization channel, we have focused on the photocyclization reaction to DHP by investigating the photophysical properties of *cis*-stilbene homologs which can photocyclize, but cannot *cis-trans* isomerize. The results of this work provide a deeper understanding of the excited state electronic hypersurface on which the two isomerization channels occur. Although stilbenes have been extensively studied, linear olefins are perhaps more appropriate model systems for photobiological processes. We have therefore investigated *all-trans*-2,4,6,8-decatetraene and have observed for the first time the flourescence excitation spectrum of the 2^1A_g state; this will help us to define the electronic surface on which the isomerization occurs. A final example of an important chemical transformation is the Twisted Intramolecular Charge Transfer (TICT) state formation in 4-(N,N-dimethylamino)benzonitrile (DMABN). We investigated the effect of solvation in polar solvent molecule clusters on the charge transfer state formation. A further element in understanding isomerization reactions in solution is the effect of solvent viscosity on large amplitude motion. We have developed a technique for investigating solvent effects on chemical reactions by measuring reaction rates in clusters; we apply the technique to the *cis-trans* isomerization of stilbene.

III-A-1 Non-Radiative Decay of *cis*-Stilbene through Photocyclization to Dihydrophenanthrene

Hrvoje PETEK, Keitaro YOSHIHARA, Yoshihisa FUJIWARA *(Kanazawa Univ.)*, Zhe LIN *(West Virginia Univ.)*, John H. PENN *(West Virginia Univ.)*, and John H. FREDERICK *(Nevada Univ.)*

Photophysical properties of *cis*-stilbene and several homologs (1,2-diphenylcycloalkenes) have been investigated in supersonic expansions as free molecules and in large Ar clusters. Assignment of sharp vibrational structure in the spectra of 1,2-diphenylcyclobutene (DPC-4) to long progressions in phenyl twisting and bending vibrations shows that in the S_1 state *cis*-stilbene phenyl twist angles are more planar and the phenyl ethylene bend angles are more bent than in the S_0 state (Figure 1). The spectra do not show a large change in the ethylene torsional angle, which is associated with the *cis-trans* isomerization coordinate. On the basis of the assignment of the DPC-4 and the similarity between the non-radiative decay of *cis*-stilbene and 1,2-diphenylcyclopentene, a new mechanism is proposed for the decay of S_1 state of *cis*-stilbene through the photocyclization to dihydrophenanthrene (DHP) and *cis-trans* isomerization channels. It is proposed that the initial motion of a wave packet excited to the S_1 surface of *cis*-stilbene is along the reaction coordinate for photocyclization to DHP; repulsive interactions between phenyl rings convert the initial motion into motion along the *cis-trans* isomerization coordinate (See III-A-2).[1]

Reference
1) H. Petek, K. Yoshihara, Y. Fujiwara, Z. Lin, J.H. Penn, J.H. Frederick, *J. Phys. Chem.* **94**, 7539 (1990).
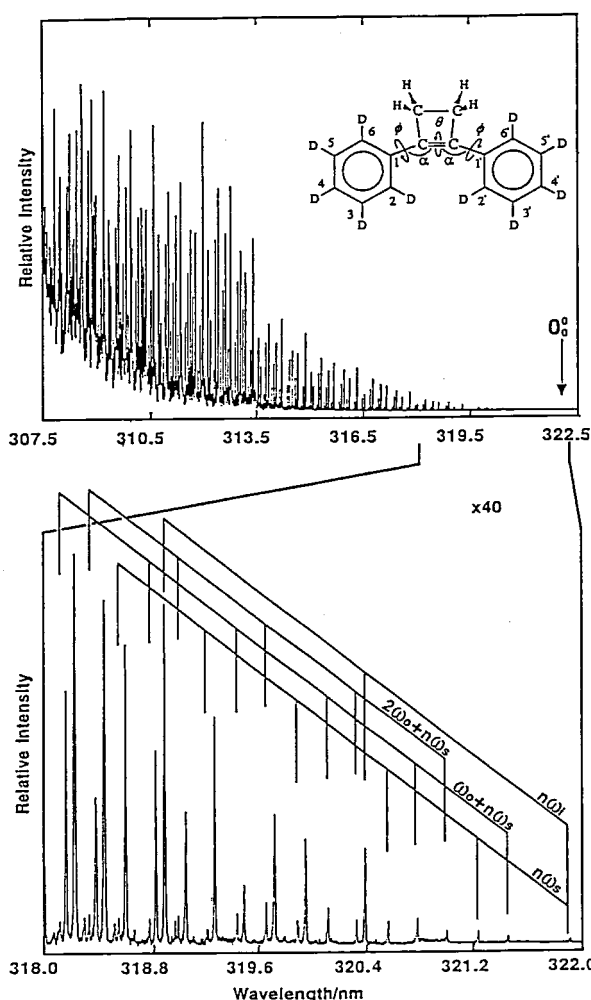
Figure 1. The fluorescence excitation spectrum of 1,2-diphenylcyclobutene d_{10}. Most of the observed transitions can be assigned to fundamentals, overtones, and combination bands of in-plane and out-of-plane phenyl bends (ω_i and ω_o), and the symmetric phenyl twist (ω_s) vibrations.

III-A-2 Modeling of The Phenyl Ring Vibrations in cis-Stilbene and Related Molecules

John H. FREDERICK *(Nevada Univ.)*, **Hrvoje PETEK**, and **Keitaro YOSHIHARA**

[*J. Phys. Chem.*, in press]

For the low frequency modes of large molecules, it is extremely difficult to generate quantitatively accurate potential energy surfaces for the ground electronic state, much less any of the excited states, using *ab initio* or even semi-empirical methods. Most molecular systems of interest have a geometry that is determined by a sensitive balance of steric effects and conjugative effects due to an extended π-electron system. To fashion an empirical potential which reproduces experimentally observed quantities, we will treat these effects as additive, leading to an expression of the form;

$$V = V_{steric} + V_{conj} + V_{other}$$

For example for 1,2-diphenylcyclobutene (DPC-4; see III-A-1), we have $V = V_{HH} + V_{conj} + V_{bend}$, where we use the forms

$$V_{HH} = \Sigma V_{vdW}(r_i);$$

where $V_{vdW}(r_i) = \begin{cases} V_r e^{-\beta r_i} + C/r_i^6 & r_i < 1.1506\text{Å} \\ V' e^{-\beta r_i} & r_i \le 1.1506\text{Å} \end{cases}$

$V_r = 3680$ kcal, $\beta = 3.704$ Å^{-1}, $C = -52.06$ kcal/mol·Å^6, $V' = 555.4$ kcal, $\beta = 2.553$ Å^{-1}, $V_{conj} = V_2 \sin^2\phi + V_4 \sin^2 2\phi$ and $V_{bend} = \frac{1}{2}k_\alpha(\alpha - \alpha_b)^2$ for the individual parts of the potential.

In this potential, V_r, β, and C are the values used in the MM3 force field,[1] while V_2, V_4, k_α, and α_b are adjustable parameters. The values of these parameters are determined so that the resulting surface reproduces the observed vibrational frequencies and the molecular geometry. For DPC-4, a preliminary fit used the values: $V_2 = 1600$ cm^{-1}, $V_4 = 200$ cm^{-1}, $k_\alpha = 99 \times 10^5$ cm^{-1}/rad^2, and $\alpha_b = 140°$ and is shown in Figure 1. Modeling of the DPC-4 spectrum in this manner will help to define the potential for simiulating the phenyl ring dynamics in *cis*-stilbene and related molecules.

Reference
1) N.L. Allinger, Y.H. Yuh, and J.-H. Lii, *J. Am. Chem. Soc.* **111**, 8551 (1989).

Empirical Potential Surface for S_1 State of DPC-4

ϕ (in degrees)
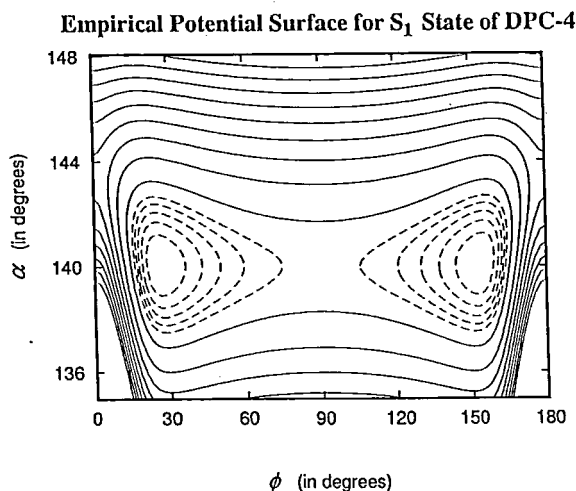
Figure 1. The model potential in phenyl bending (α) and twisting (ϕ) coordinates for modelling the DPC-4 fluorescence excitation spectrum (see III-A-1 Figure 1). The potential is described by the above equations and parameters.

III-A-3 Isomerization of cis-Stilbene in Rare Gas and Organic Solvent Clusters. Direct Measurements of trans-Stilbene Formation Rates on a Picosecond Time Scale

Hrvoje PETEK, Keitaro YOSHIHARA, Yoshihisa FUJIWARA, and Jeremy G. FREY (Southampton Univ.)

Photochemical isomerization of cis-stilbene in Ar, Kr, methanol, ethanol, propanol, iso-propanol, and hexane clusters has been studied by selectively measuring the trans-stilbene formation rate with less than 1 ps time resolution. Previous measurements of the cis-stilbene isomerization rate have been made by observation of the cis-stilbene S_1 state decay. This study was undertaken to determine whether the trans-stilbene formation rate corresponds to the cis-stilbene S_1 state decay rate, and to observe the effect of the environment on the trans-stilbene formation rate. The experimental apparatus for this experiment is described in greater detail in III-E-1. The observed rise times of trans-stilbene in Ar and Kr clusters are biexponential; the results are presented in Table I. The fast component, which is solvent dependent, is tentatively assigned to the solvent friction dependent torsion around the central C = C bond. The slow component, which is solvent independent is ascribed to the decay of the 90° twisted intermediate state. The rise times in organic clusters show a strong dependence on the solvent viscosity. Possibly due to higher temperature in the organic clusters, the production rate can be fit with a single exponential. Quantitative studies of the viscosity effect on the isomerization rate in clusters are proceeding.

Table I. Parameters obtained by fitting trans-stilbene rise times in Ar and Kr clusters to a biexponential production rate.

Excitation wavelength	Solvent	Amplitude (fast)/%	Amplitude (slow)/%	τ_{fast}/ps	τ_{slow}/ps
297.0 nm	Ar	59±5	41±5	1.73±0.28	15.8±0.9
	Kr	60±4	40±4	2.93±0.11	15.2±0.4
302.5 nm	Ar	57±4	43±4	1.79±0.39	16.1±0.8
	Kr	59±6	41±6	3.03±0.37	16.7±0.9

III-A-4 Spectroscopic and Dynamical Study of Decatetraene S_1 and S_2 States in Supersonic Molecular Beams

Hrvoje PETEK, Keitaro YOSHIHARA, and Ronald L. CHRISTENSEN (Bowdoin College)

Fluorescence excitation and emission spectra of all-trans-2,4,6,8-decatetraene have been obtained in free jets and in inert gas clusters. In isolated decatetraene, excitation into 1^1B_u (S_2) results in emission from both S_2 ($1^1B_u{\rightarrow}1^1A_g$) and S_1 ($2^1A_g{\rightarrow}1^1A_g$) on a time scale that is faster than the 10 ns experimental resolution. In clusters, decatetraene only exhibits long-lived (360 ns) emission from thermally relaxed levels of S_1. Direct excitation of low lying, S_1 vibronic levels in isolated molecules also results in long-lived $S_1{\rightarrow}S_0$ fluorescence, as expected for this symmetry-forbidden transition. The $2^1A_g{\leftarrow}1^1A_g$ fluorescence excitation spectrum of free decateraene is shown in Figure 1. Analysis of this spectrum suggests that the $S_1{\leftarrow}S_0$ transition not only is made allowed by vibronic coupling involving low frequency (b_u) polyene skeletal vibrational modes (Herzberg-Teller coupling), as seen for other polyenes in condensed phase, but also gains intensity by interactions between the electronic motion and the hindered rotations (torsions) of the terminal methyl groups. Preliminary analysis suggests that the barriers to internal rotation of the methyl groups must be substantially reduced in the 2^1A_g (S_1) state. The emission lifetimes and intensity in the LIF spectrum of the S_1 state decrease with increasing vibrational energy above origin suggesting that a non-radiative decay channel, such as cis-trans isomerization, is present at low excess energies. The role of low frequency, non-totally symmetric modes in accelerating the non-radiative decay is suggested. The extension of such studies to other intermediate length polyenes is essential for understanding the structure and dynamics of polyenes in photobiological systems.

Decatetraene S₁←S₀Fluorescence Excitation Spectrum
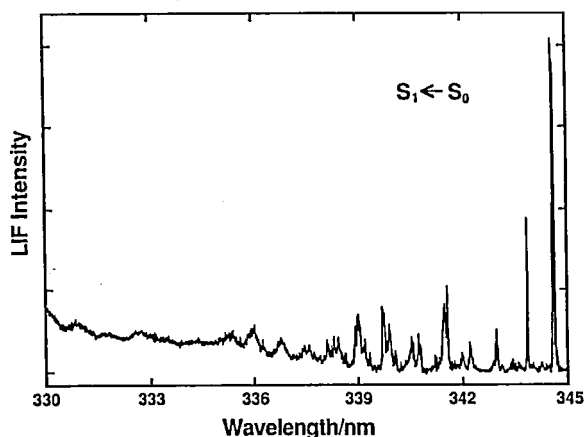
Figure 1. The $2^1A_g \leftarrow 1^1A_g$ fluoresence excitation spectrum of *all-trans*-2,4,6,8-decatetraene in a free jet expansion.

III-A-5 Twisted Intramolecular Charge Transfer (TICT) State Formation in 4-*(N,N*-dimethylamino)benzonitrile Solvated in CCl₃H and CCl₂H₂ Clusters

Hrvoje PETEK, Keitaro YOSHIHARA, Rachel HOWELL *(Imperial College)*, and David PHILLIPS *(Imperial College)*

4-(N,N-Dimethylamino)benzonitrile (DMABN) and related molecules have a dual emission in polar solvents. The most widely accepted explanation for this phenomenon is that in polar solvents a low lying charge transfer state is stabilized and can be populated by non-radiative decay of the locally excited S_1 state. The energy ordering of the locally excited and TICT states is strongly dependent on the solvent polarity and the degree of solvation. Therefore it is expected that the charge transfer state formation can be induced by solvation of DMABN in polar solvent molecule clusters.

We have investigated DMABN in clusters of both polar and non-polar molecules formed by supersonic expansion of the solvent-solute-He mixture. Surprisingly, dual emission is observed in both polar and non-polar clusters, however the anomalous emission in most cases is not associated with the TICT state formation. Concentration dependence studies show that in most cases the anomalous emission has a superlinear dependence on the DMABN concentration, suggesting that the spectra are due to formation of excimers in aggregates of DMABN. By contrast, for CCl₃H, and CCl₂H₂, but not CCl₄, the anomalous emission has a larger red shift than the excimer emission, and it is linear with DMABN concentration, therefore we assign it to the TICT state. It is surprising that in polar solvents such as CH₃OH, acetone, and CH₃CN, for which TICT emission is observed in solution phase, show only excimer emission in clusters.
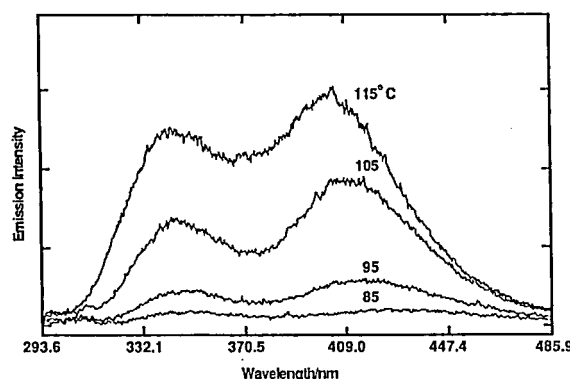
Figure 1. Emission spectra from DMABN:CCl₃H clusters as a function of supersonic nozzle temperature (DMABN concentration). The high energy maximum is due to the locally excited state, and the red-shifted maximum is due to the TICT state emission. The ratio of two emissions does not change with DMABN concentration, precluding that the red-shifted emission is from DMABN aggregates.

III—B   Excited State Dynamics and Photochemistry of Dyes at Various Environmental Conditions

In the past few years we have been studying picosecond dynamics of dyes at various environmental conditions, especially adsorbed on substrates like organic single crystals, inorganic semiconductors, silver bromides, and glasses. By controlling substrate materials, surface qualities, and dye coverage, we can observe surface energy transfer and electron transfer between dye and substrate. We pointed out that the system with fixed donor-acceptor with diffusionless semi-rigid character may serve as a model for biological electron transfer. In this issue we firstly report on the spectral sensitization in photography on the basis of electron transfer from J-aggregates of cyanine dye to AgBr single crystals.

We were able to separate the rate of sensitization (electron transfer to AgBr) from that of other processes (radiative and non-radiative deactivation) as a function of the degree of aggregation. Secondly, we describe a novel "transient isoemissive point" observed with a cyanine J-aggregate on silica gel, namely the non-exponential fluorescence decays intersect in a well defined point with temperature dependent experiment. Thirdly, we report that a triphenyl methane dye, malachite green, serves as highly sensitive environmental probe of free-volume in the adsorbed state and in solid matrix. Fourthly, we report entropy driven dimerization of xanthene dyes in non-polar solvent and equilibrium between monomer and two kinds of dimers with different solvents. All of the above studies were performed by time-resolved fluorescence (TRF) method. Recently we have introduced time-resolved surface second harmonic generation (TRSSHG) as a truly surface specific optical method. TRSSHG permits studies of the reaction dynamics in adsorbates with picosecond time resolution. We report for the first time preliminary observation of monolayer photo-reactions at the solid-liquid intereface with picosecond time resolution. We finally described photochemistry of rhodamine 6G on quartz in air upon laser excitation studied by SSHG.

III-B-1   Picosecond Kinetics of Light-Induced Electron Transfer from a J-Aggregated Cyanine Dye to AgBr Microcrystal as a Function of Aggregate Size

Tadaaki TANI (Fuji Photo Film Co.), Takeshi SUZUMOTO (Fuji Photo Film Co.), Klaus KEMNITZ, and Keitaro YOSHIHARA

The energy gap dependence of the quantum efficiency [$\phi_r = k_s/(k_s+k_L)$] of light-induced electron transfer from J-aggregates of 5,5'-dichloro-9-ethyl-thiacarbocyanine (Dye 1) and related dyes to octahedral AgBr microcrystals obeyed the Marcus theory with a small rearrangement energy λ. The size of J-aggregates of Dye 1 on the microcrystals was increased by increasing agitation temperature. The size dependence of the picosecond kinetics of the electron transfer was studied by use of a time-correlated single photon counting system. For a J-aggregate consisting of about 5 molecules, ϕ_r, the rate constant of the electron transfer process, k_s and of the competing deactivation channels, k_L, were 0.62, 2.6 $\times$ 10^{10} s^{-1} and 1.5 $\times$ 10^{10} s^{-1} respectively. For a J-aggregate consisting of about 15 molecules, ϕ_r, k_s and k_L were obtained as 0.08, 1.5 $\times$ 10^{10} s^{-1} and 17.6 $\times$ 10^{10} s^{-1}. It is thought that proportionality of the rate constant of radiative decay, k_r, to aggregate size made a large contribution to the increase in k_L and to the decrease in ϕ_r, when the aggregate size is increased as shown in Figure 1. The obtained results support the mechanism of aggregate-partitioning supersensitization.
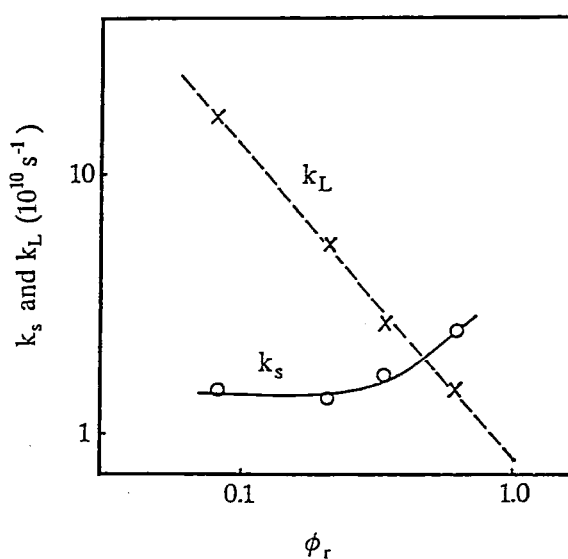
Figure 1.   Change of k_s [O] and k_L [X] with change in ϕ_r of the J-aggregates of Dye 1 formed on octahedral AgBr microcrystals in emulsions, which were digested for 20 min at 40, 50, 60, and 70°C.

III-B-2   Transient Isoemissive Point Observed in the Temperature-Dependent Fluorescence Decays of J-Aggregates Adsorbed on Silica Gel

Klaus KEMNITZ, Keitaro YOSHIHARA, and Tadaaki TANI (Fuji Photo Film Co.)

The fluorescence decay of cyanine J-aggregates adsorbed on silica gel and other inert substrates is nonexponential, with typically 90% contribution of 25 ps decay,[1] when excited near the maximum of the J-aggregate absorption band. The fluorescence decays are independent of excitation and emission wavelength but strongly dependent on temperature, with the lifetime of the fast component increasing to 120 ps at 25 K. Below that temperature the fluorescence decay is independent of temperature down to 4 K.[1] The preexponential factors in a three-exponential analysis are almost independent of temperature. When excited at the high energy side of the absorption maximum, however, the fluorescence decays become dependent on excitation and emission wavelength and the decays acquired at various temperatures display a unique "transient isoemissive point" (Figure 1(a)). The integrated fluorescence decay curves are strikingly independent of temperature in contrast to the fluorescence decay itself, which displays a pronounced temperature dependence. Excitation at the maximum yields standard fluorescence decay behaviour with a steady slowdown at lower temperatures. (Figure 1 (b)).

Reference

1) K. Kemnitz, K. Yoshihara, T. Tani, *J. Phys. Chem.*, **24** 3099 (1990).
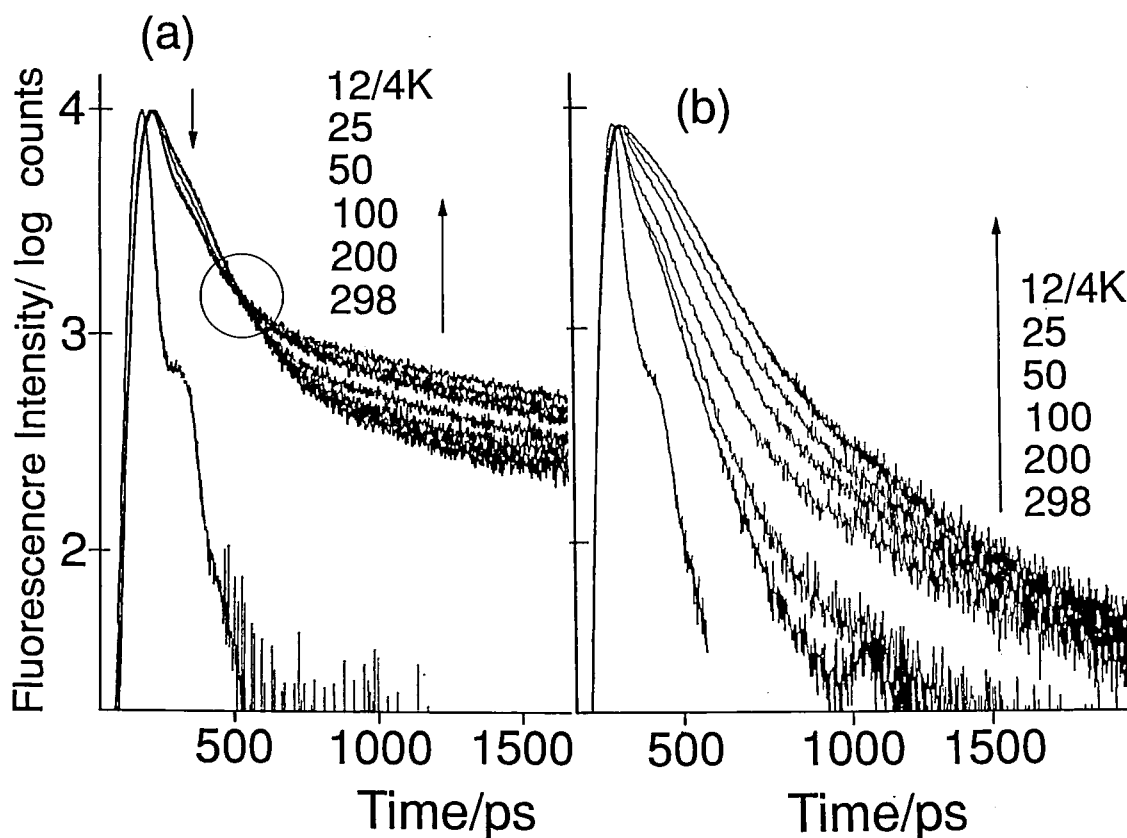
Figure 1. Fluorescence decays in the temperature range 290-4K. (a) Excitation in the monomer region at 575 nm, the circle indicates the "transient isoemissive point". (b) Excitation near the J-aggregate maximum at 620 nm. Emission is observed at 638 nm.

III-B-3 Malachite Green as a Sensitive Free-Volume Probe

Klaus KEMNITZ and Keitaro YOSHIHARA

Free-volume in polymer matrix and at interfaces, allowing the rotation of dissolved or adsorbed organic molecules, or of molecular constituents, is of considerable interest for the characterization of surfaces and for the construction of engineered molecular assemblies. Among the few free-volume probes known at present are N,N-dimethylaminobenzonitrile and its derivatives, which are able to monitor free-volume in polymer matrix[1] and in the adsorbed state,[2] by formation of the twisted intermolecular charge-transfer state. Xanthene dyes like rhodamine B can serve as probes for free-volume at distorted adsorption sites.[3] Malachite green acts as a highly sensitive free-volume probe due to the delicate dependence of its mechanism of internal conversion on the environment. A strong contrast is observed between the temperature dependence of the fluorescence decays in the adsorbed state and in solid matrix as shown in Figure 1.

References

1) K.A. Al-Hassan and W. Rettig, *Chem. Phys. Lett.* **126** 273 (1986).
2) A. Levy, K., Avnir, and M. Ottolenghi, *Chem. Phys. Lett.*, **121** 233 (1985).
3) K. Kemnitz, N. Tamai, I. Yamazaki, N. Nakashima, and K. Yoshihara, *J. Phys. Chem.*, **91**, 1423 (1987).
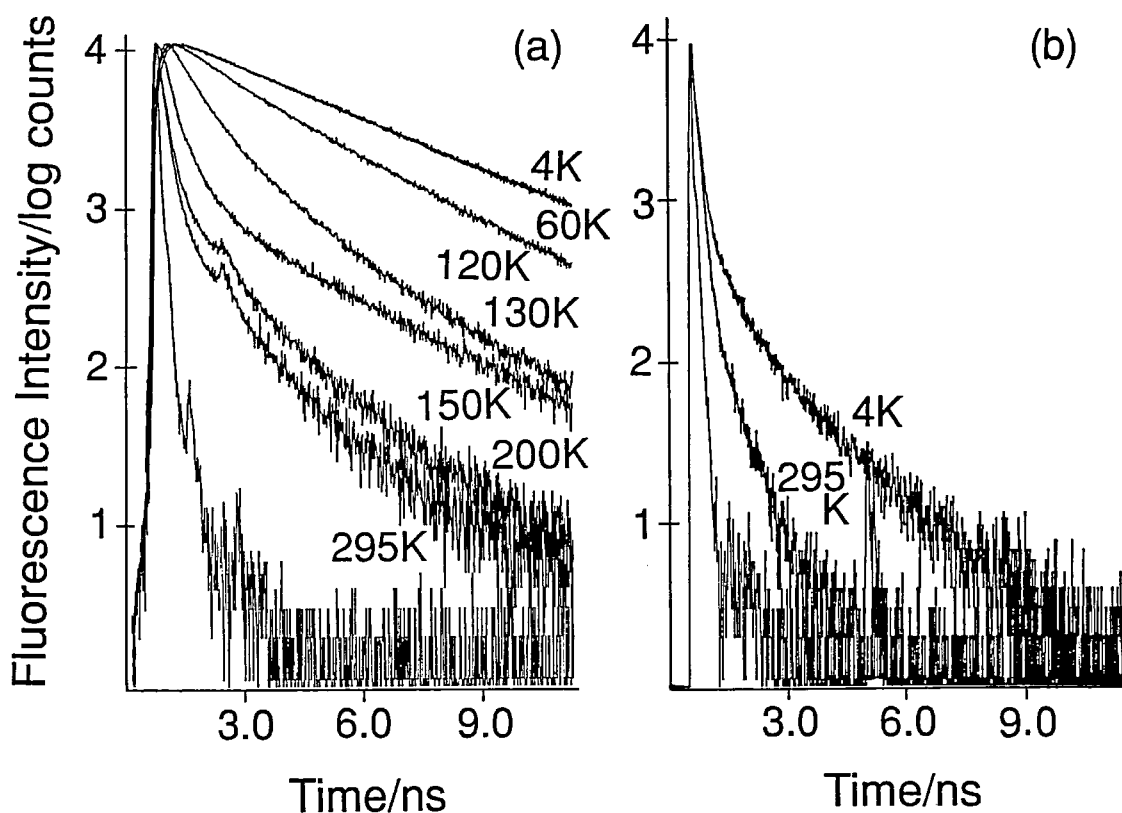
Figure 1. (a) Temperature dependent fluorescence decay of 1×10^{-6} M Malanchite green in EPA; (b) of 1/10th monolayer adsorbed on quartz, acquired by time-correlated single photon counting technique.

III-B-4　Entropy-Driven Dimerization of Xanthene Dyes in Nonpolar Solution and Temperature-Dependent Fluorescence Decay of Dimers

Klaus KEMNITZ and Keitaro YOSHIHARA

Entropy-driven dimerization has been observed in the systems of rhodamine 3B, rhodamine 6G, and pyronine B in toluene, 1-chloronaphthalene, and phenanthrene in the temperature range 22-230°C. The equilibrium constant of dimerization increases with temperature and can be as high as 1×10^8 M^{-1} at 230°C. The dimer fluorescence lifetimes display activated behaviour with $E_a \approx 2000$ cm^{-1} and decrease from about 4 ns at room temperature to 100 ps at 230°C. Kinetically detected, strongly fluorescent dimers of oblique geometry (J-dimers) of rhodamine 6G chloride are found to be in equilibrium with spectroscopically detected, nonfluorescent dimers of sandwich-type structure (H-dimers). A strong dependence of dimerization on the counter anion has been observed in rhodamine 6G solutions, where the chloride exhibits a larger equilibrium constant compared to the perchlorate, typical examples being shown in Figure 1. The lifetimes of the dimer fluorescence in the latter systems are considerably longer and only weakly dependent on temperature.
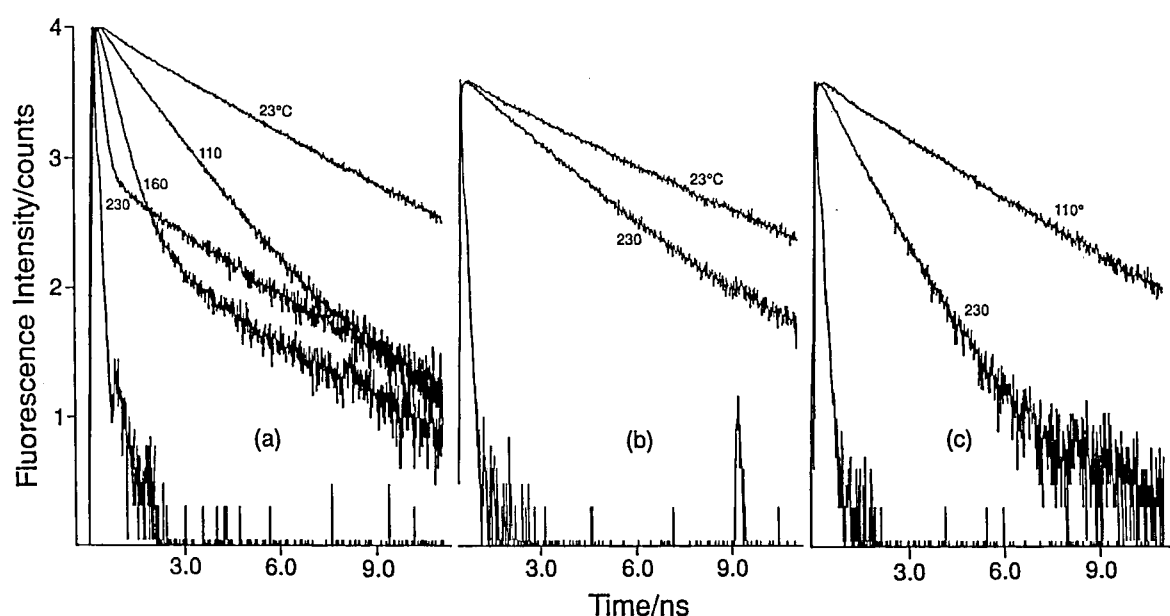
Figure 1. Effect of counter anion (a,b) and solvent (b,c) on fast fluorescent component of 1×10^{-5} M Rh6G. Chloride (a) and perchlorate (b) in chloronaphthalene, and perchlorate in phenanthrene (c) ($\lambda_{ex} = 560$ nm, λ_{em} 590 nm).

III-B-5　Picosecond Dynamics at the Solid-Liquid Interface: A Total Internal Reflection Time Resolved Surface Second Harmonic Generation Study

Stephen R. MEECH and Keitaro YOSHIHARA

[*Chem. Phys. Lett.,* in press]

We report preliminary observations of monolayer photoreactions at the solid-liquid interface with picosecond time resolution. The technique exploits the time resolved surface second harmonic generation (SSHG) method in a total internal reflection (TIR) geometry as shown in Figure 1 (a). The SSHG signal is now widely employed as a probe of surface chemistry, because SHG is forbidden in bulk media, so the signal is surface specific. A wide variety of surface and interfacial processes have been studied. Quite recently the ultrafast response of SSHG has led to its being employed as a probe of picosecond surface reaction kinetics. Malachite green photoisomerisation and rhodamine film photophysics were studied. The fast transient observed for malachite green (MG) films, as shown in Figure 1 (b), implies a heterogeneous surface layer, possibly

consisting of rhodamine dimers.
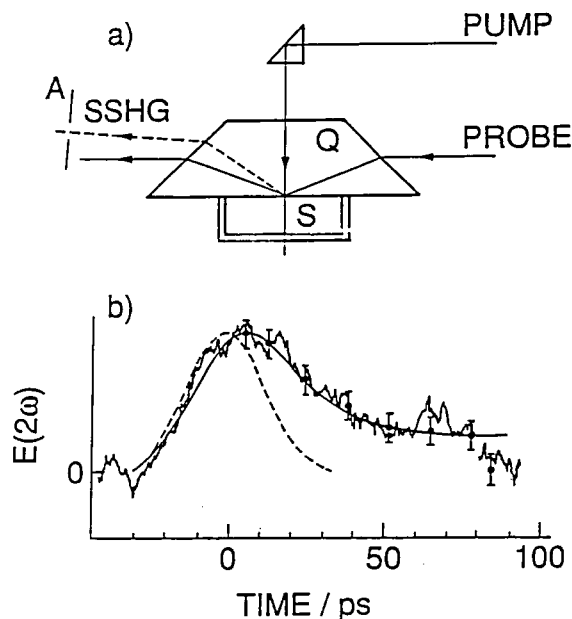
Figure 1. (a): Experimental geometry. Q, quartz dove prism, S, sample cell. The pump pulse is normally incident on the surface, to eliminate pump induced SSHG and minimize multiple reflections. The probe pulse is diffracted onto the surface at 70° to the surface normal, and is totally internally reflected. Time delay between pump and probe was determined by a variable optical delay line (not shown) under computer control. The probe generated SSHG signal was spatially filtered from the fundamental and traversed a polarisation analyser and UV bandpass filters before entering the monochromater. (b): Ground state recovery dynamics of MG adsorbed from a saturated solution of MG in diethylether. $E(2\omega)$ is plotted as a function of pump-probe delay time, t. Error bars represent the fitted curves of three measurements peak normalized. Also shown is the autocorrelation of pump and probe recorded with the dove prism removed. Simulation curve with a 40 ps component and a 3800 ps one with a 0.1 contribution. When the pump pulse was blocked at 80 ps the signal returned to the value at t < 0.

III-B-6 The Photoreaction of a Rhodamine 6G Monolayer Adsorbed on Quartz Studied by Surface Second Harmonic Generation

Stephen R. MEECH, and Keitaro YOSHIHARA

A monolayer of rhodamine 6G (R6G) on quartz in air exhibited photochemistry upon laser irradiation in the first absorption band. The course of the reaction was followed in real time by the surface second harmonic generation method. It was observed that the photoproduct had an enhanced nonlinear coefficient,

relative to R6G as shown in Figure 1. Absorption spectra showed that this was not a result of a stronger resonance enhancement of the signal by the photoproduct. Consideration of the factors to which the surface second harmonic signal is sensitive suggested that the enhancement arose from an increased charge transfer character of the photoproduct's electronic transitions, and a reorientation of its transition dipole.
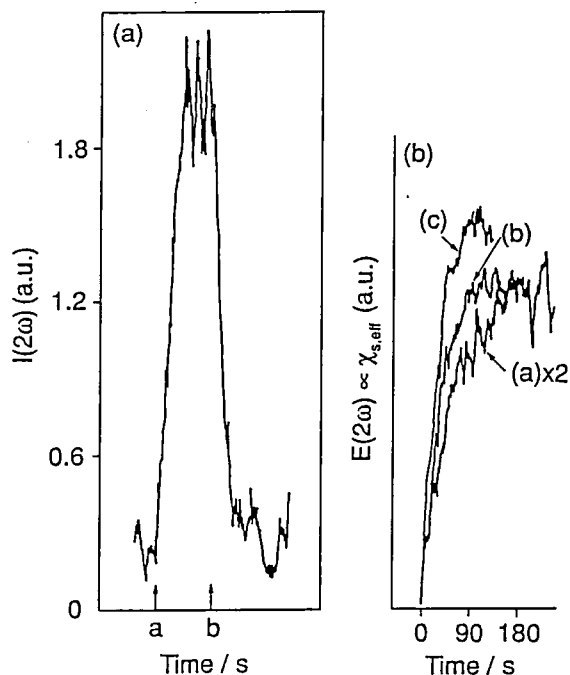
Figure 1. (a): The SSHG intensity of R6G monolayer on a rotating quartz disc is shown on the left. At point 'a' the rotation was halted and $I(2\omega)$ increased to reach a constant level. When rotation was restarted (point 'b') the signal decreased to that of R6G again. Irradiation was at 532 nm. (b): The time profile of the reaction was observed by recording $E(2\omega)=(2\omega)^{1/2} \propto \chi^{(2)}_{s,eff}$ as a function of time for different irradiation intensities. The laser was operating at 532 nm with a 3Hz repetition rate. (a) Laser intensity 35 mJ/cm^2, (b) 70 mJ/cm^2. (c) 140 mJ/cm^2. Ten shots were averaged. The mark on the vertical axis indicates the intensity due to an unirradiated R6G monolayer.

III—C Development and Applications of Femtosecond Time Resolved Coherent Raman Spectroscopy

Recent development in laser technology enables us to obtain coherent light pulses with pulse widths of less than 100 fs. The time scale correspond to a period of molecular vibration (100 fs=333 cm^{-1}, for example) and therefore this is an ultimate time scale for the study of vibrational relaxation. We have constructed a femtosecond laser system and a time resolved coherent Raman detection system. The overall time resolution is so far faster than 100 fs. This system has been used to study vibrational relaxation and rotational dynamics of various molecules in liquids and solutions, and their environmental (solvent, biological systems, etc.) dependence. Polarization experiments are sometimes very important in analysing the time resolved coherent scattering from rotating molecules (including intramolecular rotation). Therefore we have been performing polarized scattering experiments when necessary using arbitrarily tilted linearly polarized radiation.

III-C-1 Femtosecond Time-Resolved Coherent Anti-Stokes Raman Scattering from β-carotene in Solution

Hiromi OKAMOTO and Keitaro YOSHIHARA

Time-resolved pre-resonance coherent anti-Strokes Raman scattering (CARS) from β-carotene has been measured in various solvents. β-carotene has two very strong Raman bands in the fundamental region, i.e. ~ 1520 cm^{-1} (C=C stretching) and ~ 1150 cm^{-1} (C-C stretching). Single exponential decay curve is obtained, for which time constant corresponds to $T_2/2$ of the C=C stretching vibrational state, when the frequency of the Stokes radiation is turned to excite the 1520 cm^{-1} band. $T_2/2$ ws found to be ~ 0.28 ps in benzene solution, ~ 0.29 ps in carbon tetrachloride, ~ 0.30 ps in cyclohexane and ~ 0.30 ps in cyclohexane/acetone mixture (~ 1:1 v/v). This very little solvent dependence on T_2 suggests that the relaxation processes are determined mainly by intramolecular processes.

Figure 1 shows time-resolved CARS from β-carotene in carbon tetrachloride, tuning the Stokes frequency to excite ~ 1300 cm^{-1} which is in between the two Raman bands. The pump (and the probe) pulse duration is so short (~ 75 fs: therefore the pulse spectrum is so broad) that the two vibrational levels are excited coherently. The oscillating structure (11 THz = 370 cm^{-1}) observed in Figure 1 is attributed to the resulting beat of the two Raman transitions.
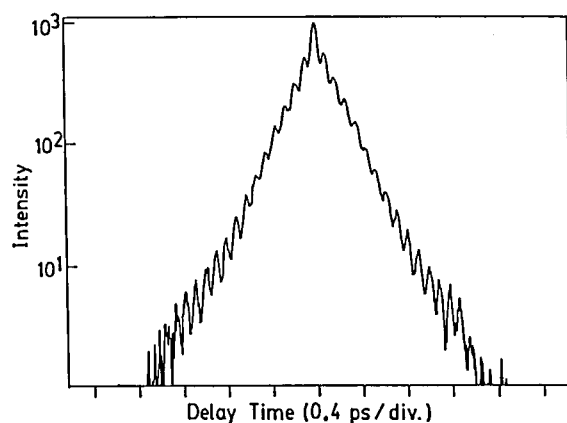
Figure 1. Anti-Stokes intensity of β-carotene CCl_4 solution (~ 10^{-3} M) as a function of delay time, the Stokes frequency is tuned to excite ~ 1300 cm^{-1}.

III-C-2 *In Vivo* Observation of Femtosecond Time-Resolved Coherent Anti-Stokes Raman Scattering from Carotenoids in Biomembrane

Hiromi OKAMOTO, Hidenori HAYASHI *(Univ. of Tokyo)*, Keitaro YOSHIHARA and Mitsuo TASUMI *(Univ. of Tokyo)*

Time-resolved coherent anti-Stokes Raman scattering (CARS) has been applied to an *in vivo* biological sample. Cell membranes of photosynthetic bacteria suspended in water (particle size ~ 50 nm), which contain carotenoids spirilloxanthin and rhodopin, were used as the sample. This sample contains bacteriochlorophylls as well. However, the contribution from the bacteriochlorophylls to the Raman intensity is negligible compared with that from the carotenoids if we

use an excitation light around 600 nm.

Figure 1 (a) is obtained when the Stokes radiation is tuned to excite the middle of the C=C and C-C stretching vibrational Raman bands (~ 1300 cm^{-1}). The oscillating structure (~ 11 THz) is due to the beating of the two Raman frequencies. Figure 1 (b) is obtained when the Stokes frequency is turned to exicite the C=C stretching band (~ 1520 cm^{-1}). The signal decays exponentially ($T_2/2 \sim 0.21$ ps) with a weak oscillating structure (possibly due to nearby weak vibrational bands). The decay is faster than that of β-carotene in solution (~ 0.3 ps) but not much different, suggesting that the relaxation process is predominantly controlled by an intramolecular process.
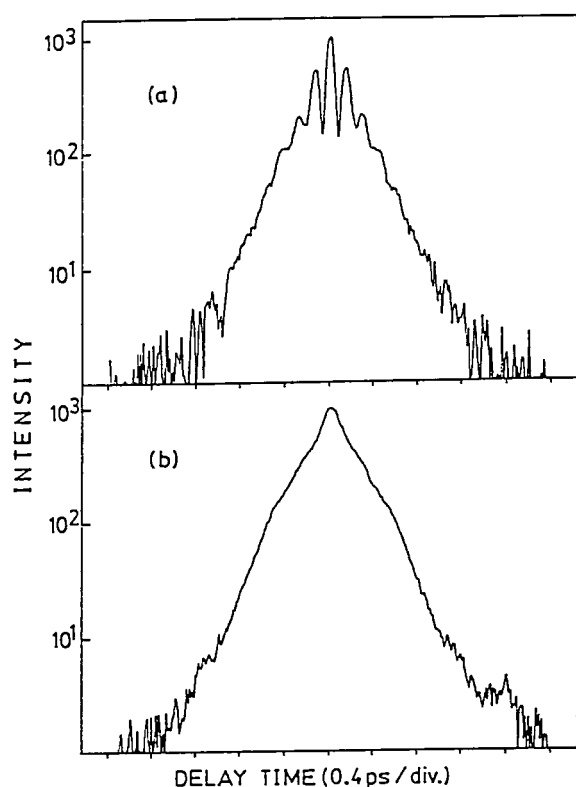
Figure 1. Time-resolved CARS from carotenoids in cell membrane of photosynthetic bacteria. Stokes frequency is tuned to of photosynthetic bacteria. Stokes frequency is tuned to (a) ~ 1300 cm^{-1}, (b) ~ 1520 cm^{-1}.

III-C-3 Observation of Femtosecond Time-Resolved Coherent Anti-Stokes Raman Scattering (CARS). Bi-Exponential Vibrational Dephasing in Acetonitrile.

Ryoji INABA *(Univ. of Tokyo and IMS)*, **Hiromi OKAMOTO, Keitaro YOSHIHARA** and **Mitsuo TASUMI** *(Univ. of Tokyo)*

In the absence of any electronic resonance, two kinds of relaxation, *i.e.* vibrational dephasing and rotational diffusion, contribute to time-resolved CARS. The effects of the vibrational dephasing are completely separated from those of the molecular rotational dynamics if the polarizations of the incident radiations are chosen properly. Figure 1 shows the anti-Stokes intensities of ν_2 (totally symmetric CN stretching mode, 2252 cm^{-1}) of neat acetonitrile as a function of the delay time between pump and probe pulses. The polarizations are so chosen that the rotational part does not contribute to the signal. The signal shows a bi-exponential decay. The faster component decays in ~ 1 ps and the slower decays in a few picoseconds. The faster component decays more rapidly when H_2O is added to acetonitrile. The signal decay tends to be faster, as the polarity of the added solvent is stronger.

For totally symmetric viberations of symmetric top molecules, rotational relaxation can be observed if another polarization condition is adopted. Studies are now under way to clarify the origin of each exponential decay component of vibrational dephasing, and to observe the rotational motion of acetonitrile in liquid-state.
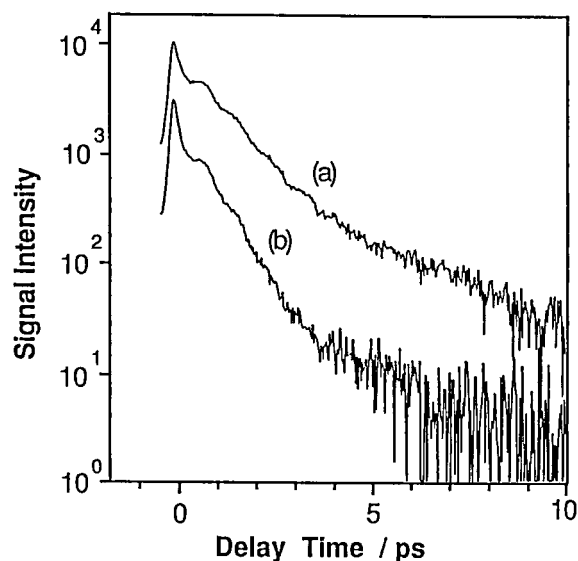
Figure 1. Anti-Stokes signals obtained for the 2252 cm^{-1} Raman transition of (a) neat acetonitrile and (b) acteonitrile/ H_2O mixture ($\sim 3:1$ v/v). The polarization of the incident radiations are so chosen that the rotational part does not contribute to the signal.

III-C-4 Theoretical Study of Polarized Time-Resolved Resonance Coherent Anti-Stokes Raman Scattering

Hiromi OKAMOTO and Keitaro YOSHIHARA

Effects of transition dipole rotation on polarized time-resolved resonance coherent anti-Stokes Raman scattering (polarized TRRCARS) is theoretically investigated. Model calculations are performed on a hypothetical system, in which the transition dipole rotates in the electronically excited state but does not rotate in the ground electronic state. We consider such a system as a model for intramolecular rearrangements (*ex.* cis-trans isomerization), intramolecular charge transfer, etc., in the electronically excited state. Figure 1 shows the calculated TRRCARS intensities as a function of delay time under various polarization conditions. This figure demonstrates that the TRRCARS profiles greatly depend on the polarization conditions if the dipole rotation is fast. Therefore, polarized TRRCARS may be used as a direct time-domain probe for initial processes of ultrafast molecular rearrangement dynamics, charge transfer, etc.
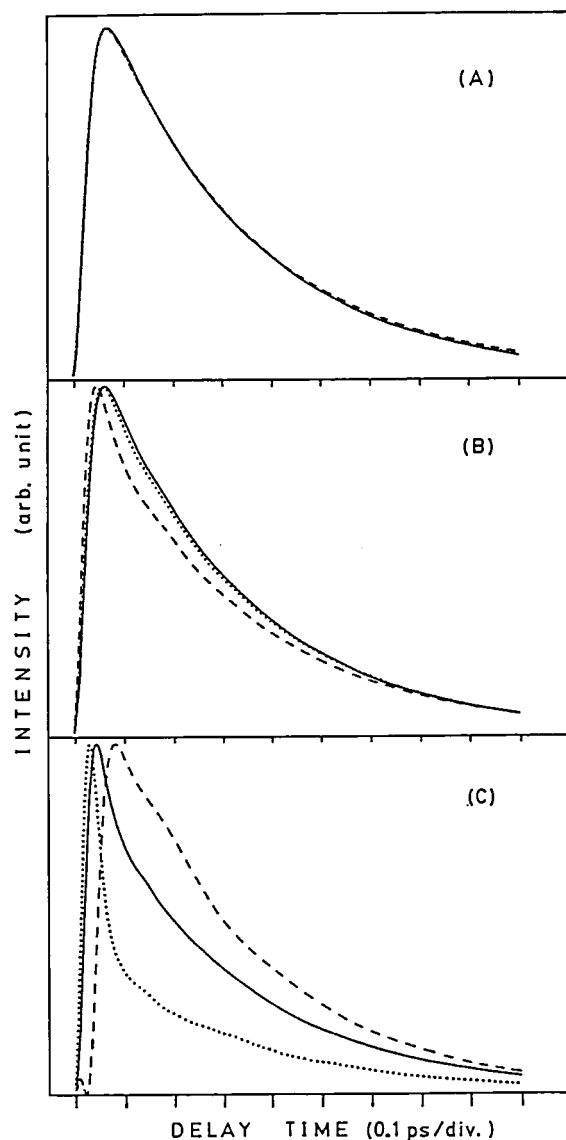
Figure 1. Calculated TRRCARS profiles. Dotted curve: [$//$, $//$] (polarization of the Stokes and probe radiations are parallel to that of the pump radiation), solid curve: [$//$, $\perp$] (the Stokes parallel to the pump and the probe perpendicular to the pump) and [$\perp$, $//$] (the Stokes perpendicular to the pump and the probe parallel to the pump), dashed curve: [$\perp$, $\perp$] (the Stokes and the probe perpendicular to the pump). The rotation of the transition dipole is slow (A), middle (B) and fast (C).

III—D   Dynamic Behavior of Electronic Excited States

Optical excitation of molecules to electronically excited states causes a variety of dynamical behavior, depending upon the nature of electronic structure and environments, some of which have been described in the previous chapters. In this chapter we describe a novel system for the study of intermolecular electron transfer, namely a dye in electron donating solvents. It was found that in some cases the intermolecular electron transfer becomes as fast as 10^{13} s^{-1}. The system has been studied by the femtosecond fluorescence spectrometer together with the subpicosecond transient absorption spectrometer. Information on both transient absorption and fluorescence gives us more complete view on the phenomena. We studied a different subject on the coenzyme environment of D-amino acid oxidase revealed by the multiple decays of FAD fluorescence.

III-D-1 Ultrafast Electron Transfer Reaction from Solvent to Solute

Tohru KOBAYASHI, Yoshihiro TAKAGI and Keitaro YOSHIHARA

In some photosynthetic bacteria, the rate of photo-induced electron transfer is found to be as fast as 1.1×10^{12} s^{-1}. In the present study, electron transfer from solvent (aniline) to solute (nile blue A; NB) is observed and the rate constant of fast component is found to be 2.5×10^{12} s^{-1}. In N,N-dimethylaniline (DMA), the rate is found to be as large as ca. 1×10^{13} s^{-1}.

The observation is carried out with fluorescence up-conversion system described in III-E-3. Ultrafast fluo-rescence decay of excited NB due to electron transfer reaction is observed as shown in Figure 1. The observed decay is non-exponential and is tentatively analyzed with two-exponentials. Possible explanations for the observed non-exponential decay are; (1) intramolecular vibrational relaxation competes with electron transfer and the observed decay is the composite of many decays of many vibrational states with different rates, (2) relative orientation of NB and aniline is not fixed and the non-exponential decay suggests the distribution in orientation which brings about distribution of reaction rate. Faster electron transfer reaction observed in DMA might come from the lower ionization potential of DMA (7.2 eV) than aniline (7.7 eV).
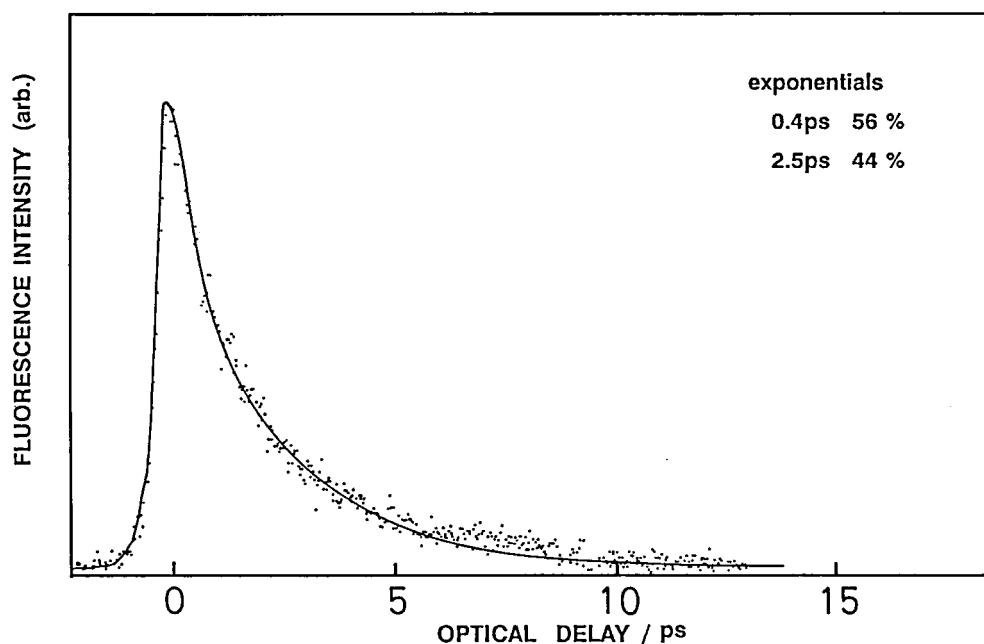
Figure 1. Fluorescence decay of excited NB dissolved in aniline. The wavelength of the excitation laser is 620 nm and the wavelength of sum frequency is 320 nm (that is, the wavelength of the detected fluorescence is 680 nm).

III-D-2 Primary Process of Nile Blue Studied by Subpicosecond Transient Absorption Measurement

Hideki KANDORI and Keitaro YOSHIHARA

Fluorescence kinetic experiments of nile blue by up-conversion technique revealed that a very fast reaction from an excited state should be present in aniline. As described above, it is likely to be electron transfer. Thus, primary reactions of nile blue molecule were also studied by subpicosecond transient absorption measurement and the following results have been obtained. (1) In methanol, an excited state of nile blue decays on nanosecond timescale. (2) In aniline, a lifetime of the excited state of nile blue is shorter than 2 ps (Figure 1(a)) which is roughly consistent with the fluorescence kinetic observation. Moreover, ground state depletion of nile blue recovered with a time constant of about 2.8 ps (Figure 1(b)), indicating that one more state (charge separated state), which is produced from

the excited state and decay to the original state, is present. The system (nile blue-aniline) provides a very fast charge separation and recombination processes which are completed within 3 ps.
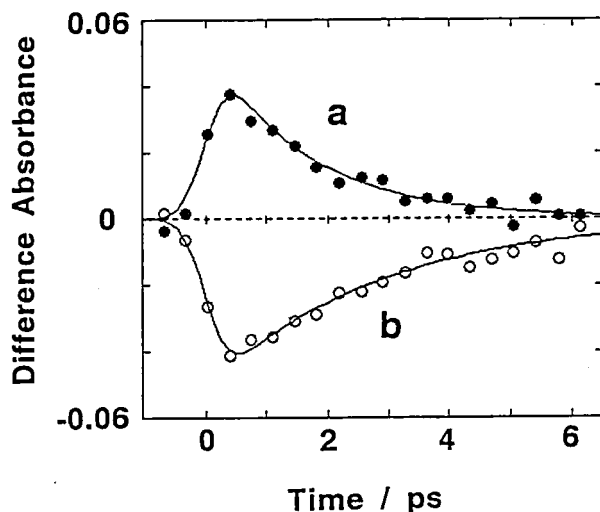
Fiugure 1. Ultrafast absorption kinetics in nile blue in aniline measured at 520 nm (a) and 655 nm (b). Solid lines are fitting curves in which the decay of the excited state is 1.6 ps (a) and recovery of ground state depletion is 2.8 ps (b).

III-D-3 Temperature-induced Changes in the Coenzyme Environment of D-amino Acid Oxidase Revealed by the Multiple Decays of FAD Fluorescence

Fumio TANAKA (Mie Nursing College), Naoto TAMAI, Iwao YAMAZAKI, Nobuaki NAKASHIMA, and Keitaro YOSHIHARA

A temperature-dependent change in the microenvironment of the coenzyme, FAD, of D-amino acid oxidase was investigated by means of steady-state and picosecond time-resolved fluorescence spectroscopy. Relative emission quantum yields from FAD bound to D-amino acid oxidase revealed the temperature transition when concentration of the enzyme was lowered. The observed fluorescence decay curves were well described by four-exponential decay functions as shown in Figure 1. The amplitude of the shortest lifetime (τ_0), ~ 25 ps, was always negative, which indicates that the fluorescence of D-amino acid oxidase at ~ 520 nm appears after a metastable state of the excited isoalloxazine decays. The other components with positive am-

plitudes were assigned to dimer or associated forms of the enzyme, monomer, and free FAD dissociated from the enzyme. Ethalpy and entropy changes of intermediate states in the quenching processes were evaluated according to the absolute rate theory. The temperature transition was much more pronounced in the monomer than in the dimer or associated forms of the enzyme.

Channel number (4.96ps/channel)
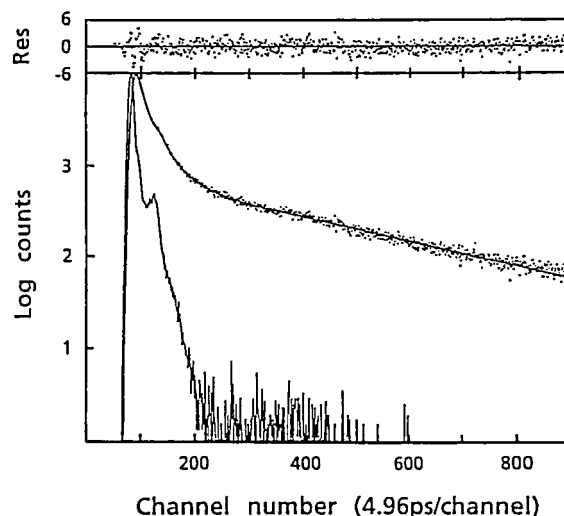
Figure 1. Fluorescence decay curve of FAD 100 μM D-amino acid oxidase. The fluorescence decay curve was measured at 40°C monitoring at 530 nm with a monochromator by means of the synchronously pumped, cavity-dumped dye laser and single-photon counting system. The enzyme was dissolved in 0.017 M pyrophosphate buffer at pH 8.3. The observed intensities are shown with dots. The decay curve was analyzed with a four-exponential decay function, using nonlinear least squares method based on Marquardt algorithm. Calculated decay curve for the best fit is illustrated with a solid curve in the dots. The exciting pulse profile (315 nm) is also shown with another solid curve. Response function of the system was ~ 30 ps. Res indicates weighed residuals between the observed and calculated fluorescence intensities.

III—E Development of Femtosecond Transient Spectroscopic Methods

It is generally recognized that many elementary processes in chemical reactions and excited state dynamics fall into femtosecond timescale. Development of ultrafast spectroscopic methods enables us to observe these phenomena in real time. We have been constructing suitable systems for the research subjects described in III-A, C and D. An apparatus for subpicosecond time resolved studies of chemical reactions in the gas phase clusters has been developed and successfully applied to the studies of *cis-trans* isomerization of *cis*-stilbene in clusters (see III-A-3). A subpicosecond transient absorption spectrometer for liquid system and a femtosecond fluorescence spectrometer by using fluorescence up-conversion method has been made and both have been used for a ultrafast electron-transfer dynamical studies in solution (see III-D-1 and 2). A femtosecond coherent anti-Stokes Raman spectrometer has been improved in experimental accuracy and several experimental results are described in III-C.

III-E-1 Construction of Apparatus for Subpicosecond Time Resolved Studies of Chemical Reactions in Clusters

Hrvoje PETEK and Keitaro YOSHIHARA

A pulsed ultrafast laser system consisting of a cw mode-locked YAG laser, hybridly mode-locked dye laser, regenerative YAG amplifier and pulsed dye laser amplifier (Figure 1a) has been assembled. The system produces ~500 fs pulses with ≤1 mJ energy at 10 Hz repetition rate. It is tunable between 570-620 nm and can be frequency doubled into uv region.

The laser system has been used for pump-probe measurements on reaction dynamics. In a typical experiment (Figure 1b), the laser is doubled into uv, the beam is split into two equal intensity pulses, one of which traverses a fixed delay while the other traverses a variable delay, and the pulses are focussed onto the molecular beam. The pump pulse initiates a chemical reaction in the clusters, such as *cis-trans* isomerization of *cis*-stilbene (see III-A-3). The probe pulse excites the fluorescence of the nascent product, such as trans-stilbene. The population of the product can be monitored either with an optical multichannel analyzer (OMA) by dispersing the fluorescence through a spectrograph, or with a photomultiplier (PMT) by detecting a portion of the spectrum through an optical filter chosen to transmit emission of a specific product. By changing the delay between pump and probe pulses, concentrations of reactants, intermediates and products can be monitored on subpicosecond time scale.

1a
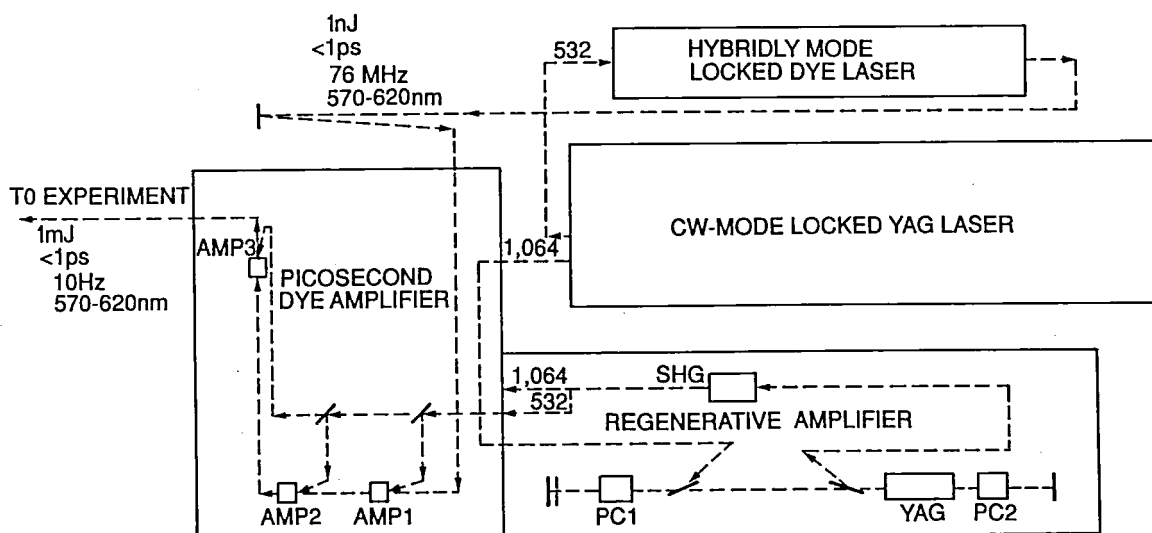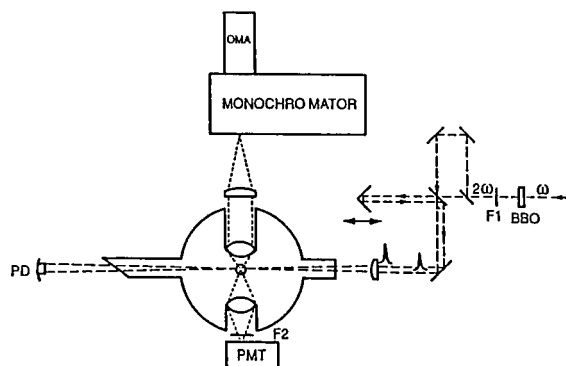
Figure 1. Experimental apparatus for measuring subpicosecond time resolved dynamics in clusters. The commercial ultrafast laser system (1a) produces pump and probe pulses that investigate reaction dynamics in clusters, which are generated by supersonic expansion in a molecular beam machine (1b).

III-E-2 Subpicosecond Transient Absorption Measurement System

Hideki KANDORI and Keitaro YOSHIHARA

An optical system for subpicosecond transient absorption measurement has been constructed. The apparatus is a double-beam spectrometer combined with a subpicosecond laser. The subpicosecond light source is shown in III-E-1. A part of the amplified laser pulse or its second harmonic (300 nm) is used for sample excitation, while the rest is used to generate a subpicosecond continuum probe pulse. The continuum was obtained by focusing the laser beam into a 1 cm cell containing H_2O. This continuum (350-1,000 nm) monitors absorbance change before and after excitation of a sample. A computer controls a stepping motor for optical delay and open/close of shutters, so that experiments are automatically carried out and time-resolved absorption spectra are obtained. The kinetic response after an excitation of a typical dye molecule (Nile Blue) suggests that actual pulse widths of excitation and probe pulses are about 0.5 ps. This system can detect subpicosecond transient if it has large enough extinction coefficient. Thus, it will be applied to study primary photochemical processes in solutions or biological systems.
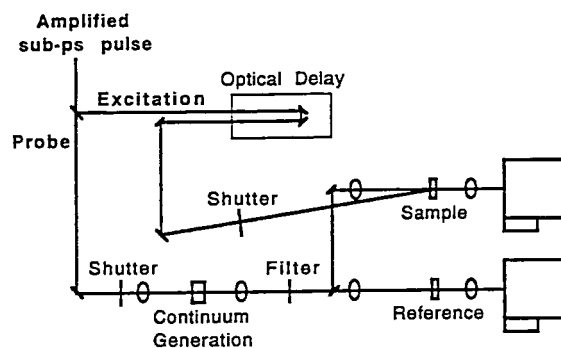
Figure 1. Block diagram of the subpicosecond transient absorption measurement system.

III-E-3 Construction of Fluorescence Up-Conversion System with Subpicosecond Time Resolution

Tohru KOBAYASHI, Yoshihiro TAKAGI and Keitaro YOSHIHARA

Some of the elementary processes in chemical reaction proceed with time constants less than 1 ps. However, conventional electro-optical instruments cannot be used in this time region due to its intrinsic limitation of time resolution. Non-linear optical effects are often applied to ultrafast spectroscopy in order to overcome this limitation. One of these techniques, fluorescence up-conversion, is applied to observe ultrafast fluorescence quenching due to electron transfer reaction. The system contains (1) non-linear crystal (BBO) with thickness of 0.5 mm to mix the fluorescence with probe laser beam, (2) pulse stage controlled by micro-computer to make optical delay of 6.7 fs/step and (3) flowing sample cell of 1 mm optical length made of quartz. The system is combined with homemade sub-ps dye laser system. Whole system is shown in the Figure 1. Time resolution is presently limited by the pulse width of dye laser output (0.3 ps) in the cavity-dumped configuration.
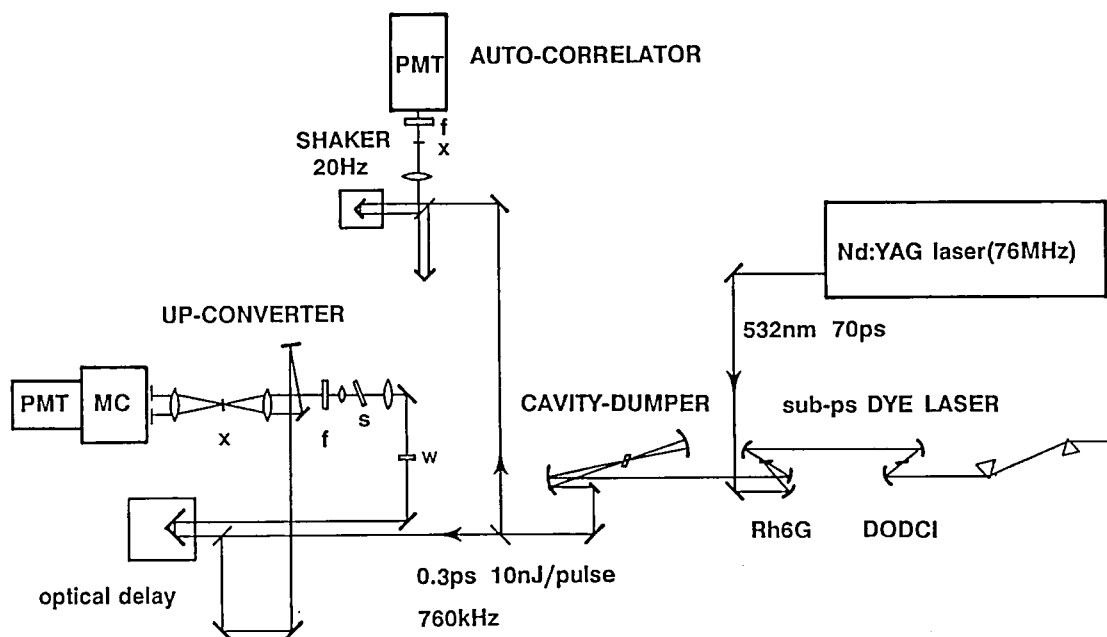
Figure 1. Whole system for fluorescence up-conversion measurement. x:non-linear crystal (BBO), s:sample, f:optical filter, and w:waveplate.

III—F Dynamical Processes in Electronically-and/or Vibrationally Excited Molecules

Fundamental molecular aspects of chemical reactions and energy transfer processes in the electronically or vibrationally excited states have been studied. Particular interest has been directed to the dynamics of vibrationally-excited weakly-coupled complexes such as van der Waals and hydrogen-bonded complexes, and the "disproportionation" reaction caused by UV irradiation of the complexes. Dynamics of highly-excited vibrational states (local modes) and chemical reaction induced by their excitation have also been subjects of research. We have also studied the nonlinear self-organizing chemical processes which exhibit temporal chemical oscillation and spatial pattern formation. The photoinduction and photoinhibition of chemically oscillating systems have been studied. The dual-frequency oscillations and uncatalysed chemical oscillations have also been studied by spectroscopic means.

III-F-1 Fluorescence-dip and SEP-LIF Spectra of van der Waals Molecules Contining Benzonitrile

Masao TAKAYANAGI and Ichiro HANAZAKI

Fluorescence-dip spectra of benzonitrile and some van der Waals complexes containing benzonitrile (benzonitrile dimers, benzonitrile·Ar, and benzonitrile·H_2O) were measured. The vibrational band widths in the fluorescence-dip spectra were found to be determined by the rotational structure and not by the rate of vibrational dissociation of the complex and/or the vibrational relaxation into the intermolecular modes. SEP-LIF (Stimulated-Emission-Pumping-Laser-Induced-Fluorescence) spectra were also measured to study the dynamical behavior of the complexes. The relaxation of the vibrational states (v_{10}, v_{12} and $v_{10}+v_{12}$ of benzonitrile) prepared by SEP was probed directly by varying the delay between the SEP and LIF laser pulses. The monomer showed slow decay which could be due to the escape of the vibrationally excited species out of the probe region. On the other hand, the dimer showed no detectable LIF signal, indicating fast relaxation of the prepared vibrationally ex-

cited state. Finite decay rates were obtained for benzonitrile · Ar and benzonitrile · H₂O, which were not sensitive to the vibrational energy.

III-F-2 Dynamics of Vibrationally Excited Anisole Investigated by the SEP-LIF Method

Masao TAKAYANAGI and Ichiro HANAZAKI
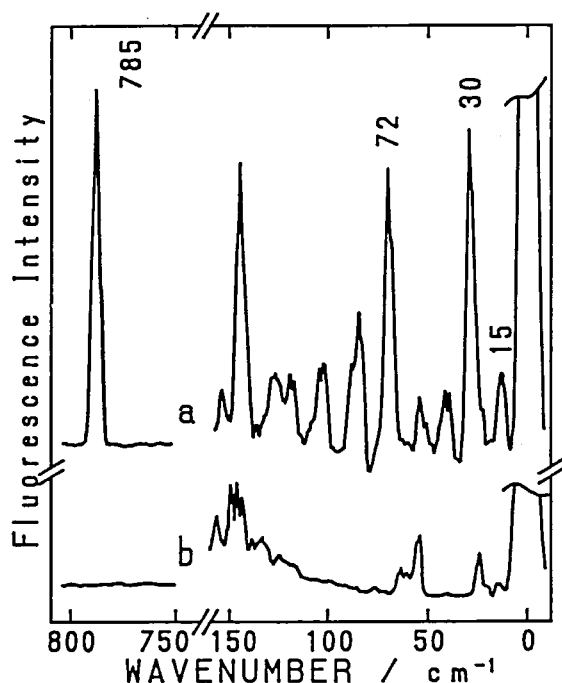
Figure 1. LIF spectra of anisole measured (a) with and (b) without the SEP excitation to the 785 cm⁻¹ vibrational level.

SEP-LIF spectra of anisole in pulsed supersonic expansion were measured. Figure 1 shows the LIF spectra of anisole measured with and without SEP excitation to the 785 cm⁻¹ vibrational level. With the SEP excitation many new bands appeared. The band at the 785 cm⁻¹ can be assigned to the 0←1 transition from the vibrational state excited by SEP. The bands in the low frequency region could be ascribed to several species since their relative intensities depend on the experimental conditions such as the stagnation pressure and the distance between the nozzle and the measuring point. Moreover, the relative intensities of the bands were found to be dependent on the delay between the SEP excitation and LIF measurement when the measurements were performed at 5 mm downstream of

the molecular beam from the nozzle, where the molecules in the expansion still collide each other. By increasing the delay, the intensity of the 30 cm⁻¹ band decayed first, then the 72 cm⁻¹ band decayed. The intensity of the 15 cm⁻¹ band increased at first with the delay shorter than 600 ns, and then began to decay. All these experimental results show that the some of the bands which appeared in LIF spectra with the SEP excitation are due to the species which are produced by the relaxation or isomerization of the initially prepared vibrationally excited species.

III-F-3 Reaction Dynamics of H + H₂O at 1.55 eV Collision Energy: Rotational Distribution of OH

Kazuhiro HONDA, Masao TAKAYANAGI, Teruhiko NISHIYA, Hiroshi OHOYAMA *(Osaka Univ.)* and Ichiro HANAZAKI

We have studied the photochemical reaction in the HI + H₂O system in a flow system. The reaction consists of two processes:

$$HI \xrightarrow{h\nu} H + I(^2P_{3/2}, {}^2P_{1/2}) \quad (1)$$
$$H + H_2O \rightarrow H_2 + OH: \Delta H=62.814 \text{ (kcal/mol)} \quad (2)$$
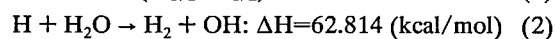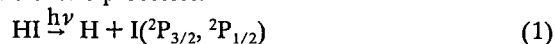
The rotational distribution of OH produced in the second process was measured by the LIF (laser-induced fluorescence) technique. Our studies had several advantages: Dissociation of HI at 266 nm yields I atoms in two spin-orbit states ($^2P_{3/2}$, and $^2P_{1/2}$), corresponding to the translational energies of the H atom of 1.55 and 0.62 eV, respectively. Since the 0.62 eV energy is less than the reaction barrier of 0.93 eV, its contribution to the OH production is expected to be minor. Figure 1 shows the rotational state distributions obtained from the R_{11}-, R_{22}- and Q_{11}-branches, which suggest relatively low rotational excitation. In order to understand the H + H₂O reaction mechanism at this collision energy, the same measurement has been performed for the H + D₂O system. The LIF spectra for this system show only the OD signal, suggesting clearly that the H + H₂O reaction at this collision energy proceeds *via* a direct reaction: *i.e.*, the colliding H extracts one of the hydrogen atoms in H₂O to leave OH.
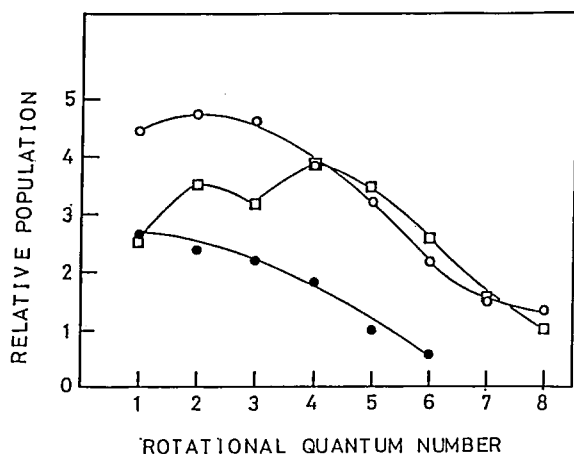
Figure 1. Nascent rotational state distributions of OH (V'=0) produced in the reaction H + $H_2O \rightarrow$ OH + H_2. Total pressure is 60 mTorr (HI:30 mTorr, H_2O:30 mTorr).
O:J=3/2, A', □:J=1/2, A', ●:J=3/2, A'' (A', A'' are the Λ-doublet components in which the unpaired electron is in-plane and out-of-plane, respectively, with respect to the plane of molecular rotation.)

III-F-4 Observation of Rotational Relaxation from the Vibrationally Excited $H^{35}Cl$ (v''=2).

Teruhiko NISHIYA, Masao TAKAYANAGI, and Ichiro HANAZAKI

F.F. Crim et al. have revealed that direct excitation is a powerful method to access the vibrational overtone states. The REMPI detection scheme has been used as a sensitive method for the determination of population distributions. We combined these two techniques [the tunable IR/UV-REMPI double resonance method] and applied it to 0.1 Torr flowing HCl. Then we could observe rotational relaxation from $H^{35}Cl$ (v''=2) with a time resolution of about 10 ns. Hydrogen second Stokes line of LD700 dye output was used to excite the v''=2, J''=0 level of $H^{35}Cl$ (P(1) branch). The excited $H^{35}Cl$ was then selectively detected with the (2+1) REMPI process via the E(v'=1)-X(v''=2) transition[1].

Figure 1 shows double-resonance REMPI spectra. IR laser was tuned by PAS and fixed at the IR transition. Then UV laser was scanned. Delay times between IR and UV lasers were (a) 5 ns, and (b) 200 ns, respectively. In (a), we can see Q(0) and S(0) lines. Besides these lines, Q(1)-Q(5) lines are also seen in (b) because of rotational relaxation. By monitoring the line intensity dependence on the delay time, we can observe the appearance and decay of each rotational level.

Their time constants were not the same as in the neighboring level, suggesting multi-quantum transitions ($|\Delta J| > 1$) to occur.

Reference
1) J. Chem Phys., 1987, **86**, 5273; ibid. 1987, **87**, 5229.
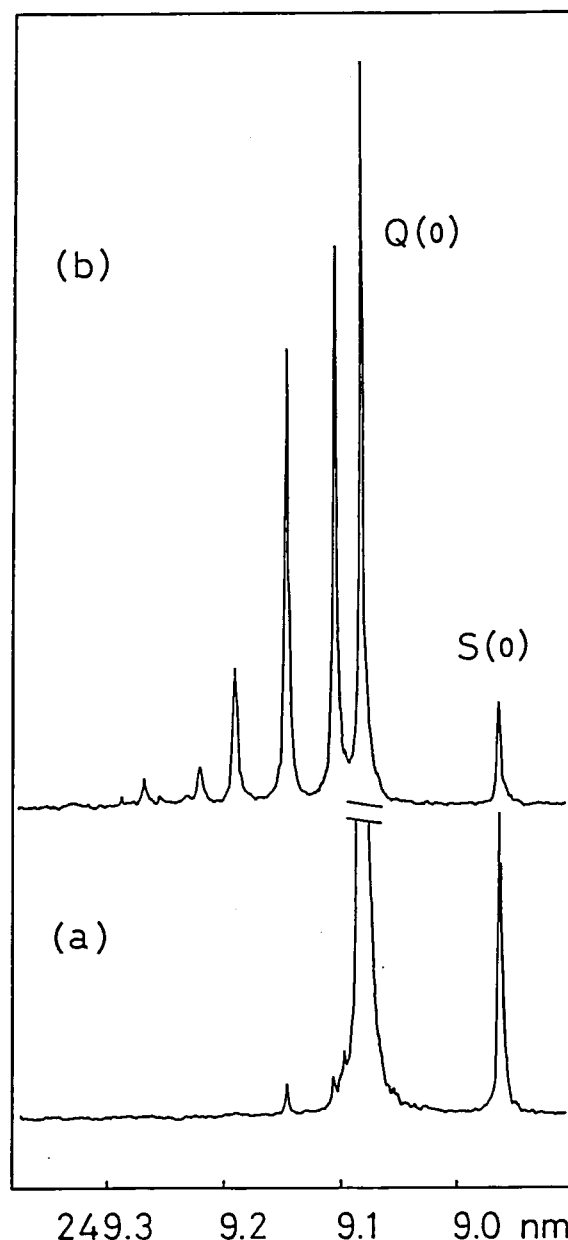
Figure 1. Double-resonance REMPI spectra. IR laser was tuned to P(1) branch of $H^{35}Cl$ (v''=2). Delay times between IR and UV lasers were (a) 5 ns, and (b) 200 ns, respectively.

III-F-5 Response of Chemical Oscillator to Irradiation

Yoshihito MORI, Prem Kumar SRIVASTAVA and Ichiro HANAZAKI
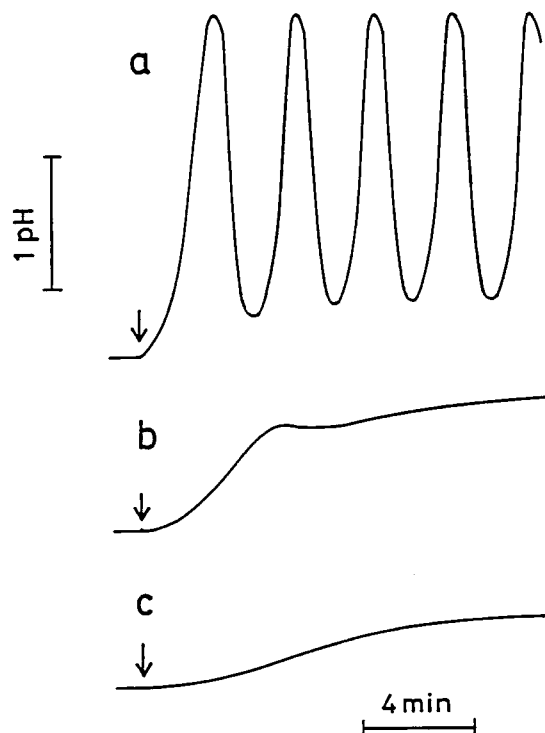
Figure 1. Time evolution of pH of the oscillator for the 290 nm irradiation. Irradiation starts at the point indicated by an arrow. Three cases correspond to the light intensity above the critical value(a), and below the critical value(b,c). Aqueous solutions of the component chemicals are input into a reactor with initial concentrations of $[Fe(CN)_6^{4-}]_0 = 3.3 \times 10^{-3}$ M, $[H_2O_2]_0 = 5.0 \times 10^{-2}$ M, $[H_2SO_4]_0 = 1.1 \times 10^{-3}$ M, at the residence time of 230 sec and T=25°C.

A photo-induced chemical oscillator (ferrocyanide-hydrogen peroxide-sulfuric acid) in a CSTR (continuously stirred tank reactor) has been reported.[1] This system is interesting in view of the general characteristic behavior of the chemical oscillation upon light irradiation, as well as of its possible application as the system which converts a steady optical energy input into an oscillatory signal. This system is more sensitive to light than similar systems reported previously. Even monochromatic light from a 500 W Xe lamp is sufficient to induce an oscillation. We have observed response of the oscillator in a CSTR to irradiation of monochro-

matic light at various wavelengths. Figure 1 shows a time evolution of pH of the oscillator at the 290 nm irradiation. In the dark, pH is in the steady state. Below the critical intensity (b,c), the value increases but reaches the steady state depending on the intensity. Above it(a), pH increases suddenly and an oscillation starts. At higher intensities, pH stays at higher steady state value without oscillation. Action spectrum can be measured for the induction and inhibition effects which would suggest the mechanism of the photosensitivity.

Reference
1) G. Rabai *et al.*, *J. Am. Chem. Soc.* **111**, 8272 (1989).

III-F-6 Spatiotemporal Pattern due to a Coupling between Photochemical Reaction and Convection

Yoshihito MORI, Prem Kumar SRIVASTAVA and Ichiro HANAZAKI

Temporal oscillation of emission has been observed for several locally irradiated solutions.[1] We have observed spatiotemporal pattern of emitting species in the locally irradiated aqueous solution of eriochrome black T(EBT) and acetone. Emission intensity and spatial pattern have been recorded for the aqueous solution of 10%(w/v) acetone and 0.033 mM EBT in a quartz cuvette (1.2×1.2×4.5 cm) locally irradiated with the light beam of 8×4.73 mm at 309 nm. Figure 1 shows a time profile of emission intensity at 450 nm and the corresponding spatial distribution of the emitting species in a single cycle of oscillation. The emitting area expands as the emission intensity increases (a-c) while, as the intensity decreases (d-f), the center part of the emitting area is pushed down out of the irradiated region and divided into two parts. This process is repeated for every cycle of oscillation. We have concluded that the emitting species is produced by an autocatalytic photochemical process(a-c), which establishes a density gradient in the solution. The convection caused by the gradient enhances the replacement of the emitting species in the irradiated zone by unreacted species(d-f).

Reference
1) I.R. Epstein *et al.*, *J. Phys. Chem.* **87**, 3955 (1983).
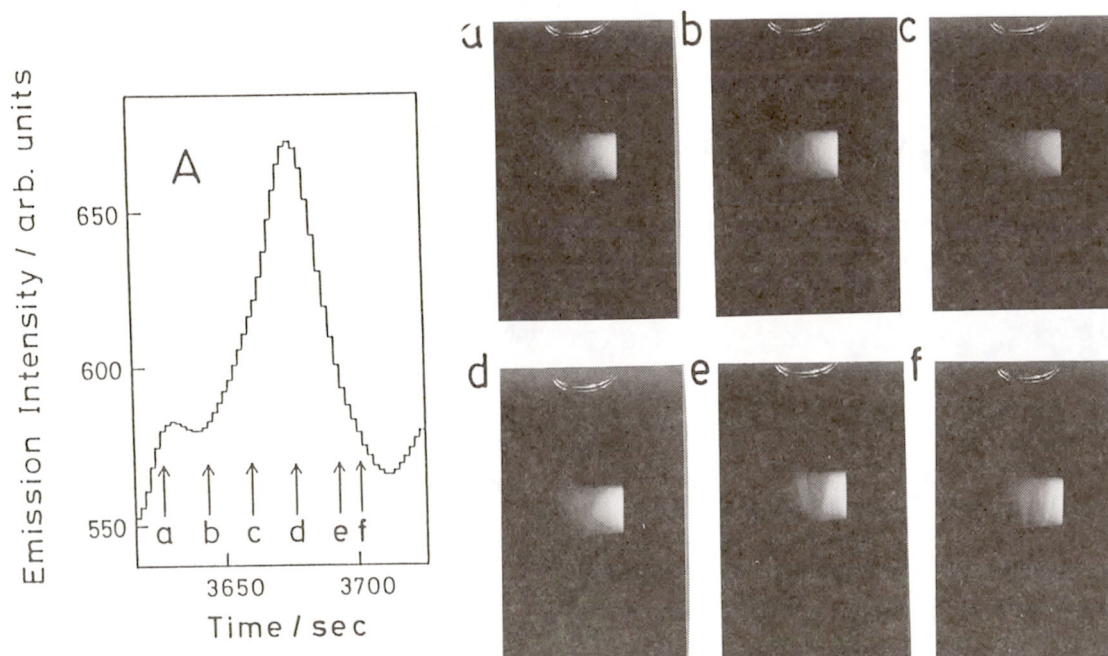
Figure 1. Time profile of emission intensity and spatial distribution of emitting species in a single cycle of oscillation. Photographs a-f were taken at points a-f, respectively, indicated in Figure 1A. The cuvette is irradiated from the right.

III-F-7 Dual-Frequency Chemical Oscillators with Acetylphenols as Substrates

Prem Kumar SRIVASTAVA, Yoshihito MORI and Ichiro HANAZAKI

The multiply oscillating system is interesting in view of the possible entrainment phenomena between oscillators coexisting in the system and of possible chaotic behaviour expected to appear as a result of competition among several oscillators. New dual frequency chemical oscillators have been found with a single organic substrate (o-acetylphenol, m-acetylphenol or p-acetylphenol) with a metal catalyst (Ce^{+4}, $Fe(phen)_3^{+2}$ or $Ru(bpy)_3^{+2}$) in a batch reactor. A typical results for o-

acetylphenol-$Fe(phen)_3^{+2}$-BrO_3^--H_2SO_4 system is shown in the figure. The system first shows high frequency oscillations and then bifurcates into a stable, non oscillatory state. After a break of a few to a few tens of minutes, it bifurcates again to an oscillatory regime with a lower frequency. Our results show that the high frequency oscillation occurs extensively for o-acetylphenol and slightly less extensively for m-acetylphenol, while only one or two spikes are observed for p-acetylphenol. It is suggested that high frequency oscillations are due to the oxidation and bromination of acetyl group, while low frequency oscillations are due to oxidation and bromination of the aromatic ring.
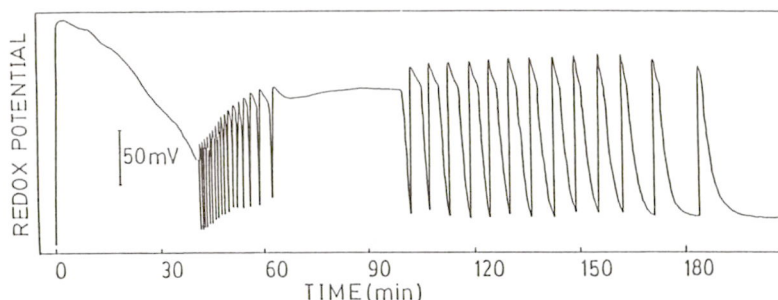
Figure 1. Dual frequency oscillation of the platinum electrode potential for o-acetylphenol(0.014M)/$Fe(phen)_3^{+2}$-(0.0005M)/BrO_3^-(0.0348M)/H_2SO_4(2.4M) in a batch reactor at 25°C. The time scale is measured from the time of addition of BrO_3^-.

III-F-8 Frequency Analyses of Dual Frequency Oscillators

Prem Kumar SRIVASTAVA, Yoshihito MORI and Ichiro HANAZAKI
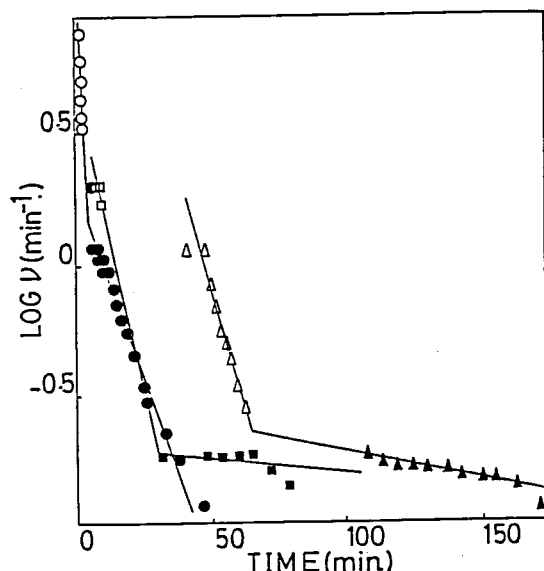
Figure 1. Variation of the frequency (ν) of oscillation with time (t) for the o-acetylphenol. Lines are the result of fitting to the equation, $\nu = \nu^0 \exp(-t/\tau)$.

O:Ce^{+4}(0.0005M)/o-acetylphenol (0.0139M)/ BrO$_3^-$(0.0349M)/H$_2$SO$_4$(2.5)

□:Ru(bpy)$_3^{+2}$(0.00014M)/o-acetylphenol(0.0112M)/ BrO$_3^-$(0.0348M)/H$_2$SO$_4$(2.5M)

△:Fe(phen)$_3^{+2}$(0.0005M)/o-acetylphenol(0.014M)/ BrO$_3^-$(0.0348M)/H$_2$SO$_4$(2.5M)

Open and closed points represent the high and low frequency oscillations, respectively.

Frequency of the dual frequency oscillators [organic substrate (o-acetylphenol, m-acetylphenol or p-acetylphenol)-metal catalyst (Ce^{+4}, Fe(phen)$_3^{+2}$ or Ru(bpy)$_3^{+2}$)-BrO$_3^-$-H$_2$SO$_4$] in a batch reactor were found to decay exponentially with time for both the high and low frequency oscillation regimes. The exponential decay of the frequencies would suggest their correlation with the lifetime of the substrate and/or some intermediate species, the concentration of which must be in a certain range for oscillation to continue. The logarithm of frequency ν(reciprocal of the time interval between neighbouring peaks) is plotted against time. A typical results for o-acetylphenol/Ce^{+4},

Fe(phen)$_3^{+2}$ or Ru(bpy)$_3^{+2}$ systems are shown in Figure 1. In some cases linear plots have been obtained for the two oscillation regimes and can be fitted to an empirical relation $\nu = \nu^0 \exp(-t/\tau)$, and parameters τ and ν^0 were determined from these plots. In some cases one or two oscillations have been obtained for the high frequency regime or the experimental points are scatterd in the low frequency regimes and cannot be fitted to the equation. A relation between the substrate concentration and the oscillation frequency was derived; if x_0 is the "initial" value of x at the begining of a single cycle of oscillation, and $x=x_T$ at t=T, then

$$\nu = k_1[RH]_0^a [\ln\{(1+1/x_0)/(1+1/x_T)\}]^{-1} \exp(-t/\tau)$$

where $x \equiv [Ce^{+4}]/[Ce^{+3}]$. Thus the decay of the oscillation frequency ν is determined by the decay of substrate RH.

III-F-9 Wavelength Dependent Photoinhibition of Chemical Oscillators

Prem Kumar SRIVASTAVA, Yoshihito MORI and Ichiro HANAZAKI

Photoinhibition and photoenhancement phenomena of oscillating chemical reactions seem to be interesting in view of the mechanistic aspects of oscillatory phenomena associated with photosensory intermediates. In order to understand the sensitivity of the systems at different wavelengths, action spectrum was determined for the two well studied uncatalyzed bromate-driven oscillators: phenol-BrO$_3^-$-H$_2$SO$_4$ and aniline-BrO$_3^-$-H$_2$SO$_4$. The light inhibition effect was discussed in relation to the absorption spectrum. It was found that the critical intensity for inhibition was decreased in proportion as the absorption of the system increased. In order to discuss the wavelength dependency in more detail, a relation between the wave length dependence of the efficiency (α) of inhibition and critical light intesity (I_{oc}) was derived as

$$\alpha = 2.303D \, \Delta S_c/I_{oc}[1-\exp(-2.303D)]$$

where, D is the opticl density of the oscillating solution and ΔS_c is the critical concentration of the particular intermediate destroyed by the critical light intensity(I_{oc}). Such a plot for the aniline-BrO$_3^-$-H$_2$SO$_4$ system

is shown in the figure, which indicates that the inhibition is more effective for shorter wavelengths where the system has higher intensity of absorption.
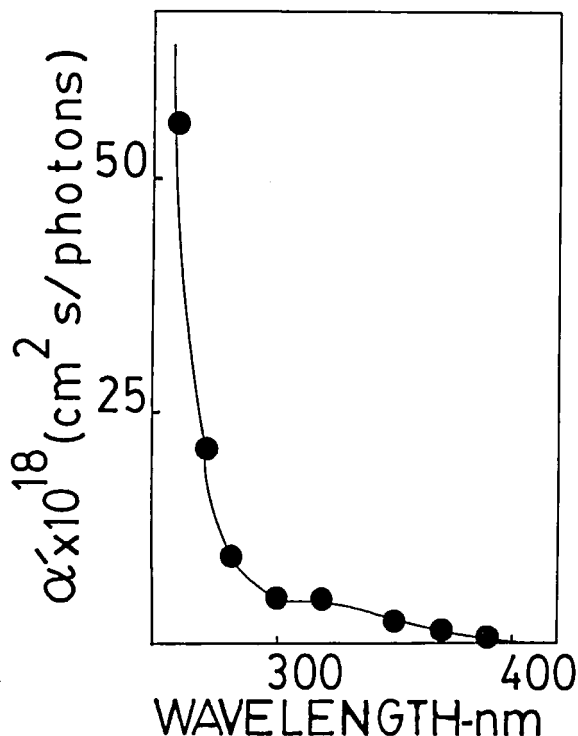
Figure 1. Wavelength dependence of relative efficiency $\alpha' =$ $D/T_{oc}[1-\exp(2.303D)]$ for inhibition of oscillation at 25°C and chemical composition; aniline (0.002M), BrO_3^- (0.021M), H_2SO_4 (2.0M).

III—G   Molecular Association and Cluster Formation in Aqueous Environments Studied by Mass-spectrometry of Liquid Fragments

Due to the unique nature of hydration or solute-solute interaction in aqueous solution, many molecules tend to produce pairs or clusters associated with other solute molecules or solvent water molecules. Adiabatic expansion of liquid droplets in vacuum dissociates molecules non-bonded or weakly bound to hydrogen-bonded clusters, and it leaves the clusters around the extended flight axis of the parent droplets. Inevitably this process is accompanied with evaporation of unstable surface molecules that causes substantial cooling or freezing of the fragment clusters. This process of the conversion of liquid to a cluster beam contains two stages of phase transition in the course of "isentropic volume expansion". The first one is the transition from liquid to a mixture of gas and liquid (free molecules and droplets) around the nozzle, and the second one is the transition of liquid state in droplets to the mixture of gas and solid (free molecules and clusters). The former process produces liquid states of droplets of which molecular association properties are analyzed through the mass-spectrometric determination of molecular composition of the fragment clusters (produced by the second "phase transition" from liquid to fragments in the high vacuum region). Previous studies on the ethanol-water and the alkyl carboxylic acids-water systems demonstrated that the observed cluster composition in each system provided good agreement with the results of many thermodynamic quantities, such as

partial molar volume, isothermal compressibilities, partial vapor pressures, and dielectric constants of aqueous mixtures.

III-G-1 Hydrophobic Hydration of Alcohols: Affinity of Alkyl Groups to Water Cages and its Shape Dependence

Nobuyuki NISHI and Kazunori YAMAMOTO

Hydrophobic hydration of 7 alkyl alcohols and their dimers has been studied by observing the cluster mass spectra of their aqueous solutions with solute-to-solvent molar ratios of 10^{-3}-10^{-2}. From the plots of the intensity ratios of monomer and dimer hydrate signals ($M^+(H_2O)_n$ and $M_2^+(H_2O)_n$) relative to $H^+(H_2O)_{n+1}$ and $M^+(H_2O)_{n+1}$, respectively, as functions of hydration number n, the stability constants of monomer and dimer hydrate clusters, κ_1 and κ_2 were obtained for methyl, ethyl, n-propyl, iso-propyl, n-butyl, t-butyl, and pentyl alcohols as shown in Table 1. The increase of κ_1 or κ_2 value with the increase of the alkyl chain length is not simple. Iso-propyl or t-butyl group exhibited much enhanced stabilities as compared with n-propyl or n-butyl alcohols, respectively. κ_m/V_w represents the stability constant divided by its van der Waals volume (expressed by a unit of volume of a water molecule). This quantity presents a measure of strength of the hydration cage and provides a rough estimate of the average number of hydrated water molecules attached to each methylene, methyl, or hydroxyl group. κ_1/V_w decreased gradually with the increase in the chain length in normal (or linear) alkyl compounds, while the alkyl groups with spherical structure, like iso-propyl and t-butyl, showed large values of κ_1/V_w. The stability of the hydration shell around an alkyl kernel must be related to the rigidity of the kernel. Lefetime of a spherical hydration shell could be much longer than that of a cylindrical shell. Similar trend was also seen in the stability of dimer hydrates, although chain-length dependence is not seen in the dimer hydration. Hydrophobic interaction between the two alkyl chains could stabilize the dimer kernel of the hydration shell.

Table 1. Stability constants of monomer and dimer hydrate clusters (κ_1 and κ_2, respectively), of alkyl-alcohols in water at 60°C.

solute	κ_1	κ_1/V_w	κ_2	κ_2/V_w
CH_3OH	5.4 ± 0.5	2.6_4	5.4 ± 0.8	1.3_5
C_2H_5OH	7.6 ± 0.8	2.5_2	8.8 ± 1.0	1.4_9
n-C_3H_7OH	9.1 ± 1.0	2.2_9	10.9 ± 1.2	1.3_9
iso-C_3H_7OH	11.1 ± 1.2	2.7_9	14.4 ± 1.5	1.8_3
n-C_4H_9OH	10.2 ± 1.5	2.0_6	14.0 ± 2.0	1.4_3
$(CH_3)_3COH$	12.0 ± 1.5	2.4_3	19.2 ± 3.0	1.9_6
n-$C_5H_{11}OH$	11.1 ± 2.0	1.8_7	16.2 ± 3.0	1.3_8

III-G-2 Hydrophobic Interaction and Hydrophobic Hydration of Butylalcohol Polymers

Nobuyuki NISHI and Kazunori YAMAMOTO

Solubility of alkyl alcohols and alkyl carboxylic acids in water exhibits marked differences depending on the size and the shape of alkyl groups. For example, t-butyl alcohol can get mixed with water in any ratio, while n-butyl alcohol can be solved only by 7.45% in water at 25°C. What is the origin of such a big difference in the solubility? Solubility is the affinity of solute molecules or solute clusters with bulk water composed of water clusters and freely rotating water molecules. An alkyl group has a large affinity with water molecules through so-called hydrophobic hydration.

Liquid fragment mass spectra were measured for the aqueous solutions with 4% butyl alcohol at 35 (± 10)°C in the mass range up to $M/Z = 1000$. Figure 1 shows parts of the mass spectra of t-butyl alcohol (top) and n-butyl alcohol (bottom) aqueous solutions. The main spectral difference is the intensity of the pure alcohol polymers ($H^+(C_4H_9OH)_m$). 4% solution of n-butyl alcohol showed a distinctive polymer sequence of $H^+(C_4H_9OH)_m$ for m=2 ~ 10, while in the spectrum of the 4% solution of t-butyl alcohol one can find this main sequence only up to m=6. The intensities of the pure t-butyl alcohol clusters with $m \geq 7$ were weaker than the hydrated polymers ($H^+(C_4H_9OH)_m(H_2O)_n$).

76

Thus one can see that linear alkyl chains tend to associate each other excluding water molecules but branched alkyl groups favor higher polymerization with intercalated water molecules. It is found that the increase of the contact surface area gives rise to the increase of the entropy in the association reactions.
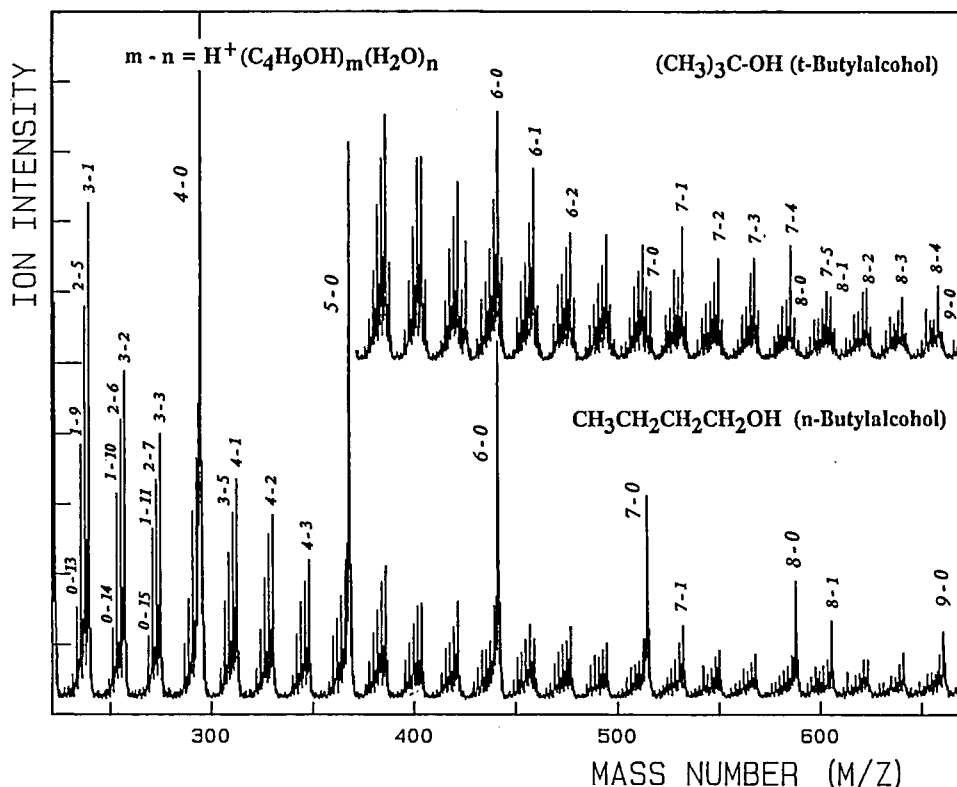
Figure 1. Mass spectra of *t*-butyl alcohol (top) and *n*-butyl alkcohol (4%) aqueous solutions at 35 (±10)°C.

III-G-3 Cluster Formation and Reactivity of Solutes with Water in Binary Mixtures of Water and Organic Solvent

Akihiro WAKISAKA *(Nat. Res. Inst. Poln. and Res.)*, Nobuyuki NISHI, Hirochika SAKURAGI *(Tsukuba Univ.)*, and Katsumi TOKUMARU *(Tsukuba Univ.)*

It has been reported that the interaction of various kinds of hydrophobic substrates with water becomes stronger remarkably at water mole fractions (X_w) higher than 0.8 in acetonitrile-water mixtures. Mass spectrometric analysis of molecular association in acetonitrile-water mixtures through the conversion of liquid to cluster beam made it clear that such behavior is due to the change of water clustering conditions with varying X_w.

Mass spectrometric analysis of acetonitrile-water mixtures containing 2-*n*-butoxyethanol (BE) was carried out for the samples of varying X_w. In $X_w > 0.8$, the intensities of $H^+(BE)(H_2O)_m$ clusters of $m < 9$ increased notably with increasisng X_w, while those of $m > 16$ did not show such enhancement. With increasing X_w, the population of smaller hydrate clusters becomes very abundant. These smaller clusters have shorter lifetimes producing bound free water molecules., These "free water" molecules can react with a substrate (solute) molecule, because they can take a configuration suited for reaction. The concentration of "free water" molecules becomes rapidly small with the addition of organic solvent molecules which in turn take a role of "free molecules" located among the cluster islands.

The deprotonation efficiency of the excited-state 2-naphthol (NpOH) in acetonitrile-water mixture is effected by the abundance of "free water" molecules. The deprotonation efficiency of the excited-state

NpOH increased drastically with increasing X_w in the region of $X_w > 0.8$. The interaction of the hydrophobic NpOH molecules with water could become active by

the effect of motional freedom of neighboring "free water". This resulted in the increase of the entropic factor.

III—H Excited State Dynamics, Reaction Pathways and Electronic Structure of Molecular Clusters

Cluster specific excited state dynamics is explored with the aid of two-color Resonance Enhanced Two-photon Ionization technique. Molecular clusters show reactions either in the intermediate excited state or in an excited (or sometimes ground) state of the ion species. Size selective excitation of molecular ion clusters enabled us to take electronic spectra of small clusters by observing the evaporation efficiency with excitation wavelength.

III-H-1 Photodissociation of Size-Selected Benzene Cluster Ions

Kazuhiko OHASHI, Pascal LABLANQUIE and Nobuyuki NISHI

Photodissociation process of size-selected benzene cluster cations, $(C_6H_6)_m^+ + h\nu \rightarrow (C_6H_6)_n^+ + (m-n)C_6H_6$, was investigated. Photodissociation spectra, i.e., photofragment yield spectra as a function of dissociation wavelength, of isolated $(C_6H_6)_2^+$ and $(C_6H_6)_3^+$ were obtained in the visible region. The experiment was carried out using a reflectron-type time-of-flight mass spectrometer (TOFMS) combined with laser multiphoton ionization (MPI) technique., Parent $(C_6H_6)_m^+$ ions were produced by MPI of neutral benzene clusters. While traveling in the acceleration region of the TOFMS, the prepared ions were crossed by a time-delayed dissociation laser (410-750 nm). Photofragment ions were analyzed by the reflectron-type TOFMS.

Figure 1 shows the photodissociation spectra of $(C_6H_6)_2^+$ and $(C_6H_6)_3^+$. In Figure 1 (a), three features can be identified; two peaks at 440 nm and 580 nm, and broad band around 600-750 nm, indicating that several different electronic transitions are involved in the photodissociation. The 440 nm and the 580 nm peaks of Figure 1 (a) can be tentatively assigned to local excitation bands of $(C_6H_6)_2^+$, corresponding respectively to the allowed $\widetilde{C}$-$\widetilde{X}$ and the forbidden $\widetilde{B}$-$\widetilde{X}$ transitions of a $C_6H_6^+$ unit. On the other hand, the feature at 600-750 nm is considered to be the tail of an intervalence transition band peaked at longer wavelength. The $\widetilde{C}$-$\widetilde{X}$ band of $(C_6H_6)_3^+$ appears to peak

slightly to the blue of the $(C_6H_6)_2^+$ absorption, while the $\widetilde{B}$-$\widetilde{X}$ band shifts to the red as shown in Figure 1 (b).
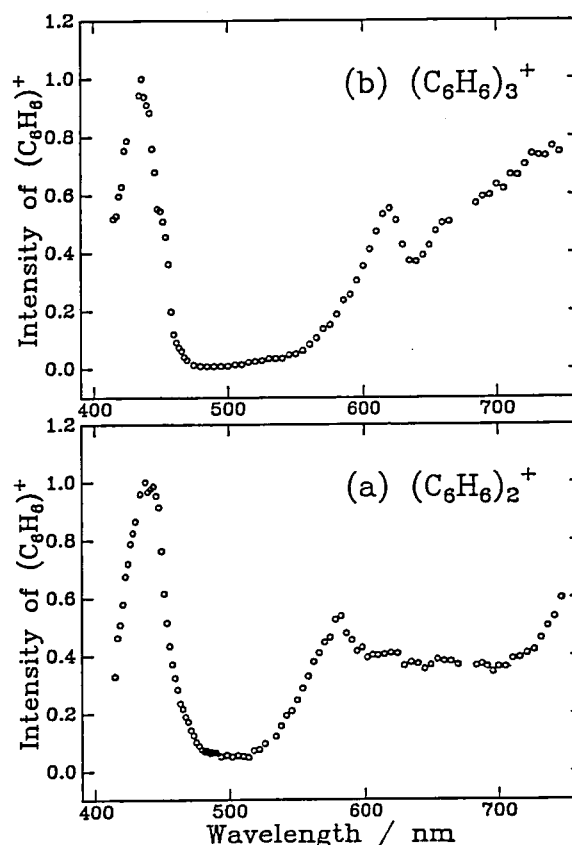
Figure 1. Photodissociation spectra of $(C_6H_6)_2^+$ (a) and $(C_6H_6)_3^+$ (b). The ordinate of the figure is the yield of $C_6H_6^+$, because the $C_6H_6^+$ is the predominant fragement in the photodissociation of $(C_6H_6)_2^+$ and $(C_6H_6)_3^+$ in the wavelength region studied here.

III-H-2 Multiple Hydrogen Transfer in Electronically Excited Pure Pyrazine Clusters.

Hidetoshi OHNO*, Kazuhiko OHASHI, Toshinobu NAKATA*, Nobuyuki NISHI, and Ryoichi SHIMADA* (*Kyushu Univ.)

It is well-known that an azine molecule such as pyrizine or pyrazine acts as a base attracting a hydrogen atom to a nitrogen site. A pyrazine molecule contains both hydrogen accepting sites and hydrogen donor sites. Although the geometrical structure of a pyrazine dimer is not known, the interaction between a non-bonding orbital localized in a nitrogen atom and a hydrogen atom of an adjacent molecule is expected to take an important role in the structure of pure pyrazine clusters. 193 nm laser pulse (10 ns) excitation of pure pyrazine cluster beam (seeded in $Ar(0.5 \sim 3$ atm.) produced cluster ion signals through a reflectron time-of-flight mass spectrometer. Figure 1 shows some parts of the spectrum taken at 1.25 atm stagnation pressure. In addition to the strong pyrazine monomer ions at 40.96

μs and the higher cluster ions with the form of $(C_4N_2H_4)_n^+$, hydrogenated clusters were observed. At the high mass side of the monomer, singly and doubly hydrogenated signals appeared with nearly the same intensity. In the pressure region higher than 0.8 atm., the clusters higher than the dimer were accompanied with hydrogenation sequencies: $(pyrazine)_n(H)_m$. Interestingly, the maximum number of m is 4 and the relative intensities of the non-hydrogenated, singly, doubly, triply and quadruply hydrogenated species were roughly the same in the dimer, tetramer and pentamer groups.; The trimer group showed the doubly hydrogenated signal intensity as strong as the singly hydrogenated one. Two color (193 nm + 442 nm) ionization study exhibited that two photons of 193 nm light produced neutral hydrogenated species (with a lifetime of $150 \sim 200$ ns for the dimers). The ion center of the clusters is likely to be composed of two pyraizine molecules which are hydrogenated up to 4, which is the same number as the nitrogen atoms in the dimer unit.
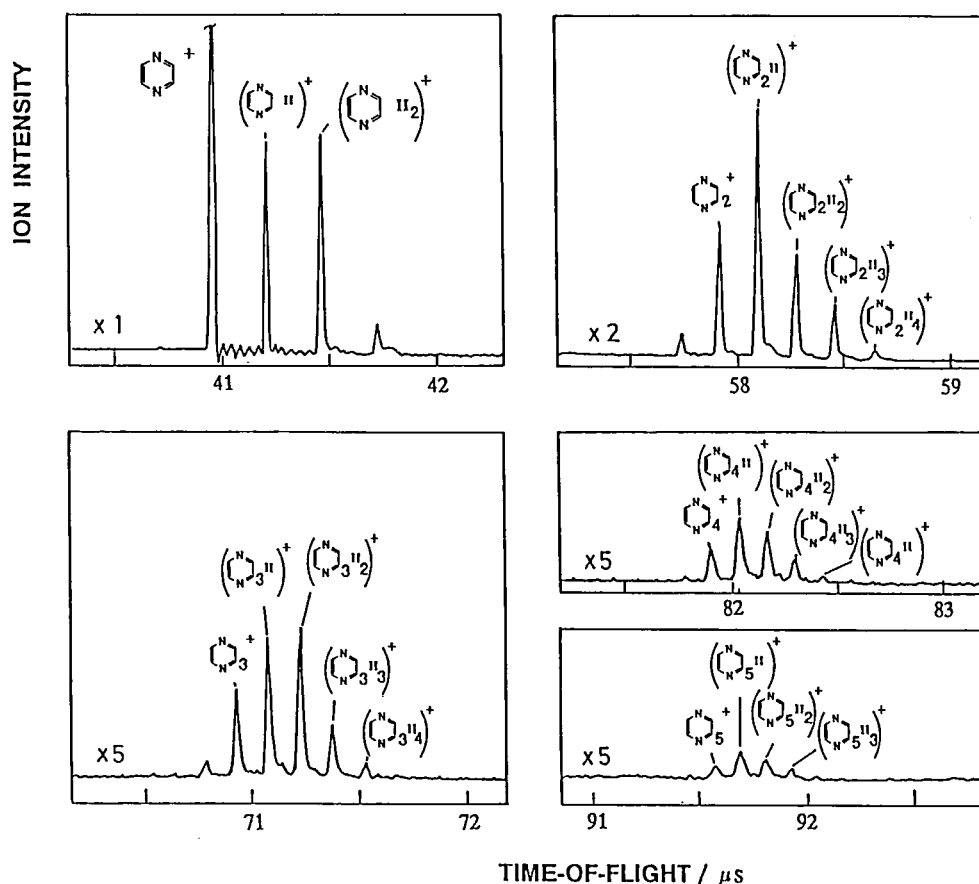
Figure 1. Some parts of one-color MPI TOF spectrum of pure pyrazine clusters excited at 193 nm. In addition to $(pyrazine)_n^+$, hydrogenated signals can be seen as dominant signals.

III-H-3 Two-color Multiphoton Ionization Study of Pyrazine-Benzene Binary Clusters

Toshinobu NAKATA,* Hidetoshi OHNO,* Kazuhiko OHASHI, Nobuyuki NISHI, and Ryoichi SHIMADA (*Kyushu Univ.)

Pyrazine-benzene binary cluster produced from an 1:4 mixture were excited to the L_a state of benzene or pyrazine at 210 nm (ω_1). After a delay of 100 ns, the second laser at 340~420 nm (ω_2) irradiated the beam at a downstream position of the ion acceleration region generating $C_6H_5^+$, $C_6H_6^+$, $C_4H_2N_4^+$, $C_4N_2H_5^+$, $(C_6H_6 \cdot C_4N_2H_4)^+$, $(C_4N_2H_4)_2^+$, and $(C_4N_2H_4)_2H^+$ as dominant signals. The observed trend of the spectral pattern and the hydration number are different from those observed in the pure pyrazine system. By fixing the detector mass positions for the ions $C_4N_2H_4^+$ and $C_4N_2H_5^+$, the ω_1 wavelengths were scanned in the region of 207~220 nm. The action spectrum of $C_4N_2H_5^+$ was nearly the same as that of $C_4N_2H_4^+$ and it also showed resemblance to that of benzene dimer. The lifetimes of the neutral parent in the excited states were 90 ± 15 ns for all the $C_6H_6^+$, $C_4N_2H_4^+$, $C_4N_2H_5^+$, and $(C_4N_2H_4)_2H^+$ ions, suggesting that these ions originate from the same or similar parent clusters. The laser power dependence of these ions were 1.0 ± 0.2 for both ω_1 and ω_2 suggesting the 1+1 ionization via neutral excited state. (Note that pure pyrazine clusters showed $2\omega_1 + 1\omega_2$ ionization for the same laser wavelengths.) Thus one could ascribe the ω_1 absorption chromophore in the binary parent clusters to a benzene-pyrazine complex unit which forms an excimer with a lifetime of ~90 ns for the excitation to the L_a state of a benzene molecule.

III-H-4 Two-Color 2+2 Photon Resonance-Enhanced Ionization of Benzene-Carbon Tetrachloride Binary Clusters

Fuminori MISAIZU, Hisanori SHINOHARA, Nobuyuki NISHI, Tamotsu KONDOW (Univ. of Tokyo), and Minoru KINOSHITA (Univ. of Tokyo)

Binary clusters produced from benzene-carbon tetrachloride (9:1) mixture are ionized by two-color (UV-VIS) excitation through the resonance pumping of the benzine S_2 state or the charge-transfer state of benzene-carbon tetrachloride complex. The observed ions are $C_6H_7^+$, $(C_6H_6)_nC_6H_6Cl^+$, $C_6H_5Cl^+$, $C_7H_6Cl^+$, and $C_7H_5Cl_2^+$ in addition to $(C_6H_6)_n^+$ (n=1,2,3...). Resonance two-photon excitation at 210 nm, in which the total energy (11.8 eV) is over the ionization potential of benzene (9.25 eV), generates neutral intermediate states with lifetimes of 250~320 ns. The visible laser ionization with a delay from the first two-photon excitation appeared to be also a two-photon resonance process, probably the first step being T←T transition of benzene. The main reason for maintaining neutral states in spite of the absorption of high energy is attributed to the double excitation of C_6H_6 and CCl_4 molecules and the subsequent dissociation of electronically excited CCl_4 in the binary clusters. Condensation reactions of the component molecules in a benzene dimer ion unit and in benzene-carbon tetrachloride binary ions are found to be highly efficient for this system.

III-H-5 Metastable Dissociation Dynamics of Molecular Cluster Ions

Hisanori SHINOHARA (Mi'e Univ.), Hiroyasu SATO (Mi'e Univ.), Fuminori MISAIZU, Kazuhiko OHASHI and Nobuyuki NISHI

The observation of metastable ("uni-cluster") dissociation of molecular cluster ions gives rise to some important clues for understanding cluster dynamics such as fragmentation, evaporation, melting, and phase transition. In this study, metastable dissociation processes of benzene, ammonia, and ammonia-water clusters are investigated by using one- and two- color RE2PI reflectron time-of-flight mass spectroscopy. All of the cluster ions studied exhibit the following metastable dissociation:

$$(C_6H_6)_n^+ \rightarrow (C_6H_6)_{n-x}^+ + x \cdot C_6H_6 \qquad (1)$$
$$(NH_3)_n^+ \rightarrow (NH_3)_{n-x}^+ + x \cdot NH_3 \qquad (2)$$
$$[(NH_3)_n(H_2O)_m] \rightarrow$$
$$[(NH_3)_{n-x}(H_2O)_m]^+ + x \cdot NH_3 \qquad (3)$$
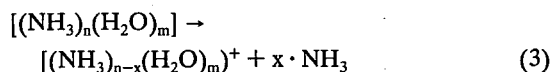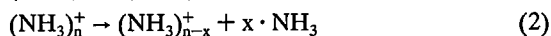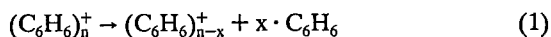
where x=1 paths dominate the dissociation processes in the excess energy range less than 2 eV. Similar results have recently been obtained by Schlag and co-workers[1] and Castleman and co-workers[2] for benzene and

ammonia clusters, respectively, at somewhat different excess energy range. Pure metastable dissociation rate constants (k) are determined for cluster size up to n=17 for reaction (12). For ammonia-water cluster ions, extensive uni-cluster dissociation processes (corresponding to reaction (3)) are found for n>5, supporting a recently proposed "binary shell-structure"

of the $(NH_3)_n(H_2O)_m$ clusters.

References
1) A. Kiermeier, B. Ernstberger, H.J. Neusser, and E.W. Schlag, *J. Phys. Chem.*, **92**, 3785 (1988).
2) S. Wei, W.B. Tzeng, and A.W. Castleman, Jr., *J. Chem. Phys.*, **93**, 2506 (1990).

III—I Photodissociation Dynamics Studied by Photofragment Time of Flight Spectroscopy

III-I-1 Time-of-Flight Spectra of Bound-to-Free Transitions in I_2

Robert J. DONOVAN *(Univ. Edinburgh)* and Nobuyuki NISHI

[*Chem. Phys. Lett.*, **169**, 74 (1990)]

Oscillatory continuum (bound-to-free) emission spectra provide a direct view of the quantum-mechanical behavior of molecular systems. In the simplest case of a repulsive lower state the observed spectrum is a reflection of the square of the upper-state wave function. In the experiment, the iodine molecule was first excited to the $\tilde{D}0_u^+$ ion-pair state by absorption of a photon at 193 nm (ArF laser). The $\tilde{D}0_u^+$ state then fluoresces back to the ground state (both bound and unbound regions) and to the repulsive $\tilde{a}'0_g^+$ state. Fluorescence to unbound lower levels leads to direct dissociation and iodine atoms are formed with a range of kinetic energies. The time-of-flight spectrum of ^{127}I following ex-

citation of I_2 at 193 nm was composed of three peaks. The most prominent peak at 250 μs is associated with transitions to unbound regions of the ground-electronic state, i.e. $I_2(\tilde{D}0_u^+ \rightarrow \tilde{X}0_g^+,$ continuum). Some broad structure is just resolved adjacent to the main peak. At shorter flight times (190 μs) a weaker peak is observed and can be assigned to the transition $\tilde{D}0_u^+ \rightarrow \tilde{a}0_g^+$. A broad peak is also observed at long flight times (499 ~ 600 μs) and this could arise from either the tails of the $\tilde{D}0_u^+ \rightarrow \tilde{X}0_g^+$ and $\tilde{D}0_u^+ \rightarrow \tilde{a}^+0_g^+$ transitions or from a hitherto unobserved transition. Results were also obtained using plane polarized light which show that the maximum yield of atoms is observed when the plane of polarization is parallel to the flight tube axis (i.e. the absorption transition is parallel in nature). For each peak in the oscillatory continuum (frequency domain) a corresponding packet of atoms, having a narrow range of velocities, is formed. Our experiment detected these packets of atoms in the time-domain.

III—J Magnetic Field Effect on Charge Recombination Process in X-irradiated Systems

III-J-1 Excimer Formation of Pyrene as a Probe to Investigate the Recombination of Geminate Pairs: ODESR and Fluorescence Study of Dilute Pyrene in Squalane

Masaharu OKAZAKI *(Gov. Ind. Res. Inst., Nagoya and IMS)*, Yutaka TAI *(GIRIN)*, Ryoichi NAKAGAKI *(IMS)*, Keichi NUNOME *(GIRIN)*, and Kazumi TORIYAMA *(GIRIN)*

[*Chem. Phys. Lett.*, **166**, 227 (1990)]

It is shown that the monomer fluorescence and the excimer fluorescence from a dilute pyrene solution in squalane at room temperature are mainly from "delayed" geminate pairs (Py^-, S^+) and (Py^-, Py^+), respectively, from the magnetic field dependence and the ESR modulation (ODESR) observed at the monomer and excimer fluorescences. The recombination time of the former pair is found to be much shorter than that of the latter from analysis of these data. This indicates that the hole (S^+) hops between the solvent molecules

towards the solute anion.

III-J-2 Dynamic Process of Delayed Geminate Pairs in X-irradiated Squalane Solution of p-Terphenyl: an ODESR Study

Masaharu OKAZAKI *(Gov. Ind. Res. Inst., Nagoya and IMS)*, Keichi NUNOME *(GIRIN)*, Kaoru MATSUURA *(GIRIN)*, and Kazumi TORIYAMA *(GIRIN)*

The magnetic field effect and the ESR modulation of the fluorescence of a X-irradiated squalane solution of p-terphenyl was observed at various temperatures, and concentrations. Analysis of the observations led us to conclude that two geminate pairs, one with a terphenyl anion and a hole, and the other with a terphenyl anion and its cation, contribute to the "delayed" charge recombination process. It is suggested that the recombination time of the former pair is much less than that of the latter due to hole hopping among the solvent molecules. Effects of kinetic processes on the ODESR spectrum are discussed.

III-J-3 Excimer Formation of Pyrene as a Probe to Investigate the Recombination of Geminate Pairs: Effect of Multicomponent Recombination on Stern-Volmer Plot

Masaharu OKAZAKI *(Gov. Ind. Res. Inst., Nagoya and IMS)*, Yutaka TAI *(GIRIN)*, Keichi NUNOME *(GIRIN)*, and Kazumi TORIYAMA *(GIRIN)*

Quenching of excimer and monomer fluorescences induced by X-ray and UV-light as well as that of ODESR amplitude was observed with freon 113 as a quencher. The Stern-Volmer plots give some precise information on the kinetic processes of the delayed geminate pairs.

III—K External Magnetic Field Effects upon Chemical Reaction

To establish external magnetic field effects upon chemical reactions, we have been studying extensively in solution phase and in gas phase. In the recent decade, we observed that the β band of NO showed one of largest external magnetic field effects ($\sim 85\%$).

III-K-1 External Magnetic Field Effects on the β Band Emission of NO.

Minoru SUMITANI, Haruo ABE *(Inst. of Phys. and Chem. Res.)*, and Saburo NAGAKURA *(Grad. Univ. for Adv. Studies)*

We studied the external magnetic field effects for the β band (B^{2}II-X^{2}II) of NO produced through next three reactions:

$$N(^4S) + O(^3P) + M \rightarrow NO(B^2II-X^2II) + M \quad (1),$$

$$NO + N_2(A^3\Sigma_u^+, B^3\Pi_g) \rightarrow NO(B^2II) \quad (2),$$

and

$$N_2O + Ar^* \rightarrow NO(B^2II) + Ar \quad (3).$$
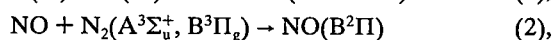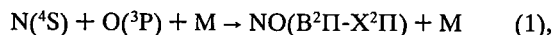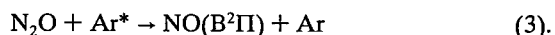
The magnetic effects are dependent on the vibrational levels of the emitting state.

The $\beta(0,n)$ band decreases its intensity to a great extent by a magnetic field commonly for the three cases.

This means that the magnetic field does not affect the formation process of the emittiing state, B^{2}II, but its decay process. From the consideration of the energy level diagram, this phenomenon can be explained in terms of the magnetically induced interaction between the B^{2}II and a^{4}II states.

In the case of the $\beta(2,n)$ band, the magnetic field effect upon β band fluorescence depends on the formation process and its intensity is increased only in the case where the emitting state is produced by the reaction between N(^{4}S) and O(^{3}P). This may be due to the magnetic enhancement of intersystem crossing b$^4\Sigma \rightarrow$ B^{2}II. This is an example in which formation of gaseous molecules in a specific excited level is enhanced by external magnetic fields.

RESEARCH ACTIVITIES IV
Department of Molecular Assemblies

IV—A   Frequency-dependent Electrical Conductivity of Organic Conductors

Frequency-dependent electrical conductivity provides the information on the transport dynamics in solid state as well as on the electronic structures. The need for this method has been increasing especially to the study of low-dimensional conductors characterized by a strong electron-electron correlation, cooperative motion of charge carriers, and disorder. As a part of ongoing program of gathering the data of frequency-dependent conductivity from dc to ultraviolet region, we have set up in this year the instruments to obtain the 1 GHz conductivity and the microspectrophotometer for measuring the reflectance spectrum from 2000-30000 cm^{-1}, subsequent to the apparatus for the dc and microwave (9.4 GHz) conductivity which was constructed last year.

IV-A-1   Construction of a Microspectrophotomeric System for Measurement of Reflectance spectrum on a Small Single Crystal

Takashi IDA, Atsushi KAWAMOTO, Akito UGAWA, and Kyuya YAKUSHI

We have constructed a microspectrophotomeric system which is designed for measurement of anisotropic reflectance spectra on a small single crystal. The block diagram is shown in Figure 1. The system covers wide range of wave-number 2150-35000 cm^{-1} by applying three light sources (Xe, halogen lamp, and globar), two gratings, two polarizers (Gran-Taylor prism and wire-grid), and three light detectors (photomultiplier, Ge-photodiode, and InSb detector). The incident light beam is precisely focused with an infrared microscope onto a sample surface as small as 20×20 μm^2 region with a 36× reflective objective. A 15× refletive objective with long working distance (24 mm) is also available which enables measurement of reflectivity at low temperatures with a cryostat (now under construction), or at high pressures using a diamond anvil cell.
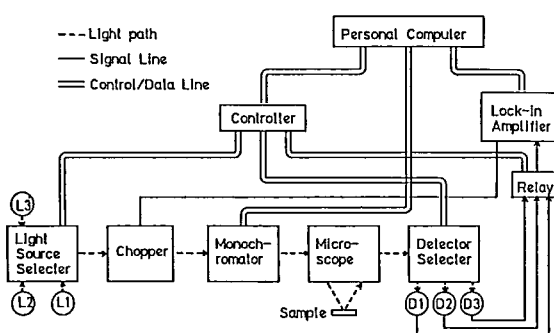
Figure 1.   Block diagram for the microspectrophotomeric system.

IV-A-2   Microwave Conductivity of the Phthalocyanine and Dicyanoquinonediimine Salts

Hideo YAMAKADO, Akito UGAWA, Takashi IDA, and Kyuya YAKUSHI

[*Proceeding of the ISSP International Symposium, Tokyo, 1989*]

The temperature dependence of microwave conductivity was measured on single crystals of phthalocyanine salts (NiPc(AsF$_6$)$_{0.5}$), PtPc(ClO$_4$)$_{0.5}$, CoPc(AsF$_6$)$_{<0.5}$), and dicyanoquinonediimine (DCNQI) salts (Cu(Me$_2$-DCNQI)$_2$, Cu(MeBr-DCNQI)$_2$, Ag(Me$_2$-DCNQI)$_2$). Phthalocyanine salts exhibit a metal-insulator transition unlike the iodine salts of phthalocyanine. DCNQI salts show qualitatively the same behavior as studied by dc conductivity.

IV—B Synthesis and Characterization of Phthalocyanine Salts

Some phthalocyanine molecules contain d-electrons in the conjugated π-electron system. Most importantly the highest occupied molecular orbital is not hybridized with the d_{z^2}-orbital although they are energetically close to each other. Owing to this special nature, the partially oxidized phthalocyanine salts in solid state may possibly have distinct natures from conventional organic conductors, say a coupling with exciton or magnon. To search for such a new type of conductor or superconductor, we have synthesized and characterized partially oxidized phthalocyanine salts and related compounds.

IV-B-1 Optical Spectra of Highly Conducting Phthalocyanine Salts

Kyuya YAKUSHI, Hideo YAMAKADO, Takashi IDA, Akito UGAWA, Hideki MASUDA, and Haruo KURODA (Univ. of Tokyo)

The polarized reflectance spectra were measured on the single crystals of unoxidized PbPc; partially oxidized phthalocyanine salts, $NiPc(AsF_6)_{0.5}$, $CoPc(AsFP_6)_{<0.5}$, $H_2Pc(AsF_6)_{0.67}$; and neutral radical LiPc. The absorption bands in the visible region are assigned by comparing these spectra. Based on this assignment, the oxidation part of $CoPc(AsF_6)_{<0.5}$ and the pressure dependence of $NiPc(AsF_6)_{0.5}$ are discussed.

IV-B-2 High-Pressure Optical Study of Partially Oxidized Metallophthalocyanines and Metallotetrabenzo-porphyrins

Takashi IDA, Hideo YAMAKADO, Hideki MASUDA, Kyuya YAKUSHI, Daisuke KANAZAWA*, Hiroyuki TAJIMA*, and Haruo KURODA* (*Univ. of Tokyo)

The reflectance spectra of (phthalocyanato)nickel(II) hexafluoroarsenate ($[Ni(Pc)]_2AsF_6$) and (tetrabenzoporphyrinato)nickel(II) hexafluoroarsenate ($[Ni(tbp)]_3(AsF_6)_2(C_{10}H_7Cl)$) were measured at high pressures. The pressure dependence of the reflectance spectrum of $[Ni(pc)]_2AsF_6$ suggests that the charge-carrying hole moves from the organic ligand to the central metal ion under high pressure.

IV—C Electronic Structures of Organic Metals

The band parameters of organic metals are fundamental quantities in a physical and chemical aspect. In a physical sense, they represent the basic field in which electrons or holes interplay along with phonons or other elementary excitations. In a chemical sense, these parameters provide the magnitude and anisotropy of an intermolecular charge-transfer interaction, which together with the ionization potential or electron affinity of candidate molecules works as the quantitative guide to design a specific architecture in the solid. This project is related to the determination of the band parameters.

IV-C-1 Relation between the Dimensionality of Electronic Structure and the Correlation Effect in (BEDT-TTF)₂X System

Akito UGAWA, Kyuya YAKUSHI, and Haruo KURODA (Univ. of Tokyo)

The optical properties of $(BEDT-TTF)_2X$ (α'-, β-, β'-, β''-, δ-, and κ-types) have been studied to elucidate the relationship between the crystal structure and the electronic structure in these charge-transfer salts. Although there is a structually two-dimensional network of mutually interacting BEDT-TTF molecules in the series compounds, the two-dimensional character of the electronic structure markedly varies depending on

the lattice type. The reflectance spectra are analyzed by the Drude-Lorentz model to describe the conduction band in terms of the effective mass approximation. The results indicate the correlation effect strongly appears when the system is of one-dimensional character, and that the screening of electron correlation becomes more efficient on increasing the dimensionality of electronic structure.

IV-C-2 Transport and Magnetization studies of β'-(BEDT-TTF)$_2$AuBr$_2$

A.G. Swanson*, J.S. Brooks*, M. Tokumoto**, A. Ugawa, and K. Yakushi (*Boston Univ., **ETL)

The de Haas van Alphen and Shubnikov de Haas frequencies of β'(BEDT-TTF)$_2$AuBr$_2$ indicate that the closed portion of the Fermi surface corresponds to 2.9% of the first Brillouin zone. The angular dependence of the data suggests a quasi three-dimensional Fermi surface. The Hall measurements yield a hole like carrier concentration of $\sim 3 \times 10^{19}$ cm^{-3}, substantially less than a carrier concentration assumming one carrier per unit cell.

IV-C-3 Polarized Reflectance Spectra of DCNQI Salts

Kyuya YAKUSHI, Akito UGAWA, Gen OJIMA*, Takashi IDA*, Hiroyuki TAJIMA*, Haruo KURODA*, Akiko KOBAYASHI*, Reizo KATO**, and Hayao KOBAYASHI** (*Univ. of Tokyo, **Toho Univ.)

Temperature dependence of the polarized reflectance spectra have been measured on the single crystals of Ag(DMe-DCNQI)$_2$, Na(DMe-DCNQI)$_2$, Cu(MeBr-DCNQI)$_2$, and Cu(DMe-DCNQI)$_2$ (DCNQI stands for dicyanoquinonediimine). The optical spectra evidence one-dimensional band structures of Ag- and Na-salts and anisotropic three-dimensional ones of Cu-salts. The dimensionality crossover is found in Cu(MeBr-DCNQI)$_2$ around the metal-insulator phase transition.

IV—D   Studies of Collisional Deactivation Processes of Electronically Excited Molecular Ions

Collisional deactivation processes of electronically excited ions are of interest because they may exhibit new aspects of molecular interactions, which are different from those of the neutral molecules, especially in connection with the existence of the charge. A time-resolved laser-induced fluorescence technique is available to obtain the rate constants for total deactivation and vibrational relaxation processes of a single ro-vibronic state. A threshold photoelectron-secondary ion coincidence technique allows direct determination of the reaction cross section as a function of the internal and collisional energies of reactants. In this project, we combine these two techniques to study individual deactivation processes of vibronically excited molecular ions separately.

IV-D-1 Collision-Induced Vibrational Relaxation Processes of CO$^+$ A$^2\Pi$ (ν=1 and 2) by He and Ar

Takashi IMAMURA, Takashi IMAJO (Kyushu Univ.), Shinzo SUZUKI (IMS and Tokyo Met. Univ.), and Inosuke KOYANO (IMS and Himeji Inst. of Tech.)

Collision-induced vibrational relaxation processes of CO$^+$A$^2\Pi$ (ν=1 and 2) by He and Ar have been studied by use of a flowing-after-glow technique combined with laser-induced fluorescence detection. The time-profile of emission from the ν=1 A$^2\Pi$ level following the excitation to the ν=2 level can be reproduced by a three level model, i.e., the population of ν=1 via an intermediate level, in addition to the direct transition from ν=2 to ν=1. In contrast to the ν=1 emission, the time-resolved fluorescence from ν=0 fol-

lowing $\nu=1$ excitation is reproducible, for the most part, by a two level model. This can be ascribed to the strong coupling between the $\nu=0$ $A^2\Pi$ and the $\nu=10$ $X^2\Sigma$ levels. The intensity ratios of the relaxed and prompt emission, $I(\nu'')/I(\nu')$, were measured as a function of the pressure of the quencher $P(Q)$, where $Q=$He or Ar. From the analysis of $I(\nu'')/I(\nu')$ vs $P(Q)$, the rate constants for the vibrational relaxation processes were obtained and are listed in Table 1. As is seen in the table, collision-induced vibrational relaxation by Ar is much more effective than by He. This may be related to the availability of the charge transfer state $(Ar^+\text{-}CO)$ in the $CO^+(A^2\Pi)+Ar$ system.

Table 1. Rate constants of vibrational relaxation of $CO^+A^2\Pi$ induced by the collision with He and Ar.

Quencher	$k_{\nu'-\nu''}/cm^3molec^{-1}s^{-1}$	
	$(v'=2)\to(v''=1)$	$(v'=1)\to(v''=0)$
He	$2.3\times10^{-12a)}$	7×10^{-13}
Ar	2.3×10^{-10}	3.3×10^{-10}

a) This value corresponds to $\sqrt{k_{2-x}\cdot k_{x-1}}$ where x represents the vibrational level of the $X^2\Sigma$ state.

IV-D-2 State-Selected Charge Transfer Reactions $CO^+(A^2\Pi\ \nu', X^2\Sigma\ \nu'') + Ar \to Ar^+ + CO$

Takashi IMAMURA, Shinzo SUZUKI *(IMS and Tokyo Met. Univ.)*, Takashi IMAJO *(Kyushu Univ.)*, and Inosuke KOYANO *(IMS and Himeji Inst. of Tech.)*

The first electronically excited state, $A^2\Pi$, of CO^+ is effectively quenched in collisions with atoms and molecules of which the ionization potentials are smaller than the binding energy of $CO^+A^2\Pi$.[1] As possible mechanisms of collisional deactivation, the reactions such as charge transfer are expected in addition to the vibrational and electronical relaxations. Ar effectively quenches the $A^2\Pi$ state of CO^+ with the quenching rate constant of about 1×10^{-9} $cm^3molec^{-1}s^{-1}$ at room temperature. Thus, the charge transfer reactions $CO^+(A^2\Pi, \nu) + Ar \to Ar^+ + CO$ (1) are expected to

be an important channel of the quenching of $CO^+A^2\Pi$. The charge transfer reaction (1) has been studied by the threshold photoelectron-secondary ion coincidence (TESICO) technique.[2] Owing to the short lifetime of the $A^2\Pi$ state of CO^+ (3-5 μs), the single chamber mode of operation has been employed. Assuming that the collection efficiencies of the primary and secondary ions are identical, the reaction cross sections were determined as shown in Figure 1 as a function of the vibrational state. A resonantly enhanced charge transfer cross section has been found at the $\nu=1$ level of the $A^2\Pi$ state. In order to explain the experimental results, it may be necessary to consider both the direct Demkov type and intimate Landau-Zener type mechanisms.

References
1) T. Imajo, T. Imamura, and I. Koyano, *Chem. Phys. Lett.*, **160**, 143 (1989).
2) I. Koyano and K. Tanaka, *J. Chem. Phys.*, **72**, 4858 (1980).
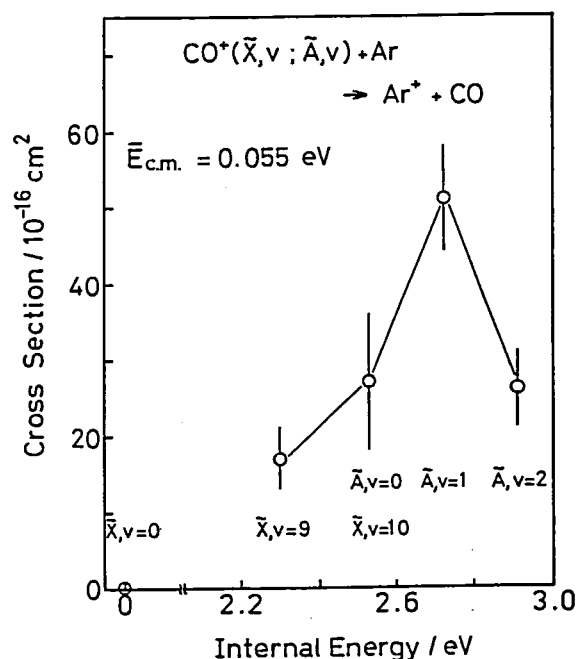
Figure 1. Cross section for the charge transfer reaction $CO^+(A^2\Pi, \nu'; X^2\Sigma, \nu'') + Ar \to Ar^+ + CO$ as a function of the vibronic state of CO^+, obtained at the average collision energies of 0.055 eV.

IV—E Studies of Ion-Pair Formation and Ionic Fragmentation in the VUV and Soft X-Ray Regions Using Synchrotron Radiation

Ion-pair formation is a very common process of highly excited molecules in the photon energy range of 10-50 eV. A great interest has been taken in the dynamics of the photodissociation into ion-pairs as half-collisional version of the electron transfer reaction. At higher photon energies, the decomposition of multiply charged ions leads to the so-called "Coulomb explosion" processes producing two or more singly charged ions and these also play an important role in the radiation induced decomposition of molecules. Synchrotron radiation is a powerful light source for these studies in the VUV and soft X-ray regions. In the present project, we aim at a systematic and extensive study of the dynamics of the ion-pair formation and dissociative photoionization of polyatomic molecules.

IV-E-1 Negative-Ion Mass Spectrometric Study of Ion-Pair Formation in the Vacuum Ultraviolet. $SF_6 \rightarrow F^- + SF_5^+$

Koichiro MITSUKE (Univ. of Tokyo), Shinzo SUZUKI (IMS and Tokyo Met. Univ.), Takashi IMAMURA, and Inosuke KOYANO (IMS and Himeji Inst. of Tech.)

[*J. Chem. Phys.* **93**, 8717 (1990)]

Ion-pair formation from photoexcitation of SF_6 has been studied by negative-ion mass spectrometry using synchrotron radiation in the 11.27-31.0 eV photon energy range. Negative ions F^-, SF_6^-, and SF_5^- have been observed. The appearance energy of the F^- ion is about 1 eV higher than the thermochemical threshold for the formation of the pair of the ground state ions F^- (^1S_g) and SF_5^+ ($\tilde{X}\,^1A_1$). The peak features observed in the F^- efficiency curve (Figure 1) are interpreted as resulting from transitions to neutral excited states with the $^1T_{1u}$ symmetry which effectively couple with ion-pair states through avoided potential crossings. The peaks assigned to diffuse Rydberg states are distinctively enhanced in the F^- efficiency curve, probably because of large transition probabilities from the dissociative Rydberg states to the ion-pair channel. Consequently, the corresponding peaks are markedly suppressed in the F^- spectrum. Assignments of the peak features in the previous photoabsorption spectra are also performed by using the term values for related Rydberg and virtual valence orbitals. Other negative ions observed, SF_6^- and SF_5^-, are produced by resonance capture of low energy electrons emitted by photoionization of the parent molecules.
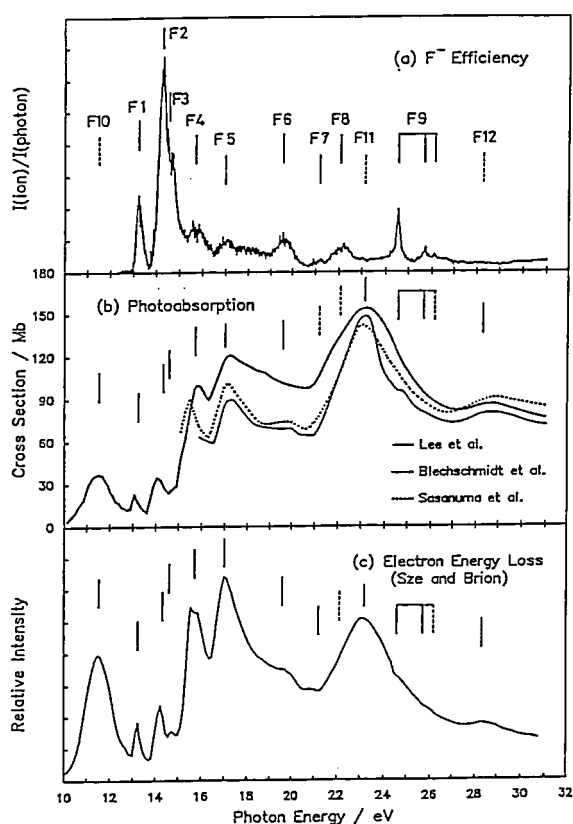
Figure 1. Comparison among (a) photodissociation efficiency curve of F^- produced from SF_6 (this work), (b) photoabsorption cross section curves taken from literatures, and (c) high resolution electron energy loss spectrum reported by Sze and Brion.

IV-E-2 Negative-Ion Mass Spectrometric Study of Ion-Pair Formation in the Vacuum Ultraviolet. $CH_3X \rightarrow X^- + CH_3^+$ (X=F, Cl, and Br)

Shinzo SUZUKI *(IMS and Tokyo Met. Univ.)*, Koichiro MITSUKE *(Univ. of Tokyo)*, Takashi IMAMURA, and Inosuke KOYANO *(IMS and Himeji Inst. of Tech.)*

Ion-pair formation processes $CH_3X \rightarrow X^- + CH_3^+$ (X=F, Cl, and Br) have been investigated in the 10.0-30.0 eV photon energy range using synchrotron radiation from the UVSOR storage ring. It has been shown that the efficiency curve for the formation of X^- has two features in this photon energy range. Figure 1 shows the efficiency curves for the formation of X^- from CH_3X in the higher energy range (about 15.0-30.0 eV). The intensities of these bands are much smaller than those of the bands observed in the lower energy range (around the ionization threshold of CH_3X). Each band seems to have at least two peaks (indicated by arrows). The peaks located at shorter wavelengths in these figures are considered to be due to the $4a_1 \rightarrow ns$ Rydberg transition in the corresponding molecules. According to the EELS study by Hitchcook and Brion,[1] several peaks assignable to the excitations to the Rydberg states of CH_3X should exist. However, our spectra in the higher photon energy range seem to contain only two peaks in each case. It may be that difference among these Rydberg states in their coupling with ion-pair states causes this discrepancy.

Reference
1) A.P. Hitchcook and C.E. Brion, *J. Electron Spectrosc. and Relat. Phenom.*, **17**, 139 (1979).
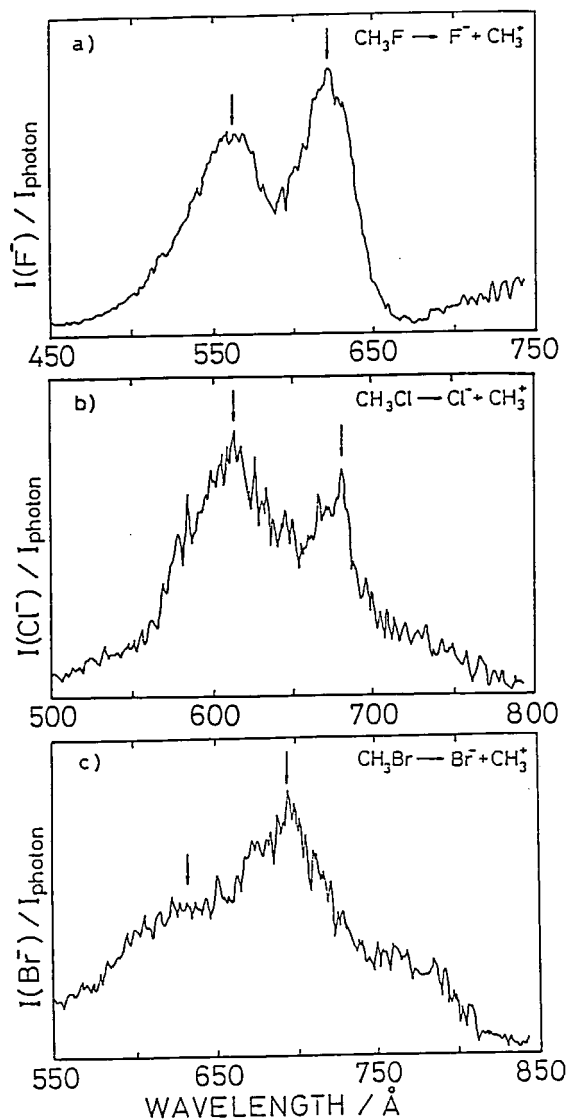
Figure 1. Photodissociation efficiency curves of X^- (X=F, Cl, Br) produced from CH_3X.

IV-E-3 Dissociative Single, Double and Triple Photoionization of SiF₄ in the Valence Shell and Si2p Regions ($h\nu$=33-133 eV)

Takashi IMAMURA, C.E. BRION *(IMS and Univ. of British Columbia)*, Inosuke KOYANO *(IMS and Himeji Inst. of Tech.)*, Toshio IBUKI *(Kyoto Univ.)*, and Toshio MASUOKA *(Osaka City Univ.)*

The photoionization of SiF_4 in the valence shell and Si2p inner shell regions has been studied using time-of-flight mass spectrometry and synchrotron radiation over the photon energy range 33-133 eV. Photoionization branching ratios are reported for stable singly and doubly charged ions arising from the various possible molecular and dissociative photoionization processes. With increasing the photon energy from the valence shell region (≤ 100 eV) to the Si2p inner shell region (≥ 106 eV), the photoionization branching ratio of SiF_3^+ decreases and those of the small fragment ions such as F^+, Si^+, Si^{2+} etc. contrarily increases (Figure 1a). Photoion-photoion coincidence (PIPICO) techniques have been used to investigate the relative yields of Coulomb explosion decomposition products and threshold energies for dissociative double photoionization in the valence shell and Si2p regions. The PIPICO branching ratios of dominant processes are shown in Figure 1b. The dominant process in the Si2p region is $(F^+ + Si^+)$. The PIPICO spectra show additional peaks

with thresholds in the Si2p region and these structures arise from the dissociation of triply charged ions into the exit channels ($F^+ + SiF_2^{2+}$), ($F^+ + SiF^{2+}$) and ($F^+ + Si^{2+}$). Of these the latter is the most probable process.
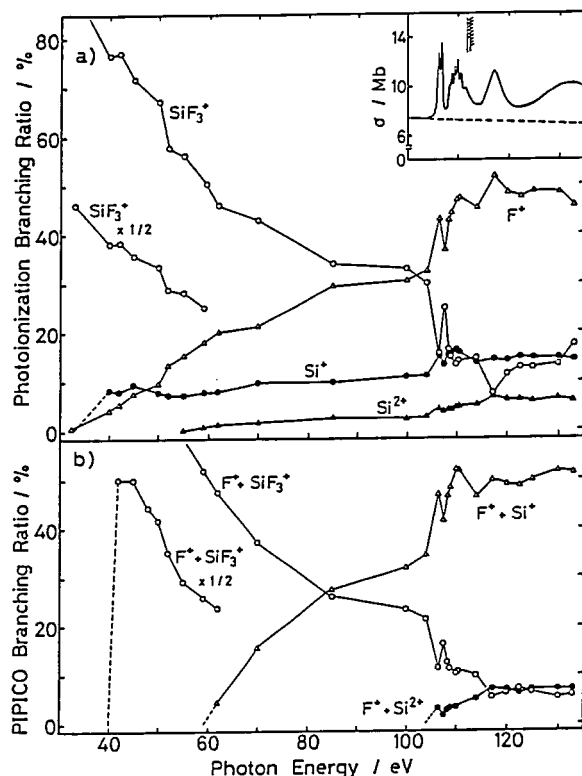
Figure 1. (a) Photoionization branching ratios for dominant stable singly and doubly charged ions. (b) PIPICO branching ratios for dominant processes.

IV-E-4 Ionic Fragmentation Following the 3p and 3s Core Excitation of $Ga(CH_3)_3$ by Soft X-Ray

Kiyoshi UEDA *(Tohoku Univ.)*, Yukinori SATO *(Tohoku Univ.)*, Shinichi NAGAOKA *(IMS and Ehime Univ.)*, Inosuke KOYANO *(IMS and Himeji Inst. Tech.)*, Akira Yagishita *(National Lab. High Energy Phys.)*, and Tatsuji Hayaishi *(Univ. of Tsukuba)*

Ionic fragmentation following the core-level photoionization of $Ga(CH_3)_3$ has been studied between 90 and 260 eV by use of monochromatized synchrotron radiation and time-of-flight mass spectrometry. The average kinetic energies of CH_n^+ (n=0-3) and H^+ produced through the ionic fragmentation are estimated to be about 4 and 7 eV, respectively. The production of H^+ is significantly enhanced by the Ga 3p and 3s photoionizations. A similar enhancement in the H^+ production was also observed previously in the fragmentation following the Sn 3d and 4p photoionization of $Sn(CH_3)_4$ and the Pb 4p and 4f photoionization of $Pb(CH_3)_4$. Thus the enhancement in the H^+ production by the deep metal-core photoionization seems to be a common feature for organometallic molecules. The H^+ production might be ascribed to a secondary decomposition of the primary fragment with high internal energy, the candidates of the latter being CH_n^+ and/or CH_n^{2+}.

IV—F   Development of High-Resolution Laser Photoelectron Spectroscopy for Excited-State Molecules

Recently we have succeded to measure laser excited-state photoelectron spectra in a resolution of "4 cm^{-1}" by using a compact capillary-type threshold photoelectron analyzer which we have newly developed in this Institute.

Laser photoelectron spectroscopy for studying excited molecules has been developed in this Institute by K. Kimura and his coworkers since 1980 [*IMS Annual Review* (1980-90); K. Kimura, *Advances in Chemical Physics*, **60**, 161 (1985)]. Since any electronically excited states can in principle be ionized by an appropriate laser to eject photoelectrons, a photoelectron spectroscopic technique is powerful for detecting not only radiative excited states but also non-radiative excited states. From such an excited-state photoelectron study, it is also possible to explore new ionic states which cannot be produced from the neutral ground-state molecules by single photons.

In this project, we have been further developing our laser photoelectron techniques by introducing the following devices: (1) tunable vacuum ultraviolet lasers, (2) a capillary-type high-resolution threshold photoelectron analyzer, and (3) a 50-100 cm time-of-flight photoelectron analyzer.

IV-F-1 New High-Ressolution Threshold Photoelectron Analyzer

Masahiko TAKAHASHI, Katsuhiko OKUYAMA, and Katsumi KIMURA

A new-type threshold photoelectron analyzer with a capillary plate has been designed to study vibrational spectroscopy of molecular cations with a two-color multiphoton ionization (MPI) technique. Figure 1 shows a schematic drawing of our threshold photoelectron analyzer. Our idea of using this analyzer is to use a capillary plate to collect threshold photoelectrons which are ejected from molecules in the absence of electric filed. Photoelectrons with kinetic energies rapidly disappear from the ionization region after each laser shot, while threshold photoelectrons (with nearly zero kinetic energies) remain in the ionization region during a certain time., The purpose of using the capillary plate to prevent most kinetic photoelectrons from reaching an electron multiplier (Ceratron) which is used for the electron detection. Applying an appropriate electric field at a certain delay time (typically at 500 ns) after each laser shot, we can more efficiently collect only the threshold photoelectrons which still remain in the ionization·volume.

With this analyzer, we have succeeded to measure a photoelectron spectrum in an energy resolution of 4 cm^{-1} (fwhm). For example, in the (1+1') resonant ionization of NO molecule via the $A^2\Sigma^+$ state (v=0, N=7), we were able to observe a rotationally-resolved photoelectron spectrum.
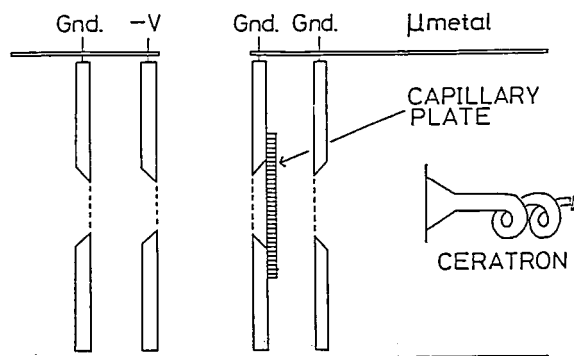
Figure 1. A compact capillary-type threshold photoelectron analyzer.

IF-F-2 MPI-TPES Study of Rotational Isomers of *n*-Propylbenzene Cation

Masahiko TAKAHASHI, Katsuhiko OKUYAMA, and Katsumi KIMURA

In the present work, we have applied our new capillary-type analyzer (see IV-F-1) to obtain high-resolution photoelectron spectra for studying low frequency vibrational modes of molecular cations with rotational isomers. In the present work, gaseous n-propylbenzene has been studied, since it is the smallest alkyl benzene which exists in both *gauche* and *trans* forms in the gas phase with different energies at the $S_1(\pi\pi^*)$ states.

Figure 1 shows threshold photoelectron spectra of *gauche* and *trans* n-propylbenzene in free jets, obtained by two-color (1+1') resonant ionization via the 0^0 level of the S_1 state, indicating a big difference in spectral pattern between the two rotational isomers in a low energy region. These photoelectron vibrational structures (Figure 1) suggest that the geometrical changes of the cations take place differently upon photoionization, and the interaction of the propyl group with the benzene ring is largely different between the *gauche* and *trans* forms. The adiabatic ionization potentials (I_a) have been determined in a resolution of 4 cm^{-1}: Namely, 9.7118 ± 0.0005 eV (*trans*) and 8.7294 ± 0.0005 eV (*gauche*). In order to understand these vibrational structures, we have been carrying out *ab initio* calculations of normal modes for the *gauche* and *trans* cations. It should be mentioned that such a high-resolution photoelectron spectroscopy provides a new "vibrational spectroscopy" for molecular cations, just corresponding to the infrared spectroscopy of molecules.
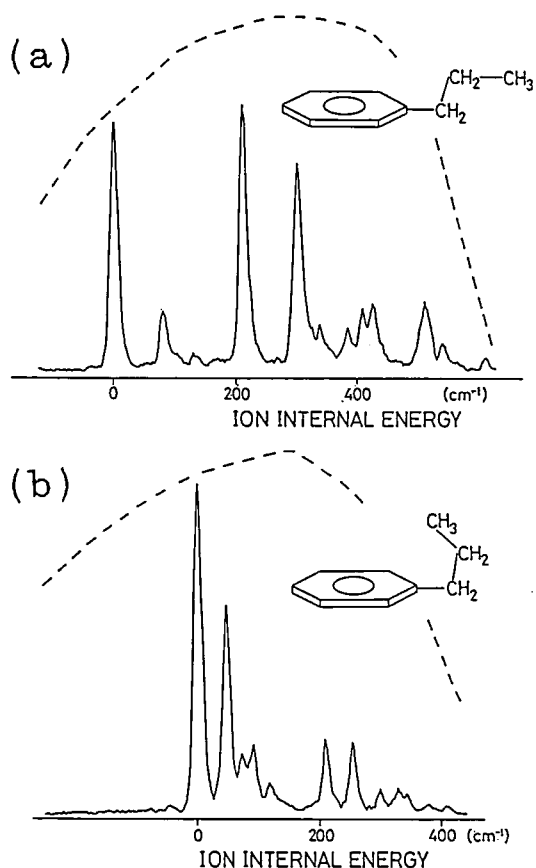
Figure 1. Threshold photoelectron spectra of n-propylbenzene: (a) *trans* form, and (b) *gauche* form. Dashed curves show the intensities of the ionization laser used.

IV-F-3 REMPI Photoelectron Spectra of Jet-cooled p-Phenylenediamine

Hiroyuki OZEKI, Katsuhiko OKUYAMA, Masahiko TAKAHASHI and Katsumi KIMURA

Resonanly enhanced multiphoton ionization (REMPI) photoelectron spectra of jet-cooled p-phenylenediamine have been observed for the first time by a time-of-flight method. The observed spectra show well-resolved structure, suggesting that the ionization transitions occur from the optically prepared single vibronic levels in the S_1 excited state. We have also found some vibrational frequencies of the cation; namely, modes 1, 6a and X. Here, X has been tentatively assigned to a symmetric inversion motion of the amino groups. The observed photoelectron peaks were almost assigned to these vibronic bands or combination bands. Comparing the vibrational frequencies in the ionic state (D_0) with those in the S_0 and S_1 states, the 6a and 1 modes are

not so different, but the X mode is very large in the D_0 state. From these assignments, we may consider that the C-N bond order in the ionic state increases, and the ion seems to form the quinoide structure.

We have also employed a threshold photoelectron technique with a time-delayed pulse method in order to determine the more accurate ionization potential. With this technique, we have obtained an ionization potential value of 6.774 ± 0001 eV.
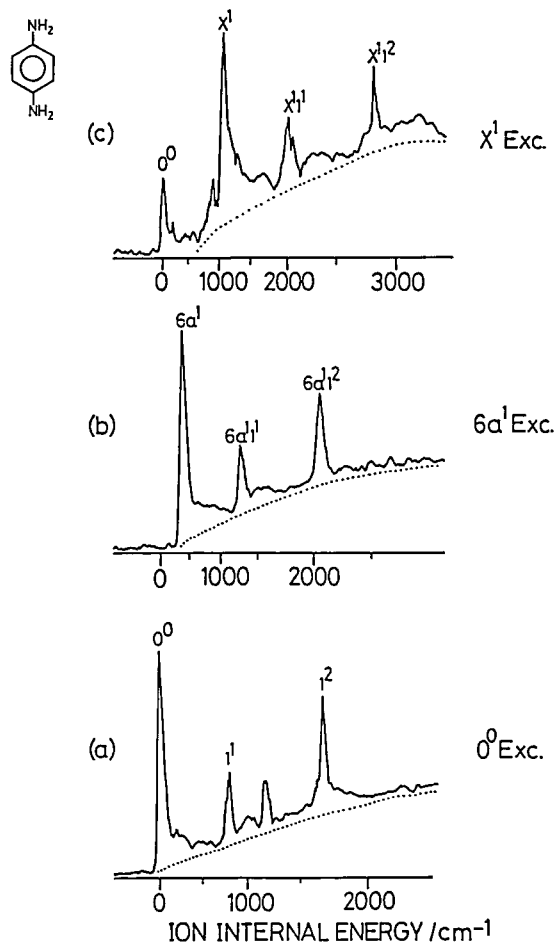
Figure 1. REMPI photoelectron spectra of p-phenylenediamine, obtained by two-color (1+1) resonant ionization via the vibronic levels of the S_1 state.

IV-F-4 A New High-Resolution TOF Photoelectron Analyzer

Katsuhiko OKUYAMA, Hiroyuki OZEKI, Masahiko TAKAHASHI and Katsumi KIMURA

A TOF (time-of-flight) photoelectron spectrometer

has an advantage of observing a photoelectron spectrum in a wide energy range. A high-resolution TOF spectrometer combining with an MPI technique is, therefore, an essential tool for studying the spectroscopy of molecular cations and pursuing the dynamic behavior of electronically excited neutral molecules. Recently we have designed and improved a high-resolution TOF photoelectron analyzer. At the present stage, we have obtained a satisfactory result in the spectral resolution. Figure 1 shows a photoelectron spectrum obtained by (1+1) resonant ionization via the 0^0 level in the lowest singlet excited state of jet-cooled p-phenylenediamine. The 0^0 band position corresponds to its adiabatic ionization potential, 6.82 eV. The spectrum shows several sharp bands on a broad background. We were able to obtain our best resolution of 4.8 meV (fwhm) at photoelectron kinetic energy of 361 meV. So far a resolution of 2.0 meV has been reported at a photoelectron energy of 180 meV [S.W. Allendorf et al., J. Chem. Phys. **91**, 2216 (1989)]. From our observed band widths we have estimated our

resolution at 180 meV to be 1.8 meV. The broad background is probably due to anomalous cascade inside the MCP detector used.
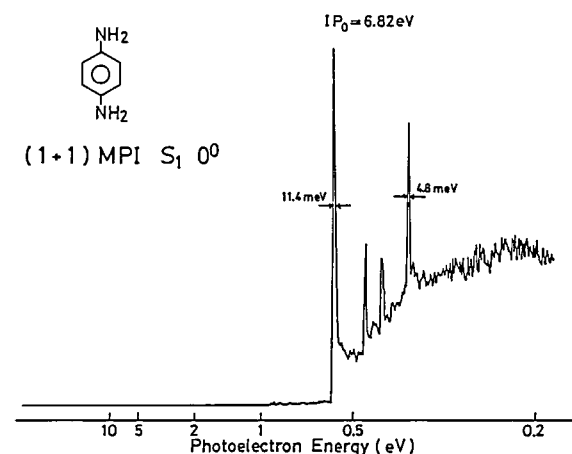
Figure 1. TOF photoelectron spectrum obtained by (1+1) resonant ionization via the 0^0 level in the lowest singlet excited state of jet-cooled phenylenediamine.

IV—G   Synchrotron Radiation Researches of Molecules and Molecular Clusters: Photoionization and Photoelectron Spectroscopy

The use of synchrotron radiation is attractive for studying photoionization and photoelectron spectroscopy of gaseous atoms, molecules and molecular clusters produced in supersonic jets. For this purpose, we have been using two kinds of photoionization apparatuses using the synchrotron radiation of the 750-MeV electron storage ring called UVSOR in this Institute. One is a molecular-beam apparatus on beamline BL2B2, using a multi-stage differential pumping system not to use any window materials between the molecular-beam apparatus and the storage ring. The other is a PEPECO apparatus on beamline 3A2, using undulator radiation. The PEPECO apparatus has been constructed to study doubly charge ions of gaseous atoms and molecules as well as to perform coincidence measurements of two photoelectrons.

IV-G-1   Decay of the *4d* Hole State of Xe Studied by Photoelectron-Photoelectron Coincidence Spectroscopy

Katsuhiko OKUYAMA, John H.D.Eland *(Oxford Univ.)* **and Katsumi KIMURA**

The formation of Xe^{2+} by decay of 4d hole states in Xe has been investigated by observing both the $N_{4,5}OO$ normal Auger spectra and the resonantly excited spectra using synchrotron radiation and a new form of electron-electron coincidence spectroscopy involving a magnetic-bottle time-of-flight analyzer. Direct double Auger processes from the resonance populate all accessible states of Xe^{2+}, while indirect processes via superexcited Xe^+ levels populate the ground and lower excited states of Xe^{2+} preferentially.

IV-G-2 Threshold Photoelectron-Photoion Coincidence Measurements for the Fragmentation Study of $CO_2^+(C^2\Sigma_g^+)$

Kenji FURUYA, Yasuhiro SAKAI *(Sophia Univ.)*, Takato HIRAYAMA *(Gakushuin Univ.)*, and Katsumi KIMURA

On the beamline BL2B2 in the UVSOR Facility, we have carried out measurements of threshold photoelectron-photoion coincidence (TEPICO) spectra in order to study the fragmentation processes of small molecules and the photoionization processes of mass-selected atomic and molecular clusters.

The fragmentation process of $CO_2^+(C^2\Sigma_g^+)$ is very interesting in the point of that the process changes in dependence with the excess energy above the C state.[1] The TEPICO spectra obtained by exciting CO_2 to the $C^2\Sigma_g^+(0,0,0)$ ($\lambda_{ex} = 63.96$ nm) and $C^2\Sigma_g^+(1,0,1)$ ($\lambda_{ex} = 62.78$ nm)[2] states are shown in Figure 1 (a) and (b), respectively. In these spectra the peak of CO_2^+ is due to false coincidence because it is known that the $C^2\Sigma_g^+$ state is fully dissociative,[1] and because at these excitation wavelengths many CO_2^+ ions are produced in comparison with O^+ and CO^+ ions; the CO_2^+/O^+ and CO_2^+/CO^+ ratios are about 50 and 150, respectively. Figure 1 (a) and (b) clearly show that the fragmenta-

tion process of the CO_2^+ $C^2\Sigma_g^+(0,0,0)$ state is quite different from that of the (1,0,1) vibrationally excited state.

References

1) J.H.D. Eland and J. Berkowitz, *J. Chem. Phys.* **67**, 2782 (1977).
2) This assignment is based on the following article: T. Baer and P.M. Guyon, *J. Chem. Phys.* **85**, 4765 (1986).
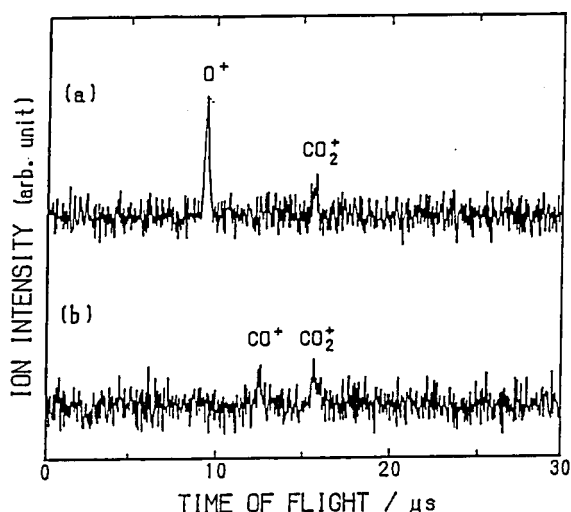
Figure 1. TEPICO spectra of CO_2 (a) at 63.96 nm ($C^2\Sigma_g^+(0,0,0)$ excitation), (b) at 62.78 nm ($C^2\Sigma_g^+(1,0,1)$ excitation).

IV—H Production, Characterization, and Spectroscopic Studies of Molecular Complexes and Clusters

There are several techniques to investigate physics and chemistry of molecular complexes and clusters. One of the most powerful techniques for producing such weakly bound complexes is supersonic expansion of a high pressure gas through a small nozzle hole, by which one can produce a large numbers of exotic molecules. However, quantitative characterization of van der Waals complexes is hard because of its weak bonding character. In this project we apply laser induced fluorescence spectroscopy combined with a nanosecond time resolved fluorescence technique to study dynamics of electronically excited rare gas clusters and solvated molecules of substituted anthracenes produced in a free jet expansion.

IV—I Molecular Beam Studies of Gas Phase and Surface Reaction Dynamics

In this project we investigate dynamics of bimolecular reactions using a crossed molecular beam technique and of surface reactions using a molecule-surface scattering technique. Experimental data obtained in this project are angular and velocity distributions of the scattered species detected by a rotatary quadrupole mass spectrometer combine with a TOF technique as functions of reactant collision energy and, in the case of surface reactions, surface conditions

such as temperature and surface structure. In order for surface experiment to be performed under ultrahigh vacuum conditions the apparatus for Molecular Beam Chemistry (model MBC-I) which have been used for crossed molecular beam experiments has been modified. In the project of dynamics of surface reactions we are especially interestd in obtaining information on interaction energies between gaseous molecules and characterized surface in relation to the reactivities.

IV—J   Vacuum UV Photochemistry of Molecules and Clusters

Photochemistry by vacuum UV (VUV) light has recently become a very active field owing to the rapid progress in and the relatively easy access to the VUV light sources such as synchrotron orbital radiation (SR) and VUV laser as well as conventional atomic resonance lines. In the present project we seek to obtain more detailed information about, 1) photodissociation dynamics of simple molecules, 2) production of emitting species from highly excited molecules, 3) excited states of clusters formed in a supersonic free-jet, and 4) excimer formation reactions of van der Waals molecules and clusters. Experimentally, absorption and fluorescence (polarization) spectroscopies of gaseous molecules in a cell and molecular clusters and/or molecular complexes are employed using the tunable and polarized VUV light from the UVSOR facility.

IV-J-1   He(I)   Photoelectron   Spectra   and VUV Absorption Cross Sections of $Ga(CH_3)_3$ and $In(CH_3)_3$

Toshio IBUKI *(Kyoto Univ.)*, Atsunari HIRAYA, Kosuke SHOBATAKE, Yutaka MATSUMI*, and Masahiro KAWASAKI *(*Hokkaido Univ.)*

He(I) photoelectron spectra (PES) and photoabsorption cross sections were measured for $Ga(CH_3)_3$ and $In(CH_3)_3$ in the 106-270 nm range. For both compounds, absorption starts at around 260 nm. Using the binding energies determined from the PES data, the broad absorption bands observed for the trimethylmetals are assigned as ns-terminating Rydberg transitions of the outer orbital electrons.

IV-J-2   Photodissociation   Dynamics   of   HCN in 135-145 nm

Takashi NAGATA*, Kazuhiro KANDA *(Iwaki Meisei Univ.)*, Tamotsu KONDOW *(*Univ. of Tokyo)*, Atsunari   HIRAYA   *(UVSOR)*,   and   Kosuke SHOBATAKE

Photodissociation dynamics of HCN was studied by the measurements of the fluorescence excitation and the optical polarization of subsequent CN(B-X)

emission in the 135-145 nm range The dispersed SR was introduced through a LiF window into a cell containing HCN gas of ~20 mTorr. Emission from the product CN(B) radical was collected at a right angle to the incident radiation. The polarization anisotropy (R) of the emission was measured with reference to the electric vector of the SR by a polarimeter developed in the present work. Figure 1 shows the observed polarization anisotropy as a function of excitation wavelength along with the fluorescence excitation spectrum. The prominent peaks appearing in the excitation spectrum were assignable to the ν_2 (bending mode) progression of the C-X transition. The non-zero base line of the spectrum is due to the underlining continuum. The R value was observed to be positive for the ν_2 progression, whereas negative for the continuum. This indicates that the C sate belongs to A' symmetry and the continuum to A" symmetry. The vibrational structures observed in the polarization anisotropy are probably ascribed to the $(0\nu_2 1)$ and the $(1\nu_2 0)$ progressions, while they are not distinct in the excitation spectrum. Careful examination of the R values for the $(0\nu_2 0)$ progression revealed that predissociation from K=1 levels proceeds much faster than that from K=0 levels of the C states, indicating heterogeneous predissociation.
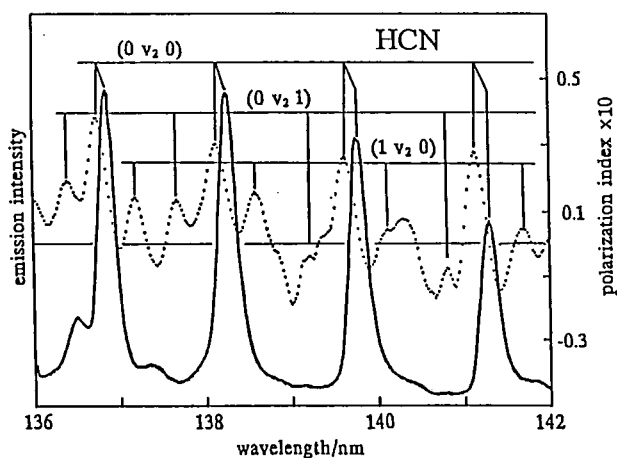
Figure 1. Fluorescence excitation (solid line) and polarization (dotted line) spectra of HCN in the wavelength range of 135-145 nm.

IV-J-3 Photodissociative Excitation Processes of BrCN in the 107-155 nm Region Studied by Absorption, Fluorescence Excitation and Fluorescence Polarization Spectral Measurements

Kazuhiro KANDA*, Takashi NAGATA**, Hiroshi OZAKI *(Natl. Environ. Res. Inst.)*, Shunji KATSUMATA *(*Iwaki Meisei Univ.)*, Tamotsu KONDOW *(**Univ. of Tokyo)*, Atsunari HIRAYA *(UVSOR)*, and Kosuke SHOBATAKE

Photodissociative excitation processes of BrCN are studied by the measurements of the fluorescence excitation and the optical polarization of subsequent CN(B-X) emission in the 107-155 nm range. The dispersed SR was introduced through a LiF window into a cell containing BrCN gas. Emission from the CN(B) product radical was collected at a right angle to the incident radiation. The polarization anisotropy (R) of the emission was measured with reference to the electric vector of the SR by a polarimeter developed in the previous work. Figure 1 shows the observed (a) polarization anisotropy R, (b) quantum yield, and (c) intensity of CN(B-X) fluorescence against excitation wavelength. We find that at around 145 nm the quantum yield at a fluorescence peak exhibits a dip, which is indicative of the presence of a broad continuum state having a high quantum yield for CN(B) formation under the Rydberg transition. The bands are assigned as shown in Figure 1 from the quantum defect and polarization anisotropy. It is noted that the assignements

of the bands have been made more reliable because of the additional information of polarization anisotropy obtained in the present work.
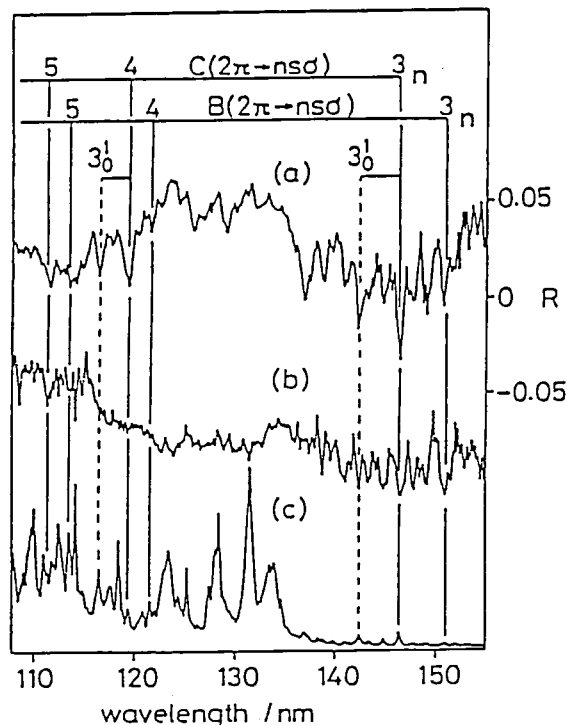
Figure 1. (a) Polarization anisotropy R, (b) quantum yield, and (c) intensity of CN(B-X) fluorescence against excitation wavelength of BrCN in the 107-155 nm region.

IV-J-4 Photochemistry of Rare Gas-Dihalogen van der Waals Molecules. I. Absorption and Fluorescence Excitation Spectra of Rg_n-Cl_2 Clusters

Kiyohiko TABAYASHI, Atsunari HIRAYA *(UVSOR)*, and Kosuke SHOBATAKE

We report the preliminary results on the measurements of absorption and fluorescence excitation spectra for Rg_n-Cl_2 clusters generated in supersonic free jets of binary Cl_2/Rg gas mixtures. The VUV spectra of Xe_n clusters in pure Xe jets have been studied in the wavelength region 1050-1550 Å and the dimer and cluster excitation bands were reasonably assigned[1]. The Xe_n cluster (n > ~200) bands have been found to closely correspond to those of the excitons in solid Xe crystals. When a small amount of Cl_2 (~1%) gas was added to the Xe flow (**Figure 1**), the broad excitonic feature still

appears in the absorption spectrum although it shows slightly deformed and faint in intensity. In contrast, the fluorescence excitation spectrum shows a very low level of fluorescence for the cluster bands and has a rather flat base line. These are indicative of low quantum yield for the radiative decay channels from the excited Xe_n-Cl_2 clusters with large n. It is also concluded that the Förster-Dexter type intra-cluster energy transfer of the excitons to the impurity Cl_2 should be followed by a non-radiative process such as dissociation of Cl_2. Similar absorption and fluorescence results as above have been observed in Kr/Cl_2 system.

Reference
1) A. Hiraya and K. Shobatake, UVSOR Activity Report, **15**, 27 (1987).
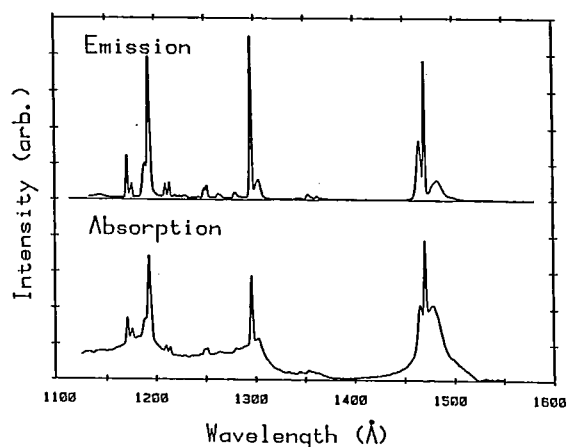
Figure 1. Absorption and fluorescence excitation spectra of a free jet of 1.0% Cl_2/Xe gas mixture at the same stagnation conditions, P_0 = 400 Torr and T_0 = 3°C.

IV-J-5 Photochemistry of Rare Gas-Dihalogen van der Waals Molecules. II. VUV Excitation of Xenon Dichloride (Xe-Cl_2)

Kiyohiko TABAYASHI, Atsunari HIRAYA (UVSOR), and Kosuke SHOBATAKE

Absorption and fluorescence excitation spectra originated from (1:1) Xe-Cl_2 VDWM in the VUV region have been studied in free jets of regulated Cl_2/Xe/Ne mixtures. Figure 1(A) illustrates absorption spectra for some $[Cl_2]/[Xe]/[Ne]$ concentration conditions, in which the absorption bands due to free Cl_2 molecule are substracted such that the sharp feature for the Cl_2 transitions disappears. In lean Xe and Cl_2 mixtures, two broad bands in the 1250-1550 Å region are intrinsic and its intensities are found to be proportional both to $[Cl_2]$ and [Xe], hence they are assigned to (1:1) Xe-Cl_2VDWM excitation. In Figure 1(B) we show typical

fluorescence excitation spectra obtained with detection of 180-650 nm radiation. Although shaded band tail resulted from $Cl_2(X^1\Sigma^+_g\text{-}1^1\Sigma^+_u)$ excitation is superimposed in the lower spectral region, the broad feature of Xe-Cl_2 and a new banded system at ~ 1425 Å, which has not been found in the absorption due to the limited detection ability, are clearly seen in the figure. From the same consideration of $[Cl_2]$ dependence for the fluorescence intensity as described above for the absorption bands, 1425 Å band is also attributed to Xe-Cl_2 excited state. The broad bands are tentatively assigned to the transitions to charge-transfer states of $XeCl^+Cl^-$ and/or $Xe^+Cl_2^-$ entities, the presence of similar $RgCl^+Cl^-$ complex has been proposed in the environment of Cl_2 trapped in Ar/Ne matrices[1]. Further spectroscopic search for the photo-induced reactions for this VDWM system is under way to clarify the outcome of excited VDWM and the origin for the relevant chemiluminescent processes.

Reference
1) P. Gurtler, H. Kunz, and J. Le Calve, *J. Chem. Phys.* **91**, 6020 (1989).
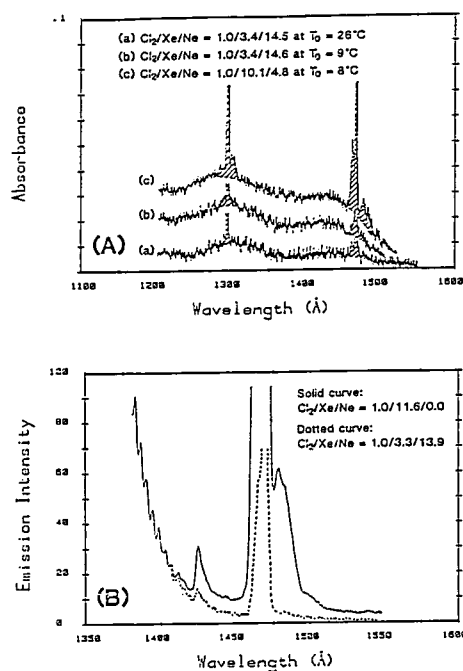
Figure 1. (A) Absorption spectra of Xe-Cl_2 VDWM observed in free jets of Cl_2/Xe/Ne gas mixtures at P_0 = 530-590 Torr. Here, absorption bands of free Cl_2 are reasonably substrated but those of Xe_n(n≥1, hatched bands) remain in the figure. (B) Fluorescence excitation spectra of free jets of Cl_2/Xe/Ne gas mixtures at P_0 = 480-500 Torr and T_0 = 1°C.

IV—K Synchrotron Orbital Radiation-Assisted Surface Reactions

Synchrotron orbital radiation (SR) is still a new light source from the viewpoint of promoting chemical reactions on solid surfaces although lithography of resist materials by means of SR has been known for about a decade. In this project we explore the possibilities of promoting surface reactions, such as etching reactions, or making new types of thin films using SOR as a light source, and furthermore seek to clarify the mechanisms of photochemical reactions which occur on solid surfaces. The experiments are done using an apparatus for photochemical surface reactions installed on the Beam Line BL8A or BL31 at the UVSOR facility. when the apparatus is connected to the beam line BL8A, unfocused synchrotron radiation is irradiated upon the solid sample at 5.85 m from the source point. On the beam line BL3A1 we use pseudo-monochromatic undulator radiation for the etching reactions as well as photochemical vapor deposition.

IV-K-1 Polystyrene Thin Film Formed by Synchrotron Radiation Chemical Vapor Deposition

Hitomi YAMADA*, Makoto NAKAMURA*, Hisato KATOU*, Tetsuo HAYASAKA*, Shinzo MORITA*, Shuzo HATTORI* (*Nagoya Univ.), Haruhikoi OHASHI**, and Kosuke SHOBATAKE

Formation of polystyrene thin films from styrene monomer was investigated by synchrotron radiation chemical vapor-deposition. Polystyrene film was deposited in the irradiated area and the visinity along the irradiation area on a Si substrate. The deposition rate depends on the monomer gas pressure, substrate temperature, and x-ray wavelength. Polystyrene film formed in the irradiated area was insoluble in benzene solvent, while that in the unirradiated area was easily solved. A patterned film deposition could be successfully performed upon irradiation of SR through a Ni mesh mask. The pattern profile was influenced by the gap between the Si substrate and the mask and a clear pattern was obtained after benzene treatment.

**Visiting graduate student from Toyohashi Univ. of Tech.

IV-K-2 Synchrotron Radiation-Excited Etching Reactions

Kosuke SHOBATAKE

The present status of the research on synchrotron radiation-excited etching reactions of SiO_2 and various Si surfaces initiated at the KEK-Photon Factory and at UVSOR is reviewed, although it is at a primitive stage of development. The recent results obtained for etching reaction of SiO_2/SE_6 system — a) the pressure and temperature dependences of the etch rates, and b) cross-sectional profiles of the etched surfaces as a function of SF_6 pressure, and c) wavelength and pressure dependence of the etch rates using pseudo-chromatic undulator radiation — are described and the reaction mechanisms are discussed. From the results so far obtained it has been concluded that excitation of the SiO_2 surface covered by reactive species such as F atoms is essential in promoting the etching reaciton. The etching reactions of various Si materials by Cl_2 and SF_6 gases are also presented and a possible contribution of surface excitation is discussed. However it is pointed out that more experiments are needed to clarify the mechanisms of etching reactions of Si surfaces.

IV-K-3 Synchrotron Radiation-Excited Etching of SiO_2 with SF_6 Using Undulator Radiation. II.

Haruo OHASHI*, Kiyohiko TABAYASHI, and Kosuke SHOBATAKE

The photo-excited etching reaction of SiO_2 surface is studied using undulator light from beam line BL3Al.

We have obtained the pressure, wavelength, and gas layer thickness dependences of the etch rate of SiO_2 with SF_6 gas using undulator radiation (UR) as a continuation of the previous work[1]. We have also carried out SR-excited etching experiment by flowing microwave discharged SF_6 and F_2 gas upon the SiO_2 surface in the hope of promoting surface reactions by supplying excess amount of F atoms around the surface. In summary we have found that a) as the etchant pressure of SF_6 is decreased below 0.015 Torr the etch rate charply drops since the etch rate is limited by the supply rate of F atoms, b) etch rate decreases with the thickness of the etchant gas layer through which SR passes before reaching the surface, and c) the maximum etch rate we could obtain even by flowing microwave-discharged F_2 (30%) gas in He was about 2Å/mA min, which is equivalent to a quantum yield of etching reaction (ie. SiO_2 moiety removed/photon) of as much as 2%. The latter two results support the importance of surface excitation by UR[1].

Reference

1) K. Shobatake et al. *Appl. Phys. Lett.* **56**, 2189 (1990).

*Visiting graduate student from Toyohashi Univ. of Tech.

IV-K-4 Echantless Etching of SiO_2 by Irradiation of Synchrotron Radiation

Haruo OHASHI**, Kenichi KATO**, Akira YOSHIDA *(Toyohashi Univ. of Tech.)*, and Kosuke SHOBATAKE

Previously we have reported synchrotron radiation (SR) excited etching reactions of semiconductor surfaces such as various polycrystalline Si and SiO_2. Now we have found that SR-excited etching reaction of SiO_2 proceeds at room temperature even in vacuum (at 1×10^{-8} Torr), ie. without echant gas around a solid sample. Figure 1 shows the normalized depth of the SiO_2 sample etched by mere irradiation of unfocused SR (3 mm in diameter) from beam line BL8A upon SiO_2. Figure 1a exhibits the SiO_2 thickness vs position when the scan is made horizontally in the electron beam orbit plane. As expected we find no variation in the etch depth. However it is noted that the etch rate obtained reaches as high as 3×10^{-3} Å/mA stored current /min, which is about 1/66 of the etch rate observed when SF_6 was used as etchant. This value

obtained for etchantless etching is very large. Figure 1b shows the profile when the scan is made vertically across the orbit plane. We find that the etch rate changes with irradiated position and shows maximum at the center position or on the orbit plane, which is indicative of wavelength dependence of etching efficiency over the wavelength range 5-2000 Å. In fact the experiment is in progress irradiating undulator radiation from BL3A1 in stead of SR from the bending magnet. With the undulator radiation which supplies photons below 200 eV, the etch rates attained are at least factor 10 lower than that for bending magnet SR, which is explained by the importance of the inner core excitation of Si and/or O atoms.

**Visiting graduate student from Toyohashi Univ. of Tech.
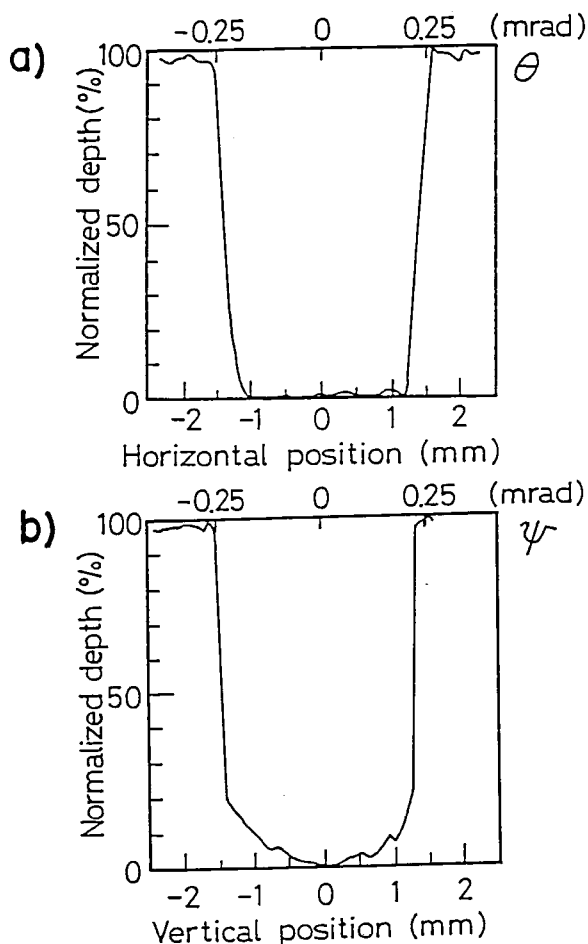
Figure 1. Cross sectional profiles of SiO_2 irradiated by SR through a channel (3 mm in diameter) from the bending magnet on the beam line BL8A. Normalized etch depth is plotted against deviated position (mm) as well as deviated angle (mrad) when measured a) horizontally in the electron orbit plane, and b) vertically across the orbit plane.

IV—L Synthesis and Electrical Properties of Organic Conductors

In order to obtain the knowledge required for the further development of new organic conductors, charge-transfer complexes and radical salts of OCNAQ and phthalocyanines have been prepared and their structural and electrical properties have been studied.

IV-L-1 Design of Two-Dimensional Stacking Structures: Twin-Type Molecules and Steric Interaction of Axial Substituents

Tamotsu INABE, Tsutomu MITSUHASHI *(Univ. of Tokyo)*, **and Yusei MARUYAMA**

Two kinds of novel approaches to constructing a two-dimensional molecular array are presented. The first approach is based on the interleaved stacking of twin-type molecules, which are composed of two units of a donor or an acceptor. The second approach is based on the slipped stacking due to the steric interaction of axial substituents. As examples, charge transfer complexes of OCNAQ, which is a twin-TCNQ-type acceptor, and radical salts of an axially substituted phthalocyanine are presented.

IV-L-2 Multi-Dimensional Stacking Structures in Phthalocyanine-Based Electrical Conductors, $K[Co(phthalocyaninato)(CN)_2]_2 \cdot 5CH_3CN$ and $Co(phthalocyaninato)(CN)_2 \cdot 2H_2O$

Tamotsu INABE and Yusei MARUYAMA

Two kinds of electrically conducting crystals have been obtained by the electrochemical oxidation of potassium dicyanophthalocyaninatocobalt(III), $KCo(Pc)$-$(CN)_2$. Oxidation in acetonitrile gives $K[Co(Pc)(CN)_2]_2 \cdot 5CH_3CN$, in which the phthalocyanine rings are two-dimensionally stacked. Since some of the acetonitrile molecules can be easily removed from the lattice, the crystal is not stable outside of the solution. Mosaically distorted crystals, which are exposed to air, show relatively high conductivities ($\sim 10 \Omega^{-1}$ cm^{-1} at room temperature). On the other hand, oxidation in benzonitrile in the presence of dibenzo-18-crown-6 yields $Co(Pc)(CN)_2 \cdot 2H_2O$, in which the phthalocyanine rings are three-dimensionally stacked. The water molecules in this crystal form hydrogen bonds, and the crystal is stable against drying. The conductivity of this crystal is $\sim 1 \Omega^{-1}$ cm^{-1} at room temperature. The multi-dimensionalities observed in these two kinds of crystals arise from a slipped stacking of phthalocyanine, due to steric interactions of the axial substituents.

IV—M Synthesis and Characterization of Proton-Transfer/Charge-Transfer System

Hydrogen-bonded systems, in which the proton transfer is coupled with the π-electron configurational change, are the subject of this study. If the interaction between the molecules is sufficiently strong in the crystalline state, the proton motion is expected to modulate the electronic properties of the crystal. In order to examine such a possibility, a number of compounds which have a comon framework of salicylideneaniline have been synthesized as the intramolecular proton transfer system. In order to extend the system to the intermolecular cases, charge transfer complexes of aromatic amines have also been prepared and subjected to structural, electrical, magnetic, and optical studies.

IV-M-1 Reversible Self-Isomerization Induced by Proton Transfer: Correlation between the Structures and Optical Properties

Tamotsu INABE, Naomi HOSHINO *(Hokkaido Univ.)*, Tadaoki MITANI, Hiroshi OKAMOTO, Isabelle GAUTIER-LUNEAU, and Yusei MARUYAMA

N-Salicylideneaniline derivativies and their charge transfer complexes have been prepared, and subjected to structural and optical studies. It is demonstrated that the intramolecular proton transfer is strongly influenced by the electronic state of the molecule, suggesting possibilities to create a novel type of electrical conduction system.

IV-M-2 Structure and Optical Properties of Thermochromic Schiff Bases. Charge Transfer Interaction and Proton Transfer in the *N*-(Tetrachlorosalicylidene)aniline and *N*-Tetrachlorosalicylidene-l-pyrenylamine Crystals

Tamotsu INABE, Isabelle GAUTIER-LUNEAU, Naomi HOSHINO *(Hokkaido Univ.)*, Kaoru OKANIWA, Hiroshi OKAMOTO, Tadaoki MITANI, Umpei NAGASHIMA, and Yusei MARUYAMA

Two kinds of *N*-salicylideneaniline derivatives, *N*-(tetrachlorosalicylidene)aniline (CL4SA) and *N*-tetrachlorosalicylidene-l-pyrenylamine (CL4SPY), have been prepared and subjected to structural and optical studies in the crystalline state. A thermochromic-type behavior of the former crystal has been observed as a shift of the absorption edge, while that of the latter crystal is much less pronounced. Fairly short O-H $\cdots$ N hydrogen bonds are found in both compounds from the crystallographic studies, which may be mainly due to a steric effect of the chlorine substituents. The difference in the proton transfer behavior of CL4SA and CL4SPY should presumably be caused by an intermolecular charge transfer interaction in the latter crystal.

IV-M-3 Charge Transfer Complexes of Salicylindeneaniline Derivatives

Tamotsu INABE, Naomi HOSHINO *(Hokkaido Univ.)*, Isabelle GAUTIER-LUNEAU, Hiroshi OKAMOTO, Kaoru OKANIWA, Tadaoki MITANI, and Yusei MARUYAMA

Since some of the salicylideneaniline derivatives have been found to have rather low ionization potential, they have been employed as a donor component of charge transfer complexes. There is a clear relationship between the charge transfer energy and the equilibrium position of the proton in the O-H $\cdots$ N hydrogen bond. The NH and OH forms are obtained when the charge tranfer energy is high, while the intermediate case is observed when the energy is low. In the latter case, the coupling between the proton motion and conduction electrons is expected to lead a novel type of eletrical properties.

IV-M-4 Charge Transfer Complexes with Intermolecular Hydrogen Bonds

Tamotsu INABE, Hironori OGATA, Kaoru OKANIWA, Hiroshi OKAMOTO, Tadaoki MITANI, and Yusei MARUYAMA

In order to examine the possibility of coupling between the proton motion and conduction electrons in the intermolecular hydrogen-bond systems, charge transfer complexes of aromatic amines have been prepared and subjected to structural, electrical, magnetic, and optical studies. The donors employed so far are 1,6-pyrenediamine, 3,3',5,5'-tetramethylbenzidine, and 3,3'-dimethylbenzidine, and the accceptors are derivatives of *p*-benzoquinone and derivatives of TCNQ. All complexes structurally studied have a hydrogen-bond network in the lattice. Depending on the combination and the crystal structure, the complexes show a wide range of electrical conductivity. A systematic study of these complexes is expected to provide the relationship between the hydrogen-bond structure and the electrical properties, and is now under way.

IV—N Ultra-Thin Organic Film Systems Prepared by Molecular Beam Epitaxy (MBE) Technique

As a strategy for the development of new types of organic materials, we have undertaken a fabrication of ultra-thin organic multi-layer systems with the use of the "MBE" technique. We are expecting new types of charge transfer compounds and/or intercalation compounds (hybrid compounds), and also the realization of novel 2-dimensional materials in such systems. As an initial step of the study, we have prepared ultra-thin well-oriented phthalocyanine films on alkali halide single crystal substrates.

IV-N-1 The Structure and Properties of Phthalocyanine Films Grown by Molecular Beam Epitaxy Technique. Part I. Preparation and Characterization

Anthony J. DANN *(Univ. of Nottingham and IMS)*, Hajime HOSHI and Yusei MARUYAMA

[*J. Appl. Phys.*, **67**, 1371 (1990)]

Ultra-thin films of the cofacially stacked F-bridged Al-pathalocyanine polymer, $(AlPcF)_n$, have been grown using the highly controlled technique of MBE. A parallel orientation of the polymer backbone to the substrate surface occurs in films on silicon and quartz, but epitaxy is not apparent. On single crystal alkali-halide substrates, the backbone is perpendicular to the substrate surface and an epitaxial relationship exists which is influenced by the interaction between the substrate and phthalocyanine molecule. The TEM studies indicate that the most highly ordered films are produced on KBr(100) which have good continuity and unidirectional crystallite orientation.

IV-N-2 The Structure and Properties of Phthalocyanine Films Grown by Molecular Beam Epitaxy Technique. Part II. UV/Visible Spectroscopic Study

Hajime HOSHI, Anthony J. DANN *(Univ. of Nottingham and IMS)* and Yusei MARUYAMA

[*J. Appl. Phys.*, **67** 1845 (1990)]

Ultra-thin films of F-bridged Al-phthalocyanine polymer, $(AlPcF)_n$, grown by the MBE technique show unusual spectroscopic properties which can be described by the possibility of pseudomorphic layer for-mation at the thin film/substrate interface. A change in the electronic structure of the molecules of this layer is presumed to occur. The existence of the layer is directly related to the degree of epitaxy.

IV-N-3 The Structure and Properties of Phthalocyanine Films Grown by the Molecular Beam Epitaxy Technique. Part III. Preparation and Characterization of Lutetium Diphthalocyanine Films

Hajime HOSHI, Anthony J. DANN *(Univ. of Nottingham and IMS)* and Yusei MARUYAMA

[*J. Appl. Phys.*, **67**, 6871 (1990)]

Two types of epitaxial films of lutetium diphthalocyanine, $LuPc_2$, have been obtained on KBr, $LuPc_2/$ KBr, and on the film of fluoro-bridged aluminium phthalocyanine polymer, $(AlPcF)_n$, on KBr, $LuPc_2/$ $(AlPcF)_n/KBr$, by the molecular beam epitaxy technique. Their structures have been studied by scanning electron microscopy as well as transmission electron microscopy. The phase of $LuPc_2/KBr$ is bidirectionally oriented tetragonal; $KBr(100)(\sqrt{10}\times\sqrt{10})R\pm27°$ $-LuPc_2$. The phase of $LuPc_2/(AlPcF)_n/KBr$ is predominantly unidirectionally oriented tetragonal; $KBr(100)(3\times3)R45°-LuPc_2/(AlPcF)_n$, but some bidirectional orthorhombic phase, $KBr(100)C(6\times3)R45°$ $-LuPc_2/(AlPcF)_n$, is also present.

IV-N-4 A New Type Epitaxial Growth in Lithium Phthalocyanine Film on KBr(100) Prepared by the Molecular-Beam Epitaxy

Hajime HOSHI, Yusei MARUYAMA, Hideki MASUDA, and Tamotsu INABE

A new type epitaxial growth is found in lithium phthalocyanine (LiPc) film on KBr(100) prepared by the molecular-beam epitaxy. The structure is directly observed by transmission electron microscopy and two epitaxial phases are noticed. One is bidirectional tetragonal phase, KBr(100)($\sqrt{10}\times\sqrt{10}$)R$\pm27°$—LiPc. The other one is a new type of tetradirectional monoclinic phase, ($\sqrt{10}\times\sqrt{12.5}$), where LiPc lattices match with both K$^+$ and Br$^-$ ions, which form unusual unit meshes.

IV-N-5 Epitaxial Growth of Chloroaluminum Phthalocyanine Films on Alkali Halide Single Crystals by the Molecular-Beam Epitaxy Technique

Hajime HOSHI and Yusei MARUYAMA

Epitaxial chloroaluminum phthalocyanine (AlPcCl) films have been prepared on NaCl, KCl, KBr, and KI(100) surfaces by the molecular-beam epitaxy technique. Their structures have been studied by scanning electron microscopy and transmission electron microscopy. The films consist of densely packed crystallites and seem to be continuous. The predominant phase of AlPcCl/NaCl is newly found bidirectionally oriented tetragonal, NaCl(100)($\sqrt{13}\times\sqrt{13}$)R$\pm11°$—AlPcCl. The phase of AlPcCl/KCl and AlPcCl/KBr is bidirectionally oriented tetragonal, KCl(100)($\sqrt{10}\times\sqrt{10}$)R$\pm27°$—AlPcCl and KBr(100)($\sqrt{10}\times\sqrt{10}$)R$\pm27°$—AlPcCl, respectively. The predominant phase of AlPcCl/KI is unidirectionally oriented tetragonal, KI(100)(3×3)R45°—AlPcCl. The epitaxial lattice di-

rections are related to the degree of lattice matching between AlPcCl and substrates.

IV-N-6 Epitaxial Growth of Vanadyl Phthalocyanine Films on Alkali Halide Single Crystals by the Molecular-Beam Epitaxy Technique

Hajime HOSHI and Yusei MARUYAMA

Epitaxial vanadyl phthalocyanine (VOPc) films have been prepared on KCl and KBr (100) surfaces by the molecular-beam epitaxy technique. Their structures have been studied by transmission electron microscopy. Every film consists of densely packed crystallites and seems to be continuous. The phase of VOPc/KCl is bidirectionally oriented tetragonal, KCl(100) ($\sqrt{10}\times\sqrt{10}$)R$\pm27°$—VOPc, while that of VOPc/KBr is unidirectionally oriented tetragonal, KBr(100) (3×3)R45°—VOPc. The preferential epitaxial lattice orientation is discussed based on the degree of lattice matching between VOPc and substrates.

IV-N-7 Measurement for SHG and THG of the Ultra-Thin Phthalocyanine Films Prepared by the MBE Technique

Hajime HOSHI, Naoki NAKAMURA *(Toyota Motor Corp. and IMS)*, and Yusei MARUYAMA

Non-linear optical effect, such as SHG or THG, has been measured for the ultra-thin phthalocyanine films prepared by the MBE technique. The effect of the molecular structure, the epitaxy and the orientation of the films for the SHG and/or THG are investigated.

IV—O Black Phosphorus

Black phosphorus is a layered structure semiconductor. We have prepared iodine intercalated compounds of black phosphorus and revealed their metallic character. Recently, inclusion or doping of silicon or germanium to black phosphorus has been undertaken.

IV-O-1 Electrical Conductivity of Black Phosphorus-Germanium Compound

Yusei MARUYAMA, Tamotsu INABE, Lin HE (General Institute for Colored Metal, Beijing, and IMS), and Kokichi OSHIMA (Okayama Univ.)

[Submitted to *Synthetic Metals*]

Single crystals of a new material, black phosphorus doped with germanium, have been prepared by a bismuth-flux method. Germanium atoms are incorporated into the black phosphorus in 2 to 4 atomic percent. The resistivity is reduced by two to three orders (ρ=6×10^{-3} Ωcm) compared with the pure black phosphorus, and its temperature dependence is metallic at low temperatures (Figure 1). There is no magnetoresistance up to 12T at 0.6K in striking contrast to the pure black phosphorus which shows negative magnetoresistance in this region. The crystal lattice constants decrease with germanium doping, especially in the interlayer direction. These facts indicate the enhanced 3-dimensionality with germanium doping.
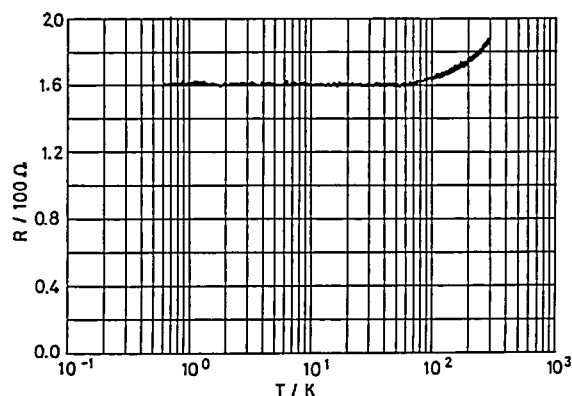
Figure 1. Temperature dependence of the electrical resistance of PGe$_x$ (x=0.03±0.01).

IV—P Preparation and Characterization of Copper Oxide High T_c Superconductor Films

After the discovery of novel high T_c superconductors, a lot of works including the film preparation have been carried out. We have carried out to fabricate thin films of such superconductors by a sputtering method and an electron-beam evaporation technique with the purpose of searching for new composition, structures, and elements in high T_c superconductors.

IV-P-1 La-Sr-Cu-O Superconducting Thin Films Preparation by MBE with Multi-Electron-Beam Gun Sources

Toshifumi TERUI, Tamotsu INABE, and Yusei MARUYAMA

La-Sr-Cu-O system seems to have crucially important physical aspects in the study of high T_c copper oxides superconductors. In this point of view, we have undertaken to construct various kinds of La-Sr-Cu-O system, especially focusing to La$_2$SrCu$_2$O$_6$ series, by the MBE technique with multi-electron-beam gun sources. Layer-by-layer deposition in the atomic order are controlled by a computer, and characterized by X-ray diffraction and ICP analysis.
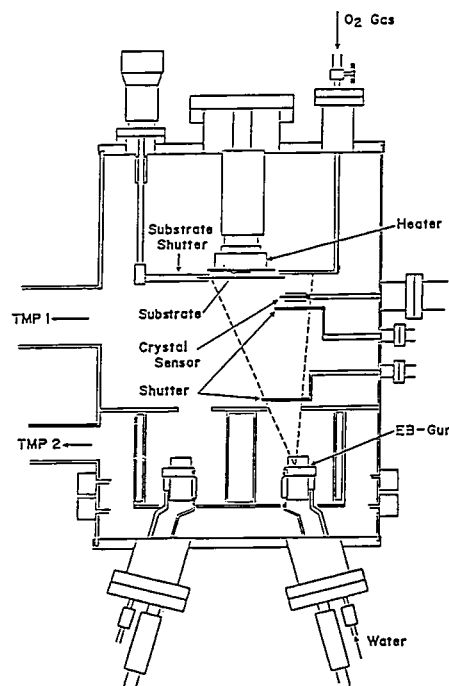
Figure 1. Vacuum deposition system with multi-electron-beam gun sources.

IV—Q STM/STS Study on Electronic Structures of Some Superconductors

Scanning tunneling microscopy (STM) and spectroscopy (STS) are very useful and direct methods to study the electronic structures of electrical conductors. We are focusing to investigate site-selective superconduting gap structures of organic or copper oxide superconductors. The system for room temperature STM/STS has been set up, and a low temperature system is now under construction.

IV-Q-1 STM/STS Study of Some Organic Superconductors at Room Temperature

Yoshihisa MORI, Hatsumi MORI *(ISTEC)*, and Yusei MARUYAMA

STM observation and STS measurement are carried out for the different crystal planes of each (BEDT-TTF)$_2$Cu(NCS)$_2$ and (BEDT-TTF)$_2$KHg(SCN)$_4$ crystal. The STM images of the former crystal are shown in Figure 1. It is still not so easy at room temperature to find out corresponding differences in the STS results due to the crystal plane differences.
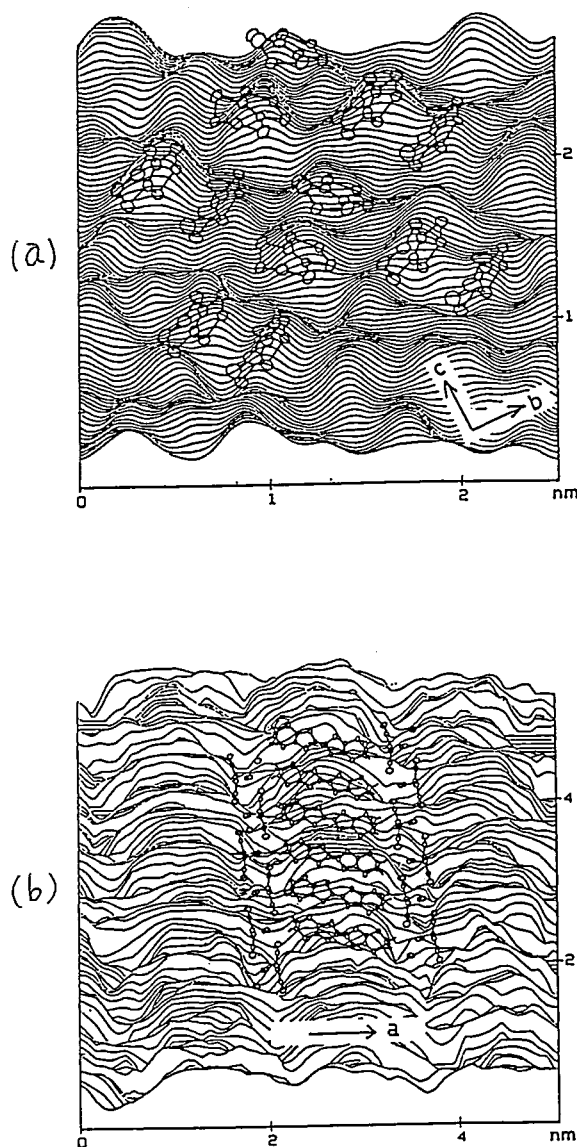
Figure 1. STM images of (BEDT-TTF)$_2$Cu(NCS)$_2$ crystal. (a) bc plane, and (b) //a plane.

IV—R   Photoelectron Spectroscopy of Organic Solids in Vacuum Ultraviolet Region

Work of ultraviolet photoelectron spectroscopy (UPS) of organic solids and graphite compounds has been proceeded. Further, using a photoelectron spectrometer combined with synchrotron radiation light source (UVSOR-UPS) the UPS spectra of organic and inorganic materials were observed.

IV-R-1   Ultraviolet Photoemission Study of Oilgothiophenes: π-Band Evolution and Geometries

Hitoshi FUJIMOTO *(Kumamoto Univ. and IMS)*, Umpei NAGASHIMA, Hiroo INOKUCHI, Kazuhiko SEKI *(Hiroshima Univ.)*, Y. CAO *(Academia Sinica, China)*, Hiroo NAKAHARA *(Saitama Univ.)*, Juzo NAKAYAMA *(Saitama Univ.)*, Masamatsu HOSHINO *(Saitama Univ.)*, and Kiyoshige FUKUDA *(Saitama Univ.)*

Ultraviolet photoelectron spectroscopy (UPS) has been applied to the investigation of the electronic structure of oligothiophenes. In a series of α-linked oilgomers (α_n with n being the number of rings), a systematic evolution of the π band is observed. Several peaks which correspond to the π band are observed in the region of 0.7-3 eV below the Fermi level (E_F) and the bandwidth becomes broader with increasing n. The non-bonding π band is observed at 3.5 eV below E_F and its energy is almost independent of n. The effect of irregularity on the π-electron system was also studied by using oligomers which contain a β linkage or a vinylene group in the middle of the molecule. The UPS spectra showed that the β linkages significantly affect the electronic structure of polythiophene, while the vinylene group does not. In order to analyze the UPS spectra and to investigate the electronic structures of oligomers, the orbital energies and the geometries of these oligomers are calculated by the empirical MNDO method.
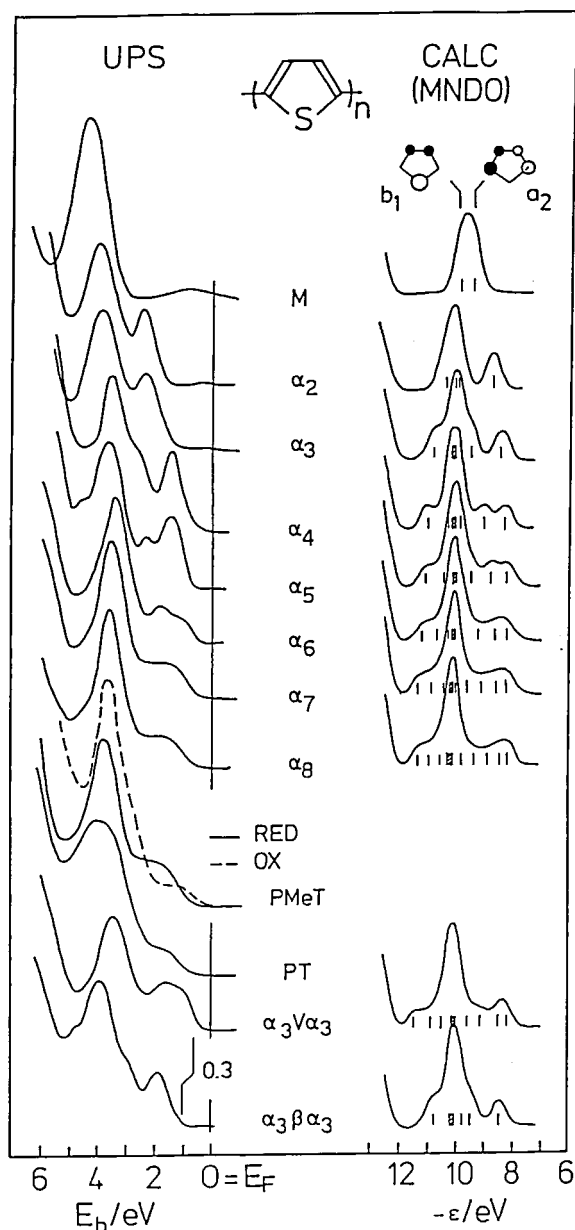
Figure 1. Obsered (left) and simulated (right) UPS spectra in the π region for oilgothiophenes used in this work. The origins of the energy scale of observed and simulated UPS spectra are taken as the Fermi level (E_F) and the vacuum level, respectively. For comparison, the observed UPS spectra of neat polythiophene (PT), reduced (solid line) and oxidized (broken line) poly(3-methylthiophene) (PMeT) are also shown.

IV-R-2 Electronic and Geometric Structures of Oilgothiophenes Studied by UPS and MNDO: π-Band Evolution and Effect of Disorder

Hitoshi FUJIMOTO *(Kumamoto Univ. and IMS)*, Umpel NAGASHIMA, Hiroo INOKUCHI, Kazuhiko SEKI *(Hiroshima Univ. and IMS)*, Hiroo NAKAHARA *(Saitama Univ.)*, Juzo NAKAYAMA *(Saitama Univ.)*, Masamatsu HOSHINO *(Saitama Univ.)*, and Kiyoshige FUKUDA *(Saitama Univ.)*

In this paper, we will report a combined experimental and theoretical study on the electronic structures of oilgothiophenes containing 4-8 thiophene rings. The systematic evolution of the π-band with increasing ring numbers and the effect of the irregularity (a β linkage and a vinylene substitution) on the π-electron systems are studied by the ultraviolet photoelectron spectroscopy (UPS). The electronic and geometric structures of these oligomers are calculated by the MNDO-SCF-MO method, and the results are discussed in comparison with the UPS results.
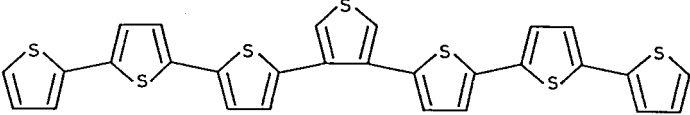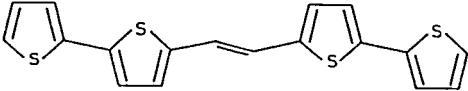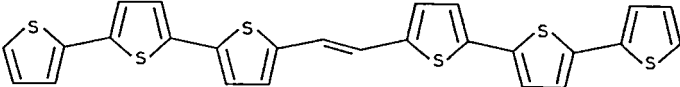
	m.p. / °C	λ max / nm (CHCl₃ soln.)
2,2':5',2'':5'',3''':4''',2'''':5'''',2''''':5''''',2''''''-septithiophene	203	370
(E)-bis(2,2'-bithiophene-5-yl)ethylene	214 - 215	423
(E)-bis(2,2':5',2''-terthiophene-5-yl)ethylene	282 - 283	460

Figure 1. ligothiophenes with irregularity. Their UV and visible absorption maxima in chloroform solutions and melting points are also given.

IV-R-3 Energy-Band Dispersion in Oriented Thin Films of Pentatriacontan-18-one by Angle-Resolved Photoemission with Synchrotron Radiation

Nobuo UENO *(Chiba Univ.)*, Kazuhiko SEKI *(Hiroshima Univ. and IMS)*, Naoki SATO *(Univ. of Tokyo)*, Hitoshi FUJIMOTO *(Kumamoto Univ. and IMS)*, Tadao KURAMOCHI *(Chiba Univ.)*, Kazuyuki SUGITA *(Chiba Univ.)*, and Hiroo INOKUCHI

Angle-resolved photoemission spectra were measured using synchrotron radiation for thin films of the pentatriacontan-18-one molecule [CH₃(CH₂)₁₆-CO(CH₂)₁₆CH₃] with their long axes perpendicular to the substrate surface. At the preparation of the films, careful studies were made on the molecular decomposition due to vacuum evaporation and on molecular orientation in the evaporated films by mass spectros-

copy, X-ray diffraction, and angle-resolved photoemission. Valence-band dispersion was observed along the long molecular axis. The results demonstrate that the chemical disorder of the C=O group in the CH_2 chain does not affect the band structure so much, and the molecule shows valence-band dispersion similar to the dispersion in an ideal polyethylene chain. Further, we observed a band which was not observed in previous work. It determines the top of the valence band at the Γ point. Comparison with theoretical results indicates that it corresponds to a band of B_1 (B_{2g} at Γ) symmetry which consists of only C2p atomic orbitals directed along the carbon chain.

IV-R-4 Angle-Resolved Photoemission from Oriented Thin Films of Long Alkyl Molecules: Valence Band Dispersion

Nobuo UENO *(Chiba Univ.)*, **Hitoshi FUJIMOTO** *(Kumamoto Univ. and IMS)*, **Naoki SATO** *(Univ. of Tokyo)*, **Kazuhiko SEKI** *(Hiroshima Univ. and IMS)*, **and Hiroo INOKUCHI**

Angle-resolved photoemission spectra were measured using synchrotron radiation for oriented thin films of hexatriacontane, $CH_3(CH_2)_{34}CH_3$, and pentatriacontan-18-one, $CH_3(CH_2)_{16}CO(CH_2)_{16}CH_3$, with their long axes perpendicular to the substrate surface. The valence band dispersion was observed along the long molecular axis over the whole Brillouin zone for both compounds. The results demonstrate that the chemical disorder caused by the C=O group in the CH_2 chain does not affect the band structure so much and both compounds show valence band dispersion similar to the dispersion in an ideal polyethylene chain. Further, we observed a band which was not observed in our previous work. It determines the top of the valence band at the Γ point. Comparison with theoretical results[1] indicates that it corresponds to a band of $B_1(B_{2g}$ at Γ) symmetry which consists of only C2p atomic orbitals directed along the carbon chain.

Reference
1) A. Karpfen, *J. Chem. Phys.*, **75**, 238 (1981).

Figure 1. Photon-energy dependence of the normal-emission photoelectron spectra of vertically oriented thin films of pentatriacontan-18-one for $\alpha=70°$.
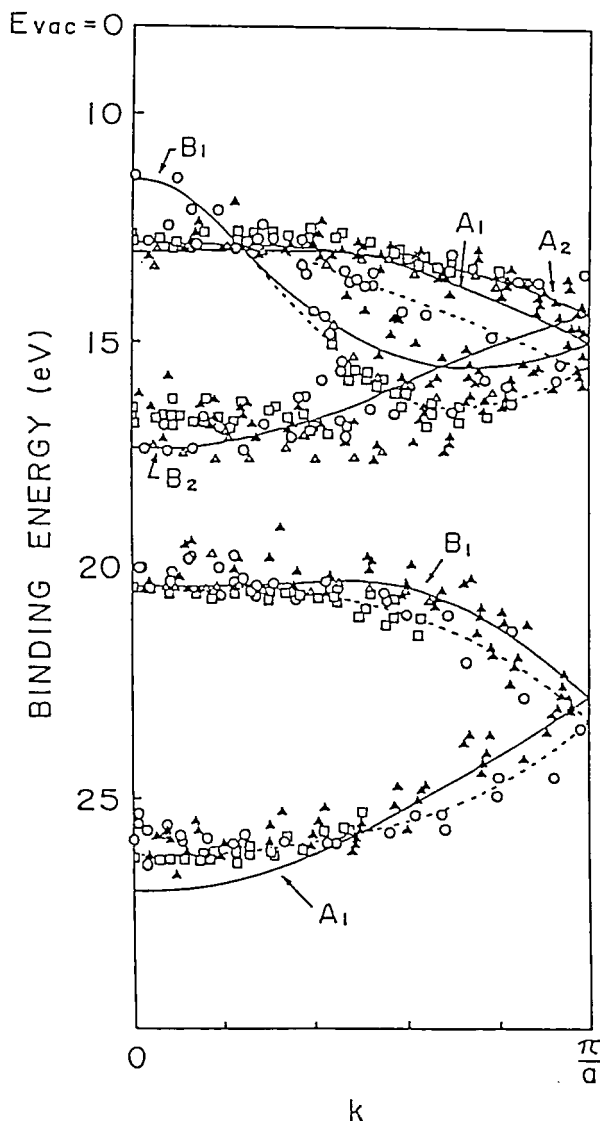
Figure 1. Experimental energy band dispersions. O: penta-triacontan-18-one. △ ▲: hexatriacontane. □: Langmuir-Blodgett film of cadmium arachidate. The binding energy is shown for pentatriacontan-18-one. The theoretical result by Karpfen[1] is shown by solid curve with some modification. The dotted curves indicate the experimentally deduced dispersion curves for the A_1 and B_1 bands.

Ultraviolet photoelectron spectra have been measured for the radical phthalocyanine dimer, Pc_2Lu, and the fluorine bridge stacked phthalocyanine polymer $(PcAlF)_n$. Samples for this work were prepared by *in situ* sublimation at very slow evaporation rates onto crystalline substrates to try to maximize the degree of sample orientation. The angle dependence of the spectra were measured and the sample structure subsequently examined using high resolution TEM. The TEM results show that the $(PcAlF)_n$ films have a much higher level of orientation than the Pc_2Lu films and this is reflected by the angle dependence of the UPS measurements. The spectra for Pc_2Lu show almost no angular dependence. Again the spectra are broadly similar to that of other Pc's with two significant differences, the lowest energy peak is split and the whole spectra is shifted to lower energy. This result will be discuussed in term of simple molecular orbital ideas. The effect of air on the spectra of both materials was examined and the spectra of $(PcAlF)_n$ was found to be particularly sensitive.

IV-R-5 Electronic Structure of Pc ₂Lu and $(PcAlF)_n$ Oriented Thin Films Using Angle Resolved Photoelectron Spectroscopy

Michael Richard FAHY *(Univ. of Nottingham and IMS)*, Hitoshi FUJIMOTO *(Kumamoto Univ. and IMS)*, Anthony John DANN *(Univ. of Nottingham and IMS)*, Hajime HOSHI, Hiroo INOKUCHI, Yusei MARUYAMA, and Martini Richard WILLIS *(Univ. of Nottingham)*
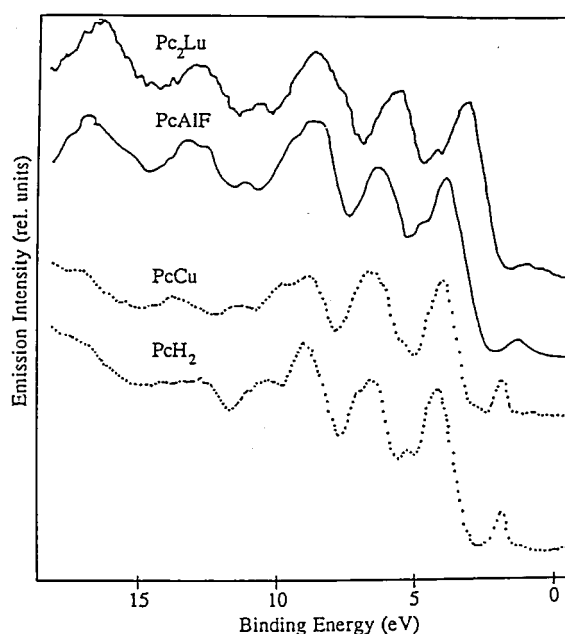
Figure 1. The spectra of 100 Å films of $(PcAlF)_n$ and Pc_2Lu with $h\nu=40$ eV. For comparison measurements on PcH_2 and PcCu using HeII radiation ($h\nu=40.8$ eV) are shown. The topmost curve is the XPS of Pc_2Lu and quite clearly shows the doublet due to Lu 4f. The zero of binding energy is the Fermi level of a gold film prepared *in situ*.

IV-R-6 Ultraviolet Photoelectron Spectroscopy of Perylene Anion in Cs-perylene Solid

Hiromichi YAMAMOTO, Hiroo INOKUCHI, Kazuhiko SEKI (Hiroshima Univ. and IMS), Hidetsugu TANAKA*, and Kichisuke NISHIMOTO* (*Osaka City Univ.)

Ultraviolet photoelectron spectra have been measured of a Cs-perylene complex prepared by Cs-exposure of perylene. The observed spectral features of the perylene anion could not be explained by the rigid band picture used previously for this kind of compound. Instead, a localized picture gives a reasonable explanation, in which the features are examined with the reported energies of the singlet and triplet excited states and the MO calculations of neutral perylene. It is shown that this kind of measurements performed on anions can be used as a technique of probing the triplet states of a neutral molecule.

IV-R-7 Photopolymerization of Long-Chain Diacetylene Monocarboxylic Acid in Langmuir-Blodgett Films Studied By UV Photoelectron spectroscopy and X-ray Absorption Near-Edge Structure

Kazuhiko SEKI (Hiroshima Univ. and IMS), Ikuo MORISADA*, Hiroshi TANAKA*, Kunishige EDAMATSU*, Masahiko YOSHIKI*, Yasutaka TAKATA*, Toshihiko YOKOYAMA*, Tosiaki OHTA*, Satoshi ASADA, Hiroo INOKUCHI, Hiroo NAKAHARA**, and Kunishige FUKUDA** (*Hiroshima Univ.) (**Saitama Univ.)

The UV photopolymerization of cadmium salt Langmuir-Blodgett (LB) films of a diacetylene long-chain compound tricosa-10,12-diynoic acid was studied with UV photoelectron spectroscopy (UPS) and X-ray absorption near-edge structure (XANES), and the results are compared with those for evaporated films of the same threshold energy from 6.7 eV (monomer) to 5.1 eV (polymer in both blue and red forms) owing to the formation of a delocalized π band, which is similar to the results for evaporated films. The XANES spectra indicate that polymerization does not proceed regularly in the topmost surface layer of the LB films probed by XANES, possibly owing to disordered surface structure. This is in contrast to the results for evaporated films, where a clear change of XANES spectra is observed owing to the formation of a delocalized π^* band.

IV-R-8 UV Photoemission Spectroscopy of Poly(p-phenylene vinylene)(PPV)

Kazuhiko SEKI (Hiroshima Univ. and IMS), Satoshi ASADA, Takehiko MORI, Hiroo INOKUCHI, Ichiki MURASE*, Toshihiro OHNISHI*, and Takanobu NOGUCHI* (*Res. Assoc. Basic Polym. Tech.)

UV photoemission spectra of poly(p-phenylene vinylene) were measured for films prepared by (i) vacuum evaporation and (ii) in-situ pyrolysis of precursor polymer. The results were analyzed using the theoretical band calculations, the data of other phenyl-containing polymers, and reported XPS spectrum. The effect of further heat-treatment of the PPV film was also examined.

IV-R-9 UV Photoelectron Spectroscopy of Photoconducting Polymers and 1:1 Alternating Copolymers Containing Pendant π-Electron Systems

Yasuhiko SHIROTA*, Yasuyo MATSUMOTO*, Toshio TANAKA*, Naoki NOMA*, Kazuhiko SEKI (Hiroshima Univ. and IMS), Hiromichi YAMAMOTO, and Hiroo INOKUCHI (*Osaka Univ.)

Threshold ionization potentials of photoconducting polymers, an electrochemically-doped polymer, and 1:1 alternating copolymers containing pendant π-electron systems in thin films have been determined by UV photoelectron spectroscopy; the results are discussed in relation to their properties and molecular structures.

IV-R-10 Impurity-State-Like Nature of Fermi-Liquid States in $Bi_2Sr_2CaCu_2O_8$ Observed by Photoemission and X-ray Absorption

H. MATSUYAMA *(Tohoku Univ.)*, T. TAKAHASHI *(Tohoku Univ.)*, H. KATAYAMA-YOSHIDA *(Tohoku Univ.)*, T. KASHIWAKURA *(Tohoku Univ.)*, Y. OKABE *(Tohoku Univ.)*, S. SATO *(Tohoku Univ.)*, N. KOSUGI *(Kyoto Univ.)*, A. YAGISHITA *(Photon Factory, National Inst. for High-Energy Phys.)*, K. TANAKA *(Photon Factory, National Inst. for High-Energy Phys.)*, H. FUJIMOTO *(Kumamoto Univ. and IMS)*, and H. INOKUCHI

Photoemission and X-ray absorption spectroscopy have been performed on $Bi_2Sr_2Ca_{1-x}V_xCu_2O_8$ in which the hole concentration is controlled by the ratio between Ca and Y atoms. It was found that the density of electronic states at the Fermi level gradually increases as the hole concentration with almost no rigid shift of the electronic structure with respect to the Fermi level. This suggests that the electronic states at the Fermi level (Fermi-liquid states) would not be simple one-electron states but be a kind of impurity states produced through the strong hybridization between doped $O2p$ hole orbitals and empty $Cu3d$ orbitals.

IV-R-11 Ultraviolet Photoelectron Spectroscopy of N,N-Diphenyl-N'-picrylhydrazine

Hiromichi YAMAMOTO *(Nippon Petrochemicals Co., Ltd.)*, Umpei NAGASHIMA, Hiroo INOKUCHI, and Naoki SATO *(Univ. Tokyo)*

UV photoelectron spectra of N,N-diphenyl-N'-picrylhydrazine ($DPPH_2$) have been measured in the solid and gas phases. The solid-state spectra, as shown in Figure 1, depend on the preparation conditions of the evaporated films, *i.e.* the different deposition rates of (a) 2.8, (b) 85, and (c) 140 nm/min, and differ from the gas-phase spectrum. Comparison of the observed spectra with the results of theoretical calculations indicates that the electronic structure of this molecule is modified in the solid state by change in the molecular conformation.
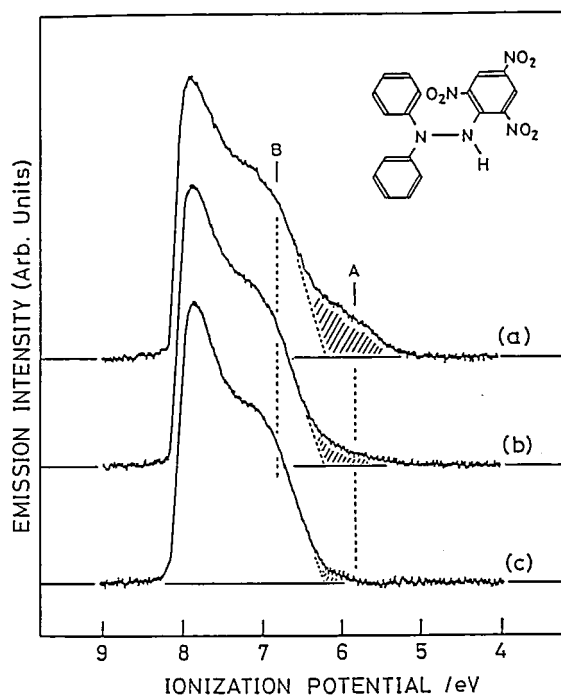
Figure 1. UPS spectra of $DPPH_2$ in the solid state measured with photon energy of 8.16 eV using the films prepared at different evaporation rates. The abscissa is the ionization energy relative to the vacuum level. The ionization threshold in (a) determiend by linear extrapolation is 5.5_2 eV, and the value extrapolated by the broken line is 6.1_8 eV.

IV—S   Electrical Conduction of Organic Solids

The main works of electrical conduction of organic solids in 1989-1990 are those of "molecular fasteners".

IV-S-1 Organic Semiconductors, Conoductors and Superconductors

Hiroo INOKUCHI

The two major categories of organic solids are known to offer the present of good electrical conduction. The first group consists of charge-transfer com-

plexes. Conductivity measurements on a large number of the charge-transfer complexes have been carried out. Among them, organic conductors (synthetic metals) and also organic superconductors have been discovered. The other group comprises single component materials; typical examples are polycyclic aromatic compounds and phthalocyanines. Their conductivities, generally speaking, are not as good as those of the charge transfer kind. We recently discovered a series of single component organic semiconductors having fairly good conductivity, which we call molecular fasteners. We also present the experimental work on the ionization energy and carrier mobility measurements for the purpose of elucidating the conducting mechanism.

IV-S-2 Charge-Carrier Drift Mobilities and Phase Transition in Tetrakis(octylthio)tetrathiafulvalene, TTC$_8$-TTF, Crystal

Yongfang LI, Chikako NAKANO, Kenichi IMAEDA, Hiroo INOKUCHI, Yusei MARUYAMA, Naoko IWASAWA*, and Gunzi SAITO* (*ISSP, Tokyo Univ.)

Temperature dependence of the charge-carrier mobility in tetrakis(octylthio)tetrathiafulvalene crystals has been observed in the temperature range −100-45°C by the time-of-flight measurement of transient photocarriers. The mobility shows a clear jump at the crystal phase transition which is found in the electrical conductivity measurement. This fact may lead a quantitative analysis of the correlation between the conductivity jump and the phase transition.

IV-S-3 Infrared Spctra of Tetrakis(alkylthio)tetrathiafulvalenes

Kenichi IMAEDA, Tadaoki MITANI, Chikako NAKANO, Hiroo INOKUCHI, and Gunzi SAITO (Univ. of Tokyo)

Infrared spectra were measured for tetrakis(alkylthio)tetrathiafulvalenes (abbreviated TTC$_n$-TTFs (n=1-18)) as power samples and single crystals. In the compounds with n=1-6, the stretching vibrational bands of the CH$_2$ and CH$_3$ groups and their relative intensities vary with n. The compounds with $n \gtrsim 7$-9 show nearly identical spectra, where the stretching and deformation vibrations of the CH$_2$ groups develop and approach those in polyethylene. This observation suggests that the high electrical conduction by the molecular fastener effect in the long-chain compounds of TTC$_n$-TTF correlates significantly with the development of polyethylene-like alkyl chains in the crystal.

IV-S-4 Phase Transition of Tetrakis(octylthio)tetrathiafulvalene (TTC$_8$-TTF)

Chikako NAKANO, Kenichi IMAEDA, Takehiko MORI, Yusei MARUYAMA, Hiroo INOKUCHI, Naoko IWASAWA (ISSP, Univ. of Tokyo), and Gunzi SAITO (Kyoto Univ.)

Tetrakis(octhylthio)tetrathiafulvalene (TTC$_8$-TTF) crystallizes in the two differnt phases of plate and needle forms. A plate crystal undergoes a phase transition around 33°C with the steep increase in the resistivity and the decrease in the drift mobility together with the small endothermic heat. The power X-ray diffraction study confirms that this transition is caused by the structure transformation from the plate-like phase to the needle-like phase. The microscopic origin of the phase transition is ascribed to the subtle repulsive motion in the nearest-neighbor octyl chains, which results in the decrease in the transfer integrals between the neighboring π-electron moieties of TTC$_8$-TTF molecules within a segregated column.

IV—T   Electron Transport in Cytochromes

The measurement of electronic conduction of cytochromes in the solid state has been carried out continuously in our group. Recently we found a conductivity jump phenomena of cytochrome c551 films as function of temperature. The result of DSC analysis of this cytochrome showed a large enthalpy change accompanied with the conductivity jump. This enthalpy change is reversible.

IV—U   Physics and Chemistry of Graphite Intercalation Compounds

Graphite-alkali metal intercalation compounds absorb hydrogen chemisorptively, leading to the occlusion of hydrogen in intercalate layers. The investigation of properties of the alkali metal-hydrogen-graphite ternary intercalation compounds has been carried out.

IV-U-1   Hydrogen-Alkali-Metal-Graphite Ternary Intercalation

Toshiaki ENOKI *(Tokyo Inst. of Technology)*, Seiichi MIYAJIMA *(Nihon Univ.)*, Mizuka SANO *(Kumamoto Univ.)*, and Hiroo INOKUCHI

Alkali-metal graphite intercalation compounds (alkali-metal-GIC's) absorb hydrogen in two ways: physisorption and chemisorption. Hydrogen uptake through the physisorption process occurs at low temperatures below about 200 K in higher stage alkali-metal-GIC's, where hydrogen molecules are stabilized to form a two-dimensional condensed phase in the galleries of the graphitic sheets. In the case of hydrogen uptake through the chemisorption process, dissociated hydrogen species are stabilized in the intercalate spaces. The introduction of hydrogen generates a charge transfer from the host alkali metal-GIC's to the hydrogen since hydrogen has strong electron affinity. The inserted two-dimensional hydrogen layer is suggested to consist of H^- ions with a weakly metallic nature. The hydrogen-absorption in alkali-metal-GIC's is an interesting phenomena in comparison with that in transition metal hydrides from the point of hydrogen storage. the hydrogen-alkali metal-ternary GIC's obtained from hydrogen absorption have novel electronic properties and lattice structures which provide attractive problems for GIC research.

IV-U-2   Two-Dimensional Metallic Hydrogen in the Potassium-Hydrogen-Graphite Ternary Intercalation Compound

Seiichi MIYAJIMA*, Masashi KABASAWA*, Takehiko CHIBA*, Toshiaki ENOKI *(Tokyo Inst. of Technology)*, Yusei MARUYAMA, and Hiroo INOKUCHI *(*Nihon Univ.)*

A proton NMR study was carried out in the stage-I potassium-hydrogen-graphite intercalation compound C_4KH_x, prepared through direct intercalation of potassium hydride into graphite. Lineshape analysis revealed extremely dense two-dimensional packing of negatively charged hydride ions where hydrogen-hydrogen direct contact takes place. The metallic nature of hydrogen was observed through the Korringa term $(T_1 T)^{-1} = 6.4 \times 10^{-4} s^{-1} K^{-1}$, where T_1 is the spin-lattice relaxation time. C_4KH_x is thus proved to be an exmple of two-dimensional metallic hydrogen.

IV-U-3   Positron Annihilation in Potassium-Intercalated Graphite

Hideoki MURAKAMI*, Ikuzo KANAZAWA*, Mizuka SANO *(Kumamoto Univ.)*, Toshiaki ENOKI *(Tokyo Inst. Tech.)*, and Hiroo INOKUCHI *(*Tokyo Gakugei Univ.,)*

The peak of the Doppler broadening spectrum of

KC$_{24}$ is depressed by 10% upon hydrogen physisorption into its interstices. The depression shows the positrons are distributed in the potassium layers. The lifetime of positrons in KC$_8$ is measured to be 290 ps which is longer than the lifetime in graphite. It is, therefore, deduced that the positrons are not confined in a special area, but distributed over negatively charged graphitic carbon layers and also positively charged potassium layers in KC$_{24}$ and KC$_8$. The narrow component of the spectrum is assigned to the annihilation of positrons with electrons in potassium layers. Imperfections included in the intercalant layers of KC$_8$ are detected as defects in which the positrons have a long lifetime of 530 ps.

IV—V Organic Metals

In an attempt to develop new organic superconductors and to explore the related phenomena, new organic conductors have been prepared and their structural and physical properties have been investigated. The structural and physical properties of (BEDT-TTF)$_2$$M$Hg(SCN)$_4$ series salts were prepared, and their structural and physical properties were studied; among them (BEDT-TTF)$_2$NH$_4$Hg(SCN)$_4$ was found to be a superconductor at T_c = 0.8 K. A new organic superconductor κ-(BEDT-TTF)$_2$Ag(CN)$_2$H$_2$O $(T_c$ = 5.0 K) was also discovered.

IV-V-1 Fermi Surface and Thermoelectric Power of Two-Dimensional Organic Conductors

Takehiko MORI and Hiroo INOKUCHI

Electronic band structures and Fermi surface of organic conductors are discussed on the basis of the single-band tight-binding approximation. The band structures of (BEDT-TTF)$_2$Cu$_5$I$_6$ and (BEDT-TTF)$_4$Hg$_3$Cl$_8$ are calculated according to this approximation.

IV-V-2 Unsymmetrically Substituted Ethylenedioxytetrathiafulvalenes

Takehiko MORI, Hiroo INOKUCHI, Aravinda M. KINI, and Jack M. WILLIAMS

Seven new electron donors, 4,5-ethylenedioxytetrathiafulvalenes where 4′,5′-substituents are trimmethylenedithio, ethylenedithio, methylenedithio, 2-oxatrimethylenedithio, methylthio, hydrogen, and methyl carboxylate, are prepared, and their electrochemical properties are investigated.

IV-V-3 Crystal and Electronic Structures of Mercury Thiocyanate Salts of BEDT-TTF

Hatsumi MORI*, Shoji TANAKA*, Kokichi OSHIMA**, Masashi OSHIMA***, Gunzi SAITO***, Takehiko MORI, Yusei MARUYAMA, and Hiroo INOKUCHI (*ISTEC, **Okayama Univ., ***ISSP, Tokyo Univ.)

A new series of BEDT-TTF salts with a cation (Li$^+$, K$^+$, NH$_4$$^+$, Rb$^+$, and Cs$^+$) as well as an anion [Hg(SCN)$_4$]$^{2-}$, were prepared. The crystal structures of (BEDT-TTF)$_2$[MHg(SCN)$_4$] $(M$ = K at 298 K and 104 K and M = NH$_4$ at 298 K) were determined by X-ray analyses. A donor layer and an anion sheet stack alternately along the b axis. The packing pattern of the donors is close to α-phase, while the anion sheet constructs a thick two-dimensional polymer plane parallel to (010). The band structure calculation indicates the existence of both a closed and an open Fermi surfaces, similarly to κ-(BEDT-TTF)$_2$Cu(NCS)$_4$. The superconductivity of (BEDT-TTF)$_2$NH$_4$Hg(SCN)$_4$ at 0.8 K was confirmed by means of the transport measurement.

IV-V-4 Thermoelectric Power of (BEDT-TTF)₂MHg(SCN)₄ [M = K, Rb, and NH₄]

Takehiko MORI, Hiroo INOKUCHI, Hatsumi MORI*, Shoji TANAKA*, Masashi OSHIMA**, and Gunzi SAITO*** (*ISTEC, **ISSP, Univ. Tokyo, ***Univ. Kyoto)

Anisotropy of thermoelectric power of a series of organic metals (BEDT-TTF)₂MHg(SCN)₄ [M = K, Rb, and NH₄] is measured and compared with a simulation based on the two-dimensional tight-binding band calculation.

IV-V-5 A New Ambient-Pressure Organic Superconductor, κ-(BEDT-TTF)₂Ag(CN)₂H₂O (T_c = 5.0 K)

Hatsumi MORI*, Izumi HIRABAYASHI*, Shoji TANAKA*, Takehiko MORI, and Hiroo INOKUCHI (*ISTEC)

Superconductivity of κ-(BEDT-TTF)₂Ag(CN)₂H₂O is observed by zero electrical resistivity and the Meissner effect. The critical temperature is determined to be 5.0 K at the midpoint of the resistance drop under an ambient pressure. The Meissner signal is observed below 5.0 K under the magnetic field of 5 Oe.

IV—W   High Temperature Oxide Superconductors

Extensive studies on the physical properties of high temperature superconductors have been continued to understand the nature of their strongly correlated and low density carrier system and to elucidate the mechanism of the high-T_c superconductivity. Because the problems involve quite difficult but new physics, we have not confined ourselves to certain special method to approach the problem: We used various kinds of studies from rather broad view points as can be known below, where the abstracts of our publications are mainly shown.

IV-W-1 Magnetic Correlations in YBa₂Cu₃O₆₊ₓ at Superconducting Concentrations

G. SHIRANE*, J. ALS-NIELSEN**, M. NIELSEN*, J.M. TRANQUADA*, H. CHOU*, S. SHAMOTO and M. SATO (*Brookhaven National Laboratory, **Risø National Laboratory)

Neutron-scattering measurements have been carried out on three large single crystals of YBa₂Cu₃O₆₊ₓ with superconducting transition temperatures T_c=25, 45, and 50 K. Strong two-dimensional magnetic correlations are found in the first two, and the magnetic cross sections at low temperatures are almost as strong as in compounds with smaller x. However, the magnetic intensities at low energies below 10 meV decrease considerably on heating to 300 K. A large decrease of the magnetic inelastic cross section was observed in the third sample (T_c=50 K) relative to the first two at these low energies. The implications of these results are discussed.

IV-W-2 Spin Fluctuations in Superconducting YBa₂Cu₃O₆.₅

J.M. TRANQUADA*, W.J.L. BUYERS**, H. CHOU*, T.E. MASON***, M. SATO, S. SHAMOTO and G. SHIRANE* (*Brookhaven National Laboratory, **Atomic Energy of Canada Limited, Chalk River, ***McMasster Univ.)

Antiferromagnetic spin fluctuations in superconducting YBa₂Cu₃O₆₊ₓ have been studied using inelastic neutron scattering. In a crystal with x=0.5 and T_c=50 K, we have observed spin fluctuations at 12 K having a cross section which increases with increasing excitation energy. The data are consistent with highly overdamped spin waves and a very short spin-spin correlation length.

IV-W-3 Effect of Ni or Zn Substitution for Cu in Nd-Ce-Cu-O and Bi-Sr-(Ca,Y)-Cu-O Systems

S. YAMAGATA, K. ADACHI*, M. ONODA, H. FUJISHITA**, M. SERA, Y. ANDO and M. SATO (*Nagoya Univ., **Kanazawa Univ.)

Doping effect on the transition temperature T_c of $Nd_{1.85}Ce_{0.15}CuO_4$ and Bi-Sr-(Ca,Y)-Cu-O systems has been studied. The rates of T_c-suppression by Zn doping to electron carrier and hole carrier systems are found to be similar to those by Ni doping to hole carrier and electron carrier systems, respectively. This kind of electron-hole symmetry suggests the similarity of the natures of the holes and the electrons. For the samples with nominal formula of $Bi_2Sr_2Ca_{1-y}Y_y(Cu_{1-x}Ni_x)_2O_8$, the value of dT_c/dx is independent of y or the nominal carrier concentration. This result and other existing data indicate the possible phase separation in this system.

IV-W-4 High Energy Spin Excitations in the Insulating Phases of High-T_c Superconducting Cuprates and La_2NiO_4

S. SUGAI*, M. SATO, T. KOBAYASHI**, J. AKIMITSU**, T. ITO+, H. TAKAGI+, S. UCHIDA+, S. HOSOYA++, T. KAJITANI++, and T. FUKUDA++ (*Osaka Univ., **Aoyama-Gakuin Univ., +Univ. of Tokyo, Institute for Materials Research, Tohoku Univ.)

High-energy spin excitations up to above 8000 cm^{-1} were measured by polarized Raman scattering in the insulating phases of $S=\frac{1}{2}$ copper oxides, La_2CuO_4, $YBa_2Cu_3O_{6.2}$, $Bi_2Sr_2Ca_{0.5}Y_{0.5}Cu_2O_{8+y}$, Nd_2CuO_4, and Pr_2CuO_4, and an $S=1$ nickel oxide La_2NiO_4. All the copper oxides commonly show anomalous spectra, especially the secondary scattering peaks near $4J$ (J is the two-spin superexchange energy). Those anomalies are caused by the large four-spin cyclic exchange interactions. The present experiments demonstrated that the four-spin exchanges show distinctive characteristics in cuprates as compared to other materials.

IV-W-5 Electronic Raman Scattering from the Hole-Spin Composite States in $La_{2-x}Sr_xCuO_4$

S. SUGAI*, T. IDO**, H. TAKAGI**, S. UCHIDA**, and M. SATO (*Osaka Univ., **Univ. of Tokyo)

Electronic Raman scattering was measured in the insulator, superconductor, and "normal metal" phases of $La_{2-x}Sr_xCuO_4$. When holes are doped, the A_{1g} spectra show non-"normal Fermi liquid" behavior. The imaginary part of the experimentally obtained susceptibility is composed of the ω-proportional part below $\omega \sim T$ and the weakly ω-dependent part up to over 7000 cm^{-1}. The initial gradient increses, on cooling, as in the case of the marginal Fermi liquid model, although the exact ω/T-dependence was not obtained. The B_{1g} spectra have leading edges of which energies decrease with the increase of doping.

IV-W-6 Thermal Conductivity of High-T_c Oxides

M. SERA, S. SHAMOTO, M. SATO, I. WATANABE*, S. NAKASHIMA* and K. KUMAGAI* (*Hokkaido Univ.)

The thermal conductivity of $La_{2-x}Sr_xCuO_4$ and $La_{2-x}Ba_xCuO_4$ has been measured. In the small x region, the thermal current is considered to be mainly carried by phonons, while for $x>0.3$ in $La_{2-x}Sr_xCuO_4$, the contribution of the electron carriers becomes dominant. For $La_{1.88}Ba_{0.12}CuO_4$, the enhancement of the thermal conductivity is observed below the transition temperature from the orthorohmbic to the low temperature tetragonal phase, which may be due to the decrease of the carrier number. The anisotropy of the thermal conductivity has also been studied for $YBa_2Cu_3O_{6.7}$ and Nd_2CuO_4 single crystals.

IV-W-7 Carrier Concentration Dependence of Doping Effect and the Critical Concentration of Metal-Insulator Transition in $La_{2-x}Sr_xCu_{1-x}Ni_xO_4$

M. SATO, H. FUJISHITA* and M. SERA (*Kanazawa Univ.)

The carrier concentration dependence of the Ni-doping effect have been studied by using $La_{2-y}Sr_yCu_{1-x}Ni_xO_4$. Various experimental results support that the localization effect mainly suppresses the superconducting transition temperature T_c. The y-dependence of the critical Ni-concentration x_c of the metal-insulator transition due to the electron localization does not indicate the existence of the drastic change of the Fermi surface across the superconducting-nonsuperconducting metallic phase boundary of $La_{2-y}Sr_yCuO_4$.

IV-W-8 On the Magnetoconductance at the Spin Structure Change in La-Ba-Cu-O System

M. SATO, M. SERA, S. YAMAGATA, S. SHAMOTO and K. OKA* (*Electrotechnical Laboratory)

Magnetoconductance of a Ba-doped La_2CuO_4 crystal at the field of the spin structure change has been studied to examine its carrier concentration dependence. The present hole system which has the much larger conductivity than that of pure La_2CuO_4, also exhibits very large magnetoconductance. From the Hall voltage measurements, it is known that the excess high filed conductance is mainly due to the increase of the carrier mobility.

IV-W-9 Two Spin Superexchange and Four Spin Cyclic Exchange Interactions in High-T_c Superconducting Cuprates and Isostructural La_2NiO_4

S.SUGAI*, M. SATO, T. ITO**, T. IDO**, H. TAKAGI**, S. UCHIDA**, T. KOBAYASHI***, J. AKIMITSU***, Y. HIDAKA+, T. MURAKAMI+, S. HOSOYA ++, T. KAJITANI++ and T. FUKUDA++ (*Osaka Univ., **Univ of Tokyo, ***Aoyama-Gakuin Univ., +NTT Opto-Electronics Laboratories, ++Institute for Materials Research, Tohoku Univ.)

Raman spectra in the antiferromagnetic insulator phases of $S=1/2$ high T_c superconducting cuprates were compared with $S=1$ La_2NiO_4. The anomalous magnon spectra in cuprates suggest that the four-spin cyclic exchange interactions are very large. the doped carriers in cuprates show non-Fermi liquid behavior.

IV-W-10 Spin and Carriers in Oxide Superconductors Studied by Raman Scattering

S. SUGAI*, M. SATO, T. ITO**, T. IDO**, H. TAKAGI**, S. UCHIDA**, T. KOBAYASHI+, J. AKIMITSU+, Y. HIDAKA++, T. MURAKAMI++, S. HOSOYA***, T. KAJITANI*** and T. FUKUDA*** (*Osaka Univ., **Univ. of Tokyo, +Aoyama-Gakuin Univ., ++NTT Opto-Electronics Laboratories, ***Institute for Materials Research, Tohoku Univ.)

The spin and doped charge states in copper oxide superconductors were investigated by Raman spectroscopy. The anomalous magnon scattering in the antiferromagnetic insulator phases, such as the second peaks near $4J$ (J is the two-spin superexchange energy) in the B_{1g} spectra and the large scattering intensities in the A_{1g} spectra, suggests the existence of four-spin cyclic exchange interactions. When carriers are doped, the A_{1g} spectra, suggests the existence of four-spin cyclic exchange interactions. When carriers are doped, the A_{1g} spectra show non-"normal Fermi liquid" behavior. The imaginary part of the experimentally obtained susceptibility have ω-proportional part from $\omega \sim 0$. The gradient increases, on cooling, as in the case of the marginal Fermi liquid.

IV-W-11 Pressure Dependence of CDW of Na-Purple Bronze

H. FUJISHITA*, C. MURAYAMA**, N. MÒRI** and M. SATO (*Kanazawa Univ., **Institute for Solid State Physics, Univ. of Tokyo)

Electrical resistivities of low dimensional conductors $(Na_{1-x}Li_x)_{0.9}Mo_6O_{17}$ (x=0, 0.2) have been measured between 4.2 K and 300 K under hydrostatic pressure. Magnitude of resistivity anomaly associated with the charge density wave(CDW) transition became smaller with increasing the pressure, while the tansition temperature itself was found to be enhanced by the pressure in contrast to the simple cases of the inorganic low dimensional conductors.

IV-W-12 Neutron Investigation of the Charge Density Wave Dynamics in the Blue Bronze $K_{0.3}MoO_3$

J.P. POUGET*, B. HENNION**, C. ECRIBE-FILIPPINI*** and M. SATO (*Laboratoire de Physique des Solides, Univ. Paris-Sud. **Laboratoire Lèon Brillouin, CEN Saclay, ***CNRS, Grenoble)

The quasi one dimensional conductor $K_{0.3}MoO_3$ undergoes a Peierels transition at T_c = 183 K. Using cold neutron scattering we have succeeded for the first time to resolve in frequency and for wave vectors in reciprocal chain direction the pretransitional dynamics and the collective excitations of the phase and of the amplitude of the charge density wave (CDW) modulation below T_c. The pretransitional dynamics consists in the softening of a Kohn anomaly at the water vector $2k_F$ together with the critical growth of a central peak in the vinicity of T_c, In addition we observed just above T_c a beginning of decoupling between the flucuations of the phase and of the amplitude of the CDW. These features are discussed in the framework of recent model calculations of the dynamics of the Peierls chain. The amplitude mode is clearly observed below T_c with a quasiharmonic frequency v_A and a damping γ_A which perfectly agree with that found in a previous Raman scattering investigation of the blue bronze. By continu-ity with the behavior of the pretransitional fluctuations, v_A does not soften at T_c. The dispersion of the phase mode has also been measured in chain direction near T_c. In this temperature range the phason velocity is quite high: about one tenth of the Fermi velocity, giving a CDW mass enhancement of ~ 100. High resolution measurements show that the phason response is overdamped at $2k_F$ with a small gap which estimated value corroborates that recently found for the high frequency pinning mode of the blue bronze by millimeter wave length range conductivity measurements.

IV-W-13 Symmetry Breaking on the Phonon Raman Spectra Only at the Superconductor Compositions in $La_{2-x}Sr_xCuO_4$

S. SUGAI*, S. SHAMOTO, M. SATO, T. IDO**, H. TAKAGI** and S. UCHIDA** (*Osaka Univ., **Univ. of Tokyo)

Phonons in $La_{2-x}Sr_xCuO_4$ were systematically invstigated by Raman and infrared spectroscopy covering from the insulator, superconductor, to normal metal compositions. In the Raman spectra, modes which appear only at the superconductor compositions were found. Many of those modes were assigned to the infrared active transverse optical modes with the polarization vectors parallel to the CuO_2 plane. The Raman and infrared activity is mutually exclusive in the crystal with inversion symmetry as in the present crystal structure. The appearance of the infrared active modes in the Raman spectra implies that the doped carriers take the states which break the inversion symmetry of phonons only at the super-conductor compositions. The larger scattering intensity of those modes than of the natively active modes indictes that the deformation-potential-type electron-phonon interactions are very large. The experimental fact that the longitudinal optical modes do not appear in the Raman spectra indicates that the Fröhlich-type electron-phonon interactions induced by the macroscopic electric field of the longitudinal optical modes do not work.

IV-W-14 On the Possible Mechanism of the Successive Structural Transitions of La$_{2-x}$Ba$_x$CuO$_4$: Study by the Li Substitutions for Cu

S. SHAMOTO, M. SERA and M. SATO

Transport and magnetic properties of La$_{2-x}$Ba$_x$Cu$_{1-y}$Li$_y$O$_4$ have been studied with varying both the hole concentration and the ratio of Ba to La, independently. The depression of the superconducting transition temperature is always found around a fixed hole concentration for the series of samples with different values of Ba/La. This fact suggests that the atomic ordering of La and Ba is not primarily important, even if it exists, for the realization of the low temperature tetragonal phase. A brief comment which excludes the possibility that only in the narrow range of x around 0.15 the superconductivity appears, is also given.

IV-W-15 On the Magnetic Field Induced Spin Structure Change and the Related Magnetoconductance in La-M-Cu-O System (M=Ba and Sr)

M. SATO, M. SERA, S. YAMAGATA, S. SHAMOTO and K. OKA* (*Electrotechnical Laboratory)

Transport and magnetic properties have been studied on La$_{2-x}$M$_x$CuO$_4$ crystals. The jump of the magnetization ΔM, observed at the spin structure change induced by the magnetic field perpendicular to the CuO$_2$ plane was found to decrease below $T=T_1 \lesssim 30$ K in certain x region, suggesting the development of a new low temperature magnetic phase. Significant increase in the conductance at the spin structure change was observed even for the doped crystals with conductivity much larger than the La$_2$CuO$_4$ crystals studied previously, which suggests that it is an intrinsic behavior of the whole system of the doped holes. The Hall coefficient measured as a function of H up to about 7 tesla shows that the conductivity change is mainly due to the increase of the carrier mobility.

IV-W-16 Neutron Scattering Study of Spin Fluctuations in Superconducting YBa$_2$Cu$_3$O$_{6+x}$ (x=0.40, 0.45 and 0.50)

H. CHOU*, J.M. TRANQUADA*, G. SHIRANE*, T.E. MASON**, W.J.L. BUYERS***, S. SHAMOTO and M.SATO (*Brookhaven National Laboratory, **McMaster Univ., ***AECL Research, Chalk River)

We show by inelastic neutron scattering that dynamic spin correlations coexist with superconoductivity in YBa$_2$Cu$_3$O$_{6+x}$ (x=0.4, 0.45, 0.5). The inelastic magnetic intensity at $\Delta E=6$ meV does not show any change near T_c and is approximately constant from 250 K to 10 K, in contrast to earlier data on superconducting La$_{1.85}$Sr$_{0.15}$CuO$_4$ ($T_c=35$ K) which showed a decrease of the integrated intensity at a temperature well above T_c. The inelastic magnetic cross section observed here can be consistently modeled as 2D spin waves overdamped by short correlation lengths. The correlation length in the $x=0.5$ sample is an order of magnitude smaller than in the $x=0.40$ and $x=0.45$ samples, indicating a drastic disruption of planar copper spin-spin correlation upon hole-doping. The temperature dependence of the correlation length deduced from our measurements is consistent with an interpretation of NMR data as proposed by Millis et al.

IV-W-17 Crystal Structures of Pb$_2$Sr$_2$-YCu$_3$O$_{8+\delta}$ (δ=0 and 1.67)

H. FUJISHITA*, S. YAMAGATA and M. SATO (*Kanazawa Univ.)

Crystal Structures of Pb$_2$Sr$_2$YCu$_3$O$_{8+\delta}$ (δ=0 and 1.67) were analysed by X-ray Rietveld method. The sample with δ=1.67 obtained by an oxygen annealing has a tetragonal lattice. The analysis has been made with the assumption that absorbed oxygen atoms occupied the sites in the oxygen deficient Cu layer. We used the space group P4/mm. The analysis of the sample with δ=0 obtained by a quenching shows almost the same structure as the one presented previously. However, introduction of slight monoclinic distortion was found to give much better fit to the observed profile. The distance between the Cu and the Pb layers in the structure with δ=1.67 was found to be longer than that

with δ=0.

Large single crystals of YBa $_2$Cu $_3$O $_x$ for neutron inelastic scattering have been successfully grown, where following requirements are fulfilled. (i) The mosaic spread should be smaller than 2 degrees. (ii) The crystals volume should be larger than 0.1 cm ^{3}. (iii) The flux inclusion could be very small. The obtained crystals gave us valuable information on the dynamical magnetic natures of the compounds: First, the magnetic be-

haviors in the antiferromagnetic phase ($x < 6.4$) were clarified. The overdamped nature of the spin fluctuations, which exist even in the superconducting phase with $T_c \approx 60$ K was revealed. Now, the magnetic behaviors in the compounds with $T_c \approx 90$ K are being clarified. Trials of the growth of La $_{2-x}$Sr $_x$CuO $_4$ crystals with x larger than 0.3 have also been made. In this case, only the small crystals have been obtained. One of the most serious difficulties we have encountered in the larger ($\lesssim 10\%$) inclusion of Pt atoms from the used crucible. Then, it may be important to adopted other methods which do not use crucibles for getting high quality crystals.

IV—X   Development of Surface Molecular Dynamics Sensitive to the Structure of Reaction Sites

The structure of reaction sites on solid surfaces is one of the most important pieces of information for designing new functional catalysts. This structure should be analyzed through dynamic properties of surface processes, since it is not provided by structural information of non-reacting surface species obtained with various spectroscopies, diffraction methods, and so on. We have expected that the spatial distribution of the desorption flux of product molecules will open new reaction dynamics sensitive to the structure of reaction sites in the first stage. In fact, the distribution has been found to depend on (a) the arrangement of reactants around the reaction site and also on (b) the arrangement of substrate atoms constructing the reaction site. We have studied the correlation between the orientation of the reaction site and the spatial distribution. The model reaction utilized is the oxidation of carbon monoxide over platinum metals. We have succeeded in confirming that the orientation is well preserved in the spatial distribution of the desorption flux of carbon dioxide produced on Pt(110)(1×2) and Ir(110)(1×2) reconstructed surfaces.

IV-X-1   The Angular Distribution of the Product Desorption and the Orientation of Terraces; the Oxidation of Carbon Monoxide over Platinum(110)(1×2) Reconstructed Surfaces

Tatsuo MATSUSHIMA and Yuichi OHNO

The angular distribution of the desorption flux of CO_2 produced on Pt(110)(1×2) reconstructed surfaces was studied in both crystal azimuths of [1$\bar{1}$0] and [001] by means of angle-resolved thermal desorption. This surface consists of (111) terraces declining about $\pm 30°$ in the [001] direction. Heating the surface covered by CO and oxygen adatoms yields four peaks of CO_2 formation in the range from 160 to 430K. The desorption

of the product in each peak yielded a sharp angular distribution collimated along the bulk surface normal in the [1$\bar{1}$0] direction. On the other hand, the desorption of CO_2 produced in the dilute co-adlayer showed two maxima in the angular distribution curves in the [001] direction. Such two-directional collimation is due to the reactive desorption from terraces declining on the reconstructed surfaces.

IV-X-2   The Spatial Distribution of the Product Desorption in the Oxidation of Carbon Monoxide on Platinum(110)(1×2) Reconstructed Surfaces

Tatsuo MATSUSHIMA

The spatial distribution of the desorption of carbon dioxide produced on platinum(110)(1×2) reconstructed surfaces was studied in the wide range of the reactant coverages by means of angle-resolved thermal desorption and low-energy electron diffraction. Heating the surface covered by oxygen atoms and carbon monoxide yields four peaks in the CO_2 formation: P_1- around 400K, P_2- (300K), P_3- (250K), and P_4-CO_2 peaks (170K). The desorption of each CO_2 indicated a sharp angular distribution collimated along the bulk surface normal in the $[1\bar{1}0]$ direction. On the other hand, the desorption of P_1- and P_2-CO_2 produced at small coverages showed two-directional desorption collimated at either about +23 or −23 degrees off the bulk surface normal in the [001] direction. It indicates that the reactive desorption takes place on declining terraces of the reconstructed plane. The desorption of P_3- and P_4-CO_2, and also of P_2-CO_2 produced at high initial CO coverages, showed a single peak in the angular distribution curve in the same direction, which was collimated along the bulk surface normal. This suggests that the reconstruction is at least partly lifted during heating procedures, and CO_2 is formed on the non-reconstructed as well as the reconstructed plane. It was supported by low-energy electron diffraction observations.

IV-X-3 Spatial Distribution of Reactive Carbon Dioxide Desorption on Pt(110)(1×2) Surfaces

Tatsuo MATSUSHIMA

The spatial distribution of the desorption flux of product molecules was studied for the oxidation of carbon monoxide on Pt(110)(1×2) reconstructed surfaces by means of angle-resolved thermal desorption and low-energy electron diffraction. Two-directional desorption, which was collimated at either about +23 or −23 degrees off the bulk surface normal, was observed in the [001] direction for CO_2 produced at small CO coverages. At high CO coverages, where the transformation of (1×2) into (1×1) was significant, the

observation of the above desorption was obscured by the contribution of reactive CO_2 desorption from (1×1) patches. No dependence on the oxygen coverage was found in the spatial distribution. The distribution in the $[1\bar{1}0]$ direction is always collimated along the bulk surface normal. It has been confirmed that the orientation of the reaction site is preserved in the spatial distribution of the product desorption.

IV-X-4 The Spatial Distribution of Reactive Carbon Dioxide Desorption on Iridium(110)(1×2) Reconstructed Surfaces

Tatsuo MATSUSHIMA, Yuichi OHNO, and Kiyoshi NAGAI

The spatial distribution of the desorption flux of carbon dioxide produced on Ir(110)(1×2) reconstructed surfaces was studied by means of angle-resolved thermal desorption and low-energy electron diffraction. A single CO_2 formation peak appeared around 380K while heating the coadlayer of CO(a) and O(a). This CO_2 shows two-directional desorption collimated at about ±26 degrees off the bulk surface normal in the [001] direction. The orientation of the reaction site is well preserved in the spatial distribution of the product desorption.

IV-X-5 Spatial Distribution of Reactive Carbon Dioxide Desorption on Palladium(100) Surfaces

Yuichi OHNO and Tatsuo MATSUSHIMA

The desorption of CO_2 produced by the interaction of oxygen adatoms with CO admolecules on Pd(100) was studied with angle-resolved thermal desorption. The spectra of CO_2 formation showed four peaks; P_1- (around 380K), P_2-(~325K), P_3-(~260K), and P_4-CO_2(~220K). Each CO_2 desorption showed a different angular distribution. The distribution is sharply collimated normal to the surface and isotropic with respect to the crystal azimuth.

IV-X-6 Transformation of Iridium(110)(1×1) into (1×2) and Spatial Distribution of Reactive Carbon Dioxide Desorption

Tatsuo MATSUSHIMA, Yuichi OHNO, and Kiyoshi NAGAI

The spatial distribution of the desorption flux of CO_2 produced on Ir(110)(1×1) and (1×2) surfaces was studied by means of angle-resolved thermal desorption and low-energy electron diffraction. The distribution is collimated along the bulk surface normal on (1×1). It is sharp in the [001] direction and sharper in the [1$\bar{1}$0] direction. This distribution is consistent with the model that the reactive desorption occurs on a short bridge site. On (1×2) surfaces, two-directional desorption was observed, which was collimated along the axis at the polar angle of 26 degrees in both [001] and [00$\bar{1}$] directions as shown in Figure 1. The distribution in the [1$\bar{1}$0] direction is collimated along the bulk surface normal. The reactive desorption was suggested to take place on a three-fold hollow site on the declining terrace. The spatial distribution changed from the (1×1) type to the (1×2) type during the transformation of the surface structure. This structure change was confirmed by low-energy electron diffraction.
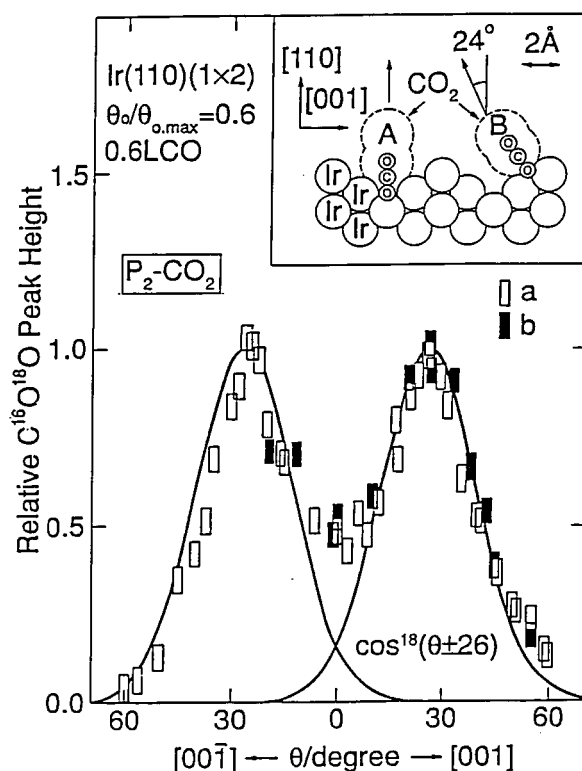
Figure 1. Angular distribution of the P_2-CO_2 desorption flux in the [001] direction on Ir(110)(1×2) reconstructed surfaces. Results in two series are summarized. θ is the desorption angle (the polar angle). $\theta_0/\theta_{0.MAX}$ is the relative oxygen coverage. The inserted figure shows a side view of the reconstructed surface and also the reaction site on (A) a long bridge site in the trough and (B) a three-fold hollow site on the declining terrace.

IV-X-7 Dissociation of Oxygen Admolecules on Platinum(110)(1×2) Reconstructed Surfaces at Low Temperatures

Yuichi OHNO and Tatsuo MATSUSHIMA

The desorption and dissociation of oxygen admolecules were studied on Pt(110)(1×2) reconstructed surfaces at low temperatures by using thermal desorption combined with an isotope tracer method. The desorption from the molecular adsorption state yields two main peaks at 180 and 200K. The dissociation occurs in the range of 180-220K, where the latter desorption peak appears. The desorption due to the recombination of dissociated oxygen takes palce above 650K.

IV-X-8 Angle and Speed Distributions of Hydrogen Desorbing Thermally from Metal Surfaces
I. Quantum Mechanical Transition State Theory

Yuichi OHNO, Takashi NAKAMURA *(Hokkaido Inst. Tech.)*, and Hideaki KITA *(Hokkaido Univ.)*

A quantum theoretical treatment of the angle and speed distributions of recombinatively desorbing hydrogen from metal surfaces is proposed. The desorption rate is discussed in the framework of the transition state theory. The recombinative reaction process of hydrogen due to thermal activation leads to the formation of an activated complex in the transition state. In the vicinity of a saddle point on a three-dimensional potential energy surface, the translational motion of the acti-

vated complex in the direction perpendicular to the metal surface is accompanied by its center-of-mass vibrational motion parallel to the metal surface. In order to carry out the quantum mechanical calculation, the potential surface is replaced by a simiplified model potential, which provides a square potential barrier along the surface normal. It is shown that, on leaving the potential barrier, the activated complex is reflected by the boundary of the potential barrier with a certain probability and, at the same time, the center-of-mass modes of vibration are coupled with the translational motion along the surface normal. Vibrational wave functions in the momentum representation are used to calculate the transmission coefficient, which is incorporated into the conventional rate formula. The angle-dependent speed distributions of desorbing molecules are derived from the rate formula.

IV-X-9 Angle and Speed Distributions of Hydrogen Desorbing Thermally from Metal Surfaces
II. Application to D_2 Desorbing from a Ni(111) Surface

Yuichi OHNO, Takashi NAKAMURA *(Hokkaido Inst. Tech.)*, and Hideaki Kita *(Hokkaido Univ.)*

On the basis of the theory developed in the above work, the angle and speed distribution of D_2 molecules desorbing thermally from the Ni(111) surface are numerically calculated in the present work. The dynamical motion of the activated complex of the recombinative desorption process is calculated by using a model potential surface, which involves a few parameters introduced to describe the necessary features of the potential surface at the transition state. Numerical calculations are carried out, and the results show that the present dynamical theory reproduces very well a variety of the characteristic features of the experimental results, e.g., sharply focused angular distribution, mean translational energy lower than $2k_BT$ at grazing angle, and the non-Maxwellian profile of the TOF distribution.

IV-X-10 Thermal Desorption Spectrum of Hard Hexagon Model

Kiyoshi NAGAI

The theoretical basis in statistical mechanical analysis of thermal desorption spectra is not yet established. In fact, there have been disputes between two groups of transition state reaction rate theory. The rate expression in the first group is a statistical mechanical extension of the Polanyi-Wigner rate, in which the local interaction energy is taken into account and the effect of adsorbate's entropy is ignored. The second is proportional to the activity of adsorbate, which takes account of both energy and entropy. Using these two theories, we calculated the thermal desorption spectra for the **hard hexagon model** (the triangular lattice gas with infinite first neared neighbor repulsion) which was solved exactly by R.J. Baxter (1982). A large difference was found in the resultant spectra; the first group gives a trivial spectrum identical with that of the ideal gas, which is physically unreasonable in view of the different thermodynamics of the ideal gas and the hard hexagon. In contrast, the second gives an extra sharp peak which originates from the critical behavior of the hard hexagon model. Experiments for CO/Ru(001) supports the latter results.

IV-X-11 Construction of an Apparatus for Thermal Desorption Studies at Low Temperatures

Tatsuo MATSUSHIMA, Yuichi OHNO, and Kiyoshi NAGAI

An apparatus for thermal desorption measurements in the temperature range from 50K to 1000K was constructed. The desorption of oxygen admolecules on Pd(100) was studied by using this apparatus. The desorption from physisorbed molecules was detected at $60 \sim 70$K. The desorption from chemisorbed molecules was confirmed in the range of $100 \sim 170$K.

IV-X-12 Construction of an Apparatus for Velocity Distribution Measurements of Molecules Produced during Thermal Desorption

Tatsuo MATSUSHIMA, Kosuke SHOBATAKE, Yuichi OHNO, and Kiyoshi NAGAI

An apparatus for velocity distribution measurements of surface reaction products desorbing during heating procedures of reactant co-adlayers was constructed. It consists of three ultra-high vacuum chambers; a reaction chamber, a chopper chamber, and an analyzer chamber. The first has a rotatable crystal holder with a cold stage, optics for low-energy electron diffraction and Auger electron spectroscopy, and facilities for sample cleaning. The second has a correlation chopper for pseudo-random time-of-flight measurements, in order to get a high transmission. A mass-spectrometer was set in the third chamber. This apparatus will be used to get velocity distribution curves of desorbing product molecules from well-defined metal surfaces, as a function of desorption angle and crystal azimuth.

IV—Y Photochemistry of Organometallic Complex Adsorbed on Solid Surfaces

Photochemistry of organometallic complex adsorbed on slid surfaces has received increasing attention in recent years. The driving force behind this stems from its potential use in catalysis and microelectronics. Interest in the surface photochemistry also arises from the fact that its products are often quite different from those observed in gas phase or in liquid solution. We have studied the photolysis of metal carbonyls adsorbed on metal oxide powders to investigate catalytic effects of the surface on a photochemical secondary process.

IV-Y-1 Surface Photochemistry of Metal Cabronyls. I. Photolysis of Iron Carbonyls Adsorbed on Alumina and Silica

Shinri SATO and Tadayoshi OHMORI

Photolysis of $Fe(CO)_5$, $Fe_2(CO)_9$, and $Fe_3(CO)_{12}$ adsorbed on alumina and silica has been studied by FTIR spectroscopy. On alumina, $Fe(CO)_5$ photolysis by visible and near-UV light gives a mixture of $Fe_2(CO)_9$ and $Fe_3(CO)_{12}$, while it leads mainly to the formation of $Fe_3(CO)_{12}$ on silica. The photolysis by deep-UV light from a D_2 lamp or SOR eliminates $Fe_3(CO)_{12}$ formation, whereas it gives little effect on the product on silica. On hydrated alumina a hydride complex is formed due to the basic property of alumina surface. Adsorbed $Fe_2(CO)_9$ and $Fe_3(CO)_{12}$ are fairly stable under illumination, though they are slowly decomposed in the dark. These results are discussed in terms of the catalytic properties of surface.

IV-Y-2 Photochemical Formation of $[HFe_3(CO)_{11}]^-$ and $[HFe(CO)_4]^-$ from $Fe(CO)_5$ Adsorbed on Hydrated Alumina

Shinri SATO and Tadayoshi OHMORI

Photolysis of $Fe(CO)_5$ adsorbed on hydrated alumina produced simultaneously hydride species, $[HFe_3(CO)_{11}]^-$ and $[HFe(CO)_4]^-$, and intermediate species, $Fe(CO)_4$ adsorbed on the basic sites of alumina. While $[HFe_3(CO)_{11}]^-$ was labile under dynamic vacuum in the dark probably due to its reversion to $Fe(CO)_5$, $[HFe(CO)_4]^-$ and $Fe(CO)_4$ were stable.

IV-Y-3 FTIR Study on the Photochemistry and Adsorption States of Iron Carbonyls Adsorbed on Alumina

Shinri SATO and Tadayoshi OHMORI

The behaviors of iron carbonyls adsorbed on alumina have been studied in the dark and under illumination by FTIR spectroscopy. Photolysis products of adsorbed $Fe(CO)_5$ are affected by hydration of surface as well as by their stability on alumina. On hydrated surfaces the photolysis leads to the formation of $[HFe_3(CO)_{11}]^-$, $[HFe(CO)_4]^-$, and $Fe(CO)_4$, which can be thermally produced at a smaller rate by base catalysis. The photo- and thermochemical formation of $[HFe(CO)_4]^-$ requires stronger basic sites than that of $[HFe_3(CO)_{11}]^-$. The photolysis of $Fe(CO)_5$ on dehydrated alumina results in predominant formation of $Fe_2(CO)_9$ with concomitant formation of a small amount of $Fe_3(CO)_{12}$, though the latter is exclusively formed on illuminated silica. This is because $Fe_3(CO)_{12}$ undergoes a disproportionation reaction on dehydrated alumina. These photo-products appear to be formed not at the outermost surface of alumina but inside the sample disc. The results are discussed with reference to those obtained for silica in terms of catalytic properties of surfaces.

IV-Y-4　Effects of Surface Acid and Basic Sites on the Photolysis of Iron Carbonyls Adsorbed on Silica

Tadayoshi OHMORI and Shinri SATO

Photolysis of iron carbonyls adsorbed on various types of silica was investigated by IR spectroscopy. In $Fe(CO)_5$ photolysis, $Fe_3(CO)_{12}$ was exclusively produced on any types of silica samples irrespective of hydration of the sample as already reported before. In the presence of gas phase water, a small amount of $[HFe_3(CO)_{10}]^-$ was formed on one of the samples used (denoted as sample A), while another sample still gave $Fe_3(CO)_{12}$ at a much smaller rate than in the absence of gaseous water. In $Fe_3(CO)_{12}$ photolysis, no appreciable change was observed on all of the samples. The addition of gas phase water, however, led to the photoformation of $[HFe_3(CO)_{10}]^-$ on sample A and to the slow photodecomposition to $Fe(CO)_5$ on the other samples. The hydride formation was suppressed by modification of the surface of sample A with a trace amount of formic acid. Modification of the surface with a trace amount of pyridine, on the other hand, made another sample possible to photo-produce the hydride.

These results indicate that the photo-formation of the hydride on sample A is due to a trace of weak basic sites formed probably by impurity.

IV-Y-5　Adsorption States of $Fe(CO)_5$ on TiO_2

Yuji UKISU, Shinri SATO and Tadayoshi OHMORI

The adsorption states and the reactivity of $Fe(CO)_5$ on TiO_2 have been studied by FTIR spectroscopy. When adsorbed $Fe(CO)_5$ is illuminated by visible light which wavelength is longer than the absorption edge of TiO_2, the IR spectrum of its photolysis products is not observed, indicating that $Fe(CO)_5$ is completely photodecomposed to Fe on TiO_2 as has been observed on Si. The adsorption of $Fe(CO)_5$ on semiconductors is, therefore, thought to be more labile than on insulators such as silica, probably because of electronic effects of semiconductor. In connection with this, we have found significant shift of the IR band of adsorbed $Fe(CO)_5$ to longer wavelength when TiO_2 is reduced. Since such shift of IR band implies the formation of anionic species, a charge-transfer complex of $Fe(CO)_5$ with Ti^{3+} may be formed. The new species formed on reduced TiO_2 is so reactive that a ligand exchange reaction with NO readily occurs at room temperature.

IV-Y-6　Construction of an Apparatus for Surface VUV-Photochemistry

Shinri SATO, Makoto WATANABE, Tadayoshi OHMORI and Yuji UKISU

To study the VUV-photochemistry of molecules adsorbed on solid surfaces, a UHV apparatus connected to a beam line of UVSOR has been constructed. Synchrotron orbital radiation is introduced directly or through various type of filters to the apparatus. The apparatus is equipped with a polarization-modulation FTIR reflection-absorption spectrometer to monitor surface species and with a manipulator which is able to control temperature of a sample from ca. 90 to 1300K.

RESEARCH ACTIVITIES V
Department of Applied Molecular Science

V—A New Multi-Stage Redox Systems

Interdisciplinary cooperation between synthetic chemistry, physical chemistry, and solid state physics opens a new field of science which can explore new materials having interesting electrical, magnetic, and optical properties in the solid state. Correlation between molecular and solid state properties discloses the importance of conjugated electronic systems having multi-stage redox nature, which can transfer electrons smoothly by multi-stage manners. Recently, we have designed and synthesized two classes of new multi-stage redox systems, such as peri-condensed Weitz type donors and amphoteric multi-stage redox systems. The former redox system is designed by replacing two of the sp^2 carbon atoms in a polycyclic arene by two sulfur atoms. Such peri-condensed heterocycles have produced new organic molecular metals which contain non-TTF and non-TCNQ type components. The latter redox system is designed so as to decrease the difference between the oxidation and the reduction potentials of a molecule. We already reported the conjugated hydrocarbons with the highest amphotericity. Design and synthesis of new type of multi-stage redox systems, and investigation of their solid state properties are actively continued.

V-A-1 Synthesis and Properties of 3,9-Dithiaperylene: A Third Isomer of Peri-Condensed Weitz-Type Donors Based on Perylene Skeleton

Kazuhiro NAKASUJI, Akio ODA,[a] Jiro TOYODA, Ichiro MURATA[a] (*a Osaka Univ.*)

Peri-condensed Weitz-type donors, such as dithiaperylene (DTPR) and dithiapyrene (DTPY), have produced a variety of organic conductors ranging from semiconductors to molecular metals. DTPR contains four reasonably stable isomers. We already reported synthesis of two isomers, 3,10- and 1,7-DTPR. A third isomer, 3,9-DTPR, has been synthesized from 1,5-dichloroanthraquinone through four steps by employing titanium-induced dicarbonyl cyclization as a key step. Comparison of the physical properties of the three isomers of DTPR's provides good correlation between their electronic and structural characteristics. Three donors, 3,9-, 1,7-DTPR, and 3,10-DTPR, in this order, show increasing oxidation potentials. Such a feature coincides with the structural consideration that the anthracene moiety in the C$_{2h}$ isomers contributes to raise their HOMO's to a larger extent than the phenanthrene moiety in the C$_{2v}$ isomer. The MNDO calculations for the HOMO energies are consistent with the behavior of the experimental data. Although preliminary studies for charge transfer complexes of 3,9-DTPR are in progress, a single crystal of the iodine complex showed a relatively high conductivity (7 Scm^{-1}).

3,9-DTPR
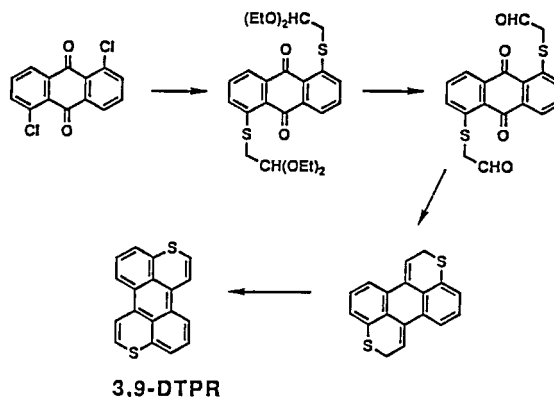
V-A-2 Crystal Structure and Electronic Structure of Radical Salts of 2,7-Bis(methylthio)-1,6-dithiapyrene (MTDTPY) and 2,7-(methylseleno)-1,6-dithiapyrene (MSDTPY)

Atsushi KAWAMOTO,[a] Jiro TANAKA,[a] Akio ODA,[b] Ichiro MURATA,[b] Kazuhiro NAKASUJI (*a Nagoya Univ., b Osaka Univ.*)

Radical salts of 2,7-bis(methylthio)-1,6-dithiapyrene (MTDTPY) with PF_6^- and 2,7-bis(methylseleno)-1,6-dithiapyrene (MSDTPY) with AsF_6^- and $[Au(CN)_2]^-$ were prepared using an electrochemical method. The crystal structures of these salts were determined with an X-ray method. MTDTPY-$(PF_6)_{0.67}$ and MSDTPY-$(AsF_6)_{0.67}$ form uniform segregated stacks of MTDTPY and MSDTPY molecules with interplanar distances of 3.40 and 3.59 Å, respectively. Short S...S contacts of 3.46-3.56 Å and 3.54-3.61 Å, respectively, were observed between the columns. The optical reflection spectra of these crystals were measured with polarized light both parallel and perpendicular to the stacking axis. In spite of the short intercolumnar S...S contacts, the spectra showed strong one dimensional character. The optical conductivity spectra and real part of the dielectric constant along the stack axis were obtained by means of Kramers-Kronig transformation. These results were analyzed with a one-dimensional electron localization model in a disordered system.
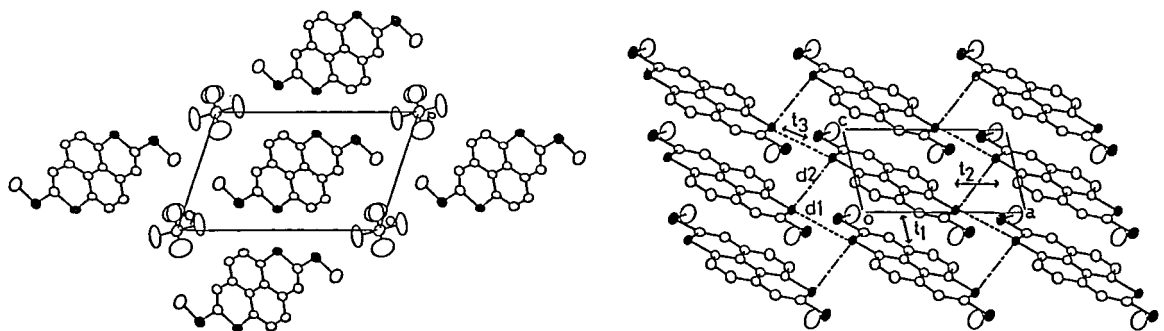
Figure 1. Crystal structure of MTDTPY-$(PF_6)_{0.67}$.

V-A-3 Electronic Structure of 2,7-Bis(methylthio)-1,6-dithiapyrene (MTDTPY) Charge Transfer Complexes

Atsushi KAWAMOTO,[a] Jiro TANAKA,[a] Mitsuru SASAKI,[b] Ichiro MURATA,[b] Kazuhiro NAKASUJI ([a]Nagoya Univ., [b]Osaka Univ.)

Polarized reflection spectra were measured on two charge transfer complexes of 2,7-MTDTPY with chloranil and TCNQ, which showed metallic conductivity. In spite of short intercolumnar S...S contacts, the spectra showed strong one-dimensional character. The optical conductivity spectra and real part of the dielectric constant along the stack axis were obtained by means of Kramers-Kronig transformation. These results were analyzed with a one-dimensional electron localization model in a disorderd system.

V-A-4 Conformational Adaptation: A New Aspect of Substituent Effects

Satoshi INAGAKI,[a] Takehiko OKAJIMA,[a] Kimiaki YAMAMURA,[b] Hideyoshi MIYAKE,[b] Kazuhiro NAKASUJI, Ichiro MURATA[c] ([a]Gifu Univ., [b]Kobe Univ., [c]Osaka Univ.)

Methoxyl (CH_3O-) substituent on unsaturated molecules was suggested by ab initio molecular orbital calculation and qualitative orbital interaction theory to change from coplaner to vertical conformation on electron acceptance. The conformational adaptation can make it possible that methoxy group is less electron-donating than methyl group.

V—B   New Stable Neutral Conjugated Radicals and Their Redox States

Design and synthesis of new stable neutral conjugated radicals have been attracted much attention to explore new materials having potentially interesting solid state properties, for example single component conductors, and magnetically interesting materials. While exploration of totally new molecules are always important for synthetic chemists, chemical modifications for known electronic systems are also important. Recently, we have utilized odd alternant hydrocarbon, phenalenyl, as the basic skeleton for neutral radicals, and modified the phenalenyl skeleton by introducing donor and acceptor substituents to suppress the thermodynamic and kinetic instability. Such modifications are sometimes applied in physical organic chemistry to stabilized unstable electronic systems.

V-B-1   Synthesis and Characterization of Phenalenyl Cations, Radicals, and Anions Having Donor and Acceptor Substituents: Three Redox States of Modified Odd Alternant Systems

Kazuhiro NAKASUJI, Masakazu YAMAGUCHI,[a] Ichiro MURATA,[a] Kizashi YAMAGUCHI,[a] Takayuki FUENO,[a] Hiroaki OHYANISHIGUCHI,[b] Tadashi SUGANO,[c] and Minoru KINOSHITA[c]

([a]Osaka Univ., [b]Kyoto Univ., [c]ISSP)

	R_1	R_2	R_3
a	OCH_3	H	H
b	OCH_3	H	OCH_3
c	OCH_3	OCH_3	OCH_3
d	SCH_3	H	H

Synthesis and characterization of the phenalenyl cations, anions, and radicals having the donor and the acceptor substituents are reported. The donor, methoxy or methylthio, groups and the acceptor, cyano, group are introduced at the electronically active α-positions of phenalenyl. The synthetic procedures are the construction of β-cyanonaphthalenes with the suitable substituents 5, and their conversions into the corresponding phenalenes 9 keeping the cyano group intact. The cations, 2a$^+$, 2b$^+$, 2c$^+$, 2d$^+$, were isolated by treatment of 9 with trityl perchlorate. The anions, 2a$^-$, 2b$^-$, 2c$^-$, 2d$^-$, were generated by treatment of 9 with n-BuLi. The radicals, 2a$^\circ$, 2b$^\circ$, 2c$^\circ$, 2d$^\circ$, were generated by applying the electrochemical oxidation technique to 9. Both the NMR and EPR spectra reveal that these modified phenalenyl species still maintain the characteristics as odd alternant electronic systems. The cation salt $(2d)_1(ClO_4)_{0.7}$ was paramagnetic not only in the solid state but also in a solution. In addition, the salt showed semiconducting behavior $(\sigma = 10^{-5}$ S cm^{-1}, $E_a = 0.3$ eV).
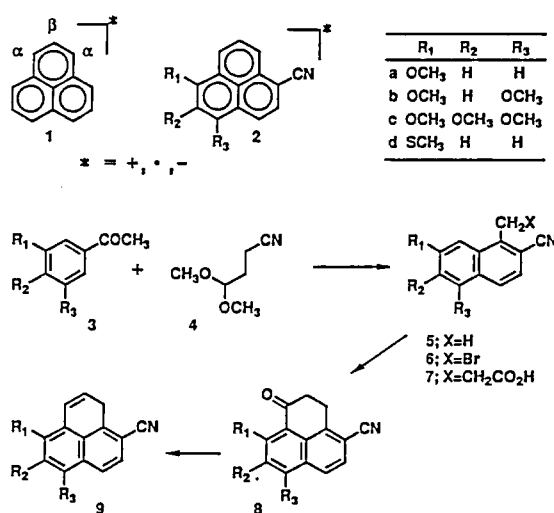
V—C New Cooperative Proton-Electron Transfer (PET) Systems

Recent discovery of a new phase transition in quinhydrone under pressure has opened an interdisciplinary area between organic chemistry and solid state physics to explore new materials having potentially interesting solid state properties. Molecular level considerations for such a cooperative phenomena in solids lead to new molecular design strategies. Thus, as one of general strategies, the exploration of the stable neutral radicals having hydrogen bonding networks is important. As a first step, the donor and acceptor substituted quinones and hydroquinones were synthesized and their physical properties were investigated. As a next step, the extended conjugated quinhydrones, for example, naphthoquinhydrones have been prepared. We are now improving the molecular level concept and constructing new materials.

V-C-1 Amphoteric Redox Nature of *p*-benzoquinones with Donor- and Acceptor-Substituent

Toshikazu KITAGAWA, Jiro TOYODA, Kazuhiro NAKASUJI, Hiroshi YAMAMOTO,[a] Ichiro MURATA[a] (*[a]Osasa Univ.*)
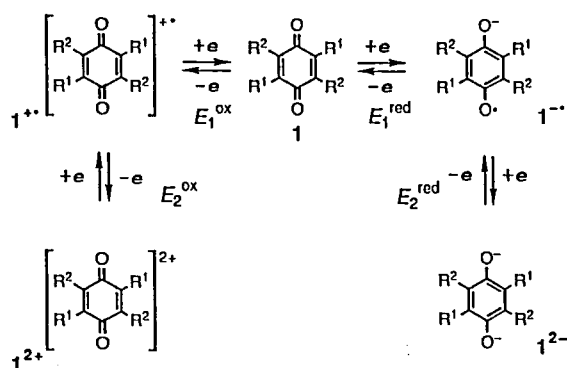
For the precise control of the electronic properties of quinonoid type acceptors, knowledge about the effect of substituents on the electrochemical behavior of quinoid compounds, *e.g p*-benzoquinones, seems essential. In this study, the redox properties of sixteen substituted *p*-benzoquinones, which include four newly synthesized *p*-benzoquinones, were measured by cyclic voltammetry. Despite the presence of bulky substituents E_1^{red} showed a good linear correlation with a Hammett constant, $\Sigma(\sigma_m + \sigma_p)/2$. Linear relationship was also obtained for the potential of the second reduction (E_2^{red}) against $\Sigma(\sigma_m + \sigma_p)/2$. It is noteworthy that most of the quinones showed the oxidation peak potentials (E_1^{ox}). Good linearity was also obtained for

the first oxidation potentials, E_1^{ox}. In addition, a measure of amphotericity, $E^{sum} = E_1^{ox} - E_1^{red}$, is a linear function of $\Sigma(\sigma_m + \sigma_p)/2$. This suggests narrow HOMO-LUMO gaps of quinones with stronger electron-donating substituents.

V-C-2 General Strategies to Design and Construct New Cooperative Proton-Electron Transfer Systems

Kazuhiro NAKASUJI, Kenichi SUGIURA, Jiro TOYODA, and Tadaoki MITANI
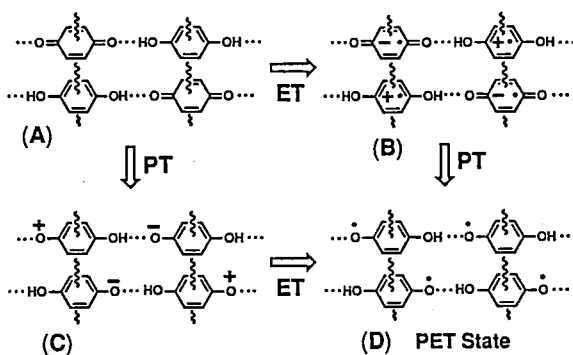
Cooperative proton-electron transfer (PET) reactions in hydrogen-bonded systems have been a prolonged subject of experimental and theoretical interests. Our particular attention is concentrated on stabilization of a PET state by using the chemical interactions present in the solid and on exploration of new materials based on the hydrogen-bonded electronic systems. Considering the reaction as if it were stepwise, we can visualize the phases transition found for quinhydrone,

as shown in the Figure. The final PET state (D) can be characterized by a molecular assembly of H-bonded neutral radicals. Therefore, two reasonable molecular design strategies for realization of such cooperative PET systems in the solid state are revealed; the exploration of (a) a quinone-hydroquinone pair with a smaller intermolecular CT gap and/or (b) an electronic modification to stabilize H-bonded neutral radicals.

V-C-3 New Cooperative Proton-Electron Transfer Systems: Pyrenoquinhydrones as Extended Conjugated Quinhydrones

Toshikazu KITAGAWA, Kenichi SUGIURA, Jiro TOYODA, Kazuhiro NAKASUJI, Hiroshi OKAMOTO, Kaoru OKANIWA, and Tadaoki MITANI

1,6-PYQH   1,8-PYQH
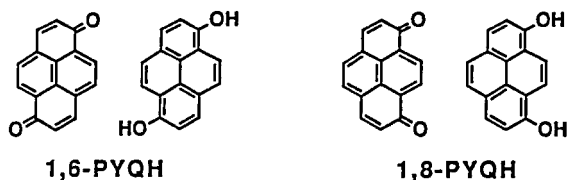
We utilized one of molecular design strategies, that is, construction of a quinone-hydroquinone pair with a smaller intermolecular CT gap, for realization of cooperative PET systems in the solid state. For this purpose, we prepard two extended conjugated quinhy-

drones, 1,6- and 1,8-pyrenoquinhydrones. Their solid state CT transition energies are 1.43 and 1.42 eV, respectively. Apparently, smaller energies of the CT gaps are observed, compared with that of benzoquinhydrone (2.34 eV). Single crystals of pyrenoquinhydrones were in progress by a diffusion method. Similarly to benzoquinhydrone, the pyrenoquinhydrones have shown pressure-response infrared and electronic absorption spectral characteristics.

V-C-4 Cooperative Proton-Electron Transfer System Containing Bis(4-hydroxyphenyl)disulfide as Donor Component

Kenichi SUGIURA, Jiro TOYODA, Kazuhiro NAKASUJI, Kaoru OKANIWA, Hiroshi OKAMOTO, Tadaoki MITANI

In order to expand the range of cooperative PET systems, the search for new donors with proton donating character are now in progress. A new donor, bis(4-hydroxyphenyl)disulfide, has been designed and synthesized. Its CT complexes with benzoquinone derivatives gave a large-size of single crystals of black cubics. X-ray crystal structure analysis showed the presence of unique CT and H-bonding networks of the components. Pressure-response infrared absorption spectral characteristic was observed.

V—D Transition Metal Oxide Clusters

The surfaces of metal oxides bound organometallic species are of interest not only as important heterogeneous catalysts but also as targets to model in coordination compounds because they have three-dimensional framework of mixed metals (soft and hard metals) and mixed valence multicenters, which cause cooperative phenomena during catalytic hydrocarbon transformations.

We have continued to study the integrated cubane type of clusters as a model compound for the inorganic oxide-bound RhCp* groups that is much more active and selective for hydroformylation.

V-D-1 Second Ionization Mass Spectroscopy (SIMS) for the Integrated Cubane Type of Clusters

Yoshihito HAYASHI, Yoshiki OZAWA, and Kiyoshi ISOBE

SIMS spectra of $[(MCp^*)]_4V_6O_{19}]$ (M = Rh(1),

Ir(2)) were recorded on a HITAC M4000 high resolution double-focusing mass spectrometer. Milligram samples were dissolved in 100 μL of CH_3OH, and 1-2 μL of this solution was added to 10 μL of m-nitrobenzyl alcohol matrix placed on the target. An 8 kV Xe^+ ion beam was used to bombard the target matrix and positive ions produced are detected. The spectra of cluster 1 and 2 are shown in Figure 1a and 1b, respectively. Both the spectra contain the $[M+H]^+$ ions with characteristic isotopic distribution patterns and the most abundant mass ion peaks appear at m/Z 1563 and 1921, respectively, as the base peaks. Interestingly,

a major fragmentation pathway clearly displays sequential loss of oxygen atoms (m/Z = 16) from these $[M+H]^+$ ions to form the $[M-O]^+$ and $[M-2O]^+$ ions. A daughter ion search (B/E method) by a linked scan method revealed that the $[M+H]^+$ and $[M-O]^+$ ions selectively produce the $[M-O]^+$ and $[M-2O]^+$ ions, respectively. Thus SIMS as well as FABMS is particularly noted for its outstanding sensitivity of chemical and isotopic detection, and it provides a rapid and accurated analytical method for determining the elemental composition and molecular weights of the oxide clusters.
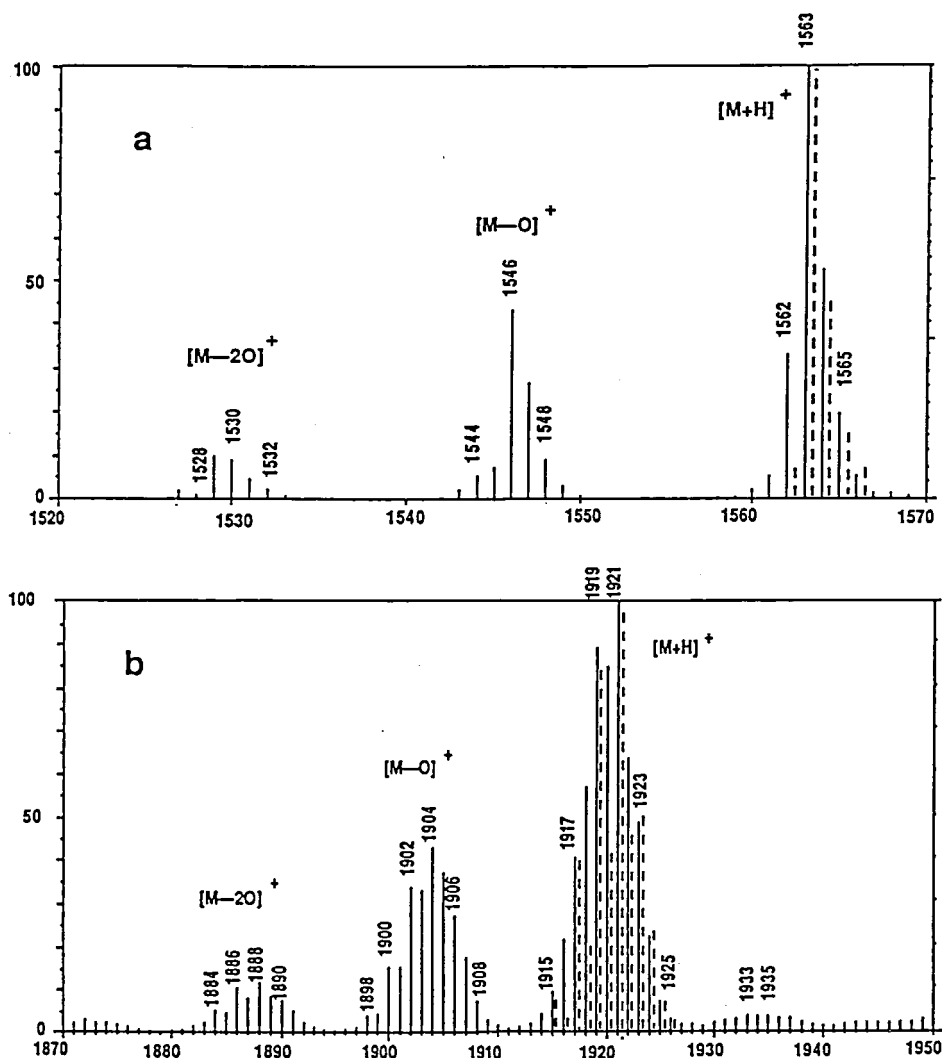
Figure 1. Positive-ion SIMS spectra of (a) $[(RhCp^*)_4V_6O_{19}]$ and (b) $[(IrCp^*)_4V_6O_{19}]$. The dotted lines are theoretical distributions of the molecular ion peaks.

V-D-2 Study of Oxidative Dehydrogenation of Methanol on Molybdenum Trioxide Surfaces by Use of the Triple Cabane Type Oxide Cluster as a Model Compound

Youngkyu DO *(KAIST and IMS)*, Yoshiki OZAWA, Xiao-Zeng YOU *(Nanjing University and IMS)*, Cuiji ZHANG *(ICAS and IMS)*, Yoshihito HAYASHI, and Kiyoshi ISOBE

$$[Cp^*RhMoO_4]_4$$
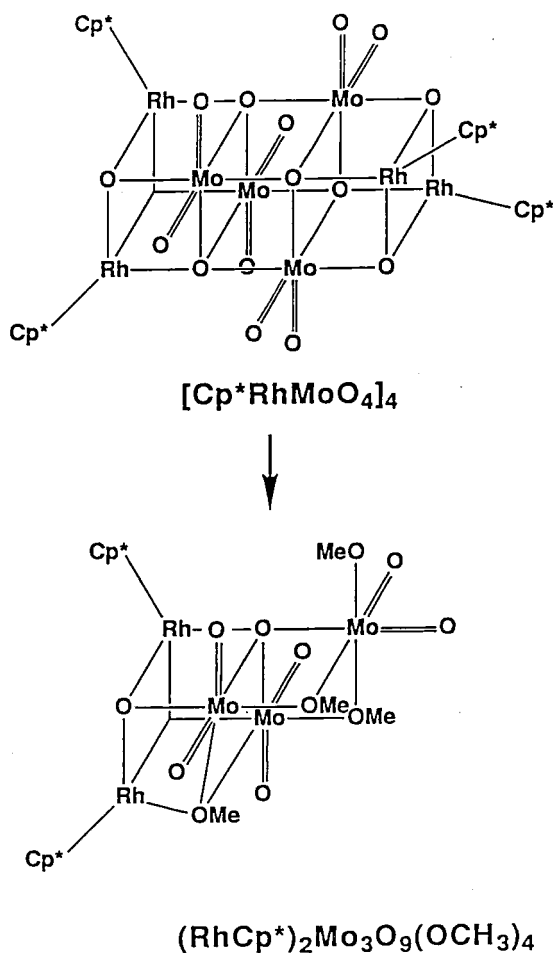
$$(RhCp^*)_2Mo_3O_9(OCH_3)_4$$

Figure 1. Simplified drawings of $[RhCp^*MoO_4]_4$ and $[(RhCp^*)_2Mo_3O_9(OCH_3)_4]$.

The integrated cubane type cluster $[Cp^*RhMoO_4]_4$ (**1**) whose structure is similar to that of the fragment of MoO_3. We are trying to explore the possible role of cluster **1** in the oxidative dehydrogenation of CH_3OH to CH_2O to mimic the heterogenous catalyst MoO_3. Reaction of **1** with CH_3OH in the presence of p-hydroquinone gave $[Rh(Cp^*)_2 Mo_3O_9(OCH_3)_4]$ **2** which represents an important intermediate step on the metal

oxide surfaces. X-ray crystal structure analysis showed the fragmentation of the triple cubane type framework took place in the reaction (Figure 1). Crystallographic data: orthorhombic, space group $P2_12_12_1$, $a = 13.701$ (1), $b = 21.743$ (2), $c = 11.599$ (1) Å, $V = 3455.3$ (5) Å^3, Z = 4, $Dc = 2.04$ g cm^{-3}.

V-D-3 Structure of Quadruple Cubane Type Cluster with Mixed Organometallic Groups

Yoshihito HAYASHI, Yoshiki OZAWA, and Kiyoshi ISOBE
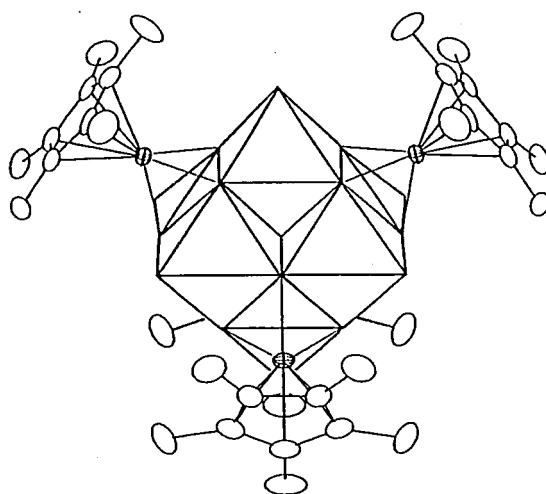
Figure 1. Poyhedra model for $[(RhCp^*)_3(IrCp^*)V_6O_{19}]$.

The oxide cluster $[(RhCp^*)_4V_6O_{19}]$ (**1**) is air-stable both in solid and in solutions. However, treatment of **1** with $[IrCp^*(H_2O)_3]^{2+}$ in a 1:1.3 molar ratio in acidic water gives mainly $[(RhCp^*)_3(IrCp^*)V_6O_{19}](2)$ as well as other minor products, $[(RhCp^*)_{4-n}(IrCp^*)_nV_6O_{19}]$ (n=2,3,4).

Black cubic crystals of $2 \cdot 3CH_3CN \cdot H_2O$ were recrystallized from acetonitrile. X-ray crystal structure analysis reveals that cluster **2** has a quadruple cubane type framework. Crystallographic data: orthorhombic, space group $Pmmn$ (No.59), $a = 15.169(3)$, $b = 18.632(4)$, $c = 11.681(1)$ Å, $V = 3301.3(9)$ Å^3, Z = 2, $Dc = 1.80$ g cm^{-3}. The RhCp* and IrCp* groups in $2 \cdot 3CH_3CN \cdot H_2O$ are disordered with respect to each other on the four alternate faces of the V_6O_{19} core. The four metal atoms in the MCp* units form a tetraheral

131

array (M_{1i}-M_{1ii} = 5.937(2) Å), whereas the vanadium atoms are disposed in an octahedral arrangement (V_{1i}-V_{1ii} = 3.175(2) Å) with briding oxygens.

V-D-4 Strcture of Hexamolybdorhodate(III)

Yoshiki OZAWA, Yoshihito HAYASHI, and Kiyoshi ISOBE

The Anderson-type heteropolyanion $[XMo_6O_{24}]^{n-}$ is a model for metal oxide surface. Many transition metal atoms can be incorporated in the anion as a XO_6 type coordination. Pale yellow prismatic crystals of $(NH_4)_3[H_6RhMo_6O_{24}] \cdot 6H_2O$ were obtained from a mixed aqueous solution at pH 4 containing $RhCl_3 \cdot 3H_2O$ and $(NH_4)_6Mo_7O_{24} \cdot 4H_2O$ (Rh:Mo= 1:6). Crystal data for $(NH_4)_3[H_6RhMo_6O_{24}] \cdot 6H_2O$: monoclinic $P2_1/c$, a=11.435(3), b=11.017(2), c=11.789(2)Å, β=100.02(2)°, V=1462.6(6)Å^3, Z=2, D_x=2.79, D_m=2.83 g cm^{-3}, μ=3.08 mm^{-1}, R=0.042 for 2248 reflections. The polyanion (Figure 1) has approximately D_{3d} symmetry. Six hydrogen atoms are

bound to oxygen atoms in RhO_6. The RhO_6 octahedron located in the center of the polyanion is slightly compressed along a trigonal axis of the anion.
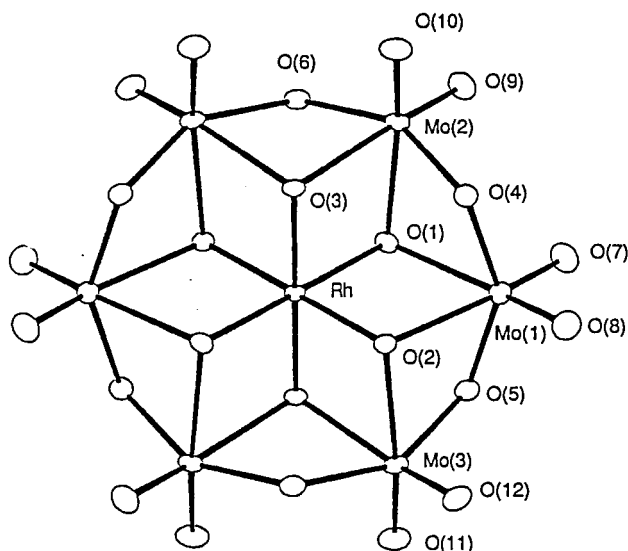
Figure 1 ORTEP drawing of $[H_6RhMo_6O_{24}]^{3-}$. Selected bond distances are: Rh—Mo 3.343(1)—3.364(1), Rh—O 2.013(6)—2.029(6), Mo—O(terminal) 1.698(8)—1.721(7), Mo—O(bridge) 1.927(6)—1.958(7), Mo—O(Rh bound) 2.267(6)—2.317(6)Å.

V—E   Transition Metal Sulfide Compounds

Although the M-S groups are present in nitrogen-fixing enzymes, industrial hydrotreating catalysis, and mineralogical processes, their functionality has not been revealed so far. We have therefore been interested in developing the solube transition metal complexes that have M-S, M-SH, and M-SR bonds to elucidate the M-S bond character.

V-E-1 Structure and Electrochemical Properties of Cp*Rh-QS$_4$ (Q=Mo, W) Complexes

Yoshiki OZAWA, Yoshihito HAYASHI, and Kiyoshi ISOBE

Reaction of the high-valent transition metal sulfide anion QS_4^{2-}(Q=Mo, W) with organometallic groups gave various complexes. These structures dependes mainly on the number of available coordination sites of organometallic groups. $Cp*Rh^{III}P(OC_2H_5)_3^{2+}$ provides two available coordination sites for formation of metal sulfide clusters. Crystal data for $Cp*RhP(OEt)_3MoS_4$:

monoclinc $P2_1/c$, a=14.560(3), b=15.183(2), c=11.452(2) Å, β=105.10(1)°, V=2440.7(8) Å^3, Z=4. The Rh—Mo bond distance shows no direct metal-metal interaction (Figure 1). Cyclic voltammograms for these complexes show two distinct one-electron reduction steps. The second redox wave is quasi-reversible. In the presence of excess amount of $P(OEt)_3$ ligand in the solution, the first wave shows also quasi-reversible. (Figure 2) The dissociation of $P(OEt)_3$ occurs in the first reduction stage. Both two electron transfers occurs at the Rh atom and their redox potentials are little influenced by neighboring Mo or W atoms.
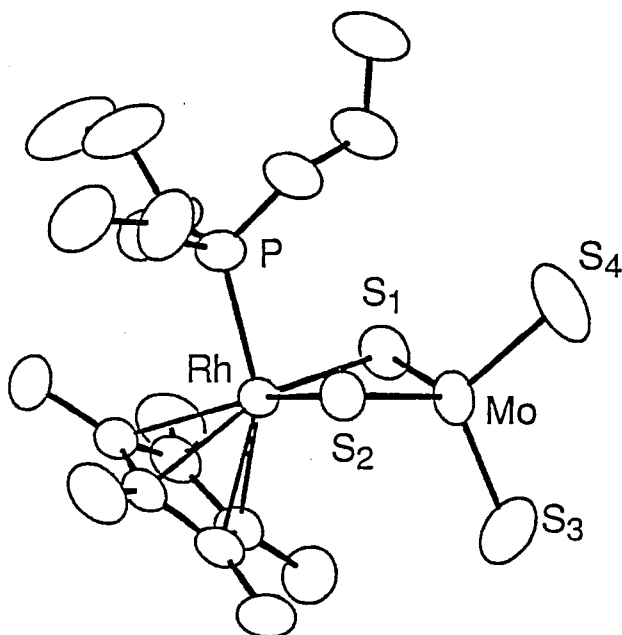
Figure 1. ORTEP drawing of Cp*RhP(OC₂H₅)₃MoS₄. Selected bond distances and angles are Rh—Mo 2.880(1), Rh—(μ-S) 2.393(2), 2.382(2), Mo—(μ-S) 2.243(2), 2.247(2), Mo—(S terminal) 2.127(3), 2.132(2) Å , S—Rh—S' 96.20(6), Rh—S—Mo 76.76(5), 76.90(5)°.
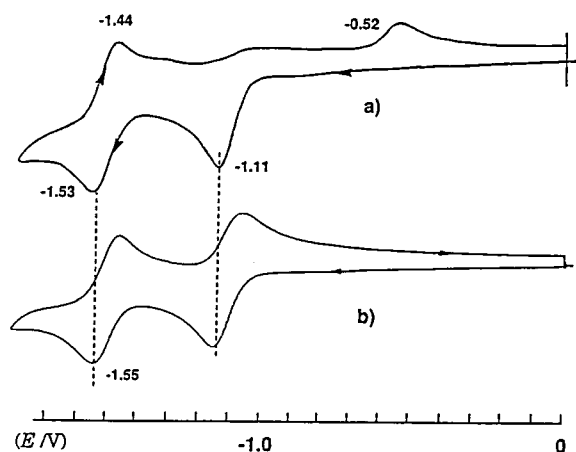
Figure 2. a) Cyclic voltammogram of RhCp*P(OC₂H₅)₃MoS₄ (1mmol) in CH₃CN. [0.1M (n-Bu)₄NPF₆, potentials v.s. Ag/AgCl]
b) Addition of excess amount of P(OC₂H₅)₃.

V-E-2 Rhodium μ-Methylene Complex with SH and SH₂ Ligands

Amelio VAZQUEZ DE MIGUEL, *(University of Alcala of Henares and IMS)*, Yoshihito HAYASHI, Yoshiki OZAWA, and Kiyoshi ISOBE

The reactivity of μ-CH₂ group in the intramolecular

coupling reaction of [RhCp*(μ-CH₂)(CH₃)]₂ **1** has been disclosed from either side of experimental and theoretical studies.[1),2)] We report here an interesting interaction between two H₂S ligands in [RhCp*(μ-CH₂)(H₂S)]₂Cl₂ **2** and formation of [RhCp*(μ-CH₂)(HS)]₂ **3** from **2**.

The reaction of [RhCp*(μ-CH₂)Cl]₂ with H₂S gas in methanol gave **2** which loses easily H₂S gas. ¹H and ¹³C NMR data of **2** in CD₃OD support that adduct **2** has cis geometry, in which the H₂S proton (H₂) and the lone pair electrons of another H₂S interact with each other as shown in Figure 1a. Treatment of **2** with NEt₃ in methanol gave **3** immediately, and its trans structure was determined by X-ray diffration (Figure 1b).

References
1) P.M. Maitlis, Pure & Appl. Chem., **61**, 1747 (1989).
2) N. Koga and K Morokuma, "Abstracts of Papers", 34th Symposium on Organometallic Chemistry, Kyoto, Novermber 1987, PA203.
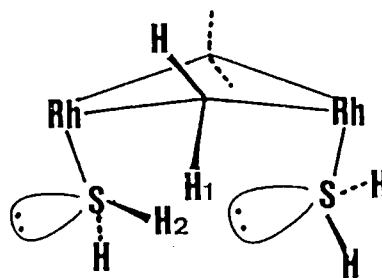
a
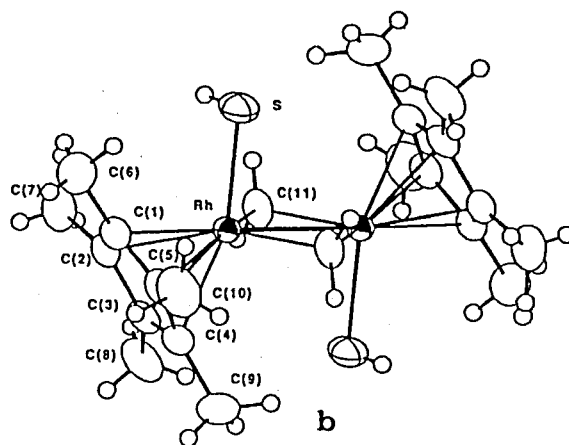
b

Figure 1. Schematic drawing of the skeleton of [RhCp*(μ-CH₂)(H₂S)]₂Cl₂: **a** and ORTEP diagram of [RhCp*(μ-CH₂)(SH)]₂: **b**.

133

V-E-3 Synthesis and Structure of Thiolate Complexes Containing $(\eta^5\text{-}C_5Me_5)Rh^{III}$ Groups

Zhaomin HOU,[1] Yoshiki OZAWA, and Kiyoshi ISOBE

Reaction of $[Cp^*RhCl_2]_2$ $(Cp^*=\eta^5\text{-}C_5Me_5$ with NaSMe in $H_2O\text{-}MeOH$ (1:1 by volume) gave $[Cp^*Rh(\mu\text{-}SMe)_3RhCp^*]Cl \cdot 3H_2O$ which was converted to $[Cp^*Rh(\mu\text{-}SMe)_3RhCp^*]_2[W_3S_9]$ **1** by treatment with WS_4^{2-}. In the presence of MoO_3 the reaction led to formation of $[Cp^*RhCl(\mu\text{-}SMe)_2RhCp^*Cl]$ **2**. X-Ray structure analyses revealed that $[Cp^*Rh(\mu\text{-}SMe)_3RhCp^*]_2[W_3S_9]$ has three μ_2-bridged SMe ligands (Figure 1) and that $[Cp^*RhCl(\mu\text{-}$ SMe)_2RhCp^*Cl] has a syn-planar conformation with two μ_2-bridged SMe ligands (Figure 2). Crystal data: **1**; $F.\ W.$ = 2075.522, monoclinic, $C2/m$, λ = 0.71069 Å, a = 26.149 (4), b = 12.681 (3), c = 11.136 (1) Å, β = 113.30 (1), V = 3391 (1) Å^3, Z = 2, Dc = 2.03 g cm^{-3}, $\mu(MoK_\alpha)$ = 65.88 cm^{-1}. **2**; $F.\ W.$ = 577.248, monoclinic, $A2/a$, λ = 0.71069 Å, a = 19.015 (2), b = 15.571 (2) c = 8.541 (1) Å, β = 98.70 (1), V = 2499.8 (16) Å^3,Z = 4, Dc = 1.704 g cm^{-3}, $\mu(MoK_\alpha)$ = 16.88 cm^{-1}.

Referance
1) IMS graduate student from Kyushu University for 1988.
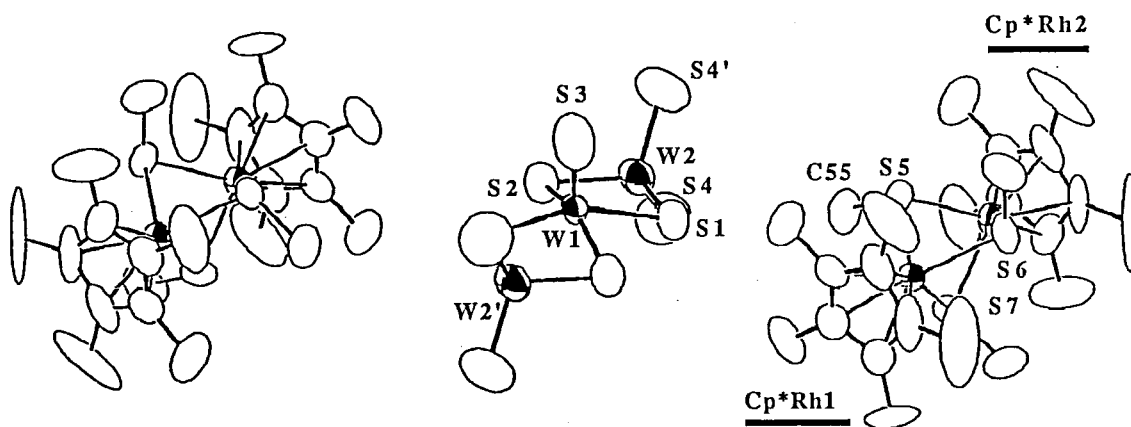
Figure 1. ORTEP view for **1**. Selected bond distances (Å) and angles (°): Rh1—S5 = 2.373(7), Rh1—S6 = 2.389(9), Rh1—S7 = 2.356(7), S5—C55 = 1.80(3), Rh1—Cp* (ring) = 2.19(av.) Rh1—S5—Rh2 = 85.8(3), Rh1—S6—Rh2 = 85.1(3), Rh1—S7—Rh2 = 86.5(3), S5—Rh1—S6 = 78.4(3), S5—Rh1—S7 = 78.9(3), S6—Rh1—S7 = 79.4(3), W1—W2 = 2.964(1), W1—S3 = 1.86(3), W1—S1 = 2.398(6), W1-S2 = 2.410(8), W2—S4 = 2.135(7), W2—W1—W2' = 158.09(7), S1—W1—S2 = 94.9(2), S1—W2—S2 = 103(3), S4—W2—S4' = 112.2(3).
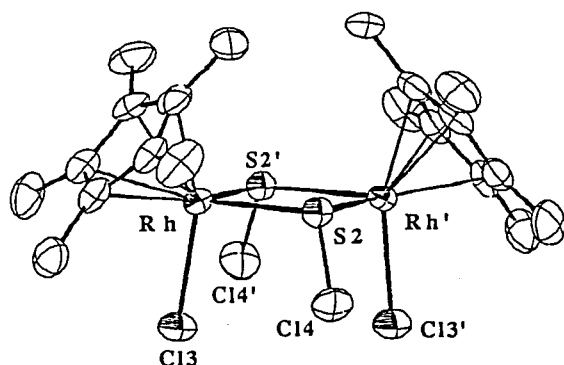
Figure 2. ORTEP view for **2**. The molecule has a C_2 symmetry. Selected bond distance (Å) and angles (°): Rh...Rh' = 3.640(1), Rh—S2 = 2.381(2), Rh—C13 = 2.387(2), S2—C14 = 1.828(7), Rh—Cp* (ring) = 2.19(av.), Rh—S2—Rh' = 99.85(6), S2—Rh—C13 = 96.06(6)

V—F   Halogen-Bridged Mixed-Valence Compounds
with Linear Chain Structures

In the past ten years, much interest has been focused on the linear-chain halogen-bridged M^{II}-X-M^{IV} mixed valence compounds (M=Pt, Pd or Ni) in the field of solid state physics and chemistry from the viewpoints of low-dimensional materials having extremely strong electron-lattice interactions. They show various charactersitic features such as the strong intervalence CT absorption and the luminescence with large Stokes shifts.

Recently, it has been prepared a new type of halogen-bridged mixed-valence compounds of $K_4[Pt_2X(pop)_4] \cdot 3H_2O$ (X=Cl, Br, or I) which are constituted of binuclear Pt complexes. The X-ray structure analyses revealed that the crystals consist of a linear chain of a repeating unit of -Pt-Pt-X-Pt-Pt-, where the bridging halogen atoms are deviated from the center between two Pt dimers. It has been proposed that the mixed valence structure consists of a $\cdots Pt^{2+}$-$Pt^{2+}\cdots\cdots$X-Pt^{3+}-Pt^{3+}-X$\cdots\cdots$ repeating unit based on some physical properties. They show semiconductive behaviors with smaller activation energies and electrical resistances than those of the halogen-bridged mixed valence compounds consisting of mononuclear Pt complexes.

In the course of growing up single crystals of the trihydrate compounds, we obtained another crystals with different shapes, that is, the dihydrate compounds of $K_4[Pt_2X(pop)_4] \cdot 2H_2O$ (X=Cl or Br).

V-F-1 Crystal Structures of Linear-Chain Halogen-Bridged Binuclear Platinum Complexes, Dihydrate Forms of $K_4[Pt_2X(pop)_4] \cdot 2H_2O$ (X=Cl and Br)

K. TORIUMI and M. YAMASHITA (Nagoya Univ.)

Crystal structures of the potassium catena-μ-halogenotetrakis(μ-diphosphonato-P,P)-diplatinum(4-) dihydrate, $K_4[Pt_2X(pop)_4] \cdot 2H_2O$ (X=Cl (1) and Br (2); pop=$P_2O_5H_2^{2-}$), have been determined by single crystal X-ray diffraction method. The complexes are isomorphous to each other and crystallize in orthorhombic, space group Pbnm, Z=4: for (1), a=9.553(2), b=15.440(3), c=17.123(3) Å, V=2525.6(8) Å^3 at room temperature; for (2), a=9.510(1), b=15.338(2), c=17.125(2), V=2497.9(6) Å^3 at 125 K. The structures consist of linear chains with a repeating unit of $\cdots Pt^{II}$-$Pt^{II}\cdots\cdots$X-Pt^{III}-Pt^{III}-X$\cdots\cdots$ along the c axes. The linear chains are not straight but a little bent to form zigzag chain structures, the bent angles defined by the Pt-Pt bonds and the c-axes being 3.34(1)° for (1) and 3.11(1)° for (2), respectively. The Pt-Pt separations, which are bridged by four pyrophosphato ligands ($P_2O_5H_2^{2-}$), are 2.835(1) Å for (1) and 2.834(1) Å for (2). The bridging halogen atoms are disordered over two sites in the chains, giving short Pt-X and long Pt$\cdots$X separations: 2.406(4) and 3.362(4) Å for (1) and 2.539(1) and 3.217(1) Å for (2), respectively. The deviations of the bridging halogen atoms from the midpoints between two Pt dimers are significantly larger than those of the trihydrate modifications.

Figure 1. ORTEP drawing of a portion of the infinite chain along c with surrounding K^+ ions and water molecules of $K_4[Pt_2Cl(pop)_4] \cdot 2H_2O$ at room temperature. The dashed lines correspond to hydrogen bonds and the dotted lines to short contacts between K^+ ions and O atoms of pop ligands or water molecules. The thermal ellipsoids are 50% probability surfaces.

V—G Magnetic and Electronic Interactions through Organic Ligand in Multi-nuclear Copper(II) Complexes

Control of electronic and magnetic interaction between metal ions in multi-nuclear metal complexes can be a basic technology to synthesize molecular assemblies which have interesting physical properties. In this project, we have aimed to control an oxidation state in binulclear copper(II) complexes by modifying the ligand structures, and to propagate a ferromagnetic interaction in oxalato bridged copper(II) complex with one dimensional zigzag chain structure by modifying a coordination structure.

V-G-1 Syntheses, Crystal Structures, and Electrochemical Properties of Binuclear Copper(II,II) [Cu₂L¹Cl₂](ClO₄)₂ · 4CH₃CN and Copper(I,I) [Cu₂L¹](ClO₄)₂ Complexes (L¹= 2,5-Bis[N,N-bis(2′-pyridylethyl)aminomethyl]-pyrazine)

Hiroki OSHIO

Binuclear copper (II,II) and copper(I,I) complexes [Cu₂L¹Cl₂](ClO₄)₂ · 4CH₃CN (**1**) and [Cu₂L¹](ClO₄)₂ (**2**) (L=2,5-bis[N,N-bis(2′-pyridylethyl)aminomethyl]-pyrazine) have been synthesized. Crystal structures of both complexes have been determined. Complex (**1**) crystallizes in the triclinic space group $P\bar{1}$ with a=13.140(3), b=13.541(4), c=8.217(2)Å, α=101.43(4), β=87.44(3), γ=117.50(2)°, and Z=1, and complex (**2**) crystallizes in the triclinic space group $P\bar{1}$ with a=10.264(6), b=12.473(5), c=9.213(2)Å,

α=89.92(2), β=113.19(3), γ=113.74(3)°, and Z=1. The complex cations in the both crystals have centrosymmetric binuclear structures with copper atoms in distorted square-pyramidal and pyramidal geometries for (**1**) and (**2**), respectively. E.p.r. and magnetic susceptibility data of (**1**) do not show a strong magnetic interaction between copper atoms. Complex (**1**) in acetonitrile shows a quasi-reversible cyclic voltammogram which has E_{pc} and E_{pa} at −0.09 and 0.06 V vs. Ag-AgCl. A Controlled-potential electrolysis for (**1**) result proves that the process involves two electron transfer. The two-step reduction potentials to Cu^{II}-Cu^{I} and Cu^{I}-Cu^{I} from Cu^{II}-Cu^{II} were estimated to be 0.04 and −0.07 V, respectively. The ligand L¹ has two ethylene groups connecting a tertiary amine with pyridine ring, so a flexible ligand is of great advantage to modifying the co-ordination structure as the copper reduced, hence easier reduction of (**1**) and stabilization of Cu(I) complex (**2**).
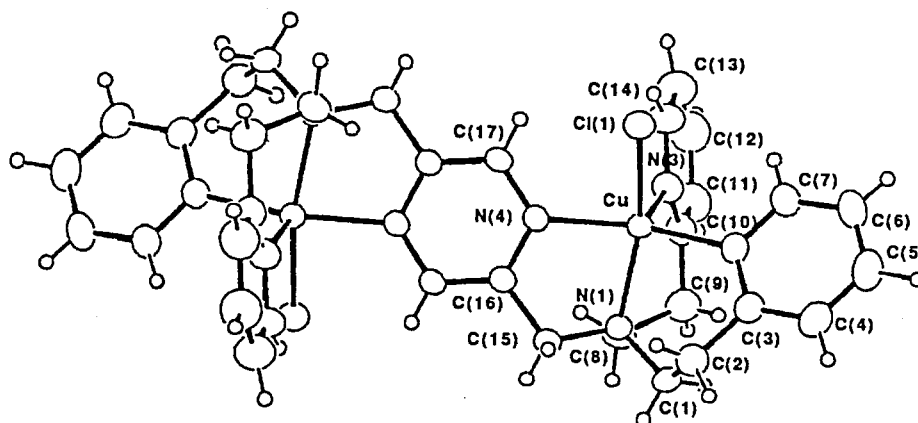
(1)
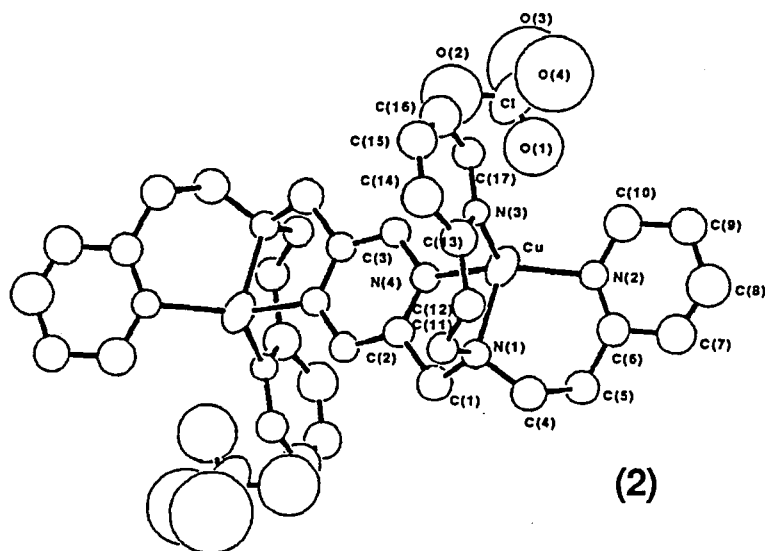
Figure 1. Molecular Structure of $[Cu_2L^1Cl_2]^{2+}$ (1) and $[Cu_2L^1](ClO_4)_2$ (2).

V-G-2 Ferromagnetic Interaction in Oxalate Bridged [Cu(bpy)(ox)] · 2H₂O with a Zigzag Chain Strucure

Hiroki OSHIO

Molecular based ferromagnetic material has been continuing interest. Oxalate ligand has been proved to propagate a strong magnetic interaction and this anion is promising bridging ligand to built a molecular assembly which has interesting magnetic properties. Magnetic susceptibility data of [Cu(bpy)(ox)] · 2H₂O (bpy:bipyridine; ox:oxalate) with an oxalate bridged zigzag chain stricture(Figure 1) indicates that the complex is a ferromagnetic $S=1/2$ Heisenberg linear chain$(J=+1.22$ cm^{-1} and $g=2.185$)(Figure 2) and magnetization experiment at 2.0 K reveals that spin multiplicity(S) is greater than 3/2 at this temperature. There are many contributions to the ferromagnetic interaction. The two short Cu-O bonds(1.984(2) and 1.993(2) Å), which might propagate the antiferromagnetic exchange interaction by the σ-path way, is in the trans position with respect to the C-C bond of the oxalate ligand. This structural restriction including the absence of d_{z^2} mixing causes a negligible overlap of the magnetic orbitals which lead to the week antiferromagnetic exchange interaction. The spin density of a copper atom is delocalized on the O(3)′ or O(4)′ atoms, which coordinate to the adjcacent copper atom from the d_{z^2} direction. The delocalized spin density on O(3)′ O(4)′ can induce the spin on the d_{z^2} orbitals of the adjacent copper atoms, which is orthogonal to its $d_{x^2-y^2}$ orbital. This orthogonality of the induced spin and its own $d_{x^2-y^2}$ spin on the copper atom is responsible for the ferromagnetic intrachain interaction.
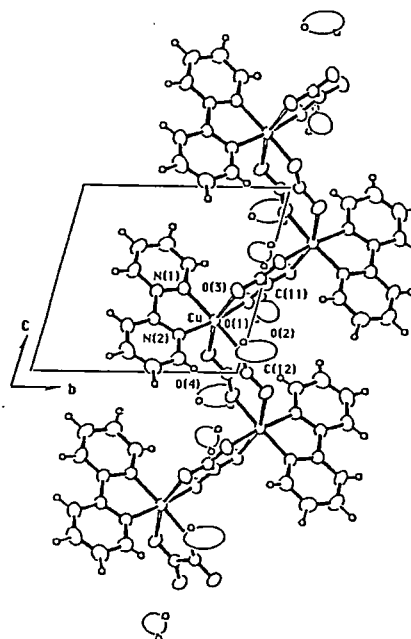
Figure 1. Projection view of [Cu(bpy)(ox)] · 2H₂O on the bc-plane.

137
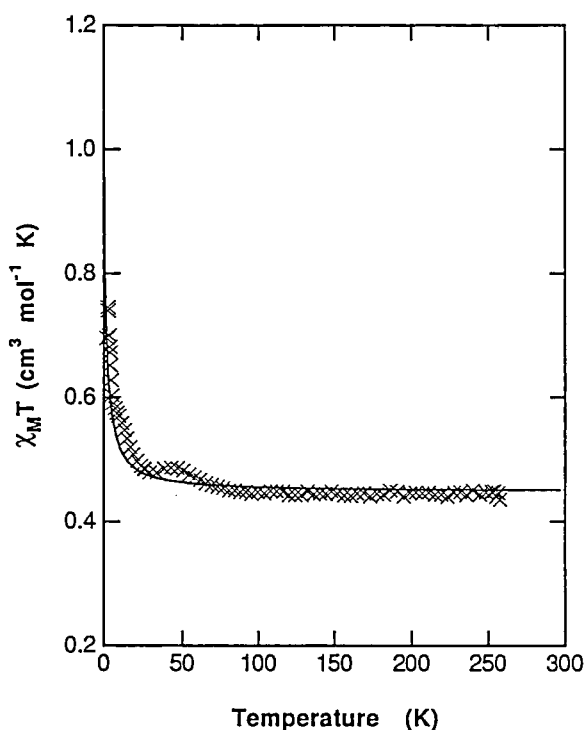
Figure 2. Plots of X_mT vs. temperature(T) of [Cu(bpy)(ox)] · 2H$_2$O. The solid line was generated from the best fit calculation using the Padé expansion series for the S=1/2 Heisenberg Model.

$$X_mT = Ng^2\mu_B{}^2T\left[\frac{1+a_1K+a_2K^2+a_3K^3+a_4K^4+a_5K^5}{1+b_1K+b_2K^2+b_3K^3+b_4K^4}\right]^{2/3}$$

where $K = J/2k_BT$, a_i and b_i are expansion coefficient, g is g factor, μ_B is the Bohr magnetron, k_B is the Boltzmann constant, and J is the intrachain-exchange coupling constant.

V—H   Thermodynamic Stabilities of Carbocations in the Gas Phase

Thermochemical properties of organic ions in the gas phase provide the most precious basis for investigation of an essential relationship between structure and chemical reactivity. In this project, thermodynamic stabilities of a series of benzylic carbocations, Ar-C$^+$(R^1)R^2, including phenonium ions have been determined by measuring equilibrium constants of proton- or halide-transfer reactions using a homemade pulsed ion cyclotron resonance spectrometer. The gas phase substituent effects have been analyzed in detail by means of the Yukawa-Tsuno LArSR equation.

$$\delta\Delta G° = \rho(\sigma° + r\Delta\bar\sigma_R^+) \tag{1}$$

where the r value is a measure of π-interaction between the aryl π-system and reaction site. Furthermore, gas-phase results have been compared with those for the corresponding S$_N$1 solvolysis to establish the basic concept for relating the solvolysis transition states to their carbocationoid intermediates.

138

V-H-1 Substituent Effect on the Gas Phase Basicity of α, α, α-Trifluoroacetophenone. Intrinsic Nature of Resonance Demand

Masaaki MISHIMA, Mizue FUJIO (Kyushu Univ.), and Yuho TSUNO

Gas phase basicities of α, α, α-trifluoroacetophenones were determined based on the proton transfer equilibrium method. Unsubstituted derivative is 7.7 kcal mol^{-1} less basic than benzaldehyde, being attributed to strong electron-withdrawing effect of the CF$_3$ group. The LArSR analysis of the substituent effect provided an r=1.20 higher than that for benzaldehyde (r=1.04). The r values for a series of benzylic carbocations, ArC$^+$ (R^1)R^2, could be correlated in terms of a following equation except for the R^1=NMe$_2$ R^2=OH system.

$$r = 0.40\Sigma\sigma° + 0.60\Sigma\Delta\bar{\sigma}_R^+ + 1.30$$

where $\Sigma\sigma°=\sigma°(R^1) + \sigma°(R^2)$ and $\Sigma\Delta\bar{\sigma}_R^+=\Delta\bar{\sigma}_R^+(R^1) + \Delta\bar{\sigma}_R^+(R^2)$. It is concluded that resonance demands of the benzylic carbocations depend on electronic effects of R^1 and R^2 substituents and that the positive charge formed at the benzylic position is stabilized complementarily by π-delocalization into the ary π-system and into α-substituents.

V-H-2 Thermodynamic Stabilities of Phenonium Ions in the Gas Phase

Masaaki MISHIMA, Mizue FUJIO (Kyushu Univ.), and Yuho TSUNO

Thermodynamic stabilities of phenonium ions (ethylenebenzenium ion) which are generated from 2-arylethyl bromides by electron impact ionization at low energies have been determined by measuring equilibrium constants for bromide-transfer reactions in the gas phase. Phenonium ion has been found to be 2.4 kcal mol^{-1} more stable than t-butyl cation. The LArSR analysis of the effects of ring substituents on the stability of phenonium ion gave a ρ of -17.5 and an r or 0.60. This ρ value is significantly larger than that for ordinary benzylic carbocation system, e.g., -13 for α-cumyl cation, but is nearly identical to that for the benzenium ion. An r value of 0.60 indicates clearly the existence of direct π-interaction between the positive charge and the para π-donor substituents, and this value is in complete agreement with that for the k$_\Delta$ process (via an intermediate phenonium ion) in the solvolysis of the β-phenylethyl tosylate.

V-H-3 Gas Phase Basicities of α-Trimethylsilylstyrenes. Effects of α-Trimethylsilyl Group on the Stability of a Carbocation

Masaaki MISHIMA, Toshifumi ARIMA (Kyushu UNiv.), Yuho TSUNO, and Kiyoshi KIKUKAWA (Kinki Univ.)

Gas phase basicities of α-trimethylsilylstyrenes have been determined by proton transfer equilibrium method to explore instrinsic effect of α-trimethylsilyl group on the stability of a carbocation. Unsubstituted trimethylsilylstyrene was found to be 2.8 kcal mol^{-1} more basic than ammonia. This means that the stability of 1-trimethylsilyl-1-phenylethyl cation (conjugate acid ion of the styrene) is 4.5 kcal mol^{-1} higher than 1-phenylethyl cation and comparable with α-cumyl cation, leading to the conclusion that α-trimethylsilyl group can stabilize the positive charge in a carbocation as well as methyl group. This is consistent with experimental observations for the solvolysis of 2-adamantyl system. In addition, the effect of ring substituent on the stability of 1-trimethylsilyl-1-phenylethyl cation was found to be parallel to that for the α-cumyl cation.

V—I Structure-Reactivity Relationship in Solvolysis

The substituent effect in the systems where the direct π-interaction between the aryl and carbocationic center is possible, can be generally described by the LArSR equation.

$$\log k/k_o = \rho(\sigma° + r\Delta\bar{\sigma}_R^+) \qquad (1)$$

The real significance of the substituent effect in organic chemistry is that the correlation results are related with reaction mechanisms. It is therefore of importance to establish an essential relation between the LArSR correlation results

and the structure of transition state. From this point of view, the substituent effects have been examined in detail for the solvolysis rates of various systems.

V-I-1 Highly Electron-Deficient Cabocation Solvolyses

Akihisa MURATA*, Shin-ichi SAKAGUCHI*, Ryoji FUJIYAMA (Kochi Univ.), Masaaki MISHIMA, Mizue FUJIO* (*Kyushu Univ.), and Yuho TSUNO

The solvolysis rates of 1-aryl-2,2,2-trifluoroethyl tosylates (I-OTs) and m-nitrobenzenesulfonates (I-ONs) were determined conductometrically in aqueous ethanol and aqueous 2,2,2-trifluoroethanol. While the Brown $\rho^+\sigma^+$ equation does not give a simple linear plot but a remarkably split pattern, there is a linear free energy relationship between solvolyses of I-OTs and α-CF$_3$-α-arylethyl OTs (II) with a slope of unity over a wide range (10^8 in reactivity) of substituents from p-MeO to unsubstituted derivatives. The substituent effect on the solvolysis of I should be closer to that on the solvolysis of II, rather than to the σ^+ substituent effect. The ρ value for this system was estimated to be identical to the value of -6.3 assigned for II, and the r value to be comparable with or even higher than the r=1.4 of II. The enhanced r value of this system must be caused from strong destabilization of the transition state by α-CF$_3$ substituent.

V-I-2 Substituent Effects in the Solvolysis of Benzyl Tosylates

Mizue FUJIO*, Toshihiro SUSUKI* (*Kyushu Univ.), Masaaki MISHIMA, and Yuho TSUNO

The substituent effect on the rates of solvolysis of substituted benzyl tosylates in acetic acid was analyzed based on the Yukawa-Tsuno LArSR equation. Neither the LArSR nor simple σ^+ treatment was capable of providing any linear correlation plot for the full range of substituents. Since any mechanistic transition with substituents should bring about a single continuous curve when plotted against an appropriate substituent constant scale, the split pattern observed in the σ^+ plot is not in line with an interpretation in terms of a mechanistic transition. On the other hand, the LArSR plots with r=1.3 coalesced into a single smooth curve including the meta correlation curve. For the reactive substituents down to p-halogens, a sufficiently linear plot can be obtained against a set of substituent constants with r=1.3 which can be referred to the substituent effect correlation for the k_c mechanism of this system. An identical r value was likewise assigned for the k_c mechanism of the hydrolysis of a more severely restricted range of activating substituents down to the 4-MeS-3-CN group.

V-I-3 Solvolysis Mechanism of 1-Arylcyclobutylcarbinyl Brosylates

Yoshihiro SAEKI, Mizue FUJIO (Kyushu Univ.), Masaaki MISHIMA, and Yuho TSUNO

The acetolysis rats of 1-arylcyclobutylcarbinyl brosylates were determined for a series of substituents. The nonlinear substituent effect behavior was reasonably account for on the basis of two linear LArSR relationships; for the aryl-assisted (k_A) and -unassisted processes. Nonlinear least squares analysis gave a ρ of -3.99 and an r of 0.56 for the k_A process, and a ρ of -1.26 (r=0.20) for the aryl-unassisted process. Results for the k_A process are identical to those for the neophyl solvolysis. This is consistent with our conclusion that the resonance demand of aryl-assisted transition state can be characterized in terms of the intermediate value of 0.5 ± 0.1. A ρ value for the aryl-unassisted process is larger than that for solvent-assisted process (k_s) in the solvolysis of β-arylalkyl systems, suggesting that the aryl-unassisted process in the present system is close to the limiting S_N1 (k_c) mechanism rather than the k_s mechanism.

V-I-4 Solvolysis Mechanism of Benzyl Chlorides

Izumi AKASAKA, Mizue FUJIO *(Kyushu Univ.)*, Masaaki MISHIMA, and Yuho TSUNO

The rates of solvolyses of a series of substituted benzyl chlorides were determined in 50% aqueous acetone and in 97% aqueous trifluoroethanol (TFE). The substituent effects in both solvents could not be correlated linearly for the full range of substituents with any substituent constants. This substituent effect behavior was reasonably account for by the mechanistic shift with substituents in the same way as that for the benzyl tosylate. In 50% acetone the plots of para π-donors against an appropriate $\bar{\sigma}^+$ scale with r=1.24 coalesced into a single smooth curve including the *meta* correlation curve. A linear LArSR plot with r=1.24 for the reactive substituents down to p-t-butyl group can be referred to the substituent effect correlation for the k_c mechanism of this system. In 97% TFE a single linear LArSR plot with r=1.23 can cover the reactive substituents down to H whereas the corresponding plot for the benzyl tosylate covers down to p-halogens. In spite of varying critical point of the mechansitic transition from the k_c to the k_s depending on leaving groups and solvents, the resonance demand of the k_c mechanism of the benzyl system appears to be constant.

V—J Solvent Effects on Reactivity of Solvolysis

Solvent effect on solvolysis rates have generally been analyzed in terms of the Winstein-Grunwald equation.

$$\log k/k_o = mY + lN \qquad (1)$$

where Y is a measure of the ionizing power of the solvent and N is its nucleophilicity. m and l are the susceptibility of the solvolysis of RX to solvent ionizing power Y and to solvent nucleophilicity N, respectively. In this project we have investigated a relation between solvent effect behavior and reaction mechanism in order to establish the theory of kinetic solvent effcts as a mechanistic probe of the solvolytic process.

V-J-1 Solvent Effects on the Solvolysis of Neophyl Tosylates

Mizue FUJIO*, Mutsuo GOTO*, Kimito FUNATSU*, Takanori YOSHINO* *(*Kyushu Univ.)*, and Yuho TSUNO

Solvolysis rates of neophyl and p-methoxyneophyl tosylates were determined in a wide variety of solvents and solvent effects were analyzed based on the Winstein-Grunwald equation. Despite the nucleophilically limiting nature of aryl-participation mechanism, the solvent effect on both k_Δ solvolyses failed to give a single linear correlation to adamantyl Y_{OTs} parameter. There is dispersion behavior with respective binary solvent series. The way of dispersion cannot be explained by simply invoking nucleophilic solvent assistance. The response to the solvent polarity *(m* value) in each solvent series is significantly lower for both methoxy and unsubstituted derivaties than m=1.0 for limiting k_c solvolysis, and appreciably lower for the methoxy derivative than for the unsubstituted one.

V-J-2 Solvent Effect on the Solvolysis of α-t-Butylbenzyl Tosylate

Yutaka TSUJI*, Mizue FUJIO* *(*Kyushu Univ.)*, and Yuho TSUNO

Solvolysis rates of α-t-butylbenzyl tosylate were determined for a wide range of solvent series. The results have been analyzed in comparison with those for 1-adamantylmethylcarbinyl and pinacolyl tosylates. α-t-Butylbenzyl and 1-adamantylmethylcarbinyl solvolyses afford the same solvent effects, on the other hand, the decreases of the slope and the deviations of fluorinated alcohols are shown in pinacolyl solvolysis. the different solvent effects must presumably be attributed to the fact that the α-butylbenzyl and 1-adamantylmethylcarbinyl solvolyses have a crowded, planar carbocation transition state whereas the pinacolyl solvolysis has a different type of transition state such as Me-bridged structure.

V-J-3 Solvolysis Mechanism of 1,1,3,3-Tetramethylindan-2-yl Arenesulfonates

Ken-ichi YATSUGI*, Yuka KIKUTA*, Yutaka TSUJI*, Mizue FUJIO* (*Kyushu Univ.), and Yuho TSUNO

The solvolysis rates of title compounds were determined in a variety of solvents, and solvent effect was analyzed in terms of the Winstein-Grunwald equation. The correlation against Y failed to give a single straight line with an m value of 1.00 but gave a characteristic dispersion pattern with small m values of ca. 0.8 for different binary solvent series. The splits for respective solvent series could not be ascribed to the nucleophilicities of solvents. Closeness of the solvent effects of k_Δ substrate such as neophyl system suggests that this system also involves the aryl-participation at the rate-determining step. The dispersion of the mY plot may be attributed to the effective dispersal of cationic charge at the transition state by the bis-homoallylic π-interaction.

V—K   Organic Synthesis with Samarium

Recent progress on the utilization of lanthanides in organic synthesis has aroused a growing interest among organic chemists. Of these lanthanides, samarium has been one of the most attractive elements because of its unique properties: Samarium(II) has a moderate oxidation potential which falls between those of magnesium and zinc, being suitable for the reduction of a variety of organic functionalities. The oxophilicity of samarium, which falls between those of aluminum and titanium, is also significant. This property can be advantageous in the activation of oxygenated organic functions. It has high coordination number and quite large ionic radius compared to d-block transition metals. These properties should find some new reactions difficult to accomplish by any other available methodologies. In this project, we have developed some SmI_2-promoted electron transfer reactions for the reduction of organic functionalities and for the formation of carbon-carbon bonds.

V-K-1   SmI$_2$-Promoted Site-Selective Deacetoxylation of Polyacetylsugar Lactones

Junji INANAGA, Junko KATSUKI, Masaru YAMAGUCHI (Kyushu Univ.), and Yuho TSUNO

Convenient and highly site-selective deacetoxylation of polyacetylsugar lactones was accomplished by utilizing SmI_2-promoted electron transfer reaction thus providing a variety of deoxysugar lactones such as 2-deoxy-, 2,3-dideoxy-, and 2,3-dehydro-2,3-dideoxy-sugar lactones which are expected to be not only biologically interesting but also synthetically very useful as chiral synthons or versatile templates for the preparation of other types of chiral intermediates.
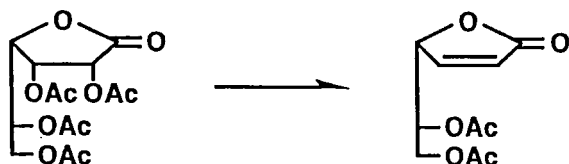
V-K-2   SmI$_2$-Induced Aryl Radical Cyclization. A New Entry into Heterocycle Formation

Junji INANAGA, Osamu UJIKAWA [a], and Masaru YAMAGUCHI[a] ([a]Kyushu Univ.)

Benzofuran, naphthofuran, and indole derivatives and their dihydro compounds were expediently constructed from arene bromides with ortho substituents containing double or triple bonds via radical cyclization process promoted by SmI_2.
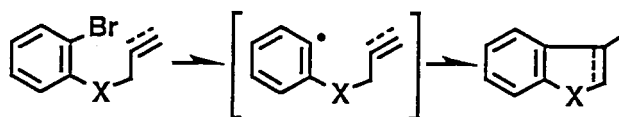
X=O, NH, NAc, NR

V-K-3 Combination of Cobalt(II) Catalyst and Samarium(II) for the Stereoselective Reduction of Acetylenes

Junji INANAGA, Yasuo YOKOYAMA[a], Yoshiyasu BABA[a], and Masaru YAMAGUCHI[a] (*[a]Kyushu Univ.*)

Cobalt-catalyzed reduction of alkynes to Z-alkenes proceeded highly stereoselectively with the aid of SmI_2 in the presence of proton sources under extremely mild conditions. The conditions also effected the conversion of 1,6-diynes to the corresponding five-membered carboxylic compounds.

$$R-\!\!\equiv\!\!-R' \quad \xrightarrow{Co^{II}cat.} \quad R\diagup\!=\!\diagdown R'$$
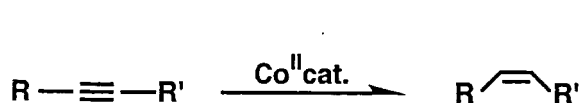
V-K-4 SmI_2-Promoted Highly Efficient Cyclization for the Synthesis of Medium and Large Carbocyclic Compounds

Junji INANAGA, Yasuo YOKOYAMA, Yuichi HANDA[a], Masaru YAMAGUCHI[a] and Yuho TSUNO (*[a]Kyushu Univ.*)

Medium as well as large carbocyclic compounds whose ring skeletons are composed entirely of sp^3 carbons have been prepared in high yields under mild conditions by utilizing SmI_2-promoted intramolecular Reformatsky reaction.

$$(n = 6 - 13)$$
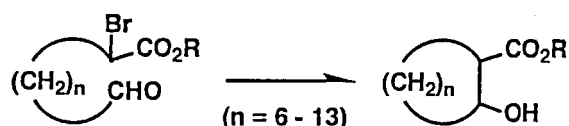
V—L   Studies on the Configuration and Reaction of Ketyl Radicals

Because of the great potential of radical reaction in organic synthesis, carbon-carbon bond-forming reactions via radical process have received much attention and recently been actively studied, especially on the regio- and stereochemically controlled formation of functionally substituted systems with five-membered rings by utilizing tin hydride-initiated free radical cyclization. However, stereocontrol of intermolecular radical reactions has been believed to be quite difficult mainly because of the lack of the knowledge to control the stereochemistry and reactivity of radical intermediates, and has remained as a challenging and important problem in organic synthesis. By using the SmI_2-THF-HMPA electron transfer system, we tried and succeeded to trap ketyl radicals directly with tributyltin hydride, olefins, or acetylenes, thus providing an important information about the configuration of ketyls.

V-L-1 Ketyl Radical Addition to Carbon-Carbon Triple Bonds

Junji INANAGA, Junko KATSUKI[a], and Masaru YAMAGUCHI[a] (*[a]Kyushu Univ.*)

A mild and convenient method for the preparation of allylic alcohols has been developed by utilizing SmI_2-promoted intermolecular carbonyl-alkyne reductive coupling reaction, where neutral alkynes can be used as the corresponding vinyl anion equivalents, some of which are hardly accessible by the conventional methodologies. Mechanistic study revealed that hydrogen atom-transfer or electron transfer to the vinyl radical intermediates (produced by ketyl-alkyne cou-

pling) is the rate determining step.
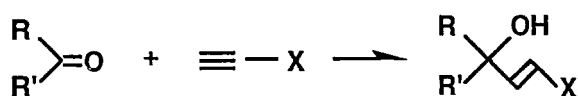
V-L-2 Samarium-Mediated Acyclic Stereocontrol in Intermolecular Radical Reaction: Highly Stereoselective Reductive Coupling of Aldehydes with β-Monosubstituted Acrylates

Junji INANAGA, Yuichi HANDA[a], Kenji OTSUBO[a] and Masaru YAMAGUCHI[a] (*[a]Kyushu Univ.*)

Intermolecular reductive carbon-carbon bond formation between carbonyl carbon and the β-carbon of α,β-unsaturated esters was effected by the use of SmI_2 to afford, after acidic workup, the corresponding γ-lactones in high yields. The addition of HMPA dramatically accelerated the reaction. Very interestingly, when the reaction of aldehydes with β-monosubstituted acrylates was conducted in the absence of HMPA, remarkably high stereoselection was realized to give 3,4-cis-γ-lactones almost exclusively. The selectivity may be explained by considering the interaction between SOMO of the ketyls and LUMO of the unsaturated esters, which takes place on the coordination sphere of samarium. Thus, high level of acyclic stereoselection in the intermolecular radical reaction was attained for the first time by utilizing the distinct property of samarium.

V-L-4 Samarium-Mediated Acyclic Stereoselection in Ketyl Addition Reaction: 1,3-Asymmetric Induction

Junji INANAGA, Osamu UJIKAWA, and Yuho TSUNO

Configuration of the ketyls (anion radicals) generated by SmI_2 reduction of β-hydroxy ketone derivatives, whose hydroxyl groups are protected as diethyl phosphate or N,N,N',N'-tetramethylphosphorodiamidate, can be fixed through samarium-involved eight-membered chelate formation which is effected by highly oxophilic nature of Sm^{3+} and high coordination ability of phosphate or phosphorodiamidate oxygen. Consequently, the subsequent carbon-carbon bond-forming reaction with methyl acrylate takes place highly stereoselectively affording high degree of 1,3-asymmetric induction. The present achievement may lead to a new phase in the area of acyclic stereoselection via radical process.

V-L-3 Studies on the Configuration of Ketyls

Junji INANAGA, Osamu UJIKAWA, and Masaru YAMAGUCHI (Kyushu Univ.)

Ketyls generated from both cyclic and acylic ketones by one electron transfer from SmI_2 can be directly trapped with tributyltin hydride or with styrene making carbon-hydrogen or carbon-carbon bonds, respectively, under mild conditions. By analysis of the products, it became obvious that ketyls (produced by one-electron transfer) and the corresponding carbanions (produced by two-electron transfer) have often the opposite stereochemistry.

RESEARCH ACTIVITIES VI
Coordination Chemistry Laboratories

The Coordination Chemistry Laboratories have accepted several new members. Dr. Koji Tanaka moved on the 16th of March, 1990 from Osaka University as the professor of the laboratory of Functional Coordination Chemistry and Dr. Hirotaka Nagao of Sophia University was appointed to be a research associate of Prof. Tanaka on the 1st of July, 1990. Professor Eiichi Kimura and Associate Professor Ryuichi Ikeda, who had been transferred from Hiroshima University and Nagoya University, respectively, finished their two years term and returned to the original positions of their universities at the end of March, 1990. However, both of them continue their contributions to the Coordination Chemistry Laboratories as adjunct staffs of the Laboratory of Complex Catalysis. Instead, Dr. Yoshihiko Kushi of Osaka University and Dr. Fumio Kawaizumi of Nagoya University joined us as the adjunct Professor and the adjunct Associate Professor, respectively, of the Laboratory of Synthetic Coordination Chemistry, together with Dr. Tatsuya Kawamoto, a research associate of Prof. Kushi. Dr. Shionoya, a research associate of Prof. Kimura, came back to Hiroshima University with his supervisor. Mr. Hiromasa Kurosaki stopped his work as a technical staff at the end of July, 1990, but is still remaining for some months in the Laboratory of Complex Catalysis as a research co-worker of Prof. Ohtaki.

VI—A   Structural Studies of Liquids

Structures of liquids and liquid mixtures have been investigated by the X-ray diffraction method.

VI-A-1 Liquid Structure of 2,2,2-Trifluoroethanol-Dimethyl Sulfoxide Mixtures As Studied by X-Ray Diffraction

Tamas RADNAI*, Shin-ichi ISHIGURO* (*Tokyo Institute of Technology), and Hitoshi OHTAKI

The liquid structure of 1:1 and 2:1 molar mixtures of 2,2,2-trifluoroethanol (TFE) and dimethyl sulfoxide (DMSO) has been investigated by X-ray diffraction at 25°C. The nearest neighbor structure in the mixtures involves the O-H...O type H-bonds between TFE and DMSO molecules besides the relatively long-range intermolecular ordering, which is characteristic of both pure TFE and DMSO, in their mixtures. The long-range interactions may arise from H-bonding between TFE and DMSO clusters, both consisting of a few molecules of each component liquid. No evidence was found for the short-range interaction between the S atom of DMSO and the O atom of TFE.

VI—B   Structure of Solvated Metal Ions and Complexes in Solution

Structures of solvated metal ions and complexes in aqueous and nonaqueous solutions have been investigated by the X-ray diffraction method.

VI-B-1 An X-Ray Diffraction Study on the Structure of Solvated Cadmium(II) Ion and Tetrathiocyanatocadmate(II) Complex in *N,N*-Dimethylformamide

Kazuhiko OZUTSUMI*, Toshiyuki TAKAMUKU*, Shin-ichi ISHIGURO* *(*Tokyo Institute of Technology)*, and Hitoshi OHTAKI

The structure of solvated cadmium(II) ion and the tetrathiocyanatocadmate(II) complex in *N,N*-dimethylformamide (DMF) has been determined by means of X-ray diffraction at 25°C. The radial distribution curve for a cadmium(II) perchlorate DMF solution was well explained in terms of the presence of the octahedral $[Cd(dmf)_6]^{2+}$ complex with the Cd-O bond length of 229.6(4) pm, which was practically the same as that within $[Cd(dmso)_6]^{2+}$ in DMSO and $[Cd(H_2O)_6]^{2+}$ in H_2O. It is also found that the tetrathiocyanatocadmate(II) complex has a tetrahedral structure, $[Cd(NCS)_3(SNC)]^{2-}$, with three Cd-N and one Cd-S bonds, the distances being 223(2) and 257(2) pm, respectively. The coordination structure of the complex in DMF was different from that found in aqueous solution, $[Cd(NCS)_2(SCN)_2]^{2-}$.

VI-B-2 Structure Determination of Zinc Iodide Complexes Formed in Aqueous Solution

Hisanobu WAKITA *(Fukuoka Univ.)*, Georg JOHANSSON*, Magnus SANDSTRÖM* *(*Royal Inst. Technol.)*, Peter GOGGIN *(Univ. Bristol)*, and Hitoshi OHTAKI

Structures of the complexes formed in aqueous solutions between zinc(II) and iodide ions have been determiend from Raman, far-IR and large-angle X-ray scattering measurements. The coordination in the hydrated Zn^{2+} hexaaqua ion and in the first iodide complex, $[ZnI]^+$, is octahedral but is changed into tetrahedral in the higher complexes, $[ZnI_2(H_2O)_2]$, $[ZnI_3(H_2O)]^+$ and $[ZnI_4]^{2-}$. The Zn-I bond length is 263.5(4) pm in $[ZnI_4]^{2-}$ and slightly shorter, 259.2(6) pm, in the two lower tetrahedral complexes. In the octahedral

$[ZnI(H_2O)_5]^+$ complex the Zn-I bond length is 290(1) pm. The Zn-O bonding distances to the aqua ligands in the complexes are approximately the same as in the hydrated Zn^{2+} ion, 210(1) pm.

VI-B-3 An X-Ray Diffraction Study on Zinc(II) Complexes with α-Alaninate Ion in Aqueous Solution

Tamas RADNAI*, Kenta INOUE* *(*Tokyo Inst. Technol.)*, and Hitoshi OHTAKI

The structure of mono(α-alaninato)zinc(II), bis(α-alaninato)zinc(II), and tris(α-alaninato)zinctate(II) complexes in aqueous solutions were determined by the X-ray diffraction method. All the three complexes have the octahedral structure in the form $[Zn(α-ala)(H_2O)_4]^+$, $[Zn(α-ala)_2(H_2O)_2]$, and $[Zn(α-ala)_3]^-$. The structures of the complexes were different from those of the glycinato complexes of zinc(II) ion, which were all regular octahedral. The length of the Zn-O bond in the α-alaninato complexes was shorter than that of the Zn-N bond due to the inductive effect of the substituted methyl group at the α-carbon on the oxygen atom in the amino acid. The lengths of the Zn-O and Zn-N bonds in the complexes determined are, respectively, as follows: $[Zn(α-ala)(H_2O)_4]^+$, 202 and 214 pm; $[Zn(α-ala)(H_2O)_2]$, 203 and 214 pm; $[Zn(α-ala)_3]^-$, 202 and 213 pm.

VI-B-4 An X-Ray Diffraction Study on the Structure of 18-Crown-6 Ether Complexes with Alkali Metal Ions in Aqueous Solution

Kazuhiko OZUTSUMI*, Masahiko NATSUHARA* *(*Tokyo Inst. Technol.)*, and Hitoshi OHTAKI

The structure of 1,4,7,10,13,16-hexaoxacyclooctadecane (18-crown-6) and its complexes with alkali metal ions in aqueous solution has been investigaged by X-ray diffraction and Raman spectroscopic methods at 25°C. The X-ray scatttering data and Raman spectrum for an aqueous 18-crown-6 solution show that free 18-crown-6 has a conformation of C_i or D_{3d} sym-

metry. The molecule seems to be flexible and may be present as a mixture of the two conformations in aqueous solution. The structure of the lithium complex was not conclusive because of a weak scattering power of lithium atoms and weak complex formation between lithium ion and 18-crown-6. The sodium 18-crown-6 complex is estimated to have a structure similar to that found in crystal. The 18-crown-6 ring within the complex adopts the C_1 conformation, where five oxygen atoms within 18-crown-6 coordinate to the sodium ion at the equational position and an oxygen atom within the 18-crown-6 and a water molecule at the axial one. The structure of the potassium complex is also similar to that in crystal in which the D_{3d} conformation is taken. The potassium ion is located at the center of the mean plane of the 18-crown-6 and one or two water molecules solvate the potassium ion above and/or below the plane of the 18-crown-6. It is suggested that the structure of the caesium complex is with either C_1 or D_{3d} symmetry, where the caesium ion is apart from the mean plane of the 18-crown-6. The rubidium complex was not examined because of a strong fluorescent X-ray emission from rubidium atoms when studied. The 18-crown-6 ring in the sodium and potassium complexes is rather rigid probably because the cavity of the ring well fits to the metal ions, while the ring coordinating to the large caesium ion becomes more flexible than that in the sodium and potassium complexes due to weaker interaction with the caesium ion.

VI-B-5 The Structure of Nickel(II) and Copper(II) Complexes with 1,4,8,11-Tetraazacyclotetradecane in Aqueous Solution As Studied by the X-Ray Diffraction Method

Hitoshi OHTAKI and Hiroyuki SEKI (Tokyo Inst. Technol.)

The structure of 1,4,8,11-tetraazacyclotetradecane (cyclam) complexes with nickel(II) and copper(II) ions in aqueous solution has been determined by the X-ray diffraction method at 25°C. The [Ni(cyclam)]$^{2+}$ complex has a square-planar structure with four nitrogen atoms of the cyclam and the Ni-N bond length has been determined to be 198 pm. By the addition of ammonia the color of the nickel(II)-cyclam solution turns to deep purple and the [Ni(NH$_3$)$_2$(cyclam)]$^{2+}$ complex is formed, which has a regular octahedral structure around the nickel(II) ion with the additional two NH$_3$ molecules along the axis vertical to the cyclam plane, and the Ni-N(NH$_3$ and cyclam) bond lengths are 209 pm. The copper(II)-cyclam complex in the aqueous solution is distorted octahedral with two water molecules along the elongated axis. The axial Cu-O and equatorial Cu-N bond lengths are 277 and 210 pm, respectively.

VI—C   Structural Studies of Ionic Melts, Glasses and Crystals

Structures of ionic melts, glasses and crystals have been determined by the X-ray diffraction method and EXAFS.

VI-C-1   Structural Studies of Superionic Glass AgI-Ag$_2$O-MoO$_3$

A. RAJALAKSHMI*, M. SESHASEYEE*, G. ARAVAMUDAN* (*Indian Inst. Technol.), Toshio YAMAGUCHI (Fukuoka Univ.), Masaharu NOMURA (Natl. Lab. High Energy Physics), and Hitoshi OHTAKI

Superionic conducting glass of the mole percent 60%AgI-20%Ag$_2$O-20%MoO$_3$ was prepared by rapid quenching from the melt. EXAFS and X-ray RDF studies indicate the presence of strong Ag-I interactions with $r_{Ag-I}=287$ pm. Two Ag-O interactions whose distances differ by 38 pm are also indicated. X-Ray RDF studies also yield $r_{Mo-O}=210$ pm and the coordination number of oxygen around Mo, $n_{Mo-O}=5.7$. A model is proposed which consists of a three dimensional network of distorted MoO$_6$ octahedra, which are 6-, 4-, and 2-corner shared leading to

large channels in the structure. The Ag^+ ions form bonds and secondary interactions with both non-bridging and bridging oxygen atoms in the network. The I^- ions surround the Ag^+ ions in the voids created by the glass network. The results show that Ag^+ and I^- ions are highly dispersed in the glass network and cluster formation was not found as proposed by earlier workers.

VI-C-2　Characterization of Highly Selective Cu-Ni Amination Catalysts

Hiroshi ABE *(Kao Corporation)*, Satoko HOSHI*, Kazunari DOMEN*, Ken-ichi MARUYA*, Hitoshi OHTAKI, and Takaharu ONISHI* (*Tokyo Inst. Technol.)

The characterization of Cu-Ni amination catalysts has been done by using TEM, XPS, and EXAFS. The Cu-Ni catalyst whose nickel atoms were hard to be reduced even at high temperatures under a hydrogen atmosphere gave a high selectivity in the reaction between dodecyl alcohol and dimethylamine to produce *N,N*-dimethyldodecylamine.

VI-C-3　In-situ Observations of the Phase Transition among Cobalt(II) Dichloride Hydrates and Crystal Structures of the Tetra- and Hexahydrates

Kenji WAIZUMI*, Hideki MASUDA, Hitoshi OHTAKI, Katsuo TSUKAMOTO*, and Ichiro SUNAGAWA* (*Tohoku Univ.)

Transformation among hexa-, tetra- and dihydrate crystals of cobalt(II) dichloride in aqueous solutions equilibrated with the crystals was studied by the optical microscopic method and X-ray crystallographic structural analysis. The solution-mediated transformation between $CoCl_2 \cdot 6H_2O$ and $CoCl_2 \cdot 2H_2O$ could be observed under a microscope, but the phase transition of $CoCl_2 \cdot 6H_2O$ or $CoCl_2 \cdot 2H_2O$ to $CoCl_2 \cdot 4H_2O$ was not observable under the present experimental conditions. The crystal structure of $CoCl_2 \cdot 4H_2O$ was determined by the X-ray diffraction method. The structure

of $CoCl_2 \cdot 6H_2O$ was reexamined because previously reported results had a relatively large *R*-factor. The crystal of $CoCl_2 \cdot 4H_2O$ is monoclinic, space group $P2_1/a$ with $a=11.543(1)$Å, $b=9.342(1)$Å, $c=6.056(1)$Å, $\beta=110.79(1)°$, and $Z=4$. The complex has a slightly distorted octahedral geometry about Co^{2+} ion and two Cl^- ions are located at the cis-position. The crystal of $CoCl_2 \cdot 6H_2O$ is monoclinic, space $C2/m$ with $a=10.380(2)$Å, $b=7.048(1)$Å, $c=6.626(1)$Å, $\beta=122.01(1)°$, and $Z=2$. The geometry around the cobalt ion is also octahedral with four water molecules at the equatorial positions and two chloride ions at the axial positions. The remaining two water molecules are linked to the two Cl^- ions by hydrogen-bonding. The narrow range of formation of $CoCl_2 \cdot 4H_2O$ crystals in the phase diagram was explained in terms of the relatively unstable cis-dichloro structure of the $[CoCl_2(H_2O)_4]$ moiety compared with the other two hydrates which have the trans-form.

VI-C-4　Structure of $MgCl_2 \cdot RbCl \cdot 6H_2O$

Kenji WAIZUMI *(Tohoku Univ.)*, Hideki MASUDA, Hitoshi OHTAKI, K. A. BURKOV*, and M. Y. SCRIPKIN* (*Leningrad Univ.)

$MgCl_2 \cdot RbCl \cdot 6H_2O$, $M_r324.22$, triclinic, $P1$, $a=6.672(5)$, $b=13.282(15)$, $c=6.639(5)$Å, $\alpha=89.83(8)$, $\beta=91.72(6)$, $\gamma=90.41(8)°$, $V=588.0(14)$Å^3 and $Z=2$, $D_x=1.831$ Mg m^{-3}, λ(Mo Kα)=0.71073Å, $\mu=51.7$ cm^{-1}, F(000)320, $T=253$ K. $R(F)=0.78$ for 2604 independent reflections with $|F_o| > 3\sigma(|F_o|)$. The crystal consists of a network of top-sharing $[RbCl_6]$ network, and isolated $[Mg(H_2O)_6]^{2+}$ octahedra occupying holes in the $[RbCl_6]$ network. The Rb^+ ion is coordinated with six Cl^- ions and each Cl^- ion is surrounded by two Rb^+ ions and four oxygen atoms of water molecules. The Mg-O bond length varies from 1.982(14) to 2.115(13)Å in the $[Mg(H_2O)_6]^{2+}$ octahedron. Each H_2O molecule is hydrogen-bonded to two Cl^- ions.

VI-C-5　Crystallographic Investigation on $MgCl_2 \cdot XCl \cdot 6H_2O$ Double Salts ($X^+ = K^+$,

Rb$^+$, Cs$^+$, NH$_4^+$). Crystal Structure of MgCl$_2$ · CsCl · 6H$_2$O

Kenji WAIZUMI *(Tohoku Univ.)*, Hideki MASUDA, Hitoshi OHTAKI, M. Y. SCRIPKIN*, and K. A. BURKOV* *(*Leningrad Univ.)*

The crystal structure of MgCl$_2$ · CsCl · 6H$_2$O double salt complex has been determined by the X-ray diffraction method. The crystal has the triclinic space group $P1$ with a unit cell of the dimensions a=6.749(1), b=13.531(6), c=6.764(2)Å, α=90.09(3), β=90.01(2), γ=90.17(3)°. The crystal structure consists of a network of top-sharing [CsCl$_6$] octahedra and isolated [Mg(H$_2$O)$_6$]$^{2+}$ octahedra which occupy holes in the [CsCl$_6$] network. The structure is similar to those of MgCl$_2$ · RbCl · 6H$_2$O and MgCl$_2$ · NH$_4$Cl · 6H$_2$O, but it differs from that of MgCl$_2$ · KCl · 6H$_2$O (carnallite). From the comparison of X$^+$ - Cl$^-$ distances (X$^+$=K$^+$, Rb$^+$, Cs$^+$, NH$_4^+$) in their double salts, the difference among the structures of MgCl$_2$ · XCl · 6H$_2$O double salts is explained in terms of different ionic sizes of the X$^+$ cation. Rubidium and ammonium ions seem to have the most favorable ionic radius to form MgCl$_2$ · XCl · 6H$_2$O double salt crystals by constructing the [XCl$_6$] top-sharing network. Incorporation of Rb$^+$ and Cs$^+$ ions into carnallite occurs by replacing K$^+$ ions with these ions.

VI—D   Molecular Dynamics Simulations of Electrolyte Solutions

Molecular dynamics simulations have been used to elucidate structures and dynamics of ions and solvent molecules in electrolyte solutions.

VI-D-1 Dissolution of Alkali Fluoride and Chloride Crystals in Water Studied by Molecular Dynamics Simulations

N. FUKUSHIMA *(Tokyo Inst. Technol.)*, Y. TAMURA, and H. OHTAKI

Dissolution processes of the rock-salt type NaF, KF, CsF, LiCl, NaCl, and KCl crystals consisting of 32 cations and 32 anions in an isolated box containing 216 water molecules were studied at 298 K by molecular dynamics simulations in order to elucidate the dissolution mechanism of alkali halide crystals in water. The side-lengths of the box were 1938(NaF), 1975(KF), 2019(CsF), 1963(LiCl), 1993(NaCl), and 2039(KCl) pm. The simulations were demonstated for 12 ps for NaF, CsF, and LiCl and for 20 ps for KF, NaCl, and KCl after the equilibrium was reached between the water molecules and the crystals. The ion-ion, ion-water and water-water interactions were described in terms of the Tosi-Fumi, Kistenmacher-Popkie-Clementi, and Matsuoka-Clementi-Yoshimine potentials, respectively. It was observed that anions *dissolved* in case of the LiCl, NaCl and CsF systems, but no dissolution of ions was found in the NaF, KF and KCl systems during the simulation periods. The mass effect of ions was examined in the dissolution process of CsF by introducing caesium ions having the same atomic weight as fluouride ion, 18.998. The positions of caesium ions fluctuated in the crystal and a less number of fluoride ions dissolved in case of the *lighter* system than in the normal one.

VI—E Thermodynamic and Spectroscopic Studies of Metal Complexes in Nonaqueous Solutions

Formation constants, enthalpies, and entropies of complexation reactions and structures of the complexes formed in aqueous and nonaqueous solvents have been investigated by calorimetry, spectrophotometry, and NMR.

VI-E-1 Solvation and Complexation of Copper(II) and Chloride Ions in 2,2,2-Trifluoroethanol-Dimethyl Sulphoxide Mixtures

Honoh SUZUKI*, Shin-ichi ISHIGURO* (*Tokyo Inst. Technol.), and Hitoshi OHTAKI

The formation of copper(II) chloro-complexes has been studied by calorimetry and spectrophotometry in various 2,2,2-trifluoroethanol (TFE)-dimethyl sulphoxide (DMSO) mixtures at 25°C. It was shown that as the mole fraction of TFE, x, in the mixtures increased, the formation constant of $[CuCl]^+$ gradually decreased to $x=0.8$. The result is contrary to that obtained for acetonitrile (AN)-DMSO mixtures. This is ascribed to the decresed entropy of formation of $[CuCl]^+$ in the TFE-DMSO mixtures in contrast to the increased entropy in the AN-DMSO mixtures with decreasing DMSO content. The corresponding enthalpy of formation of $[CuCl]^+$ remaines practically unchanged over the wide range of the solvent composition in the TFE-DMSO mixtures, as well as in the AN-DMSO mixtures. The different variation trends in the entropy of formation of $[CuCl]^+$ in the TFE-DMSO and AN-DMSO mixtures may be explained in terms of the different intermolecular interactions between solvent molecules in the bulk.

VI-E-2 Formation of Binary and Ternary Complexes of Cadmium(II) with Halide Ions and 2,2′-Bipyridine in N,N-Dimethylformamide

Shin-ichi ISHIGURO*, Kazuhiko OZUTSUMI*, Makoto MIYAUCHI* (*Tokyo Inst. Technol.), and Hitoshi OHTAKI

The formation of binary and ternary complexes of cadmium(II) with halide ions (X) and 2,2′-bipyridine (bpy) has been studied by calorimetry in *N,N*-di-

methylformamide (DMF) containing 0.1 mol dm^{-3} $(C_2H_5)_4NClO_4$ as an ionic medium at 25°C. The formation of ternary $[CdX(bpy)]^+$, $[CdX_2(bpy)]$, $[CdX_3(bpy)]^-$, $[CdX(bpy)_2]^+$, and $[CdX_2(bpy)_2]$ complexes is proposed, together with binary halogeno $[CdX_n]^{(2-n)+}$(n=1-4; X=Cl, Br, I) and 2,2′-bipyridine $[Cd(bpy)_n]^{2+}$ (n=1-3) ones, and their formation constants, enthalpies, and entropies are obtained. The geometry is suggested to be six-coordination for $[CdX(DMF)_5]^+$ and four-coordination for $[CdX_2(DMF)_2]$, $[CdX_3(DMF)]^-$, and $[CdX_4]^{2-}$; i.e., the change from octahedral to tetrahedral occurs at the formation of $[CdX_2]$. The ternary complexes are six-coordinated, except for $[CdX_3(bpy)]^-$, which is five-coordinated. The $[CdX_3(bpy)]^-$ complex is formed as the dominant species in the chloride and bromide systems, while the formation of the corresponding iodide complex is practically negligible. Affinities of halide ions with Cd^{2+}, $[Cd(bpy)]^{2+}$, or $[Cd(bpy)_2]^{2+}$ are compared in view of the effect of bound 2,2′-bipyridine molecules on the Cd(II)-X interactions.

VI-E-3 Formation of Chloro Complexes of Manganese(II), Cobalt(II), Nickel(II) and Zinc(II) in Dimethyl Sulphoxide

Honoh SUZUKI*, Shin-ichi ISHIGURO* (*Tokyo Inst. Technol.), and Hitoshi OHTAKI

The formation of chloro complexes of Mn(II), Co(II), Ni(II) and Zn(II) in dimethyl sulphoxide (DMSO) has been studied by calorimetry and spectrophotometry at 25°C. The formation constants, enthalpies and entropies for $[MCl_n]^{(2-n)+}$(n=1-4; M=Mn, Co, Ni, Zn) were determined and electronic spectra for the individual Co(II) and Ni(II) complexes were extracted. It is revealed that the coordination structure of $[CoCl]^+$, $[NiCl]^+$, and $[NiCl_2]$ is octahedral and that of

[CoCl₂], [CoCl₃]⁻, [CoCl₄]²⁻, [NiCl₃]⁻ and [NiCl₄]²⁻ is tetrahedral. Thus, an octahedral to tetrahedral geometry change occurs at the second step for Co(II) and at the third step for Ni(II). The log K_1 values for the formation of [MCl]⁺ vary in the order Mn > Co > Ni < Cu > Zn, which is different from the Irving-Wil liams series. The overall log β_4 values follow the sequence Mn < Co > Ni < Cu < Zn. Complexation entropies of these metal systems are appreciably smaller in DMSO than in N,N-dimethylformamide (DMF), which is ascribed to stronger solvent-solvent interactions in DMSO.

VI—F   Electrochemistry of Metal Complexes

Electrochemistry of metal complexes in aqueous and nonaqueous solutions has been investigaed with various methods.

VI-F-1   Electrocatalytic Reduction of Nitrous Oxide to Dinitrogen at a Mercury Electrode Using Ni(II) Complexes of Macrocyclic Polyamines

Isao TANIGUCHI*, Takashi SHIMPUKU*, Kenichi YAMASHITA* (*Kumamoto Univ.), and Hitoshi OHTAKI

Reduction of N₂O takes place efficiently at an Hg electrode to give only N₂ in current yields close to 100% in the presence of a small amount of Ni(II) complex of [15 or 14]aneN₄ ([15 or 14]aneN₄=1,4,8,12(or 11)-tetra-azacyclopenta(or tetra)decane) in aqueous solutions.

VI—G   Developments of Novel Multi-functionalized Macrocycles and Their Metal Complexes

Novel functions are attached to the classical macrocyclic polyamines for further extention of useful polyamine chemistries. Thus, developed new ligands and their metal complexes have shown unique chemical properties.

VI-G-1   Mono-, Di- and Tetrafluorinated Cyclams

Mitsuhiko SHIONOYA (Hiroshima Univ.), Eiichi KIMURA (Hiroshima Univ., and IMS), and Yoichi IITAKA (Teikyo Univ.)

The synthesis of the mono-(F1-), di-(F2-) and tetra-(F4-) fluorinated dioxocyclams (2 ~ 4) and cyclams (6 ~ 8) has been succeeded. An electron-withdrawing effect and a lipophilic effect of fluorine atoms on ligand properties were demonstrated by the weakened amine basicities and LF strengths with successive fluorinations with respect to those for nonfluorinated 1 and 5. The fluorinated 2 ~ 4 exhibit higher formation constants of square planar [Cuᴵᴵ(H₋₂L)]⁰ complexes. In their kinetics in acetate buffers (4.7 < pH < 5.7), the fastest overall complexation was observed with 4, where the contribution of the unprotonated ligand form is most determining. With Ni(II) complexes of cyclams 5 ~ 8 in aqueous solution, the ratio of the octahedral, high spin state increases with more fluorines. The F4-cyclam Ni(II) complex is in almost 100% high spin state. The fluorination strongly affects redox properties of Cu(II) and Ni(II) complexes, where the higher oxidation states become successively destabilized and the lower oxidation states successively stabilized. The X-ray structure of the F4-cyclam Ni(II) complex showed an octahedral, high spin form, where the bonding parameters are simi-

lar to those for the nonfluorinated complex. A preliminary test, where the present Ni(II) complexes were used as electrocatalysts for CO_2 reduction to CO in H_2O, suggests a promising application of fluorinated cyclams in redox-involving cyclam chemistry.

1 2 3 4

5 6 7 8
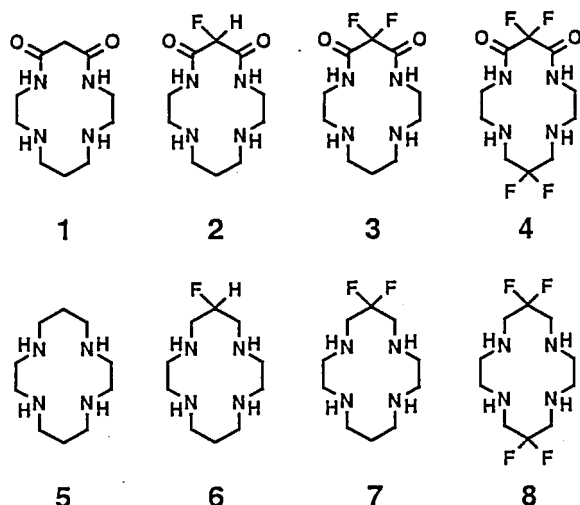
VI-G-2 Novel Cyclam-Ni(II) Complexes Appended with Photoactive Ru(II) Complex

Eiichi KIMURA *(Hiroshima Univ. and IMS)*, Mitsuhiko SHIONOYA *(Hiroshima Univ.)*, Toshikazu TAKAHASHI *(Hiroshima Univ.)*, Shinobu MARUYAMA *(Hiroshima Univ.)*, Makoto HARUTA *(Hiroshima Univ.)*, and Yoichi IITAKA *(Teikyo Univ.)*

A new class of heterometallo-bi- or trinuclear complexes (1 ~ 3) containing photoactive Ru(II) complexes have been synthesized as new complexes for use in photocatalysts; ^{1}H NMR, X-ray, cyclic voltammograms and emission studies show some efficient interactions between intramolecularly linked functionalities.

Referecne
E. Kimura, S. Wada, M. Shionoya, T. Takahashi and Y. Iitaka, *J. Chem. Soc., Chem. Commun.*, 397 (1990).

1

2

3
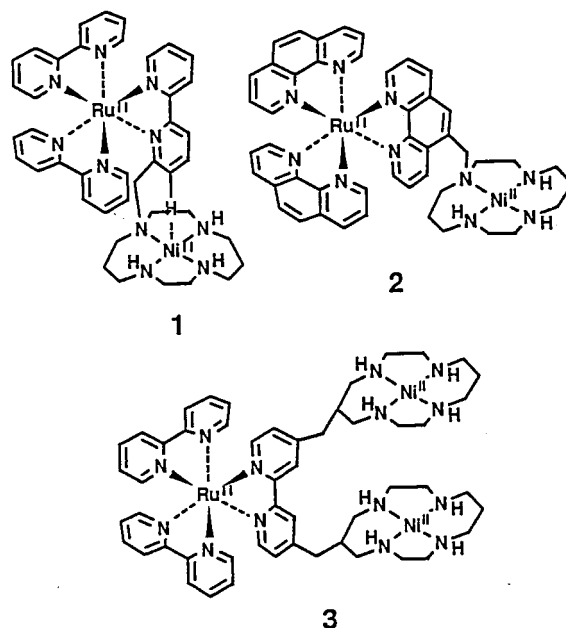
VI-G-3 A Novel Cyclam Appended with 3-Hydroxypyridine, An Ambident Donor Ligand Comprising of A Pyridyl N and A Pyridinolate O^- Donors

Eiichi KIMURA *(Hiroshima Univ., and IMS)*, Yoshihiko KOTAKE, Tohru KOIKE, Mitsuhiko SHIONOYA *(Hiroshima Univ.)*, and Motoo SHIRO *(Shionogi Research Labs)*

A new cyclam appended with an ambident donor 3-hydroxypyridine (1) has been synthesized to determine which adjacent donor, i.e. pyridyl N or pyridinolate O^-, apically binds with metal ions in the cyclam and how the pendant donor influences the complex structure and chemical behavior. With Ni^{II} ion, a *cis*-cyclam complex 2 is formed as a kinetic product, which converts to a thermodynamically more stable *trans*-cyclam complex 2. Crystalline Ni^{II} complex 2 was isolated from pH 9 solution and its X-ray analysis was conducted. Crystals of 2 ($C_{15}H_{26}N_5ONi \cdot ClO_4 \cdot 3H_2O$) are monoclinic, space group Pc, with two molecules in the unit cell of dimensions a=8.127(1) Å, b=12.056(1) Å, c=11.553(1) Å, and β=97.53(1)°. The structure was solved by the heavy atom method and refined anisotropically to R=0.035, R_w=0.048 for 1877 independent reflections. The crystal structure of 2 reveals a folded *cis*-cyclam configuration and the pyridyl N at

the fifth coordination site. The pyridyl N donor serves to enhance the rate of Ni^{II} complexation with cyclam and keeps binding with Ni^{II} without switching to the pyridinolate O^- donor in the Ni^{II}/Ni^{III} redox process. With Cu^{II} and Zn^{II}, the pyridyl N donor also is the exclusive fifth donor.
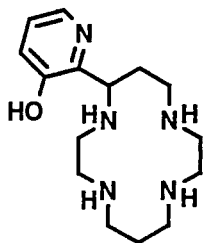
1
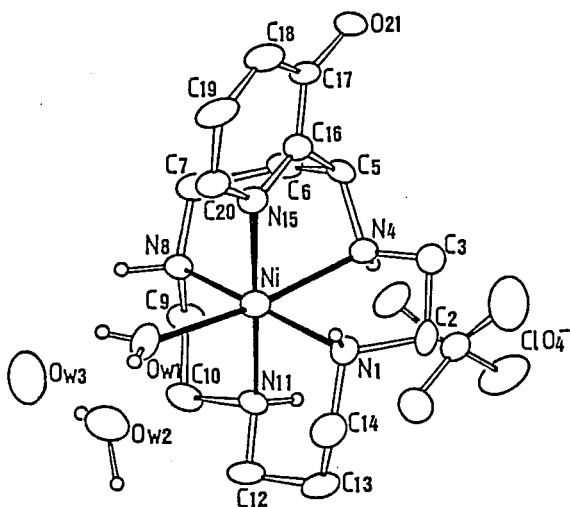
X-ray Structure of cis complex 2

VI-G-4 A Novel Synthesis of N_2S_3-type Ligand and Its Unique X-ray Structure of Pt(II) Complex

Eiichi KIMURA *(Hiroshima Univ. and IMS)*, Yasuhisa KUROGI *(Hiroshima Univ.)*, Mitsuhiko SHIONOYA *(Hiroshima Univ.)*, and Motoo SHIRO *(Shiono Research Labs)*

Highly selectivity for Pt^{II} and Pd^{II} complexations against Cu^{II}, Ni^{II} and Co^{II} has been previously found with "Dioxo[14]N_2S_2" (**1** is its Pt^{II} complex). Such a unique complexation behavior combined with amide groups have not yet reported. Recently, a new type of $(N^-)_2S_3$ macrocyclic ligand, "Dioxo[16]N_2S_3", and its Pt^{II} complex **2** have been synthesized. The $(N^-)_2S_2$ square-planar structure of **2** (S(4) is out of the plane) was clarified by the X-ray analysis.

Reference
E. Kimura, Y. Kurogi, S. Wada and M. Shionoya, *J. Chem. Soc., Chem. Commun.*, 781 (1989).
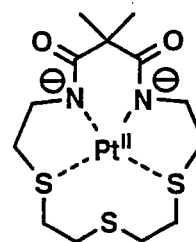
1   **2**
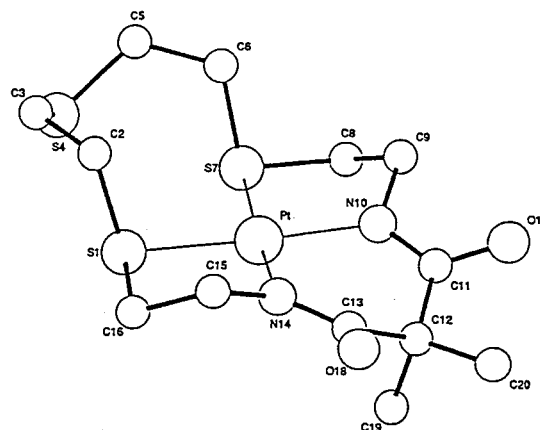
X-ray Structure of 2

VI—H Pharmaceutical Applications of Macrocyclic Polyamines

We have recently shown the biochemical usefulness of macrocyclic polyamines. Macrocyclic ligands are of great advantage to separation of lanthanides, magnetic resonance imaging as contrast-enhancing agents and radiopharmaceuticals.

VI-H-1 Effect of Polyamine Related Tetraamines on Anti-Ulcerogenic Activity and Anti-H$^+$, K$^+$-ATPase Activity

Tomohito KAKEGAWA *(Chiba Univ.)*, Seiyu HIROSE *(Chiba Univ.)*, Eiichi KIMURA *(Hiroshima Univ. and IMS)*, Hironaka AIHARA *(Taisho Research Labs)*, Yoshihiko ISOBE *(Taisho Research Labs)*, and Kazuei IGARASHI *(Chiba Univ.)*

The relationship between the structure of polyamine related tetraamine and their anti-ulcerogenic activity in rats was studied. Among the tetraamines tested, linear tetraamines had stronger anti-ulcerogenic activity in both restraint stress-induced gastric ulceration and ulceration in pylorus-ligated rats. Macrocyclic tetraamines and polycyclotetraamines had less anti-ulcerogenic activity. Correlation was detected between the inhibitory effect of tetraamines on gastric secretion in pylorus-ligated rats and their inhibitory effect on H$^+$, K$^+$-ATPase activity in rat gastric mucosa. Thermine and spermine were the most effective in these two inhibitions. Thus, it is suggested that primary amino groups are important in both anti-ulcerogenic activity and anti-H$^+$K$^+$-ATPase activity.

VI-H-2 Thermodynamic and Kinetic Studies of Lanthanide Complexes of 1,4,7,10,13-Pentaazacyclopentadecane-N,N′,N″,N‴,N⁗-pentaacetic Acid and 1,4,7,10,13,16-Hexaazacyclooctadecane-N,N′,N″,N‴,N⁗,N⁗′-hexaacetic Acid

Mutsuo KODAMA *(Hirosaki Univ.)*, Tohru KOIKE *(Hiroshima Univ.)*, Anung B. MAHATMA *(Hiroshima Univ.)*, and Eiichi KIMURA *(Hiroshima Univ. and IMS)*

The lanthanide complexes with macrocyclic tetraaminotetracarboxylate such as **DOTA** (3) or **TETA** (4) are currently attracting much attention in separation of lanthanides, magnetic resonance imaging as contrast-enhancing agents and radiopharmaceuticals. In comparison with linear analogues **EDTA** (1) or **DTPA** (2), these macrocyclic ligands have the great advantage of forming more stable complexes. **DOTA** forms more stable complexes with lanthanides than does the larger ring chelate **TETA**. An X-ray crystal structure of Eu(III)-**DOTA** shows a rigid nine-coordinate structure with an additional coordination of H$_2$O. However, one of the common drawbacks with these macrocyclic ligands is in their slow complexation rates. This may pose a serious setback in their practical use.

In our current efforts in searching for new chelating agents, we have synthesized macrocyclic pentaamine **PEPA** (5) and hexaamine homologue **HEHA** (6) and tested their complexation with Ln(III) and Y(III). It was found that the complexation of these new macrocycles seemed much quicker, while maintaining the extraordinary thermodynamic stabilities.
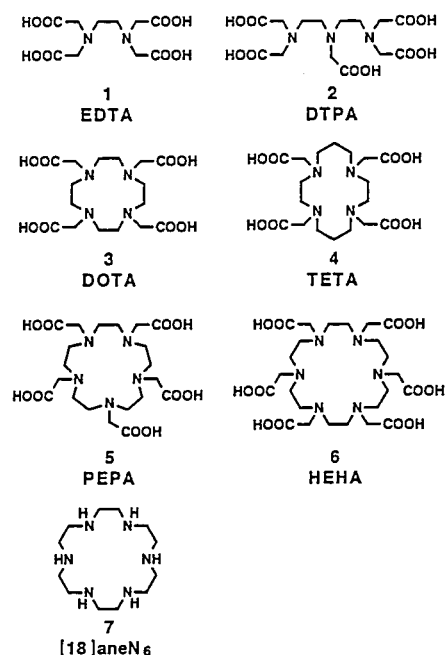
VI—I Biomimetic Studies Using Polyamine Complexes

A model study of active sites of metalloenzymes (*e.g.* Zn^{II}-containing carbonic anhydrase) using macrocyclic polyamine complexes was undertaken to clarify the crucial factor in enzyme functions.

VI-I-1 A Zinc(II) Complex of 1,5,9-Triazacyclododecane ([12]aneN₃) as a Model for Carbonic Anhydrase

Eiichi KIMURA *(Hiroshima Univ. and IMS)*, Takeshi SHIOTA *(Hiroshima Univ.)*, Tohru KOIKE *(Hiroshima Univ.)*, Motoo SHIRO *(Shionogi Research Labs)*, and Mustuo KODAMA *(Hirosaki Univ.)*

1

Molecular structure of (1)(ClO₄)₃HClO₄ with the 3-fold axis
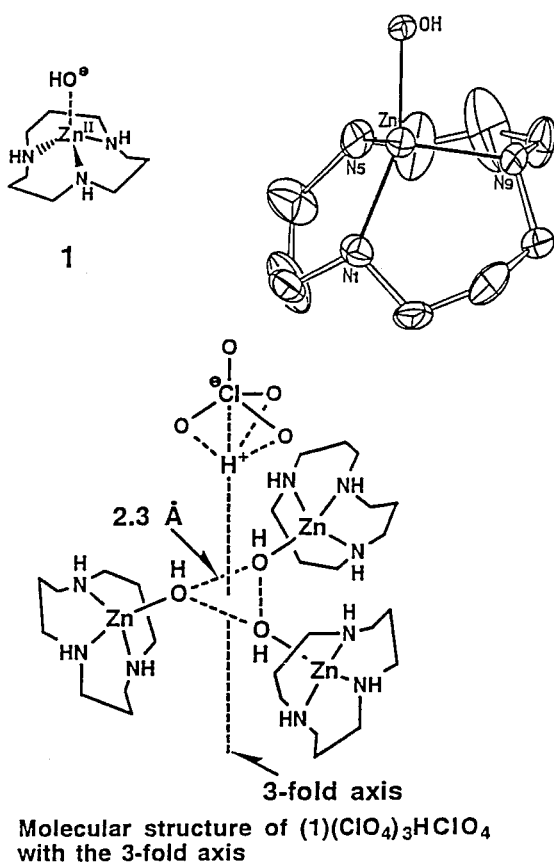
Among macrocyclic tri- and tetraamines tested, [12]aneN₃ is the most appropriate ligand that mimics the ligand field surrounding Zn^{II} in carbonic anhydrase. In its 1:1 $Zn^{II}L$ complex, the H_2O bound at the fourth coordination site deprotonates with the pK_a value of 7.30 at 25°C, I=0.1 (NaClO₄), almost the same value

being reported for the Zn^{II}-enzymes. The resulting hydroxo complex, precipitated as a trimer from pH 8 aqueous solution with a formula of $[Zn^{II}L(OH)]_3(ClO_4)_3 \cdot HClO_4$, has been analyzed by X-ray study. Anion binding affinity to the $Zn^{II}L$ complex is determined by pH titration to have an order of $OH^-=(\log K=6.4) \gg CH_3COO^-(2.6) > SCN^-(2.4) > I^-(1.6) > Br^-(1.5) > F^-(0.8)$, which is almost comparable with the anion inhibition order and magnitude reported for carbonic anhydrase activities. Moreover, like the Zn^{II}-enzymes, the $[Zn^{II}L(OH)]^+$ species (**1**) catalyzes methyl acetate hydrolysis and acetaldehyde hydration, where the Zn^{II}-bound OH^- commonly acts as a nucleophile to the carbonyl carbons. The plots of these rate constants vs pH in either case show the kinetic pK_a values of $Zn^{II}L(OH_2)$ to be nearly the same as the thermodynamically obtained values of 7.3 at 25°C and 7.9 at 0°C. Various outstanding properties of Zn^{II} in enzymes have been well demonstrated by the present complex behaviors.

VI-I-2 Acid Properties of Zinc(II) and Cadmium(II) in Complexation with Macrocyclic Oxopolyamine Ligands

Eiichi KIMURA *(Hiroshima Univ. and IMS)*, Tohru KOIKE *(Hiroshima Univ.)*, Takeshi SHIOTA *(Hiroshima Univ.)*, and Yoichi IITAKA *(Teikyo Univ.)*

The pH-metric titration study of the interaction of Zn^{II} and Cd^{II} ion with a series of dissociable (acidic) hydrogen-containing macrocyclic polyamines has served to distinguish inherent acid and coordination properties of these two metal ions. In complexation with monooxocyclam below pH 8, Zn^{II} ion can replace the amide hydrogen and forms a planar 1:1 monooxocyclam complex $[ZnH_{-1}L]^+$ containing the hitherto unknown deprotonated amide N^--Zn^{II} coordination, while Cd^{II} ion does not yield such a complex. A square-pyramidal N_5 Zn^{II} complex $[ZnH_{-1}L]^+$ **3** is

formed with a pyridyl-pendnat monooxocyclam **1** at pH < 8, as confirmed by X-ray structure analysis. In contrast, the larger and less acidic Cd^{II} displaces the amide proton of the same ligand to yield $[CdH_{-1}L]^+$ **5** at pH > 10. The intermediate complex **4** containing Cd^{II}-O(amide) bond was isolated and characterized by X-ray structure analysis. A larger-sized 16-membered macrocyclic monooxopentaamine initially (pH < 6) binds more strongly with Cd^{II} than with Zn^{II} using the four secondary nitrogen donors to form $[ML]^{2+}$. At higher pH, however, the more acidic Zn^{II} yields a more stable 5-coordinate amide-deprotonated complex $[ZnH_{-1}L]^+$ than the less acidic Cd^{II} does to $[CdH_{-1}L]^+$.

tropically to $R = 0.044$, $R_w = 0.062$ for 1551 independent reflections. The complex assumes a five-coordinate, square pyramidal geometry, where zine(II) is surrounded by cyclam moiety in a planar fashion and by the pendant phenolate anion occupying an axial position. An extremely short Zn-O(phenolate) bond distance 1.983 Å, in conjunction with the 0.225 Å deviation of Zn^{2+} above the cyclam N_4 plane toward the phenolate, accounts for the extremely low pK_a value of 5.8 for the pendant phenol. These facts about **1**, in comparison with the previous findings with Ni^{2+} and Cu^{2+} complexes of the same ligand, well illustrate the characteristics of Zn^{2+} coordination properties.
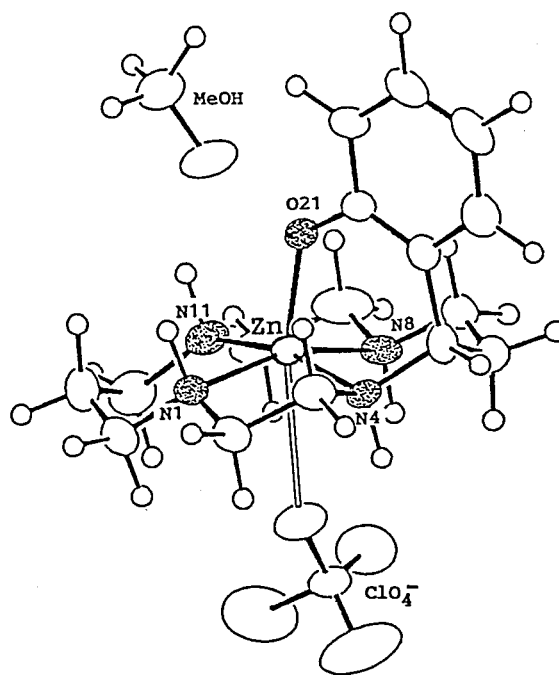
X-ray Structure of (1) · ClO₄ · CH₃OH

VI-I-3 X-Ray Structural Study of Zinc(II) Inclusion Complex of a Phenolate-pendant Cyclam

Eiichi KIMURA *(Hiroshima Univ. and IMS)*, Hiromasa KUROSAKI, Tohru KOIKE *(Hiroshima Univ.)*, and Koshiro TORIUMI

Molecular structure of phenol-pendant cyclam-zinc(II) complx **1** has been determined by X-ray structure analysis. Crystals of **1** · ClO₄ · CH₃OH ($C_{16}H_{27}N_4OZn$ · ClO₄ · CH₃OH) are monoclinic, space group $P2_1/n$, with four molecules in the unit cell of dimensions $a = 31.198(2)$ Å, $b = 8.426(1)$ Å, $c = 8.214(1)$ Å, and $\beta = 93.96(1)°$. The structure was solved by the heavy atom method and refined aniso-

VI-I-4 Synthesis, Properties and Complexation Studies of a New Imidazole Attached to a Macrocyclic 12-Membered Triamine Ligand

Eiichi KIMURA *(Hiroshima Univ. and IMS)*, Yasuhisa KUROGI *(Hiroshima Univ.)*, Mitsuhiko SHIONOYA *(Hiroshima Univ.)*, and Motoo SHIRO *(Shionogi Research Labs)*

The new imidazole attached to a 12-membered ring triamine ([12]aneN₃) **1** has been synthesized. The properties and complexation behaviors of its imidazole

were studied, in particular, the easiness with which the imidazolate anion is generated in free form and in metal complex form and their esterolysis activities. An X-ray crystal study of the Zn(II) complex 1 shows close equatorial coordination of the imidazole (2.025 Å) in a distorted trigonal bipyramidal structure with an additional axial chloride ion: crystal data; $Pna2_1$, a=14.574, b=9.079, c=13.506(Å), Z=4, R=0.030 and R_w=0.040.

1
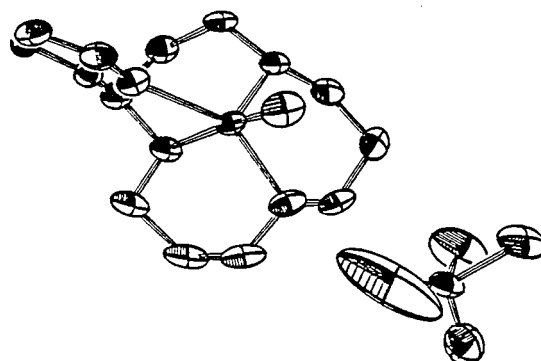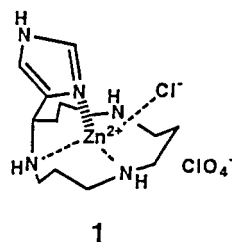
VI—J Dynamic Behavior of Ions and Electrons in Crystals

Diffusional and reorientational motions of molecular ions and electron migration in crystals have been investigated by means of nuclear magnetic and nuclear quadrupole resonance techniques. From these studies, the following dynamically highly-disordered states having intermediate properties between solid and liquid have been obtained in ionic crystals. The rotator phase of n-butylammonium chloride containing uniaxially rotating rod-like cations has been shown to be a low-dimensional plastic crystal, that can be considered as a new type of mesophase between the plastic crystal and the liquid crystal. A novel ionic plastic phase was found in $[(CH_3)_4N]SCN$ in which rapid 3D self-diffusion and overall rotation of the bulky cations take place.

VI-J-1 Studies of the Anisotropic Self-Diffusion and Reorientation of Butylammonium Cations in the Rotator Phase of Butylammonium Chloride Using ^1H Nuclear Magnetic Resonance, Electrical Conductivity, and Thermal Measurements

Mineyuki HATTORI*, Shin-ichi FUKADA*, Daiyu NAKAMURA*, and Ryuichi IKEDA (*Nagoya Univ.)

Butylammonium chloride crystals annealed by a slow scanning through the phase transitions many times were shown to exhibit a simple thermogram having a single phase transition at 241 K (T_{tr}) on heating from ca. 100 K up to the melting temperature T_m (487 K). AC electrical conductivity measurements on single crystals revealed that ionic conduction takes place in the 2D layers of the room-temperature phase (rotator phase) which have a lamellar-type double-layer structure. The observed ^1H NMR T_1 and $T_{1\rho}$ data were explained well by applying the theory of 2D diffusion by MacGillivray and Sholl in the low vacancy-concentration limit. The averaged jump times for the cationic self-diffusion were derived from T_1 and $T_{1\rho}$ data to be 5×10^{-3} s at room temperature and 3×10^{-7} s at T_m. The transition entropies at T_{tr} and T_m determined by differential scanning calorimetry were 26 and 19 J K^{-1} mol^{-1}, respectively. These results imply that the rotator

phase is a kind of plastic crystal.

VI-J-2 A Novel Ionic Plastic Phase of [(CH₃)₄N]SCN Attainable above 455 K

Toshitaka TANABE*, Daiyu NAKAMURA*, and Ryuichi IKEDA (*Nagoya Univ.)

A new high-temperature solid phase of tetramethylammonium thiocyanate was found above the phase transition at 455 K, where a large entropy change (15 JK mol^{-1}) was observed by thermal analysis. X-Ray powder patterns recorded at ca. 470 K showed that the crystals of this phase form a CsCl-type cubic lattice with a = 6.00 Å indicating that the SCN$^-$ anions take highly disordered orientations. Presence of rapid 3D self-diffusion as well as overall reorientation of the cations in this phase were revealed by the temperature dependence studies of ^{1}H NMR spin-lattice relaxation times, T_1 and $T_{1\rho}$, the second moment of NMR absorptions, and the electrical conductivity. A large ionic diffusion constant of the order of 10^{-13} m^{2}s^{-1} obtained around 490 K is roughly the same as those in "ionic plastic crystals" already reported. An activation energy of ca. 100 kJ mol^{-1} was determined for the cationic self-diffusion. From these data, it can be concluded that this new phase is the first example of the ionic plastic crystal containing tetramethylammonium cations.

VI-J-3 Chlorine Nuclear Quadrupole Relaxation Studies on Ionic Dynamics and Phase Transition in NH₄AuCl₄

Atsushi ISHIKAWA*, Tetsuo ASAJI*, Daiyu NAKAMURA*, and Ryuichi IKEDA (*Nagoya Univ.)

Chlorine NQR frequencies, and NQR spin-lattice and spin-spin relaxation times (T_{1Q} and T_{2Q}) were measured for NH₄AuCl₄ crystals at various temperatures between 4.2 and 337 K. Each of two resonance lines observed at room temperature was split into a doublet below T_c = 29 K indicating the occurrence of phase transition. A rapid decrease of T_{1Q} observed

above ca. 290 K is attributable to 90° reorientational jumps of the complex anions about its pseudo C₄ axis. The activation energy of 80 kJ mol^{-1} was obtained for this motion. ^{35}Cl T_{1Q} exhibited a minimum at T_c. The T_{1Q} isotope ratio $T_{1Q}(^{37}$Cl$)/T_{1Q}(^{35}$Cl$)$ became 1.6 and 1.0 in the high- and low-temperature sides of this minimum, respectively. These results were explained by the fluctuation of the electric field gradient produced at the chlorine nuclei originating from the reorientational jumps of the NH₄$^+$ ions. The motion of the cations is much faster and much slower than the resonance frequencies in the high- and low-temperature sides, respectively. This conclusion suggests that the phase transition is an order-disorder type relating to the orientation of the NH₄$^+$ ion.

VI-J-4 Chlorine Nuclear Quadrupole Relaxation due to the Motion of Pyridinium Cations in Pyridinium Hexachlorometallates(IV): (pyH)₂MCl₆ (M = Sn, Pb, Te)

Yutaka TAI*, Tetsuo ASAJI*, Daiyu NAKAMURA*, and Ryuichi IKEDA (*Nagoya Univ.)

The temperature dependence of chlorine quadrupole spin-lattice relaxation time T_{1Q} was observed for one of the three ^{35}Cl NQR lines of [pyH]₂MCL₆ (M = Sn, Pb, Te). Each T_{1Q} curve can be devided into three temperature regions. In the low- and high-temperature regions, T_{1Q} is dominantly determined by the relaxation mechanism due to the libration and reorientation of [MCl₆]$^{2-}$, respectively. In the intermediate temperature region, T_{1Q} results from the modulation of chlorine electric field gradient by the motion of the neighboring pyridinium cations. This way the reorientational motion of the cation between potential wells with nonequivalent depths is precisely characterized.

VI-J-5 A Highly Disordred New Solid Phase Containing Isotropically Reorienting Cations in (CH₃NH₃)₂CdBr₄ Studied by ^{1}H NMR and Thermal Measurements

Hiroyuki ISHIDA*, Kentaro TAKAGI*, Mifune TERASHIMA**, Daiyu NAKAMURA**, and Ryuichi IKEDA (*Okayama Univ, **Nagoya Univ.)

Measurements of the ¹H spin-lattice relaxation time, the line-width parameter, the second moment of ¹H NMR absorption, differential thermal analysis, and differential scanning calorimetry were performed on methylammonium tetrabromocadomate(II) crystals. A new solid phase was found between 482 K and its melting point (493 K). ¹H NMR measurements revealed the presence of overall reorientation of methylammonium cations in this phase. In the room temperature phase, a 120° reorientational jumps of the CH₃ and NH₃⁺ groups was detected.

VI-J-6 Motion of Methylammonium Ions in (CH₃NH₃)₂ZnBr₄ Crystals Studied by ¹H NMR and Thermal Measurements

Hiroyuki ISHIDA*, Kentaro TAKAGI*, Tadashi IWACHIDO*, Mifune TERASHIMA**, Daiyu NAKAMURA**, and Ryuichi IKEDA (*Okayama Univ., **Nagoya Univ.)

Measurements of the ¹H spin-lattice relaxation time T_1, the linewidth parameter T_2^*, the second moment of ¹H NMR absorption, differential thermal analysis, and differential scanning calorimetry were performed on methylammonium tetrabromozincate(II) crystals from 58 to above 500 K. A solid-solid phase transition was located at 456 K. In the room temperature phase, 120° reorientational jumps of CH₃ and NH₃⁺ groups in the cation about its C-N bond axis were detected. In the high-temperature phase, the cations undergo overall reorientation as well as translational self-diffusion. The

activation energy for the cationic self-diffusion wasevaluated to be 18 kJ mol⁻¹.

VI-J-7 Solid State ¹³C High Resolution NMR in One-Dimensional Halogen-Bridged Nickel Complexes and Palladium(II)-Palladium(IV) Mixed Valence Complexes

Ryuichi IKEDA, Tomomi TAMURA*, and Masahiro YAMASHITA** (*Bruker Japan, **Nagoya Univ.)

Solid state high-resolution ¹³C NMR (CP/MAS) spectra were measured on one-dimensional halogen-bridged complexes [Ni(R,R-chxn)₂X]X₂ (X: Cl, Br; R,R-chxn: 1R,2R-cyclohexanediamine) to elucidate the metal valence state. The observed spectra were compared with those of Pd(II)-Pd(IV) mixed-valence complexes: [Pd(R,R-chxn)₂][PdX₂(R,R-chxn)₂]Y₄ (X: Cl, Br; Y: ClO₄, Cl) and [Pd(en)₂][PdX₂(en)₂] (ClO₄)₄ (X: Cl, Br; en: ethylenediamine) together with a monomer Pd(II) complex [Pd(R,R-chxn)₂]Cl₂. The one-dimensional Pd complexes showed a clear 1:1 doublet ¹³C signal for en ligands and also for the α-carbons in chxn ligands indicating the presence of two kinds of Pd valence states: Pd(II) and Pd(IV). On the other hand, a sharp singlet line was observed for the α-carbons in the Ni complexes and the Pd monomer complex. These results mean that all Ni atoms in the chain are equivalent and the paramagnetic Ni(III) state is formed. Small chemical shifts observed in the Ni complexes comparable to those in the diamagnetic Pd complexes imply the presence of strong antiferromagnetic interactions between neighboring Ni(III) sites in the one-dimensional chain.

VI—K Synthesis of Optically Active Complexes and Their Catalytic Use in the Asymmetric Oxidation

The enantioselective synthesis of organic compounds using chiral transition metal complexes has received attention. We are interested in the asymmetric epoxidation of olefins and oxidation of prochiral sulfides. In this project, the synthesis of new optically active complexes and their catalytic activites on the asymmetric oxidation reactions are investigated.

VI-K-1 Preparation and Characterization of Optically Active Schiff Base-Oxovanadium(IV) and -Oxovanadium(V) Complexes and Catalytic Properties of These Complexes on Asymmetric Oxidation of Sulfides into Sulfoxides with Organic Hydroperoxides

Kiyohiko NAKAJIMA, Katsuhide KOJIMA*, Masaaki KOJIMA*, and Junnosuke FUJITA*
(*Nagoya Univ.)

Oxovanadium(V) complexes, V ^{V}O(Schiff base)Y (Y=ClO$_4$, Cl, NO$_3$), with quadridentate Schiff base ligands derived from optically active 1,2-diamines and salicylaldehyde or its derivatives were prepared by oxidizing corresponding V^{IV}O (Schiff base) with Ce^{IV} in acetonitrile followed by the addition of HY. The complexes were characterized by ^{1}H NMR, IR, UV-Vis, and circular dichroism spectra, and electrochemistry. Reversible reduction potentials (V^{5+}/V^{4+}) obtained by cyclic voltammetry for a series of oxovanadium(V) complexes with Schiff base ligands derived from 5-substituted salicylaldehydes showed a linear dependence on the Hammett parameter. Both vanadium(IV) and vanadium(V) complexes catalyze asymmetric oxidation of sulfides into the corresponding sulfoxides with organic hydroperoxides. The vanadium(IV) complexes gave better results than the vanadium(V) complexes and in most cases the optical yields (e.e.) ranged between 20 and 40%. In the reaction of V^{IV}O(Schiff base) with an organic hydroperoxide the complex is finally converted into the oxovanadium(V) species, and a dark brown intermediate is suggested to be the catalytically active species.

VI—L   Chemistry of Polyoxoanions

One area of current interest is the solution dynamics of polyoxoanions, especially those of Anderson and/or Lindqvist type structure. Efforts are also underway to synthesize polyoxoanions having novel structures and molecular properties using non-aqueous synthetic methods.

VI-L-1 Synthesis and Structure of a Novel Polymolybdate which Contains Penta-Coordinated Mo(VI)

Hikaru ICHIDA (Univ. of Tokyo) and Atsushi YAGASAKI

Reaction of Te(OH)$_6$ with [(n-C$_4$H$_9$)$_4$N]$_4$[α-Mo$_8$O$_{26}$] in acetonitrile yields [(n-C$_4$H$_9$)$_4$N]$_4$-[TeMo$_8$O$_{29}$] · H$_2$O. X-ray structural analysis revealed the presence of discrete [TeMo$_8$O$_{29}$]$^{4-}$ anions having the structure shown in the Figure. The striking feature of this structure is the presence of a coodination number of five for hexavalent molybdenum [Mo(7)], which has never been reported for any polymolybdate before. The distortion of the TeO$_6$ octahedron also seems worthy of mention. The Te-O(1) distance is significantly longer than the other five Te-O bond lengths.
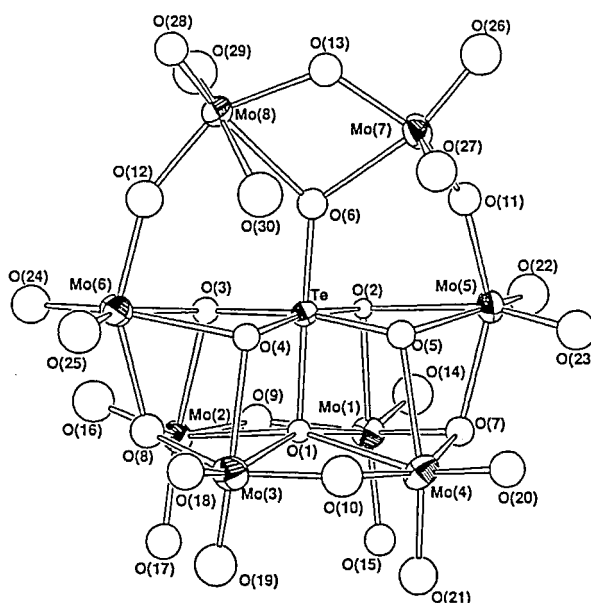
Figure 1. The structure of [TeMo$_8$O$_{29}$]$^{4-}$. Ellipsoids and spheres are drawn to encompass 30% of the electron density. O(30) is the oxygen atom of water molecule.

VI—M Synthesis, Characterization and Stereoselectivity of the Metal Complex with Chiral Ligand

New metal complexes with chiral ligand having an asymmetric center at the N-terminal moiety are synthesized and the stereoselectivity of these complexes are studied.

VI-M-1 Syntheses, X-ray Crystal and Molecular Structures, Absolute Configurations and Stereoselectivities of Octahedral Cobalt(III) Tris-Chelate Complexes of N-(R)-1-Phenylethylsalicylaldimine, N-(R)-sec-Butylsalicylaldimine and N-(S)-sec-Heptylsalicylaldimine

Tatsuya KAWAMOTO, Akira TAKEUCHI*, Hiro KUMA*, and Yoshihiko KUSHI (*Osaka Univ.)

Octahedral tris-bidentate chelate cobalt(III) complexes of optically active Schiff base ligand have been synthesized and their crystal and molecular structures have been determined. The central cobalt atoms of all complexes have a N_3O_3 type meridional coordination. The absolute configuration along the pseudo three-fold axis is found to be Λ-SSS form for the N-(S)-sec-heptyl complex from the X-ray analysis. The stereoselectivity about these complexes depends considerably on the bulkiness of the N-terminal groups. The effect of the functional group which introduced into the salicyl moiety are also studied, and found that the 5-nitro group tends to decrease the stereoselectivity considerably.

Λ -SSS Λ -SSS Λ -SSS

VI-M-2 Syntheses, X-ray Crystal and Molecular Structures, Absolute Configurations and Stereoselectivities of Pseudo-Tetrahedral Copper(II) Bis-Chelate Complexes of N-(R)-1-Phenylethylsalicylaldimine and N-(S)-sec-Butylsalicylaldimine

Tatsuya KAWAMOTO, Akira TAKEUCHI*, Hiro KUMA*, and Yoshihiko KUSHI (*Osaka Univ.)

Six pseudo-tetrahedral bis-bidentate chelate copper(II) complexes of optically active Schiff base ligand have been synthesized and their crystal and molecular structures have been determined. The central copper atoms of all complexes have a N_2O_2 type trans coordination. The absolute configuration along the pseudo two-fold axis is found to be Δ-RR form for the N-(R)-1-phenylethyl complex from the X-ray analysis. The effect of the functional group which introduced into the salicyl moiety are studied, and found that the 5-nitro group tends to decrease the stereoselectivity considerably.

VI-M-3 The Effect of the Asymmetric Center on the Molecular Structure of Meso- and Optically Active-trans Bis(succinimidato)-bis(1-phenylethylamine)palladium(II)

Hiroshi SHIMOMURA*, Seiko KOMORITA*, Hiro KUMA*, and Yoshihiko KUSHI (*Osaka Univ.)

A pair of palladium(II) succinimidato complex with 1-phenylethylamine ligand has been newly prepared and both crystal structures were determined by X-ray analyses. Both palladium(II) have a trans 4N-type planar coordination and two trans succinimidato ligands also form a plane with including the Pd atom. The planar geometry around the central Pd atom affects the asymmetric center on the 1-phenylethylamine ligand. Three possible staggered rotamers of 1-phenylethylamine ligand have been found in these complexes, and the different interligand repulsions of those rotamers have been confirmed: the Pd-N(phenea) bond lengths 2.039(7) Å for meso form (i) and 2.029(6) Å and 2.079(7) Å for optically active form (ii) an (iii) respectively.

(i)   (ii)   (iii)

VI-M-4 The Effect of the Asymmetric Center on the Molecular Structure of Meso-trans Bis(succinimidato)bis(1-phenylethylamine)copper(II) and Optically active-trans Bis(hydantoinato)bis(1-phenylethylamine)copper(II)

Hiroshi SHIMOMURA*, Seiko KOMORITA*, Hiro KUMA*, and Yoshihiko KUSHI (*Osaka Univ.)

Two new copper(II) imidato complexes with meso- and optically active 1-phenylethylamine ligand have been prepared, and both crystal structures were determined by X-ray analyses. Both complexes have a tetrahedrally distorted trans 4N-type coordination. It is interested to note that the lack of cener of symmetry in the tetrahedrally distorted coordination affects the molecular structure around the assymmetric ligand. Thus, in contrast to the planar Pd(II) complexes, the distortion around the asymmetric ligand in the meso-Cu(II) complex is larger than that found in the optically active-Cu(II) complex.

VI—N   Thermodynamic Properties of Solutions and Solute-Solvent Interactions

Molecular interactions in solutions were investigated mainly from the static, thermodynamic properties of solutions. Special emphasis was placed on the following two points: (1) Experimental division of the partial molar volume V_2^0 of an electrolyte MX into the cationic $V_2^0(M^+)$ and anionic $V_2^0(X^-)$ contributions based on the measurement of an electric potential called "Sedimentaion Potential" which arises from the difference in the movement of dissolved ionic species in the applied gravitational field. (2) Elucidation of the phenomena of hydration in aqueous solution and selective solvation in mixed solvent systems.

VI-N-1   Sedimentation Potential of Complexes of Nitroamminecobalt(III) in Aqueous Solution at 25°C

Hiromitsu HIRAKAWA   (Kagoshima   Univ.),
Hiroyasu NOMURA   (Nagoya Univ.), and Fumio
KAWAIZUMI

Sedimentation potentials(SP) were measured for a series of nitroamminecobalt(III) salts containing $[Co(NO_2)_n(NH_3)_{6-n}]^{3-n}$ ions in aqueous solution. The magnitudes of the sedimentation potentials varied with the number of NO_2^- ligands in the complexes and a definite positive signal was observed for a neutral complex $[Co(NO_2)_3(NH_3)_3]^0$. The division of the partial molar volumes of nitroamminecobalt(III) complexes based on the observed SP values resulted in comparable values of the partial molar volumes for the Cl^- ion, suggesting no appreciable hydrolysis nor ionic association occur for these nitroamminecobalt(III) complexes.

VI-N-2   On the Partial Molar Volumes of Univalent Ions in Water-Acetone Mixtures Based on the Sedimentation Potential Measurements

Hiromitsu HIRAKAWA   (Kagoshima   Univ.),
Hiroyasu NOMURA   (Nagoya Univ.), and Fumio
KAWAIZUMI

Early work on the determination of partial molar volumes V_2^0 of $Na[BPh_4]$ and $[Ph_4P]Cl$ dissolved in water-acetone system up to 50 wt% of acetone showed that the V_2^0 of $Na[BPh_4]$ increases with acetone con-tent, while values of V_2^0 remain constant for such salts as NaCl, NaBr, and $[Ph_4P]Cl$. To solve this problem, sedimentation potentials were measuerd for tetraphenyl complexes $Na[BPh_4]$, $[Ph_4P]Cl$, $[Ph_4P]Br$ as well as NaCl and NaBr dissolved in water-acetone system. The V_2^0 of the cation $[Ph_4P]^+$ remained constant with variation of solvent composition, while an abrupt increase in V_2^0 was observed for the anion $[BPh_4]^-$ in solvents with acetone content from 10 to 30 wt% of acetone. Values fo $V_2^0([Ph_4P]^+)$ are smaller than $V_2^0([BPh_4]^-)$ in water and 10 wt% of acetone but the former becomes larger than the latter in solvents containing more than 20 wt% of acetone. The conventional assumption that molar properties are set to be equal for the two large ions $[Ph_4P]^+$ and $[BPh_4]^-$ is not always acceptable for V_2^0 in water-acetone system.

VI-N-3   Ion-Solvent Interactions in Water-Methanol and Water-Acetonitrile from the Point of Ionic Partial Molar Volumes

Fumio KAWAIZUMI, Yoshitomo INOUE*, and
Hiroyasu NOMURA* (*Nagoya Univ.)

Using the digital precision densitometer, measurements of densities of solution of $AgNO_3$ and $Ca(NO_3)_2$ in the mixed solvents water-methanol and water-acetonitrile were carried out at 25°C and the partial molar volumes V_2^0 of these electrolytes were determined on taking account of the concentration dependence of the apparent molar volumes as predicted by the Debye-Hückel theory. The ionic partial molar volumes of Ag^+, Ca^{2+}, and NO_3^- were evaluated by combining our results obtained earlier and those obtained in this work. The solvent composition dependence of V_2^0 of each

ion was far remarked in water-acetonitrile than in water-methanol and characteristic behaviors were observed for Ag^+ and Ca^{2+} ions in water-acetonitrile system.

VI-N-4 A New Method of Determination of Enthalpy for the Proton Dissociation in Solution

Motoharu TANAKA*, Hiroyasu NOMURA* (*Nagoya Univ.), and Fumio KAWAIZUMI
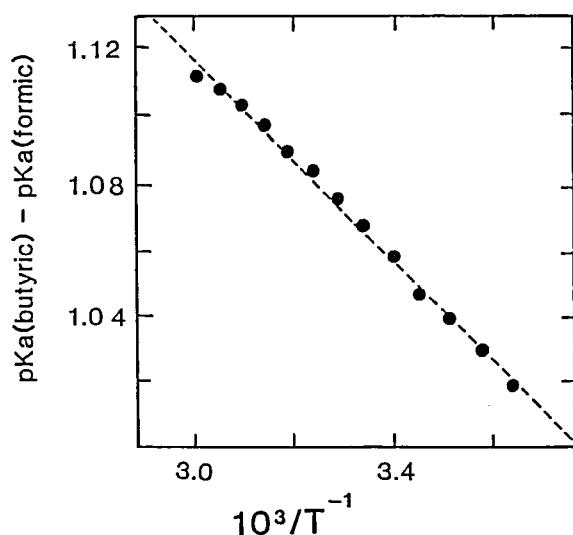
Figure 1. pKa(Butyric acid) − pKa(Formic acid) plotted against reciprocal temperature.

A method is proposed for evaluation of the enthalpy for the proton dissociation of an acid HB in solutions; Instead of differentiating pKa value with respect to temperature, an appropriate acid HA is selected as a reference and the quantity X = pKa(HB) - pKa(HA) is plotted as a function of reciprocal temperature. Figure.

1 is an example of such plot where formic acid corresponds to reference acid. As seen in Figure 1, the plot is regarded as linear with sufficient accuracy for most non-charged or negatively charged acids of which pKa is expressed as a complex function of temperature. ΔH^0 values are thus easily evaluated by the linear least-squares fitting. Theoretical foundation of this method was discussed.

VI-N-5 Hydration of Methyl Cellulose

Shinobu KODA*, Takeo HORI*, Hiroyasu NOMURA* (*Nagoya Univ.), and Fumio KAWAIZUMI

Methyl cellulose(MC) is one of the most familiar samples of cellulose derivatives. It dissolves easily in water at lower temperatures but it becomes progressively less soluble at higher temperatures, showing that the hydration of MC is strongly hydrophobic in nature. To evaluate the hydration number of MC as a function of degree of substitution, that is, the number of $-OCH_3$ group in a cellulose unit, the compressibility method was applied for solutions of MC with different degree of substitution. From the data of sound velocity and density of solution of MC, the partial molar volume and partial molar adiabatic compressibility of methyl cellulose have been evaluated. The partial molar volume of MC increased with the degree of substitution but it was independent of temperature. The amount of hydration of MC was calculated after evaluating the compressibility of the dehydrated MC which was estimated from the temperature dependence of the partial molar adiabatic compressibility. The hydration number of MC decreased with the degree of substitution.

VI—O Analysis of Microscopic Aspects of Fluid Flow

Theoretical treatment was developed for fluid flow related to the complicated geometries with the intention of getting formulae applicable for practical cases.

VI-O-1 Theoretical Analysis of Turbulent Flow and Heat Transfer around a Surface-mounted Obstacles

Tsutomu ARAGAKI*, Shuichi IWATA*, Hideto TANGE*, Setsuro HIRAOKA*, Ikuho YAMADA* (*Nagoya Inst. Tech.), and Fumio KAWAIZUMI

To estimate the distribution of turbulent eddy viscosity in the flow related to the complicated geometries, a simple model was developed based on the mixing-length hypothesis. This model was applied to two cases of turbulent separated flows around a surface-mounted obstacle of circular cross-section. The first one is film flow on the outer wall of a vertical tube, and the second is flow between parallel plates. Calculations were performed by using Galerkin finite element method. In view of heat transfer augmentation, structure of the separating and reattaching flow around a surface-mounted obstacle was investigated in details, together with the corresponding temperature field. It was shown that the reattachment length depends on Reynolds number; isothermal contours are strongly distorted and pushed down toward the wall due to the back flow in recirculating zone; maximum Nusselt number locates on the upstream side of the reattachment point; and the augmentation effect due to the obstacle is remarkable only in a limited range of relatively lower Reynolds number.

VI—P Bioinorganic Studies on Electronic and Molecular Structures of Metal Complexes as a Model for Active Site in Some Metalloproteins

Metal-containing proteins have been found to be widely distributed in both plants and animals and have been related to such metabolic processes as hydroxylation, oxygen transport, electron transfer, oxidative catalysis, and so on. In this project the electornic and molecular structures for several metal complexes are studied as a model of several metallo-proteins or metallo-enzymes by some physico-chemical methods.

VI-P-1 Aromatic Ring Stacking and Its Control in Ternary Copper(II) Complexes with Phenylalanine Derivatives and Aromatic Diamines

Hideki MASUDA, Tamotsu SUGIMORI*, Akira ODANI*, and Osamu YAMAUCHI* (*Nagoya Univ.)

Interactions between aromatic rings play important roles in the processes of biological recognition of molecules and subsequent specific reactions. We have been interested in the ternary metal(II) complexes involving p-substituted phenylalanines as models for aromatic ring stacking and its control in biological system. We now investigated the effects of ring substituents on stabilization of complexes due to stacking interactions in Cu(II)(DA)(AA), where DA = 2,2'-bipyridine (bpy) or 1,10-phenanthroline (phen), and AA = p-substituented phenylalanines, by synthetic, spectroscopic and crystallographic methods.

Six complexes were isolated as single crystals: Cu(bpy)(DL-Iphe)NO$_3$(1)(DL-IPhe = p-iodo-DL-phenylalanine), Cu(bpy)(DL-BrPhe)NO$_3$(2)(DL-BrPhe = p-bromo-DL-phenylalanine), Cu(bpy)(L-NH$_2$Phe)NO$_3$(3)(L-NH$_2$Phe = p-amino-L-phenylalanine), Cu(bpy)(L-Tyr)ClO$_4$(4)(L-Tyr = L-tyrosine), Cu(phen)(L-Tyr)ClO$_4$(5), and Cu(bpy)(L-phe)NO$_3$(6)(L-Phe = L-phenylalanine). The crystal structures of the six complexes have been determined by the X-ray diffraction method.

The geometries around the Cu(II) ions in all complexes are five-coordinate square-pyramidal. The most remarkable structural difference between the former two complexes, 1 and 2, and the latter four complexes, 3, 4, 5, and 6, is the presence of intramolecular stacking in the latter complexes between the phenyl ring and aromatic rings of bpy or phen with the average spacing of about 3.5 Å between the mean planes. The former two complexes do not show such an interaction. This structural difference may be attributed to the charge transfer due to the electron density difference interacting rings or the steric effect of substituent groups which is large for IPhe or BrPhe. The present findings suggest the possibility that stacking interactions in biological systems may be controled by the changes of aromatic ring electron density and steric effects due to introduction of bulky groups.

VI-P-2 Multiple Intermolecular Interactions around Metal Complexes. Adduct Formation between Pt(II) Complexes with Aromatic Rings and Indole Derivatives

Akira ODANI*, Tetsuo SEKIGUCHI*, Osamu YAMAUCHI* (*Nagoya Univ.), Shin-ichi ISHIGURO** (**Tokyo Inst. Tech.), and Hideki MASUDA

Pt(II) complexes involving an aromatic diamine are well-known as intercalators of DNA, but the mode of interactions are not fully understood. For further introduction of multiple functions into them multi-site recognitions seem important. To obtain more information about this possibility we studied adduct formations between Pt(phen)(A) complexes (phen = 1,10-phenanthroline; A = ethylenediamine (en) or L-2,3-diaminopropionate (dap)) and indole derivatives (indoleacetate (I-COO⁻), tryptamine hydrochloride, or tryptophan (Trp)) by calorimetric, spectroscopic, and X-ray methods.

Absorption and CD spectra for systems involving Pt(phen)(A) and indole derivatives showed deviation from additivity based on each component in H_2O. NMR spectra exhibited upfield shifts of ^1H and ^{13}C signals due to aromatic ring currents and indicated adduct formation involving stacking interactions in solution. The crystal structure of Pt(phen)(en)·I-COO⁻·Cl re-

vealed the stacking between the phen and indole rings and the hydrogen bonds between COO⁻(I-COO⁻), and the NH_2(en) and indole NH(I-COO⁻) groups of the adjacent molecule. No direct Pt(II)-indole interactions were observed. The thermodynamic parameters for 1:1 and 1:2 Pt(II) complex-indole adduct formations were obtained by the combination of the calorimetric and absorption spectral methods. All the systems showed large negative enthalpy changes indicating the contribution of stacking involving charge transfer. With respect to the electrostatic interaction involving the indole side chain in solution a more negative enthalpy term for the Pt(phen)(A)-I-COO⁻ system showed the effect of the electrostatic interaction involving the COO⁻(I-COO⁻) and Pt^{2+}. However, the COO⁻ group in Pt(phen)(dap) had almost no influence on parameters probably due to lower basicity. Other charged groups did not exhibit appreciable effects and accordingly the stereoselectivity for D/L-Trp was not observed. These results coincided with ^{195}Pt, ^1H and ^{13}C chemical shifts.

From these observations we concluded that the combination of stacking and electrostatic interactions play an important role in adduct formation but that its specificity may depend on various factors including steric requirements.

VI-P-3 Structural Evidence for the Intramolecular Charge-Transfer Interaction Involving an Indole Ring in Ternary Copper(II) Complexes with L-Tryptophan and Aromatic Diamines

Hideki MASUDA, Tamotsu SUGIMORI*, Akira ODANI*, and Osamu YAMAUCHI* (*Nagoya Univ.)

With a view to understanding the precise binding mode and strength of the stacking interaction in the ternary copper(II) complexes comprising an aromatic diamine such as 2,2'-bipyridine (bpy) and 1,10-phenanthroline (phen) and an aromatic amino acid such as L-phenylalanine, L-tyrosine, and L-tryptophan (L-trp), the crystal structure of [Cu(bpy)(L-trp)]ClO_4 and the circular dichroism (CD) and absorption spectra of

[Cu(bpy)(*L*-trp)]ClO₄ and [Cu(phen)(*L*-trp)]ClO₄ have been investigated. The complex [Cu(bpy)(*L*-trp)]ClO₄ crystallizes in the monoclinic space group, $P2_1$, with two molecules in a unit cell of dimensions a = 13.022(1), b = 7.753(1), c = 10.533(1) Å, and β = 91.18(1)°. The Cu(II) ion is five-coordinate square-pyramidal, with the two nitrogen atoms of bpy and the nitrogen and oxygen atoms of the amino acid coordinated at the equatorial positions in a slightly distorted square-planar form and the carboxylate oxygen atom of the neighboring molecule at the axial position. The most interesting structural feature of the complex is the existence of the intramolecular stacking interaction between the aromatic rings of *L*-trp and bpy with the average spacing of 3.67 Å from the vacant axial position. The CD spectra in the *d-d* region for [Cu(bpy)(*L*-trp)]ClO₄ and [Cu(phen)(*L*-trp)]ClO₄ in aqueous solution showed a large negative peak at 587 and 598 nm, respectively, and the magnitudes were greatly reduced in dioxane-water, which indicates that the aromatic ring stacking interaction is weakened in a hydrophobic environment. The absorption bands due to the charge transfer (CT) interaction between the indole ring and the aromatic diamine have been observed in the difference spectra in the near ultraviolet region. The strength of the stacking interactions has been demonstrated by the CT band intensity and the distance between the stacked rings to be in the order [Cu(phen)(*L*-try)]ClO₄ > [Cu(bpy)(*L*-trp)]ClO₄ both in solution and in the solid state.

VI-P-4 Indole-Metal and Indole-Aromatic Ring Interactions in Palladium(II) and Platinum(II) Complexes

Hideki MASUDA, Masako TAKANI* *(*Kanazawa Univ.)*, **Tetsuo SEKIGUCHI****, and **Osamu YAMAUCHI**** *(**Nagoya Univ.)*

Indole is an electron-rich aromatic ring involved in tryptophan (Trp) and physiologically active natural products such as ergot alkaloids. Recently it has been shown to coordinate to Pd(II) through the nitrogen in the 3H-indole form. We present spectroscopic and X-ray crystallographic evidence showing that 3-indoleacetate (IA) forms a novel dimeric Pd(II) complex with Pd(II)-IA bonds and an adduct with Pt(phen)(en) (phen = 1,10-phenanthroline; en = ethylenediamine) where IA is bound to the Pt(II) complex through aromatic ring stacking and hydrogen bonds. Pd₂(IA)₂(py)₂(1) (py = pyridine) was isolated as orange needles by recrystallization from CHCl₃ of crystals obtained from py and NaPd(IA)Cl in methanol. X-ray crystal structure analysis revealed a unique structure, where IA coordinates to Pd(II) through the nitrogen, carboxylate oxygen and carbon (C(3)) atoms. The indole ring assumes a 3H-indole form with C(3) as an sp³ carbon. The UV absorption spectrum showed a peak at 267 nm but no peaks at 280-290 nm corresponding to the indole ring. On the other hand, an aqueous solution containing Pt(phen)(en)Cl₂ and IA in the ratio of 1:1 gave Pt(phen)(en)(IA)Cl · H₂O (2) as orange-red plates. The molecular structure of 2 showed non-covalent interactions between Pt(phen)(en) and IA; the indole ring and coordinated phen are bound by stacking with the distance of 3.6 Å, and the carboxylate oxygens of IA are hydrogen-bonded to the neighboring NH₂ group of en and the indole NH group. The above two complexes indicate possible modes of interactions in which indole derivatives may be involved in biological and synthetic systems.

VI—Q Reactivity of Fe and Mo Sites fo MoFeS Cluster and Physical Properties of FeS Clusters

Both MoFeS and FeS clusters play key roles in nitrogen cycle and Co_2 assimilation. Elucidation of the reactivity of Fe and Mo sites of MoFeS clusters may bring about fundamental knowledges about those biological redox reactions. In the present project, CO_2 fixation and NO_3^- reduction catalyzed by MoFeS clusters are investigated.

VI-Q-1 Assimilatory and Dissimilatory Reductions of NO_3^- and NO_2^- on Iron and Molybdenum Sites fo MoFeS Clusters

Koji TANAKA, Nobutoshi KOMEDA *(Osaka Univ.)*, and Tatsuji MATSUI

Both NO_3^- and NO_2^- are selectively reduced to NH_3 by $(Bu_4N)_3[Mo_2Fe_6S_8(SPh)_9]$ (1) and $(Bu_4N)_4[MoFe_3S_4(SPh)_3(O_2C_6Cl_4)]_2$ (2) modified with glassy carbon electrodes under controlled potential electrolysis at -1.25 V *vs.* SCE in H_2O (pH 10.0), while NO_2^- is reduced to N_2O by 1 at -1.10 V and N_2 by 2 at -1.00 V. A nitrite ion binds to Fe of 1 with nitrogen (nitro form) and to Mo of 2 with oxygen (nitrito form). A current-potential curve detected on a ring electrode of rotating ring-disk electrodes (RRDE),

clearly evidenced the formation of free NH_2OH and NO intermediates in the reduction of NO_2^- by the 1 and 2 modified glassy carbon disk electrodes, respectively, of the RRDE ($\omega = 1000 \sim 2000$ rpm) under electrolysis at -1.50 V. Such the dissociations of NH_2OH from Fe of 1 and NO from Mo of 2 are reasonably explained by removal of the terminal-oxygen of the nitro moiety on Fe of 1 and the either terminal- or bound-oxygen of the nitrito moiety on Mo of 2 (Scheme 1). NO has been proposed to be a free obligatory intermediate in the reduction of NO_2^- by dissimilatory nitrite reductases. Accordingly, evolution of NO from nitrite reductases may be accounted for the formation of a nitrito adduct with the active center of the enzyme.

Scheme 1
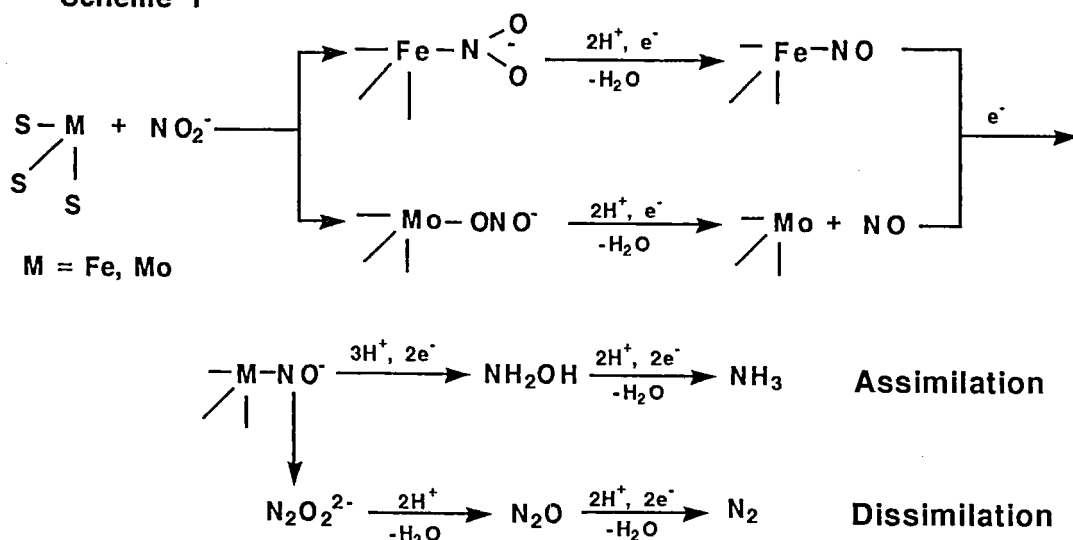
VI-Q-2 Redox Behavior of Fe_4S_4 Cluster in Hydrophilic and Hydrophobic Spheres

Koji TANAKA and Satoshi TANAKA (Osaka Univ.)

The redox behavior of $[Fe_4S_4(SC_6H_4\text{-}t\text{-}Bu)_4]^{2-}$ adsorbed on a surface of a mercury electrode was examined in H_2O in an aqueous micellar solution and in a CH_2Cl_2 layer of the CH_2Cl_2/H_2O two phase system. In the CH_2Cl_2 layer of the CH_2Cl_2/H_2O system, the $E_{1/2}$ value of the (2-/3-) redox couple of the cluster is -0.83 V $vs.$ SCE in the pH region higher than 7.0 of the H_2O phase, while it is shifted by -60 mV/pH in the pH region lower than 7.0 (Figure 1). This can be explained by a reversible protonation of sulfur of the reduced Fe_4S_4 core at pH lower than 7.0 in the H_2O

phase. The break point of the plot of $E_{1/2}$ $vs.$ pH, therefore, corresponds to the proton dissociation constant of the protonated cluster in the CH_2Cl_2, phase. The pK_a of the cluster is shifted to 7.9 and 8.9 in an aqueous Triton X-100 micellar solution and in H_2O respectively. The increase in the pK_a in the order, H_2O saturated CH_2Cl_2 < micellar solution < H_2O, can be associated with the proton concentrations around the Fe_2S_4 core in those media. The $E_{1/2}$ value at pH higher than the pK_a is -0.66 V in both H_2O and the micellar solution, and the value is essentially consistent with the redox potentials of 4Fe-ferredoxins. This observation suggests that hydrophobic spheres around the Fe_4S_4 core largely control the pK_a value of the cluster but hardly affect the redox potential of the Fe_4S_4 cluster.
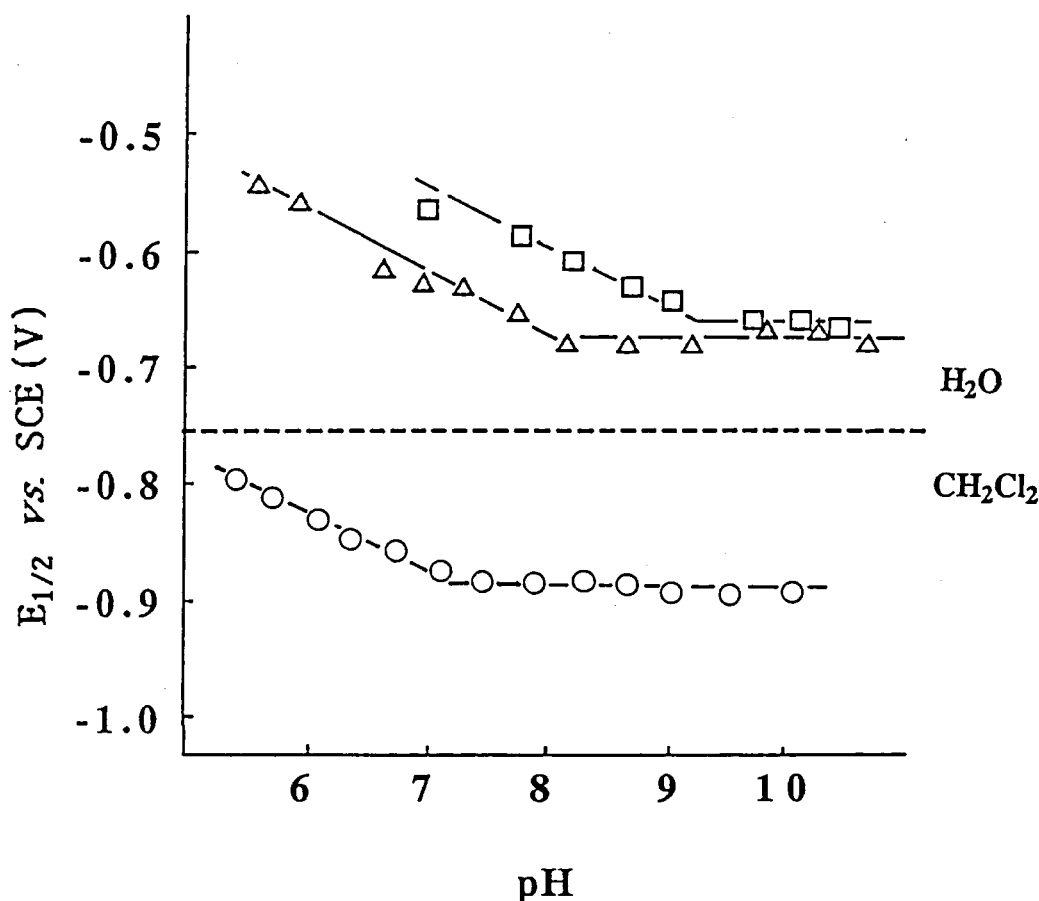
Figure 1. $E_{1/2}$ values of the (2-/3-) redox couple of $[Fe_4S_4(SC_6H_4\text{-}t\text{-}Bu)_4]^{2-}$ adsorbed on an Hg electrode in H_2O (□), in an aqueous micellar solution (△), and in a CH_2Cl_2 phase in the CH_2Cl_2/H_2O two phase system (O) at various pH.

VI-Q-3 1,2-Addition of CO_2 to methyl acrylate

Koji TANAKA, Hirotaka NAGAO, and Hajime MIYAMOTO *(Osaka Univ.)*

The controlled potential electrolysis at $-1.6 \sim -1.7$ V vs. SCE of a CO_2 saturated CH_3CN solution containing $(Bu_4N)_2[Mo_2Fe_6S_8(SEt)_9]$ and methyl acrylate $(CH_2=CHC(O)OCH_3)$ was performed using a glassy carbon electrode as a working electrode. Four reaction products, $CH_3OC(O)CH_2CH_2L$, $CH_3CH[C(O)-OCH_3](L)$, $CH_3OC(O)CH_2CH[C(O)OCH_3](L)$, and CH_3CH_2L ($L = C(O)OCH_3$) were identified with current efficiencies $\eta = 8.2, 12.8, 2.8,$ and 58.3%, respectively, after the reaction mixture was converted to the corresponding esters by treatment of the crude products with either HCl/MeOH or HCl followed by

CH_2N_2 in diethyl ether. Before esterification of the crude products, the formation of $HOOCCH_2CH_2L$ was hardly confirmed in the analysis of the reaction mixture by HPLC. Most of $CH_3OC(O)CH_2CH_2L$ detected after esterification, therefore, is considered to result from the decarboxylation of $HOOCCH_2CH(COOH)(L)$. The CO_2 fixation to methyl acrylate may proceed via an apparent nucleophilic attack of either CO_2 or H^+ activated by the reduced form of the MoFeS cluster to a positively polarized terminal carbon of $CH_2=CHC(O)OCH_3$, followed by an electrophilic attack of free CO_2 or H^+ in the solution to the negatively charged β-carbon of the corresponding $YCH_2\overset{\ominus}{C}HC(O)OCH_3$ ($Y=COO^-$, H). Thus, CO_2 functions as not only electrophile but also nucleophile in the 1,2-addition of CO_2 to olefinic carbons of methyl acrylate.

VI—R Novel Reactivity of Molybdenum and Tungsten Dinitrogen Complexes

Reactivity of coordinated dinitrogen in molybdenum and tungsten complexes of the type $[M(N_2)_2(L)_4]$ (M = Mo, W; L = phosphine) has been investigated.

VI-R-1 Novel Disilylation and Germylation of Coordinated Dinitrogen in cis-$[W(N_2)_2(PMe_2Ph)_4]$

Hiroyuki OSHITA*, Yasushi MIZOBE* (*Tokyo Univ.), and Masanobu HIDAI (Tokyo Univ. and IMS)

[*Chem. Lett.*, 1303 (1990)]

When treated with a mixture of $ClMe_2SiCH_2CH_2SiMe_2Cl$ and excess NaI, cis-$[W(N_2)_2(PMe_2Ph)_4]$ (**1**) afforded mer-$[WI_2(N\overline{NSiMe_2CH_2CH_2Si}Me_2)(PMe_2Ph)_3]$, the structure of which was determined by the X-ray analysis. On the other hand, treatment of (**1**) with Me_3GeCl in the presence of excess NaI gave two germylated dinitrogen complexes trans-$[WI(NNGeMe_3)(PMe_2Ph)_4]$ and mer-$[WI_2(NNHGeMe_3)(PMe_2Ph)_3]$.

VI-R-2 Regioselective Alkylation of Tungsten Diazoalkane Complexes via Alkenyldiazenido Complexes

Youichi ISHII*, Hidekazu MIYAGI* (*Tokyo Univ.), and Masanobu HIDAI (Tokyo Univ. and IMS)

[*Chem. Commun.*, in press]

Tungsten alkenyldiazenido complexes, which are obtained by the deprotonation of diazoalkane complexes trans-$[WF(NN=CRR')(Ph_2PCH_2CH_2PPh_2)_2]$ with lithium di-isopropylamide or $NaN(SiMe_3)_2$, undergo regioselective alkylation to give the C-alkylated diazoalkane complexes.

VI—S Synthesis, Structure, and Properties of Metal Complexes with Suger Type Ligands

Sugar and sugar-type compounds form complexes with metal ions. The metal-sugar complexes play an important biological role in the transport phenomena of vital metal ions across cell membranes. The structure and properties of metal-sugar complexes are investigated by electronic spectra, Mössbauer, and X-ray absorption fine structure methods.

VI-S-1 EXAFS and XANES Studies of Copper(II) Complexes Formed with Adenosine and Uridine

T. YAMAGUCHI*, L. NAGY**, M. NOMURA***, and H. OHTAKI (*Fukuoka Univ. and IMS, ***A. József Univ., ***KEK-PF)

Interactions between adenosine or uridine and copper(II) ion have been studied by Cu K-XANES and -EXAFS measurements at different pH in water-DMSO solutions. From the analysis of the EXAFS spectra it was concluded that the oxygen coordination geometry around copper(II) ion is probably square-planar, irrespective of pH values. The copper(II)-oxygen bond lengths within the copper(II)-complexes are slightly shorter (~ 190 pm) than those of the hexaaqua copper(II) ion (195 pm). EXAFS Fourier transforms have clearly shown a peak ascribed to non-bonded Cu(II)......C interactions, indicating the formation of chelate rings of ribose moiety of nucleosides around copper(II) ion. The most likely structure of copper(II)-nucleoside complexes is proposed.

VI-S-2 The Local Structure of Diorganotin(IV) Complexes Formed with Carbohydrate in the Solid State

L. NAGY[a], B. GRURCSKI[a], K. BURGER[a], S. YAMASHITA[b], T. YAMAGUCHI[c], H. WAKITA[b], and M. NOMURA[d] ([a]A. József Univ., [b]Fukuoka Univ., [c]Fukuoka Univ. and IMS, [d]KEK-PF)

Eight different kinds of diethyltin(IV) complexes with carbohydrate ligands (aldoses, polyalcohols, sugar acids, sugar amines, and disaccharides) were prepared. The analytical data showed that complexes are formed containing the diethyltin moiety and carbohydrate ligand in 1:1 ratio. Their local structure has been determined by the extented X-ray absorption fine structure (EXAFS) technique in solid state. The results showed that the dioxastannolane units are associated into an infinite ribbon polymer, in which the tin is bonded by two carbon atoms and three or four oxygen atoms in a highly distorted octahedral or trigonal bipyramidal arrangement. This observation agreed with Mössbauer results published earlier. Within each unit the average Sn-O,C bond length is 200 pm, while the Sn...C distance (278 pm) in the second shell is acceptable as values of diorganotin(IV) complexes formed with carbohydrate obtained by X-ray diffraction. On the basis of structural data the most likely structure of the complexes was proposed which is recoinciled with the Mössbauer parameters.

VI—T   Neutron Diffraction of Electrolyte Solutions

Neutron diffraction method is one of the powerful means in elucidating ion-solvent and ion-ion interactions of an electrolyte solution, when it is combined with isotopic substitution technique. Since the scattering length of a deuterium atom (in neutron diffraction the deuterium atom is used instead of a hydrogen atom because of large incoherent scattering cross section of the latter) is comparable with those of heavy metals, the neutron diffraction method can uniquely reveal the structure involving hydrogen atom, e.g. the orientational correlation of water molecules in the hydration sphere.

VI-T-1   Pulsed Neutron Diffraction Studies on Lanthanide(III) Hydration in Aqueous Perchlorate Solutions

T. YAMAGUCHI[a], S. TANAKA[b], H. WAKITA[b], M. MISAWA[c], I. OKADA[d], A. K. SOPER[e], and S. W. HOWELLS[e] ([a]Fukuoka Univ. and IMS, [b]Fukuoka Univ., [c]KEK-BSF, [d]Tokyo Inst. Tech., [e]Rutherford Appleton Lab.)

Neutron diffraction measurements were performed at room temperature on aqueous 2 molar perchlorate solutions in D_2O of Pr^{3+}, Nd^{3+}, Tb^{3+}, Dy^{3+}, Tm^{3+}, and Yb^{3+} ions by use of pulsed neutron sources. The first order difference technique with respect to the isomorphous ions was employed to derive the metal ion related pair correlation functions in the systems. The metal-oxygen and metal-deuterium distances and the hydration number are determined for the ions from the correlation functions (Figure 1). The neutron scattering data are consistent with the trend that the hydration number changes from ~ten for the light elements to ~eight for the heavy ones in the series. The dipoles of water molecules coordinated to the ions are orientated on the average by $10 \sim 20$ degrees from the M-O bonds; the values are significantly smaller than those found for uni- and divalent ions. The present results are compared with neutron isotopic substitution, X-ray diffraction, and X-ray absorption data, and discussed on the structure of hydrated lanthanide(III) ions in solution.
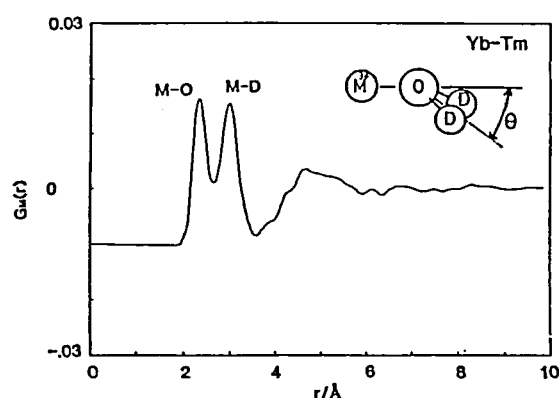
Figure 1. The radial distribution function, $G_M(r)$, for 2.56 molar solutions of Tm(III) and Yb(III) perchlorates in heavy water.

VI—U   Structure and Properties of Electrolyte Solutions in the Undercooled and Glassy States

Glassy solutions formed by quick vitrification of liquid solutions, which have often been used in Mössbauer and ESR spectroscopies, are of considerable interest in the fields of solution chemisty, biochemistry, and coordination chemistry since the motions of ions and solvent molecules and the chemical reactions are suppressed in the glassy state. The electrolyte solutions in the undercooled state is metastable between liquid and crystals, and thus their structural similarities between the three states may be a key to understand crystallization process. We have developed a cryostat of solution samples for X-ray diffraction and X-ray absorption measurements.

VI-U-1 A Cryostat for Liquid X-ray Diffraction

T. YAMAGUCHI*, K. KAMIHATA**, and H. WAKITA** (*Fukuoka Univ. and IMS, **Fukuoka Univ.)

Figure 1 shows a cryostat designed for X-ray diffraction measurements of solution samples. A solution sample is kept in gold-plated cell at ambient pressure in a sample chamber sealed with o-ring and a Mylar window to prevent vaporization of the sample. The sample cell is connected to a copper cold finger, which is attached to a stainless vessel filled with liquid nitrogen. The temperature is measured with a copper-constantan thermocouple and controlled within ±1°C by two ribbon type heaters over the range −140 to −5°C. This temperature range covers the undercooled region of most electrolyte solutions.
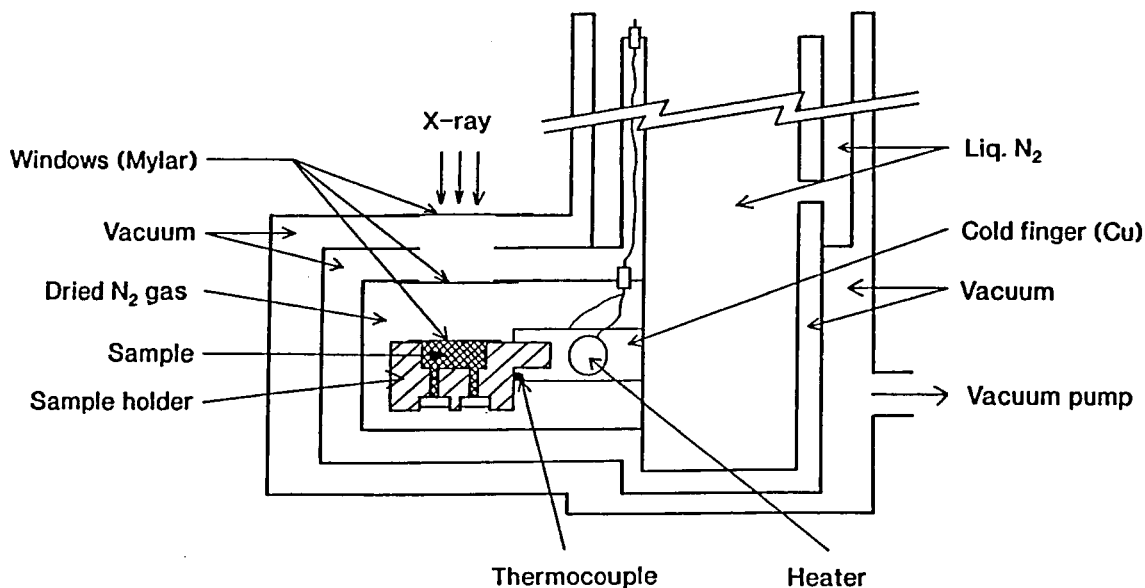
Figure 1. Drawing of Cryostat

VI-U-2 Structure of Zinc(II) Chloride Complexes in Aqueous Liquid and Glassy Solutions

T. YAMAGUCHI, O. YATA*, H. WAKITA*, and M. NOMURA** (Fukuoka Univ. and IMS, *Fukuoka Univ., **KEK-PF)

Sample solutions of compositions of $ZnCl_2 \cdot RH_2O$ ($R=3.5$, 4.5, 10) and $ZnCl_2 \cdot 3LiCl \cdot 20H_2O$, and of crystalline $ZnSO_4 \cdot 7H_2O$ (structure standard) were measured at Zn K-absorption edge using synchrotron radiation at KEK-PF. The octahedral hexaaqua Zn(II) and tetrahedral $[ZnCl_4]^{2-}$ ions are stable in both liquid and glassy states. The $Zn-OH_2$ and $Zn-Cl$ distances are 2.08 and 2.26 Å, respectively, and do not change in vitrification. For the solutions of $ZnCl_2 \cdot RH_2O$ ($R=3.5$, 4.5, 10) the Zn-Cl distance does not change significantly. On the contrary, the distance and coordination number of the $Zn-OH_2$ interactions differ in liquid and glassy states; the coordination number increased from 3.3 to 4.5 and the $Zn-OH_2$ distance increased from 2.04 to 2.08 Å in vitrification. This result indicates that the hexaaqua and tetrachloro Zn(II) complexes coexit in the glassy solutions, while the di- and trichloro complexes predominantly form in the liquid state.

173

VI—V Laboratory EXAFS and Its Applications

A laboratory EXAFS system has proved to be very useful for studying the local structure around a specific atom. We have developed an EXAFS spectrometer equipped with a rotating anode type X-ray generator. The technique has been applied for characterization of several materials.

VI-V-1 EXAFS Measurement with Laboratory Equipment: Problems and their Countermeasures

T. OKAMOTO[a], S. YAMASHITA[b], T. YAMAGUCHI[c], and H. WAKITA[b] ([a]Toyota Central Res. Lab., [b]Fukuoka Univ., [c]Fukuoka Univ. and IMS)

Experimental techniques for eliminating the characteristic X-rays emitted from impurities in cathode and anode materials in the vicinity of the X-ray absorption edge were studied with a laboratory EXAFS spectrometer using a rotating anode. Two methos are proposed for this purpose, a current-control system and a filter method involving the use of a material that selectively absorbs characteristic X-rays. The former method was applied to the Co, Ni and Zn K absorption spectra and the latter to a Pd K absorption spectrum, and the results were compared with those obtained from conventional measurements. The change in the nearest neighbour structure of Pd in a Pd-Al_2O_3 catalyst accompanied by oxidation or reduction was clarified by EXAFS and XANES measurements with the use of the filter method.

VI-V-2 A Structural Study of a Series of Bis(2,3-alkanedione dioximato)-nickel(II) Complexes in the Crystal and the Liquid States by X-ray Absorption Spectroscopy

S. YAMASHITA*, Y. YANASE*, T. YAMAGUCHI**, and H. WAKITA* (*Fukuoka Univ., **Fukuoka Univ. and IMS)

The structures of a series of bis(2,3-alkanedione dioximato)nickel(II) complexes, [Ni(R,R'-dioxH)₂], with dioxH=C(=NOH)—C(=NO), R and R'=H(A, R=CH₃ and R'=H(B), CH₃(C), C₂H₅(D), n-C₃H₇(E), n-C₄H₉(F), n-C₅H₁₁(G), n-C₆H₁₃(H), or n-C₁₀H₂₁(I), were investigated in crystals, pyridine solution, and melt (160°C) by means of extended X-ray absorption fine structure (EXAFS) and X-ray absorption near edge structure (XANES), magnetic susceptibility, and UV/visible spectra. The magnetic susceptibility of complexes C, F, and H in crystals revealed a diamagnetic character. The electronic spectra of crystalline samples E, F, and H changed with the alkyl substituents of the glyoximato ligands, while the corresponding spectra in a pyridine solution were very similar to each other, independent of the glyoximato ligands. The EXAFS data showed that the average Ni-N distance within nickel(II) glyoximato complexes is 1.85-1.88 Å, practically independent of alkyl substituents of the glyoximato ligands. The XANES spectra were found to correlate with the molecular packing structures of nickel(II) glyoximato complexes in crystals, pyridine solutions, and melt.

Table 1. Composition of [Ni(R,R'-dioxH)₂]

	Complex	R	R'
A	[Ni(gH)₂]	H	H
B	[Ni(mgH)₂]	CH₃	H
C	[Ni(dmgH)₂]	CH₃	CH₃
D	[Ni(emgH)₂]	CH₃	C₂H₅
E	[Ni(mprgH)₂]	CH₃	n-C₃H₇
F	[Ni(bmgH)₂]	CH₃	n-C₄H₉
G	[Ni(mpegH)₂]	CH₃	n-C₅H₁₁
H	[Ni(hxmgH)₂]	CH₃	n-C₆H₁₃
I	[Ni(decmgH)₂]	CH₃	n-C₁₀H₂₁

VI—W Steric Control of Axial Coordinations in Transition Metal Complexes of syn-Crown Thioethres

The axial sites of transition metal complexes of quadridentate crown thioethers adopting syn conformation are in stereochemically different environments; the site surrounded by the ring carbon atoms is congested while the opposite site is uncongested. Accordingly, the ligands possessing different steric demands may be discriminated at the axial sites if we choose suitable ring size.

VI-W-1 Ring Size Effect of Crown Thioethers upon Recognition of Hydrido and Chloro Ligands at Stereochemically Different Axial Sites in trans-RuH(Cl)L (L=syn-Me$_4$[14]aneS$_4$, syn-Me$_8$[16]aneS$_4$)

Toshikatsu YOSHIDA *(Univ. Osaka Pref. and IMS)*, Tomohiro ADACHI*, Tatsuo UEDA*, and Toshihiro TANAKA* *(*Univ. Osaka Pref.)*

Hydrido and chloro ligands in trans-RuH(Cl)(syn-Me$_4$[14]aneS$_4$)(1) coordinates selectively at the stereochemically congested and uncongested axial sites, respectively, while the corresponding 16-membered analogue trans-RuH(Cl)(syn-Me$_8$[16]aneS$_4$) exists as a mixture of two geometrical isomers 2a and 2b.
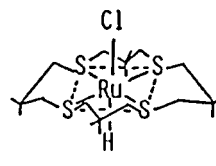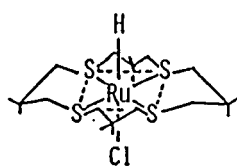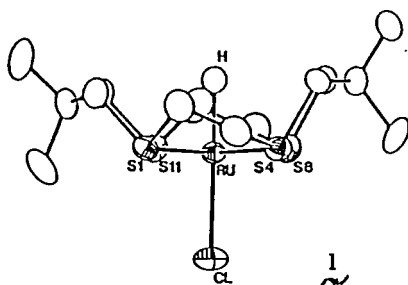
VI-W-2 trans-Mo(η^2-O,C-PhNCO)(η^2-C,N-PhNCO)(syn-Me$_8$[16]aneS$_4$): Steric Control on C=O and C=N Discrimination of PhNCO by Crown Thioether Complex in syn-Conformation

Toshikatsu YOSHIDA *(Univ. Osaka Pref. and IMS)*, Tomohiro ADACHI*, Kenzi KAWAZU*, Akira YAMAMOTO, and Tatsuo UEDA* *(*Univ. Osaka Pref.)*

Treatment of trans-Mo(N$_2$)$_2$(syn-Me$_8$[16]aneS$_4$) with PhNCO gave trans-Mo(η^2-O,C-PhNCO)(η^2-C,N-PhNCO)(syn-Me$_8$[16]aneS$_4$)(1). The crystal structure shows that the η^2-O,C-PhNCO ligand, the coordination mode of which is sterically less demanding than η^2-C,N-PhNCO, occupies specifically at the congested axial sites. The η^2-C=O and -N=C bonds are mutually staggered and each eclipses a trans-S-Mo-S vector. Extended Hückel MO calculations on the model trans-Mo(η^2-O,C-HNCO)-(η^2-C,N-HNCO)(syn-SH$_2$)$_4$ and one of its isomers trans-Mo(η^2-C,N-HNCO)$_2$(syn-SH$_2$)$_4$ indicate that the latter is stable by 3.6 kcal/mol in energy compared to the former. By contrast, the strain energy of 1 assessed from molecular mechanics calculations is 12.3 kcal/mol less than that estimated for trans-Mo(η^2-C,N-PhNCO)$_2$(syn-Me$_8$[16]-aneS$_4$). Thus, the discrimination of two functional groups of PhNCO at the axial sites of 1 can be rationalized in terms of steric control rather than electronic one.
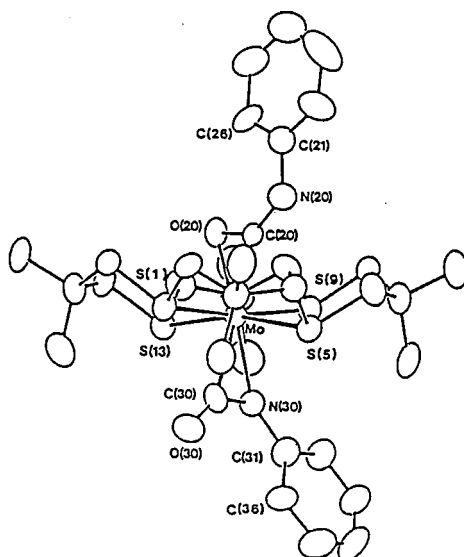
VI—X Nucleic Acid Structure and DNA - Ligand Interactions at the Molecular Level

DNA recognition by ligands plays a key role in various biological processes, whether the ligands are large proteins or small molecules. Many of the DNA - ligand interactions are DNA base-sequence specific. We have been designing and synthesizing novel compounds which can interact with DNA in specific manner, in order to understand the mechanism of the DNA - ligand interactions. The compounds we have been looking at include intercalators which insert themselves between the DNA base-pairs, DNA groove binders and the compounds which cleave DNA strands either by oxidation or uv/vis irradiation. For the analyses, we have been employing various methodology, including X-ray crystallography, spectroscopy, enzymology and computer graphics.

VI-X-1 DNA Binding and Interaction by Novel Porphyrins: Role of Charge and Substituents Probed by DNase I Footprinting and Topoisomerase I Unwiding

Reiko KURODA *(Tokyo Univ. and IMS)*, Eitaro TAKAHASHI *(Tokyo Univ.)*, Caroline A. AUSTIN *(Univ. London)*, and L. Mark FISHER *(Univ. London)*

Porphyrins carrying four charged sidechains, *e.g.*, mesotetrakis[4-*N*-methylpyridiniumyl]- and meso-tetrakis[4-*N*-(2-hydroxyethyl)pyridiniumyl]porphyrin, bound and intercalated similarly into DNA as measured by helix stabilization and DNA unwinding studies in the presence of DNA topoisomerase I. Despite their different bulky sidechains, these complexes gave essentially identical DNase I footprinting patterns (Figure 1). In contrast, tetrasubstituted porphyrins carrying three phenyl rings and a single positively charged pyrimidiumyl sidechain did not intercalate and exhibited little affinity for DNA. Thus, the presence of charged sidechains on the porphyrin rather than their indentity appears to be crucial for efficient DNA intercalation. The results are discussed in regard to current models for the porphyrin-DNA intercalation complex.

B

```
AGCTTTAATGCGGTAGTTTATCACAGTTAAATTGCTAACGCAG
      40.                    60.              ▼   ▼▼
    *ⓐAATTACGCCATCAAATAGTGTCAATTTAACGATTGCGTC
                  ↑↑           ↑↑         ↑↑↑

TCAGGCACCGTGTATGAAATCTAACAAT GCGCTCATCGTCAT
▼▼▼80.                   90.           ▼           ▼
AGTCCGTGGCACATACTTTAGATTGTTA CGCGAGTAGCAGTA
    ↑ ↑ ↑  ↑    ↑↑↑ ↑↑  ↑↑ ↑

CCTCGGCACCGTCACCCTGGATGCTGTAGGCATAGGCTTGGT
   120·            ▼      ▼    14 9·          ▼
GGAGCCGTGGCAGTGGGACCTACGACATCCGTATCCGAACCA
                            ↑  ↑

TATGCCGGTACTGCCG
160·
ATACGGCCATGACGGCCCG
```

Figure 1. A) Site-specific binding of +4 positively charged porphyrins to DNA revealed by DNase I footprinting. B) Summary of footprinting data for the labelled DNA strand.

VI-X-2 Photocleavage of DNA by the *p*-Nitrobenzoyl Group: Selective Attack in the Major or the Minor Groove of DNA

Reiko KURODA *(Tokyo. Univ. and IMS)* **and Miho H. SHINOMIYA** *(Tokyo Univ.)*

We have designed and synthesized a series of new DNA photo-cleaving compounds which control the site of attack on DNA (Figure 1). **1a,b** are expected to place their sidechain and hence the photocleaver in the major groove of DNA, whereas **2a,b** in the minor groove. Compound **3b** is thought not to intercalate the acridine moiety between the base-pairs of DNA. The compounds were characterized by elemental analysis, ^{1}H-NMR and UV-visible absorption spectroscopy. Intercalation of the acridine moiety between the base-pairs of DNA was checked by absorption spectroscopy, DNA unwinding study using topoisomerase I and viscometry. Binding constants were much the same for **1a**, **1b**, **2a**, and **2b**.

The photocleavage efficiency was determined by the degree of nicking of supercoiled pBR322 DNA. Compounds **1a,b**, and **2a,b** induced DNA scission on UV irradiation, while **3b** did not show the activity. When the acridine moiety and the sidechain were not covalently linked but present separately in the reaction mixture, no photocleavage was observed. Thus, DNA cleavage by the *p*-nitro benzoyl group occurs only when this moiety is positioned close to DNA. Different photocleavage activity was observed depending on the site of attack on DNA as well as the group linking the *p*-nitrobenzoyl group to the polymethylene chain (Figure 2).

Sequence specificity of the photocleavage was analysed by polyacrylamide gel electrophoresis using ^{32}P-labeld DNA fragment. The data clearly showed different cleavage sites for **1b** and **2b**.
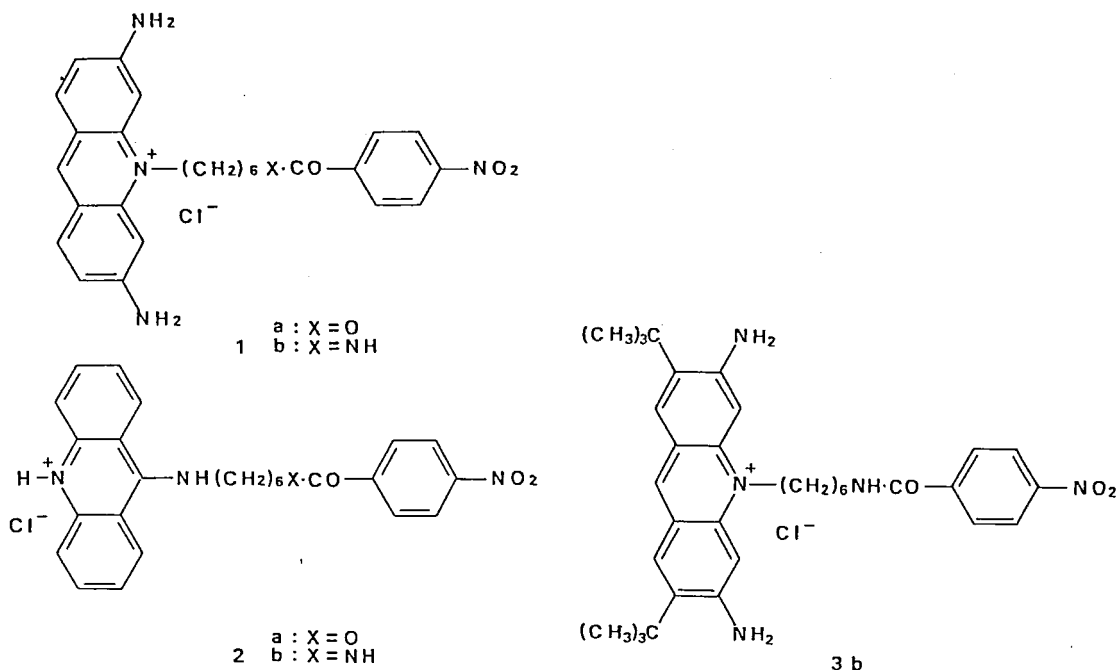
Figure 1. Molecular structure of designed photocleaving agents.
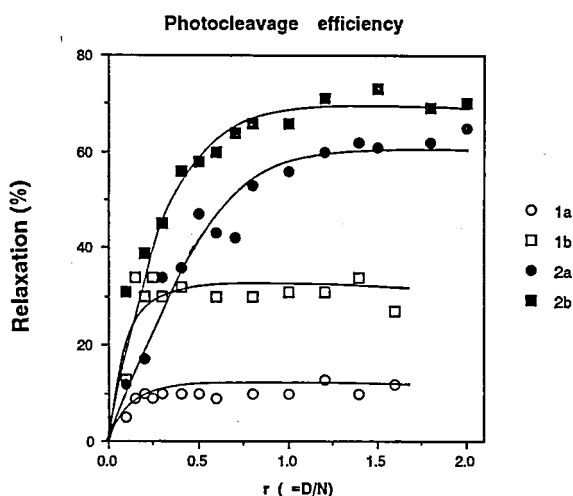
Figure 2. Comparison of photocleavage efficiency at various r values (r= [drug] / [DNA in bp]).

VI-X-3 Crystal Strucure of a DNA Binding Compound: (9-[[6-(4-nitrobenzoyloxy)hexyl]-amino]acridine hydrochloride monohydrate

Reiko KURODA *(Tokyo Univ. and IMS)*, and Miho H. SHINOMIYA *(Tokyo Univ.)*

We have been studying synthetic compounds which cleave DNA on UV irradiation. To study the mode and mechanism of interaction between the compounds and DNA, we have determined the crystal structure of one of the photocleavers.

Crystals were obtained from 1:1 chloroform/ethanol solution. It was difficult to obtain a large crystal suitable for X-ray diffraction study, hence a rotating anode Cu source was employed. Crystal data: $C_{26}H_{28}N_3O_5Cl$, F.W. = 497.98, triclinic, a = 9.4810(8), b = 14.495(2), c = 9.225(1) Å, α = 95.48(1), β = 98.17(1), γ = 101.781(1)°, U = 1222.3(5) Å^3, space group $P\bar{1}$ (No. 2), Z = 2, μ = 17.34 cm^{-1}. Intensity data were collected on an Enraf-Nonius CAD-4, using Cu $K\alpha$ radiation (λ = 1.5418 Å). 2θ-ω scan mode was employed, up to 2θ = 139.7°. The structure was solved by a direct method and refined by full matrix least-squares procedures, assuming anisotropic temperature factor for the non-hydrogen atoms. Final R factor was 0.052 for 3589 reflections observed with $I > 3\sigma(I)$. The hexamethylene chain bents at a paticular bond (C_{15}-C_{16}-C_{17}-C_{18} = −66.8°). Both p-nitrobenzoyl group and acridine moiety are almost planar and almost perpendicular to each other (98.7°) (Figure 1).

178
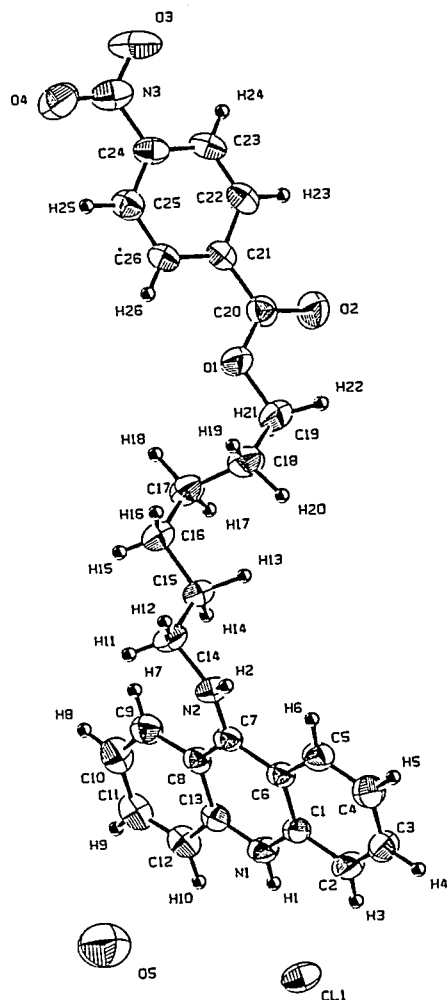
Figure 1. *ORTEP* drawing of the molecular structure of 9-[[6-(4-nitrobenzoyloxy)hexyl]amino]acridine hydrochloride monohydrate.

VI-X-4 Chiral Discriminations of Complexes with D_3 Symmetry. Molecular Structure and Crystal Packing Mode of (−)$_{589}$-tris[(−)-cyclic-O,O'-1(R),2(R)dimethylethylenedithiophosphato]-chromium(III), {Cr[(−)bdtp]$_3$}

Reiko KURODA *(Tokyo Univ. and IMS)* and **Paolo BISCARINI** *(Universita Bologna)*

The molecular structure and crystal packing mode of the title complex have been determined from single-crystal X-ray diffraction data and refined by full-matrix least-squared methods to R 0.0435. The optically active crystal has unit-cell dimensions $a = 11.699(1)$, $b = 12.738(2)$, $c = 16.827(2)$ Å, $U = 2507.6(6)$ Å^3, space

group $P2_12_12_1$, and $Z = 4$. The ligand has two ring planes: an inner four-membered chelate ring and an outer five-membered ring. The complex exhibits approximate D_3 symmetry and the three inner rings and the three outer rings each form a propeller of opposite handedness. The crystal packing mode and the chiral recognitions have been compared with those of D_3 tris(chelate) metal complexes involving a single propeller system (Figure 1).
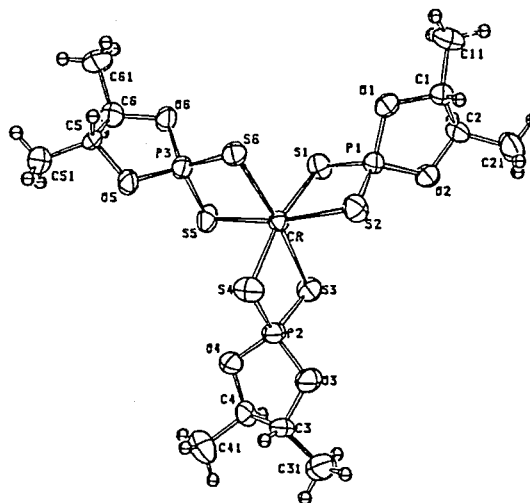
Figure 1. *ORTEP* drawing of the molecular structure of Λ-{Cr[(−)$_{589}$bdtp]$_3$}.

VI-X-5 Gold(I) Complexes of 1-Diphenylphosphino-2-diphenyl-arsinoethane-(appe):Solution Studies, X-ray Crystal Structures and Cytotoxicity of [(AuCl)$_2$(appe)] · 0.5DMA and [Au(appe)$_2$]Cl · 2H$_2$O

Orla M. NI DHUBHGHAILL *(Birkbeck College)*, **Peter J. SADLER** *(Birkbeck College)*, and **Reiko KURODA** *(Tokyo Univ. and IMS)*

The Au(I) phosphinoarsines, [(AuCl)$_2$(appe)] (**1**) and [Au(appe)$_2$]Cl (**2**) where appe is Ph$_2$PCH$_2$CH$_2$AsPh$_2$ have been prepared and characterized by n.m.r. spectroscopy (^{31}P{^{1}H}, ^{1}H, and ^{13}C{^{1}H}), and by X-ray crystallography. ^{31}P{^{1}H} n.m.r. spectroscopy shows that complex (**1**) is converted to complex (**2**) on titration with appe in CDCl$_3$ at a Au:appe ratio of 1:2. At higher Au:appe ratios there is exchange between complex (**2**) and the excess ligand.

179

Such rapid ligand exchange is also indicated by the ^{1}H n.m.r. data. Crystals of (**1**) are monoclinic, space group *Cc* with $a = 19.385(3)$, $b = 11.011(2)$, $c = 27.260(1)$Å, $\beta = 96.40(1)°$, and $Z = 8$. The ligand coordinates two Au-Cl units with a Au-Au contact of 3.21Å. The P and As atoms are disordered and there appears to be conformational flexibility about the ethane bridge (Figure 1-a). Crystals of (**2**) are monoclinic, space group $P2_1/n$, $a = 10.192(1)$, $b = 21,797(7)$, $c = 21.683(10)$Å, $\beta = 94.14(3)°$, and $Z = 4$ and contain bis chelated Au(I) in a distorted tetrahedral environment; again the P and As atoms are disordered (Figure 1-b). Complexes (**1**) and (**2**) are significantly more toxic towards L1210, WS, and V.79 cells in vitro than the free ligand, appe, and are comparable to [Au(dppe)$_2$]Cl in their toxicity towards WS and V.79 cell-lines.

a

b
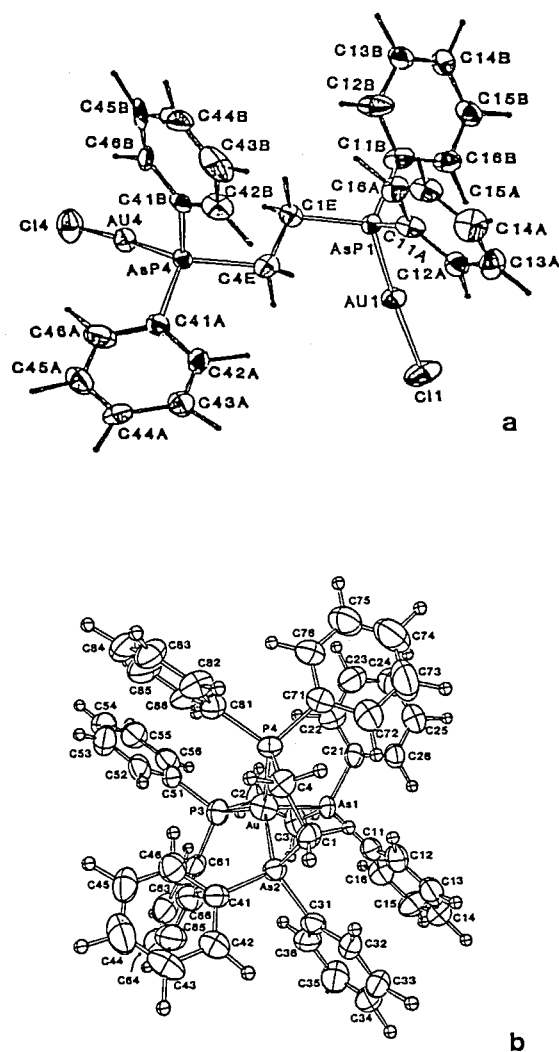
Figure 1. Molecular Structures of a) **1** and b) **2**.

RESERACH ACTIVITIES VII
Computer Center

VII—A Theoretical Investigations of Structures and Properties of Molecular Assemblies

Structures and properties of molecular clusters, liquids, solutions and solids are studied using the molecular dynamics and the Monte Calro technique. A new intermolecular potential function for the molecular simulations is developed based on the *ab initio* molecular orbital theory.

VII-A-1 Monte Carlo Simulation of Liquid Water and an Evaluation of the Thermodynamic Properties

Kazuhiko HONDA, Kazuo KITAURA and Kichisuke NISHIMOTO *(Osaka City Univ.)*

Monte Carlo simulations were performed on liquid water using a new intermolecular potential function which is expressed in terms of intermolecular overlap integrals over localized orbitals of constituent molecules and electrostatic potentials between fractional point charges on the atoms. The potential function can reproduct *ab initio* interaction energies accurately.

For the evaluation of the thermodynamic properties of liquid water, we propose a simple expression of partition function which involves some parameters to be evaluated using the results of MC simulation. Various thermodynamic properties including heat capacities and compressibility were obtained from the partition function. Our simple partition function reproduces the thermodynamic properties of liquid water satisfactorily. In the present study, it was shown the contribution from the hydrogen bond term is significant for C_v and also for other anomalous thermodynamic properties of liquid water.

VII-A-2 An Improvement for a Large Scale Random Sparse Symmetric Matrix Diagonalization Based on Jennings' Method: AV=EV

Umpei NAGASHIMA

For a large scale random sparse symmetric matrix diagonalization: AV=EV, where the size of matrix is about $10^{10} \sim 10^8$, a new program has been developed by using Jennings' method to remove computational limitations: CPU time and main memory requirements.

Since Jennings' method is one of power methods, the most time consuming step is the part of matrix multiplication to trial eigenvectors. In the general procedures of a large scale symmetric matrix diagonalization, matrix elements are kept on disk units as a dataset and trial eigenvectors are kept on main memory as an array. The size of available main memory gives an upperlimit of matrix size because two arrays at the very least should be kept to evaluate only one eigenvalue and only one eigenvector. For example, 8 M byte is required for an array where vector size is 10^6.

In order to remove the limitation, vectors are divided some blocks and these blocks of vectors are kept on desk. Block size are determined to be able to keep four blocks of vectors on the available main memory. A large matrix A is also divided to some samll blocks corresponding to the partition of the trial eigenvector. Only non zero elements of matrix A are also kept on disk space. The matrix A is read from disk only once in each iteration.

In the examination of actual performance. 10^2 eigenvalues and eigenvectors of 10^7 orderd random sparse matrix are evaluated on a vector type supercomputer: HITAC S-820/80 where maximum speed is 2 G Flops. The nonzero rate of the matrix is about 10^{-6}. CPU times of the 64 M byte and 32 M byte main memory size are 4228 and 5703 seconds on scalar computer, and 110 and 164 seconds on vector computer, respectively. Acceleration ratio between scalar

and vector computer is about 38 and 34.7. Vectorization ratio is about 94%. this program is quite efficient on the vector computer.

According to the partition, this algorithm is easily applicable to parallel computing and can automatically avoid the introduction of the numerical error.

Chemical Materials Center

VII—B Preparation and Properties of Novel Heterocyclic Compounds

Heterocyclic compounds are useful as components of functional materials such as organic conductors because heteroatoms in their rings are helpful to stabilize ions or ion-radical species, and intermolecular interactions caused by heteroatom contacts may form unique molecular assemblies. In this project novel electron acceptors and donors containing heterocycles were synthesized and their properties including those of the charge-transfer complexes or ion-radical salts were investigated.

VII-B-1 N-Methyl Derivatives of [1,2,5]Thiadiazolo[3,4-b]quinoxaline and the Selenium Analogues

Yoshiro YAMASHITA, Kenichi SAITO*, Toshio MUKAI*, and Tsutomu MIYASHI* (*Tohoku Univ.)

A benzene ring of 5,10-dimethyl-5,10-dihydrophenazine (DMPH), which is a strong electron donor due to the 16 π-electron system, was replaced by 1,2,5-thiadiazole or selenadiazole to give a new type of electron donors 1a,b. The similar replacement of a benzene ring of N-methylphenazinium (NMP), which is a cation to form an organic metal with TCNQ, gave heterocyclic cations 2a,b. The first oxidation potentials of 1a,b are almost the same with that of dibenzotetrathiafulvalene although they have electron withdrawing heterocycles. The cation radicals of the donors 1a,b are stable and that of 1b was isolated as a 1:1 perchlorate salt. The cations 2a,b have extremely high electron affinities. The radical formed by reduction of 2a was detected by ESR.
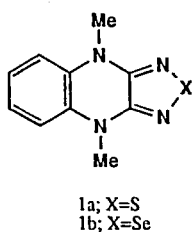
VII-B-2 Benzo[g][1,2,5]thiadiazolo[3,4-b]quinoxaline-5,10-dione and Its Selenium Analogue. An Unusual Type of Quinones

Yoshiro YAMASHITA, Yoshiaki TSUBATA*, Takanori SUZUKI*, Tsutomu MIYASHI*, Toshio MUKAI*, and Shoji TANAKA (*Tohoku Univ.)

The title compounds 1a,b were prepared from 2,3-diamino-1,4-naphthoquinones in good yields. The reduction potentials of 1a,b are considerably higher than those of the related naphthoquinones. Their semiquinone formation constants are significantly larger than those of the naphthoquinones. These facts indicate that upon reduction of 1a,b electrons are first accepted at the heterocyclic part. This is supported by ab initio calculations using STO-3G basis set.

1a; X=S
1b; X=Se

1a; X=S
1b; X=Se

2a; X=S
2b; X=Se
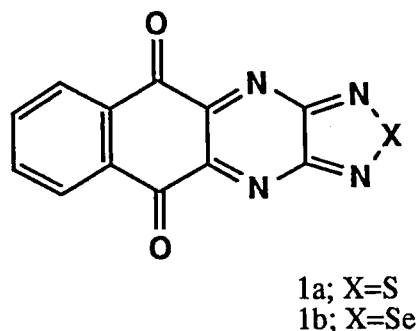
VII-B-3 4,7-Dimethyl-4,7-dihydro[1,2,5]thiadiazolo[3,4-b]pyrazine. A Novel Electron Donor with a 12 π-Electron Ring System

Yoshiro YAMASHITA, Junko EGUCHI*, Takanori SUZUKI*, Chizuko KABUTO*, Tsutomu MIYASHI*, and Shoji TANAKA (*Tohoku Univ.)

The title compound 1 was prepared by reduction of the corresponding thiadiazolopyrazine with potassium followed by methylation with methyl iodide. The first oxidation potential is very low (E_{ox}=+0.15 V vs. SCE) due to the 12 π-electron ring system. The donor 1 gave no complex with TCNQ, but gave conducting complexes with acceptors such as 2 containing a 1,2,5-thia-diazole ring. The X-ray structural analysis reveals that 1 is a completely planar molecule and forms a sheet-like network by S • • • N contacts and hydrogen bondings.

1   2
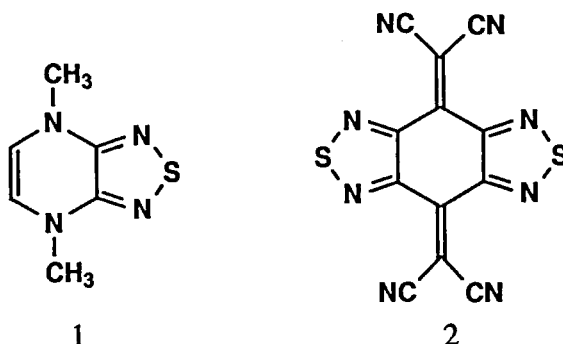
VII-B-4 Preparation and Properties of p-Quinodimethane Analogues of Tetrathiafulvalene Containing Alkylthio Groups

Yoshiro YAMASHITA, Shoji TANAKA, and Masaaki TOMURA

A Tetrathiafulvalene (TTF) analogue (QBT) containing a quinodimethane structure is of interest because it is a extremely strong elecron donor and has extended π-conjugation to decrease on-site Coulomb repulsion.[1] Alkylthio substituents of TTF play an important role in increasing intermolecular interactions as found in bis(ethylenedithio)TTF (BEDT-TTF). We have now introduced alkylthio groups to the skeleton of QBT to afford 1a-c.

The donors 1 were synthesized by a retro Diels-Alder reaction of cyclopentadiene adducts 2 which were prepared by using the Wittig-Horner reaction of phosphorous compounds 3. The oxidation potentials of the donors were lower than those of the corresponding TTF. However, they were unstable and rapidly changed to polymeric materials even in solid state at room temperature. In order to enhance the stability of 1, the benzo derivatives 4a,c were prepared by the analogous methods. They were stable in solid state under air, and 4a formed a highly conducting complex with TCNQ.

Reference
1) Y. Yamashita, Y. Kobayashi, and T. Miyashi, Angew. Chem. Int. Ed. Engl., 28, 1052 (1989).

QBT: R=H
1a: R=SCH₃
1b: R=S(CH₂)₉CH₃
1c: R,R=SCH₂CH₂S

2

3

4a: R=SCH₃
4c: R,R=SCH₂CH₂S
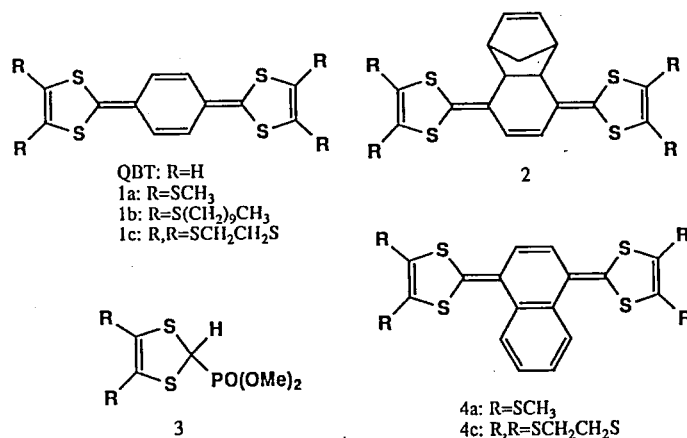
VII-B-5　Synthesis and Physical Properties of Thieno[3,4-c][1,2,5]thiadiazole

Shoji TANAKA, Masaaki TOMURA, and Yoshiro YAMASHITA

We have synthesized 'non-classical' thieno[3,4-c][1,2,5]thiadiazole **1** and elucidated the electronic characters by means of UV, NMR spectroscopies and cyclic voltammetry combined with MO calculations. This heterocyclic molecule is a logical candidate for novel conducting polymer **2** which would have a narrow band-gap due to the quinoid character of the thiophene ring and the S· · ·N interactions between the polymer chains. Reaction of 3,4-diaminothiophene with N-thionylaniline, followed by dehydration with chlorotrimethylsilane, gave the parent compound **1** which is stable in solution for a day. This compound was isolated by sublimation at $-20°C(10^{-6}$ mmHg), but the initially formed yellow sublimate rapidly decom-

posed to colorless insoluble material at room temperature. The MO calculations (MNDO and RHF/STO-3G) predict that the thienothiadiazole should have a small HOMO-LUMO energy gap compared to thiophene and isothianaphtene. The comparison of the UV spectra and redox potentials of these compounds confirms this prediction.
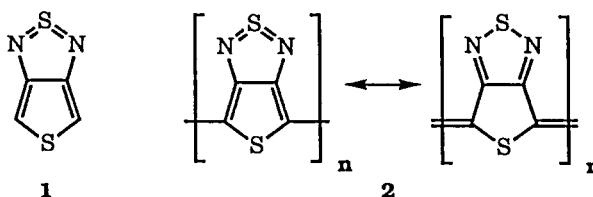
Instrument Center

VII—C　Studies of Solvated Metal Clusters

Solvated metal ions and metal cluster ions afford a particularly interesting collection of systems for study because they bridge the gap between bare, isolated ions and ionic solids and electrolyte solutions. From the point of view of cluster chemistry, the question of charge delocalization, the formation of solvation shells, and the interaction of solvent with metal surfaces appear especially attractive.

In order to investigate the spectroscopy and photodynamics of solvated metal cluster ions, we have constructed a molecular beam apparatus with adopting a laser vaporization technique.

VII-C-1　Construction of a System of Metal Cluster Beam Source and Reflectron Time-of-Flight Mass Spectrometer for the Studies of Solvated Metal Clusters

Fuminori MISAIZU, Keizo TSUKAMOTO *(Keio Univ.)* and Kiyokazu FUKE

We have constructed a high vacuum apparatus for the purpose of investigating the geometrical and electronic structure and the reaction dynamics of solvated metal clusters by spectroscopic methods. The system is composed of a three-stage differentially evacuated chamber involving a metal cluster beam source by laser

vaporization and a reflectron-type time-of-flight (TOF) mass spectrometer (see Figure 1). Metal vapor produced by irradiation of second harmonic of Nd:YAG laser to the metal rod is co-expanded with ca. 6 atm of He gas mixed with solvent vapor through a 2 mm diameter nozzle. Resultant solvated metal clusters are ionized by irradiation of an ArF excimer laser in the acceleration region of the TOF mass spectrometer. Accelerated ions fly through the reflectron TOF mass spectrometer and are detected by dual microchannel plates.

Some preliminary results are obtained for aluminum and aluminum-D_2O binary clusters. Aluminum cluster

ions, Al_n^+, are observed up to the size of $n \sim 60$. A mass resolution $(m/\Delta m)$ of about 1000 was achieved in the normal measurement. Dissociative binary cluster ions, Al_nD^+, Al_nOD^+, and $Al_nD_3O^+$ are detected in addition to the nondissociative ion, $Al_nD_2O^+$.
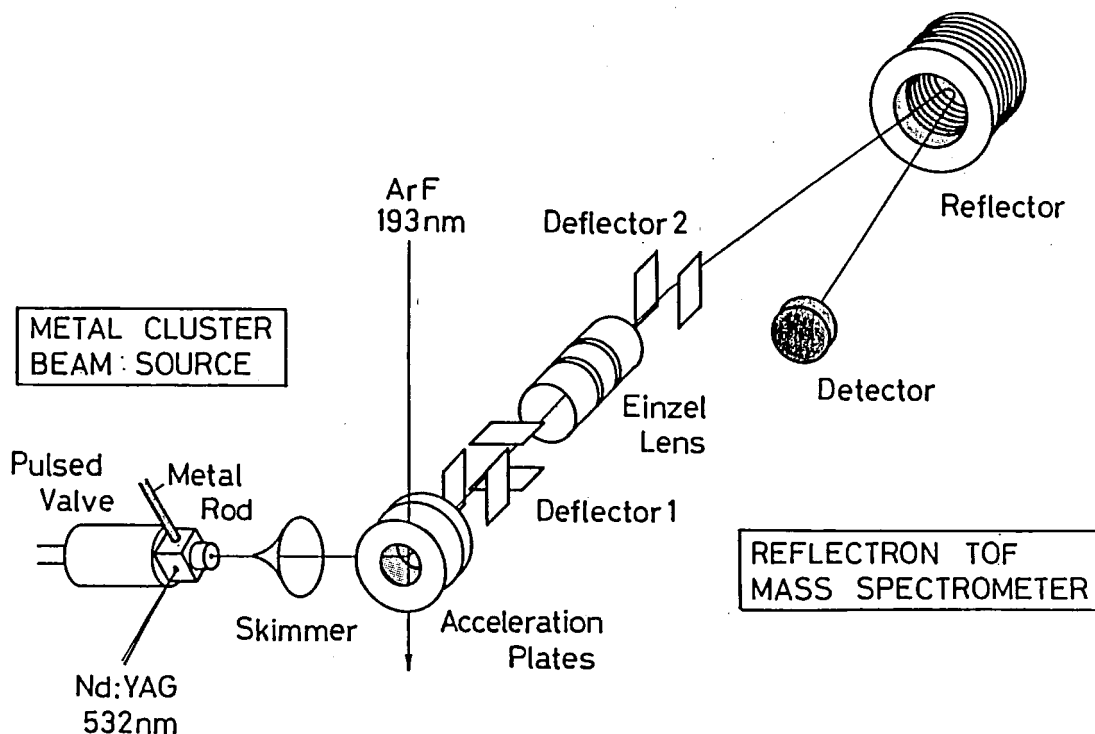
Figure 1. Schematic diagram of the apparatus.

VII—D   Dynamics of Proton-Transfer Reaction in a Model Hydrogen-Bonded Base Pair

Proton-transfer reaction (PTR) has known to play a predominant role in many chemical and biological systems. With the advent of a picosecond laser spectroscopy, a wealth of kinetic data in solution has been accumulated and produced a good qualitative description of the PTR process in the form of reaction mechanism. However, a dynamical aspect of PTR still remains to be unveiled, especially, the role of cooperative motion of proton and a frame of heavy nuclei. To manifest the dynamics of PTR, we have been studying the PTR of model hydrogen-bonded base pairs such as 7-azaindole and 1-azacarbazole (1-AC) dimers and their heterodimer in supersonic jet by using a laser induced fluorescence method. In this issue we report on the picosecond real-time study of the PTR of jet-cooled 1-AC dimer.

VII-D-1   Real-Time Probing of Proton-Transfer Reaction of Jet-Cooled 1-Azacarbazole Dimer: Vibrational Level Dependence

Kiyokazu FUKE, Fuminori MISAIZU, Keizo TSUKAMOTO*, and Koji KAYA* (*Keio Univ.)

In the previous report it has been shown that 1-AC dimer exists as the two conformational isomers in a jet and only the isomer having a near coplanar structure selectively undergoes the proton-transfer reaction (PTR) even from the zero vibrational level of the S_1

185

state. The symmetric stretching vibration (109 cm^{-1}) in the hydrogen bond has found to promote the PTR rate dramatically from the analysis of LIF spectra monitoring the primary (370 nm) and tautomeric fluorescence (500 nm).[1] In order to obtain more quantitative information on the vibrational level dependence of the PTR of jet-cooled 1-AC dimer, picosecond fluorescence measurements were performed using a time correlated single-photon counting technique.

Figure 1 shows the decays and fits of total emission induced by the excitations of the 0_0 (a) and +109 cm^{-1} (b) vibrational bands of the reactive isomer. The slow decay components, τ=2.2 ns in both excitations, were attributed to the decay of tautomer fluorescence. The fast decay components were assigned to the primary fluorescence from the excited-state dimer; the lifetimes of the 0_0 and 109 cm^{-1} vibrational levels were 330 and 130 ps, respectively. Moreover, the lifetime of the 2×109 cm^{-1} level was found to be less than 65 ps. Since the PTR has found to be the dominant process in the decay of the S_1 state of the reactive isomer, the decrease in lifetime with increasing the quantum number of the 109 cm^{-1} vibration confirms the previous assertion that this vibration is the promoting mode of PTR. Detailed lifetime measurements for the other vibrational modes are underway.

Figure 1. Time-resolved emission traces for jet-cooled 1-AC dimer induced by the excitation of the 0_0 (a) and +109 cm^{-1} (b) vibrational levels. The solid lines are computer fits of the data that take into account the time response of our apparatus.

Reference
1) K. Fuke and K. Kaya, *J. Phys. Chem.* **93**, 614 (1989).

VII—E   Interatomic Potentials and Intramultiplet Mixing of Zn-Rare Gas Systems

VII-E-1   Intramultiplet Mixing of Zn(4^{3}P$_J$) by Collisions with ^{4}He and ^{3}He

Hironobu UMEMOTO, Akira MASAKI, Toshiharu OHNUMA, Toshiyuki TAKAYANAGI *(Tokyo Inst. of Tech.)*, Shin SATO *(Chiba Univ.)*, Fuminori MISAIZU, and Kiyokazu FUKE

The intramultiplet mixing processes of Zn(4^{3}P$_J$) by collisions with ^{4}He and ^{3}He were studied by employing pulsed laser techniques. The following cross sections were obtained:

Zn(4^{3}P$_1$) + ^{4}He → Zn(4^{3}P$_2$) + ^{4}He: 3.1;
Zn(4^{3}P$_1$) + ^{4}He → Zn(4^{3}P$_0$) + ^{4}He: 1.5;
Zn(4^{3}P$_1$) + ^{3}He → Zn(4^{3}P$_2$) + ^{3}He: 4.7;
Zn(4^{3}P$_1$) + ^{3}He → Zn(4^{3}P$_0$) + ^{3}He: 1.8;
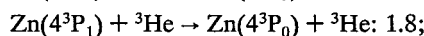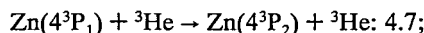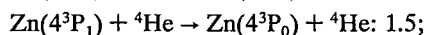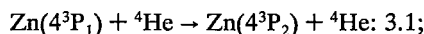
in units of 10^{-17} cm^2. A quantum calculation was carried out within a close-coupling treatment to evaluate the mixing cross sections. The agreement between the calculated and the experimental cross sections was very good for electrostatically allowed transitions; i.e., those for the production of Zn(4^{3}P$_2$) from Zn(4^{3}P$_1$), for both ^{4}He and ^{3}He. The calculated cross sections for the production of Zn(4^{3}P$_0$) were found to be smaller than the experimental ones.

VII-E-2 The Intramultiplet Mixing of Zn(4³P_J) by Collision with Ar

Hironobu UMEMOTO, Akira MASAKI, Toshiharu OHNUMA *(Tokyo Inst. of Tech.)*, Fuminori MISAIZU, and Kiyokazu FUKE

The intramultiplet mixing processes of $Zn(4^3P_J)$ by collisions with Ar were studied by employing pulsed laser techniques. The following cross sections were ob-tained:

$$Zn(4^3P_1) + Ar \rightarrow Zn(4^3P_2) + Ar: 5.5;$$
$$Zn(4^3P_1) + Ar \rightarrow Zn(4^3P_0) + Ar: 2.2;$$
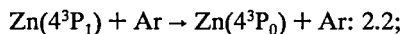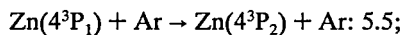
in units of 10^{-19} cm². These experimentally obtained cross sections were compared with the results of a close-coupling calculation. It is suggested that not only $^3\Pi$ states but also $^3\Sigma$ states of ZnAr are slightly attractive.

VII—F   Studies of Ultrafine Particles

The physical properties of fine particles, the size of which is less than ten nm, are affected by the quantum size effect, surface effect and a fluctuation of a thermodynamical property due to low dimensionality. These effects were studied as functions of particle species, supporting organic liquids and preparation techniques.

VII-F-1 Magnetic Properties of Iron: From Clusters to Bulk

Keisaku KIMURA

The magnetic moments of iron clusters are studied as a function of clusters size and temperature. At zero Kelvin, the magnetic moment is a monotonous increasing function of decreasing size. The temperature dependence of magnetic moment of clusters and bulk materials is given. The size dependence of the Curie temperature (T_c) of small particles is derived. All these magnetic characteristics are combined to give a phase diagram as a function of size and temperature. A valley structure in magnetic moment is found in this diagram in the cluster size range of 10^1-10^2 atoms per particle. The size and temperature dependence of the magnetic state of bulk Fe above T_c is discussed.

VII-F-2 Deviation of Spin Susceptibility of Small Metallic Particles as Predicted by the Random-Matrix Theory

Keisaku KIMURA

The spin susceptibility of small metallic particles is studied that takes into account the contribution of the clustering of particles, size distribution of the sample,

shape effect on the electronic energy distribution, spin-orbit coupling interaction, and magnetic field effect within the framework of random-matrix theory. It is found that each of these effects contributes to enhance the spin susceptibility. From the analyses stated above of the Cu Knight-shift data, the spin-orbit coupling energy is derived and compared with those derived from ESR measurements. The two-level correlation function that is proportional to the spin susceptibility given by Efetov is used to analyze both the Knight-shift data of Cu and Al small particles under a strong magnetic field which gives the orthogonal energy-level distribution rather than the symplectic one.

VII-F-3 Fractal Analysis of the Coagulation Process of Au Nano-Meter Particles Dispersed in 2-Propanol

Naoki SATOH *(Kao Corp.)*, Hiroyuki HASEGAWA *(Kao Corp.)*, Kaoru TSUJII *(Kao Corp.)*, and Keisaku KIMURA

The coagulation process of Au small particles (11 nm in size) dispersed in 2-propanel is analyzed via fractal analysis. It was found that the particle network grows one dimensionally at an initial step and three dimensionally later. Ostwald's ripening was found at the beginning of the growth process. The absorption

band at around 750 nm gradually increases at the expense of the decrease of 523 nm plasmon band with the growth of particle network.

VII-F-4 ESR Study of Spin Assembly in a Finite System: Decrease of the Neel's Temperature Observed in Ultrafine MnF_2 Particles

Shunji BANDOW and Keisaku KIMURA

We studied the size dependence of phase transition phenomenon of a spin system. Samples were prepared by the vacuum evaporation technique using electron beam heating. 99.99% of MnF_2 was deposited on an evaporated quartz film with a thickness of a few nm. In this process, MnF_2 was grown on a quartz film with the island structure. Diameter of the particles was changed by the evaporation thickness. Crystal structure of the MnF_2 particles was found to be α-PbO_2-type (metastable phase[1,2]) by the electron diffraction. Usual bulk MnF_2 has rutile type crystal structure. The Neel's temperatures for these particles were determined by the finite size scaling using the relation $\Delta H \propto (T\text{-}T_N)^{-\alpha}$ with maximizing the range of $\log(T\text{-}T_N)$ over which the data points in a $\log(\Delta H)$ vs $\log(T\text{-}T_N)$ plot form a straight line. The result is shown in Figure 1. From this figure, the relation between T_N and particle diameter d was found to be represented by $T_N \propto d^{-3}$. T_N for the bulk α-PbO_2-type MnF_2 is also found to be 62 K and T_N disappears at the size of 2.8 nm (ca. 400 MnF_2 molecules are included in this size of particle). The latter finding suggests that the long range spin-ordering does not exist in extremely small MnF_2 particles.

References
1) L.M. Azzaria and F. Dachille, *J. Phys. Chem.*, **65**, 889 (1961).
2) S.S. Kabalkina, L.F. Vershchagin, and L.M. Lityagia, *Soviet Phys.-Solid State*, **11**, 847 (1969).
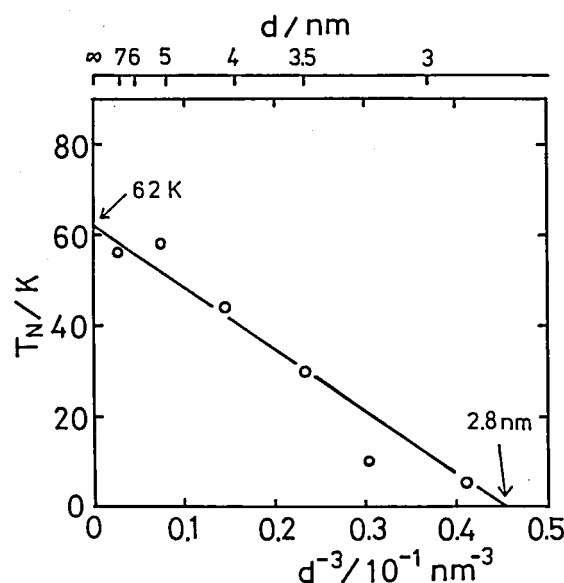
Figure 1. Size dependence of the Neel's temperature. Neel' temperature T_N is represented by a functional relation of particle diameter d as $T_N \propto d^{-3}$. Bulk T_N is 62 K and T_N disappears at 2.8 nm in diameter.

VII-F-5 Size Effect of the Magnetic Moment Determined by the Analysis of Magnetization Curve in Ultrafine Magnetite Particles

Shunji BANDOW and Keisaku KIMURA

In magnetite UFP's (ultrafine particles), it was found that FMR spectra disappeared in the particles with diameter less than 3.1 nm. This finding from FMR experiment suggests that the long range spin-order (bulk ferromagnetic state) does not realize in such a small particle system. A simple question arises from this fact that how does the magnitude of magnetic moment change around the diameter of 3.1 nm. We focused the problem on this pint and meausred the magnetizations to determine the average magnetic moment in a particle. The results are shown in Figure 1. Fitting curves using Langevin function are indicated by the solid line. In the particle larger than 3.4-nm diameter, we could not fit the experimental results by a single magnetic moment, but they can be fitted by using two kinds of magnetic moments as indicated in the figure. The magnetic moment for 2.4-nm particle should be ca. 400 μ_B from the calculation of bulk approximation. However, analyzed result for 2.4-nm particle showed that the magnetic moment was 90 μ_B, much smaller than the above value. This fact suggests that four

magnetic domains with the magnetic moment of 90 μ_B exist in 2.4-nm particle. Based on the same consideration stated above, the number of magnetic domains for each particle is indicated in the figure. From these

analyses, we can say that the picture of mono-magnetic-domain is no longer useful for the small particles. Mono-domain character will gradually grow up starting from ca. 3-nm particles with increasing particle size.
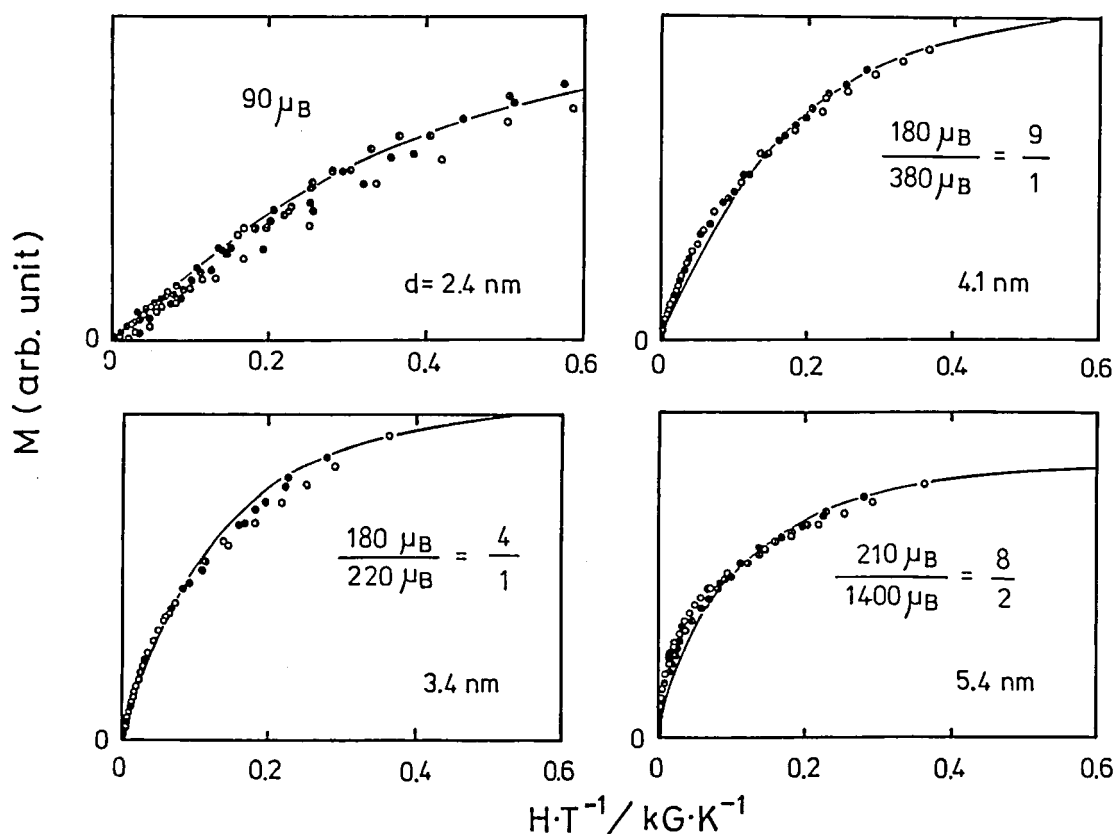
Figure 1. Magnetization curves of ultrafine magnetite particles. Solid lines are the fitting curves using Langevin functions. Data points in the figure are for the various temperatures, 60 to 140 K, 100 to 220 K, 100 to 220 K and 140 to 260 K for 2.4-, 3.4-, 4.1- and 5.4-nm particles, respectively, with different kinds of circles. In these analyses, it is necessary to use two kinds of magnetic moments in the particle with the size larger than 3.4 nm and their ratios are indicated in the figure.

VII-F-6 ESR and CESR Observed in Ultrafine Mg Particles

Shunji BANDOW and Keisaku KIMURA

Electron spin resonance (ESR) of ultrafine Mg particles prepared in ultrahigh vacuum condition are measured. An asymmetrical ESR line (linewidth: 16 G) which has been ascribed to the quantum size effect (QSE), is assigned to the O_2^- ion adsorbed on the particle surface. Another ESR spectrum with the linewidth of 1 G is also observed with the sample prepared under leaking O_2 gas. Quantum narrowing of the ESR line-

width is not perceivable even for the particles having 3-nm diameter. Instead, a very broad conduction ESR line is observed, the intensity of which indicates a typical QSE. The reason for the absence of quantum narrowing is discussed in relation to the shape effect on the energy level statistics.

VII-F-7 Temperature Dependence of ESR Absorption Intensity of Ultrafine Zn and Mg Particles

Shunji BANDOW and Keisaku KIMURA

189

Recently reported temperature dependence of spin susceptibilities of ultrafine particles (UFP's) of Zn and Mg exhibiting Curie-like behavior is found not to originate from the quantum size effect of conduction electrons but from an impurity effect. The microwave power saturation, especially enhanced in the smaller UFP's, suppresses the ESR intensity at low tempera-

ture and gives a complicated temperature dependence. ESR signal from the conduction electrons (CESR) can not be detectd in Zn UFP's, but observed in Mg UFP's with very broad linewidth. These phenomena are explained in relation to the size and shape effects of UFP's combining with the nature of CESR observed in bulk for both metals.

Low-Temperature Center

VII—G   Instrumentation for Low Temperature Experiments

VII-G-1   Development of the Data-Monitoring System for the Helium Liquefier

Kiyonori KATO, Hisashi YOSHIDA, Takashi TAKAYAMA, Keiichi HAYASAKA, Kunio AWAGA and Yusei MARUYAMA

We installed a large scale helium liquefier system (capacity 150 1/h) in 1989. The system is fully-automatically controlled, but no monitoring system was set in. In this year we have developed a monitoring system for the liquefier in order to seize the running state of the machine and to forebode possible failures.

The sixty-four digital control bits are sent from the controller of the liquefier to a digital data selector developed for this purpose. The transformed data are sent to NEC PC-9801 microcomputer through an I/O card.

The pressures and temperatures of the system, open-close of the Joule-Thomson valve, amount of liquid helium, speed of two turbines, and oxygen concentration and dew point of the process gas are monitored. These analogue data are recorded by a CHINO AA hybrid recorder with which the computer comunicates through GPIB. These informations are processed and displayed on the screen as four pictures. The analogue data are printed out. The digitally controlled data are stored in a disk to inspect the function of the liquefying system.

We are grateful to the staffs of the Equipment Division and the Construction Division of Administration Bureau for their helpful collaborations.

Reference
Treating manual for the IMS helium liquefier, KOBE STEEL WORKS (1989).
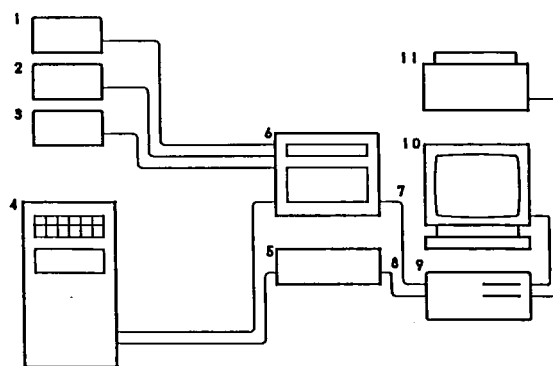
Figure 1.   Schematic diagram of the data-monitoring system: 1. Dew point meter. 2. Oxygen concentration meter. 3. Liquid helium level meter. 4. Controller of the liquefier. 5. Digital data selector. 6. CHINO AA hybrid recorder. 7. GPIB line. 8. Digital I/O line. 9. NEC PC-9801 computer. 10. Color display with 21 inch CRT. 11. Printer.

VII-G-2   Development of Multi Purpose ^{3}He Cooling System in the 12 Tesla Magnet

Kiyonori KATO, Koukichi OOSHIMA (Okayama Univ.), Kyoji ARAKI (Okayama Univ.), Hitoshi YAMAZAKI (Okayama Univ.), Kyuya YAKUSHI, and Yusei MARUYAMA

A multi purpose ^{3}He cooling system was set up and linked to a cryostat with a superconducting magnet. Electrical conductivity and magnetic susceptibility are

able to be measured under variable magnetic fields and at variable temperatures ranging from room temperature to 0.5 K. The magnetic field-strength is changeable from 0 to 12 Tesla arbitrarily. The lowest temperature to be obtainable by this single-cycle type cooling system after 30 minutes from the start of cooling is about 0.5 K. The system retains this temperature more than three hours. The calibrated germanium thermometer and ^{3}He vapour pressure are used for determination of temperatures. The sample holder is rotatable through the leading shaft, and a sample can be exchanged without warming up the magnet.

The ^{3}He chamber can be carried out very simple because the lower part of the chamber is insulated by permanent vacuum. The 100 1 ^{4}He enables four days experiments continuously. The system will be open to use for the IMS staff in near future. Another measurement cells for specific heat and AC magnetic susceptibility will be made for the future.

We are grateful to the staff of Equipment Development Center for their useful suggestions.
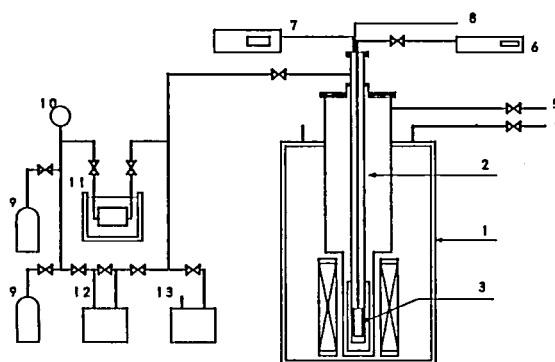
Figure 1. Schematic diagram of the ^{3}He cooling system installed into a cryostat with superconducting magnet: 1. Cryostat (IGC magnet) 2. ^{3}He chamber. 3. Measurement cell and sample holder. 4. ^{4}He recovery line. 5. ^{4}He pumping line. 6. Absolute pressure gauges and a readout (Baratron 122A, 127A and PDR-C-2C). 7. Temperature controller (LakeShore DRC-93C). 8. Connections to measurement system. 9. ^{3}He cylinder. 10. Compound pressure gauge. 11. Cold trap (liquid N_2). 12. ^{3}He pump (DAIA CRP S50). 13. Auxiliary pump.

VII—H   Ferromagnetic Interaction in Molecular Crystal

The study of the ferromagnetic intermolecular interaction in organic molecular solids should bring us important knowledge, not only to the establishment of molecular ferromagnet but also to the understanding about radical reactions. In the present project, we investigate the factors controlling ferromagnetic and antiferromagnetic behaviors in the solids.

VII-H-1   Magnetic Susceptibility Measurement System under High Pressure

Kunio AWAGA and Yusei MARUYAMA

The magnetic measurement under high pressure might be useful and important for the study of molecular/organic ferromagnetism. The pressure dependence of the ferromagnetic behavior could give us important information about the ferromagnetic interaction and, in some case, about the magnetic ordering. We have set up a magnetic susceptibility measurement system suitable for this purpose. A hydrostatic pressure is maintained by using a miniature Be-Cu pressure clamp cell. The pressure was calibrated with a Manganin gauge at room temperature. The decay of pressure at 7 K was about 3% of its initial pressure clamped at room temperature. The magnetic data of this clamp cell were experimentally determined as follows; the diamagnetic susceptibility $\chi_d=-7.2\times10^{-8}$ emu g^{-1} and the Curie constant $C=3.0\times10^{-6}$ emu K g^{-1}. Static magnetic susceptibility and magnetization under high pressure are measured by a standard Faraday susceptometer using Oxford superconducting magnets and a Cahn 1000 electric microbablance. The construction of the susceptometer system is schematically illustrated in Fig. 1. Temperature and magnetic field dependence measurement can be performed automatically.
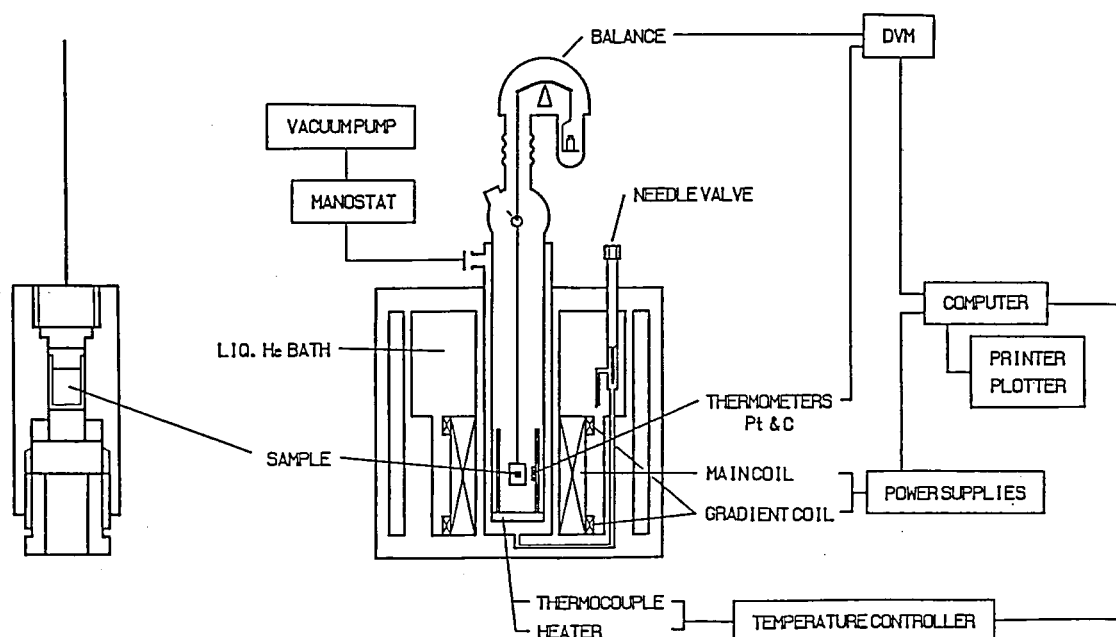
Figure 1. Magnetic susceptibility measurement system under high pressure, combined of a Faraday susceptometer and a Be-Cu high-pressure clamp cell.

VII-H-2 Pressure-Induced Enhancement of the Ferromagnetic Intermolecular Interaction in an α-Nitronyl Nitroxide Organic Radical

Kunio AWAGA and Yusei MARUYAMA

The effect of high pressure on the ferromagnetic properties of a crystal of an organic radical, 2-(4-nitro-phenyl)-4,4,5,5-tetramethyl-4,5-dinhydro-1H-imidazo-lyl-1-oxy 3-oxide (NPNN), has been studied with the use of the combined system of a Faraday suscep-tometer and a Be-Cu high-pressure clamp cell. The magnetic susceptibility of the crystal NPNN remarkably increases with increasing pressure at low temperatuers, and furthermore, its increment increases monotonically with decreasing temperature down to about 5 K. The Weiss constant under the pressure of 9 kbar corresponds to the 40% increase in the ferromagnetic inter-molecular interaction in the crystal of NPNN, and the magnetization at 9 kbar also comes to saturation more rapidly compared with the behavior under an ambient pressure. The simple calculation of the intermolecular overlap integrals between the frontier orbitals, can semi-quantitatively interpret the pressure-induced en-hancement of the ferromagnetic coupling in the crystal of NPNN.
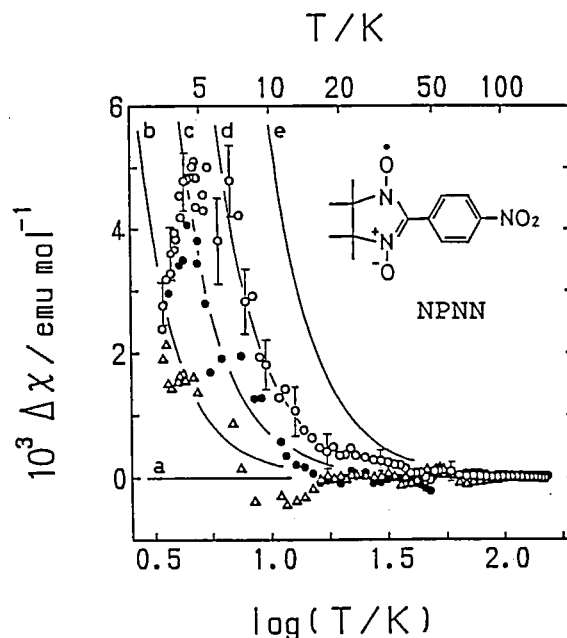
Figure 1. Temperature dependence of the magnetic suscepti-bility of NPNN at three different high pressures: 9 kbar (O), 6 kbar (●) and 3 kbar (△). The difference in magnetic suscepti-bility between ambient pressure is plotted as a function of com-mon logarithm of temperature. The solid curves, a-e, are the theoretical ones for the Weiss constants of $\theta(P)$=0.90 (a), 0.95 (b), 1.05 (c), 1.25 K (d) and 2.00 K (e), respectively.

VII-H-3 Magneto-Structural Correlation in the α-Nitronyl Nitroxide Organic Radicals

Kunio AWAGA, Tamotsu INABE, Toshihiko YOKOYAMA (Hiroshima Univ.,) and Yusei MARUYAMA

Three kinds of α-nitronyl nitroxides, 2-R-4, 4,5,5-tetramethyl-4,5-dihydro-1H-imidazolyl-1-oxy 3-oxide [with R=phenyl (I), 3-nitrophenyl (II) and 4-nitrophenyl (III)], with different types of magnetic coupling, have been structurally characterized. The nitroxide I crystallizes in the P2₁/c space group [a=21.070(3) Å, b=10.239(5) Å, c=12.311(2) Å, β=105.56(1)°, Z=8], forming centrosymmetric tetramers. The nitroxide II belongs to the non-centrosymmetric P2₁ space group [a=10.314(3) Å, b=11.130(2) Å, c=6.138(2) Å, β=106.70(1)°, Z=2], with two-dimensional (2-D) sheets parallel to the bc plane. The nitroxide III crystallizes in the non-centrosymmetric Fdd2 space group [a=10.960(3) Å, b=19.350(3) Å, c=12.347(5) Å, Z=8]. This radical has a complex 3-D structure with the combination of the 2-D network linked by the O^{δ-}...N^{δ+} contacts and the 3-D hydrogen bonding network. The intermolecular conformations in I-III are determined by the Coulombic attraction forces between the polarized charges. The magneto-structural correlation in the three α-nitronyl nitroxides can be qualitatively interpreted by the competition between the antiferromagnetic coupling caused by the intermolecular contact between the NO groups, and the ferromagnetic one caused by the contact between the NO group and the substituent at the α-position.

Equipment Development Center

VII—I   Studies of Quasi-1-D Organic Semiconductors

VII-I-1   Optical and Magnetic Properties of the Halogen-Bridged Metal Complexes Modified by Hydrogen Bondings; {M(chxn)₂Br}Br₂ (M=Pt, Pd and Ni)

Hiroshi OKAMOTO, Koshiro TORIUMI, Tadaoki MITANI, and Masahiro YAMASHITA* (*Nagoya Univ.)

Polarized reflection and ESR measurements have been carried out on the single crystals of newly synthesized halogen-bridged one-dimensional (1-D) metal complexes {M(chxn)₂Br}Br₂ (M=Pt, Pd, Ni: chxn=1R, 2R-cyclohexanediamine), which have tight hydrogen bonds between ligands (chxn) and counter anions (Br⁻) and construct a two-dimensional hydrogen-bond network. Both of the polarized reflection spectra and the temperature dependent ESR signals indicate that the electronic state of M=Ni is essentially different from that of M=Pt (or Pd). From the analysis of these results, it can be concluded that the complex for M=Ni is in a mono-valent state, where a Mott-insulator is formed in a (-Ni³⁺-Br⁻-) regular chain, in contrast to the mixed valent state (-M²⁺-Br⁻-M⁴⁺-Br⁻-) for M=Pt and Pd. Thermally excited paramagnetic spins observed for the Pd complex can be explained by the soliton-kink model under the influence of the 2-D hydrogen-bond network.

VII-I-2   Photo-Induced Gap State in the Mott-Hubbard System of Halogen-Bridged Ni³⁺ Complex ({Ni(chxn)₂Br}Br₂)

Hiroshi OKAMOTO, Kaoru OKANIWA, Tadaoki MITANI, Koshiro TORIUMI, and Masahiro YAMASHITA* (*Nagoya Univ.)

Photo-induced IR absorption measurements have been made on the bromo-bridged Ni³⁺ complex ({Ni(chxn)₂Br}Br₂: chxn=cyclohexanediamine), which has the one-dimensional Mott-Hubbard-type ground state. A photo-induced absorption band was observed around 0.25 eV, which is a considerably lower energy than the lowest exciton transition at 1.3 eV. In the Mott-Hubard system, this is the first observation of the gap state, which can be ascribed to the formation of

small polarons accompanied by the displacements of the bridging bromine ions after photo-excitation of an electron-hole pair. This interpretation is supported by both the observed results of the laser-intensity dependence of the photoinduced signals and the quantum-yield spectra of photoconductivity.

VII-I-3 Optical and Magnetic Studies of H-bonded Charge-Transfer Complex, DAP-TCNQ

Kaoru OKANIWA, Hiroshi OKAMOTO, Tadaoki MITANI, Tamotsu INABE, Kunio AWAGA, and Yusei MARUYAMA

In order to interpret anomalous semiconducting behavior of DAP(1,6-diaminopyrene)-TCNQ crystal which has hydrogen bonds (H-bonds) between TCNQ and DAP columns, optical and magnetic measurements were made. The results suggest that the TCNQ columns dimerize in low temperature region although X-ray diffraction signals related to the dimerization could not been detected. This might be attributable to the specific nature of the system; the degree of charge transfer ρ is very close to unity and the lattice undergoes the discommensulate-type dimerization. And the electronic state with $\rho \sim 1$ might be stabilized by the interchain H-bonds. Nevertheless, this complex involves some unsolved problems in the physical properties associated with the electron-proton interaction. Discussion of these problems is being developed by studying the substitution effect of the donner by DMTCNQ or $TCNQF_4$ in order to modify both the degree of charge transfer and the strength of H-bond.

VII-I-4 IR Study of the H-bond Coupled with the Mixed-Valence State of Halogen-Bridged Metal Complexes

Kaoru OKANIWA, Hiroshi OKAMOTO, Tadaoki MITANI, Koshiro TORIUMI and Masahiro YAMASHITA* (*Nagoya Univ.)

IR spectroscopic measurements were made on the halogen bridged metal complexes of $[M(chxn)_2Br]Br_2$ (M=Pt, Pd and Ni) which have interchain N-H...Br bond strongly coupled with the electronic state of chains. the splitting of the N-H stretching bands for Pt and Pd complexes show a good correlation with the amplitude of CDW in the chain. No splitting of the N-H band was observed for the Ni complex, which is an evidence of transformation from the mixed-valence (CDW) state to the mono-valence (the Mott-Hubbard) state by replacement of M=Pt (or Pd) by Ni. The IR studies under hydrostatic pressures indicate that an application of the pressure leads to reduction of the amplitude of the CDW.

VII—J Development of Nonlinear Techniques for Ultrashort Optical Pulse Measurement

VII-J-1 Application of Nonlinear Photoelectric Effect to Ultrashort Optical Pulse Measurement

Yoshihiro TAKAGI, Tohru KOBAYASHI, and Keitaro YOSHIHARA

The nonlinear photoelectric effect (NPE) has been applied to an intensity correlation measurement of ultrashort optical pulse in various solids in wide spectral range from IR to UV. NPE was first found with a photocathode of photomultiplier by Sonnenbert et al.[1] over two decades ago. This effect was applied to measurement of the second-order autocorrelation function of a cw mode-locked Ar ion laser[2]. When the photon energy of the incident optical pulse satisfies a condition $2h\nu > W > h\nu$, where W is the work function of the photoelectric material, the photocurrent should be proportional to the square of the input power. We manufactured evaporated films of various materials attached to an electron multiplier contained in a vacuum chamber. Figures 1 and 2 show input power dependences of photocurrent and signals of 2nd and 3rd-order autocorrelation functions for PbI_2 and CsI. Light sources are 2nd to 5th harmonics of a mode-locked

Nd:YAG laser. These data indicate that the NPE can be applied to the autocorrelator for the deep UV spectral region by making use of a photoelectric material with large work function, that is not accessible by the ordinary SHG autocorrelator.

References

1) H. Sonnenberg, H. Heffner, and W. Spicer, Appl. Phys. Lett., **5**, 95 (1964).
2) W. Bennett, D. Carlin, and G. Collins, IEEE J. Quantum Electron., **QE-1097** (1974).
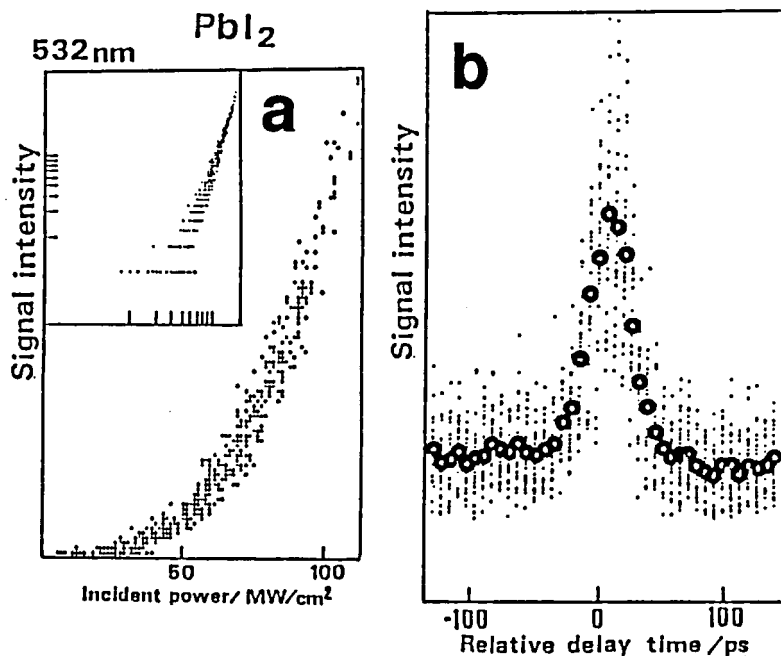
Figure 1. (a) Input power dependence of photoemission intensity and (b) autocorrelation profile of PbI_2 film. Light source is a frequency-doubled Nd:YAG laser.
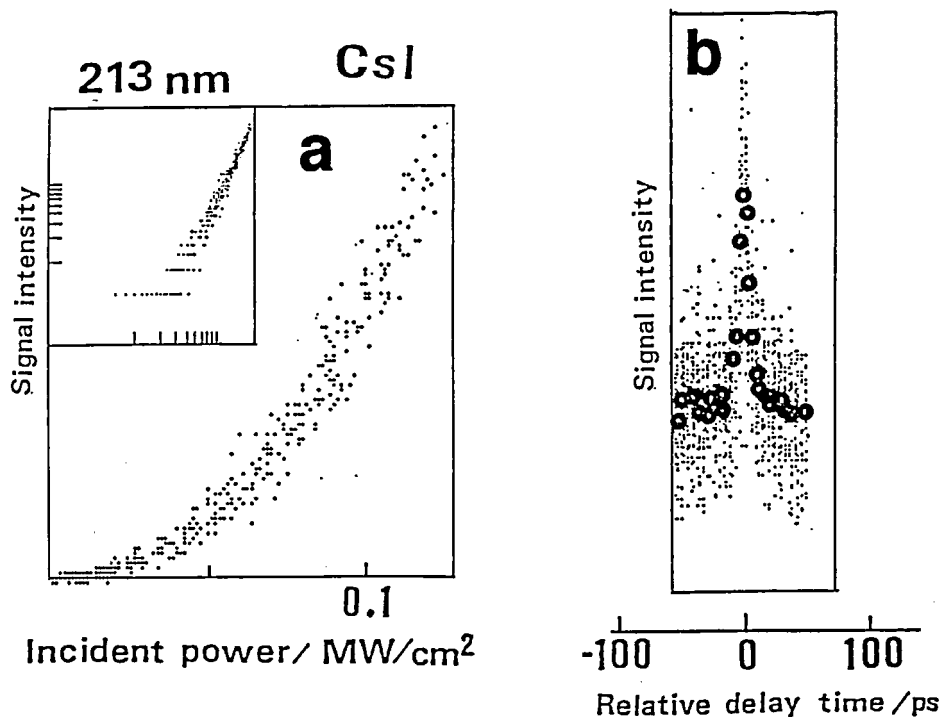
Figure 2. (a) Input power dependence of photoemission intensity and (b) autocorrelation profile of CsI film. Light source is a fifth-harmonic of Nd:YAG laser.

VII-J-2 Application of Nonlinear Photoconductivity for Ultrashort Optical Pulse Measurement

Yoshihiro TAKAGI, Tohru KOBAYASHI, and Keitaro YOSHIHARA

[submitted to *Appl. Phys. Lett.*]

Two-photon-induced conductivity has been observed in Si and GaAsP photodiodes and a CdS photocondutive cell and applied to an ultrafast optical pulse measurement with a simplified Michelson-type optical arrangement. Efficiency of the two-photon conductivity is found to be 3×10^{-14} I Ampere/Watt for a GaAsP photodiode, where I is the intensity of the incident pulse in Watt/cm^2. A single-shot pulsewidth measurement is also performed with a combination of a Si CCD camera and a diffraction grating. These nonlinear devices will prove a versatile intensity correlator for ultrafast optical pulse measurement because of its high time-resolution and simplicity in optical arrangement and in operation.

VII—K Development of Experimental Devices

VII-K-1 Development of a Pulsewidth Stabilizer for Subpicosecond Laser System

Kazuo HAYAKAWA

The subpicosecond laser system constructed in the department of electronic structure at IMS had a problem of pulsewidth fluctuation (40-%-increase in 20 minutes after turn on) due to a thermal expansion in the optical bench of the order of one micrometer. This is a serious problem for high time-resolution spectroscopy. We have developed an electronics circuit for feedback-stabilizing laser pulsewidth that controls the cavity length using a piezo device. The circuit consists of a control unit of one-board microcomputer and a driver for the piezo device. Control parameters are obtained by digitizing output of an autocorrelator used in the pulsewidth measurement. The autocorrelator outputs a voltage proportional to the square of pulse intensity as a function of the time in the pulse profile. This signal is sampled with a fixed time interval and reproduced as a digitized pulse profile. A full-width at half maximum is read from this profile and used for a control parameter. A piezo device (7 μm/150 volts) was attached to the end-mirror in the cavity. As a result, using this feedback controller the pulse-width fluctuation is limited within 5% and the laser can be operated for a few hours without manual adjustment.

Ultraviolet Synchrotron Orbital Radiation Facility

VII—L Development of UVSOR Light Source

VII-L-1 New Superconducting Wiggler

Eiken NAKAMURA, Goro ISOYAMA, Osamu MATSUDO

A new superconducting wiggler of the wavelength-shifter type was recently installed in place of the old one. The maximum magnetic field at the central pole is 4 T and the critical energy of the synchrotron radiation is 1.5 keV at the beam energy of 750 MeV. The new device has a semi-closed helium liquefying system utilizing two refrigerators. Therefore no additional supply of liquid helium is necessary. The beam can be injected with the wiggler excited up to 3.6 T without appreciable decrease of the injection speed. After injection at 600 MeV, the beam is accelerated to 750 MeV and then the wiggler is excited at the full rating, 4 T. A

three-dimensional drawing of the wiggler is shown in Figure 1. The vessel, in which the superconducting coils are soaked in liquid helium, is surrounded by two thermal isolation plates cooled to 20 K and 80 K, respectively, with one of the refrigerators installed on the top of the device. The other refrigerator is used for liquefying evaporated helium gas. The cooling system can confine helium in the vessel completely.

SUPERCONDUCTINC WICCLER

Rupture Disk

Safty Valve

Refrigerator
(SRD 220)

Heat Exchanger

Liq.He Vessel

Iron Yoke

Electron Beam

Beam Duct

Support

Power Lead

Heat Exchanger

Refrigerator.
(SRJ 803)

80K Shield plate

Heat Exchanger

20K Shield plate

Vacuum Vessel

Support

20K Shield plate

80K Shield plate

Vacuum Vessel

Superconducting
Magnet

Circulation pump
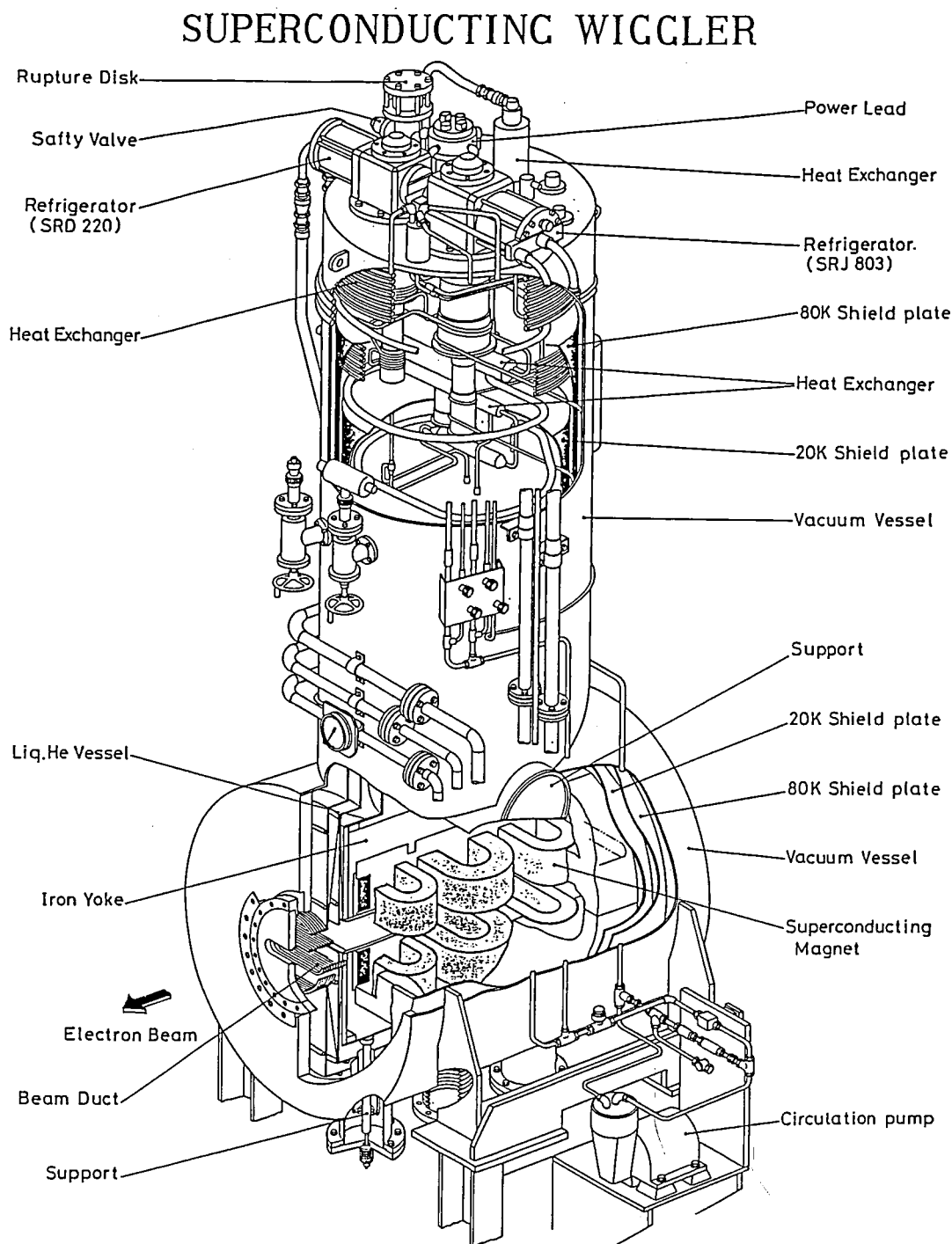
Figure 1. Three-dimensional drawing of the new superconducting wiggler.

VII-L-2 Free Electron Laser Experiment

Shirou TAKANO, Goro ISOYAMA, and Akihiko LIN

An FEL experiment at the wavelength of 488 nm using the UVSOR storage ring is under way. The electron energy for the experiment is chosen to be 500 MeV. The beam current of more than 50 mA is stored in the single bunch operation mode by the full energy injection, which corresponds to the peak current of about 15 A. The beam lifetime at the current is about 20 minutes. We are now preparing for an amplification experiment of the light injected by an Ar ion laser of 1 W output power. An undulator made of the permanent magnet with the period length of 111 mm and the number of periods of 19 is used for the experiment. The gain is estimated to be about 10^{-3} for the beam current of 10 mA. For the next step, the undulator magnetic blocks will be rearranged into the optical klystron configuration in order to improve the gain. The central part of the undulator will be modified into the dispersive section and the magnet gap there will be adjusted independently of that of the normal undulator sections. After an amplifier experiment with this optical klystron, we will proceed to an oscillator experiment.

VII—M   Researches by the Use of UVSOR

Researches of IMS staff other than UVSOR staff are reported at some other places in this issue. Details of all researches preformed by inside and outside users will be reported in UVSOR Activity Report 1990.

VII-M-1   Constant Initial State Spectra of Crystalline GeTe Thin Film

Kazutoshi FUKUI, Yasuo FUJII (Osaka City Univ.), and Makoto WATANABE

Constant initial state (CIS) spectra of crystalline GeTe are investigated at excitation photon energies between 26 and 48 eV at room temperature. Figure 1 shows energy distribution curve (EDC), the CIS and total yield spectra. The number attached to each curve represents the binding energy E_b of the peak of valence band structure in the EDC. The structures around 30 eV in the total yield spectrum are due to the transition from Ge $3d$ level to the conduction band and those around 40 eV, the transition from Te $4d$ level. The CIS spectra of the upper valence bands $(E_b = 1.5, 3.4$ eV$)$ do not have prominent structure. The spectrum at $E_b = 5.5$ eV has two peaks around 32 and 42 eV corresponding to Ge $3d$ and Te $4d$ transitions. The CIS spectra of the deep valence bands $(E_b = 8.7, 12.0$ eV$)$ have close resemblance to the yield spectrum. The results show that the strong resonant effect is found in the case of the deep valence bands for both Ge $3d$ and Te $4d$ excitation, but no effect was found in the case of the upper valence bands. It means that the wave function of the upper valence bands spreads widely in the crystal and that of the deep valence bands is localized both at Ge and Te sites. The upper valence bands mainly consist of Ge $4p$ and Te $5p$ orbitals and the deep valence bands, Ge $4s$ and Te $5s$ orbitals. Therefore, it is concluded that the p orbitals of both constituent atoms are highly mixed, but s orbitals still have individual characters.
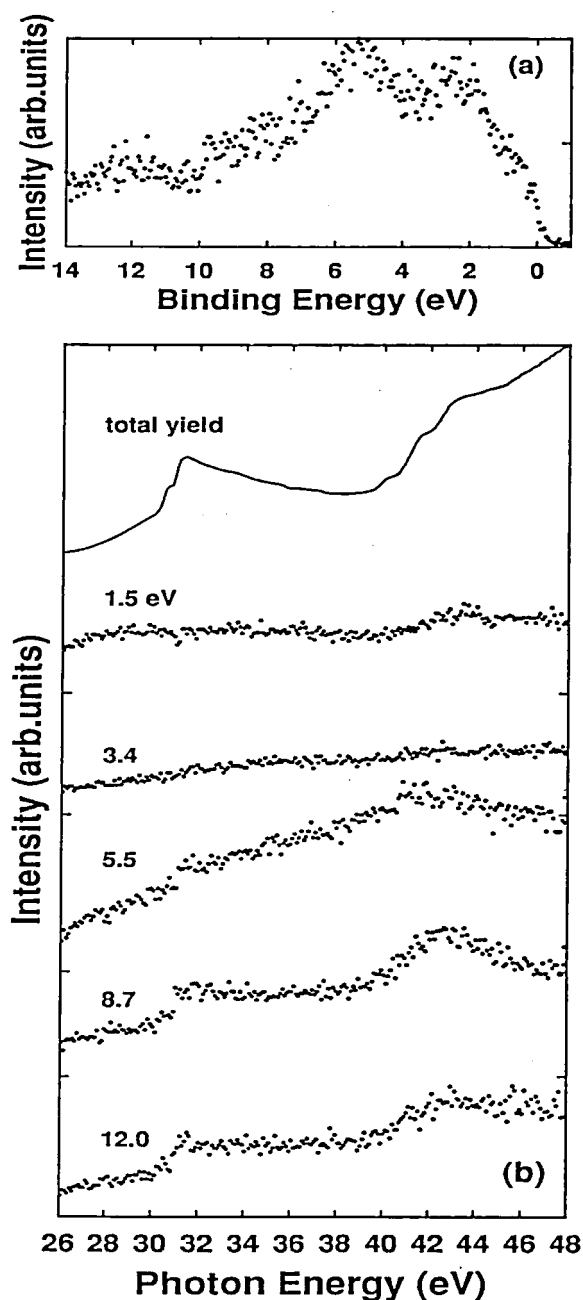
Figure 1. (a) Energy distribution curve at excitation photon energy 29.0 eV and (b) CIS and total yield spectra of crystalline GeTe thin film. Numbers in CIS spectra represent the binding energies.

VII-M-2 Sputtering of Excited Sodium Atoms from Na-Halides Irradiated with Synchrotron Radiation

Masao KAMADA, Sayumi HIROSE *(Univ. Osaka Pref.)*, and Osamu AITA *(Univ. Osaka Pref.)*

The sputtering of constituent atoms from sodium halides irradiated with synchrotron radiation was investigated. Single crystals of sodium halides were irradiated with a quasi-monochromatized light of 36 eV from the undulator. A Jobin-Yvon HR-320 monochromator was used for the measurement of emission spectra. The emission spectra consist of broad bands of bulk origin and a sharp line at 2.1 eV, as shown in Figure 1. The sharp line is attributed to the Na D line, indicating that the excited sodium atoms are sputtered from irradiated sodium halides. It should be noted that the sharp line can be seen strongly in NaF, weakly in NaCl, but is not appreciable in NaBr and NaI. This result is in good agreement with the efficiency of defect formation. Therefore, we conclude that the sputtering of the excited sodium atoms is closely related to the defect-formation process induced by electronic transition. Similar experiments on potassium halides are under way.
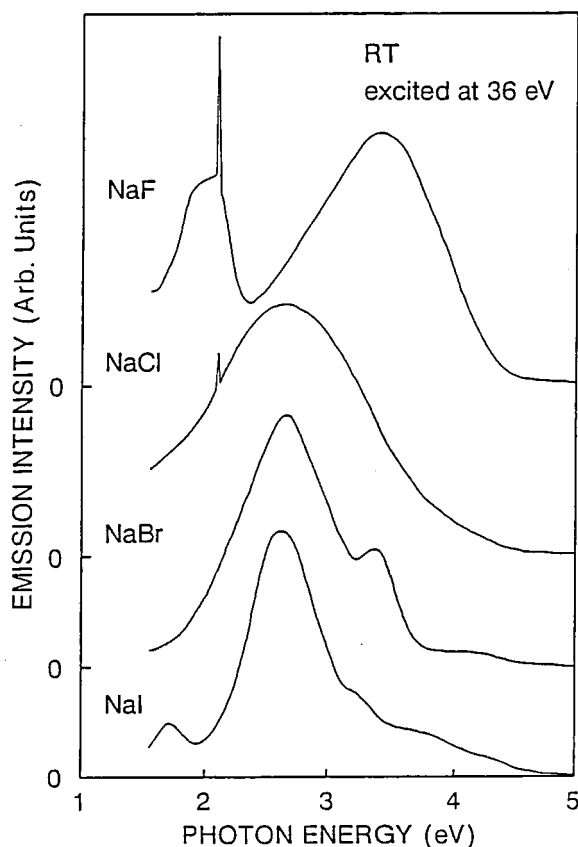
Figure 1. Emission spectra of sodium-halide crystals irradiated with undulator radiation of 36 eV.

VII-M-3 Electronic Structure of Poly(tetrafluoroethylene) Studies by UPS, VUV Absorption, and Band Calculations

Kazuhiko SEKI *(Hiroshima Univ. and IMS)*, Hiroshi TANAKA*, Toshiaki OHTA*, Yuriko AOKI*, Akira IMAMURA*, Hitoshi FUJIMOTO, Hiromichi YAMAMOTO, and Hiroo INOKUCHI *(*Hiroshima Univ.)*
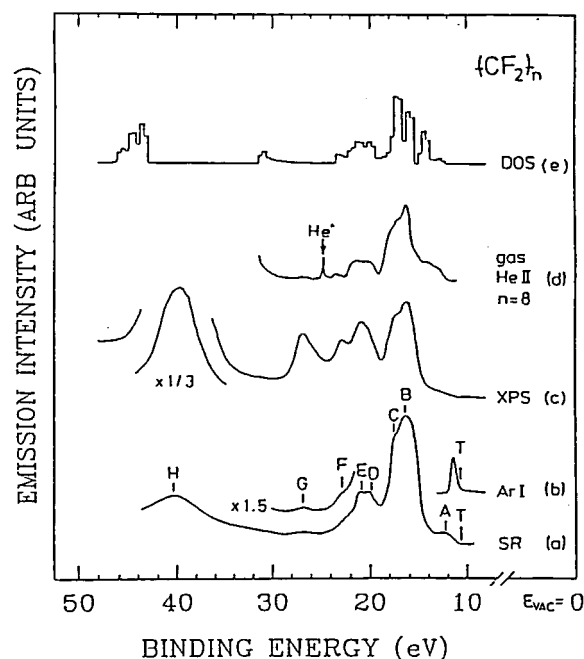
Figure 1. UPS spectra of poly(tetrafluorethylene) (PTFE) evaporated films using ArI radiation (hv = 11.7 eV)(a) and synchrotron radiation of 101.2 eV (b). Also shown are the XPS spectrum of PTFE (Ref.1) and vapor HeII (hv = 40.8 eV) UPS spectrum of n-C_8F_{18} (Ref.2)(d) and the density of occupied states derived from the present band calculation.

The electronic structure of poly(tetrafluoroethylene) (PTFE) was studied by UV photoelectron spectroscopy (UPS), vacuum-UV absorption, and ab-initio MO calculations. The UPS spectra (Figure 1(a) and (b)) give a photoemission threshold energy of 10.6 eV, with deeper valence band features consistent with the reported XPS (Figure 1(c)) and the oligomer vapor UPS spectra (Figure 1(d)). The UPS spectra are also consistent with the density of states derived from the calculated band structure (Figure 1(e)), which indicates that the uppermost part of the valence band is formed from the C and F 2p orbitals with C-C bonding and

C-F antibonding combination. The VUV absorption spectrum shows an intense peak at 7.7 eV, which most probably corresponds to the valence excitation from the top of the valence band to the bottom of the conduction band. With these data, the structure of the occupied and vacant states are deduced.

References
1) J.J. Pireaux, J. Riga, R., Caudano, J.J.Verbist, J.M. Andre, J. Delhalle, and S. Delhalle, J. Electron Spectrosc., **5**, 531 (1974).
2) M.B. Robin and N.A. Kueler, private communication.

VII-M-4 UV Photoelectron Spectroscopic Study of the Electronic Structure of Poly(dimethylsiloxane) and the Comparison with Related Silicon Compounds

Tohmei SUGANO*, Kazuhiko SEKI *(Hiroshima Univ. and IMS)*, Toshiaki OHTA*, Hitoshi FUJIMOTO, and Hiroo INOKUCHI *(*Hiroshima Univ.)*

The electronic structure of poly(dimethylsiloxane) was studied by UV photoelectron spectroscopy. The results using rare gas resonance lines give an accurate ionization energy of 8.3 eV, while the spectrum by synchrotron radiation gives the whole valence electronic structure. From the comparison with the data of related compounds and with the density of states of unsubstituted polysiloxane calculated by Takeda and Shiraishi, the spectral features are assigned. The comparison of the present results with those of poly(dimethylsilylene) shows that the σ conjugation in poly(dimethylsilylene), which leads to the low ionization thrshold energy and high conductivity upon doping, is effectively broken in poly(dimethylsiloxane), resulting in good insulating property. The localized nature of the electronic states in the Si-O systems leads to the increase of the ionization threshold from poly(dimethylsiloxane) SiO_2 by the removal of electron donating methyl groups, in contrast to the decrease in the catenated silicon systems from poly(dimethylsilylene) to silicon due to more effective delocalization in the three-dimensional system than in the one-dimensional system.

RESEARCH FACILITIES

For the sake of brevity the present issue includes only the newly installed facilities and the activities since September 1989. Concerning the activities and facilities before September 1989, please refer to older IMS Annual Review issues (1978 ~ 1989).

Computer Center

The main computers at the Center are a supercomputer HITAC S-820/80 and a general purpose computer HITAC M-680H. S-820, with a peak speed of 3 GFLOPS, has a 256 mega byte main memory and a 4 giga byte extended storage(solid state disk), while M-680H has a 128 mega byte main memory with a speed of about 14 MFLOPS. The disk memory has been expanded in June 1989 from 85 to 140 giga byte. In July 1989, the computers have been linked to the Japanese inter-university network. The Center is equiped with a few workstations including a Silicon Graphics IRIS-4D/70GT. The Center also provides a BITNET service (nodename:JPNONRI) for in-house staff members via a VAX at NIBB.

The Computer Center has been supporting development, porting and improvement of computer programs for molecular science. About 200 programs are available for immediate execution. Recent additions include GAUSSIAN86, GAUSSIAN88, CRYSTAL88 and FLAPW (self- consistent energy band calculation).

Databases in molecular science are also available at the Computer Center. These include the Quantum Chemistry Literature Database(QCLDB), Carnegie-Mellon Quantum Chemistry Archive(CMQCA), Infrared Spectra Database(IR2), Steric Chemical Calculation Database(STERIC) and Quantum Chemistry Basis Function Database(QCBDB). QCLDB, which has been developed by the Center in collaboration with the QCDB Group and had in the past been distributed only to academic institutions on a trial basis, is now available to all the interested organizations throughout the world including industrial laboratories.

About 35% of the computer time is used by the research staff at IMS, and the remaining 65% is given out as research grants free of charge to scientists outside the Institutes in related fields. As of March 1990, the number of project group was 239, consisting of 690 users.

Chemical Materials Center

The Chemical Materials Center plays an important role in the synthesis and purification of chemical substances in IMS. The scientists and technical associates of this facility support other people in IMS to carry out the above works. Upon request, technicians carry out elemental and mass spectrometric analyses of new compounds prepared at IMS. They also carry out their own researches on synthesis of new interesting compounds, developments of new selective chemical transformations, elucidation of reaction mechanisms, and application of new methodologies developed in IMS to the analysis of chemical substances and reactions. Part of the scientific activities are presented in the Section VII.

Instrument Center

For the efficient use of instruments, the Center is equipped with various types of instruments for general use. [1] Four instruments have been newly installed in 1990.

1) **Pulsed Dye Laser and Wavelength Extenders** (Quanta-Ray PDL-3, WEX-1, and IR-WEX)

Coupled with the Quanta-Ray DCR Nd:YAG laser (equipped in this Center), the dye laser provides tunable laser radiation from 380 nm to 960 nm. The tuning range is further extended, from 215 nm in the UV to 4.5 μm in the mid-infrared, by the WEX wavelength extender.

2) **Excimer Laser** (Lambda Physik LPX 100)

The excimer laser generates a pulse with pulse energy of 200 mJ/pulse at 193 nm(ArF) and with repetition rate up to 100 Hz.

3) **X-ray Powder Diffractometer** (MAC Science MXP^{3VA})

This diffractometer enables to use the analysis of powder and thin-film samples under computer control. The measurement temperature covers the range from 300 K to 90 K.

4) **Auger Electron Spectrometer and Ultraviolet Photoelectron Spectrometer** (VG Microtech)

AES and UPS parts were purchased from VG Microtech Inc. and installed in a VG ESCALAB MKII XPS system. The available energies are 21.2 eV and 40.8 eV for UV region and 5 kV (maximum) for AES. SEM function can be used at a spatial resolution of 10 μm.

Reference
1) *List of Instruments*, No.7, IMS Instrument Center (1989).

Low-Temperature Center

1. The new helium liquefier system installed in 1989 is in steady operation without any serious troubles. The total monitoring system for liquefying conditions will be completed in this year. The supplied amount of liquid helium in 1989 was about 23,000 1 in excess of 5,000 1 compared with that in 1988.
2. A new technical associate, Mr. Takashi Takayama has been enrolled in this center since Jan. 1st, 1990.

Equipment Development Center

A number of research instruments have been designed and constructed by making use of the mechanical, electric and glass-blowing technologies at this Facility. Representative instruments developed during this fiscal year of 1989 are listed below.

He Cryostat with Cleavage Device.
Water-Cooled Mirror Holders for Synchrotron Radiation Use.
Construction of a new Cryostat for EXAFS Study.
Sample Adjuster for Magnetic Measurement.
Sputtering System for the Ultrafine Particles.
Capillary Waveguide Raman Shifter.
Wiley-Mclaren Type TOF-MS Spectrometer.
An Apparatus for Velocity Distribution Measurements.
A Rotatable Crystal Holder with a Cold Stage.
Beam Source of Metal Clusters and Their Ions.
Ion Optics of Reflectron Time-of-Flight Mass spectrometer.

High Precision Delay Pulse Generator.

MCPD Data Acquisition System.

Interface for Transient Digitizer.

Pulsewidth Stabilizer for Subpicosecond Laser system.

Potentiostat for High-Speed Cyclic Voltammetry.

Molecular Beam Valve Controller.

Transition Sell for EXAFS Studies of Liquid Sample.

Several Type Glow Sell with Jacket.

Ultraviolet Synchrotron Orbital Radiation Facility

The UVSOR light source is usually operated at an electron energy of 750 MeV with an initial current of 150 mA. Single bunch operation has been performed with a frequency of 1 week per 2 months. A new beam line, BL4A has served as a irradiation port for photo-catalysis experiments in the vacuum ultraviolet region. The Activity Report 1989 has been published in this April.

SPECIAL RESEARCH PROJECTS

IMS has special research projects supported by national funds. Three projects presently in progress are:

(1) Development and evaluation of molecular synergistic systems and their application to chemical energy conversion (1985-1990).

(2) Fundamental research of molecular devices (1985-1990).

(3) Molecular science of primordial chemical evolution and selforganization (1987-1991).

These projects are being carried out with close collaboration between research divisions and facilities. Collaborators from outside also make important contributions. Research fellows join these projects. The results in 1989 are reviewed in this report.

(1) Development and Evaluation of Molecular Synergistic Systems and their Application to Chemical Energy Conversion

Dynamical Molecular Structure and Control of Reactive Molecules

Eizi HIROTA*, Chikashi YAMADA, Yasuki ENDO *(Univ. Tokyo and IMS)*, Masaharu FUJITAKE, Haruhiko ITO, Toshinori SUZUKI, and Wyn LEWIS-BEVAN *(Southern Illinois Univ. and IMS)*

Infrared diode laser kinetic spectroscopy was employed to unravel the mechanisms of the $O(^1D)$ or $O(^3P)$ + CH_4 reaction (II-A-2) and also of the CH_3I photolysis (II-A-8), where the CH_3 radical ν_2 bands were mainly employed to diagnose the reactions. This method was also used to study the CDO ν_3 band (II-A-7) and the CCD bands in 2400-2900 cm^{-1} (II-A-12). A molecular-beam apparatus for infrared diode laser spectroscopy was newly constructed to investigate transient molecules of relatively large size (II-B-1). A laser-induced-fluorescence spectrometer was used to detect two Ge-containing transient molecules, HGeCl (II-A-3) and HGeBr (II-A- 4).

(1) Studies on Structure and Dynamical Processes of Highly Excited Atoms and Molecules
(2) Studies of Laser Cooling and Trapping of Atoms

Norio MORITA, Asuka FUJII, and Mitsutaka KUMAKURA

Theoretical analysis on the spectra of doubly excited states of Ca atom so far observed has been continued through the R-matrix calculation as well as the CI-calculation. The behavior of the electron correlation has extensively been investigated by drawing charge density plots. Some quite unusual angular correlation patterns observed in the previous CI-calculations have been confirmed by more precise R-matrix calculations.

On the other hand, experimental studies on highly electronic-excited states of molecules have been started with interest in their autoionizing and predissociating properties. High Rydberg states of the NO molecule have been excited and then the nitrogen atom resulting from the predissociation has been observed through laser multiphoton ionization. With this observation, the dependence of each final state of the nitrogen atom on the initial NO states has extensively been studied.

An apparatus for the laser cooling and trapping of He atom has been constructed. A transition used for the cooling and trapping is the one from a metastable $2s^3S_1$ state to $2p^3P_2$, and its wavelength is 1.083 μm. There is no commercial single-mode lasers which can generate this wavelength with adequate intensity, so that a ring-type single-mode laser with a gain medium of an LNA crystal has also been constructed. Helium atom is so light that adequate cooling of the atom requires too long distance in usual conditions. In our apparatus, therefore, the helium source is cooled by liquid nitrogen, and helium atoms are excited by elec-

tron bombardment to the metastable state. Consequently, a very slow beam (910 m/s) of the metastable helium atoms has successfully been obtained. By using this apparatus, the laser cooling and trapping are now being tried.

Construction of a New Cryostat for in-situ EXAFS Study

Nobuo MIZUTANI, Toshio HORIGOME, Takanori MIZUSHIMA, Kazuyuki TOHJI, and Yasuo UDAGAWA
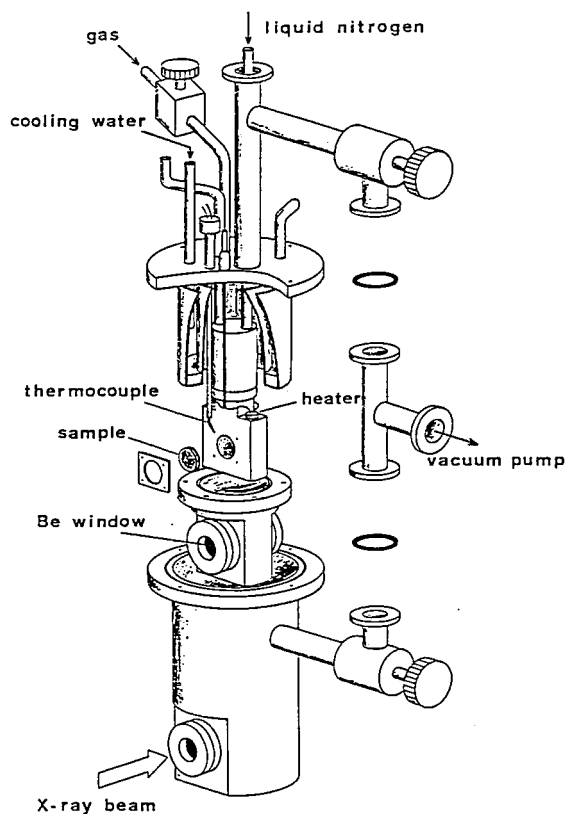
Figure 1. A schematic diagram of the cryostat.

A new cryostat for catalyst study by EXAFS spectroscopy has been constructed. The cryostat, whose schematic diagram is shown in Figure 1, uses liquid nitrogen as a refrigerant and has the following features.

1. It is small enough to fit the space on the crystal monochromators.
2. A series of catalyst treatments, e.g. calcination, reduction, and gas adsorption is possible inside the cryostat without exposing the sample to air.
3. The sample can be heated up to 800 K and can be cooled below 150 K.
4. Liquid nitrogen is continuously fed during scanning of the monochromator, making long data accumulation period possible.

Development of Non-linear Spectroscopy for Studies on Ultrafast Phenomena

Hiromi OKAMOTO, Yoshihiro TAKAGI and Keitaro YOSHIHARA

Firstly, a femtosecond time resolved CARS (coherent anti- Stokes Raman scattering) measurement system has been constructed. The second harmonic of a home made CW mode-locked Nd:YAG laser excites two dye lasers. The linear cavity hybridly mode-locked dye laser produces ultrashort light pulses (~ 595 nm, ≥ 75 fs) and is used as pump and probe pulses for the CARS process. Another ordinary synchronously pumped dye laser ($600 \sim 700$ nm tuneble, ~ 5 ps) is used as a Stokes radiation. The pump, Stokes and probe radiations are focused into the sample, and the resulting anti-Stokes signal intensity is recorded as a function of the delay time between the pump and probe pulses. This system has been used for studies on vibrational relaxation of carotenoids, acetonitrile, etc., and rotational motions of symmetric top molecules in liquid. It is also demonstrated that the method can be applied to properly prepare *in vivo* biological samples. The details are described in III-C.

Secondly a new method of measuring ultrafast light pulses has been developed. Two-photon induced conductivity replaced to the ordinary second harmonic generation in the Michelson-type autocorrelator. Commecial Si and GaAsP photodiodes and a CdS photoconductive cells are used for appropriate wavelength region. The details are described in the Equipment Development Center section.

Picosecond Reaction Dynamics of Excited Molecules in Clusters

Hrvoje PETEK and Keitaro YOSHIHARA

While the understanding of reaction dynamics in

isolated mlecules has greatly advanced in recent years, similar progress in understanding of reaction dynamics in solution awaits development of more powerful experimental and theoretical techniques. A fruitful approach for studying condensed phase reactions is to investigate well characterized solvent - solute clusters under supersonic molecular beam conditions. This approach is particularly useful because it can reveal specific solvent - solute interactions that are otherwise obscured, and because such well characterized systems can be modeled by theoretical methods. We have made preliminary measurements on cis-stibene isomerization in Ar and Kr clusters using picosecond pump-probe techniques (III-A-3 and III-E-1). The dynamics observed in clusters are significantly different than in room temperature solutions, suggesting that this technique may provide new information on this important reaction. In other systems we have made preliminary measurements on solvent effects on intramolecular charge transfer, $S_2 \to S_1$ and $S_1 \to S_0$ internal conversion rates, vibrational relaxation rates, etc. The investigation of these fundamental solution phase processes using picosecond pump-probe techniques on well characterized cluster systems will proceed.

External Magnetic Field Effects upon Chemical Reactions

Masaharu OKAZAKI (Government Industrial Research Inst., Nagoya and IMS), Ryoichi NAKAGAKI, Minoru SUMITANI, and Saburo NAGAKURA (Grad. Univ. for Adv. Studies)

In the present research project, we have investigated magnetic field effects on photo-redox reactions, involving biradical reaction intermediates for a series of bichromophoric chain species. Since extremely small interactions such as the Zeeman energy and hyperfine interaction may give rise to a remarkable change in the product distribution, the magnetic field effects have some potential for application, e.g., control of reaction yields or selection of reaction pathways. Two different intramolecular photoreactions have been observed for p-O_2N-C_6H_4-$O(CH_2)_{12}$-$NBzC_6H_5(Bz=*CX_2C_6H_5, *C=$ ^{12}C or ^{13}C, X=H or D), namely, photo-redox reactions involving benzylic and methylene chain oxidation and nitro to nitroso reduction. The end product ratio

for two competitive processes depends on the magnetic field strength and the nuclear magnetic moments within biradical intermediates.

We have also investigated a mechanism of magnetic field effects on the emission intensity of NO in the $B^2\Pi$ excited state, which was populated through collisional dissociation of N_2O with metastable Ar atoms.

Dynamics in Ion-Molecule Systems

Inosuke KOYANO, Takashi IMAMURA, and Shinzo SUZUKI

In the present research project, we have investigated the gas phase ion-molecule reactions of great interest both in the intersteller chemistry and reaction dynamics. The $C_3H_3^+$ ion, an ubiquitous molecular ion in the mass spectra of hydrocarbons, is considered to play an important role in the formation of the intersteller molecules. The time-of- flight coincidence spectra of $C_3H_3^+$ produced by the reactions of $C_3H_4^+ + C_3H_4$ showed abnormally broad features and seem to consist of at least two broad peaks. These two broad peaks were also observed in the system of $C_3H_4^+$ C_3D_4 and are considered to correspond to the two isomers of $C_3H_3^+$, probably those having cyclic and linear structure.

We have also studied the collisional deactivation of the electronically excited $A^2\Pi$ state of CO^+. The collisions with He are followed by the production of vibrationally relaxed states of $A^2\Pi$ that occurs via an adjacent vibrational level of the $X^2\Sigma$ state. In contrast to the case of He, the charge transfer state of $(CO-Ar^+)$ is found to play an important role in the collisional deactivation of CO^+ $A^2\Pi$ by Ar.

Development of Laser High-Resolution Photoelectron Spectroscopy for Vibrational Analysis of Jet-Cooled Molecular Ions

Katsumi KIMURA, Katsuhiko OKUYAMA, Masatoshi TAKAHASHI, and Hiroyuki OZEKI

Since 1980, in this Institute we have been studying excited-state photoelectron spectroscopy with UV/ visible pulse lasers for jet-cooled molecules as well as

for van der Waals molecules, using a time-of-flight photoelectron analyzer. Photoelectron spectra thus observed are due to specific radiative and non-radiative excited states, providing new information about photophysics and photochemistry (IMS Annual Review, 1980-90).

In the present project, we have been developing a new high-resolution photoelectron analyzer to improve the photoelectron resolution up to a few cm^{-1} (1 cm^{-1}: 0.12 meV). If a photoelectron spectrum is observed in such a high resolution, it is possible to perform vibrational analysis for any molecular ions just like in the infrared spectroscopy of molecuels.

Recently we have succeeded to develop a compact capillary-type analyzer which collects threshold photoelectons in a resolution of 3 cm^{-1} as a function of laser wavelength. This photoelectron analyzer can be used for two purposes: One is to use a vacuum ultraviolet laser to observe photoelectron spectra for ground- state molecules, while the other is to carry out two-color resonant photoionization expriments to observe photoelectron spectra of excited-state molecules. The laser high-resolution photoelectron spectroscopy is now regarded as a "new vibrational spectroscopy". (See IV-F)

Molecular Beam Study of Surface Reaction Dynamics

Kosuke SHOBATAKE, Kiyohiko TABAYASHI, Haruhiko OHASHI, Hiroshi YOSHIKAWA, Kunikazu KONDO, Kenichi KATOH and Yukio INOKUCHI

In the present project we are studying etching reactions of semiconductor (Si and SiO_2) surfaces stimulated by synchrotron radiation or bombarding translationally hot halogen beams with ultimate goals of clarifying their dynamics and further finding ways to control surface reactions. Molecular beam techniques are applied since the state selection of the reactants is relatively easily done under the ultra-clean conditions. As to the synchrotron radiation excited etching reactions of SiO_2 surfaces we have so far found that etching reactions are stimulated by exciting the surface layer of SiO_2 by synchrotron radiation in the atomsphere of echant gas such as SF_6 and F_2. Recently we have found

that etching of SiO_2 occurs even without echant gas present (See IV-K-4). We have constructed detector chambers to detect the nascent species (neutral as well as charged ions) desorbed from the surface irradiated by synchrotron radiation.

We have just finished modifying the molecular beam chemistry apparatus (Model MBC-I) to carry out molecule-surface non-reactive and reactive scattering experiments under ultrahigh vacuum conditions. We wish to accumulate data on the interaction energies between gaseous molecules and solid surface and also measure activation energies for the surface reactions from scattering experiments.

Preparation and Propeties of New Types of Transition Metal Oxide and Sulfide Clusters by Use of Hydrothermal Synthesis

Kiyoshi ISOBE, Yoshiki OZAWA, and Yoshihito HAYASHI

We have synthesized new classes of organometallic oxide and sulfide clusters at ordinary temperature and pressure. They have a novel structure with integrated cubane type framworks and exhibit interesting physicochemical properties, for example, Second Harmonic Generation (SHG), multi stage redox states, and catalysis for the oxidation of hydrocarbons.

In order to prepare the clusters having higher integrated cubane type frameworks, which are supposed to be excellent in optical and electrochemical properties, we are constructing an apparatus for hydrothermal synthesis in cooperation with NIKKISO CO., LTD (Figure 1). The apparatus is designed to use both in aqueous and in nonaqueous solvents. We are carring out the reaction of $[Cp^*RhCl_2]_2$ with ReO_4^- in water.

207

700
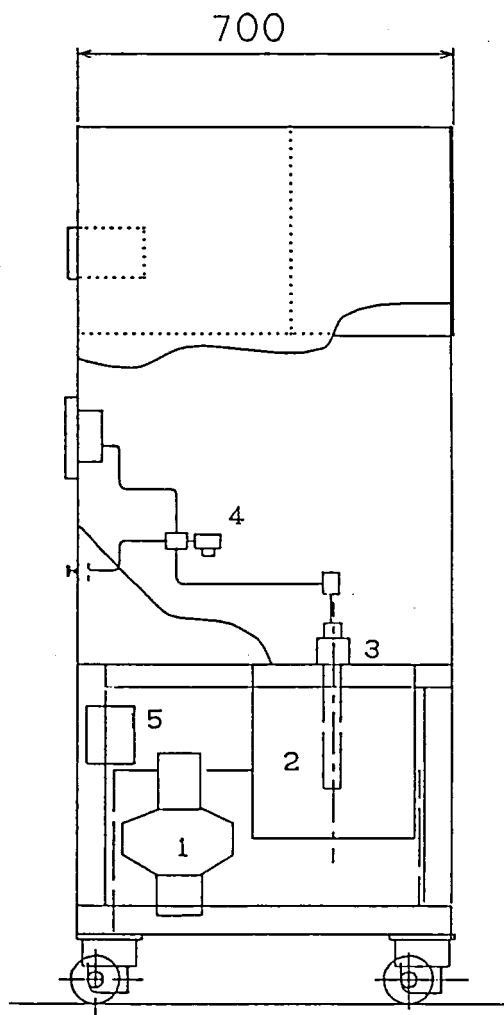
Figure 1. A schematic side view of an apparatus for hydrothermal synthesis. 1: water pump, 2: electric furnance, 3: reactor, 4: safety valve, 5: water tank.

Development of Computer Programs for Molecular Simulations

Kazuo KITAURA

Computer programs has been developed for studying molecular clusters, liquids and solids by the molecular simulations. A new intermolecular potential function, which is expressed by intermolecular overlap integrals and point charge interactions, is employed in the programs.

The programs include;

1. generation of initermolecular potentials based on the *ab initio* MO calculations,
2. geometry optimization for molecular clusters,
3. normal mode analysis and partition function for molecular clusters,
4. lattice energy minimization for molecular crystals,
5. Monte Carlo simulation for molecular clusters and liquids.

The program for molecular dynamics simulations using the new intermolecular potential function is udner development.

Dynamics of Solvated Metal Cluster Ions

Kiyokazu FUKE and Fuminori MISAIZU

Metal ions are intimately involved in chemistry and biochemistry and play a crucial role in many reactions. Although there has been extensive progress in the thermodynamic and kinetic studies of solvated metal ions, the study of microscopic aspect of solvation dynamics has been rather limited. Spectroscopic studies of the solvated metal ion clusters as a specific function of cluster size can provide detailed information on energetic and dynamics of solvation. The advent of mass spectrometer and metal cluster beam techniques in conjunction with laser probes now allow an attack on the problem for the solvation of metal ions and metal cluster ions through studies that probe energy levels and dynamical processes occurring in solvated metal clusters.

In order to investigate the solvation dynamics of metal cluster ions, we have constructed a molecular beam apparatus and an angular reflectron TOF mass spectrometer in collaboration with the Equipment. Development Center of IMS. We adopted a recently developed laser vaporization technique to produce metal cluster ions. The details are described in VII-C.

(2) Fundamental Research of Molecular Devices

Study of Novel Organic Conductors

Hiroo INOKUCHI

We are studying extensively to find new-type organic conductors/semiconductors in single component organic material. In this period, 1989-1990, we found two kinds of single component organic semiconductor. One of them is cytochrome c_{551} derivatives and the other is "quasi-covalent bond" molecular material. Using cytochrome c_{551} film, we found a conductivity jump in the temperature range of 40-60°C. The results of DSC analysis and also infra-red absorption spectra show great changes accompanied with the conductivity jump and these phenomena are reversible.

Elucidation of the Coupling Between the Proton- and Electron-Transfers in Cytochrome Oxidase

Teizo KITAGAWA, Takashi OGURA, Satoshi TAKAHASHI, and Shinya YOSHIKAWA (Himeji Inst. Tech.)

Cytochrom oxidase, the terminal enzyme in the respiratory chain of aerobic organisms, is known to translocate protons through membrane upon the electron transfer from cytochrom c to molecular oxygen. The ratio of the transferred protons to the transferred electrons is reported to be nearly unity. As a part of studies for elucidating the mechanism by which the enzyme holds this stoichiometry, we investigated resonance Raman (RR) spectra of reaction intermediates in this year. The intermediates were generated by using our original "artificial cardiovascular system" and their RR and absorption spectra were monitored at the same time. Upon excitation at 425 nm, we succeeded in observing an oxygen isotope-sensitive band at 569 cm^{-1} for $^{16}O_2$ and 540 cm^{-1} for $^{18}O_2$ for the earliest intermediate and another one at 787 cm^{-1} for $^{16}O_2$ and 748 cm^{-1} for $^{18}O_2$ for a later intermediate. The former and latter were assigned to the $Fe^{II}-O_2$ and $Fe^{IV}=O$ stretching vibrations, respectively. On the basis of the simultaneously observed absorption spectra, we could demonstrate that the compound A and compound B have the $Fe^{II}-O_2$ and $Fe^{IV}=O$ hemes, respectively.

d-π Interaction in Molecular Metals

Kyuya YAKUSHI, Akito UGAWA, Takashi IDA, and Hideo YAMAKADO

Magnetic interaction between conduction electrons and localized spins brings forth sometimes an interesting phenomena such as a Kondo effect and heavy fermion superconductivity. In this special research project we are studying organic materials containing transition metal ions as well as itinerant π-electrons. We have investigated so far the radical salts of metallo-phthalocyanine (MPc) and Cu salts of DCNQI (dicyanoquinonediimine). In the case of phthalocyanine salts, a transition metal is incorporated in the π-conjugated molecule. In the salts of CoPc such as $CoPc(AsF_6)_{0.5}$ having unpaired electrons on the cobalt ions, we found evidence for a strong d-π interaction. We consider that the semiconductive band gap of this salt originates from the ferromagnetic interaction between the antiferromagnetic one-dimensional Co chain and the itinerant π-electron in the ligand chain. In the case of DCNQI salts, Cu ion is tetrahedrally coordinated by cyano groups of four DCNQIs. This salt has been considered a one-dimensional metal. By means of spectroscopic method, however, we verified the strong hybridization between the copper d-orbital and DCNQI π-orbital. The magnitude of the interchain interaction was proved to be much lager than that of $(TMTSF)_2X$.

Fabrication of Novel Organic Molecular Assemblies with the Use of the Molecular Beam Epitaxy Technique

Yusei MARUYAMA, Hajime HOSHI, Naoki NAKAMURA (Toyota Motor Corp. and IMS), and Tamotsu INABE

In order to prepare new materials which could be useful for molecular devices elements, we have started to design and fabricate ultra-thin organic multi-layered systems. In the first place, we have prepared ultra-thin

single component phthalocyanine thin films to investigate epitaxial growth conditions on alkali halide single crystals. Fairly well oriented, uni-or bi-directionally, crystalline films are obtainable on the alkali halide substrates. Based on this kind of mono-film, we are going to fabricate a multi-layered system.

The SHG and/or THG of the films are investigated from the view point of the molecular structure and the epitaxy or orientation of the films.

Fabrication of High T_c Metal Oxide-Superconducting Films by Layer-by-Layer Deposition from Multi-electron-Beam Gun Sources

Toshifumi TERUI and Yusei MARUYAMA

Successive deposition of each component of metal oxides has been undertaken to achieve the layer-by-layer construction for high T_c oxide superconductors. The high vacuum evaporation machine is equiped with three electron-beam guns and it can be operated under a differential pumping when oxygen inclusion is required. As an initial trial, La-Sr-Cu-O system is now investigated.

High Temperature Oxide Superconductors

Masatoshi SATO, Masafumi SERA, Masashige ONODA, Shin-ichi SHAMOTO and Shin-ichi YAMAGATA

Various experimental studies of high-T_c oxides have revealed that they have quite unusual physical properties in their normal states, which stem from their very strong electron correlations, their low carrier densities and the low dimensional nature of the systems. Then, a fundamental question has arisen in the course of the works if the carriers in the systems which exhibit superconductivity can be described by the usual Fermi liquid picture or not. To answer it, has been one of the important issues for the udnerstanding of the supercondsuctivity with the surprisingly high T_c. On the other hand, the rough features of the BCS's mean field type theory with s-wave symmetry, where most behaviors in the superconducting state do not reflect the direct information on the microscopic origin of the Cooper pair formation. Then, it seems to be another important issue

to clarify, through careful and detailed studies, if the superconducting behaviors of the high-T_c oxides have certain characteristic difference from those of ordinary superconductors. If any difference exists, it may become a useful clue to elucidate the mechanism of the superconductivity. Keeping these things in minds, we have continuously carried out the extensive studies both in the normal and the superconducting strates and clarified various subjects which would be important for the description of their electron systems and for the understanding of the high-T_c superconductivity.

Exploration of New Cooperative Proton-Electron Transfer (PET) Systems

Kazuhiro NAKASUJI, Kenichi SUGIURA, Jiro TOYODA, and Yasushi MORITA

From the recent finding of a new phase transition for 1,4-benzoquinhydrone under pressure, which can be assigned to cooperative proton-electron transfer (PET) phenomena, we have developed a general strategy to explore new materials based on quinhydrones characterized as hydrogen-bonded CT complexes. Thus, from the stepwise consideration of the PET phenomena, two reasonable molecular design strategies for realization of such cooperative PET systems in the solid state are revealed; the exploration of (a) a quinone-hydroquinone pair with a smaller intermolecular CT gap and/or (b) an electronic modification to stabilize H-bonded neutral radicals. As a former approach (a), we prepared four extended conjugated quinhydrones, 1,5-dichloro and 1,5-dibromo-2,6-naphthoquinhydrones and 1,6- and 1,8-pyrenoquinhydrones. Smaller energies of the CT gaps were observed for these four quinhydrones compared with that (2.34 eV) of the prototype, benzoquinhydrone. Single crystals of 1,5-dichloro- and 1,5-dibromo-2,6-naphthoquinhydrones were grown by a diffusion method in benzene as black lustrous plates. Their crystal structure analysis showed that these are the first examples of extended conjugated quinhydrones whose characteristic features are similar to benzoquinhydrone. Similarly to benzoquinhydrone, the four quinhydrones have shown pressure-response infrared and electronic absorption spectral characteristics.

Coupled Proton and Electron Transfer in the Crystals of Salicylideneaniline Derivatives and their Complexes

Tamotsu INABE, Hironori OGATA, Naomi HOSHINO *(Hokkaido Univ.)*, Kaoru OKANIWA, Hiroshi OKAMOTO, Tadaoki MITANI, and Yusei MARUYAMA

Our interest in this particular area of research on molecular devices lies in the possibility of furnishing molecular assemblies with novel physical properties through an appropriate modification of the constituent molecules. Proton-transfer process was chosen as the molecule-based function, and its coupling to the assemble-based properties has been investigated. A framework of salicylideneailine has such a function of intramolecular proton transfer. The thermochromic behavior observed in many of the derivatives gives a clue for changes in the π-electron state accompanying the

proton transfer. Thus, the work has been devoted to the crystal structure determination at varied temperature and elucidation of possible cooperation in proton- and electron-transfer processes in the crystal of these compounds by means of optical measurements. Since the assembly-based properties depend largely on the intermolecular interaction, some derivatives have been employed as a donor component of the charge-transfer complexes with various acceptors in order to introduce stronger intermolecular interaction. The structural and optical studies of the complexes have provided the information about the correlation between the proton motion and the electronic state, which suggests possibilities of constructing a novel type of electrical conductors. Similarly, the structures and the optical and electrical properties of some charge-transfer complexes with intermolecular hydrogen-bonds have been studied. Details of the work are given in Section IV-M.

Creation of Intelligent Supermolecules

Eiichi KIMURA *(Hiroshima Univ. and IMS)*, Mitsuhiko SHIONOYA *(Hiroshima Univ.)*, Hiromasa KUROSAKI, Yasuhisa KUROGI *(Hiroshima Univ.)* and Cynthia J. BURROWS *(Univ. of New York at Stony Brook)*

In the current efforts to combine cyclams with other functional molecules to develop efficient photo- and electrocatalysis systems, we have succeeded in the synthesis of a number of novel supermolecular ligands and new prototype of mononuclear or hetello-metallo-bi-

or trinuclear complexes possessing photoactive and/or redox-active metal centers. Ni(II)- cyclam complexes can act as catalysts for the reduction of CO_2 to CO, the oxidation of alkenes to epoxides, and a variety of other interesting transformations. It has become feasible to achieve a wide range of photo- or electrochemical redox-reaction by minute structural modifications with various functionalities.

Photocatalysts

Electrocatalysts
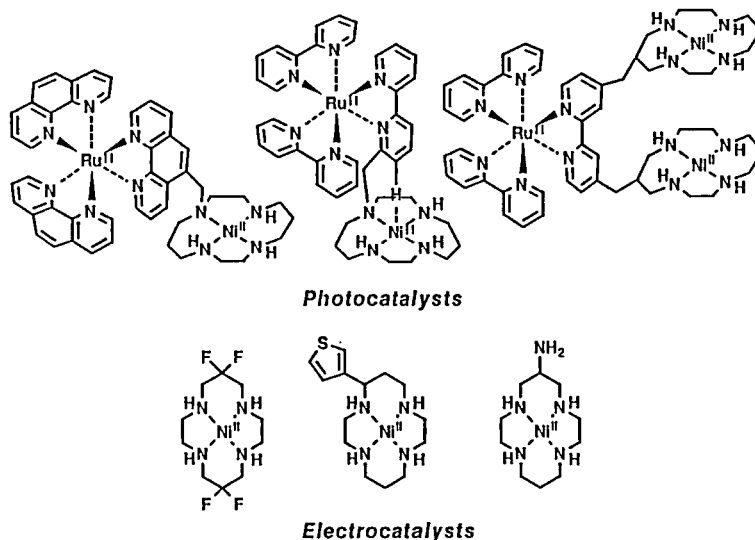
A Study of Ultrafine Particles

Keisaku KIMURA and Shunji BANDOW

Small particles are produced by the gas evaporation method and by the sputtering method conbined with a solution trap giving a dispersion in organic liquids. The ratio of the number of atoms at surface to the total atoms in nm particles exceeds 50% resulting in the enhanced surface effects. We have observed that the NMR line width of ionic crystals of AlF_3 sample was split lines. The smaller the particles, the lower field the chemical shift position becomes. This finding meets the fact that the chemical bonding of ultrafine particles are somewhat covalent and was substantiated by the X-ray photoelectron spectroscopic observation. The sputtering method gave kinds of ultrafine particles with high melting points.

Research of the Electron-Proton Interaction in H-bonded Molecular Crystals

Tadaoki MITANI and Hiroshi OKAMOTO

The H-bonded molecular systems have attracted our attention for design and creation of new molecular functions by using the unique electron-proton interaction.[1] By introducing strong H-bonds into halogen-bridged mixed-valence metal-complexes, a new one-dimensional (1-D) electronic system has been revealed by our IMS's group.[2] (See Figure 1) In this system, the 1-D instability due to the Peirls distortion is completely suppressed for M=Ni, and $X^-=Br^-$ and Cl^-. As the results, the electronic state becomes essentially equivalent to that of the CuO_2 sheet of the high T_c compounds except for dimensionality of the systems, and shows unusual properties, such as a fairly high conductivity (ca. 0.2 S/cm at R. T.) in spite of a large optical gap (ca. 1.3 eV), a highly anisotropic photoconductivity, and an antiferromagnetic coupling of spins with a extremely large J value (J=3600 K).[3] Furthermore, the photo-induced absorption measurement of this system has been successfully made for the first time (see VII-I-2). Further chemical modifications of these complexes for carrier dopping are in progress.

References
1) T. Mitani, *Mol. Cryst. Liq. Cryst.* **171**, 343 (1989).
2) K. Toriumi et al., *J. Am. chem. Soc.* **111**, 2341 (1989).
3) H. Okamoto et al., *Phys. Rev. B.*, in press.
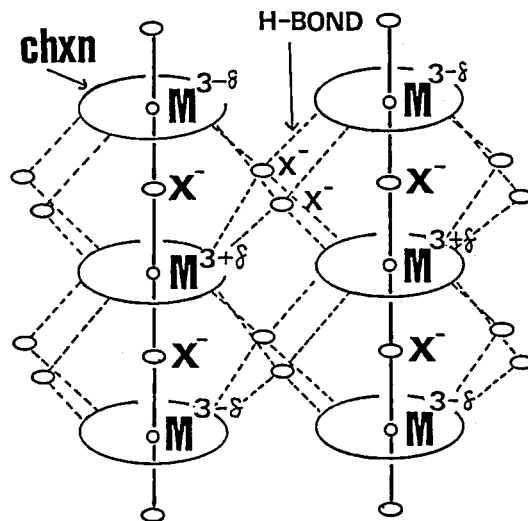
Figure 1. Schematic structure of the halogen-bridged metal complex having strong H-bonds ([M(chxn)$_2$X]X$_2$: chxn=cyclohexanediamine).

Ferromagnetism in Organic Molecular Solids

Kunio AWAGA and Yusei MARUYAMA

The study of ferromagnetic interaction in organic molecular solids is basically important to develop organic ferromagnets. We have chosen single crystal systems of organic radicals in which the ferromagnetic interaction is involved and of which structure can be well defined. Details of the work are described in VII- section.

(3) Molecular Science of Primordial Chemical Evolution

Synchronization of Chemical Oscillators

Yoshihito MORI, Minoru YOSHIMOTO *(Nagoya Univ.)*, Kenichi YOSHIKAWA *(Nagoya Univ.)*, and Ichiro HANAZAKI

Synchronization is well known in coupled nonlinear oscillators in physics and in coupled heart cells or plasmodia of Physarum polycephalum in biology. Synchronization appears in various ratios of frequencies of two or more coupled oscillators. Although several experimental results have been reported for two coupled chemical oscillators, the chemical nature of the coupling has not been clarified. We have focused here on two coupled oscillator modes (in phase and out of phase) in the 1:1 synchronization. Two CSTR's (continuously stirred tank reactors) are controlled independently by changing temperature, residence time and the reactor volume. Two reactors are then coupled by exchanging the solution between the reactors by a pump in order to control the coupling quantitatively. This reactor configuration is important to observe the relative stability of the two modes which may depend on the coupling and the ratio of the characteristic frequencies of oscillations in two reactors. Figure 1 shows typical results of synchronization for the in phase(a) and out of phase(b) couplings in the 1:1 ratio of two chemical oscillators containing the Belousov-Zhabotinsky solution. These systematic experiments would allow us to elucidate the mechanism of chemical coupling in the synchronization phenomenon.
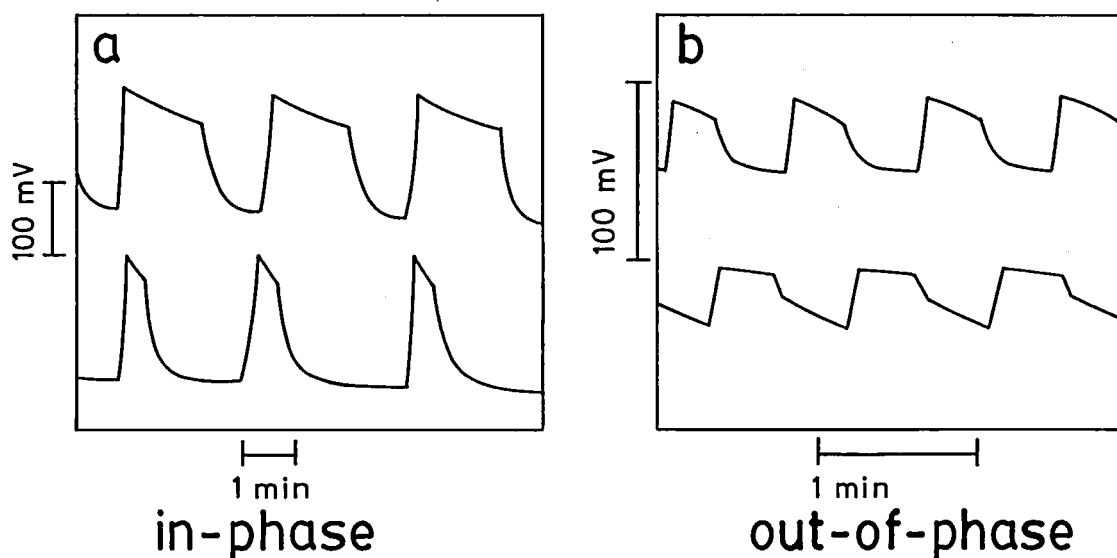
Figure 1. Synchronizaion of two chemical oscillators. Component chemicals are input into each reactor with initial concentrations of $[KBrO_3]_0$=0.1 M, [malonic acid]$_0$=0.1 M, $[Ce^{4+}]_0$=1 mM, $[H_2SO_4]_0$=1.5 M. (a) Residence times=20 min(upper) and 10 min(lower), exchage rate=3.3 ml/min, T=25°C; (b) Residence time=10 min, exchage rate=1.6 ml/min, T=35°C(upper) and 25°C(lower).

Photoinhibition in Uncatalysed Bromate Driven Oscillator: Rhodamine B Base/BrO$_3^-$/H$_2$SO$_4$ system

Prem Kumar SRIVASTAVA, Yoshihito MORI and Ichiro HANAZAKI

Uncatalysed chemical oscillations have been found in the Rhodamine B base/BrO$_3^-$/H$_2$SO$_4$ system in a batch reactor. The oscillation was found to be inhibited by light irradiation. A decrease of oscillation frequency was observed with moderate intensity. On increasing light intensity the oscillation was completely abolished beyond a critical value. The transition between the os-

cillatory state and steady state was found to be reversible. Wavelength dependency of the critical light intensity required to inhibit the oscillation was measured as in the figure(1d) together with absorption spectra of the oscillatory solution(1c), Rhodamine B Base in water(1a) and in acidic solution(1b). The intense peak at 556 nm in the acidic solution disappeared immediately after addition of BrO_3^- and a weak band probably due to a trace of residual dye appeared at 550 nm in the reaction mixture. The two additional absorption bands were observed at 342 nm and 265 nm which appeared instantaneously after mixing of BrO_3^- and decreased exponentially with time during the course of reaction. The wavelength dependency for the inhibition of oscillation indicates that the inhibition is effective for the intermediate band at 342 nm and 265 nm and negligibly small for visible light. The effect seems to be more pronounced for shorter wave length bands.
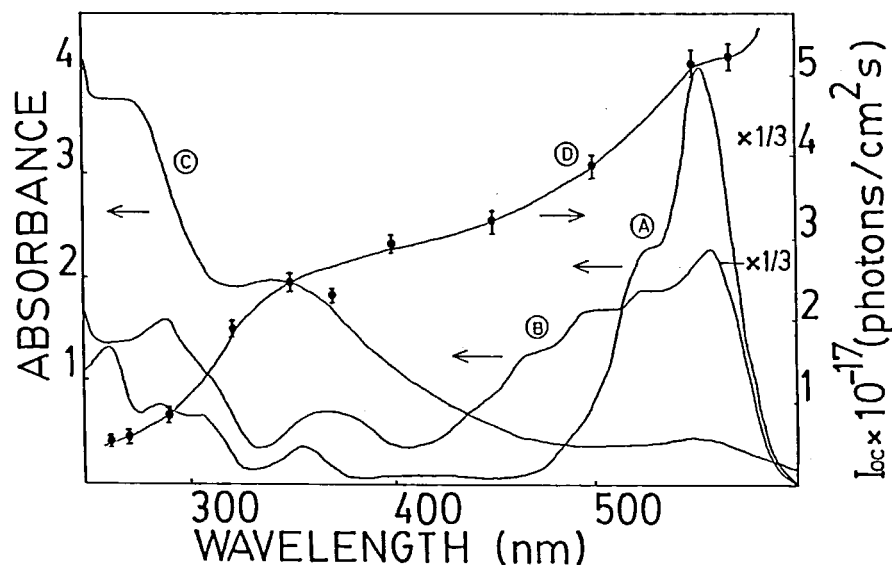
Figure 1. Wavelength dependence of critical intensity and absorption spectra.
(A) Absorption spectrum of Rhodamine B Base (0.00287M) in water.
(B) Absorption spectrum of Rhodamine B Base (0.00287M) in (1.5M) H_2SO_4.
(C) Absorption spectrum of reaction mixture for the chemical composition Rhodamine B Base (0.00287M), BrO_3^- (0.0265M) and H_2SO_4 (1.5M).
(D) Wavelength dependence of critical light intensity for the reaction mixture with the same chemical composition as in (C) at 25°C.

Spectrophotometric Oscillations in Uncatalyzed Bromate Driven Oscillators

Prem Kumar SRIVASTAVA, Yoshihito MORI and Ichiro HANAZAKI

Uncatalyzed bromate driven B-Z chemical oscillations have been reported in terms of redox potential, Br^- potential and temperature in a number of phenol and aniline derivatives, but it is not known that which species correspond to redox potential oscillation. We have found an optically detectable oscillating intermediates in the phenol-BrO_3^--H_2SO_4 and aniline -BrO_3^--H_2SO_4 systems. On addition of BrO_3^- to the acidic solution of phenol, the absorption band of phenol at 210 nm and 270 nm disappeared immediately and three new bands appeared at 244 nm, 290 nm and 388 nm. The absorption intensity of 388 nm band was increased during the induction period and then decreased in an oscillatory manner and finally disappeared. Oscillation in absorbance of this band was found to be in phase with redox potential oscillations as shown in the figure. This oscillating intermediate was assumed to be phenoxy radical. The oxidation-reduction step between phenol and this radical was suggested to be responsible for the redox potential oscillations. On the other hand, in the case of the aniline-BrO_3^--H_2SO_4 system, the intensity of aniline band at 252 nm increased and a new band appeard at 320 nm on addition of BrO_3^- to the acidic solution of aniline. The intensity of 320 nm intermediate band was increased in

an oscillatory manner and then decreased.
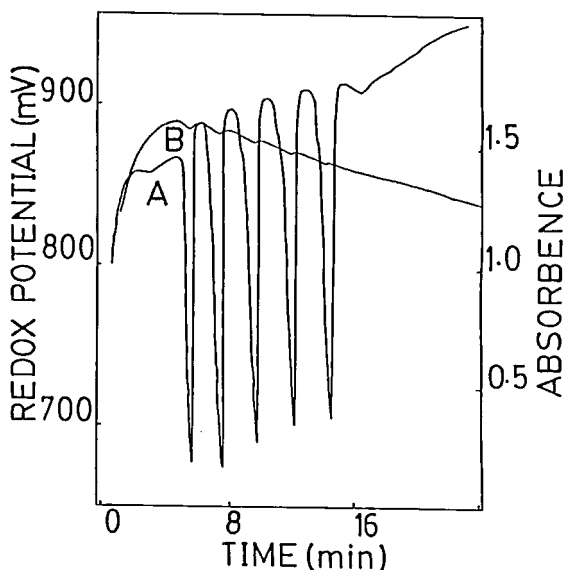
Figure 1. (A) Uncatalyzed chemical oscillation for phenol at 25°C: phenol (0.002M), BrO$_3^-$ (0.025M) and H$_2$SO$_4$ (1.0M). (B) Uncatalyzed chemical oscillation in absorbance for the phenol system at 25°C for the chemical composition given in (A). The reaction mixture volume is 2.5 ml and the optical path length is 1.0 cm. The time scale is measured from the time of addition of the BrO$_3^-$ solution.

Self-Association, Micro-Micelle and Lamellar Structure Formation of Solute Molecules in Aqueous Solutions

Nobuyuki NISHI and Kazunori YAMAMOTO

Development of a new tool has made it possible to analyse the molecular compositions of strongly associated solute-solute or solute-solvent aggregates so that we can now discuss about the structural specificity and the origin of the aggregation of various molecules in aqueous environment. In the early stage of this project we found that the water molecules in acetonitrile exist mostly in the form of water clusters associated with acetonitrile molecules at the surface sites of the clusters. In particular, linear-chain type clusters were expected in the low water concentration region of X$_w$ < 0.05. Two types of amphiphilic substances, such as alkyl alcohols and alkyl carboxylic acids were shown to self-associate with the aid of water molecules. When water partial volume becomes to be less than 50%, the solute-associates tend to be dissociated and mostly small solute clusters (dimer and trimers) were found.

Water medium is indispensable to the formation of large solute clusters. Enthalpy and entropy changes for the association process of A$_m$(H$_2$O)$_n$ + A(H$_2$O)$_{n'-1}$ $\rightleftarrows$ A$_{m+1}$(H$_2$O)$_{n-1}$ + (H$_2$O)' were obtained for m=1 ~ 5 in the system of alkyl carboxylic acids. With increasing m, the enthalpy change stayed nearly constant, while the entropy change on the association reaction increased rather drastically for larger m values. This increase of entropy is ascribed to the destruction of hydrogen bonding networks of pure water clusters. Thus the solute association is not "self"- association. In t-buthlalcohol-water mixtures, micro-micelle type solute association was deduced from the mass spectrometric analysis. Mixture of ethanol and water with the mixing ratios of 1:10 ~ 1:1 presented a common spectral pattern which suggests the existence of lamellar type structure of hydrophobic and aqueous layers.

Self-organization of Ions and Molecules in Solutions under High Pressures and High Temperatures

Hitoshi OHTAKI, Toshio YAMAGUCHI *(Fukuoka Univ. and IMS)*, Georg JOHANNSON *(Roya. Inst. Technol., Sweden and IMS)*, Nobuhiro FUKUSHIMA *(Tokyo Inst. Technol. and IMS)*, and Kenji WAIZUMI *(Tohoku Univ. and IMS)*

Ordering and organization of ions and molecules in solutions have mostly been investigated at room temperature and under an atmospheric pressure and extremely limited information has been presented for intermolecular interactions in solutions under high pressures and high temperatures. In this project we have undertaken to study structures of liquids and aqueous electrolyte solutions under supercritical conditions. A high-pressure-high-temperature cell which can be used up to 400°C and 8000 atmospheric pressures was made and set up on an X-ray diffractometer equipped with a rotatory anode. Tests of the cell and the whole apparatus for X-ray diffraction measurements of solutions are being examined.

Novel Electron Donors and Acceptors Containing Fused-heterocycles

Yoshiro YAMASHITA, Shoji TANAKA, and Masaaki TOMURA

Electron donors and acceptors containing fused heterocycles such as thiadiazole and pyrazine are of interest since the presence of the fused heterocycles enlarges the π-electron ring system and reduces Coulmbic repulsion. Intermolecular interactions can be also expected by heteroatom contacts. We have now prepared several novel compounds containing a fused [1,2,5]thiadiazole and the selenium analogues. For example, 4,7-dimethyl-4,7-dihydro[1,2,5]thiadiazolo-[3,4-b]pyrazine is a strong electron donor with a low oxidation potential due to the 12 π-electron ring system although it has an electron withdrawing heterocycle. The thiadiazole ring in this compound plays an important role in enhancing the stability of the ring system and forming a unique molecular assemble which was revealed by an X-ray crystal analysis. The benzo derivative with 16 π-electron ring system was also prepared. The first oxidation potential is almost the same with that of dibenzo-TTF. A naphthoquinone fused with a thiadiazolopyrazine and its selenium analogue are novel quinones in which electrons are first accepted at the heterocyclic part upon reduction. Details of these works are described in VII-B section.

OKAZAKI CONFERENCES

"Okazaki Conferences" are principal symposia at IMS, which are held on the subjects related to the "Special Research Projects". They are held two or three times a year, with a moderate number of participants around 50, including several invited foreign speakers. The formal language for the conference in English. Outlines of the thirty-sixth and thirty-seventh conferences are as follows.

The Thirty-sixth Okazaki Conference

Novel Solid State Phenomena Induced by Hydrogen-Electron Cooperation
(November 13-15, 1989)

Organizers: **T. MITANI** *(IMS)*, **T. ENOKI** *(Tokyo Inst. Tech.)* and **Y. NAKASUJI** *(IMS)*
Invited Speakers: **A.J. Epstein** *(Ohio State Univ.)*, **J. Halpern** *(Univ. Chicago)*, **S.I. Chan** *(California Inst. Tech.)*, **T. Haeberlen** *(Max-plank Inst.)*, and **F. Fillaux** *(C.N.R.S.)*

The main subject of the conference was to predict and control the behavior of "hydrogen in solids": (1)

Background and/or prospect of hydrogen-electron (H-E) interaction in solids, (2) H-E interaction in metals or graphite, (3) Solid state phenomena related with H-bonding, (4) H-E interaction in metal complexes, (5) Porton and electron transfer in biological system, and (6) design of molecules and molecular assemblies for H-E interaction systems. The conference provided a good opportunity for researchers in different fields to exchange information and to gain insight into the unique H-E intraction in solids. Simultaneously, this Okazaki conference greatly contributed to make a nucleus for the studies of "Novel Solid State Phenomena Induced by H-E Cooperation".
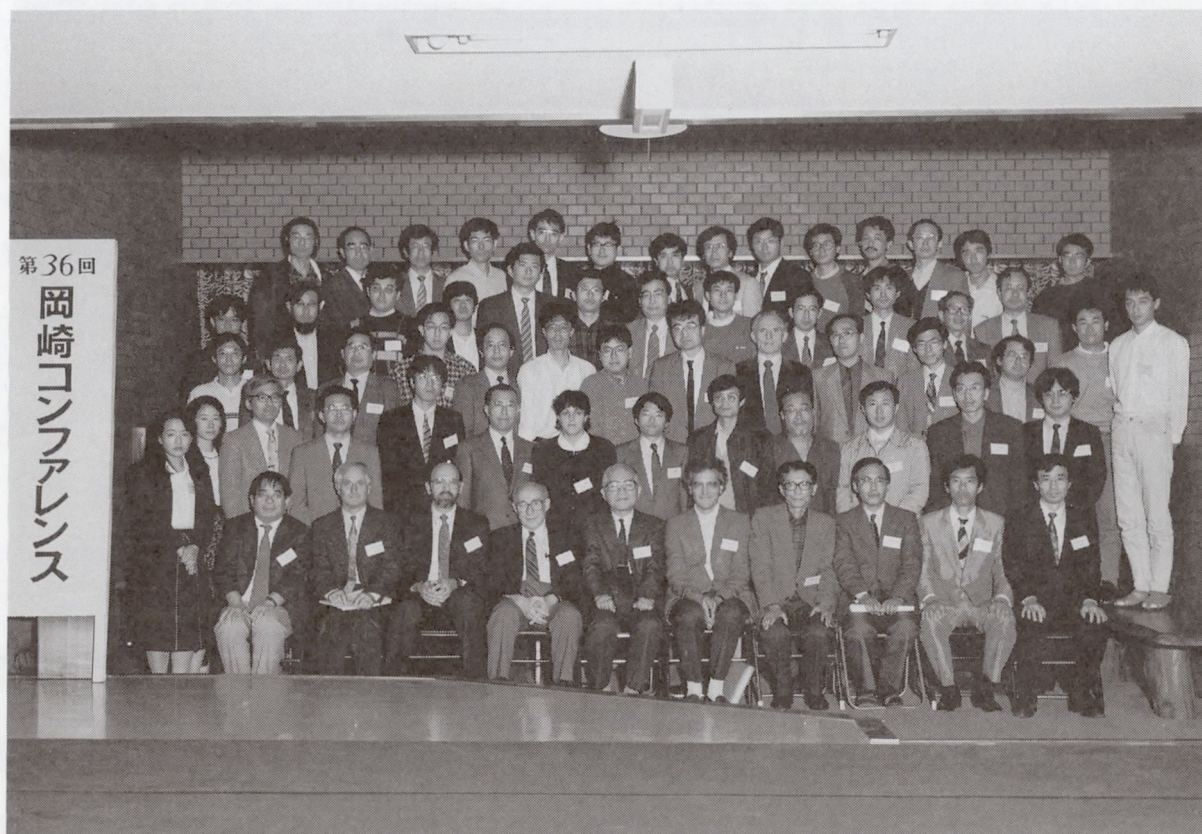
The Thirty-seventh Okazaki Conference

High Temperature Oxide Superconoductors -Materials and Mechanism of the Superconductivity-
(February 13-15, 1990)

Organizers: J. TANAKA *(Nagoya Univ.)*, **F. TAKEI** *(Univ. Tokyo)*, **and K. KITAZAWA** *(Univ. Tokyo)*
Invited Speakers: T. TÍMUSK *(McMaster Univ.)*, **N.P. Ong** *(Princeton Univ.)*, **F.J. Himpsel** *(IBM)*, **N. NÜCKER** *(Kernforshungszentrum Karlsruhe)*, **J.M. TRANQUADA** *(Brookhaven National Lab.)*, **and C. VETTIER** *(ILL)*

It is one of the most interesting and challenging tasks in the scientific research area to properly describe the normal state properties of the high temperature superconductors and to understand the mechanism of the superconductivity. The conference was hold to exchange the information and discuss on the materials and the physical properties of these oxides.

Although much attention was paid to special experimental studies such as neutron scattering and photoemission in the selection of the invited speakers from abroad, the domestic participants were chosen from almost all area of the basic physical research. All of them eagerly discussed this difficult but quite attractive subject for three days.

JOINT STUDIES PROGRAMS

As one of the important functions of an inter-university research institution, IMS undertakes joint studies programs for which funds are available to cover research expenses as well as travel and living expenses of individuals. The proposals from domestic scientists are reviewed and controlled by the inter-university commitee. The programs are carried out under one of five categories:

1) Joint Studies on special projects (a special project of significant relevance to the advancement of molecular science can be carried out by a team of several groups of scientists).
2) Research Symposia (on timely topics in collaboration with both outside and IMS scientists).
3) Cooperative Research (carried out in collaboration with both outside and IMS scientists).
4) Use of Facility (the Computer Center, Instrument Center and other research facilities at IMS are open to all researchers throughout the country).
5) Joint studies programs using UVSOR facilities.
   a) Special Project, b) Cooperative Research, c) Use of UVSOR Facility.

In the fiscal year 1989, numbers of joint studies programs accepted amounted to 1, 9, 137 and 240 for categories 1)-4), respectively and 2, 21 and 107 for 5a)-5c), respectively.

1) Special Projects

Studies of Elementary Chemical Reaction Processes by Development of New Spectroscopic Methods

Coordinators: Soji TSUCHIYA *(Univ. Tokyo)*, Seiichiro KODA *(Univ. Tokyo)*, Okitsugu KAJIMOTO *(Univ. Tokyo)*, Yasuki ENDO *(Univ. Tokyo and IMS)*, Kaoru YAMANOUCHI *(Univ. Tokyo)*, Eizi HIROTA, and Hiroki NAKAMURA

This research project aims at development of new spectroscopic methods which enable us to open a new field in chemical kinetic studies.

1. Generation of Tunable Vacuum Ultraviolet (VUV) laser and Its Application to Spectroscopic and Kinetic Studies.

Intense and tunable VUV laser has been generated by 2-photon resonant 4-wave mixing of visible or ultraviolet laser beams in a non-linear medium. We have found that the convenient non-linear media for the 200-170, 170-145, 145-120, and 125-115 nm regions are Sr, Mg, Kr, and Hg, respectively. The generated coherent VUV light has a resolution of 0.05 cm^{-1} with use of etalons for the fundamental lasers and that of 0.5 cm^{-1} without etalons. The conversion efficiency of the fundamental lasers is about 10^{-3}.

The C-X and D-X bands of XeRg(Rg = Ne, Ar, and Kr) van der Waals complexes in the VUV region are observed to determine the interatomic potentials.[1] The similar studies are made also on the C-X transitions of HgRg.[2] In some electronically highly excited van der Waals complex, the interatomic distance of the complex takes a value comparable or smaller than the diameter of the electron orbit. this suggests a picture that the complex is close to an ionic dimer with an electron surrounding it.

The detailed interatomic potential of Cl_2 in the optically allowed state $^1\Sigma_u^+$ is determined from the REMPI spectrum in the VUV region considering interactions between the ion-pair and the Rydberg state.[3]

The photofragment excitation (Phofex) spectra of $O(^3P_j)$ from NO_2 is observed by monitoring the LIF of $O(^3P_j)$ in the VUV region. The spectrum shows a clear wavelength threshold of the photolysis laser light which corresponds to the energy requirement for formation of $O(^3P_j)$ + NO(Ω=1/2, v, J). Moreover, a complicated level structure is found in the Phofex spectra indicating that excited NO_2 predissociates. The j distribution of $O(^3P_j)$ is dependent on these predissociating levels, and differs from the statistical one.

2. Microwave Kinetic spectroscopy of Reaction Kinetics of Atomic Oxygen with Olefins.

O(^{3}P) atom reactions with ethylene, propylene and 1-butene are studied by measuring time evolutions of vinoxy, HCO and H_2CO through the microwave spectroscopy. A reaction scheme has been concluded as follows. Initially a triplet biradical is produced through O(^{3}P) attack to the terminal carbon atom of the C=C double bond, which is then converted to a signlet biradical. Subsequently, a hydrogen atom migrates and then the C-C bond adjacent to the original C=C double bond dissociates to yield the vinoxy and corresponding alkyl radicals.[4]

3. UV Laser-Microwave Double Resonance Spectroscopy of Electronically Excited Molecules.

In order to discuss electronic excitation of a rotationally state-selected molecule, the UV laser-microwave double resonance method is developed. The method is first applied to the C-X transition of SO_2. A number of level splittings are found for a single vibronic level of $SO_2(\widetilde{C})$ whose rotational state is chosen to a certain specific level. These splittings are dependent on the rotational state of $SO_2(\widetilde{X})$. The data enable us to discuss the details of the coupling scheme in the SO_2 $\widetilde{C}$ state.

The same method is applied to observation of the predissociation rate of $NH_3(\widetilde{A})$ as a function of the initial rotational state. The predissociation rate is clearly determined from the line broadening. The rate increases at higher J's independent of K.[5]

References
1) T. Tsuchizawa, K. Yamanouchi, and S. Tsuchiya, *J. Chem. Phys.* **92**, 1560 (1990).
2) T. Tsuchizawa, K. Yamanouchi, and S. Tsuchiya, *J. Chem. Phys.* **89**, 4646 (1988).
3) T. Tsuchizawa, K. Yamanouchi, and S. Tsuchiya, *J. Chem. Phys.* **93**, 111 (1990).
4) S. Koda, Y. Endo, S. Tsuchiya, and E. Hirota, *J. Phys. Chem.* to be published.
5) Y. Endo, M. Iida, and Y. Ohshima, *Chem. Phys. Lett.* to be published.

2) Research Symposia

1. Construction of Novel Conjugate Electron System in Search of Novel Material with Novel Properties
   (December 5th-7th, 1989)
   Organizer: K. Nakasuji (IMS)
2. Electronically Highly Excited States of Atoms and Molecules—Electron Correlation and Dynamical Processes
   (March 19th-20th, 1990)
   Organizer: M. Matsuzawa (The Univ. of Electro-Communications and IMS)
3. Mini-Symposium on TTC_nTTF
   (February 24th-25th, 1990)
   Organizer: Y. Maruyama (IMS)
4. Design and Construction of Organic Constituent Molecules in Fundamental Material Science
   (March 23rd, 1990)
   Organizer: K. Nakasuji (IMS)
5. Electron Correlation and Electron-lattice Interaction in One-dimensional Systems
   (March 26th, 1990)
   Organizer: T. Mitani (IMS)
6. Symposium on Theoretical Chemistry for the Younger Generation in Molecular Science
   (May 29th, 1990)
   Organizer: T. Kato (Kyoto Univ.)
7. Setup for Promotion of Chemical Research
   (June 23rd, 1990)
   Organizer: H. Inokuchi (IMS)
8. New Metal Complexes and Their Properties in Solid Phase
   (July 14th, 1990)
   Organizer: K. Yakushi (IMS)
9. Is It Possible to Synthesize Super-molecular Multi-dimensional and Multi-functional Compounds by Utilizing Metal Complexes?
   (August 25th, 1990)
   Organizer: K. Isobe (IMS)

3) Cooperative Research

This is one of the most important programs IMS undertakes for conducting its own research of the common interest to both outside and IMS scientists by using the facilities at IMS. During the first half of fiscal

year of 1989 ending on September 30, 64 outside scientists including 1 invited collaborated with IMS scientists; and during the second half of the fiscal year, 73 outside scientists worked in collaboration with IMS scientists, the names and the affiliations of these collaborators are found in the Research Activities.

4) Use of Facility

The number of projects accepted for the Use of Facility Program of the Computer Center during the fiscal year of 1989 amounted to 156 (503 users), and the computer time spent for these projects is 5444 hours (converted to the HITAC M-680 time), and amounts to 51% of the total annual CPU time used.

Seventy nine projects (220 users) were accepted for the Use of Facility Program of the Instrument Center during the fiscal year of 1989.

5) UVSOR

Joint studies programs using UVSOR facilities are carried out under one of three categories: 5-a) UVSOR Special Project, 5-b) UVSOR Cooperative Research, and 5-c) Use of UVSOR Facility.

The 11th UVSOR Research Symposium, organized by K. Kimura (IMS), was held during December 8th-9th, 1989.

5-a) UVSOR Special Project

Analysis of the Electronic Structures of Molecular Assemblies with Photoelectron Spectroscopy Using Synchrotron Radiation

Coordinators: **Kazuhiko SEKI** *(Hiroshima Univ. and IMS),* **Makoto WATANABE** *(UVSOR Facility)*

This year was the final year of the 3 year project of using the angle-resolving photoelectron spectrometer at the beamline 8B2 for the analysis of the electronic structures of organic molecular assemblies. Successful measurements were carried out on the following subjects, thanks to the efforts of Drs. H. Fujimoto and K.

Kamiya who took care of the instruments.

(i) Vinylthiophene oligomers embedded in Langmuir-Blodgett (LB) films or Cd stearate: This subject is an extension of the study of oligothiophenes and vinylene-including oligothiophenes, which serve as good models for elucidating the evolution of the electronic structure of polythiophene and the effect of disorder. This spectra showed some angle dependence, reflecting the molecular orientation.

(ii) LB films of Cu tetrakis(n-butoxycarbonyl)phthalocyanines: In these films, molecules are oriented even in the azimutal angle. The spectra showd anisotropy by the rotation around vertical axis to the substrate. Analysis of these results are now underway.

(iii) Lu phthalocyanine and poly(Al phthalocyanine fluoride): In the former, the splitting of the highest occupied molecular orbital of phthalocyanine by the interring interaction has been observed. The latter showed rather similar spectra of other phthalocyanines.

(iv) Poly(p-phenylene) evaporated films: the density of states of the topmost valence band region has been clearly observed, with consistent results with those estimated from the data for oligomers.

Also studies has started on perylenetetracarboxylicacid dianhydride and poly(perynaphthalene), indicating some interesting results.

Through the three year term, the electronic structures of many interesting molecular and polymeric solids have been clarifield. The next step will be more detailed studies of films grown on well characterized surfaces, and improvements of the instruments in this direction has started.

Photo-Induced Transient Spectroscopy of Organic Solids

Tadaoki MITANI, Hiroshi OKAMOTO, and **Youji ACHIBA** *(Tokyo Metropolitan Univ. and IMS)*

Delay-time modulation spectrometer using a cw mode-locked Nd:YAG laser synchronized with the synchrotron radiation (SOR) from an electron storage-ring has been constructed for the first time.[1] An application of this technique to IR photo-induced absorption measurements on organic materials, such as polyacetylene films, has been successfully made under an irradiation of the laser. The spectra obtained by

steady-state laser excitations were almost in agreement with those previously reported. However, reliable time-resolved IR signals could not be detected due to the weak photon-flux of the SOR pulses. To improve this experimental situation, the FT-IR spectrometer, which is expected to lead to an effective increase of SOR flux by two orders of magnitude, has been constructed at the UVSOR IR beam line. As an experimental test of the ability of the FT-IR system, the photo-induced absorption spectra of one-dimensional halogen-bridged metal complexes have been measurd by using a conventional IR light source. (see VII-I-2) This results indicate that the transient photo-induced absorption measurements with a time resolution of ca. 500 ps might become possible by a combination of the FT-IR spectrometer and the SOR in a low energy region down to the far IR (ca. 50 cm^{-1}).

Reference
1) T. Mitani et al., *Rev. Sci. Instrum.* **60**, 1569 (1989).

5-b) UVSOR Cooperative Research

During the first half of fiscal year of 1989, 11 outside scientists including 2 invited collaborated with IMS scientists; and during the second half of the fiscal year, 10 outside scientists worked in collaboration with IMS scientists.

5-c) Use of UVSOR Facility

The number of projects accepted for the Use of UVSOR Facility Program during the fiscal year of 1989 amounted to 53.

FOREIGN SCHOLARS

Vistors from abroad play an important role in research activities and are always welcome at IMS. The following is the list of foreign scientists who visited IMS in the past year (Aug. 1989-July 1990). The sign *1 indicates an attendant to an Okazaki Conference, *2 an IMS or Japan Society for the Promotion of Science Invited Foreign Scholar, *3 an IMS councillor, *4 an IMS visiting scientist and *5 an IMS adjunct professor or associate professor from abroad (period of stay is from 9 to 12 months). Scientists who wish to visit IMS under programs 2 and 5 are invited to make contact with an IMS faculty in a related field.

Dr. P.K. Srivastava*2	Dept. of Chem., Bauaras Hindu Univ.	(India)	Apr. 1989 -
Prof. J.L. Sessler	Univ. of Texas at Austin	(USA)	Aug. 1989
Dr. V. Zhulego	Phys. Dept., Moscow State Univ.	(USSR)	Aug. 1989
Dr. M. MacDonald*2	Daresbury Lab.	(UK)	Aug. 1989
Dr. S.S. Ramamurthi*2	Centre of Advanced Tech., Indore	(India)	Aug. 1989
Prof. A.J. Ashe, III	Univ. of Michigan	(USA)	Aug. 1989
Dr. M.H. Palmer	Univ. of Edinburgh	(UK)	Aug. 1989
Prof. Y. Petroff	LURE	(France)	Aug. 1989
Dr. J.H.D. Eland	Univ. of Oxford	(UK)	- Aug. 1989
Dr. E.I. von Nagy-Felsobuki	Univ. of Newcatle	(Australia)	- Aug. 1989
Dr. E. Anni*4	Training Program of EC committee	(Greece)	Aug. 1989 - Feb. 1990
Prof. S.L. Anderson *2	State Univ. New York at Stony Brook	(USA)	Aug. 1989 - Feb. 1990
Dr. C.J. Burrows	State Univ. of New York at Stony Brook	(USA)	Aug. 1989 - Feb. 1990
Prof. X.-Z. You	Nanjing Univ.	(China)	Aug. - Sep. 1989
Prof. W. Lewis-Bevan*2	Southern Illinois Univ.	(USA)	Aug. - Nov. 1989
Dr. I.G. Luneau	LIESG, Domaine Univ.	(France)	Aug. - Dec. 1989
Prof. J. Hudecek	Charles Univ.	(Czechoslovakia)	- Aug. 1990
Dr. Yonfang Li*4	Inst. of Chem., Acad. Sinica	(China)	Aug. 1989 -
Prof. P. Rosmus*2	Univ. of Frankfurt	(FRG)	- Aug. 1989
Prof. Byoung-Jip Yoon*2	Kanreng Natl. Univ.	(Korea)	- Aug., Dec. 1989 - Jan. 1990
Dr. J. Frey	Southampton Univ.	(UK)	Sep. 1989
Prof. Zhang Wu	HESYRL, Chin. Univ. of Sci. & Tech. (CUST)	(China)	Sep. 1989
Prof. Feng Lan Lin	HESYRL, CUST	(China)	Sep. 1989
Prof. Guo Cong Liang	HESYRL, CUST	(China)	Sep. 1989
Dr. A. Andronais	CNRS	(France)	Sep. 1989
Prof. H. Bock	Univ. of Frankfurt	(FRG)	Sep. 1990
Prof. Jiang, Fenglin*2	Fudan Univ.	(China)	Sep. - Oct. 1989
Mr. Fushi Zhang*4	Tsinghua Univ.	(China)	Sep. - Dec. 1989
Dr. L.S.P. Mirashi*4	Poona Univ.	(India)	Sep. - Dec. 1989
Prof. A.V. de Miguel*2	Univ. of Alcala de Henares	(Spain)	- Sep. 1989
Prof. P. Gütlich*2	Johannes Gutenberg Univ.	(FRG)	Oct. 1989
Prof. W. Linert*2	Tech. Univ. of Vienna	(Austria)	Oct. 1989
Dr. T. Amano	NRC	(Canada)	Oct. 1989
Prof. J.H. Espenson	Iowa State Univ.	(USA)	Oct. 1989

Prof. R. Poilblanc	Univ. Paul Sabatier - Toulouse	(France)	Oct. - Nov. 1989
Miss R. Howell	Imperial College	(UK)	Oct. - Dec. 1989
Dr. Li, Zhen Xiauy[2]	Changchun Inst. of Appl. Chem.	(China)	Oct. - Dec. 1989
Prof. R. Ramaswamy[5]	Jawaharlal Nehru Univ.	(India)	Oct. 1989 - May, Jul. - Aug. 1990
Prof G. Johansson[2]	Dept. of Inorganic Chem., Royal Inst. of Tech.	(Sweden)	Oct. 1989 - Sept. 1990
Prof. Chen. Cong Xiang	CUST	(China)	Nov. 1989
Prof. K.H. Welge	Univ. Bielefeld	(FRG)	Nov. 1989
Dr. L.E. Brus	AT & T Bell Lab.	(USA)	Nov. 1989
Prof. Mu-Shik Jhon	KAIST	(Korea)	Nov. 1989
Prof. E.F. Hayes	Rice Univ.	(USA)	Nov. 1989
Prof. B.M. Deb[2]	Panjab Univ.	(India)	Nov. 1989
Prof. J. Halpern[1]	Univ. of Chicago	(USA)	Nov. 1989
Prof. A.J. Epstein[1]	Ohio State Univ.	(USA)	Nov. 1989
Prof. S.I. Chan[1]	Calif. Inst. of Tech.	(USA)	Nov. 1989
Dr. U. Haeberlen[1]	Max-Planck Inst.	(FRG)	Nov. 1989
Dr. F. Fillaux[1]	CNRS	(France)	Nov. 1989
Prof. C.T. Llaguno[2]	Univ. of the Philippines System	(Philippine)	Nov. - Dec. 1989
Dr. F.H. Mies[2]	NIST	(USA)	Nov. 1989 - Jan., Feb. - Mar. 1990
Prof. R.J. Fleming[5]	Monash Univ.	(Australia)	- Nov. 1989
Dr. S.N. Rai[2]	North Eastern Hill Univ.	(India)	- Nov. 1989
Prof. J.T. Yates Jr.	Univ of Pittsburgh	(USA)	Dec. 1989
Dr. R.E. Wright	3M Corporate Research Lab.	(USA)	Dec. 1989
Dr. J.T. Hougen	NIST	(USA)	Dec. 1989
Dr. D.N. Luneau	Toulouse Univ.	(France)	- Dec. 1989
Dr. Kwang Oh Koh	Soonchunhyang Univ.	(Korea)	Dec. 1989 - Feb. 1990
Prof. C. Nordling	Univ. of Uppsala	(Sweden)	Jan. 1990
Prof. J. Frederick[4]	Univ of Nevada, Reno	(USA)	Jan., May - Jun. 1990
Prof. Ho-In Lee	Seoul Natl. Univ.	(Korea)	Feb. 1990
Prof. P. Dhez[2]	LURE, Univ. Paris-Sud	(France)	Feb. 1990
Dr. Mazurenko	Sci. Res. Inst. of Phys. Problems	(USSR)	Feb. 1990
Prof. G. Kulipanov	Inst. of Nuclear Phys., Novosibirsk	(USSR)	Feb. 1990
Prof. N.P. Ong[1]	Princeton Univ.	(USA)	Feb. 1990
Prof. T. Timusk[1]	McMaster Univ.	(Canada)	Feb. 1990
Dr. F.J. Himpsel[1]	IBM	(USA)	Feb. 1990
Dr. C: Vettier[1]	Laue · Langevin Inst.	(France)	Feb. 1990
Dr. J.M. Trauquada	Brookheaven Natl. Lab.	(USA)	Feb. 1990
Dr. N. Nucker[1]	Inst. of Nuclear Phys.	(FRG)	Feb. 1990
Prof. R.L. Christensen[2]	Bowdoin College	(USA)	Feb. - May 1990
Prof. C.E. Brion[2]	Univ. of British Columbia	(Canada)	Feb. - May 1990
Prof. Wang, Yu	Natl. Taiwan Univ.	(Taiwan)	Mar. 1990
Prof. Peng. Shie-Ming	Natl. Taiwan Univ.	(Taiwan)	Mar. 1990
Prof. Chang, Shin-Lin	Natl. Tsing Hua Univ.	(Taiwan)	Mar. 1990
Prof. Lee, Tsong-Jen	Natl. Tsing Hua Univ.	(Taiwan)	Mar. 1990
Prof. Wang, Sue-Lein	Natl. Tsing Hua Univ.	(Taiwan)	Mar. 1990

Prof. Shiu, Kom-Bei	Natl. Cheng Kung Univ.	(Taiwan)	Mar. 1990
Dr. Liu, Ling-Kang	Inst. of Chem., Acad. Sinica	(Taiwan)	Mar. 1990
Dr. Lii, Kwang-Hwa	Inst. of Chem., Acad. Sinica	(Taiwan)	Mar. 1990
Dr. Chien, Fan-Z	Tam Kang Univ.	(Taiwan)	Mar. 1990
Mr. Lee, Yean-Jang	Natl. Sci. Council, Executive Yuan	(Taiwan)	Mar. 1990
Mr. Wu, Fei-Sheng	Association of East Asian Relations	(Taiwan)	Mar. 1990
Dr. S. Kotaiah*[2]	Center of Advan. Tech., Indore	(India)	Mar. 1990
Prof. D. Phillips	Imperial College	(UK)	Mar. 1990
Prof. R.J. Donovan	Univ. of Edinburgh	(UK)	Mar. 1990
Prof. W.J. Hehre	Univ. of California	(USA)	Mar. 1990
Prof. P.R. Schleyer*[2]	Univ. of Erlangen	(FRG)	Mar. 1990
Prof. H.A. Staab*[3]	Max-Planck-Gesellschaft	(FRG)	Mar. 1990
Prof. C. Leforestier*[2]	Univ. of Paris-Sud	(France)	Mar. - Apr. 1990
Prof. S. Nespurek*[5]	Inst. of Macromolecular Chem., Czechoslovakia Sci. Acad.	(Czechoslovakia)	Mar. - Nov. 1990
Prof. J. Barthel	Univ. of Regensburg	(FRG)	Apr. 1990
Prof. M. Ya Amusia*[2]	Ioffe Inst. -Leningrad	(USSR)	Apr. 1990
Prof. J. Rabinowitz	Univ. of Geneve	(Switzerland)	Apr. 1990
Prof. C.O'Connor	Univ. of Auckland	(New Zealand)	Apr. 1990
Dr. K. Heinzinger	Max-Planck-Inst. for Chem.	(FRG)	Apr. 1990
Prof. P. Botschwina	Univ. of Goettingen	(FRG)	Apr. 1990
Dr. J. Evans	Univ. of Southampton	(UK)	Apr. 1990
Dr. Thompson	NSF	(USA)	Apr. 1990
Prof. P.M. Maitlis	Sheffield Univ.	(UK)	Apr. 1990
Dr. P. Lablanquie*[4]	Centre Univ. Paris-Sud	(France)	Apr. 1990 -
Prof. H. Weinstein	Mount Sinal School of Medicine	(USA)	May 1990
Dr. F. Galsbøl*[2]	Copenhagen Univ.	(Denmark)	May 1990
Prof. R. Bersohn	Columbia Univ.	(USA)	May 1990
Prof. G. Davis	Northeastern Univ.	(USA)	May 1990
Ms. T.C. Kavanaugh*[4]	Massachusetts Inst. of Tech.	(USA)	May 1990 -
Prof. P.M. Champion*[2]	Northeastern Univ.	(USA)	May - Aug. 1990
Prof. Kee Hag Lee*[2]	Wonkwang Univ.	(Korea)	Jun. 1990 -
Dr. A. Douhal*[4]	Kadi Ayad Univ.	(Morocco)	Jun 1990 -
Prof. Ng, Cheuk-Yiu*[2]	Iowa State Univ.	(USA)	Jun. - Sept. 1990
Prof. S. Forsen	Univ. of Lund	(Sweden)	Jul. 1990
Dr. D.D. Bhawalker*[2]	Centre of Advan. Tech., Indore	(India)	Jul. 1990
Dr. Dongho Kim	KSRI	(Korea)	Jul. 1990
Prof. K.-H. Jung	KAIST	(Korea)	Jul. 1990
Prof. J. Ku	Pohan Inst. of Sci. and Tech.	(Korea)	Jul. 1990
Prof. H. Kang	Pohan Inst. of Sci. and Tech.	(Korea)	Jul. 1990
Prof. Nam-Soo Lee	Chungbuk Natl. Univ.	(Korea)	Jul. - Aug. 1990
Prof. Xin Sun*[5]	Fudan Univ.	(China)	Jul. 1990 -
Ms. Ping Wang*[4]	Inst. of Chem., Acad. Sinica	(China)	Jul. 1990 -

AWARD

Prof. Kimura's Scientific Achievements

Prof. Katsumi Kimura of Photochemistry Laboratory, Department of Molecular Assemblies, received the Award of the Chemical Society of Japan for 1990 for his contribution of "Studies on Excited Molecules by Multiphoton Ionization Photoelectron Spectroscopy.".

In 1980 Prof. Kimura succeeded in developing a technique of laser multiphoton ionization photoelectron spectroscopy (MPIPES) and has applied the technique to solve a variety of problems of excited molecules which cannot be solved by other means. Some of his achievements are the following:

1) Prof. Kimura measured the photoelectron spectra due to one- or two-photon inonization of the excited states of some typical molecules, such as NO, NH_3, benzene, naphthalene and established that the MPIPES spectra reflect the electronic and vibrational structures of both the excited and ionized molecules.

2) He thus found the ways to produce vibrational state-selected molecular ions.

3) The dynamic behaviors of the electronically excited states of complex molecules, such as benzene and naphtalene, are often studied by laser induced fluorescence and/or MPI mass spectroscopies. From the photoelectron spectra of the electrons emitted from the excited states of benzene in the channel-3 region, Dr. Kimura has shown that information on the vibronic structures before undergoing internal conversion or intersystem crossing can be obtained and has found that the intramolecular vibrational redistribution is the fastest process.

4) From the measurement of photoelectron spectra of electrons emitted from the autoionization states of NO, he has succeeded in obtaining information on the repulsive potential surface of the molecule.

Prof. Tsuno's Scientific Achievements

Prof. Yuho Tsuno received the Award of the Chemical Society of Japan in 1990 for his contributions to "Structure Reactivity Relationships in Organic Chemistry".

Since 1950's Prof. Tsuno continues his works on the linear free energy relationship between structure and reactivity in organic chemistry. In 1959 he proposed a new idea that the degree of the direct π-interaction between the aryl group and the charge developed at a reaction center on the side chain reactions of benzene derivatives must vary with the system. This idea had been realized in the LArSR equation well-known as the Yukawa-Tsuno equation.

$$\log k/k_o = \rho(\sigma^o + r^+ \Delta \bar{\sigma}_R^+ + r^- \Delta \bar{\sigma}_R^-)$$

The concept of varying resonance demand had unified all Hammett-type equations proposed so far, and thereby the theory of the substituent effect had progressed into a new stage. Furthermore, Prof. Tsuno presented the LSFE equation as an alternative descrition of his idea on the basis of an assumption that the

substituent constant must be divided into σ- and π-electronic effects. This formulation had enabled correlation of not only reactivities in aromatic, heteroaromatic, and aliphatic systems but also physical properties such as IR, NMR, and so on. Thus, Prof. Tsuno's idea has been accepted widely as the most important theory in the analysis of the substituent effects in organic chemistry. The real significance of the LArSR equation is that the results of the LArSR correlation can be closely related to reaction mechanism, and the structure of transition state. He had analyzed in detail reaction mechanisms of a variety of organic reactions such as rearrangement, elimination, and substitution reactions by means of the LArSR equation, and mechanistic problems remained unexplicit for a long time had been solved clearly.

Recently Prof. Tsuno introduced a new technique, ion cyclotron resonance spectroscopy, into this field in order to separate the structural effects from solvent effects in organic reactions, and he determined thermochemical properties of various ionic species in the gas phase. Throughout these studies the physical significance of the LArSR equation had been confirmed, and also had been discovered many important facts which provided a new insight into the theory with respect to solvent effects in organic chemistry.

Professor Ohtaki's Scientific Achievements

Professor H. Ohtaki received the Takei Prize (gold medal) from the Electrochemical Society of Japan in April, 1990 for his outstanding contribution to solution chemistry of electrolytes in aqueous and nonaqueous solvents.

In spite of an extensive use of aqueous and nonaqueous electrolyte solutions in electrochemistry, very limited knowledge has been given to udnerstand reactivities of electrolytes in connection with solvent structures and properties, as well as with the structure of the species existing in solutions. Professor Ohtaki used liquid X-ray and neutron diffraction, and EXAFS methods for determining structures of solvents and complexes in solution in order to elucidate reactivities of electrolyts in solutions at a molecular level.

His contributions to electrolyte solution chemistry can be divided into three parts. (1) Structural investigations of liquids and electrolyte solutions by the diffraction and EXAFS methods and molecular dynamics simulations (2) Thermodynamic and spectroscopic studies of complex formation reactions in solutions. (3) Studies on ion exchange equilibria. His activities in the field of fundamental electrochemistry at the international standpoint was also highly evaluated.

LIST OF PUBLICATIONS

N. KOGA and K. MOROKUMA, "Ab Initio Molecular Orbital Studies of Intermediates and Transition States of Organometallic Elementary Reactions and Homogeneous Catalytic Cycles", in "Topics in Physical Organometallic Chemistry", Vol. 3, ed. M.F. Gielen (Freund Publishing House, London), p.1 (1989).

T. YAMAGUCHI, Y. SASAKI, A. NAGASAWA, T. ITO, N. KOGA and K. MOROKUMA, "Facile Regioselective Ligand Substitution for the In-Plane Bridging Acetates in Octakis (μ-acetato-O,O') tetraplatinum (II)", *Inorg. Chem.* **28**, 4311 (1989).

K. YAMASHITA and K. MOROKUMA, "A Theoretical Study of Transition State Spectroscopy: Laser Dressed Potential Energy Surface and Surface Hopping Trajectory Calculations on K + NaCl and Na + KCl", *J. Chem. Phys.* **91**, 7477 (1989).

A.E. DORIGO and K. MOROKUMA, "Theoretical Studies of the Role of Complexation in the Conjugate Addition of Dialkylcuprates to Electron-deficient C=C Bonds. Influence on the Stereochemistry of the Reaction", *J. Chem. Soc. Chem. Comm.* 1884 (1989).

K. YAMASHITA, Y. SHIRAISHI, I. KUSUNOKI and K. MOROKUMA, "Ab Initio Potential Energy Surfaces of Charge-Transfer Reactions: $F^+ + CO \rightarrow F + CO^+$", *J. Chem. Phys.* **92**, 2505 (1990).

M.B. COOLIDGE, K. YAMASHITA, W.T. BORDEN and K. MOROKUMA, "Ab Initio MCSCF and CI Calculations of the Singlet-Triplet Energy Differences in Oxyallyl and in Dimethyloxyallyl", *J. Am. Chem. Soc.* **112**, 1751 (1990).

D.A. HROVAT, W.T. BORDEN, R.L. VANCE, N.G. RONDAN, K.N. HOUK and K. MOROKUMA, "Ab Initio Calculations of the Effects of Cyano Substituents on the Cope Rearrangement", *J. Am. Chem. Soc.* **112**, 2018 (1990).

M. OHSAKU and K. MOROKUMA, "Parallel and Cross Cycloaddition of Triplet Penta-1,4-diene. An Ab Initio MO Study", *J. Chem. Soc. Perkin Trans.* **2**, 735 (1990).

N. KOGA and K. MOROKUMA, "Ab Initio Potential Energy Surface and Electron Correlation Effect in CH Activation of CH_4 by Coordinatively Unsaturated $RhCl(PH_3)_2$", *J. Phys. Chem.* **94**, 5454 (1990).

B. WEIS, P. ROSMUS, K. YAMASHITA and K. MOROKUMA, "Theoretical Potential Energy and Electric Dipole Moment Functions of HCF (X $^1A'$ and a $^3A''$)", *J. Chem. Phys.* **92**, 6635 (1990).

K. YAMASHITA and K. MOROKUMA, "Ab Initio Study of Transition State Spectroscopy: $ClHCl^-$ Photodetachment Spectrum", *J. Chem. Phys.* **93**, 3716 (1990).

M. HANDA, N. KOGA and S. KIDA, "Study of the Effect of Structural Factors on the Magnetism of Di-μ-alkoxodicopper (II) Complexes by Ab Initio MO Calculations", *Bull. Chem. Soc. Jpn.* **61**, 3853 (1988).

D. JAYATILAKE, R.D. AMOS and N. KOGA, "Analytic Second Derivatives with Model Potentials at SCF and MP2 Level", *Chem. Phys. Lett.* **163**, 151 (1989).

H. TANAKA and I. OHMINE, "Potential Energy Surfaces for Water Dynamics: Reaction Coordinates, Transition States, and Normal Mode Analyses", *J. Chem. Phys.* **91**, 6318 (1989).

M. AOYAGI, I. OHMINE and B. KOHLER, "Frequency Increase of the C=C a_g Stretch Mode of Polyenes in the $2^1A_g^-$ States: Ab Initio MCSCF Study of Butadiene, Hexatriene, and Octatetraene", *J. Phys. Chem.* **94**, 3922 (1990).

M. SASAI, "Nonlinear Phase Excitations in the PPP Model of Polyacetylene", *Int. J. Quantum Chem.* **37**, 559 (1990).

M. IWAI and H. NAKAMURA, "Cranking Model of Collective Rotational Motion of Atomic Electrons", *Phys. Rev.* **A40**, 6695 (1989).

T. SHIRAI and H. NAKAMURA, "Ionization of Low-Rydberg-state He Atoms by Dipole-forbidden Rotational Deexcitation of NH_3", *Phys. Rev.* **A40**, 7377 (1989).

S.C. PARK, H. NAKAMURA and A. OHSAKI, "Quantum Mechanical Study of the Light-atom Transfer Reactions, $O(^3P)+XCl \rightarrow OX+Cl$ (X=H,D). I. Reactions in the Ground Vibrational States", *J. Chem. Phys.* **92**, 6538 (1990).

M. NAKAMURA and H. NAKAMURA, "Application of the Independent Events Approximation to Rotational Transitions in the $H+H_2$ and $D+H_2$ Reactions", *Chem. Phys.* **143**, 271 (1990).

A. MISHIMA and K. NASU, "Formation Process of a Bipolaron and Light-Absorption Bands in Halogen-Bridged Mixed-Valence Metal Complexes," *Phys. Rev.* **B40**, 5593 (1989).

C. WU, X. SUN and K. NASU, "Reply to the Comment on Electron Correlation and Bond Alternation in Polymers." *Phys. Rev. Letters* **63**, 2534 (1989).

K. NASU, "S-wave Pairing Mediated by Double Excitation of Triplet in Two Band Systems with Intermediate Electron Correlation." *Physica* **C162-164**, 815 (1989).

K. YAMAGUCHI, H. NAMIMOTO, T. FUENO, S. YAMAMOTO and K. NASU, "N-bands Hubbard Models for Doped Transition Metal Oxides. Cooperation of Charge and Spin Fluctuations for the High-T_c Superconductivity." *Physica* **C162-164**, 1333 (1989).

M. SUZUKI and K. NASU, "Dynamics of Charge Transfer from Molecule to Semiconductor at Surface: Numerical Method for Nonadiabaticity and Irreversibility in Discrete Continuum Transition." *J. Chem. Phys.* **92**, 4576 (1990).

K. HIRAO, "Interative Method for the Solution of Large Systems of Linear Equations", *J. Comp. Phys.* **80**, 232-242 (1989).

J.A. SUNNER, P. KEBARLE and K. HIRAO, "Hydride-Transfer Reactions. Temperature Dependence of Rate Constants for $i\text{-}C_3H_7^+ + HC(CH_3)_3 = C_3H_8 + C(CH_3)_3$", *J. Phys. Chem.* **93**, 4010-4016 (1989).

K. HIRAO and P. KEBARLE, "S_N2 Reaction in the Gas-phase. Transition States for the Reactions: $Cl^- + RBr = ClR + Br^-$ where $R = CH_3$, C_2H_5 and $iso\text{-}C_2H_7$, from Ab Initio Calculations and Comparison with Experiments", *Can. J. Chem.* **67**, 1261-1267 (1989).

H. WASADA and K. HIRAO, "Computational Studies of Satellite Peaks of the Inner-valence Ionization of C_2H_4. C_2H_2 and H_2S using the SAC-CI Method", *Chem. Phys.* **138**, 277-290 (1989).

S. SAKAKI and K. OHKUBO, "Ab Initio MO Study of CO_2 Insertion into a Cu(I)-H Bond. Semiquantitative Understanding of Changes in Geometry, Bonding, and Electron Distribution during the Reaction", *Inorg. Chem.* **28**, 2583 (1989).

S. SAKAKI and K. OHKUBO, "Ab Initio Molecular Orbital Configuration Interaction Study of $Ni(PH_3)_2(N_2)$. Differences in Electron Correlation Effects between η^1- End-on and η^2-Side-on N_2 Coordination", *J. Phys. Chem.* **93**, 5655 (1989).

S. SAKAKI and K. OHKUBO, "Ab Initio MO Study of CO_2 Insertion into a $Cu^I\text{-}CH_3$ Bond. Critical Difference from CO_2 Insertion into a $Cu^I\text{-}H$ Bond", *Organometallics*, **8**, 2970 (1989).

C. YAMADA, M. FUJITAKE and E. HIROTA, "The Microwave Spectrum of the LiO Radical", *J. Chem. Phys.* **91**, 137 (1989).

Y. ENDO, H. KANAMORI and E. HIROTA, "Millimeter- and Submillimeter-Wave Spectra of the Vibrationally Excited CCD Radical", *Chem. Phys. Lett.* **160**, 280 (1989).

S. KODA, S. SUGA, S. TSUCHIYA, T. SUZUKI, C. YAMADA and E. HIROTA, "The $SiH_4 + O(^1D)$ Reaction Studied by Infrared Diode Laser Kinetic Spectroscopy", *Chem. Phys. Lett.* **161**, 35 (1989).

K. KAWAGUCHI, K. MATSUMURA, H. KANAMORI and E. HIROTA, "Diode Laser Spectroscopy of C_3: The $\nu_2 + \nu_3 - \nu_2$, $2\nu_2 + \nu_3 - 2\nu_2$, and $2\nu_2 + \nu_3$ Bands", *J. Chem. Phys.* **91**, 1953 (1989).

M. TANIMOTO, H. TAKEO, C. MATSUMURA, M. FUJITAKE and E. HIROTA, "Microwave Spectroscopic Detection of Dichlorosilylene $SiCl_2$ in the Ground State", *J. Chem. Phys.* **91**, 2102 (1989).

M. FUJITAKE and E. HIROTA, "The Millimeter- and Submillimeter-Wave Spectrum of Dichlorocarbene CCl_2: Electronic Structure Estimated from the Nuclear Quadrupole Coupling Constants", *J. Chem. Phys.* **91**, 3426 (1989).

E. TIEMANN, H. KANAMORI and E. HIROTA, "Infrared Diode Laser Spectroscopy of SCl Generated by the Photolysis of S_2Cl_2 and SCl_2,", *J. Mol. Spectrosc.* **137**, 278 (1989).

C. YAMADA, H. KANAMORI, E. HIROTA, N. NISHIWAKI, N. ITABASHI, K. KATO and T. GOTO, "Detection of the Silylene ν_2 Band by Infrared Diode Laser Kinetic Spectroscopy", *J. Chem. Phys.* **91**, 4582 (1989).

H. KANAMORI, Y. ENDO and E. HIROTA, "The Vinyl Radical Investigated by Infrared Diode Laser Kinetic Spectroscopy", *J. Chem. Phys.* **92**, 197 (1990).

C. YAMADA, E.A. COHEN, M. FUJITAKE and E. HIROTA, "The Microwave Spectrum of the AlO Radical", *J. Chem. Phys.* **92**, 2146 (1990).

N. ITABASHI, N. NISHIWAKI, M. MAGANE, S. NAITO, T. GOTO, A. MATSUDA, C. YAMADA and E. HIROTA, "Spatial Distribution of SiH_3 Radicals in RF Silane Plasma", *Jpn. J. Appl. Phys.* **29**, L505 (1990).

N. ITABASHI, N. NISHIWAKI, M. MAGANE, T. GOTO, A. MATSUDA, C. YAMADA and E. HIROTA, "SiH_3 Radical Density in Pulsed Silane Plasma", *Jpn. J. Appl. Phys.* **29**, 585 (1990).

M. MAGANE, N. ITABASHI, N. NISHIWAKI, T. GOTO, C. YAMADA and E. HIROTA, "Measurements of the CF Radical in DC Pulsed CF_4/H_2 Discharge Plasma Using Infrared Diode Laser Absorption Spectroscopy", *Jpn. J. Appl. Phys.* **29**, L829 (1990).

N. MORITA and T. SUZUKI, "Laser Spectroscopic Observation and Large-Scale Configuration-Interaction Calculation of Doubly Excited $msns$ $^1S^e$ States of Ca Atoms", *Phys. Rev.* **A41**, 2370 (1990).

T. OGURA, S. YOSHIKAWA and T. KITAGAWA, "Raman/Absorption Simultaneous Measurements for Cytochrome Oxidase Compound A at Room Temperature with a Novel Flow Apparatus", *Biochemistry* **28**, 8022 (1989).

P. ANZENBACHER, J.H. DAWSON and T. KITAGAWA, "Towards a Unified Concept of Oxygen Activation by Heme Enzymes: The Role of the Proximal Ligand", *J. Mol. Struct.* **214**, 149 (1989).

P. ANZENBACHER, J.H. DAWSON and T. KITAGAWA, "Heme Enzymes Examined by Vibrational Spectroscopy — Role of the Fifth Heme Iron Ligand" in "Spectroscopy of Biological Molecules — State of the Art" (A. Bertoluzza, C. Fagnano and P. Monti Eds.) pp.295-298, Esculapio, Bologna (1989).

T. KITAGAWA, S. KAMINAKA and T. OGURA, "Time-resolved UV Resonance Raman Study of Quaternary Structure Change of Hemoglobin" in "Spectroscopy of Biological Molecules — State of the Art" (A. Bertoluzza, C. Fagnano and P. Monti Eds.) pp.295-298, Esculapio, Bologna (1989).

K. IMAI, K. ISHIMORI, K. FUSHITANI, G. MIYAZAKI, T. KITAGAWA, Y. WADA, H. MORIMOTO, I. MORISHIMA, D. SHIH, J. TAME and K. NAGAI, "Manipulation of Hemoglobin Function by Protein Engineering" in "Protein Structural Analysis, Folding and Design" (M. Hatano Ed.) pp.185-195, Japan Sci. Soc. Press (1990).

M. NAGAI, T. KITAGAWA and Y. YONEYAMA, "Molecular Parthology of Hemoglobin M Saskatoon Disease", *Biomed. Biochim. Acta* **49**, 2/3 S317 (1990).

S. KAMINAKA, T. OGURA and T. KITAGAWA, "Time-resolved Ultraviolet Resonance Raman Study of the Photolysis of Carbonmonoxy Hemoglobin: Relaxation of the Globin Structure", *J. Am. Chem. Soc.* **112**, 23 (1990).

K. KAMOGAWA and T. KITAGAWA, "A New Device for Raman Difference Spectroscopy and Its Application to Observe Frequency Shifts due to Isotope Mixing", *J. Phys. Chem.* **94**, 3916 (1990).

T. OGURA, V. FIDLER, Y. OZAKI and T. KITAGAWA, "Alcohol Catalyzed Photoreduction of Iron Porphyrin Complexes Revealed by Resonance Raman and Absorption Spectroscopies", *Chem. Phys. Lett.* **169**, 457 (1990).

N. KITAJIMA, H. FUKUI, Y. MORO-OKA, Y. MIZUTANI and T. KITAGAWA, "A Synthetic Model for Dioxygen Binding Site of Non-heme Proteins. X-ray Structure of $Fe(OBz)$ $(MeCN)[HB(3,5-iPr_2pz)_3]$ and Resonance Raman Evidence for Reversible Formation of Peroxo Adduct", *J. Am. Chem. Soc.* **112**, 6402 (1990).

T. EGAWA, Y. IMAI, T. OGURA and T. KITAGAWA, "Resonance Raman Study on Mutant Cytochrome P-450 Obtained by Site Directed Mutagenesis", *Biochim. Biophys. Acta.* **1040**, 211 (1990).

T. OGURA. S. TAKAHASHI, K. SHINZAWA, S. YOSHIKAWA and T. KITAGAWA, "Observation of the Fe^{II}-O_2 Stretching Raman Band for Compound A of Cytochrome Oxidase at Room Temperature", *J. Am. Chem. Soc.* **112**, 5630 (1990).

Y. MIZUTANI, S. HASHIMOTO, Y. TATSUNO and T. KITAGAWA, "Resonance Raman Pursuit of the Change for Fe^{II}-O_2 to Fe^{III}-OH via Fe^{IV}=O in Autoxidation of Ferrous Iron-porphyrin", *J. Am. Chem. Soc.* **112**, 6809 (1990).

T. OGURA, S. TAKAHASHI, K. SHINZAWA-ITOH, S. YOSHIKAWA and T. KITAGAWA, "Observation of the Fe^{4+}=O Stretching Raman Band for Cytochrome Oxidase Compound B at Ambient Temperature", *J. Biol. Chem.* **265**, 14721 (1990).

S. TOKUTOMI, Y. MIZUTANI, E. ANNI and T. KITAGAWA, "Resonance Raman Scattering from Large Pea Phytochrome at Ambient Temperature: Difference in Chromophore Protonation between Red- and Far-red Light Absorbing Forms", *FEBS Lett.* **269**, 341 (1990).

T. MIZUSHIMA, K. TOHJI, Y. UDAGAWA, A. UENO and M. HARADA, "Characterization and Catalytic Properties of Silica Supported Iron-Nickel Catalysts through EXAFS and Formic Acid Decomposition", MRS It'l Mtg. on Adv. Mats. **2**, 375 (1989).

Z. NAKAGAWA, H. MORIKAWA, T-H. SUNG, M. YOSHIMURA, F. MARUMO and Y. UDAGAWA, "EXAFS Study of Coordination of Cu Atom in Amorphous $BiSr_2CaCu_2O_x$ (in Japanese)", *J. Chem. Soc. Jpn.* **1989**, 2085.

T. MIZUSHIMA, K. TOHJI, Y. UDAGAWA and A. UENO, "An EXAFS Study on the CO Adsorption Induced Morphology Change in Ru Clusters Supported on Alumina", *J. Phys. Chem.* **94**, 4980 (1990).

K. TOHJI, T. MIZUSHIMA and Y. UDAGAWA. "An Improved Double Crystal Spectrometer for Laboratory EXAFS Spectroscopy (in Japanese)", *Adv. in X-ray Analysis* **21**, 29 (1990).

K. TOHJI, Y. UDAGAWA, T. MATSUSHITA, M. NOMURA and T. ISHIKAWA, "Anisotropic Effect in X-ray Raman Scattering from Graphite", *J. Chem. Phys.* **92**, 3233 (1990).

K. SHINOZAKI, O. OHNO, Y. KAIZU, H. KOBAYASHI, M. SUMITANI and K. YOSHIHARA, "Excited-State Lifetime of the Nonemissive Complex [2,2'-4H-Bipyrazinium(1+))bis(2,2'-bipyridine)ruthenium(II)](3+)", *Inorg. Chem.* **28**, 3680 (1989).

K. KEMNITZ, N. NAKASHIMA, K. YOSHIHARA and H. MATSUNAMI, "Temperature Dependence of Fluorescence Decays of Isolated Rhodamine B Molecules Adsorbed on Semiconductor Single Crystals", *J. Phys. Chem.* **93**, 6704 (1989).

F. TANAKA, N. TAMAI, I. YAMAZAKI, N. NAKASHIMA and K. YOSHIHARA, "Temperature-Induced Changes in the Coenzyme Environment of D-Amino Acid Oxidase Revealed by the Multiple Decays of FAD Fluorescence", *Biophys. J.* **56**, 901 (1989).

K. KEMNITZ, K. YOSHIHARA and T. TANI, "Short and Excitation-Independent Fluorescence Lifetimes of J-Aggregates Adsorbed on AgBr and SiO_2,", *J. Phys. Chem.* **94**, 3099 (1990).

A. GRABOWSKA, A MORDZINSKI, N. TAMAI and K. YOSHIHARA, "Reversible Intramolecular Proton-Transfer Reactions of Electronically Excited "Double" Benzoxazoles: A Direct Observation of the Effect of the Intrinsic Barrier", *Chem. Phys. Lett.* **169**, 450 (1990).

S.R. MEECH and K. YOSHIHARA, "Time-Resolved Surface Second Harmonic Generation: A Test of the Method and Its Application to Picosecond Isomerization in Adsorbates", *J. Phys. Chem.* **94**, 4913 (1990).

H. PETEK, K. YOSHIHARA, Y. FUJIWARA and J. FREY, "Isomerization of *cis*-Stilbene in Rare Gas Clusters. Direct Measurements of *trans*-Stibene Formation Rates on Picosecond Time Scale", *J. Opt. Soc. Am.* **B7**, 1540 (1990).

H. OKAMOTO and K. YOSHIHARA, "Femtosecond Time-Resolved Coherent Raman Scattering under Various Polarization and Resonance Conditions", *J. Opt. Soc. Am.* **B7**, 1702 (1990).

H. PETEK, K. YOSHIHARA, Y. FUJIWARA, Z. LIN, J.H. PENN and J.H. FREDERICK, "Is the non-Radiative Decay of S_1 cis-Stilbene Due to the Dihydrophenanthrene Isomerization Channel? Suggestive Evidence from Photophysical Measurements on 1,2-Diphenylcycloalkens.", *J. Phys. Chem.* **94**, 7539 (1990).

K. KEMNITZ, K. YOSHIHARA and T. TANI, "Transient Isoemissive Point Observed in the Temperature-Dependent Fluorescence Decays of J-Aggregates Adsorbed on Silica Gel", *Chem. Lett.* **1990**, 1785.

K. KEMNITZ and K. YOSHIHARA, "Malachite Green as a Sensitive Free-Volume Probe", *Chem. Lett.* **1990**, 1789.

H. PETEK, D.J. NESBITT, J.C. OWRUTSKY, C.S. GUDEMAN, X. YANG, D.O. HARRIS, C.B. MOORE and R.J. SAYKALLY, "A Study of the Structure and Dynamics of the Hydronium Ion by High Resolution Infrared Laser Spectroscopy. III. The v_3 Band of D_3O^+", *J. Chem. Phys.* **92**, 3257 (1990).

H. PETEK, D.J. NESBITT, D.C. DARWIN, P.R. OGILBY, C.B. MOORE and D.A. RAMSAY, "Analysis of $CH_2 \tilde{a}$ $^1A_1$ (1,0,0) and (0,0,1) Coriolis-Coupled States, $\tilde{a}$ $^1A_1$- $\tilde{X}$ $^3B_1$ Spin-Orbit Coupling, and the Equilibrium Structure of $CH_2 \tilde{a}$ $^1A_1$ State." *J. Chem. Phys.* **91**, 6566 (1989).

H. OKAMOTO, H. HAMAGUCHI and M. TASUMI, "Resonance Raman Studies on Tetradesmethyl-β-carotene Aggregates", *J. Raman Spectrosc.* **20**, 751 (1989).

H. OHOYAMA, M. TAKAYANAGI, T. NISHIYA and I. HANAZAKI, "Chemical Reaction of Weakly Bound Complexes: $HI \cdot N_2O + h\nu \to OH + N_2 + I$", *Chem. Phys. Lett.* **162**, 1 (1989).

M. TAKAYANAGI and I. HANAZAKI, "Fluorescence-dip and Stimulated-emission-pumping Laser-induced-fluorescence Spectra of van der Waals Molecules Containing Benzonitrile", *J. Opt. Soc. Am.* **B7**, 1898 (1990).

H. SHINOHARA and N. NISHI, "Excited State Lifetimes and Appearance Potentials of Benzene Dimer and Trimer", *J. Chem. Phys.* **91**, 6743 (1989).

M. KAWASAKI, K. KASATANI, A. SATO, H. SATO and N. NISHI, "Mechanistic Study of Laser Chemical Vapor Desorption of Trimethylindium", *Mat. Res. Soc. Symp. Proc.* **129**, 69 (1989).

K. YAMAMOTO and N. NISHI, "Hydrophobic Hydration and Hydrophobic Interaction of Carboxylic Acids in Aqueous Solution: Mass Spectroscopic Analysis of Liquid Fragments Isolated as Clusters", *J. Am. Chem. Soc.* **112**, 549 (1990).

N. NISHI, "Aqueous Molecular Clusters Isolated as Liquid Fragments by Adiabatic Expansion of Liquid Jets", *Z. Phys.* **D15**, 239 (1990).

R.J. DONOVAN and N. NISHI, "Time-of-flight Spectra of Bound-to-Free Transitions in I_2", *Chem. Phys. Lett.* **169**, 74 (1990).

R. NAKAGAKI, K. MUTAI and S. NAGAKURA, "Magnetic Field Effects upon Photoredox Reactions of Bifunctional Chain Molecules Containing Anilino and Nitro-aromatic Chromophores", *Chem. Phys. Lett.* **167**, 439 (1990).

Y. TANIMOTO, M. UEHARA, M. TAKASHIMA, M. ITOH, M. HIRAMATSU, R. NAKAGAKI, T. WATANABE and S. NAGAKURA, "Magnetic Field Effects on the Intramolecular Photoreaction of n-Alkyl Anthraquinone-2-carboxylates", *Bull. Chem. Soc. Jpn.* **63**, 2164 (1990).

M. OKAZAKI, Y. TAI, R. NAKAGAKI, K. NUNOME and K. TORIYAMA, "Excimer Formation of Pyrene as a Probe to Investigate the Recombination of Geminate Pairs: ODESR and Fluorescence Study of Dilute Pyrene in Squalane", *Chem. Phys. Lett.* **166**, 227 (1990).

M. OKAZAKI, K. NUNOME, K. MATSUURA and K. TORIYAMA, "Dynamic Process of Delayed Geminate Pairs in X-irradiated Squalane Solution of p-Terphenyl: an ODESR Study", *Bull. Chem. Soc. Jpn.* **63**, 1396 (1990).

M. OKAZAKI, Y. TAI, K. NUNOME and K. TORIYAMA, "Excimer Formation of Pyrene as a Probe to Investigate the Recombination of Geminate Paris: Effect of Multicomponent Recombination on Stern-Volmer Plot", *Chem. Phys. Lett.* **171**, 537 (1990).

K. YAKUSHI, A. UGAWA, G. OJIMA, T. IDA, H. TAJIMA, H. KURODA, A. KOBAYASHI, R. KATO and H. KOBAYASHI, "Polarized Reflectance Spectra of DCNQI Salts", *Mol. Cryst. Liq. Cryst.* **181**, 217 (1990).

T. IDA, H. YAMAKADO, H. MASUDA, K. YAKUSHI, D. KANAZAWA, H. TAJIMA and H. KURODA, "High-Pressure Optical Study of Partially Oxidized Metallophthalocyanines and Methallotetrabenzoporphyrins", *Mol. Cryst. Liq. Cryst.* **181**, 243 (1990).

A. UGAWA, K. YAKUSHI and H. KURODA, "Relation between the Dimensionality of Electronic Structure and the Correlation Effect in (BEDT-TTF)$_2$ X System", *Mol. Cryst. Liq. Cryst.* **181**, 269 (1990).

K. YAKUSHI, H. YAMAKADO, T. IDA, A. UGAWA, H. MASUDA and H. KURODA, "Optical Spectra of Highly Conducting Phthalocyanine Salts", in *Proceedings of the ISSP International Symposium, Tokyo,* 1989 [Proceedings in Physics **51**, pp.54-57, Springer-Verlag].

H. YAMAKADO, A. UGAWA, T. IDA and K. YAKUSHI, "Microwave Conductivity of the Phthalocyanine and Dicyanoquinonediimine Salts", in *Proceedings of the ISSP International Symposium, Tokyo,* 1989 [Proceedings in Physics **51**, pp.311-314, Springer-Verlag].

S. NAGAOKA, S. SUZUKI, U. NAGASHIMA, T. IMAMURA and I. KOYANO, "Ionic Fragmentation Processes in Organometallic Molecules of Group II-IV Elements Following (n-1)d Core Photoionization", *J. Phys. Chem.* **94**, 2283 (1990).

K. UEDA, E. SHIGEMASA, Y. SATO, S. NAGAOKA, I. KOYANO, A. YAGISHITA and T. HAYAISHI, "Ionic Fragmentation Following Core-Level Photoionization of Sn(CH$_3$)$_4$ by Soft X-rays", *Phys. Scripta* **41**, 78 (1990).

S. NAGAOKA, I. KOYANO and T. MASUOKA, "Dissociative Double Ionization Following Valence and Al:2p Core Level Photoionization of Al(CH$_3$)$_3$", *Phys. Scripta* **41**, 472 (1990).

K. UEDA, E. SHIGEMASA, Y. SATO, S. NAGAOKA, I. KOYANO, A. YAGISHITA and T. HAYAISHI, "Ionic Fragmentation Following the Photoionization of Sn(CH$_3$)$_4$ in the 60-260 eV Region", *Chem. Phys. Lett.* **166**, 391 (1990).

K. UEDA, Y. SATO, S. NAGAOKA, I. KOYANO, A. YAGISHITA and T. HAYAISHI, "Ionic Fragmentation Following the 3p and 3s Core Excitation of Ga(CH$_3$)$_3$ by Soft X-Rays", *Chem. Phys. Lett.* **170**, 389 (1990).

K. MITSUKE, S. SUZUKI, T. IMAMURA and I. KOYANO, "Negative-Ion Mass Spectrometric Study of Ion Pair Formation in the Vacuum Ultraviolet. I. N$_2$O → O$^-$ + N$_2^+$", *J. Chem. Phys.* **92**, 6556 (1990).

K. MITSUKE, S. SUZUKI, T. IMAMURA and I. KOYANO, "Negative-Ion Mass Spectrometric Study of Ion Pair Formation in the Vacuum Ultraviolet. II. OCS → S$^-$ + CO$^+$, O$^-$ + CS$^+$ and CO$_2$ → O$^-$ + CO$^+$", *J. Chem. Phys.* **93**, 1710 (1990).

K. MITSUKE, S. SUZUKI, T. IMAMURA and I. KOYANO, "Negative-Ion Mass Spectrometric Study of Ion Pair Formation in the Vacuum Ultraviolet. III. SF$_6$ → F$^-$ + SF$_5^+$", *J. Chem. Phys.* **93**, 8717 (1990).

K. KIMURA, Y. ACHIBA and H. SHIROMARU, "Synchrotron Radiation Apparatus for Supersonic-Jet Experiments", *Rev. Sci. Instrum.* **60**, 2205 (1989).

K. KIMURA, M. TAKAHASHI, K. OKUYAMA and I. PLAZIBAT, "Application of MPI Photoelectron Spectroscopy to Excited Molecules. Use of Tunable VUV Laser Radiation", *J. Electron Spectrosc.* **51**, 383 (1990).

M. UKAI, K. KAMETA, K. SHINSAKA, Y. HATANO, T. HIRAYAMA, S. NAGAOKA and K. KIMURA, "Photoionization of (O$_2$)$_2$, (O$_2$)$_3$, and Ar-O$_2$ in the 50-100 nm Region: State Selective Ionization of O$_2$ in a Framework of van der Waals Molecules", *Chem. Phys. Lett.* **167**, 334 (1990).

K. OKUYAMA, J.H.D. ELAND and K. KIMURA, "Decay of the 4d Hole States of Xe Studied by Photoelectron-Photoelectron Coincidence Spectroscopy", *Phys. Rev. A* **41**, 4930 (1990).

H. OHASHI, K. INOUE, Y. SAITO, A. YOSHIDA, H. OGAWA and K. SHOBATAKE, "Synchrotron Radiation Assisted Deposition of Carbon Films", *Appl. Phys. Lett.* **55**, 1644 (1989).

F. TANAKA, S. HIRAYAMA and K. SHOBATAKE, "Microscopic Solvent Effects on the S$_1$-T$_2$ Intersystem Crossing of 9,10-Diphenylanthracene in Supersonic Free Jets", *Chem. Phys. Lett.* **164**, 335 (1989).

S. HIRAYAMA, F. TANAKA and K. SHOBATAKE, "Electronic Relaxation in Isomers of 9,10-Dimethoxyanthracene and their Rare-Gas Complexes", *J. Phys. Chem.* **94**, 1317 (1990).

H. YAMADA, M. NAKAMURA, H. KATOH, T. HAYASAKA, S. MORITA, S. HATTORI, H. OHASHI and K. SHOBATAKE, "Polystrene Thin Film Formed by Synchrotron Radiation Chemical Vapor Deposition", *J. Appl. Phys.* **67**, 2613 (1990).

K. UNO, T. HIKIDA, A. HIRAYA and K. SHOBATAKE, "Formation of $NH(c^1\Pi)$, $NH(A^3\Pi)$, and $NCO(A^2\Sigma)$ in the VUV Photolysis of HNCO", *Chem. Phys. Lett.* **166**, 475 (1990).

T. IBUKI, A. HIRAYA and K. SHOBATAKE, "Photexcitation of $M(CH_3)_2$ (M=Zn, Cd. Hg) Compounds in the 106-270 nm", *J. Chem. Phys.* **92**, 2797 (1990).

T. IBUKI, A. HIRAYA, K. SHOBATAKE, Y. MATSUMI and M. KAWASAKI, "Vacuum Ultraviolet Photochemistry of $CHFCl_2$ and $CHFBr_2$: Absorption Spectra and $CHF(\tilde{A}\ ^1A'')$ Radical Formation", *J. Chem. Phys.* **92**, 4277 (1990).

K. SHOBATAKE, H. OHASHI, A. HIRAYA, N. HAYASAKA, H. OKANO, A. YOSHIDA and H. KUME, "Synchrotron Radiation-Excited Etching of SiO_2 with SF_6 at 143 and 251 Å", *Appl. Phys. Lett.* **56**, 2189 (1990).

S. HIRAYAMA, Y. IUCHI, F. TANAKA and K. SHOBATAKE, "Natural Radiative Lifetimes of Anthracene Derivatives and their Dependence on Refractive Index", *Chem. Phys.* **144**, 401 (1990).

T. INABE, N. HOSHINO, T. MITANI, H. OKAMOTO, I. G.-LUNEAU and Y. MARUYAMA, "Reversible Self-Isomerization Induced by Proton Transfer: Correlation between the Structures and Optical Properties" in "Molecular Electronics — Science and Technology" A. Aviram Ed., Engineering Foundation, pp.63-69 (1989).

Y. MARUYAMA, T. INABE, H. MORI, H. YAMOCHI and G. SAITO, "Tunneling Spectroscopic Study of the Superconducting Gap of $(BEDT-TTF)_2Cu(NCS)_2$ Crystals" in "The Physics and Chemistry of Organic Superconductors" G. Saito and S. Kagoshima Ed., Springer-Verlag, pp.163-166 (1990).

T. INABE, T. MITSUHASHI and Y. MARUYAMA, "Design of Two-Dimensional Stacking Structures: Twin-Type Molecules and Steric Interaction of Axial Substituents" in "The Physics and Chemistry of Organic Superconductors" G. Saito and S. Kagoshima Ed., Springer-Verlag, pp.408-411 (1990).

T. INABE and Y. MARUYAMA, "Multi-Dimensional Stacking Structures in Phthalocyanine-Based Electrical Conductors, $K[Co(phthalocyaninato)(CN)_2]_2 \cdot 5CH_3CN$ and $[Co(phthalocyaninato)(CN)_2]_2 \cdot 2H_2O$", *Bull. Chem. Soc. Jpn.* **63**, 2273 (1990).

N. HOSHINO, H. MURAKAMI, Y. MATSUNAGA, T. INABE and Y. MARUYAMA, "Liquid Crystalline Copper(II) Complexes of N-Salicylideneaniline Derivatives. Mesomorphic Properties and a Crystal Structure", *Inorg. Chem.* **29**, 1177 (1990).

A.J. DANN, H. HOSHI and Y. MARUYAMA, "The Structure and Properties of Phthalocyanine Films Grown by the Molecular Beam Epitaxy Technique. I. Preparation and Characterization", *J. Appl. Phys.* **67**, 1371 (1990).

H. HOSHI, A.J. DANN and Y. MARUYAMA, "The Structure and Properties of Phthalocyanine Films Grown by the Molecular Beam Epitaxy Technique. II. Ultraviolet/Visible Spectroscopic Study", *J. Appl. Phys.* **67**, 1845 (1990).

H. HOSHI, A.J. DANN and Y. MARUYAMA, "The Structure and Properties of Phthalocyanine Films Grown by the Molecular Beam Epitaxy Technique. III. Preparation and Characterization of Lutetium Diphthalocyanine Film", *J. Appl. Phys.* **67**, 6871 (1990).

H. HOSHI, Y. MARUYAMA, H. MASUDA and T. INABE, "A New Type of Epitaxial Growth in Lithium Phthalocyanine Film on KBr(100) Prepared by the Molecular-Beam Epitaxy", *J. Appl. Phys.* **68**, 1396 (1990).

T.R. THURSTON, R.J. BIRGENEAU, D.R. GABRE, H.P. JENSSEN, M.A. KASTNER, P.J. PICONE, N.W. PREYER, J.D. AXE, P. BONI, G. SHIRANE, M. SATO, K. FUKUDA and S. SHAMOTO, "Neutron Scattering Study of Soft Optical Phonon in $La_{2-x}Sr_xCuO_{4-y}$", *Phys. Rev.* **B39**, 4327 (1989).

Y. ANDO, M. SERA, S. YAMAGATA, S. KONDOH, M. ONODA and M. SATO, "Normal State Properties of $La_{2-x}Sr_xCuO_4$ and $La_2SrCu_2O_y$", *Solid State Commun.* **70**, 303 (1989).

A. FUJIMORI, H. EISAKI, H. TAKAGI, S. UCHIDA, S. TAKEKAWA and M. SATO, "Origin of the Electronic States near the Fermi Level in High-T_c Supercounductors", *Phys. Rev.* **40**, 7303 (1989).

P. BONI, J.D. AXE, G. SHIRANE, R.J. BIRGENEAU, D.R. GABBE, H.P. JENSSEN, M.A. KASTNER, P.J. PICONE, T.R. THURSTON, M. SATO and S. SHAMOTO, "Lattice Instability in Single Crystal $La_{2-x}Sr_xCuO_4$", *Physica* **B156&157**, 902 (1989).

S. SUGAI and M. SATO, "Phonon Raman Spectroscopy in $Bi_2Sr_2Ca_{1-x}Y_xCu_2O_{8+y}$", *Jpn. J. Appl. Phys.* **28**, L1361 (1989).

M. SERA, S. SHAMOTO and M. SATO, "Small Electronic Specific Heat in the Electron Doped Cu-Oxide Superconductors", *Solid State Commun.* **72**, 749 (1989).

M. SATO, S. SHAMOTO, M. SERA and H. FUJISHITA, "On the Anomalous Magnetic Behaviors of High-T_c Oxides", *Solid State Commun.* **72**, 689 (1989).

G. SHIRANE, J. ALS-NIELSEN, M. NIELSEN, J.M. TRANQUADA, H. CHOU, S. SHAMOTO and M. SATO, "Magnetic Correlations in $YBa_2Cu_3O_{6+x}$ at Superconducting Concentrations", *Phys. Rev.* **B41**, 6547 (1990).

J.M. TRANQUADA, J. ALS-NIELSEN, W.J.L. BUYERS, H. CHOU, T. MASON, M. NIELSEN, M. SATO, S. SHAMOTO and G. SHIRANE, "Spin Fluctuations in Superconducting $YBa_2Cu_3O_{6.5}$", *Phys. Rev. Lett.* **64**, 800 (1990).

S. YAMAGATA, K. ADACHI, M. ONODA, H. FUJISHITA, M. SERA, Y. ANDO and M. SATO, "Effect of Ni or Zu Substitution for Cu in Nd-Ce-Cu-O and Bi-Sr-(Ca,Y)-Cu-O Systems", *Solid State Commun.* **74**, 177 (1990).

S. SUGAI, M. SATO, T. KOBAYASHI, J. AKIMITSU, T. ITO, H. TAKAGI, S. UCHIDA, S. HOSOYA, T. KAJITANI and T. FUKUDA, "High Energy Spin Excitations in the Insulating Phases of High-T_c Superconducting Cuprates and La_2NiO_4", *Phys. Rev.* **B42**, 1045 (1990).

M. SERA, S. SHAMOTO and M. SATO, "Thermal Conductivity of High-T_c Oxides", *Solid State Commun.* **74**, 951 (1990).

M. SATO, H. FUJISHITA and M SERA, "Carrier Concentration Dependence of Doping Effect and the Critical Concentration of Metal-Insulator Transition in $La_{2-x}Sr_xCu_{1-x}Ni_xN_4$", *Physica* **B165&166**, 1531 (1990).

M. SATO, M. SERA, S. YAMAGATA, S. SHAMOTO and K. OKA, "On the Magnetoconductance at the Spin Structure Change in La-Ba-Cu-O System", *Physica* **B165&166**, 1189 (1990).

S. SUGAI, M. SATO, T. ITO, T. IDO, H. TAKAGI, S. UCHIDA, T. KOBAYASHI, J. AKIMITSU, Y. HIDAKA, T. MURAKAMI, S. HOSOYA, T. KAJITANI and T. FUKUDA, "Two Spin Superexchange and Four Spin Cyclic exchange Interactions in High T_c Superconducting Cuprates and Isostructural La_2NiO_4", in *Proc. Yamada Conf. XXV on the Magnetic Phase Transition, Osaka, Japan, April 1990.*

S. SUGAI, M. SATO, T. ITO, T. IDO, H. TAKAGI, S. UCHIDA, T. KOBAYASHI, J. AKIMITSU, Y. HIDAKA, T. MURAKAMI, S. HOSOYA, T. KAJITANI and T. FUKUDA, "Spin and Carriers in Oxide Superconductors Studied by Raman Scattering", *Physica* **B165&166**, 1263 (1990).

H. FUJIMOTO, U. NAGASHIMA, H. INOKUCHI, K. SEKI, Y. CAO, H. NAKAHARA, J. NAKAYAMA, M. HOSHINO and K. FUKUDA, "Ultraviolet Photoemission Study of Oligothiophenes: π-Band Evolution and Geometries", *J. Chem. Phys.* **92**, 4077 (1990).

H. FUJIMOTO, U. NAGASHIMA, H. INOKUCHI, K. SEKI, N. NAKAHARA, J. NAKAYAMA, M. HOSHINO and K. FUKUDA, "Electronic and Geometric Structures of Oligothiophenes Studied by UPS and MNDO: π-Band Evolution and Effect of Disorder", *Physica Scripta*, **41**, 105 (1990).

N. UENO, K. SEKI, N. SATO, H. FUJIMOTO, T. KURAMOCHI, K. SUGITA and H. INOKUCHI, "Energy-Band Dispersion in Oriented Thin Films of Pentatriacontan-18-one by Angle-Resolved Photoemission with Synchrotron Radiation", *Phys. Rev.* **B41**, 1176 (1990).

N. UENO, H. FUJIMOTO, N. SATO, K. SEKI and H. INOKUCHI, "Angle-Resolved Photoemission from Oriented Thin Films of Long Alkyl Molecules: Valence Band Dispersion", *Physica Scripta*, **41**, 181 (1990).

M.R. FAHY, H. FUJIMOTO, A.J. DANN, H. HOSHI, H. INOKUCHI, Y. MARUYAMA and M.R. WILLIS, "Electronic Structure of Pc$_2$Lu and (PcAlF)$_n$ Oriented Thin Films Using Angle Resolved Photoelectron Spectroscopy", *Physica Scripta*, **41**, 550 (1990).

H. YAMAMOTO, H. INOKUCHI and K. SEKI, "Ultraviolet Photoelectron Spectroscopy of Perylene Anion in Cs-Perylene Solid", *Mol. Cryst. Liq. Cryst. Lett.* **6**, 171 (1989).

K. SEKI, I. MORISADA, H. TANAKA, K. EDAMATSU, M. YOSHIKI, Y. TAKATA, T. YOKOYAMA, T. OHTA, S. ASADA, H. INOKUCHI, H. NAKAHARA and K. FUKUDA, "Photopolymerization of Long-chain Diacetylene Monocarboxylic Acid in LB Films Studied by UV Photoelectron Spectroscopy (UPS) and X-ray Absorption Near Edge Structure (XANES)", *Thin Solid Films*, **179**, 15 (1989).

K. SEKI, S. ASADA, T. MORI, H. INOKUCHI, I. MURASE, T. OHNISHI and T. NOGUCHI, "UV Photoelectron Spectroscopy of Poly(p-phenylene Vinylene) (PPV)", *Solid State Commun.* **74**, 677 (1990).

Y. SHIROTA, Y. MATSUMOTO, T. TANAKA, N. NOMA, K. SEKI, H. YAMAMOTO and H. INOKUCHI, "UV Photoelectron Spectroscopy of Photoconducting Polymers and 1:1 Alternating Copolymers Containing Pendant π-Electron Systems", *Mol. Cryst. Liq. Cryst.* **183**, 227 (1990).

H. MATSUYAMA, T. TAKAHASHI, H. KATAYAMA-YOSHIDA, T. KASHIWAKURA, Y. OKABE, K. KOSUGI, A. YAGISHITA, K. TANAKA, H. FUJIMOTO and H. INOKUCHI, "Impurity-State-Like Nature of Fermi-Liquid States in Bi$_2$Sr$_2$CaCu$_2$O$_8$ Observed by Photoemission and X-ray Absorption", *Physica* **C160**, 567 (1989).

H. INOKUCHI, "Organic Semiconductors, Conductors, and Superconductors", *Int. Rev. Phys. Chem.* **8**, 95 (1989).

Y. LI, C. NAKANO, K. IMAEDA, H. INOKUCHI, Y. MARUYAMA, N. IWASAWA and G. SAITO, "Charge-Carrier Drift Mobilities and Phase Transition in Tetrakis(octylthio)tetrathiafulvalene, TTC$_8$-TTF, Crystal", *Bull. Chem. Soc. Jpn.* **63**, 1857 (1990).

T. ENOKI, S. MIYAJIMA, M. SANO and H. INOKUCHI, "Hydrogen-Alkali-Metal-Graphite Ternary Intercalation Compounds", *J. Materials Res.* **5**, 435 (1990).

S. MIYAJIMA, M. KABASAWA, T. CHIBA, T. ENOKI, Y. MARUYAMA and H. INOKUCHI, "Two-Dimensional Metallic Hydrogen in the Potassim-Hydrogen-Graphite Ternary Intercalation Compound", *Phy. Rev. Lett.* **64**, 319 (1990).

H. MURAKAMI, I. KANAZAWA, M. SANO, T. ENOKI and H. INOKUCHI, "Positron Annihiration in Potassium-Intercalated Graphite", *Synth. Metals.* **32**, 135 (1989).

T. MORI and H. INOKUCHI, "Fermi Surface and Thermoelectric Power of Two-Dimensional Organic Conductors", in "The Physics and Chemistry of Organic Superconductors", G. Saito and S. Kagoshima Eds., Springer, Berlin (1990), p.204.

H. TAJIMA, M. TAMURA, H. KURODA, T. MORI and H. INOKUCHI, "The Reflectance Spectra of (BEDT-TTF)$_5$Hg$_3$Br$_{11}$ and (BEDT-TTF)HgBr$_3$. The Estimation of Effective On-Site Coulomb Interaction", *Bull. Chem. Soc. Jpn.* **63**, 538 (1990).

T. MORI, H. INOKUCHI, A.M. KINI and J.M. WILLIAMS, "Unsymmetrically Substituted Ethylenedioxytetrathiafulvalenes", *Chem. Lett.* **1990**, 1279.

H. MORI, S. TANAKA, M. OSHIMA, G. SAITO, T. MORI, Y. MARUYAMA and H. INOKUCHI, "Crystal and Electronic Structures of (BEDT-TTF)$_2$[MHg(SCN)$_4$] (M = K and NH$_4$)", *Bull. Chem. Soc. Jpn.* **63**, 2183 (1990).

H. MORI, S. TANAKA, K. OSHIMA, M. OSHIMA, G. SAITO, T. MORI, Y. MARUYAMA and H. INOKUCHI, "Electrical Properties and Crystal Structures of Mercury(II) Thiocyanate Salts Based upon BEDT-TTF with Li$^+$, K$^+$, NH$_4^+$, Rb$^+$, and Cs$^+$", *Solid State Commun.* **74**, 1261 (1990).

T. MORI, H. INOKUCHI, H. MORI, S. TANAKA, M. OSHIMA and G. SAITO, "Thermoelectric Power of (BEDT-TTF)$_2$$M$Hg(SCN)$_4$ [M = K, Rb, NH$_4$]", *J. Phys. Soc. Jpn.* **59**, 2624 (1990).

H. MORI, I. HIRABAYASHI, S. TANAKA, T. MORI and H. INOKUCHI, "A New Ambient-Pressure Organic Superconductor, κ-(BEDT-TTF)$_2$Ag(CN)$_2$H$_2$O (T_c = 5.0 K)", *Solid State Commun.* **76**, 35 (1990).

S. SATO, A. SOBCZINSKI, J.M. WHITE, A.J. BARD, A. CAMPION, M.A. FOX, T.E. MALLOUK and S.E. WEBBER, "Photochemical Properties of Ultrathin TiO_2 Films Prepared by Chemical Vapor Deposition", *J. Photochem. Photobio. A. Chem.* **50**, 283 (1989).

S. SATO and T. OHMORI, "Surface Photochemistry of Metal Carbonyls. I. Photolysis of Iron Carbonyls Adsorbed on Alumina and Silica", *Shokubai (Catalyst)* (in Japanese), **32**, 67 (1990).

S. SATO and T. KADOWAKI, "Photoevolution of Oxygen from a Suspension of Metal Oxide Semiconductor in Aqueous Silver-Salt Solution", *Denki Kagaku* (in Japanese), **57**, 12 (1989).

T. OHMORI, Y. NODASAKA and M. ENYO, "Electro-Oxidation of Methanol on Pt Electrodes Modified by Metal Oxides and Noble Metals", *J. Electroanal. Chem.* **281**, 331 (1990).

T. MATSUSHIMA, "Crystal Azimuth Dependence of the Angular Distribution of the Desorption Flux of Carbon Dioxide Produced on Palladium (110) Surfaces", *J. Chem. Phys.* **91**, 5722 (1989).

T. MATSUSHIMA, "Crystal Azimuth Dependence of the Desorption Flux of Carbon Dioxide Produced on Palladium (110) and (111) Surfaces", *Vacuum* **41**, 275 (1990).

T. MATSUSHIMA and Y. OHNO, "The Angular Distribution of the Product Desorption and the Orientation of Terraces: the Oxidation of Carbon Monoxide over Platinum (110)(1×2) Reconstructed Surfaces", *Chem. Phys. Lett.* **169**, 569 (1990).

T. MATSUSHIMA, "The Spatial Distribution of the Product Desorption in the Oxidation of Carbon Monoxide on Platinum (110)(1×2) Reconstructed Surfaces", *J. Chem. Phys.* **93**, 1464 (1990).

Y. OHNO, T. NAKAMURA and H. KITA, "Angle and Speed Distributions of Hydrogen Desorbing Thermally from Metal Surfaces I. Quantum Mechanical Transition State Theory", *Appl. Phys.* **A50**, 551 (1990).

Y. OHNO, T. NAKAMURA and H. KITA, "Angle and Speed Distributions of Hydrogen Desorbing Thermally from Metal Surfaces II. Application to D_2 Desorbing from a Ni(111) Surface", *Appl. Phys.* **A51**, 35 (1990).

K. NAKASUJI, M. YAMAGUCHI, I. MURATA, K. YAMAGUCHI, T. FUENO, H. OHYA-NISHIGUCHI, T. SUGANO and M. KINOSHITA, "Synthesis and Characterization of Phenalenyl Cations, Radicals, and Anions Having Donor and Acceptor Substituents: Three Redox States of Modified Odd Alternant Systems", *J. Am. Chem. Soc.* **111**, 9265 (1989).

K. NAKASUJI, A. ODA, I. MURATA, K. IMAEDA and H. INOKUCHI, "Synthesis and Properties of 1,7-Dithiaperylene: a New Pericondensed Weitz-Type Donor", *J. Chem. Soc., Chem. Commun.* 1553 (1989).

H. HARADA, H. ODA, K. NAKASUJI and I. MURATA, "Interchoromophoric Homoconjugation Effect and Intramolecular Change-transfer Transition of the Triptycene System Containing a Tetracyanoquinodimethane Chromophore", *J. Chem. Soc., Perkin Trans. II*, 1449 (1989).

K. NAKASUJI, "Design of Organic Molecular Metals Based on New Multi-Stage Redox Systems in the Non-TTF Family: Peri-Condensed Weitz-Type Donors", *Proc. ISSP Int. Symp. on the Physics and Chemistry of Organic Superconductors* 1989 Tokyo, Springer-Verlag, p.399.

K. NAKASUJI, "New Multi-Stage Redox Systems and New Molecular Metals", *Pure & Appl. Chem.* **62**, 477 (1990).

K. NAKASUJI, A. ODA, J. TOYODA and I. MURATA, "Synthesis and Properties of 3,9-Dithiaperylene: A Third Isomer of Peri-Condensed Weitz-Type Donors Based on the Perylene Skeleton", *J. Chem. Soc., Chem. Commun.* 366 (1990).

A. KAWAMOTO, J. TANAKA, A. ODA, H. MIZUMURA, I. MURATA and K. NAKASUJI, "Crystal Structure and Electronic Structure of Radical Salts of 2,7-Bis(methylthio)-1-6-dithiapyrene (MTDTPY) and 2,7-(methylseleno)-1-6-dithiapyrene (MSDTPY)", *Bull. Chem. Soc. Jpn.* **63**, 2137 (1990).

A. KAWAMOTO, J. TANAKA, M. SASAKI, I. MURATA and K. NAKASUJI, "Electronic Structure of 2,7-Bis(methylthio)-1,6-dithiapyrene (MTDTPY) Cherge Transfer Complexes", *Bull. Chem. Soc. Jpn.* **63**, 2146 (1990).

T. KITAGAWA, J. TOYODA, K. NAKASUJI, H. YAMAMOTO and I. MURATA, "Amphoteric Redox Nature of *p*-Benzoquinones with Donor- and Acceptor-Substituents", *Chem. Lett.* 897 (1990).

S. INAGAKI, T. OKAJIMA, K. YAMAMURA, H. MIYAKE, K. NAKASUJI and I. MURATA, "Comformational Adaptation: A New Aspect of Substituent Effects", *Bull. Chem. Soc. Jpn.* **63**, 2099 (1990).

W.E. ACREE, Jr., S.A. TUCKER, L.E. CRETELLA, A.I. ZVAIGNE, K.W. STREET, Jr., J.C. FETZER, K. NAKASUJI and I. MURATA, "Polycyclic Aromatic Hydrocarbons and Polycyclic Aromatic Sulfur Heterocycles: Examination of Molecular Structure-Fluorescence Probe Character Correlations", *Appl. Spectrosc.* **44**, 951 (1990).

C. ZHANG, Y. OZAWA, Y. HAYASHI and K. ISOBE, "Oxidation of Cyclohexene with t-Butyl Hydroperoxide Catalyzed by Transition Metal Oxide Clusters", *J. Organomet. Chem.* **373**, C21 (1989).

Y. OZAWA, Y. HAYASHI and K. ISOBE, "Synthesis and Structure of Novel Organometallic Sulfide Cluster $[(\eta^5\text{-}C_5Me_5)MWO(\mu\text{-}S_2)(\mu\text{-}S)_2]_2$ (M=Rh,Ir) Containing High-Valent Tungsten Atoms", *Chem. Lett.* 249 (1990).

K. KITAMURA-BANDO, K. ASAKURA, H. ARAKAWA, Y. SUGI, K. ISOBE and Y. IWASAWA, "Direct Observation of Unusual CO Insertion on an New SiO_2-Attached Rh Dimer Catalyst by FTIR", *J. Chem. Soc., Chem. Commun.* 253 (1990).

K. ASAKURA, K. KITAMURA-BANDO, K. ISOBE, H. ARAKAWA and Y. IWASAWA, "Metal-Assisted CO Insertion Reaction on a New Surface Rhodium Dimer Catalyst Observed by an *in situ* Extended X-Ray Absorption Fine Structure Technique", *J. Am. Chem. Soc.* **112**, 3242 (1990).

K. UMAKOSHI and K. ISOBE, "Reactivity of Pentamethylcycropentadienyltetrachloromolybdenum(V). Synthesis, Structure and Electrochemical Properties of $[(\eta^5\text{-}C_5Me_5)MoOCl]_2O$", *J. Organomet. Chem.* **392**, 115 (1990).

N. KITAJIMA, K. FUJISAWA, Y. MORO-OKA and K. TORIUMI, "$\mu\text{-}\eta^2{:}\eta^2$-Peroxo Binuclear Copper Complex, $[Cu(HB(3,5\text{-}iPr_2pz)_3)]_2(O_2)$", *J. Am. Chem. Soc.* **111**, 8975 (1989).

K. TORIUMI, H. OKAMOTO, T. MITANI, S. BONDOW, M. YAMASHITA, Y. WADA, Y. FUJII, R.J.H. CLARK, D.J. MICHAEL, A.J. EDWARD, D. WATKIN, M. KURMOO and P. DAY, "Syntheses, Structures and Solid State Properties of One-Dimensional Halogen-Bridged Ni^{III}-X-Ni^{III} Compounds (X=Cl and Br)", *Mol. Cryst. Liq. Cryst.* **181**, 333 (1990).

T. NAGATA, A. OSUKA, K. MARUYAMA and K. TORIUMI, "Structure of 3,5,7,13,15,17-Hexamethyl-2,8,12,18-tetramethylporphinato-copper(II)", *Acta. Crystallogr.* **C46**, 1745 (1990).

M. MIKURIYA, K. KUSHIDA, H. OKAWA and H. OSHIO, "Preparation, Electronic Properties and Crystal Structure of Imidazolebis(1,10-phenanthroline)copper(II) Bis(hexafluorophosphate)", *Inorg. Chim. Acta.* **159**, 149 (1989).

M. SUZUKI, T. SUGISAWA, H. SENDA, H. OSHIO and A. UEHARA, "Synthesis and Characterization of a Novel Tetranuclear Manganese(II,III,III,II) Mixed Valence Complex", *Chem. Lett.* 1091 (1989)

N. MATUMOTO, Y. MAEDA, H. OKAWA, T. AKUI, T. KAWAJI, A. OHYOSHI, M. KODERA, H. OSHIO and S. KIDA, "Synthesis and Characterization of Imidazolate-bridged Iron(III)-Copper(II) and Manganese(III)-Copper(II) Binuclear Complexes", *J. Chem. Soc., Dalton Trans.* 943 (1989).

T. KAMIUSUMI, H. OKAWA, E. KITAURA, M. KOIKAWA, N. MATUMOTO, S. KIDA and H. OSHIO, "Binuclear Copper(II) Complexes of New Dinucleating Ligands with a Pyrazolate Group as an Endogenous Bridge. Effects of Exogenous Azide and Acetate Bridges on Magnetic Properties", *J. Chem. Soc., Dalton Trans.* 2077 (1989).

H. OSHIO, K. TORIUMI and Y. HAYASHI, "Synthesis, Crystal Structure, and Electrochemical Properties of μ-{2,5-Bis[N,N-bis(2'-pyridylmethyl)aminomethyl]pyrazine}bis[chlorocopper(II)] Perchlorate", *J. Chem. Soc., Dalton Trans.* 293 (1990).

H. OKAWA, M. KOIKAWA, S. KIDA, D. LUNEAU and H. OSHIO, "Synthesis, Structure, and Spectral and Magnetic Properties of Trinuclear Copper(II) Complexes bridged by Glyoximate Groups", *J. Chem. Soc., Dalton Trans.* 469 (1990).

H. OSHIO, K. TORIUMI, S. BANDOW, K. MIYAGAWA and S. KURITA, "Structural, Magnetic, and Optical Studies of New Mixed Valence Copper(II)-Platinum(IV) Complexes with One-dimentional Chain Structures", *J. Chem. Soc., Dalton Trans.* 1013 (1990).

M. MIKURIYA, S. SHIGEMATU, K. KAWANO, T. TOKII and H. OSHIO, "Synthesis, Structure, and Magnetic Properties of a Novel Manganese(IV) Complex with the Schiff-base Ligand Containing Two Phenolic Oxygen", *Chem. Lett.* 729 (1990).

M. MIKURIYA, T. FUJII, S. KAMISAWA, Y. KAWASAKI, T. TOKII and H. OSHIO, "Synthesis, Structure, and Magnetic Properties of Novel Binuclear and Mononuclear Manganese(II) Complexes with 2,6-Bis[N-(2-pyridylethyl)iminomethyl]4-methylphenol", *Chem. Lett.* 1181 (1990).

D. LUNEAU, H. OSHIO, H. OKAWA and S. KIDA, "Synthesis, Structure, and Magnetism of Trinuclear Copper(II) Complexes [Cu(CuL)$_2$](ClO$_4$)$_2$ (H$_2$L = 3,3'-(Trimethylenedinitrilo)bis(2-butanoneoxime))", *J. Chem. Soc., Dalton Trans.* 2283 (1990).

H. OSHIO and U. NAGASHINA, "Magnetic Property of a Pyrazine-Bridged Dinuclear Copper(II) Compound. X-ray Structure of μ-2,5-Bis[[(dimethylamino)methyl]pyrazine]bis[(diethylenetriamine)-copper(II)]perchlorate", *Inorg. Chem.* **29**, 3321 (1990).

D. LUNEAU, H. OSHIO, H. OKAWA, M. KOIKAWA and S. KIDA, "Synthesis, Structure and Magnetism of Binuclear Cu(II)Cu(II), Cu(II)Ni(II) and Ni(II)Ni(II) Complexes Doubly Bridged by Oxymate Groups", *Bull. Chem. Soc. Jpn.* **63**, 2212 (1990).

M. SORAI, Y. MAEDA and H. OSHIO, "Unusual Heat Capacity of the Ferric Spin-Crossover Complex, [Fe(acpa)$_2$]PF$_6$, Showing a Gradual but Complete Spin-State Interconversion at the Fast Spin-Flipping Rate", *J. Phys. Chem. Solids.* **51**, 941 (1990).

H. OSHIO, "Syntheses, Crystal Structures, and Electrochemical Properties of Binuclear Copper(II,II) [Cu$_2$L^{1}Cl$_2$](ClO$_4$)$_2 \cdot$ 4CH$_3$CN and Copper(I,I) [Cu$_2$L^1](ClO$_4$)$_2$ Complexes (L^1=2,5-Bis[N,N-bis(2'-pydidyl-ethyl)aminomethyl]pyrazine", *J. Chem. Soc., Dalton Trans.* 2985 (1990).

M. MISHIMA, H. INOUE, M. FUJIO and T. TSUNO, "Gas Phase Substituent Effects. Stabilities of 1-Aryl-2,2,2-trifluoroethyl Cations", *Tetrahedron Lett.* **31**, 685 (1990).

M. FUJIO, M. GOTO, M. MISHIMA and Y. TSUNO, "Substituent Effects. XVIII. The Resonance Demand in the Acetolysis of Neophyl Brosylates", *Bull. Chem. Soc. Jpn.* **63**, 1121 (1990).

A. MURATA, M. GOTO, R. FUJIYAMA, M. MISHIMA, M. FUJIO and Y. TSUNO, "Substituent Effects. XIX. Solvolysis of 1-Aryl-1-(trifluoromethyl)ethyl Tosylates", *Bull. Chem. Soc. Jpn.* **63**, 1129 (1990).

A. MURATA, S. SAKAGUCHI, R. FUJIYAMA, M. MISHIMA, M. FUJIO and Y. TSUNO, "Substituent Effects. XX. Highly Electron-Deficient Carbocation Solvolyses", *Bull. Chem. Soc. Jpn.* **63**, 1138 (1990).

M. FUJIO, M. GOTO, T. SUSUKI, I. AKASAKA, M. MISHIMA and Y. TSUNO, "Substituent Effects. XXI. Solvolysis of Benzyl Tosylates", *Bull. Chem. Soc. Jpn.* **63**, 1146 (1990).

Y. TSUJI, M. FUJIO and Y. TSUNO, "Substituent Effects. 22. The Solvolysis of α-t-Butylbenzyl Tosylates", *Bull. Chem. Soc. Jpn.* **63**, 856 (1990).

M. FUJIO, M. GOTO, S. SUSUKI, M. MISHIMA and Y. TSUNO, "Substituent Effects in the Solvolysis of Benzyl Tosylates", *J. Phys. Org. Chem.* **3**, 449 (1990).

M. FUJIO, M. GOTO, K. FUNATSU, T. YOSHINO and Y. TSUNO, "Solvent Effects on the Solvolysis of Neophyl Tosylates", *Mem. Fac. Sci., Kyushu Univ., Ser. C* **17(2)**, 255 (1990).

K. YATSUGI, Y. KIKUTA, Y. TSUJI, M. FUJIO and Y. TSUNO, "Solvent Mechanism of 1,1,3,3-Tetramethylin-dan-2-yl Arenesufonates", *Mem. Fac. Sci., Kyushu Univ., Ser. C* **17(2)**, 267 (1990).

Y. TSUJI, M. FUJIO and Y. TSUNO, "Solvent Effect on the Solvolysis of α-t-Butylbenzyl Tosylate", *Mem. Fac. Sci., Kyushu Univ., Ser. C* **17(2)**, 281 (1990).

N. SHIMIZU, S. MATSUNO, M. TANAKA and Y. TSUNO, "Configuration-dependent Stereochemistry in 2,4-Dichirolo-3-pentanone. Its Trimethylsilyl Ether Interconversion", *Chem. Lett.* 1979 (1989).

239

Y. HANDA, J. INANAGA and M. YAMAGUCHI, "Rapid and Mild Deoxygenation of Organoheteroatom Oxides with the Efficient Electron Transfer System SmI_2-Tetrahydrofuran-Hexamethylphosphoric Triamide", *J. Chem. Soc., Chem. Commun.* 298 (1989).

O. UJIKAWA, J. INANAGA and M. YAMAGUCHI, "An Efficient Intermolecular Carbon-Carbon Bond Formation via SmI_2-Promoted Anion Radical Alkylation", *Tetrahedron Lett.* 30, 2837 (1989).

K. KUSUDA, J. INANAGA and M. YAMAGUCHI, "A Highly Efficient Deoxygenation of α-Oxygenated Esters via SmI_2-Induced Electron Transfer Process", *Tetrahedron Lett.* 30, 2945 (1989).

T. RADNAL, S. ISHIGURO and H. OHTAKI, "Liquid Structure of 2,2,2-Trifluoroethanol-Dimethyl Sulphoxide Mixtures as Studied by X-Ray Diffraction", *Chem. Phys. Rev.* 159, 532 (1989).

K. OZUTSUMI, T. TAKAMUKU, S. ISHIGURO and H. OHTAKI, "An X-Ray Diffraction Study on the Structure of Solvated Cadmium(II) Ion and Tetrathiocyanatocadmate(II) Complex in N,N-Dimethylformamide", *Bull. Chem. Soc. Jpn.* 62, 1875 (1989).

K. OZUTSUMI, M. NATSUHARA and H. OHTAKI, "An X-Ray Diffraction Study on the Structure of 18-Crown-6 Ether Complexes with Alkali Metal Ions in Aqueous Solution", *Bull. Chem. Soc. Jpn.* 62, 2807 (1989).

H. SUZUKI, S. ISHIGURO and H. OHTAKI, "Solvation and Complexation of Copper(II) and Chloride Ions in 2,2,2-Trifluoroethanol-Dimethyl Sulphoxide Mixtures", *J. Chem. Soc., Faraday Trans. 1*, 85, 2587 (1989).

S. ISHIGURO, K. OZUTSUMI, M. MIYAUCHI and H. OHTAKI, "Formation of Binary and Ternary Complexes of Cadmium(II) with Halide Ions and 2,2'-Bipyridine in N,N-Dimethylformamides", *Inorg. Chem.* 28, 3258 (1989).

A. RAJALAKSHMI, M. SESHASAYEE, T. YAMAGUCHI, M. NOMURA and H. OHTAKI, "Structural Studies on Superionic Glass $AgI-Ag_2O-V_2O_5$", *J. Non-Crystal. Solid*, 113, 260 (1989).

A. RAJALAKSHMI, M. SESHASAYEE, G. ARAVAMUDAN, T. YAMAGUCHI, M. NOMURA and H. OHTAKI, "Structural Studies on Superionic Glass $AgI-Ag_2O-MoO_3$", *J. Phys. Soc. Jpn.* 59, 1252 (1990).

H. ABE, S. HOSHI, K. DOMEN, K. MARUYA, H. OHTAKI and T. ONISHI, "Characterization of Highly Selective Cu-Ni Amination Catalysts", *Chem. Lett.* 401 (1990).

H. SUZUKI, S. ISHIGURO and H. OHTAKI, "Formation of Chloro Complexes of Manganese(II), Cobalt(II), Nickel(II) and Zinc(II) in Dimethyl Sulphoxide", *J. Chem. Soc., Faraday Trans.* 86, 2179 (1990).

M. KODAMA, H. ANAN, T. KOIKE and E. KIMURA, "Complexation Reactions of Copper(II) Ions with 16-Memberd and 18-Membered Monocyclic Dioxopolyamines in an Aqueous Solution", *Bull. Chem. Soc. Jpn.* 62, 4044 (1989).

T. TAKEGAWA, S. HIROSE, E. KIMURA, H. AIHARA, Y. ISOBE and K. IGARASHI, "Effect of Polyamine Related Tetraamines on Anti-Ulcerogenic Activity and Anti-H^+, K^+-ATPase Activity", *Res. Commun. Chem. Pathol. Pharmacol.* 64, 395 (1989).

E. KIMURA, Y. KURAMOTO, T. KOIKE, H. FUJIOKA and K. KODAMA, "A Study of New bis(macrocyclic polyamine) Ligands as Inorganic and Organic Anion Receptors", *J. Org. Chem.* 55, 42 (1990).

E. KIMURA, Y. YOSHIYAMA, M. SHIONOYA and M. SHIRO, "Isolation and Unusual Stability of a New Macrocyclic Polyamine Containing a Phthalimidine", *J. Org. Chem.* 55, 764 (1990).

E. KIMURA, S. WADA, M. SHIONOYA, T. TAKAHASHI and Y. IITAKA, "A Novel Cyclam-Nickel(II) Complex Appended with a Tris-(2,2'-bipyridine)-Ruthenium(II) Complex (Cyclam = 1,4,8,11-tetra-azacyclotetradecane)", *J. Chem. Soc., Chem. Commun.* 397 (1990).

E. KIMURA, T. SHIOTA, T. KOIKE, M. SHIRO and M. KODAMA, "A Zinc(II) Complex of 1,5,9-Triazacyclododecane ($[12]aneN_3$) as a Model for Carbonic Anhydrase", *J. Am. Chem. Soc.* 112, 5805 (1990).

M. TANSHO, D. NAKAMURA and R. IKEDA, "^{1}H NMR and Thermal Studies of CH_3NH_3Br in a Metastable Solid Phase Newly Found above 483 K", *Z. Naturforsch.* 44a, 738 (1989).

H. ISHIDA, T. IWACHIDO, N. HAYAMA, R. IKEDA, M. TERASHIMA and D. NAKAMURA, "Self-Diffusion and Reorientation of Methylammonium Ions in $(CH_3NH_3)_2ZnCl_4$ Crystals as Studied by ^1H NMR", *Z. Naturforsch.* **44a**, 741 (1989).

R. IKEDA, A. KUBO and C.A. MCDOWELL, "Structure and Dynamics of Dimethylammonium Ions in Solids Using ^2H Quadrupole Echo Spectra", *J. Phys. Chem.* **93**, 7315 (1989).

R. WATANABE, T. ASAJI, Y. FURUKAWA, D. NAKAMURA and R. IKEDA, "Structural Phase Transitions and Cationic Motions in Pyridinium Dichloroiodate(I) as Studied by ^1H NMR, Differential Thermal Analysis, and Powder X-Ray Diffraction", *Z. Naturforsch.* **44a**, 1111 (1989).

Y. TAI, T. ASAJI, D. NAKAMURA and R. IKEDA, "Chlorine Nuclear Quadrupole Relaxation due to the Motion of Pyridinium Cations in Pyridinium Hexachlorometallates(IV): $(pyH)_2MCl_6$ (M = Sn, Pb, Te)", *Z. Naturforsch.* **45a**, 477 (1990).

A. ISHIKAWA, T. ASAJI, D. NAKAMURA and R. IKEDA, "Chlorine Nuclear Quadrupole Relaxation Studies on Ionic Dynamics and Phase Transition in NH_4AuCl_4", *Z. Naturforsch.* **45a**, 467 (1990).

H. ISHIDA, K. TAKAGI, T. IWACHIDO, M. TERASHIMA, D. NAKAMURA and R. IKEDA, "Motions of Methylammonium Ions in $(CH_3NH_3)_2ZnBr_4$ Crystals Studied by ^1H NMR and Thermal Measurements", *Z. Naturforsch* **45a**, 923 (1990).

K. NAKAJIMA, K. KOJIMA, M. KOJIMA and J. FUJITA, "Preparation and Characterization of Optically Active Schiff Base-Oxovanadium(IV) and -Oxovanadium(V) Complexes and Catalytic Properties of These Complexes on Asymmetric Oxidation of Sulfides into Sulfoxides with Organic Hydroperoxides", *Bull. Chem. Soc. Jpn.* **63**, 2620 (1990).

M. ZENKI, T. SHIBAHARA, M. YAMASAKI and Y. KUSHI, "Crystal Structure of Arsenazo I", *Analytical Science*, **6**, 153 (1990).

Y. YOKOYAMA, A. INABA, H. HARA, T. YAMAZAKI, H. TAMURA and Y. KUSHI, "Crystal Structure of Photosensitive Uranyl Ethoxycarboxylate Complexes", *Chem. Lett.*, 671 (1990).

H. NAKAZAWA, H. NOSAKA, Y. KUSHI and H. YONEDA, "Reaction of Nickel(0) with α-Keto Phosphonates. Syntheses, Characterization, and X-ray Crystal Structure of $(PPh_3)_2Ni(\eta^2$-(CO)RC(O)P(O)(OMe)_2)$", *Organometallics*, **9**, 1958 (1990).

T. YAMAMOTO, K. SANO, K. OSAKADA, S. KOMIYA, A. YAMAMOTO, Y. KUSHI nad T. TADA, "Comparative Studies on Reactions of α,β- and β,γ-Unsaturated Amides and Acids with Nickel(0), Palladium(0), and Platinum(0) Complexes. Preparation of New Five- and Six-Membered Nickel- and Palladium Containing Cyclic Amide and Ester Complexes", *Organometallics*, **9**, 2396 (1990).

H. HIRAKAWA, H. NOMURA and F. KAWAIZUMI, "Sedimentation Potential of Complexes of Nitroamminecobalt(III) in Aqueous Solution at 25°C", *J. Solution Chem.* **19**, 11 (1990).

K. OHE, S. UEMURA, N. SUGITA, H. MASUDA and T. TAGA, "Sodium Arenetellurolate Catalyzed Selective Conversion of Nitroaromatics to Aromatic Azoxy or Azo Compounds and Its Application for Facile Preparation of 3,3'- and 4,4'-Bis [β-(aryltelluro)vinyl]azobenzenes from (3- and 4-Nitrophenyl)acetylenes", *J. Org. Chem.* **54**, 4169 (1989).

K. YAMAMURA, S. ONO, H. OGOSHI, H. MASUDA and Y. KURODA, "Chiral Liquid Crystal Mesogens. Synthesis and Determination of Absolute Configuration of Mesogens with 4,4'-Biphenanthryl Cores", *Synlett*, **1**, 18 (1989).

O. YAMAUCHI, A. ODANI, T. KOHZUMA, H. MASUDA, K. TORIUMI and K. SAITO, "Aromatic Ring Stacking in Ternary Copper(II) Complexes [Cu(histamine)(L-AA)(ClO_4)](AA=Phenylalaninate, Tyrosinate). Structural Evidence for Intramolecular Stacking Involving a Coordinated Imidazole Ring", *Inorg. Chem.* **28**, 4066 (1989).

M. MUNAKATA, M. MAEKAWA, S. KITAGAWA, S. MATSUYAMA and H. MASUDA, "Synthesis and Structures of (2,9-Dimethyl-1,10-phenanthroline)(acetonitrile)copper(I) Perchlorate and Hexafluorophosphate. A Correlation between Bond Angles and Bond Distances in T- and Y-Shaped Three-Coordinate Copper(I) Complexes", *Inorg. Chem.* **28**, 4300 (1989).

M. EBIHARA, K. SAKURAI, T. KAWAMURA, H. KATAYAMA, H. MASUDA and T. TAGA, "Covalent Bonding of Two Ag(I) Atoms to a Square-Planar Pt(II) Atom in [Pt$_3$(S$_2$CNEt$_2$)$_6$Ag$_2$](ClO$_4$)$_2$", *Chem. Lett.* 415 (1990).

M. MUNAKATA, M. MAEKAWA, S. KITAGAWA, M. ADACHI and H. MASUDA, "Synthesis, Properties and Crystal Structures of Dicopper(I) and Disilver(I) Complexes with 1,8-Naphthyridine(napy): [Cu$_2$(napy)$_2$](ClO$_4$)$_2$ and [Ag$_2$(napy)$_2$](ClO$_4$)$_2$", *Inorg. Chim. Acta,* **167**, 181 (1990).

O. YAMAUCHI, M. TAKANI, K. TOYODA and H. MASUDA, "Indole Nitrogen-Palladium(II) Bonding. Chemical and Structural Characterization of Palladium(II) Complexes of Alkylindoles and Intermediacy of the 3*H*-Indole Ring", *Inorg. Chem.* **29**, 1856 (1990).

T. MITSUDO, A. ISHIHARA, T. SUZUKI, Y. WATANABE and H. MASUDA, "Synthesis, Structure, and Reactivity of the First Anionic Acyldihalocarbonyliron(II) Complex. Halogen-Induced Insertion of Carbon Monoxide into an Alkyl-Iron Bond" *Organometallics,* **9**, 1357 (1990).

H. MASUDA, "Raman Spectra of Copper(I) and Silver(I) Complexes with 1,5-Cyclooctadiene and the Nature of Metal-Olefin Bonds. Possibility of a Copper(I)-Olefin Bond in Cytochrome Oxidase", *J. Organomet, Chem.* **391**, 131 (1990).

S. KITAGAWA, M. MUNAKATA, H. SHIMONO, S. MATSUYAMA and H. MASUDA, "Synthesis and Crystal Structure of Hexanuclear Copper(I) Complexes of μ_3-Pyridine-2-thionate", *J. Chem. Soc., Dalton Trans.* 2105 (1990).

T. YOSHIDA, T. ADACHI, T. UEDA and T. TANAKA, "Ring Size Effect of Crown Thioethers upon Recognition of Hydrido and Chloro Ligands at Stereochemically Different Axial Sites in trans-RuH(Cl)L(L=syn-Me$_4$[14]aneS$_4$, syn-Me$_8$[16]aneS$_4$)", *J. Chem. Soc., Chem. Commun.* 342 (1990).

T. YOSHIDA, T. ADACHI, T. UEDA, M. KAMINAKA, N. SASAKI, T. HIGUCHI, T. AOSHIMA, I. MEGA, Y. MIZOBE and M. HIDAI, "N-Arylation and N, N-Dibenzylation of Coordinated N$_2$ with Organic Halides; Differences in the Reactivity of trans-[Mo(N$_2$)$_2$(Me$_8$[16]aneS$_4$] and Its Phosphine Analogues", *Angew. Chem. Int. Ed. Engl.* **28**, 1040 (1989).

K. KOMORI, S. SUGIURA, Y. MIZOBE, M. YAMADA and M. HIDAI, "Synthesis and Some Reactions of Trimethylsilylated Dinitrogen Complexes of Tungsten and Molybdenum", *Bull. Chem. Soc. Jpn.* **62**, 2953 (1989).

H. OSHITA, Y. MIZOBE and M. HIDAI, "Novel Disilylation and Germylation of Coordinated Dinitrogen in cis-[W(N$_2$)$_2$(PMe$_2$Ph$_4$)]", *Chem. Lett.* 1303 (1990).

T. YAMAMURA, M. TADOKORO and R. KURODA, "A New Synthetic Route and the Structural Analysis of Ni(tsalen). (N,N'-Ethylenenbis-(thiosalicylidenaminato))nickel(II)", *Chem. Lett.* 1245 (1989).

T. YAMAMURA, M. TADOKORO, M. HAMAGUCHI and R. KURODA, "Synthesis and the Structure of a Thiolato Amine Nickel Complex. (N,N'-Ethylenebis(*o*-mercaptobenzylaminato))nickel(II)", *Chem. Lett.* 1481 (1989).

T. YAMAMURA, R. KURODA and M. TADOKORO, "[Bis[μ-N,N'-bis(o-thiobenzoyl)ethylenediamine-S,O,O',S]-dinickel(II)]. Synthesis of a 2 × [S$_2$O$_2$] bis-complex and the Structural Analysis", *Chem. Lett.* 1807 (1989).

T. YAMAMURA, H. KURIHARA, N. NAKAMURA, R. KURODA and K. ASAKURA, "Synthesis, X-Ray Analysis, EXAFS and XANES Of [Ni(SCH$_2$CH$_2$)$_2$]$^{2-}$. An Evidence for the Mononuclear Square Planar [Ni(II)S$^-_4$] Geometry in Nickel/Alkane Thiolate System", *Chem. Lett.* 101 (1990).

T. KOJIMA, T. USUI, T. TANASE, M. YASHIRO, S. YOSHIKAWA, R. KURODA, S. YANO and M. HIDAI, "Synthesis and Characterization of Cobalt(III) Complexes Containing α-Diamine and Carbinolamine Derived from α-Aminomalonate and Ethylenediamine.", *Inorg. Chem.* **29**, 446 (1990).

J. SKELLY, D.A. SUTTER, R. KURODA, S. NEIDLE, J.F. HANCOCK and A.F. DRAKE, "Conformational Effects of Nucleotide Exchange in Ras P21 Proteins as Studied by Fluorescence Spectroscopy", *FEBS Lett.* **262**, 127 (1990).

R. KURODA, E. TAKAHASHI, C.A. AUSTIN and L.M. FISHER, "DNA Binding and Interactions by Novel Porphyrins: Role of Charge and Substituents Probed by DNase I Footprinting and Topoisomerase I", *FEBS Lett.* **262**, 293 (1990).

T. KOJIMA, M. HIDAI, R. KURODA and S. YANO, "An Unprecedented Imido-Bridged Binuclear Cobalt(III) Complex: Synthesis and Molecular Structure of p-[Co$_2$(μ(μN:η-O,O')-Imidomalonato)(tren)$_2$](ClO$_4$)$_3$.H$_2$O", *J. Amer. Chem. Soc.* **112**, 4576 (1990).

O.M.Ni DHUBHGHAILL, P.J. SADLER and R. KURODA, "Gold(I) Complexes of 1-Diphenylphosphino-2-diphenylarsinoethane(appe): Solution Studies, X-ray Crystal Structures and Cytotoxicity of [(AuCl)$_2$(appe)] · 0.5DMA and [Au(appe)$_2$]Cl · 2H$_2$O", *J. Chem. Soc., Dalton Trans.* 2913 (1990).

R. KURODA and P. BISCARINI, "Chiral Discriminations of Complexes with D$_3$ Symmetry. Molecular Structure and Crystal Packing Mode of $(-)_{589}$-tris[$(-)$-cyclic-O,O'-1(R),2(R)dimethylethylenedithiophosphato]-chromium(III), {Cr[$(-)$bdtp]$_3$}", *J. Chem. Soc., Dalton Trans.* 3393 (1990).

Y. YANASE, H. YOSHIMURA, S. KINOSHITA, T. YAMAGUCHI and H. WAKITA, "Bis(aniline)bis(2,3-hexylmethylglyoximato)cobalt(III) Chloride and Bis(aniline)bis(2,3-octhylmethylglyoximato)cobalt(III) Chloride", *Acta Crystallogr.* **C46**, 36 (1990).

S. YAMASHITA, Y. YANASE, T. YAMAGUCHI and H. WAKITA, "A Structural Study of a Series of Bis(2,3-alkanedione dioximato)nickel(II) Complexes in the Crystal and the Liquid States by X-Ray Absorption Spectroscopy", *Bull. Chem. Soc. Jpn.* **62**, 2902 (1989).

T. OKAMOTO, S. YAMASHITA, T. YAMAGUCHI and H. WAKITA, "EXAFS Measurement with Laboratory Equipment: Problems and Their Countermeasures" *X-ray Spectrometry*, **19**, 15 (1990).

T. OKAMOTO, S. YAMASHITA, T. YAMAGUCHI and H. WAKITA, "Elimination of the Characteristic X-rays for Laboratory X-ray Spectroscopy" (in Japanese), *Adv. X-ray Chem. Anal.* **21**, 69 (1990).

Y. YAMASHITA, Y. KOBAYASHI and T. MIYASHI, "p-Quinodimethane Analogues of Tetrathiafulvalene", *Angew. Chem. Int. Ed. Engl.* **28**, 1052 (1989).

T. SUZUKI, Y. YAMASHITA, C. KABUTO and T. MIYASHI, "Preparation, Properties, and Crystal Structure of a 1,2,5-Thiadiazolotetracyanoquinodimethane", *J. Chem. Soc., Chem. Commun.* 1102 (1989).

Y. YAMASHITA, K. SAITO, T. MUKAI and T. MIYASHI, "N-Methyl Derivatives of [1,2,5]Thiadiazolo[3,4-b]quinoxaline and the Selenium Analogues", *Tetrahedron Lett.* **30**, 7071 (1989).

K. SAITO, T. USHIDA, H. FUSHIHARA, Y. YAMASHITA, S. TANAKA and K. TAKAHASHI, "On the Multiplicity of Carbenes Conjugated with Pyrrole and Furan Moieties: Molecular Orbital Calculation and Reaction of 2-(1-Methyl)-pyrrolylmethylene and 2-Furylmethylene with *cis*- and *trans*-Stilbenes", *Heterocycles*, **31**, 115 (1990).

Y. YAMASHITA, Y. TSUBATA, T. SUZUKI, T. MIYASHI, T. MUKAI and S. TANAKA, "Benzo[g][1,2,5]thiadiazolo[3,4-b]quinoxaline-5,10-dione and its Selenium Analogue. An Unusual Type of Quinones", *Chem. Lett.* 445 (1990).

Y. YAMASHITA, Y. KOBAYASHI and T. MIYASHI, "Preparation and Properties of p-Quinodimethane Analogues of Tetrathiafulvalene" in "The Physics and Chemistry of Organic Superconductors", G. Saito and K. Kagoshima Eds., Springer-Verlag (1990), p. 387.

Y. YAMASHITA, J. EGUCHI, T. SUZUKI, C. KABUTO, T. MIYASHI and S. TANAKA, "4,7-Dimethyl-4,7-dihydro[1,2,5]thiadiazolo[3,4-b]pyrazine, a Novel Electron Donor with a 12 π-Electron Ring System", *Angew. Chem. Int. Ed. Engl.* **29**, 643 (1990).

H. UMEMOTO, A. MASAKI, T. OHNUMA, T. TAKAYANAGI, S. SATO, F. MISAIZU and K. FUKE, "The Intramultiplet Mixing of Zn(4^3P$_J$) by Collisions with ^{4}He and ^{3}He", *J. Chem. Phys.* **93**, 4112 (1990).

N. SATOH and K. KIMURA, "High-Resolution Solid-State NMR in Liquids. 2. ^{27}Al NMR Study of AlF$_3$ Ultrafine Particles", *J. Am. Chem. Soc.* **112**, 4688 (1990).

K. KIMURA and H. HAYASHI, "Effect of Surface State on the Spin Susceptibility of Ultrafine Metallic Particles", *Phys. Rev.* **B41**, 10185 (1990).

S. BANDOW and K. KIMURA, "ESR and CESR Observed in Ultrafine Mg Particles", *Solid State Commun.* **73**, 167 (1990).

S. BANDOW and K. KIMURA, "Temperature Dependence of ESR Absorption Intensity of Ultrafine Zn and Mg Particles", *Solid State Commun.* **75**, 473 (1990).

K. KIMURA, "Deviation of Spin Susceptibility of Small Metallic Particles as Predicted by the Random-Matrix Theory", *Phys. Rev.* **B42**, 6939 (1990).

K. AWAGA, H. OKAMOTO, T. MITANI, Y. MARUYAMA, T. SUGANO and M. KINOSHITA, "Spin-Soliton Excitation in One-Dimensional Alternation Antiferromagnetic System of Galvinoxyl Single Crystal", *Solid State Commun.* **71**, 1173 (1989).

K. AWAGA, T. INABE, U. NAGASHIMA and Y. MARUYAMA, "Two-Dimensional Network of the Ferromagnetic Organic Radical, 2-(4-Nitrophenyl9-4,4,5,5-tetramethyl-4,5-dihydro-1H-imidazol-1-oxyl 3-N-Oxide", *J. Chem. Soc., Chem. Commun.* 1617 (1989).

K. AWAGA, T. INABE, U. NAGASHIMA and Y. MARUYAMA, "Ferro- and Antiferromagnetic Intermolecular Interactions of Organic Radicals, α-Nitronyl Nitroxides" in "The Physics and Chemistry of Organic Superconductors", G. Saito and S. Kagoshima Ed., Springer-Verlag, pp. 329-332 (1990).

K. AWAGA, T. INABE and Y. MARUYAMA, "Ferromagnetic Intermolecular Interaction and Crystal Structure of α-Nitronyl Nitroxide", *Mat. Res. Soc. Symp. Proc.* **173**, 33 (1990).

K. KATO and M. SUZUI, "Automated Liquid-helium Transfer Tube Lifting System", *Rev. Sci. Instrum.* **61**, 2004 (1990).

H. YOSHIOKA and T. MITANI, "Effect of Pressure on the Properties of a Surfactant Micelle and a Lipid Membrane Studied by the Spin-Probe Method", *J. Chem. Soc., Faraday Trans. 1*, **85**, 1485 (1989).

T. MITANI, "Optical-Spectroscopy of Interacting Protons in H-Bonding System", *Mol. Cryst. Liq. Cryst.* **183**, 139 (1990).

M. FUJITA, H. NAKAGAWA, H. MATSUMOTO, T. MIYANAGA, M. WATANABE, K. FUKUI, E. ISHIGURO, Y. FUJII and Y. SAKISAKA, "Optical Spectra of Cadmium Halide Crystals in 3-30 eV Region", *J. Phys. Soc. Jpn.* **59**, 338 (1990).

K. KAN'NO, K. TANAKA, H. KOSAKA, T. MUKAI, Y. NAKAI, M. ITOH, T. MIYANAGA, K. FUKUI and M. WATANABE, "Decay Time Measurements of Intrinsic Luminescence in Alkali Halides Using Single-Bunched Light Pulses from UVSOR", *Phys. Scripta*, **41**, 120 (1990).

M. WATANABE, H. NAKAGAWA, T. MIYANAGA, H. MATSUMOTO, M. FUJITA and K. FUKUI, "Photochemical Reactions of Molecules on Alkali Halide Surfaces Induced by Undulator Radiation", *Phys. Scripta*, **T31**, 154 (1990).

M. TOBIYAMA, T. KASUGA, H. YONEHARA, M. HASUMOTO, T. KINOSHITA, O. MATSUDO, E. NAKAMURA, K. SAKAI and J. YAMAZAKI, "Suppression of Increase in Impurity in Single-Bunch Mode for the UVSOR Storage Ring", *Jpn. J. Appl. Phys.* **29**, 210 (1990).

G. ISOYAMA, "Simulation of Magnetic Field Correction Scheme for a Halbach-type Undulator", *Rev. Sci. Instrum.* **60**, 1826 (1989).

G. ISOYAMA, S. YAMAMOTO, T. SHIOYA, H. OHKUMA, S. SASAKI, T. MITSUHASHI, T. YAMAKAWA and H. KITAMURA, "Construction of a Multiundulator, Revolver No.19, at the Photon Factory", *Rev. Sci. Instrum.* **60**, 1863 (1989).

M. KAMADA and E.T. ARAKAWA, "Electron-Excited Optical Emission from H$_2$O Adsorbed on Potassium Halides at Low Temperatures", *Nucl., Instr. Methods* **B43**, 525 (1989).

M. KAMADA and E.T. ARAKAWA, "Sputtering of Excited-State Potassium Atoms from Electron-Bombarded KBr Crystals", *J. Vac. Sci. Tech.* **A8**, 3152 (1990).

M. KAMADA, H. YAMAMOTO and E.T. ARAKAWA, "Atomic and Molecular Spectra from Electron-Excited Alkali Halides", *Reviews of Solid State Science,* **4**, 603 (1990) in "Proceedings of the US-JAPAN Seminar on Atomic Processes Induced by Electronic Excitation in Non-Metallic Solids".

M. KAMADA, "Spectroscopic and Photoelectron-Spectroscopic Studies on Condensed Matters by Using Extreme Ultraviolet Radiation from Synchrotron", in "Proceedings of 2nd Int. Symp on Advanced Nuclear Energy Research, Evalution by Accelerators", p.557 (1990).

K. SEKI, H. TANAKA, T. OHTA, Y. AOKI, A. IMAMURA, H. FUJIMOTO, H. YAMAMOTO and H. INOKUCHI, "Electronic Structure of Poly(tetrafluoroethylene) Studied by UPS, VUV Absorption, and Band Calculations", *Phys. Scripta,* **41**, 167 (1990).

T. SUGANO, K. SEKI, T. OHTA, H. FUJIMOTO and H. INOKUCHI, "UV Photoelectron Spectroscopic Study of the Electronic Structure of Poly(dimethylsiloxane) and the Comparison with Related Silicon Compounds", *Nippon Kagaku Kaishi* (in Japanese), 594 (1990).

S. TANAKA, M. ONCHI and M. NISHIJIMA, "The Adsorption and Thermal Decomposition of Formic Acid on Si(100) and Si(111) Surfaces", *J. Chem. Phys.* **91**, 2712 (1989).

S. TANAKA, N. TAKAGI, N. MINAMI and M. NISHIJIMA, "Existence of Two Adsorbed States for K on the Si(100) (2X1) Surface-a Thermal Desorption Study", *Phys. Rev.* **B42**, 1868 (1990).

M.J.L. TURNER, H.D. THOMAS, B.E. PATCHETT, D.H. READING, K. MAKISHIMA, T. OHASHI, T. DOTANI, K. HAYASHIDA, H. INOUE, H. KONDO, K. KOYAMA, K. MITSUDA, Y. OGAWARA, S. TAKANO, H. AWAKI, Y. TAWARA and N. NAKAMURA, "The Large Area Counter on Ginga", *Publ. Astron. Soc. Jap.* **41**, 345 (1989).

K. HAYASHIDA, H. INOUE, K. KOYAMA, H. AWAKI, S. TAKANO, Y. TAWARA, O.R. WILLIAMS, M. DENBY, G.C. STEWART, M.J.L. TURNER, K. MAKISHIMA and T. OHASHI, "The Origin and Behavior of the Background in the Large Area Counters on Ginga and Its Effect on the Sensitivity", *Publ. Astron. Soc. Jap.* **41**, 373 (1989).

K. KOYAMA, H. KONDO, F. MAKINO, F. NAGASE, S. TAKANO, Y. TAWARA, M.J.L. TURNER and R.S. WARWICK, "Are There Many Be Star Binary X-ray Pulsars in the Galactic Ridge?", *Publ. Astron. Soc. Jap.* **41**, 483 (1989).

S. TAKANO, K. KOYAMA and K. MAKISHIMA, "Ginga Observation of X-ray Emission from the Dark Cloud Lynds 1457", *Publ. Astron. Soc. Jap.* **41**, 651 (1989).

K. MAKISHIMA, T. OHASHI, K. HAYASHIDA, H. INOUE, K. KOYAMA, S. TAKANO, Y. TANAKA, A. YOSHIDA, M.J.L. TURNER, H.D. THOMAS, G.C. STEWART, O.R. WILLIAMS, H. AWAKI and Y. TAWARA, "X-ray Spectral Study of M31 with Ginga" *Publ. Astron. Soc. Jap.* **41**, 697 (1989).

K. KOYAMA, H. INOUE, Y. TANAKA, H. AWAKI, S. TAKANO, T. OHASHI and M. MATSUOKA, "An Intense Iron Line Emission from NGC 1068" *Publ. Astron. Soc. Jap.* **41**, 731 (1989).

R.S. WARWICK K. KOYAMA, H. INOUE, S. TAKANO, H. AWAKI and R. HOSI, "Hard X-ray Emission from Markarian 348", *Publ. Astron. Soc. Jap.* **41**, 739 (1989).

K. KOYAMA, M. KAWADA, S. TAKANO and S. IKEUCHI, "Ginga Observations of a Wolf-Rayet Star HD 193793", *Publ. Astron. Soc. Jap.* **42**, L1 (1989).

Review Articles and Textbooks

K. MOROKUMA, U. NAGASHIMA, S. YAMAMOTO, N. KOGA, S. OBARA and S. YABUSHITA, "Chemical Calculation on Japanese Supercomputers", in "Methods in Computational Chemistry", Vol. 3, ed. by S. Wilson, Plenum Publishing, p.147 (1989).

H. NAKAMURA and H. TAKAGI, "Superexcited States of Molecules — Their Dynamic Processes and Quantum Defect Theory", *Butsuri* (in Japanese) **45**, 87 (1990).

A. OHSAKI and H. NAKAMURA, "Hyperspherical Coordinate Approach to Atom-diatom Chemical Reactions in the Sudden and Adiabatic Approximations", *Physics Reports* **187**, No.1, 1 (1990).

K. NASU, "Strong Electron-Phonon Coupling and Many-Body Problems.", *The Most Front of Physics*, Y. Otsuki Ed, (Kyoritsu-Shuppan, Tokyo, in Japanese) **27**, 79 (1990).

K. HIRAO, " The SCF Theory. The Cluster Expansion of a Wavefunction Formalism", in "Self-Consitent Field" R. Carbo and M. Klobukowski Eds, Elsevier, 1990.

E. HIROTA, "Japan-UK Cooperative Research on High-Resolution Spectroscopy", *Bunko-kenkyu* (in Japanese) **38**, 441 (1989).

E. HIROTA, "Transient Molecules, Free Radicals and Molecular Ions, Investigated by High-Resolution Spectroscopy", *Int. Revs. Phys. Chem.* **8**, 171 (1989).

T. GOTO and E. HIROTA, "Measurements of Non-Emissive Radicals in Silane Plasma Using Laser Absorption Spectroscopy", *Rev. Laser Eng.* (in Japanese) **17**, 595 (1989).

C. YAMADA and E. HIROTA, "Absorption Spectroscopic Measurements Using Infrared Lasers", in "Basis of Plasma Diagnosis (in Japanese)", The Japan Society of Plasma and Nuclear Fusion Research Ed., Nagoya Univ. Press, pp. 194-208 (1990).

E. HIROTA and Y. ENDO, "Molecules — their Structures and Properties (in Japanese)", Dainippon Tosho, 1990.

E. HIROTA, "The Institute for Molecular Science", *Chemistry and Industry* (in Japanese) **43**, 320 (1990).

E. HIROTA, "Future in Chemistry", *Chemistry* (in Japanese) **45**, 16 (1990).

E. HIROTA, "Si-Containing Short-Lived Molecules and Interstellar Molecules", *Organometallic News* (in Japanese) No.1, 22 (1990).

E. HIROTA, "Molecular Structure and Density of Free Radicals Determined by Laser and Microwave Spectroscopy", *Oyo Buturi* (in Japanese) **59**, 866 (1990).

E. HIROTA, "New Developments in Molecular Spectroscopy of Si-Containing Molecules", *Chemistry* (in Japanese) **45**, 572 (1990).

K. KAMOGAWA and T. KITAGAWA, "Application of Raman Difference Spectroscopy to Solution Chemistry", in "Vibrational Spectra and Structure" (J.R. Durig Ed.) **17B**, 447-472 (1989).

T. KITAGAWA and A. MAEDA, "Vibrational Spectra of Rhodopsin and Bacteriorhodopsin (Yearly Review)", *Photochem. Photobiol.* **50**, 883 (1989).

Y. UDAGAWA and K. TOHJI, "A Possibility of X-ray Raman Scattering as a Tool of Structure Determination (in Japanese)", *Hoshako* **2**, 35 (1989).

Y. UDAGAWA, K. TOHJI and T. MIZUSHIMA, "EXAFS Measurement in Laboratories (in Japanese)", *Rigaku Denki Journal* **20**, 3 (1989).

Y. UDAGAWA, "The Most Attractive work in the Year (in Japanese)" *Kagaku* **45**, 157 (1990).

K. YOSHIHARA, "Picosecond and Femtosecond Laser Spectroscopy-Application to Condensed Phases", *High Polymers*, Japan (in Japanese) **39**, 445 (1990).

K. YOSHIHARA, "Spectroscopic Measurements in Photochemistry: II. Ultrafast Photochemical Processes", *Bunko Kenkyu* (in Japanese) **39**, (1990).

H. OKAMOTO, "Time-Resolved Coherent Anti-Stokes Raman Scattering Using Femtosecond Light Pulses", *Bunko Kenkyu (J. Spectrosc. Soc. Jpn.)* (in Japanese) **38**, 437 (1989).

R. NAKAGAKI, "Photoreduction of Nitroaromatic Species. — Properties and Reactivity of Excited States —", *J. Synth. Org. Chem.* (Yuki Gosei Kagaku Kyoukai-shi, in Japanese) **48**, 65 (1990).

K. KIMURA, "Photoionization Spectroscopy of Molecules and Molecular Clusters by Synchrotron Radiation", *Hyoumenn* (in Japanese) **28**, 328 (1990).

K. KIMURA, "Diagnosis of Molecules by Laser Photoelectron Spectroscopy", *Gendai Kagaku* (in Japanese), **134**, 38 (1990).

K. SHOBATAKE, "Chemistry '90 — Dynamics of Surface Reactions", *Chemistry* (in Japanese), **45**, 62 (1990).

K. SHOBATAKE, "Synchrotron Radiation-Excited Etching Reactions", *Hoshako* (*J. Jpn. Soc. Synchrotron. Rad. Res.*) (in Japanese), **3**, 27 (1990).

K. SHOBATAKE and H. SHINOHARA, "Spectroscopic Measurements in Photochemistry. III. Molecular Beam Techniques", *J. Spectrosc. Soc. Jpn.* (in Japanese), **39** (3), 187 (1990).

K. SHOBATAKE, "Synchrotron Radiation. A Fantastic Light Source," *Chemistry* (in Japanese), **45**, 608 (1990).

M. SATO, M. SERA, S. SHAMOTO, M. ONODA, S. YAMAGATA and H. FUJISHITA, "Characteristics of Electronic Properties of High-T_c Oxides", Research Report on Mechanisim of Superconductivity March 1990 p.119.

T. TAKAHASHI, H. MATSUYAMA, H. KATAYAMA-YOSHIDA, T. WATANABE, T. EJIMA, T. KASHIWAKURA, S. SUZUKI, S. SATO, N. KOSUGI, A. YAGISHITA, K. TANAKA, H. MAEZAWA, H. FUJIMOTO, K. SEKI, K. KAMIYA, S. SHAMOTO, M. SATO and H. INOKUCHI, "Electronic Structure of High-T_c Superconductor Studied by Photoemission and X-Ray Absorption", Research Report on Mechanism of Superconductivity March 1990, p.249.

S. SATO, "Photocatalytic Activities of Titanium Dioxide Powder", *Hyomen* (in Japanese), **28**, 427 (1990).

K. NAKASUJI, "Aromaticity and Multistage Redox Systems: Dynamic Aromaticity", *Kagaku to Kogyo* (in Japanese) **42**, 1003 (1989).

K. NAKASUJI, "Solid State Physical Organic Chemistry: Union of *Synthesis* and *Solid State Properties*", *Butsuri* (in Japanese) **45**, 390 (1990).

J. TOYODA and K. NAKASUJI, "Exploration of New Conjugated Electronic Systems with Potentially Interesting Solid State Properties", *Chemistry* (in Japanese) **45**, 60 (1990).

K. NAKASUJI, "Exploration of Organic Molecular Metals", *MOL* (in Japanese) **28**, No.5, 110 (1990).

M. MISHIMA, "Chemical Reaction without Solvent", *Kagaku to Yakugaku no Kyoshitsu* (in Japanese) **No. 10**, 16 (1989), Hirokawa Shoten.

J. INANAGA, "Samarium Diiodide — A Versatile Reagent in Organic Synthesis", *Yuki Gohsei Kagaku Kyokai-shi* (in Japanese) **47**, 200 (1989).

J. INANAGA, "Reduction of Organic Functions via SmI$_2$-Promoted Electron Transfer Process", *Reviews on Heteroatom Chemistry* Vol.3, S. Oae Ed., MYU, 75 (1990).

H. OHTAKI, "Transfiguration of Solution Chemistry" (in Japanese), *Chemistry*, **44**, 356 (1989).

H. OHTAKI, "Dissolution of Electrolytes — Structures and Dynamics of Solutions" (in Japanese), *New Ceramics*, **36** (1990).

H. OHTAKI, "Structure and Reactions of Electrolytes in Solution" (in Japanese), *Denki Kagaku*, **58**, 591 (1990).

H. OHTAKI, "Ionic Hydration" (in Japanese), Kyoritsu Shuppan Co. (1990).

E. KIMURA, "Chemistry and Functions of Recently Developed Macrocyclic Polyamiens", *J. Inclusion Phenomena*, **7**, 183 (1989).

E. KIMURA, "Shape-recognition Molecules", *Kagaku*, **45**, 35 (1990).

Y. KUSHI, "The Short History of the Periodic Table — (1)", *Chemistry* (in Japanese), **45**, pp.314-319 (1990).

Y. KUSHI, "The Short History of the Periodic Table — (2)", *Chemistry* (in Japanese), **45**, pp.393-397 (1990).

H. MASUDA, "Are Origins of Oxygen-Transport Proteins Same?", *Kagaku Kogyo* (in Japanese), **43**, 673 (1990).

R. KURODA, "Determination of a Difficult Structure: A Case of Strong Correlations between Parameters", *Rigaku J.* **6**, 22 (1989).

Y. YAMASHITA, "Novel Electron Acceptors and Donors Containing Fused-heterocycles", *Yuki gohsei Kagaku Kyohkai-shi* (in Japanese), **47**, 1108 (1989).

K. FUKE, "Reations of Gas-phase Metal and Semiconductor Clusters", *Situryou Bunseki* (in Japanese), **38**, 221 (1990).

K. KIMURA, "The Effect of Shape and Size on the Electronic Properties of Ultrafine Metallic Particles", *Phase Transitions,* **24-26**, 493 (1990).

K. KIMURA, " Metal Microclusters" (in Japanese), in "Handbook of Ultrafine Particles", K. Ono Ed., Fuji Techno-System, Tokyo, 889 (1990).

K. KIMURA, "Handling of Materials" (in Japanese), in "Basic Operation II, Jikken Kagaku Kohza 2", H. Inokuchi Ed., Maruzen, Tokyo, 308 (1990).

H. OKAMOTO, "Infrared Spectroscopy of Structural Phase Transitions in Organic Charge-Transfer Crystals", *Butsuri Gakkaishi* (in Japanese) **45**, 567 (1990).

M. WATANABE, "Front End of Beamline", in "Techniques for Utilization of Synchrotron Radiation" (in Japanese), *Science Forum*, pp.81-84 (1989).

M. ANDO and M. WATANABE, "Synchrotron Radiation and Material Science", *Kagaku* (in Japanese) **60**, 419 (1990).

M. SAKURAI, S. MORITA, H. YONEZU, J. FUJITA, K. FUKUI, K. SAKAI, E. NAKAMURA, M. WATANABE, K. YAMASHITA and E. ISHIGURO, "A Beam Line for Radiometric Calibration at UVSOR", *Hoshako* (in Japanese) **2**, 13 (1989).

K. SEKI, "Photoelectron Spectroscopy of Polymers", in "Optical Techniques to Characterize Polymer Systems", H. Baessler Ed., Elsevier Amsterdam, pp.115-180 (1989).

Institute for Molecular Science, Myodaiji, Okazaki 444, Japan